Forschungszentrum Karlsruhe
in der Helmholtz-Gemeinschaft

Wissenschaftliche Berichte
FZKA 6888

Solutions of Dissimilar Material Singularity and Contact Problems

Y. Yang
Institut für Materialforschung

September 2003

Forschungszentrum Karlsruhe

in der Helmholtz-Gemeinschaft

Wissenschaftliche Berichte

FZKA 6888

Solutions of Dissimilar Material Singularity and Contact Problems

Yingyuan Yang

Institut für Materialforschung

Von der Fakultät für Maschinenbau der Universität Karlsruhe (TH)
genehmigte Habilitationsschrift
zur Anerkennung der Lehrbefähigung
im Fachgebiet Werkstoffmechanik

Forschungszentrum Karlsruhe GmbH, Karlsruhe
2003

Impressum der Print-Ausgabe:

Als Manuskript gedruckt

Forschungszentrum Karlsruhe GmbH
Postfach 3640, 76021 Karlsruhe

Mitglied der Hermann von Helmholtz-Gemeinschaft
Deutscher Forschungszentren (HGF)

ISSN 0947-8620

Solutions of Dissimilar Material Singularity and Contact Problems

Abstract

Due to the mismatch of the material properties of joined components, after a homogeneous temperature change or under a mechanical loading, very high stresses occur near the intersection of the interface and the outer surface, or near the intersection of two interfaces. For most material combinations and joint geometries, there exists even a stress singularity. These high stresses may cause fracture of the joint. The investigation of the stress situation near the singular point, therefore, is of great interest. Especially, the relationship between the singular stress exponent, the material data and joint geometry is important for choosing a suitable material combination and joint geometry. In this work, the singular stress field is described analytically in case of the joint having a real and a complex eigenvalue. Solutions of different singularity problems are given, which are two dissimilar materials joint with free edges; dissimilar materials joint with edge tractions; joint with interface corner; joint with a given displacement at one edge; cracks in dissimilar materials joint; contact problem in dissimilar materials and logarithmic stress singularity. For an arbitray joint geometry and material combination, the stress singular exponent, the angular function and the regular stress term can be calculated analytically. The stress intensity factors for a finite joint can be determined applying numerical methods, e.g. the Finite Element Method (FEM). The method to determine more than one stress intensity factor is presented. The characteristics of the eigenvalues and the stress intensity factors are shown for different joint conditions.

Lösungen für Spannungssingularitäts- und Kontaktprobleme in Stoffverbunden

Zusammenfassung

In Stoffverbunden entstehen aufgrund der unterschiedlichen Materialeigenschaften bei mechanischer Belastung oder nach einer Temperaturänderung hohe Spannungen in der Nähe des freien Randes der Grenzfläche oder in der Nähe einer inneren Ecke. In den meisten Fällen treten Spannungssingularitäten auf, die zum Versagen des Bauteils führen können. Die genaue Berechnung des Spannungsfeldes und der Einfluss der Materialeigenschaften und der Geometrie des Verbundes auf die Spannungen ist von groβer

Bedeutung für die Werkstoffauswahl und die geometrische Gestaltung des Verbundes. Die Spannungen im Nahfeld werden in analytischer Form für reelle und komplexe Eigenwerte dargestellt. Lösungen für verschiedene Probleme werden angegeben: Zweistoffverbunde mit freien Rändern oder mit belasteten Rändern, Verbunde mit inneren Ecken, Verbunde mit vorgegebener Verschiebung am Rand, Risse in Stoffverbunden, Kontakt von zwei verschiedenen Werkstoffen. Logarithmische Spannungssingularität wird auch berücksichtigt. Die Singularitätsexponenten, die Winkelfunktionen und der bei thermischer Belastung auftretende reguläre Spannungsterm können analytisch berechnet werden. Der Spannungsintensitätsfaktor wird mit der Methode der Finiten Elemente berechnet. Dies ist auch möglich, wenn mehrere singuläre Terme auftreten. Die Eigenschaft der singulären Spannungsexponenten und der Spannungsintensitätsfaktoren werden für Stoffverbunde mit verschiedenen Randbedingungen aufgezeigt.

Contents

Nomenclature

Φ	stress function
T	temperature change
E	Young's modulus
ν	Poisson ratio
α_1, α_2	thermal expansion coefficient
α,β	Dundurs parameters
r, θ	polar coordinates
θ_1, θ_2	angle of the material 1 and 2
u	displacement component in the r direction
v	displacement component in the θ direction
σ_{ij}	stress tensor
σ_{ij0}	regular stress tensor
σ	normal stress component
τ	shear stress component
λ	real eigenvalue
Λ	complex eigenvalue
A,B,C,D	coefficients in real stress function
$\mathcal{A}, \mathcal{B}, \mathcal{C}, \mathcal{D}$	coefficients in complex stress function
ω	stress exponent
f_{ij}	angular faction
g	G_2/G_1
μ	E_2/E_1
ξ_k	see the equation under Eq. (3.1.113)
t_n, p_n	real and imaginary part of the complex eigenvalue
q	see the equation under Eq.(3.2.1)
$\bar{r}$	r/R
R	R is a characteristic length of a joint
L	interface length
$\wedge$	quantities in the Mellin domain
R_0	radius with temperature change in a semi-infinite joint
$\bar{R}_0$	R_0/R
s	Mellin transform parameter
$\parallel X \parallel$	determinant of $[a_{ij}]$ in Eqs. (3.2.29 - 3.2.32)
p_{ij}, g_{ij}	see Eq. (3.2.45)
$\bar{q}$	see Eqs. (3.2.66) and (3.2.67)
K_0	unknown factor in the regular stress term
K or K_i	i=1 or 2 or L or H, stress intensity factors
H_1, H_2	height of material 1 and 2 in a quarter plane joint

σ_{ij0}^{TH}	regular stress term according to temperature change
σ_{ij0}^{RM}	regular stress term according to remote mechanical loading
σ_{ij0}^{ET}	regular stress term according to edge traction
$\sigma_{ij}^{ET}(\theta)$	$(r/R)^l \sigma_{ij}^{ET}(\theta)$ is the higher order regular stress term according to edge traction
f_{ij}	for logarithmic singularity see Eq.(7.1.5) or Eq.(7.2.11)
t_{ij}	for logarithmic singularity see Eq.(7.1.6) or Eq.(7.2.12)
l_{ij}	for logarithmic singularity see Eq.(7.1.7)
Q	for logarithmic singularity see Eq.(7.1.39) or for r^ω singularity see Eqs. (8.2.20) and (8.2.21)
η	friction coefficient

Chapter 1

Introduction

In many technical areas two or more dissimilar materials have to be joined together to take the advantage of the properties of the different materials. The joining of ceramic to metal to combine the ceramic's wear resistance, high temperature strength, and low thermal or electrical conductivity with the ductility of the metal is especially important. Examples of the application of ceramic - metal joints are heat engines [1], turbocharger rotors [2], electronic or microelectronic components [3], and nuclear fusion components [4]. Another example of materials joint is a coated structure for thermal protection, wear resistance, and corrosion resistance. In the electronic field many dissimilar material layers are joined together as chips.

With increasing use of bonded joints, their behavior is of interest in many engineering disciplines. Both mechanical and thermal loading at fabrication or in service are relevant. For the reliable design of such components, and for choosing a material combination and a joint geometry, a stress analysis is required for elastic, elastic - plastic or viscoplastic material behavior. In particular, the effect of residual stresses caused by thermal mismatch of the joined components needs to be investigated, because these residual stresses may lead to fracture of joints directly after the fabrication of cooling from high temperature.

For two-dimensional problem the stress distribution, in the range far away from the edges of a simple joint geometry, can be calculated analytically by using the plate or beam theory [5, 6, 7]. Near the bonded edges, the stresses can be calculated applying the numerical method, e.g. the Finite Element Method (FEM) or the Boundary Element Method (BEM).

Due to the mismatch of the material properties of the joined components after a homogeneous temperature change or under a mechanical loading, very high stresses occur near the intersection of the interface and the outer surface, or near the intersection of two interfaces. For most material combinations and joint geometries, there exists even a stress singularity. This intersection point is called singular point. These high stresses

may cause fracture of the joint. Therefore, the investigation of the stress situation near the singular point is of interest. Due to the singularity, the stresses directly near the singular point calculated from FEM are not accurate. To determine the stress and displacement fields in the neighborhood of the singular point, a combination of analytical and numerical methods has to be applied.

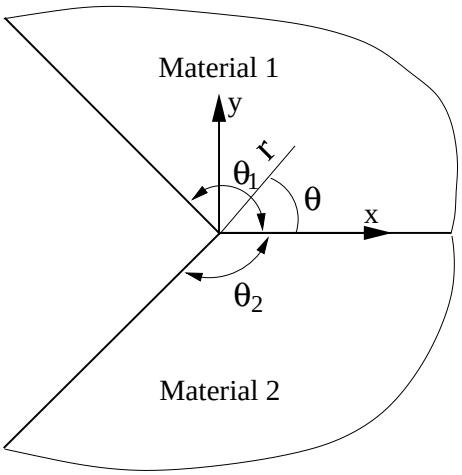

Figure 1.1: A general two dissimilar materials joint with free edges.

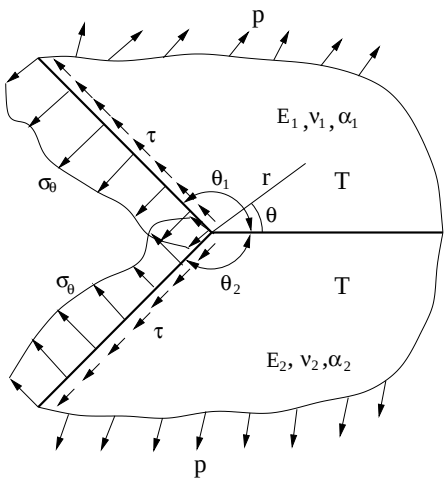

Figure 1.2: A joint with edge tractions.

In the presented work, the stress and displacement field near the singular point are studied for 2-D problem, in which the joint geometry may have arbitrary angles θ_1, θ_2 (see Figs. 1.1 - 1.9).
The focuses are:
(a) to describe the stress and displacement field near the singular point analytically with some unknown parameters, which are the so called stress intensity factors;
(b) to give the methods and solutions for calculating all quantities used to describe the stress and displacement field;
(c) developing empirical relations between the stress intensity factors, the geometry and the material properties of the joint.
The aim of this work is to give explicit solutions for calculating the stress and displacement field near the singular point. This means that, for example, to determine the singular stress exponent an explicit transcendental equation will be given, not only the determinant, or to calculate the angular function the explicit equations for the coefficients are presented, not only the linear equations system, and so on. This is convenient for the engineer to analyze the singular stress field without deriving and solving the complicated equations system.

For a given material combination and joint geometry, the singularity behavior depends on the conditions at the interface and at the outer surfaces. By selecting a suitable

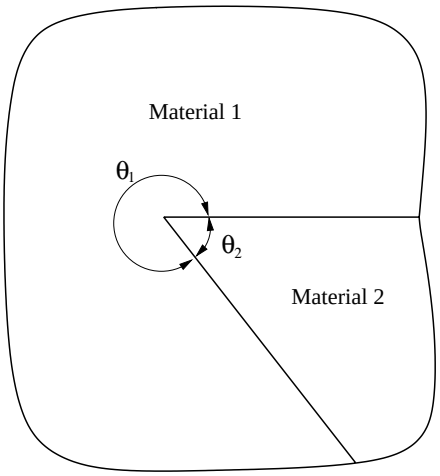

Figure 1.3: A joint with an interface corner.

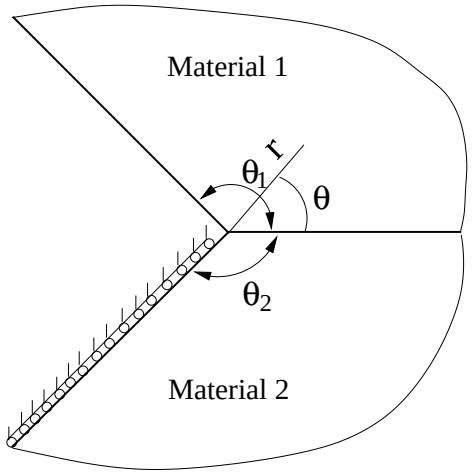

Figure 1.4: Joint with a given displacement at one edge.

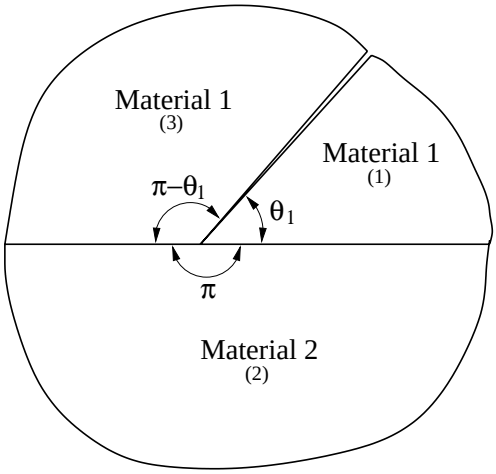

Figure 1.5: Joint with a crack terminating at the interface.

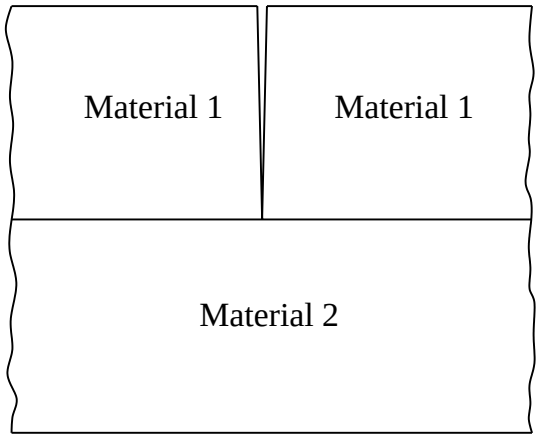

Figure 1.6: Joint with a crack perpendicular to the interface.

material combination, joint geometry and boundary conditions, stress singularities can be avoided or weakened. In the following Sections, some of the typical boundary conditions will be treated.

The usually appeared two dissimilar materials joint in the practice is a joint with perfect interface and two free edges (see Fig. 1.1), which is considered in Chapter 3. One special case, i.e. a notch or a crack in a homogeneous material, is discussed in Chapter 4. If the edges of the joint is not stress free, but with edge tractions (see Fig. 1.2) the stress analysis is given in Chapter 5. For a joint with two interfaces and having an interface corner (see Fig. 1.3), the singularity behavior differs to that one of a joint with free edges, see Chapter 6. On rare occasions, the logarithmic stress singularity appears in a dissimilar materials joint, which is investigated in Chapter 7. If the displacement at one edge of the joint is given (see Fig. 1.4), the singularity is

stronger than a joint with a free edge or edge with traction for the same joined materials and geometry (the details are described in Chapter 8). Due to the different material properties of the joined components, cracks often exist in the joint. The analytical description of the stress field near the singular point in a joint with different type of cracks (see Figs. 1.5 - 1.8) is presented in Chapter 9. Finally, a special case of a joint, i.e. the contact problem of two dissimilar materials (see Fig. 1.9), is studied in Chapter 10.

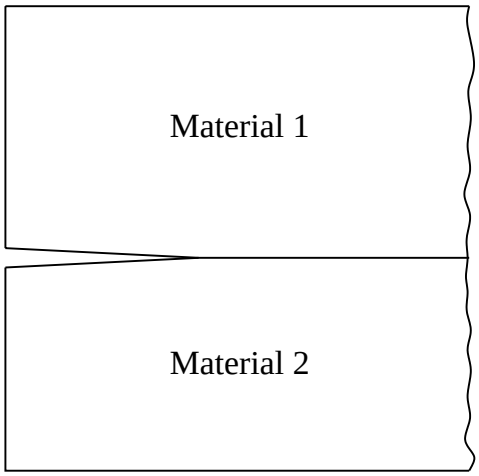

Figure 1.7: Joint with an interface crack.

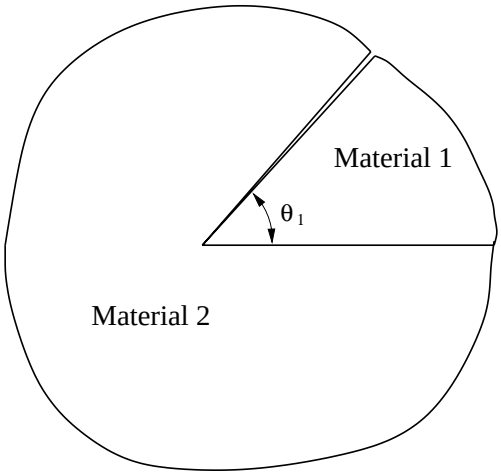

Figure 1.8: Joint with an interface corner crack.

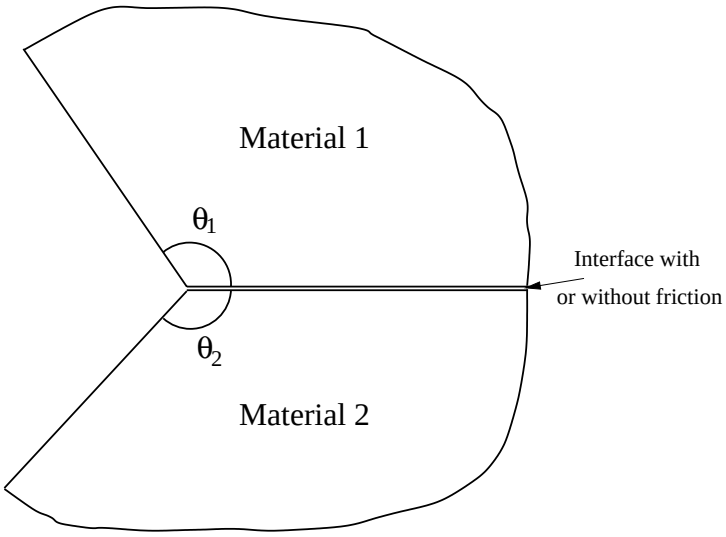

Figure 1.9: Contact problem of two dissimilar materials.

All calculations are performed for elastic isotropic material behaviour.

Chapter 2

Review on the Stress Singularities in Dissimilar Material Joints

In a dissimilar materials joint, the boundary and interface conditions may be different. The following boundary conditions may be assumed: (a) the edge is stress free; (b) the edge is loaded with tractions; (c) the edge has a given displacement. At the interface there may be a perfect bond or sliding with friction.
The methods to analyze the stresses near the edges can be divided into three groups:
(I) The approximate or semi-analytical method.
This method is based on the elasticity theory and on some assumptions (see e.g. [7] - [23]). The special assumption may be, for example, one stress component decreases exponentially with increasing distance from the interface, or the shear stress in a thin layer varies linearly [11]. In these calculations, the stress singularity is not considered. Anisotropic material has been considered in [17, 23] applying semi-analytical methods.
(II) Numerical method.
To calculate the stress distribution near the edges, conventional finite element method or the boundary element method is often used (see e.g. [24, 25, 26]). Due to the singularity, however, the stresses very close to the singular point cannot be determined accurately. Therefore, some special elements, the so-called singular elements, have be developed [27, 28, 29, 30, 31]. To use the singular element, the singularity behavior (i.e. the singular stress exponent) of the joint has to be known. For each joint, one finite element calculation has to be done to obtain the stress distribution near the edges. Another disadvantage of this method is that the dependency of the stresses on the material data, the joint geometry, and the boundary conditions is not explicit.
(III) Asymptotic description of the singular stress field.
To study the dependency of the singular stress on the material data, the joint geometry, and the boundary conditions, it is useful to find an analytical description of the stress field near the singular point. Willams [32] has found that the stress singularity can be described by the term $r^{-\omega}$, where r is the distance from the singular point and ω is called stress exponent. If $\omega > 0$, $r^{-\omega}$ approaches infinity for $r \to 0$. The well known case is a homogeneous material with a crack, where $\omega = 0.5$. For a two dissimilar

materials joint, in general, ω is not equal to 0.5, it may be smaller or larger than 0.5 (e.g. in a joint with a given displacement at one edge, or in a joint with a delamination crack, not an interface crack). In the last 20 years, numerous investigations were performed on the stress singularity of a dissimilar materials joint.

Joint with free edges

In this section, a joint with a perfect bonding at the interface and the edges being stress free is considered. Different methods have been used to determine the stress exponent ω, e.g. using an Airy's stress function, or a displacement function, or analysis complex functions, or using the Mellin transform method (see [5], [32] - [83]). The joint may be made of two dissimilar isotropic materials (see e.g., [5, 33, 34, 35, 37, 39, 40, 41, 46, 47, 55, 56, 83, 84, 86, 87]), or two dissimilar anisotropic materials (see e.g., [36, 44, 45, 49, 57, 58, 59, 60, 61]). A special case is a homogeneous (isotropic or anisotropic) material with a notch or a crack, which was considered in [32, 38, 42, 43, 48, 49, 50, 51, 52, 53, 54]. The stress exponent depends on the material data and the contact angles θ_1, θ_2. However, the stress exponent ω is not the only parameter to describe the singular stress field as it will be shown below. For convenience, the joint will be divided into two groups: (A) quarter planes joint with $\theta_1 = 90°, \theta_2 = -90°$, which is often used in engineering, (B) joint with arbitrary θ_1, θ_2.

(A) Quarter planes joint
For this joint geometry, there exists only one singular term and the singular stress field can be described by

$$\sigma_{ij}(r,\theta) = \frac{K}{(r/R)^{\omega}} f_{ij}(\theta) + \sigma_{ij0}(\theta)$$

where the stress exponent ω can be determined by solving a transcendental equation [34, 37, 62]. The angular function $f_{ij}(\theta)$ can be calculated analytically [34, 41, 62, 63, 64, 65, 66]. The regular stress term $\sigma_{ij0}(\theta)$ for thermal loading can be obtained analytically as well [34, 62, 63]. The quantity R is a characteristic length of the joint, e.g. the length of the interface. The parameter K is called stress intensity factor. This definition is different from that one used in fracture mechanics, because the distance r is divided by R. The advantage of this definition is that the value of factor K is independent of the absolute size of the joint and that the factor K has the unit of a stress. For a finite joint, in general, the factor K cannot be determined analytically. However, it can be calculated by means of numerical methods, e.g. FEM ([41, 62, 63, 67, 68, 69]), the boundary collocation method ([34, 70, 71, 72]), the weight function method [73], the boundary integral method ([74]) or the path independent integral method [75, 76, 77]. For the convenience of engineers, some empirical equations have been developed to calculate the stress intensity factors without using any numerical methods [78, 79, 80].

(B) Joint with arbitrary angle.
For a joint with arbitrary angles θ_1, θ_2, there may be more than one singular term ([39, 81]) and the analytical description of the stress field is more complicated than that one in a quarter planes joint. In general, the stresses can be calculated from

$$\sigma_{ij}(r,\theta) = \sum_{n=1}^{N} \frac{K_n}{\bar{r}^{\omega_n}} f_{ijn}(\theta) + \sigma_0 f_{ij0}(\theta)$$

for a joint with real eigenvalues [81, 82] and

$$\sigma_{ij}(r,\theta) = \sum_{n=1}^{N} \frac{K_n}{\bar{r}^{\omega_n}} \quad \Big\{ \quad \cos[p_n ln\bar{r}] f^c_{ijn}(\theta) + \sin[p_n ln\bar{r}] f^s_{ijn}(\theta) \Big\} + \sigma_0 f_{ij0}(\theta)$$

for a joint with complex eigenvalues [83], where the real part ω_n and the imaginary part p_n of the eigenvalues can be determined by solving a transcendental equation [35, 39]. The angular functions $f_{ijn}(\theta)$ can be calculated analytically [84] and $f^c_{ijn}(\theta), f^s_{ijn}(\theta)$ also [83]. The regular stress term $\sigma_0 f_{ij0}(\theta)$ can be determined analytically as well [85, 86, 87]. If there is only one singular term (i.e. N=1), the determination of factor K is easy, like for a quarter plane joint. If there are two singular terms, the factors K_1, K_2 corresponding to ω_1, ω_2 ($\omega_1 > \omega_2$) were determined in [88] as follows: (a) calculate the stresses in the whole joint by using FEM (or another numerical method); (b) determine K_1 from the stress values for very very small r by using only one term; (c) determine K_2 from the stress values for a little larger r and using the known K_1. In this process, only one factor K can be determined at each time. This method can be used only when the absolute value of ω_1 is much larger than that one of ω_2. If the values of ω_1 and ω_2 are similar, the stresses calculated from the asymptotic equation by using the determined K-factor values are accurate only for a very small distance r, which is not in the range of practical interest. In [81] a method is given to determine more than one factor K at the same time.

One special case is $\theta_1 = 180°, \theta_2 = -180°$, which is the well-known case of a joint with an interface crack (see [89] - [102]). For this case, the eigenvalues are $0.5 \pm i\varepsilon$, i.e. the eigenvalues are always complex. Due to the terms $\sin[\epsilon ln\bar{r}]$ and $\cos[\epsilon ln\bar{r}]$, the stresses oscillate in the range very, very close to the singular point. For most joint material combinations, the value of ε is very small. Therefore, the oscillation effect can be neglected [92]. To avoid the stress oscillation, some models have to be developed [91, 93, 95].

Another special case is a homogeneous (isotropic or anisotropic) material with a notch under mechanical loading. The stress singularity has been studied in many publications [32, 38, 42, 43, 103, 104, 105, 106, 107].

Joint with edge tractions

Comparing to a joint with free edges, there are a few publications considering a joint with edge tractions. Most of them focused on the study of stress singular exponents [35, 36, 37]. The stress solution has been studied only for a quarter planes joint under a constant edge traction [108, 109].
In the analytical description of the singular stress field, the stress exponent, the angular functions, and the method to determine the factor K are the same as that one in a joint with free edges. For satisfying the boundary conditions, however, higher order regular stress terms have to be considered [110].

Joint with two interfaces

There are many applications, in which the joint has an interface corner, i.e. the materials occupy an angle of 360° and there are two interfaces (see Fig. 1.3). At the intersection point of the interfaces, stress singularity exists for most cases. To describe the singular stress field analytically, the stress exponents can be determined by solving a transcendental equation [111, 112, 113]. The calculation of the angular functions is given in [114]. The regular stress term is considered in [115] and the stress intensity factor is discussed in [115, 116].

Joint with a given displacement at the edge

Investigations of a two dissimilar materials joint mostly concentrate on joints having stresses at the edges as boundary condition. If displacement is given at the edge, the singularity behavior of the joint is more complicated than that of a joint with a free edge. In [32, 38, 46, 103, 117] the determination of the stress exponent is studied. Most studies focus on a homogeneous material with a notch or a crack. For a dissimilar materials joint, there may be three singular terms and the stress exponent may be larger than 0.5.

Logarithmic stress singularity

For most material combinations and joint geometries, the stress singularity can be described by $r^{-\omega}$. For a given joint geometry, however, some material combinations exist or for a given material combination some joint geometries exist, where the singular stress field cannot be described by the type of $r^{-\omega}$ singularity. In these cases, the singular stress field should be described by ln(r) or $r^{-\omega}\ln(r)$, which are called logarithmic singularity. Bogy and Dempsey [33, 35, 46, 111, 118] described the conditions of a two dissimilar materials joint with the type of ln(r) or $r^{-\omega}$ln(r) singularity. In [45, 119, 120], the logarithmic singularity problems have also been discussed. Bogy [118] studied the type of ln(r) singularity in a quarter planes joint under edge tractions. Dempsey [121]

examined special cases with an $r^{-\omega}ln(r)$ singularity. In fact, the conditions of a two dissimilar materials joint with the type of ln(r) or $r^{-\omega}ln(r)$ singularity is also dependent on the loading condition [122].

Contact problem in dissimilar materials

For a two dissimilar materials contact problem, in which the interface is friction free or with friction, still stress singularity exists for most material combinations and contact geometries. The stress singularity can also be described by $r^{-\omega}$. Dempsey and Sinclair [33] have given the equations to determine the stress exponent ω for interfaces with and without friction. Adams and Bogy [125, 126] have studied the friction free contact problem in semi-infinity bodies, in which the stresses can be determined by solving singular integral equations. Dundurs and Lee [127] have considered the friction free contact problem with the contact geometry $\theta_2 = 180^\circ$ and θ_1 being arbitrary, in which the dependency of the stress exponent on the Dundurs parameter α is given. In [128] experimental results are presented for the contact geometry corresponding to that one used by Dundurs and Lee. Comninou [95] and [129] discussed the interface crack problem with friction.

Chapter 3

Two Dissimilar Materials Joint with Free Edges

In a two dissimilar materials joint with free edges, after a homogeneous temperature change or under a mechanical loading very high stresses occur near the intersection of the interface and the edges due to the difference of the material properties and the thermal expansion coefficients of the joined components and due to the free edge effect. In most cases, stress singularities exist at the intersection point for elastic material behaviors. It is called singular point. The stresses near the singular point can be described analytically as

$$\sigma_{ij}(r,\theta) = \sum_{n=1}^{N} \frac{K_n}{\bar{r}^{\omega_n}} f_{ijn}(\theta) + \sigma_0 f_{ij0}(\theta) \tag{3.0.1}$$

for a joint with real eigenvalues and

$$\sigma_{ij}(r,\theta) = \sum_{n=1}^{N} \frac{K_n}{\bar{r}^{\omega_n}} \Big\{ \cos[p_n ln\bar{r}] f^c_{ijn}(\theta) + \sin[p_n ln\bar{r}] f^s_{ijn}(\theta) \Big\} + \sigma_0 f_{ij0}(\theta) \tag{3.0.2}$$

for a joint with complex eigenvalues, where $\bar{r}$=r/R and R is a characteristic length of the joint. In Eqs. (3.0.1) and (3.0.2) ω_n is the stress exponent, which corresponds the real part of the eigenvalue, p_n is the imaginary part of the eigenvalue, $f_{ijn}(\theta)$, $f_{ij0}(\theta)$, $f^c_{ijn}(\theta)$ and $f^s_{ijn}(\theta)$ are the angular functions, the term $\sigma_0 f_{ij0}(\theta)$ is called regular stress term, which is independent of the distance from the singular point. K_n is called stress intensity factor and has the unit of a stress, because the distance r is divided by R (for the coordinates see Fig. 3.1). The quantities ω_n, $f_{ijn}(\theta), f_{ij0}(\theta), f^c_{ijn}(\theta), f^s_{ijn}(\theta)$, and σ_0 can be calculated analytically for an arbitrary joint geometry (with θ_1, θ_2) and for an arbitrary material combination (i.e. $E_1, E_2, \nu_1, \nu_2, \alpha_1, \alpha_2$ being arbitrary). The quantity K_n cannot be calculated analytically for a finite joint, it should be determined applying a numerical method, for instance, the Finite Element Method (FEM) or the Boundary Element Method (BEM).

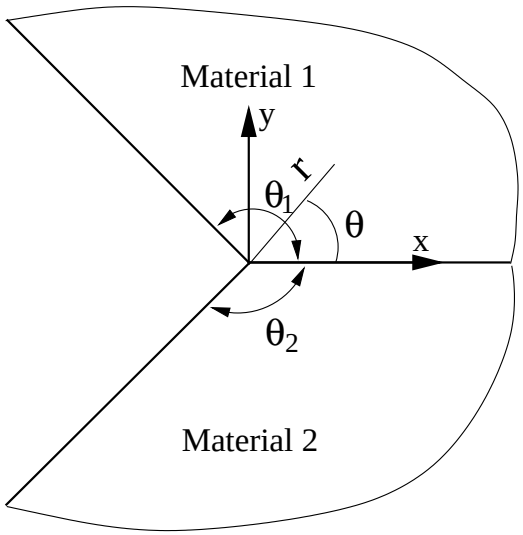

Figure 3.1: A general two dissimilar materials joint with the coordinates system.

In Sections 3.1, 3.2, 3.3 and 3.4 methods to determine the quantities ω_n, p_n, $f_{ijn}(\theta)$, $f_{ij0}(\theta)$, $f^c_{ijn}(\theta)$, $f^s_{ijn}(\theta)$, σ_0, and K_n will be given for a joint with free edges under thermal and mechanical loading.
The behaviour of the quantities ω_n and K_n for some joint geometries and material combinations will be shown in Section 3.5 to prove and apply the given methods. Especially, empirical relations will be given to calculate the stress intensity factors K_n without using FEM. In Section 3.6 the displacement field near the singular point is discussed. The size effect on the stress distribution near the singular point is presented in Section 3.7.

3.1 Determination of the Stress Exponents and the Angular Functions

3.1.1 Joint with Real Eigenvalues

For a two-dimensional problem of a joint under mechanical loading or after a homogeneous change of temperature, without body force, the stresses can be calculated from the Airy's stress function. This function has to satisfy the equation

$$\nabla^4 \Phi(r,\theta) = 0, \tag{3.1.1}$$

where in polar coordinates there is

$$\begin{aligned} \nabla^4 &= \frac{\partial^4}{\partial r^4} + \frac{2}{r}\frac{\partial^3}{\partial r^3} - \frac{1}{r^2}\frac{\partial^2}{\partial r^2} + \frac{1}{r^3}\frac{\partial}{\partial r} \\ &+ \frac{4}{r^4}\frac{\partial^2}{\partial \theta^2} + \frac{1}{r^4}\frac{\partial^4}{\partial \theta^4} - \frac{2}{r^3}\frac{\partial^3}{\partial r \partial \theta^2} + \frac{2}{r^2}\frac{\partial^4}{\partial r^2 \partial \theta^2}. \end{aligned} \tag{3.1.2}$$

For a singular stress problem, its solution in a series has the following form

$$\Phi_k(r,\theta) = \sum_n r^{(2-\lambda_n)} \quad \Big\{ \quad A_{kn}\sin(\lambda_n\theta) + B_{kn}\cos(\lambda_n\theta) + \quad C_{kn}\sin[(2-\lambda_n)\theta] + D_{kn}\cos[(2-\lambda_n)\theta]\Big\}, \tag{3.1.3}$$

where k= 1 and 2 are for materials 1 and 2. The exponent λ_n and the coefficients $A_{kn}, B_{kn}, C_{kn}, D_{kn}$ are unknown.
The stresses can be calculated from the stress function by

$$\sigma_{rr}(r,\theta) = \frac{1}{r}\frac{\partial\Phi(r,\theta)}{\partial r} + \frac{1}{r^2}\frac{\partial^2\Phi(r,\theta)}{\partial\theta^2}, \tag{3.1.4}$$

$$\sigma_{\theta\theta}(r,\theta) = \frac{\partial^2\Phi(r,\theta)}{\partial r^2}, \tag{3.1.5}$$

$$\sigma_{r\theta}(r,\theta) = -\frac{\partial}{\partial r}(\frac{1}{r}\frac{\partial\Phi(r,\theta)}{\partial\theta}). \tag{3.1.6}$$

Inserting Eq. (3.1.3) into Eqs. (3.1.4, 3.1.5, 3.1.6) yields:

$$\begin{aligned}\sigma_{rrk}(r,\theta) &= \sum_n r^{-\lambda_n}(1-\lambda_n)\Big\{A_{kn}(2+\lambda_n)\sin(\lambda_n\theta) + B_{kn}(2+\lambda_n)\cos(\lambda_n\theta)\\ &- C_{kn}(2-\lambda_n)\sin[(2-\lambda_n)\theta] - D_{kn}(2-\lambda_n)\cos[(2-\lambda_n)\theta]\Big\},\end{aligned} \tag{3.1.7}$$

$$\begin{aligned}\sigma_{\theta\theta k}(r,\theta) &= \sum_n r^{-\lambda_n}(1-\lambda_n)(2-\lambda_n)\Big\{A_{kn}\sin(\lambda_n\theta) + B_{kn}\cos(\lambda_n\theta)\\ &+ C_{kn}\sin[(2-\lambda_n)\theta] + D_{kn}\cos[(2-\lambda_n)\theta]\Big\},\end{aligned} \tag{3.1.8}$$

$$\begin{aligned}\sigma_{r\theta k}(r,\theta) &= -\sum_n r^{-\lambda_n}(1-\lambda_n)\Big\{A_{kn}\lambda_n\cos(\lambda_n\theta) - B_{kn}\lambda_n\sin(\lambda_n\theta)\\ &+ C_{kn}(2-\lambda_n)\cos[(2-\lambda_n)\theta] - D_{kn}(2-\lambda_n)\sin[(2-\lambda_n)\theta]\Big\}.\end{aligned} \tag{3.1.9}$$

The strains for plane stress can be calculated from

$$\varepsilon_{rr}(r,\theta) = \frac{1}{E}[\sigma_{rr}(r,\theta) - \nu\sigma_{\theta\theta}(r,\theta)] + \alpha T, \tag{3.1.10}$$

$$\varepsilon_{\theta\theta}(r,\theta) = \frac{1}{E}[\sigma_{\theta\theta}(r,\theta) - \nu\sigma_{rr}(r,\theta)] + \alpha T, \tag{3.1.11}$$

$$\varepsilon_{r\theta}(r,\theta) = \frac{1}{2G}\sigma_{r\theta}(r,\theta) \tag{3.1.12}$$

where E is the Young's modulus, ν is the Poisson's ratio, G is the shear modulus, α is the thermal expansion coefficient, and T is the homogeneous temperature change in the joint. For plane strain, E should be replaced by $\frac{E}{1-\nu^2}$, ν by $\frac{\nu}{1-\nu}$, and α by $\alpha(1+\nu)$. The displacements can be obtained from

$$\varepsilon_{rr} = \frac{\partial u}{\partial r}, \tag{3.1.13}$$

$$\varepsilon_{\theta\theta} = \frac{u}{r} + \frac{1}{r}\frac{\partial v}{\partial \theta}, \tag{3.1.14}$$

$$\varepsilon_{r\theta} = \frac{1}{2}\left(\frac{1}{r}\frac{\partial u}{\partial \theta} + \frac{\partial v}{\partial r} - \frac{v}{r}\right) \tag{3.1.15}$$

where u and v are the displacements in the direction of r and θ, respectively. By using the relations between the stresses, strains, and the displacements we have:

$$\begin{aligned} u_k(r,\theta) = \sum_n \frac{r^{(1-\lambda_n)}}{E_k} \quad \Big\{ & \quad A_{kn}[2(1-\nu_k) + \lambda_n(1+\nu_k)]\sin(\lambda_n\theta) \\ & + \quad B_{kn}[2(1-\nu_k) + \lambda_n(1+\nu_k)]\cos(\lambda_n\theta) \\ & - \quad C_{kn}(1+\nu_k)(2-\lambda_n)\sin[(2-\lambda_n)\theta] \\ & - \quad D_{kn}(1+\nu_k)(2-\lambda_n)\cos[(2-\lambda_n)\theta]\Big\} + r\alpha_k T \end{aligned} \tag{3.1.16}$$

$$\begin{aligned} v_k(r,\theta) = \sum_n \frac{r^{(1-\lambda_n)}}{E_k} \quad \Big\{ & \quad A_{kn}[2(1-\nu_k) + (2-\lambda_n)(1+\nu_k)]\cos(\lambda_n\theta) \\ & - \quad B_{kn}[2(1-\nu_k) + (2-\lambda_n)(1+\nu_k)]\sin(\lambda_n\theta) \\ & - \quad C_{kn}(1+\nu_k)(2-\lambda_n)\cos[(2-\lambda_n)\theta] \\ & + \quad D_{kn}(1+\nu_k)(2-\lambda_n)\sin[(2-\lambda_n)\theta]\Big\}, \end{aligned} \tag{3.1.17}$$

where the rigid body displacements are neglected by setting u=0 and $v = 0$ at r=0. In Eqs. (3.1.7, 3.1.8, 3.1.9, 3.1.16, 3.1.17), the term according to $\lambda = 0$ is not given separately as in [86].

If the exponent λ_n and the coefficients $A_{kn}, B_{kn}, C_{kn}, D_{kn}$ are known, the stress field and displacements can be calculated from Eqs. (3.1.7, 3.1.8, 3.1.9, 3.1.16, 3.1.17). To determine the unknowns, boundary conditions have to be used. For a joint with free edges the boundary conditions are:

at the interface

$$\begin{aligned} u_1(r,0) &= u_2(r,0), \\ v_1(r,0) &= v_2(r,0), \\ \sigma_{\theta\theta 1}(r,0) &= \sigma_{\theta\theta 2}(r,0), \\ \sigma_{r\theta 1}(r,0) &= \sigma_{r\theta 2}(r,0), \end{aligned} \tag{3.1.18}$$

for the free edges

$$\begin{aligned}
\sigma_{\theta\theta 1}(r,\theta_1) &= 0,\\
\sigma_{\theta\theta 2}(r,\theta_2) &= 0,\\
\sigma_{r\theta 1}(r,\theta_1) &= 0,\\
\sigma_{r\theta 2}(r,\theta_2) &= 0.
\end{aligned} \tag{3.1.19}$$

From these eight conditions the following equations hold

$$\begin{aligned}
\sum_n r^{(1-\lambda_n)} \quad \times \quad & \Big\{B_{1n}\mu[2(1-\nu_1)+\lambda_n(1+\nu_1)] - D_{1n}\mu(1+\nu_1)(2-\lambda_n)\\
& -B_{2n}[2(1-\nu_2)+\lambda_n(1+\nu_2)] + D_{2n}(1+\nu_2)(2-\lambda_n)\Big\}\\
& = rTE_2(\alpha_2-\alpha_1)
\end{aligned} \tag{3.1.20}$$

$$\begin{aligned}
\sum_n r^{(1-\lambda_n)} \quad \times \quad & \Big\{A_{1n}\mu[2(1-\nu_1)+(2-\lambda_n)(1+\nu_1)] - C_{1n}\mu(1+\nu_1)(2-\lambda_n)\\
& -A_{2n}[2(1-\nu_2)+(2-\lambda_n)(1+\nu_2)] + C_{2n}(1+\nu_2)(2-\lambda_n)\Big\} = 0
\end{aligned} \tag{3.1.21}$$

$$\sum_n r^{-\lambda_n} \times (1-\lambda_n)(2-\lambda_n)\left\{B_{1n}+D_{1n}-B_{2n}-D_{2n}\right\} = 0 \tag{3.1.22}$$

$$\sum_n r^{-\lambda_n} \times (1-\lambda_n)\left\{A_{1n}\lambda_n + C_{1n}(2-\lambda_n) - A_{2n}\lambda_n - C_{2n}(2-\lambda_n)\right\} = 0 \tag{3.1.23}$$

$$\begin{aligned}
\sum_n r^{-\lambda_n} \quad \times \quad & (1-\lambda_n)(2-\lambda_n)\Big\{A_{1n}\sin(\lambda_n\theta_1) + B_{1n}\cos(\lambda_n\theta_1)\\
+ \quad & C_{1n}\sin[(2-\lambda_n)\theta_1] + D_{1n}\cos[(2-\lambda_n)\theta_1]\Big\} = 0
\end{aligned} \tag{3.1.24}$$

$$\begin{aligned}
\sum_n r^{-\lambda_n} \quad \times \quad & (1-\lambda_n)\Big\{A_{1n}\lambda_n\cos(\lambda_n\theta_1) - B_{1n}\lambda_n\sin(\lambda_n\theta_1)\\
+ \quad & C_{1n}(2-\lambda_n)\cos[(2-\lambda_n)\theta_1] - D_{1n}(2-\lambda_n)\sin[(2-\lambda_n)\theta_1]\Big\} = 0
\end{aligned} \tag{3.1.25}$$

$$\begin{aligned}
\sum_n r^{-\lambda_n} \quad \times \quad & (1-\lambda_n)(2-\lambda_n)\Big\{A_{2n}\sin(\lambda_n\theta_2) + B_{2n}\cos(\lambda_n\theta_2)\\
+ \quad & C_{2n}\sin[(2-\lambda_n)\theta_2] + D_{2n}\cos[(2-\lambda_n)\theta_2]\Big\} = 0
\end{aligned} \tag{3.1.26}$$

$$\begin{aligned}
\sum_n r^{-\lambda_n} \quad \times \quad & (1-\lambda_n)\Big\{A_{2n}\lambda_n\cos(\lambda_n\theta_2) - B_{2n}\lambda_n\sin(\lambda_n\theta_2)\\
+ \quad & C_{2n}(2-\lambda_n)\cos[(2-\lambda_n)\theta_2] - D_{2n}(2-\lambda_n)\sin[(2-\lambda_n)\theta_2]\Big\} = 0
\end{aligned} \tag{3.1.27}$$

where $\mu = E_2/E_1$ for plane stress. Because in Eqs. (3.1.20 - 3.1.27) r is arbitrary, from Eq. (3.1.20) it follows that if $E_2T(\alpha_2 - \alpha_1) \neq 0$, there must be a solution with $\lambda_n = 0$. Therefore, the solution of this equations system is made of two groups: (I) the solution according to $\lambda_n = 0$, (II) the solution according to $\lambda_n \neq 0$.

(I) The solution according to $\lambda_n = 0$.

From Eqs. (3.1.7, 3.1.8, 3.1.9) it is known that the corresponding stresses are independent of the distance r for $\lambda_n = 0$. This stress is called regular stress term. The solution for $\lambda_n = 0$ will be discussed in Sections 3.2 and 3.3.

(II) The solution according to $\lambda_n \neq 0$.

For $\lambda_n \neq 0, 1, 2$ and for an arbitrary r, Eqs. (3.1.20 - 3.1.27) hold, if the following equations are satisfied

$$\begin{aligned} B_{1n}\mu[2(1-\nu_1) &+ \lambda_n(1+\nu_1)] - D_{1n}\mu(1+\nu_1)(2-\lambda_n) \\ &- B_{2n}[2(1-\nu_2) + \lambda_n(1+\nu_2)] + D_{2n}(1+\nu_2)(2-\lambda_n) = 0 \end{aligned} \tag{3.1.28}$$

$$\begin{aligned} A_{1n}\mu[2(1-\nu_1) &+ (2-\lambda_n)(1+\nu_1)] - C_{1n}\mu(1+\nu_1)(2-\lambda_n) \\ &- A_{2n}[2(1-\nu_2) + (2-\lambda_n)(1+\nu_2)] + C_{2n}(1+\nu_2)(2-\lambda_n) = 0 \end{aligned} \tag{3.1.29}$$

$$B_{1n} + D_{1n} - B_{2n} - D_{2n} = 0 \tag{3.1.30}$$

$$A_{1n}\lambda_n + C_{1n}(2-\lambda_n) - A_{2n}\lambda_n - C_{2n}(2-\lambda_n) = 0 \tag{3.1.31}$$

$$\begin{aligned} A_{1n}\sin(\lambda_n\theta_1) &+ B_{1n}\cos(\lambda_n\theta_1) \\ &+ C_{1n}\sin[(2-\lambda_n)\theta_1] + D_{1n}\cos[(2-\lambda_n)\theta_1] = 0 \end{aligned} \tag{3.1.32}$$

$$\begin{aligned} A_{1n}\lambda_n\cos(\lambda_n\theta_1) &- B_{1n}\lambda_n\sin(\lambda_n\theta_1) \\ &+ C_{1n}(2-\lambda_n)\cos[(2-\lambda_n)\theta_1] - D_{1n}(2-\lambda_n)\sin[(2-\lambda_n)\theta_1] = 0 \end{aligned} \tag{3.1.33}$$

$$\begin{aligned} A_{2n}\sin(\lambda_n\theta_2) &+ B_{2n}\cos(\lambda_n\theta_2) \\ &+ C_{2n}\sin[(2-\lambda_n)\theta_2] + D_{2n}\cos[(2-\lambda_n)\theta_2] = 0 \end{aligned} \tag{3.1.34}$$

$$\begin{aligned} A_{2n}\lambda_n\cos(\lambda_n\theta_2) &- B_{2n}\lambda_n\sin(\lambda_n\theta_2) \\ &+ C_{2n}(2-\lambda_n)\cos[(2-\lambda_n)\theta_2] - D_{2n}(2-\lambda_n)\sin[(2-\lambda_n)\theta_2] = 0. \end{aligned} \tag{3.1.35}$$

This equations system can be rewritten in a matrix form as

$$[A]_{8\times8}\{X\}_{8\times1} = \{0\}_{8\times1} \tag{3.1.36}$$

where there is $\{X\}_{8\times1} = \{A_{1n}, B_{1n}, C_{1n}, D_{1n}, A_{2n}, B_{2n}, C_{2n}, D_{2n}\}^t$, and $[A]_{8\times8}$ is its coefficients matrix. $\{X\}_{8\times1}$ is unknown and $[A]_{8\times8}$ includes the unknown exponent λ_n, the material properties (E_k, ν_k, k=1,2 for materials 1 and 2) and the geometry angles (θ_1, θ_2). Equation (3.1.36) has a nonzero solution, if and only if

$$\mathrm{Det}([A]_{8\times8}) = 0 \tag{3.1.37}$$

is satisfied. In Eq. (3.1.37) the only unknown is the exponent λ_n. Its solutions are the eigenvalues of this problem. Because this is a transcendental equation, there are infinite solutions of λ_n (n=1,2,3,...), and they may be real or complex. If the eigenvalues are complex, the stress function Eq. (3.1.3) cannot be used directly. In this section only the real solutions are considered.
From Eq. (3.1.16) and Eq. (3.1.17) it is known that the displacements are proportional to $r^{(1-\lambda_n)}$. Because the displacements must be finite at the singular point (r=0), there must be $1-\lambda_n \geq 0$. This means that only the solutions with $\lambda_n \leq 1$ can be used to describe the stress field. From Eqs. (3.1.7, 3.1.8, 3.1.9) we can see that if $\lambda_n = 1$, all stresses at any point are zero. On the other hand, according to $\lambda_n = 1$ the displacements are nonzero (see Eqs. (3.1.16, 3.1.17)). Therefore, the solution with $\lambda_n = 1$ refers to the rigid body displacement, which is not included in the following equations. For the description of stresses near the singular point, only eigenvalues in the range of $-0.5 \leq \lambda_n < 1$ will be used. Here, the negative eigenvalues in the range of $-0.5 \leq \lambda_n$ are considered, because they are also important to describe the stresses near the singular point (see examples given in [84]).
For an arbitrary geometry (θ_1, θ_2), the expansion of $\mathrm{Det}([A]_{8\times8}) = 0$ reads

$$\mathrm{Det}([A]_{8\times8}) = \| X \| = X_1\alpha^2 + X_2\beta^2 + X_3\alpha\beta + X_4\alpha + X_5\beta + X_6 = 0 \tag{3.1.38}$$

where

$$\begin{aligned} X_1 = {} & (s_n+1)^2F_{4s} - F_{5s} + F_{5c} - (s_n+1)^2(2s_n^2+4s_n+1)F_{4c} \\ & +2s_n(s_n+1)^2(s_n+2)F_{1p} - 2(s_n+1)^4 + 3(s_n+1)^2 - 1 \end{aligned} \tag{3.1.39}$$

$$\begin{aligned} X_2 = {} & 2\Big\{ -(s_n+1)^4F_{4c} + (s_n+1)^2F_{3p} + (s_n+1)^2s_n(s_n+2)F_{1p} \\ & -s_n(s_n+2)F_{2p} - F_{5c} - s_n^2(s_n+2)^2\Big\} \end{aligned} \tag{3.1.40}$$

$$X_3 = 2\Big\{2(s_n+1)^4F_{4c} - (s_n+1)^2F_{3p} - (s_n+1)^2(2s_n^2+4s_n+1)F_{1p} + 2s_n(s_n+1)^2(s_n+2) + (s_n+1)^2F_{2p}\Big\} \tag{3.1.41}$$

$$X_4 = 2\{-(s_n+1)^2F_{3n} + s_n(s_n+2)F_{2n}\} \tag{3.1.42}$$

$$X_5 = 2\{F_{1n} - F_{2n} + F_{3n}\}(s_n+1)^2 \tag{3.1.43}$$

$$X_6 = -(s_n+1)^2(F_{4s}+F_{4c}) + F_{5s} + F_{5c} + s_n(s_n+2) \tag{3.1.44}$$

where α, β are the Dundurs parameters (their definitions see the following). The quantities $F_{12}, F_{21}, F_{1p}, F_{2p}, ...$ are

$$F_{1n} = \cos(2\theta_2) - \cos(2\theta_1) \tag{3.1.45}$$

$$F_{2n} = \cos[2(s_n+1)\theta_2] - \cos[2(s_n+1)\theta_1] \tag{3.1.46}$$

$$F_{3n} = \cos[2(s_n+1)\theta_2]\cos(2\theta_1) - \cos[2(s_n+1)\theta_1]\cos(2\theta_2) \tag{3.1.47}$$

$$F_{1p} = \cos(2\theta_2) + \cos(2\theta_1) \tag{3.1.48}$$

$$F_{2p} = \cos[2(s_n+1)\theta_2] + \cos[2(s_n+1)\theta_1] \tag{3.1.49}$$

$$F_{3p} = \cos[2(s_n+1)\theta_2]\cos(2\theta_1) + \cos[2(s_n+1)\theta_1]\cos(2\theta_2) \tag{3.1.50}$$

$$F_{4s} = \sin(2\theta_2)\sin(2\theta_1) \tag{3.1.51}$$

$$F_{4c} = \cos(2\theta_2)\cos(2\theta_1) \tag{3.1.52}$$

$$F_{5s} = \sin[2(s_n+1)\theta_2]\sin[2(s_n+1)\theta_1] \tag{3.1.53}$$

$$F_{5c} = \cos[2(s_n+1)\theta_2]\cos[2(s_n+1)\theta_1] \tag{3.1.54}$$

$$F_{12} = \sin(2\theta_1)\cos(2\theta_2) \tag{3.1.55}$$

$$F_{21} = \sin(2\theta_2)\cos(2\theta_1). \tag{3.1.56}$$

The relation between the solution (s_n) of $\| X \| = 0$ and the singular stress exponent ω_n is

$$\omega_n = \mathrm{Re}(2 + s_n). \tag{3.1.57}$$

If we take $s_n + 1 = q_n$, the coefficients in Eq. (3.1.38) will be replaced by

$$\begin{aligned} X_1 &= q_n^2 F_{4s} - F_{5s} + F_{5c} - q_n^2(2q_n^2 - 1)F_{4c} \\ &\quad + 2q_n^2(q_n^2 - 1)F_{1p} - 2q_n^4 + 3q_n^2 - 1 \end{aligned} \tag{3.1.58}$$

$$\begin{aligned} X_2 &= 2\Big\{ - q_n^4 F_{4c} + q_n^2 F_{3p} + q_n^2(q_n^2 - 1)F_{1p} \\ &\quad - (q_n^2 - 1)F_{2p} - F_{5c} - (q_n^2 - 1)^2 \Big\} \end{aligned} \tag{3.1.59}$$

$$\begin{aligned} X_3 &= 2\Big\{ 2q_n^4 F_{4c} - q_n^2 F_{3p} - q_n^2(2q_n^2 - 1)F_{1p} \\ &\quad + 2q_n^2(q_n^2 - 1) + q_n^2 F_{2p} \Big\} \end{aligned} \tag{3.1.60}$$

$$X_4 = 2\{ - q_n^2 F_{3n} + (q_n^2 - 1)F_{2n}\} \tag{3.1.61}$$

$$X_5 = 2\{F_{1n} - F_{2n} + F_{3n}\}q_n^2 \tag{3.1.62}$$

$$X_6 = -q_n^2(F_{4s} + F_{4c}) + F_{5s} + F_{5c} + (q_n^2 - 1) \tag{3.1.63}$$

and

$$F_{1n} = \cos(2\theta_2) - \cos(2\theta_1) \tag{3.1.64}$$

$$F_{2n} = \cos[2q_n\theta_2] - \cos[2q_n\theta_1] \tag{3.1.65}$$

$$F_{3n} = \cos[2q_n\theta_2]\cos(2\theta_1) - \cos[2q_n\theta_1]\cos(2\theta_2) \tag{3.1.66}$$

$$F_{1p} = \cos(2\theta_2) + \cos(2\theta_1) \tag{3.1.67}$$

$$F_{2p} = \cos[2q_n\theta_2] + \cos[2q_n\theta_1] \tag{3.1.68}$$

$$F_{3p} = \cos[2q_n\theta_2]\cos(2\theta_1) + \cos[2q_n\theta_1]\cos(2\theta_2) \tag{3.1.69}$$

$$F_{4s} = \sin(2\theta_2)\sin(2\theta_1) \tag{3.1.70}$$

$$F_{4c} = \cos(2\theta_2)\cos(2\theta_1) \tag{3.1.71}$$

$$F_{5s} = \sin[2q_n\theta_2]\sin[2q_n\theta_1] \tag{3.1.72}$$

$$F_{5c} = \cos[2q_n\theta_2]\cos[2q_n\theta_1] \tag{3.1.73}$$

$$F_{12} = \sin(2\theta_1)\cos(2\theta_2) \tag{3.1.74}$$

$$F_{21} = \sin(2\theta_2)\cos(2\theta_1). \tag{3.1.75}$$

From Eqs. (3.1.58-3.1.75) we can see that for q_n and -q_n the quantities $X_1, X_2, ..., X_6$ and $F_{1n}, F_{2n}, ..., F_{21}$ are the same. This means that if q_n is the solution of $\parallel X \parallel = 0$, -$q_n$ is also its solution.
The relation between ω_n and q_n is

$$\omega_n = q_n + 1. \tag{3.1.76}$$

Therefore, if ω_n is the eigenvalue of the problem, $2-\omega_n = -q_n+1$ is also the eigenvalue of the problem. If ω_n is in the range of $-0.5 \leq \omega_n < 1$, however, $2-\omega_n$ is not.

For a joint with $\theta_1 = -\theta_2$ the quantities $X_1, X_2, X_3, ...$ can be simplified as

$$X_1 = s_n(s_n+1)^2(s_n+2)[\cos(2\theta_1)-1]^2 \tag{3.1.77}$$

$$\begin{aligned} X_2 &= \{\cos(2\theta_1)(s_n+1)^2 - \cos[2(s_n+1)\theta_1]\}^2 \\ &\quad + s_n(s_n+2)\{2\cos[2(s_n+1)\theta_1] - 2\cos(2\theta_1)(s_n+1)^2 + s_n(s_n+2)\} \end{aligned} \tag{3.1.78}$$

$$\begin{aligned} X_3 &= 2\Big\{ -\cos^2(2\theta_1)(s_n+1)^4 + \cos[2(s_n+1)\theta_1]\cos(2\theta_1)(s_n+1)^2 \\ &\quad + \cos(2\theta_1)(s_n+1)^2(2s_n^2+4s_n+1) - \cos[2(s_n+1)\theta_1](s_n+1)^2 \\ &\quad -(s_n+1)^2 s_n(s_n+2)\Big\} \end{aligned} \tag{3.1.79}$$

$$X_4 = X_5 = 0 \tag{3.1.80}$$

$$X_6 = (s_n+1)^2\cos^2(2\theta_1) - \cos^2[2(s_n+1)\theta_1] - s_n(s_n+2). \tag{3.1.81}$$

$$\tag{3.1.82}$$

In particular, for $\theta_1 = -\theta_2 = 90^\circ$

$$\parallel X \parallel = \Big\{\beta\cos^2(\frac{\pi}{2}s_n) + (\alpha-\beta)(s_n+1)^2\Big\}^2 + \sin^2(\frac{\pi}{2}s_n)\cos^2(\frac{\pi}{2}s_n) - \alpha^2(s_n+1)^2 \tag{3.1.83}$$

or in another form as

$$\begin{aligned}\mathrm{Det}([A]_{8\times 8}) &= (\lambda_n-2)\Big\{\beta^2[cos^2(\frac{\pi}{2}\lambda_n)-(\lambda_n-1)^2]^2+\alpha^2\lambda_n(\lambda_n-1)^2(\lambda_n-2)\\ &+ 2\alpha\beta(\lambda_n-1)^2[cos^2(\frac{\pi}{2}\lambda_n)-(\lambda_n-1)^2]+cos^2(\frac{\pi}{2}\lambda_n)sin^2(\frac{\pi}{2}\lambda_n)\Big\}=0.\end{aligned} \tag{3.1.84}$$

For ω_n=0, i.e. s_n=-2 the differential of $\parallel X \parallel$ is

$$\begin{aligned}\frac{d\parallel X\parallel}{ds_n}\mid_{s_n=-2} &= \text{constant}\times\Big\{1-\alpha^2+4\alpha\beta+2\,\alpha\Big[-1+\alpha-2\,\beta\Big]\cos(2\theta_1)\\ &-2\Big[1+\alpha\Big]\,\beta\,\theta_1\sin(2\theta_1)+2\,\alpha\Big[1+\alpha-2\,\beta\Big]\cos(2\theta_2)\\ &+2\Big[1-\alpha\Big]\,\beta\,\theta_2\sin(2\theta_2)+2\,\alpha\Big[-\alpha+\beta\Big]\cos\left[2(\theta_1+\theta_2)\right]\\ &+\Big[-1-\alpha^2+2\,\alpha\,\beta\Big]\cos\left[2(\theta_1-\theta_2)\right]\\ &+\Big[-\alpha+\beta\Big]\Big[\theta_1(1+\alpha)-\theta_2(1-\alpha)\Big]\sin\left[2(\theta_1+\theta_2)\right]\\ &+\Big[(-1-\alpha+\beta+\alpha\,\beta)\;\theta_1+(1-\alpha+\beta-\alpha\,\beta)\;\theta_2\Big]\sin\left[2(\theta_1-\theta_2)\right]\Big\}\end{aligned} \tag{3.1.85}$$

where α,β are the Dundurs parameters [130]. They are defined as

$$\begin{aligned}\alpha &= \frac{m_2-gm_1}{m_2+gm_1}\\ \beta &= \frac{(m_2-2)-g(m_1-2)}{m_2+gm_1}\end{aligned} \tag{3.1.86}$$

with

$$m=\begin{cases}\frac{4}{(1+\nu)} & \text{for plane stress}\\ 4(1-\nu) & \text{for plane strain}\end{cases}$$

and $g=\frac{G_2}{G_1}$.
Directly using the material constants

$$\alpha=\frac{E_1-E_2}{E_1+E_2} \tag{3.1.87}$$

$$\beta=\frac{1}{2}\frac{E_1(1-\nu_2)-E_2(1-\nu_1)}{E_1+E_2} \tag{3.1.88}$$

are obtained for plane stress. For plane strain, there is

$$\alpha=\frac{\frac{E_1}{1-\nu_1^2}-\frac{E_2}{1-\nu_2^2}}{\frac{E_1}{1-\nu_1^2}+\frac{E_2}{1-\nu_2^2}} \tag{3.1.89}$$

$$\beta=\frac{1}{2}\frac{E_1(1+\nu_2)(1-2\nu_2)-E_2(1+\nu_1)(1-2\nu_1)}{E_1(1-\nu_2^2)+E_2(1-\nu_1^2)}. \tag{3.1.90}$$

In general, for a two dissimilar materials joint, the four elastic constants E_1, E_2, ν_1, ν_2 can be reduced to two independent parameters. These are the Dundurs parameters α, β. Following the definition of the Dundurs parameters, α and β may take the values in the range of $-1 \leq \alpha \leq 1$ and $-0.5 \leq \beta \leq 0.5$. This means that all possible material combinations can be found as a point in the Dundurs diagram, in which α is plotted versus β. For plane stress and plane strain, the values of α and β corresponding to all possible physically relevant material combinations, are restricted to an area within a parallelogram. For plane stress, the four limit lines are

$$\begin{aligned} \alpha = -1, \qquad & \beta \quad \text{from} \ -0.5 \ \text{to} \ -0.25 \\ \alpha = 1, \qquad & \beta \quad \text{from} \ \ 0.5 \ \ \text{to} \ \ 0.25 \\ \beta &= \frac{3}{8}\alpha - \frac{1}{8} \\ \beta &= \frac{3}{8}\alpha + \frac{1}{8}, \end{aligned} \tag{3.1.91}$$

and for plane strain, the four limit lines are

$$\begin{aligned} \alpha = -1, \qquad & \beta \quad \text{from} \ -0.5 \ \text{to} \ 0 \\ \alpha = 1, \qquad & \beta \quad \text{from} \ \ 0.5 \ \ \text{to} \ 0 \\ \beta &= \frac{1}{4}\alpha - \frac{1}{4} \\ \beta &= \frac{1}{4}\alpha + \frac{1}{4}, \end{aligned} \tag{3.1.92}$$

which are plotted in the following Dundurs diagrams as dashed lines for plane stress and as solid lines for plane strain.
As now the eigenvalues λ_n are known, we can calculate the stress exponent ω_n and the angular functions $f_{ijn}(\theta)$. For a joint with real eigenvalues, the stress exponent is

$$\omega_n = \lambda_n \qquad (-0.5 \leq \lambda_n < 1). \tag{3.1.93}$$

Because Eq. (3.1.36) is a homogeneous equations system, its solution $A_{1n}, B_{1n}, C_{1n}, D_{1n}$, A_{2n}, B_{2n}, C_{2n}, and D_{2n} is not unique. To obtain unique angular functions for each given eigenvalue λ_n, they are normalized as

$$f_{rrkn}(\theta) = \frac{\sigma_{rrkn}(r,\theta)}{\sigma_{\theta\theta 1n}(r,0)} = \frac{\sigma_{rrkn}(r,\theta)}{\sigma_{\theta\theta 2n}(r,0)}, \tag{3.1.94}$$

$$f_{\theta\theta kn}(\theta) = \frac{\sigma_{\theta\theta kn}(r,\theta)}{\sigma_{\theta\theta 1n}(r,0)} = \frac{\sigma_{\theta\theta kn}(r,\theta)}{\sigma_{\theta\theta 2n}(r,0)}, \tag{3.1.95}$$

$$f_{r\theta kn}(\theta) = \frac{\sigma_{r\theta kn}(r,\theta)}{\sigma_{\theta\theta 1n}(r,0)} = \frac{\sigma_{r\theta kn}(r,\theta)}{\sigma_{\theta\theta 2n}(r,0)}. \tag{3.1.96}$$

This means that there is always $f_{\theta\theta 1n}(\theta = 0) = f_{\theta\theta 2n}(\theta = 0) = 1$. Using Eqs. (3.1.7 - 3.1.9) for each eigenvalue λ_n, the angular functions can be calculated from

$$\begin{aligned} f_{rrkn}(\theta) &= \Big\{A_{kn}(2+\omega_n)\sin(\omega_n\theta) + B_{kn}(2+\omega_n)\cos(\omega_n\theta) - C_{kn}(2-\omega_n) \times \\ &\times \sin[(2-\omega_n)\theta] - D_{kn}(2-\omega_n)\cos[(2-\omega_n)\theta]\Big\}/\{(2-\omega_n)(B_{kn}+D_{kn})\}, \end{aligned} \tag{3.1.97}$$

$$\begin{aligned} f_{\theta\theta kn}(\theta) &= \Big\{A_{kn}\sin(\omega_n\theta) + B_{kn}\cos(\omega_n\theta) + C_{kn}\sin[(2-\omega_n)\theta] \\ &+ D_{kn}\cos[(2-\omega_n)\theta]\Big\}/(B_{kn}+D_{kn}), \end{aligned} \tag{3.1.98}$$

$$\begin{aligned} f_{r\theta kn}(\theta) &= -\Big\{A_{kn}\omega_n\cos(\omega_n\theta) - B_{kn}\omega_n\sin(\omega_n\theta) + C_{kn}(2-\omega_n)\cos[(2-\omega_n)\theta] \\ &- D_{kn}(2-\omega_n)\sin[(2-\omega_n)\theta]\Big\}/\{(2-\omega_n)(B_{kn}+D_{kn})\}, \end{aligned} \tag{3.1.99}$$

with k = 1 and 2 for materials 1 and 2.
Considering all singular stress exponents (N terms) and the regular stress term, and using the definition of the angular functions $f_{ijn}(\theta)$, the stresses near the singular point can be described analytically by

$$\sigma_{ijk}(r,\theta) = \sum_{n=1}^{N} \frac{K_n}{\bar{r}^{\omega_n}} f_{ijkn}(\theta) + \sigma_0 f_{ijk0}(\theta) \tag{3.1.100}$$

where the factor K_n is unknown, which should be determined from the stress analysis of the total joint (method will be presented in Section 3.4). Here, the distance r is normalized by a characteristic length R ($\bar{r} = r/R$), so that the factor K_n has the unit of a stress. The determination of the regular stress term $\sigma_0 f_{ijk0}(\theta)$ will be discussed in Sections 3.2 and 3.3 for thermal and remote mechanical loading.
In principle, for an arbitrary geometry (θ_1, θ_2), the coefficients A_{1n}, B_{1n}, C_{1n}, D_{1n}, A_{2n}, B_{2n}, C_{2n}, and D_{2n} (according to λ_n) in Eqs.(3.1.97 - 3.1.99) can be obtained analytically by solving a 7×7 linear equations system, but they cannot be calculated from a simple explicit form.
Only for the special joint geometry $\theta_1 = -\theta_2 = 90°$, the coefficients $A_{1n}, B_{1n}, C_{1n}, D_{1n}$, A_{2n}, B_{2n}, C_{2n}, and D_{2n} can be simplified as

$$A_{kn} = \frac{A^*_{kn}}{Z} \qquad B_{kn} = \frac{B^*_{kn}}{Z} \qquad C_{kn} = \frac{C^*_{kn}}{Z} \qquad D_{kn} = \frac{D^*_{kn}}{Z} \tag{3.1.101}$$

with

$$Z = \beta[\cos^2(\frac{\pi}{2}\omega_n) + (1-\omega_n)(3-\omega_n)] - \alpha(2-\omega_n)(1-\omega_n) - 1 + \cos^2(\frac{\pi}{2}\omega_n) \tag{3.1.102}$$

$$A^*_{1n} = Z \tag{3.1.103}$$

$$B^*_{1n} = -\tan(\frac{\pi}{2}\omega_n)\Big\{\beta[\cos^2(\frac{\pi}{2}\omega_n) + (1-\omega_n)^2] - \alpha(2-\omega_n)(1-\omega_n) + \cos^2(\frac{\pi}{2}\omega_n)\Big\} \tag{3.1.104}$$

$$C^*_{1n} = -\beta[\frac{4-3\omega_n}{(2-\omega_n)}\sin^2(\frac{\pi}{2}\omega_n) - (2-\omega_n)\omega_n] - \alpha\omega_n(1-\omega_n) + \sin^2(\frac{\pi}{2}\omega_n) \tag{3.1.105}$$

$$\begin{aligned} D^*_{1n} &= \tan(\frac{\pi}{2}\omega_n)\Big\{ -\frac{\beta}{(2-\omega_n)}[\cos^2(\frac{\pi}{2}\omega_n)(3\omega_n-4) - \omega_n(1-\omega_n)^2] \\ &- \alpha\omega_n(1-\omega_n) - \cos^2(\frac{\pi}{2}\omega_n)\Big\} \end{aligned} \tag{3.1.106}$$

$$\begin{aligned} A^*_{2n} &= -\frac{1}{1+\alpha}\Big\{\alpha^2(2-\omega_n)(1-\omega_n)(2\omega_n-1) \\ &+2\beta^2[-(2-\omega_n)\sin^2(\frac{\pi}{2}\omega_n) + (2-\omega_n)^2\omega_n] \\ &+\alpha\beta[\cos^2(\frac{\pi}{2}\omega_n)(2\omega_n-3) + 4(2-\omega_n)^3 - 9(2-\omega_n)^2 + 6(2-\omega_n) - 1] \\ &+\alpha[-\cos^2(\frac{\pi}{2}\omega_n)(2\omega_n-3) + (2-\omega_n)^2 - 3(2-\omega_n) + 1] \\ &+\beta[-\sin^2(\frac{\pi}{2}\omega_n)(2\omega_n-3) - (2-\omega_n)^2] + \sin^2(\frac{\pi}{2}\omega_n)\Big\} \end{aligned} \tag{3.1.107}$$

$$\begin{aligned} B^*_{2n} &= -\frac{\tan(\frac{\pi}{2}\omega_n)}{1+\alpha}\Big\{\alpha^2(2-\omega_n)(1-\omega_n)(2\omega_n-1) \\ &+2\beta^2[(1-\omega_n)\cos^2(\frac{\pi}{2}\omega_n) - (2-\omega_n)^3 + 3(2-\omega_n)^2 - 3(2-\omega_n) + 1] \\ &+\alpha\beta[\cos^2(\frac{\pi}{2}\omega_n)(2\omega_n-3) + 4(2-\omega_n)^3 - 11(2-\omega_n)^2 + 10(2-\omega_n) - 3] \\ &+\alpha[-\cos^2(\frac{\pi}{2}\omega_n)(2\omega_n-3) - (2-\omega_n)^2 + (2-\omega_n)] \\ &+\beta[\cos^2(\frac{\pi}{2}\omega_n)(2\omega_n-3) + (2-\omega_n)^2 + 2\omega_n - 3] + \cos^2(\frac{\pi}{2}\omega_n)\Big\} \end{aligned} \tag{3.1.108}$$

$$\begin{aligned} C^*_{2n} &= -\frac{1}{1+\alpha}\Big\{\alpha^2\omega_n[2(2-\omega_n)^2 - 3(2-\omega_n) + 1] \\ &+2\beta^2\omega_n[-\cos^2(\frac{\pi}{2}\omega_n) + (2-\omega_n)^2 - 2(2-\omega_n) + 1] \\ &-\frac{\alpha\beta}{(2-\omega_n)}[\cos^2(\frac{\pi}{2}\omega_n)(2\omega_n^2 - 5\omega_n + 4) - 4\omega_n^4 + 17\omega_n^3 - 26\omega_n^2 + 17\omega_n - 4] \\ &+\alpha[\cos^2(\frac{\pi}{2}\omega_n)(1-2\omega_n) - (2-\omega_n)^2 + (2-\omega_n) + 1] \\ &+\frac{\beta}{(2-\omega_n)}[\cos^2(\frac{\pi}{2}\omega_n)(2\omega_n^2 - 5\omega_n + 4) + \omega_n^3 - 6\omega_n^2 + 9\omega_n - 4] - \sin^2(\frac{\pi}{2}\omega_n)\Big\} \end{aligned} \tag{3.1.109}$$

$$
\begin{aligned}
D^*_{2n} \;=\; & \frac{\tan(\frac{\pi}{2}\omega_n)}{1+\alpha}\Big\{\alpha^2\omega_n[2(2-\omega_n)^2-3(2-\omega_n)+1] \\
& +2\beta^2[(1-\omega_n)\cos^2(\frac{\pi}{2}\omega_n)-(2-\omega_n)^3+3(2-\omega_n)^2-3(2-\omega_n)+1] \\
& -\frac{\alpha\beta}{(2-\omega_n)}[\cos^2(\frac{\pi}{2}\omega_n)(2\omega_n^2-5\omega_n+4)-4\omega_n^4+19\omega_n^3-34\omega_n^2+27\omega_n-8] \\
& +\alpha[\cos^2(\frac{\pi}{2}\omega_n)(1-2\omega_n)-\omega_n(1-\omega_n)] \\
& +\frac{\beta}{(2-\omega_n)}[\cos^2(\frac{\pi}{2}\omega_n)(2\omega_n^2-5\omega_n+4)-\omega_n(1-\omega_n)^2]-\cos^2(\frac{\pi}{2}\omega_n)\Big\}.
\end{aligned}
\tag{3.1.110}
$$

3.1.2 Joint with Complex Eigenvalues

If the eigenvalues of Eq. (3.1.37) are complex, the stress function given in Eq. (3.1.3) cannot be used directly to describe the stresses near the singular point. The analysis can be performed applying complex functions for the stresses and displacements.
Based on the elasticity theory for a two-dimensional problem under thermal or mechanical loading, the stresses and displacements can be calculated from the following complex relations in Cartesian coordinates [131]

$$
\sigma_{xxk}(x,y)+\sigma_{yyk}(x,y)=2(\phi_k\prime(z)+\overline{\phi_k\prime(z)}) \tag{3.1.111}
$$

$$
\sigma_{yyk}(x,y)-\sigma_{xxk}(x,y)+2i\tau_{xyk}(x,y)=2(\overline{z}\phi_k\prime\prime(z)+\psi_k\prime(z)) \tag{3.1.112}
$$

$$
2G_k[u_{xk}(x,y)+iu_{yk}(x,y)-\varepsilon_{k0}z]=\xi_k\phi_k(z)-z\overline{\phi_k\prime(z)}-\overline{\psi_k(z)} \tag{3.1.113}
$$

with

$$
\xi_k=\begin{cases}\frac{3-\nu_k}{(1+\nu_k)} & \text{for plane stress}\\ 3-4\nu_k & \text{for plane strain}\end{cases}
$$

and

$$
z=\frac{x+iy}{R}=\bar{r}e^{i\theta} \tag{3.1.114}
$$

where R is a characteristic length of the joint and k= 1, 2 for materials 1 and 2. ε_{k0} are the thermal strains with

$$
\varepsilon_{k0}=\begin{cases}\alpha_k T & \text{for plane stress}\\ (1+\nu_k)\alpha_k T & \text{for plane strain}\end{cases}
$$

for a homogeneous change in temperature. The real and imaginary parts of the complex functions $\phi(z)$ and $\psi(z)$ are harmonical functions. For a stress singularity problem the following complex functions are chosen:

$$
\phi_k(z)=\sum_n \mathcal{A}_{\mathrm{kn}}\mathrm{z}^{\Lambda_\mathrm{n}}+\sum_\mathrm{n}\mathcal{B}_{\mathrm{kn}}\mathrm{z}^{\bar{\Lambda}_\mathrm{n}} \tag{3.1.115}
$$

$$\psi_k(z) = \sum_n \mathcal{C}_{\rm kn} {\rm z}^{\Lambda_{\rm n}} + \sum_{\rm n} \mathcal{D}_{\rm kn} {\rm z}^{\bar{\Lambda}_{\rm n}} \tag{3.1.116}$$

where n=1, 2, 3, ..., Λ_n is a complex number and $\mathcal{A}_{\rm kn}, \mathcal{B}_{\rm kn}, \mathcal{C}_{\rm kn}, \mathcal{D}_{\rm kn}$ are complex coefficients, which are unknown. $\bar{\Lambda}_n$ is the conjugate number of Λ_n. Substitution of Eqs. (3.1.115) and (3.1.116) by Eqs. (3.1.111), (3.1.112), and (3.1.113) provides for

$$\begin{aligned} \sigma_{xxk}(x,y) &+ \sigma_{yyk}(x,y) \\ &= 4Re\Big\{ \sum_n \mathcal{A}_{\rm kn}\Lambda_{\rm n} {\rm z}^{(\Lambda_{\rm n}-1)} + \sum_{\rm n} \mathcal{B}_{\rm kn}\bar{\Lambda}_{\rm n} {\rm z}^{(\bar{\Lambda}_{\rm n}-1)} \Big\} \equiv \Pi_{\rm k} \end{aligned} \tag{3.1.117}$$

$$\begin{aligned} \sigma_{yyk}(x,y) &- \sigma_{xxk}(x,y) + 2i\tau_{xyk}(x,y) \\ &= 2\sum_n \mathcal{A}_{\rm kn}\Lambda_{\rm n}(\Lambda_{\rm n}-1){\rm z}^{(\Lambda_{\rm n}-2)}\bar{\rm z} + 2\sum_{\rm n} \mathcal{B}_{\rm kn}\bar{\Lambda}_{\rm n}(\bar{\Lambda}_{\rm n}-1){\rm z}^{(\bar{\Lambda}_{\rm n}-2)}\bar{\rm z} \\ &\quad +2\sum_n \mathcal{C}_{\rm kn}\Lambda_{\rm n}{\rm z}^{(\Lambda_{\rm n}-1)} + 2\sum_{\rm n} \mathcal{D}_{\rm kn}\bar{\Lambda}_{\rm n}{\rm z}^{(\bar{\Lambda}_{\rm n}-1)} \equiv {\rm e}^{-2{\rm i}\theta}\Gamma_{\rm k} \end{aligned} \tag{3.1.118}$$

$$\begin{aligned} 2G_k[u_{xk}(x,y) &+ iu_{yk}(x,y) - \varepsilon_{k0}z] \\ &= \xi_k\Big[\sum_n \mathcal{A}_{\rm kn}{\rm z}^{\Lambda_{\rm n}} + \sum_{\rm n} \mathcal{B}_{\rm kn}{\rm z}^{\bar{\Lambda}_{\rm n}}\Big] - \sum_{\rm n} \bar{\mathcal{A}}_{\rm kn}\bar{\Lambda}_{\rm n}\bar{\rm z}^{\bar{\Lambda}_{\rm n}-1}{\rm z} \\ &- \sum_n \bar{\mathcal{B}}_{kn}\Lambda_n\bar{z}^{\Lambda_n-1}z - \sum_n \bar{\mathcal{C}}_{kn}\bar{z}^{\bar{\Lambda}_n} - \sum_n \bar{\mathcal{D}}_{kn}\bar{z}^{\Lambda_n}. \end{aligned} \tag{3.1.119}$$

The stresses and displacements in polar coordinates can be obtained by using the transformation

$$\sigma_{xxk}(x,y) + \sigma_{yyk}(x,y) = \sigma_{rrk}(r,\theta) + \sigma_{\theta\theta k}(r,\theta) \tag{3.1.120}$$

$$\sigma_{yyk}(x,y) - \sigma_{xxk}(x,y) + 2i\tau_{xyk}(x,y) = e^{-2i\theta}[\sigma_{\theta\theta k}(r,\theta) - \sigma_{rrk}(r,\theta) + 2i\tau_{r\theta k}(r,\theta)] \tag{3.1.121}$$

$$2G_k[u_{xk}(x,y) + iu_{yk}(x,y) - \varepsilon_{k0}z] = 2G_k\left[\Big(u_k(r,\theta) + iv_k(r,\theta)\Big)e^{i\theta} - \varepsilon_{k0}z\right] \tag{3.1.122}$$

In order to determine the unknown coefficients $\mathcal{A}_{\rm kn}, \mathcal{B}_{\rm kn}, \mathcal{C}_{\rm kn}, \mathcal{D}_{\rm kn}$ and the exponent Λ_n for an arbitrary joint geometry (θ_1, θ_2), the boundary conditions in polar coordinates have to be used. For a joint with free edges they are

$$[\sigma_{\theta\theta 1}(r,\theta) + i\tau_{r\theta 1}(r,\theta)]\ |_{\theta=0} = [\sigma_{\theta\theta 2}(r,\theta) + i\tau_{r\theta 2}(r,\theta)]\ |_{\theta=0} \tag{3.1.123}$$

$$[u_1(r,\theta) + iv_1(r,\theta)]\ |_{\theta=0} = [u_2(r,\theta) + iv_2(r,\theta)]\ |_{\theta=0} \tag{3.1.124}$$

$$[\sigma_{\theta\theta 1}(r,\theta) + i\tau_{r\theta 1}(r,\theta)]\ |_{\theta=\theta_1} = 0 \tag{3.1.125}$$

$$[\sigma_{\theta\theta 2}(r,\theta) + i\tau_{r\theta 2}(r,\theta)]\ |_{\theta=\theta_2} = 0 \tag{3.1.126}$$

where u and v are the displacements in the direction of r and θ, respectively. For each Λ_n, if the exponent Λ_n is not equal to 1, substituting Eqs. (3.1.117 - 3.1.119) by Eqs. (3.1.123 - 3.1.126) and due to r being arbitrary, eight equations can be obtained

$$\mathcal{A}_{1\mathrm{n}}\Lambda_{\mathrm{n}} + \bar{\mathcal{B}}_{1\mathrm{n}} + \mathcal{C}_{1\mathrm{n}} - \mathcal{A}_{2\mathrm{n}}\Lambda_{\mathrm{n}} - \bar{\mathcal{B}}_{2\mathrm{n}} - \mathcal{C}_{2\mathrm{n}} = 0 \tag{3.1.127}$$

$$\mathcal{A}_{1\mathrm{n}} + \bar{\mathcal{B}}_{1\mathrm{n}}\Lambda_{\mathrm{n}} + \bar{\mathcal{D}}_{1\mathrm{n}} - \mathcal{A}_{2\mathrm{n}} - \bar{\mathcal{B}}_{2\mathrm{n}}\Lambda_{\mathrm{n}} - \bar{\mathcal{D}}_{2\mathrm{n}} = 0 \tag{3.1.128}$$

$$g[\xi_1\mathcal{A}_{1\mathrm{n}} - \Lambda_{\mathrm{n}}\bar{\mathcal{B}}_{1\mathrm{n}} - \bar{\mathcal{D}}_{1\mathrm{n}}] - \xi_2\mathcal{A}_{2\mathrm{n}} + \Lambda_{\mathrm{n}}\bar{\mathcal{B}}_{2\mathrm{n}} + \bar{\mathcal{D}}_{2\mathrm{n}} = 0 \tag{3.1.129}$$

$$g[-\Lambda_n\mathcal{A}_{1\mathrm{n}} + \xi_1\bar{\mathcal{B}}_{1\mathrm{n}} - \mathcal{C}_{1\mathrm{n}}] + \Lambda_{\mathrm{n}}\mathcal{A}_{2\mathrm{n}} - \xi_2\bar{\mathcal{B}}_{2\mathrm{n}} + \mathcal{C}_{2\mathrm{n}}] = 0 \tag{3.1.130}$$

$$\mathcal{A}_{1\mathrm{n}}\Lambda_{\mathrm{n}} + \bar{\mathcal{B}}_{1\mathrm{n}}\mathrm{e}^{-2\mathrm{i}(\Lambda_{\mathrm{n}}-1)\theta_1} + \mathcal{C}_{1\mathrm{n}}\mathrm{e}^{2\mathrm{i}\theta_1} = 0 \tag{3.1.131}$$

$$\mathcal{A}_{1\mathrm{n}} + \bar{\mathcal{B}}_{1\mathrm{n}}\Lambda_{\mathrm{n}}\mathrm{e}^{-2\mathrm{i}(\Lambda_{\mathrm{n}}-1)\theta_1} + \bar{\mathcal{D}}_{1\mathrm{n}}\mathrm{e}^{-2\mathrm{i}\Lambda_{\mathrm{n}}\theta_1} = 0 \tag{3.1.132}$$

$$\mathcal{A}_{2\mathrm{n}}\Lambda_{\mathrm{n}} + \bar{\mathcal{B}}_{2\mathrm{n}}\mathrm{e}^{-2\mathrm{i}(\Lambda_{\mathrm{n}}-1)\theta_2} + \mathcal{C}_{2\mathrm{n}}\mathrm{e}^{2\mathrm{i}\theta_2} = 0 \tag{3.1.133}$$

$$\mathcal{A}_{2\mathrm{n}} + \bar{\mathcal{B}}_{2\mathrm{n}}\Lambda_{\mathrm{n}}\mathrm{e}^{-2\mathrm{i}(\Lambda_{\mathrm{n}}-1)\theta_2} + \bar{\mathcal{D}}_{2\mathrm{n}}\mathrm{e}^{-2\mathrm{i}\Lambda_{\mathrm{n}}\theta_2} = 0 \tag{3.1.134}$$

where g= G_2/G_1. From Eqs. (3.1.117) and (3.1.118), it is known that $\Lambda_n = 1$ corresponds to the stress term, which is independent of the distance r. It is called the regular stress term and will be treated in Sections 3.2 and 3.3.
Equations (3.1.127) to (3.1.134) can be rewritten in a matrix form as

$$[F_n]_{8\times 8}\{X_n\}_{8\times 1} = 0 \tag{3.1.135}$$

where $\{X_n\} = \{\mathcal{A}_{1\mathrm{n}}, \bar{\mathcal{B}}_{1\mathrm{n}}, \mathcal{C}_{1\mathrm{n}}, \bar{\mathcal{D}}_{1\mathrm{n}}, \mathcal{A}_{2\mathrm{n}}, \bar{\mathcal{B}}_{2\mathrm{n}}, \mathcal{C}_{2\mathrm{n}}, \bar{\mathcal{D}}_{2\mathrm{n}}\}^{\mathrm{T}}$, and $[F_n]_{8\times 8}$ is the coefficients matrix. This is a homogeneous equations system. Only if the determinant of $[F_n]$ is equal to zero, Eq. (3.1.135) has a nonzero solution. In $[F_n]$ the exponent Λ_n is the only unknown. The solutions Λ_n of

$$\mathrm{Det}([F_n]_{8\times 8}) = 0 \tag{3.1.136}$$

are the eigenvalues of the problem. For each given Λ_n ($\Lambda_n \neq 1$), the corresponding coefficients $\mathcal{A}_{1\mathrm{n}}, \bar{\mathcal{B}}_{1\mathrm{n}}, \mathcal{C}_{1\mathrm{n}}, \bar{\mathcal{D}}_{1\mathrm{n}}, \mathcal{A}_{2\mathrm{n}}, \bar{\mathcal{B}}_{2\mathrm{n}}, \mathcal{C}_{2\mathrm{n}}, \bar{\mathcal{D}}_{2\mathrm{n}}$ can be determined from Eq. (3.1.135) or Eqs. (3.1.127-3.1.134), but one of them is arbitrary.
In order to obtain the explicit form for calculation of the stresses, the quantities Λ_n and $\mathcal{A}_{\mathrm{kn}}, \mathcal{B}_{\mathrm{kn}}, \mathcal{C}_{\mathrm{kn}}, \mathcal{D}_{\mathrm{kn}}$ must be separated into a real and an imaginary part. The definitions

$$\begin{aligned}
\mathcal{A}_{\mathrm{kn}} &= \mathcal{A}^{\mathrm{R}}_{\mathrm{kn}} + \mathrm{i}\mathcal{A}^{\mathrm{I}}_{\mathrm{kn}} \\
\mathcal{B}_{\mathrm{kn}} &= \mathcal{B}^{\mathrm{R}}_{\mathrm{kn}} + \mathrm{i}\mathcal{B}^{\mathrm{I}}_{\mathrm{kn}} \\
\mathcal{C}_{\mathrm{kn}} &= \mathcal{C}^{\mathrm{R}}_{\mathrm{kn}} + \mathrm{i}\mathcal{C}^{\mathrm{I}}_{\mathrm{kn}} \\
\mathcal{D}_{\mathrm{kn}} &= \mathcal{D}^{\mathrm{R}}_{\mathrm{kn}} + \mathrm{i}\mathcal{D}^{\mathrm{I}}_{\mathrm{kn}} \\
\Lambda_n &= t_n + ip_n
\end{aligned} \tag{3.1.137}$$

are used. The stress components can be calculated from Eqs. (3.1.117), (3.1.118), (3.1.120), and (3.1.121) as

$$\sigma_{rrk}(r,\theta) = \frac{1}{2}\mathrm{Re}(\Pi_k - \Gamma_k) \tag{3.1.138}$$

$$\sigma_{\theta\theta k}(r,\theta) = \frac{1}{2}\mathrm{Re}(\Pi_k + \Gamma_k) \tag{3.1.139}$$

$$\tau_{r\theta k}(r,\theta) = \frac{1}{2}\mathrm{Im}(\Gamma_k). \tag{3.1.140}$$

After inserting Eq. (3.1.137) into Eqs. (3.1.117) and (3.1.118), then separating the real and imaginary parts, the stresses for each Λ_n can be described by

$$\sigma_{rrkn}(r,\theta) = K_n^* \bar{r}^{-\omega_n} \left\{ \cos\left[p_n \ln(\bar{r})\right] F^c_{rrkn}(\theta) + \sin\left[p_n \ln(\bar{r})\right] F^s_{rrkn}(\theta) \right\} \tag{3.1.141}$$

$$\sigma_{\theta\theta kn}(r,\theta) = K_n^* \bar{r}^{-\omega_n} \left\{ \cos\left[p_n \ln(\bar{r})\right] F^c_{\theta\theta kn}(\theta) + \sin\left[p_n \ln(\bar{r})\right] F^s_{\theta\theta kn}(\theta) \right\} \tag{3.1.142}$$

$$\tau_{r\theta kn}(r,\theta) = K_n^* \bar{r}^{-\omega_n} \left\{ \cos\left[p_n \ln(\bar{r})\right] F^c_{r\theta kn}(\theta) + \sin\left[p_n \ln(\bar{r})\right] F^s_{r\theta kn}(\theta) \right\} \tag{3.1.143}$$

where K_n^* is an unknown real constant and $\omega_n = \{(1-t_n) \mid 0 < (1-t_n) < 1\}$. The functions $F^c_{rrkn}(\theta), F^s_{rrkn}(\theta), F^c_{\theta\theta kn}(\theta), F^s_{\theta\theta kn}(\theta), F^c_{r\theta kn}(\theta), F^s_{r\theta kn}(\theta)$ can be determined as follows

$$\begin{aligned}
F^c_{rrkn}(\theta) &= e^{-p_n\theta}\Big\{ \sin[(t_n-1)\theta]\Big\{ p_n \mathcal{A}^{\mathrm{R}}_{\mathrm{kn}}(2\mathrm{t_n}-3) - \mathcal{A}^{\mathrm{I}}_{\mathrm{kn}}(\mathrm{p_n^2}-\mathrm{t_n^2}+3\mathrm{t_n}) \\
&\qquad -p_n \mathcal{B}^{\mathrm{R}}_{\mathrm{kn}} \mathrm{e}^{2\mathrm{p_n}\theta}(2\mathrm{t_n}-3) - \mathcal{B}^{\mathrm{I}}_{\mathrm{kn}} \mathrm{e}^{2\mathrm{p_n}\theta}(\mathrm{p_n^2}-\mathrm{t_n^2}+3\mathrm{t_n}) \Big\} \\
&+ \sin[(t_n+1)\theta]\Big\{ p_n \mathcal{C}^{\mathrm{R}}_{\mathrm{kn}} + \mathrm{t_n}\mathcal{C}^{\mathrm{I}}_{\mathrm{kn}} - \mathrm{p_n}\mathrm{e}^{2\mathrm{p_n}\theta}\mathcal{D}^{\mathrm{R}}_{\mathrm{kn}} + \mathrm{t_n}\mathrm{e}^{2\mathrm{p_n}\theta}\mathcal{D}^{\mathrm{I}}_{\mathrm{kn}} \Big\} \\
&+ \cos[(t_n-1)\theta]\Big\{ \mathcal{A}^{\mathrm{R}}_{\mathrm{kn}}(\mathrm{p_n^2}-\mathrm{t_n^2}+3\mathrm{t_n}) + \mathrm{p_n}\mathcal{A}^{\mathrm{I}}_{\mathrm{kn}}(2\mathrm{t_n}-3) \\
&\qquad +\mathcal{B}^{\mathrm{R}}_{\mathrm{kn}} \mathrm{e}^{2\mathrm{p_n}\theta}(\mathrm{p_n^2}-\mathrm{t_n^2}+3\mathrm{t_n}) - \mathrm{p_n}\mathcal{B}^{\mathrm{I}}_{\mathrm{kn}} \mathrm{e}^{2\mathrm{p_n}\theta}(2\mathrm{t_n}-3) \Big\} \\
&+ \cos[(t_n+1)\theta]\Big\{ -t_n \mathcal{C}^{\mathrm{R}}_{\mathrm{kn}} + \mathrm{p_n}\mathcal{C}^{\mathrm{I}}_{\mathrm{kn}} - \mathrm{t_n}\mathrm{e}^{2\mathrm{p_n}\theta}\mathcal{D}^{\mathrm{R}}_{\mathrm{kn}} - \mathrm{p_n}\mathrm{e}^{2\mathrm{p_n}\theta}\mathcal{D}^{\mathrm{I}}_{\mathrm{kn}} \Big\} \Big\}
\end{aligned} \tag{3.1.144}$$

$$F^s_{rrkn}(\theta) = e^{-p_n\theta}\Big\{ \sin[(t_n-1)\theta]\Big\{ -\mathcal{A}^{\mathrm{R}}_{\mathrm{kn}}(\mathrm{p_n^2}-\mathrm{t_n^2}+3\mathrm{t_n}) - \mathrm{p_n}\mathcal{A}^{\mathrm{I}}_{\mathrm{kn}}(2\mathrm{t_n}-3) +$$

$$
\begin{aligned}
&+\mathcal{B}^{\mathrm{R}}_{\mathrm{kn}}\mathrm{e}^{2\mathrm{p_n}\theta}(\mathrm{p_n^2}-\mathrm{t_n^2}+3\mathrm{t_n})-\mathcal{B}^{\mathrm{I}}_{\mathrm{kn}}\mathrm{e}^{2\mathrm{p_n}\theta}(2\mathrm{t_n}-3)\Big\}\\
+\;&\sin[(t_n+1)\theta]\Big\{t_n\mathcal{C}^{\mathrm{R}}_{\mathrm{kn}}-\mathrm{p_n}\mathcal{C}^{\mathrm{I}}_{\mathrm{kn}}-\mathrm{t_n}\mathrm{e}^{2\mathrm{p_n}\theta}\mathcal{D}^{\mathrm{R}}_{\mathrm{kn}}-\mathrm{p_n}\mathrm{e}^{2\mathrm{p_n}\theta}\mathcal{D}^{\mathrm{I}}_{\mathrm{kn}}\Big\}\\
+\;&\cos[(t_n-1)\theta]\Big\{p_n\mathcal{A}^{\mathrm{R}}_{\mathrm{kn}}(2\mathrm{t_n}-3)-\mathcal{A}^{\mathrm{I}}_{\mathrm{kn}}(\mathrm{p_n^2}-\mathrm{t_n^2}+3\mathrm{t_n})\\
&\quad+p_n\mathcal{B}^{\mathrm{R}}_{\mathrm{kn}}\mathrm{e}^{2\mathrm{p_n}\theta}(2\mathrm{t_n}-3)+\mathcal{B}^{\mathrm{I}}_{\mathrm{kn}}\mathrm{e}^{2\mathrm{p_n}\theta}(\mathrm{p_n^2}-\mathrm{t_n^2}+3\mathrm{t_n})\Big\}\\
+\;&\cos[(t_n+1)\theta]\Big\{p_n\mathcal{C}^{\mathrm{R}}_{\mathrm{kn}}+\mathrm{t_n}\mathcal{C}^{\mathrm{I}}_{\mathrm{kn}}+\mathrm{p_n}\mathrm{e}^{2\mathrm{p_n}\theta}\mathcal{D}^{\mathrm{R}}_{\mathrm{kn}}-\mathrm{t_n}\mathrm{e}^{2\mathrm{p_n}\theta}\mathcal{D}^{\mathrm{I}}_{\mathrm{kn}}\Big\}\Big\}
\end{aligned}
\tag{3.1.145}
$$

$$
\begin{aligned}
F^{c}_{\theta\theta kn}(\theta) \;=\;& -e^{-p_n\theta}\Big\{\sin[(t_n-1)\theta]\Big\{\mathcal{A}^{\mathrm{R}}_{\mathrm{kn}}\mathrm{p_n}(2\mathrm{t_n}+1)-\mathcal{A}^{\mathrm{I}}_{\mathrm{kn}}(\mathrm{p_n^2}-\mathrm{t_n^2}-\mathrm{t_n})\\
&\quad-p_n\mathcal{B}^{\mathrm{R}}_{\mathrm{kn}}\mathrm{e}^{2\mathrm{p_n}\theta}(2\mathrm{t_n}+1)-\mathcal{B}^{\mathrm{I}}_{\mathrm{kn}}\mathrm{e}^{2\mathrm{p_n}\theta}(\mathrm{p_n^2}-\mathrm{t_n^2}-\mathrm{t_n})\Big\}\\
+\;&\sin[(t_n+1)\theta]\Big\{p_n\mathcal{C}^{\mathrm{R}}_{\mathrm{kn}}+\mathrm{t_n}\mathcal{C}^{\mathrm{I}}_{\mathrm{kn}}-\mathrm{p_n}\mathrm{e}^{2\mathrm{p_n}\theta}\mathcal{D}^{\mathrm{R}}_{\mathrm{kn}}+\mathrm{t_n}\mathrm{e}^{2\mathrm{p_n}\theta}\mathcal{D}^{\mathrm{I}}_{\mathrm{kn}}\Big\}\\
+\;&\cos[(t_n-1)\theta]\Big\{\mathcal{A}^{\mathrm{R}}_{\mathrm{kn}}(\mathrm{p_n^2}-\mathrm{t_n^2}-\mathrm{t_n})+\mathcal{A}^{\mathrm{I}}_{\mathrm{kn}}\mathrm{p_n}(2\mathrm{t_n}+1)\\
&\quad+\mathcal{B}^{\mathrm{R}}_{\mathrm{kn}}\mathrm{e}^{2\mathrm{p_n}\theta}(\mathrm{p_n^2}-\mathrm{t_n^2}-\mathrm{t_n})-\mathcal{B}^{\mathrm{I}}_{\mathrm{kn}}\mathrm{p_n}\mathrm{e}^{2\mathrm{p_n}\theta}(2\mathrm{t_n}+1)\Big\}\\
+\;&\cos[(t_n+1)\theta]\Big\{-t_n\mathcal{C}^{\mathrm{R}}_{\mathrm{kn}}+\mathrm{p_n}\mathcal{C}^{\mathrm{I}}_{\mathrm{kn}}-\mathrm{t_n}\mathrm{e}^{2\mathrm{p_n}\theta}\mathcal{D}^{\mathrm{R}}_{\mathrm{kn}}-\mathrm{p_n}\mathrm{e}^{2\mathrm{p_n}\theta}\mathcal{D}^{\mathrm{I}}_{\mathrm{kn}}\Big\}\Big\}
\end{aligned}
\tag{3.1.146}
$$

$$
\begin{aligned}
F^{s}_{\theta\theta kn}(\theta) \;=\;& -e^{-p_n\theta}\Big\{\sin[(t_n-1)\theta]\Big\{-\mathcal{A}^{\mathrm{R}}_{\mathrm{kn}}(\mathrm{p_n^2}-\mathrm{t_n^2}-\mathrm{t_n})-\mathrm{p_n}\mathcal{A}^{\mathrm{I}}_{\mathrm{kn}}(2\mathrm{t_n}+1)\\
&\quad+\mathcal{B}^{\mathrm{R}}_{\mathrm{kn}}\mathrm{e}^{2\mathrm{p_n}\theta}(\mathrm{p_n^2}-\mathrm{t_n^2}-\mathrm{t_n})-\mathrm{p_n}\mathcal{B}^{\mathrm{I}}_{\mathrm{kn}}\mathrm{e}^{2\mathrm{p_n}\theta}(2\mathrm{t_n}+1)\Big\}\\
+\;&\sin[(t_n+1)\theta]\Big\{t_n\mathcal{C}^{\mathrm{R}}_{\mathrm{kn}}-\mathrm{p_n}\mathcal{C}^{\mathrm{I}}_{\mathrm{kn}}-\mathrm{t_n}\mathrm{e}^{2\mathrm{p_n}\theta}\mathcal{D}^{\mathrm{R}}_{\mathrm{kn}}-\mathrm{p_n}\mathrm{e}^{2\mathrm{p_n}\theta}\mathcal{D}^{\mathrm{I}}_{\mathrm{kn}}\Big\}\\
+\;&\cos[(t_n-1)\theta]\Big\{p_n\mathcal{A}^{\mathrm{R}}_{\mathrm{kn}}(2\mathrm{t_n}+1)-\mathcal{A}^{\mathrm{I}}_{\mathrm{kn}}(\mathrm{p_n^2}-\mathrm{t_n^2}-\mathrm{t_n})\\
&\quad+p_n\mathcal{B}^{\mathrm{R}}_{\mathrm{kn}}\mathrm{e}^{2\mathrm{p_n}\theta}(2\mathrm{t_n}+1)+\mathcal{B}^{\mathrm{I}}_{\mathrm{kn}}\mathrm{e}^{2\mathrm{p_n}\theta}(\mathrm{p_n^2}-\mathrm{t_n^2}-\mathrm{t_n})\Big\}\\
+\;&\cos[(t_n+1)\theta]\Big\{p_n\mathcal{C}^{\mathrm{R}}_{\mathrm{kn}}+\mathrm{t_n}\mathcal{C}^{\mathrm{I}}_{\mathrm{kn}}+\mathrm{p_n}\mathrm{e}^{2\mathrm{p_n}\theta}\mathcal{D}^{\mathrm{R}}_{\mathrm{kn}}-\mathrm{t_n}\mathrm{e}^{2\mathrm{p_n}\theta}\mathcal{D}^{\mathrm{I}}_{\mathrm{kn}}\Big\}\Big\}
\end{aligned}
\tag{3.1.147}
$$

$$
\begin{aligned}
F^{c}_{r\theta kn}(\theta) \;=\;& e^{-p_n\theta}\Big\{\sin[(t_n-1)\theta]\Big\{-\mathcal{A}^{\mathrm{R}}_{\mathrm{kn}}(\mathrm{p_n^2}-\mathrm{t_n^2}+\mathrm{t_n})-\mathrm{p_n}\mathcal{A}^{\mathrm{I}}_{\mathrm{kn}}(2\mathrm{t_n}-1)\\
&\quad-\mathcal{B}^{\mathrm{R}}_{\mathrm{kn}}\mathrm{e}^{2\mathrm{p_n}\theta}(\mathrm{p_n^2}-\mathrm{t_n^2}+\mathrm{t_n})+\mathrm{p_n}\mathcal{B}^{\mathrm{I}}_{\mathrm{kn}}\mathrm{e}^{2\mathrm{p_n}\theta}(2\mathrm{t_n}-1)\Big\}\\
+\;&\sin[(t_n+1)\theta]\Big\{t_n\mathcal{C}^{\mathrm{R}}_{\mathrm{kn}}-\mathrm{p_n}\mathcal{C}^{\mathrm{I}}_{\mathrm{kn}}+\mathrm{t_n}\mathrm{e}^{2\mathrm{p_n}\theta}\mathcal{D}^{\mathrm{R}}_{\mathrm{kn}}+\mathrm{p_n}\mathrm{e}^{2\mathrm{p_n}\theta}\mathcal{D}^{\mathrm{I}}_{\mathrm{kn}}\Big\}\\
+\;&\cos[(t_n-1)\theta]\Big\{p_n\mathcal{A}^{\mathrm{R}}_{\mathrm{kn}}(2\mathrm{t_n}-1)-\mathcal{A}^{\mathrm{I}}_{\mathrm{kn}}(\mathrm{p_n^2}-\mathrm{t_n^2}+\mathrm{t_n})\\
&\quad-p_n\mathcal{B}^{\mathrm{R}}_{\mathrm{kn}}\mathrm{e}^{2\mathrm{p_n}\theta}(2\mathrm{t_n}-1)-\mathcal{B}^{\mathrm{I}}_{\mathrm{kn}}\mathrm{e}^{2\mathrm{p_n}\theta}(\mathrm{p_n^2}-\mathrm{t_n^2}+\mathrm{t_n})\Big\}\\
+\;&\cos[(t_n+1)\theta]\Big\{p_n\mathcal{C}^{\mathrm{R}}_{\mathrm{kn}}+\mathrm{t_n}\mathcal{C}^{\mathrm{I}}_{\mathrm{kn}}-\mathrm{p_n}\mathrm{e}^{2\mathrm{p_n}\theta}\mathcal{D}^{\mathrm{R}}_{\mathrm{kn}}+\mathrm{t_n}\mathrm{e}^{2\mathrm{p_n}\theta}\mathcal{D}^{\mathrm{I}}_{\mathrm{kn}}\Big\}\Big\}
\end{aligned}
\tag{3.1.148}
$$

$$
\begin{aligned}
F^s_{r\theta kn}(\theta) &= e^{-p_n\theta}\Big\{ \sin[(t_n-1)\theta]\Big\{ -p_n\mathcal{A}^{\mathrm{R}}_{\mathrm{kn}}(2\mathrm{t_n}-1)+\mathcal{A}^{\mathrm{I}}_{\mathrm{kn}}(\mathrm{p_n^2}-\mathrm{t_n^2}+\mathrm{t_n}) \\
&\quad -p_n\mathcal{B}^{\mathrm{R}}_{\mathrm{kn}}\mathrm{e}^{2\mathrm{p_n}\theta}(2\mathrm{t_n}-1)-\mathcal{B}^{\mathrm{I}}_{\mathrm{kn}}\mathrm{e}^{2\mathrm{p_n}\theta}(\mathrm{p_n^2}-\mathrm{t_n^2}+\mathrm{t_n})\Big\} \\
&+ \sin[(t_n+1)\theta]\Big\{ -p_n\mathcal{C}^{\mathrm{R}}_{\mathrm{kn}}-\mathrm{t_n}\mathcal{C}^{\mathrm{I}}_{\mathrm{kn}}-\mathrm{p_n}\mathrm{e}^{2\mathrm{p_n}\theta}\mathcal{D}^{\mathrm{R}}_{\mathrm{kn}}+\mathrm{t_n}\mathrm{e}^{2\mathrm{p_n}\theta}\mathcal{D}^{\mathrm{I}}_{\mathrm{kn}}\Big\} \\
&+ \cos[(t_n-1)\theta]\Big\{ -\mathcal{A}^{\mathrm{R}}_{\mathrm{kn}}(\mathrm{p_n^2}-\mathrm{t_n^2}+\mathrm{t_n})-\mathrm{p_n}\mathcal{A}^{\mathrm{I}}_{\mathrm{kn}}(2\mathrm{t_n}-1) \\
&\quad +\mathcal{B}^{\mathrm{R}}_{\mathrm{kn}}\mathrm{e}^{2\mathrm{p_n}\theta}(\mathrm{p_n^2}-\mathrm{t_n^2}+\mathrm{t_n})-\mathrm{p_n}\mathcal{B}^{\mathrm{I}}_{\mathrm{kn}}\mathrm{e}^{2\mathrm{p_n}\theta}(2\mathrm{t_n}-1)\Big\} \\
&+ \cos[(t_n+1)\theta]\Big\{ t_n\mathcal{C}^{\mathrm{R}}_{\mathrm{kn}}-\mathrm{p_n}\mathcal{C}^{\mathrm{I}}_{\mathrm{kn}}-\mathrm{t_n}\mathrm{e}^{2\mathrm{p_n}\theta}\mathcal{D}^{\mathrm{R}}_{\mathrm{kn}}-\mathrm{p_n}\mathrm{e}^{2\mathrm{p_n}\theta}\mathcal{D}^{\mathrm{I}}_{\mathrm{kn}}\Big\}\Big\}.
\end{aligned}
\tag{3.1.149}
$$

The angular functions used to describe the stresses are normalized as

$$
\begin{aligned}
f^c_{rrkn}(\theta) &= \frac{F^c_{rrkn}(\theta)}{F^c_{\theta\theta 1n}(0)} \\
f^s_{rrkn}(\theta) &= \frac{F^s_{rrkn}(\theta)}{F^c_{\theta\theta 1n}(0)} \\
f^c_{\theta\theta kn}(\theta) &= \frac{F^c_{\theta\theta kn}(\theta)}{F^c_{\theta\theta 1n}(0)} \\
f^s_{\theta\theta kn}(\theta) &= \frac{F^s_{\theta\theta kn}(\theta)}{F^c_{\theta\theta 1n}(0)} \\
f^c_{r\theta kn}(\theta) &= \frac{F^c_{r\theta kn}(\theta)}{F^c_{\theta\theta 1n}(0)} \\
f^s_{r\theta kn}(\theta) &= \frac{F^s_{r\theta kn}(\theta)}{F^c_{\theta\theta 1n}(0)},
\end{aligned}
\tag{3.1.150}
$$

which means that always $f^c_{\theta\theta kn}(\theta=0)=1$. The angular functions $f^c_{rrkn}(\theta)$, $f^s_{rrkn}(\theta)$, $f^c_{\theta\theta kn}(\theta)$, $f^s_{\theta\theta kn}(\theta)$, $f^c_{r\theta kn}(\theta)$, and $f^s_{r\theta kn}(\theta)$ can be calculated analytically for each given eigenvalue Λ_n. They are dependent on the eigenvalue Λ_n, the material properties (E_k,ν_k), and the geometry (θ_1,θ_2). By considering all stress exponents ω_n, which are in the range of $-0.5<\omega_n<1$, and the regular stress term, the stresses near the singular point in a joint with complex eigenvalues can be calculated from

$$
\begin{aligned}
\sigma_{rrk}(r,\theta) &= \sum_{n=1}^{N}\frac{K_n}{\bar{r}^{\omega_n}}\left\{\cos\left[p_n\ln(\bar{r})\right]f^c_{rrkn}(\theta)+\sin\left[p_n\ln(\bar{r})\right]f^s_{rrkn}(\theta)\right\} \\
&\quad +\sigma_{rrk0}(\theta)
\end{aligned}
\tag{3.1.151}
$$

$$
\begin{aligned}
\sigma_{\theta\theta k}(r,\theta) &= \sum_{n=1}^{N}\frac{K_n}{\bar{r}^{\omega_n}}\left\{\cos\left[p_n\ln(\bar{r})\right]f^c_{\theta\theta kn}(\theta)+\sin\left[p_n\ln(\bar{r})\right]f^s_{\theta\theta kn}(\theta)\right\} \\
&\quad +\sigma_{\theta\theta k0}(\theta)
\end{aligned}
\tag{3.1.152}
$$

$$
\begin{aligned}
\tau_{r\theta k}(r,\theta) &= \sum_{n=1}^{N}\frac{K_n}{\bar{r}^{\omega_n}}\left\{\cos\left[p_n\ln(\bar{r})\right]f^c_{r\theta kn}(\theta)+\sin\left[p_n\ln(\bar{r})\right]f^s_{r\theta kn}(\theta)\right\} \\
&\quad +\tau_{r\theta k0}(\theta)
\end{aligned}
\tag{3.1.153}
$$

where k = 1 and 2 denote materials 1 and 2, $\sigma_{ijk0}(\theta)$ is the regular stress term, which will be given in the next section, and K_n are unknown constants, which can be determined from a numerical method, e.g. the Finite Element Method (FEM). From Eqs. (3.1.151) - (3.1.153) we know that due to the terms $\sin[p_n \ln(\bar{r})]$ and $\cos[p_n \ln(\bar{r})]$, if $p_n \neq 0$, the stresses oscillate in the range very near to the singular point. The frequency of the stress oscillation is dependent on the absolute value of p_n.
In [132] the complex eigenvalue problem has been studied as well, but used another method.

3.2 Determination of the Regular Stress Term for a Joint under Thermal Loading

In Section 3.1 the singular stress term, i.e. the singular stress exponent and the corresponding angular functions, have been studied in detail. But for the stresses near the singular point and in particular for a joint with free edges under thermal loading, the regular stress term, which is independent of the distance from the singular point, is also very important. In this section the method to calculate the regular stress term, which corresponds to the solution of $\lambda_n = 0$ in Section 3.1.1 and of $\Lambda_n = 1$ in Section 3.1.2, will be given for a joint with an arbitrary geometry (θ_1, θ_2) under thermal loading. For several special geometries, simple explicit forms will be presented as well.
There are three methods to determine this regular stress term, which are: (a) Method using a special Airy's stress function [86]; (b) using a general Airy's stress function and applying mathematical limit method [85]; (c) the Mellin transform method [87]. In this section the Mellin transform method will be used, because it is a more general method for the singularity problem.

Solution in the Mellin Transform Domain

When thermal loading is taken into account and body forces are disregarded, the stress function, Φ, should satisfy the equation

$$\nabla^4 \Phi + q \nabla^2 T = 0 \tag{3.2.1}$$

with

$$q = \begin{cases} \alpha E & \text{for plane stress} \\ \frac{\alpha E}{(1-\nu)} & \text{for plane strain} \end{cases},$$

where T is the temperature change, E the Young's modulus, ν Poisson ratio, and α is the thermal expansion coefficient. To use the Mellin transform, a semi-infinite bonded component with the temperature change

$$T = \begin{cases} T & \text{for r} \leq R_0 \\ 0 & \text{for r} > R_0 \end{cases}$$

is considered at first.
The Mellin transform of a function, $\Phi(\bar{r},\theta)$, is defined as

$$\hat{\Phi}(s,\theta)=\int_0^\infty \Phi(\bar{r},\theta)\bar{r}^{(s-1)}d\bar{r} \tag{3.2.2}$$

where s is a parameter of the Mellin transform, and $\bar{r}$ is dimensionless ($\bar{r}$=r/R). The parameter s should be chosen so that the integration in Eq. (3.2.2) is valid. The property of the Mellin transform is

$$\int_0^\infty \bar{r}^p\frac{\partial^q\Phi(\bar{r},\theta)}{\partial\bar{r}^q}\bar{r}^{(s-1)}d\bar{r}=(-1)^q\frac{\Gamma(s+p)}{\Gamma(s+p-q)}\hat{\Phi}(s+p-q,\theta) \tag{3.2.3}$$

where $\Gamma(x)$ is the Γ-function.
The Mellin transform of the first term in Eq. (3.2.1) is

$$\int_0^\infty \bar{r}^4\nabla^4\Phi(\bar{r},\theta)\bar{r}^{(s-1)}d\bar{r}=[s^2+\frac{\partial^2}{\partial\theta^2}][(s+2)^2+\frac{\partial^2}{\partial\theta^2}]\hat{\Phi}(s,\theta) \tag{3.2.4}$$

and the second term is

$$\int_0^\infty \bar{r}^4 q\nabla^2 T\bar{r}^{(s-1)}d\bar{r}=[(s+2)^2+\frac{\partial^2}{\partial\theta^2}]\hat{T}(s+2) \tag{3.2.5}$$

with

$$\hat{T}(s+2)=\int_0^\infty qT\bar{r}^{(s+1)}d\bar{r}=\frac{qT}{s+2}\bar{R}_0^{(s+2)} \tag{3.2.6}$$

where $\bar{R}_0=R_0/R$. The Mellin transform of Eq. (3.2.1) then reads

$$[s^2+\frac{\partial^2}{\partial\theta^2}][(s+2)^2+\frac{\partial^2}{\partial\theta^2}]\hat{\Phi}(s,\theta)+[(s+2)^2+\frac{\partial^2}{\partial\theta^2}]\hat{T}(s+2)=0. \tag{3.2.7}$$

If s is considered as a parameter, Eq. (3.2.7) is an ordinary differential equation of the variable θ. Its solution is

$$\hat{\Phi}_k(s,\theta)=A_k e^{is\theta}+\bar{A}_k e^{-is\theta}+B_k e^{i(s+2)\theta}+\bar{B}_k e^{-i(s+2)\theta}-\frac{\hat{T}_k(s+2)}{s^2} \tag{3.2.8}$$

where A_k, B_k ($\bar{A}_k, \bar{B}_k$ is the conjugate complex number of A_k, B_k) are unknown complex constants. In order to determine the unknown A_k and B_k, the boundary conditions expressed by the Mellin transform are used. For a joint with free edges they are:

for the free edges

$$\begin{aligned}\theta=\theta_1: &\quad \hat{\tau}_{r\theta 1}+i\hat{\sigma}_{\theta\theta 1}=0\\ \theta=\theta_2: &\quad \hat{\tau}_{r\theta 2}+i\hat{\sigma}_{\theta\theta 2}=0\end{aligned} \tag{3.2.9}$$

at the interface

$$\begin{aligned} \theta = 0: \quad & \hat{\tau}_{r\theta 1} + i\hat{\sigma}_{\theta\theta 1} = \hat{\tau}_{r\theta 2} + i\hat{\sigma}_{\theta\theta 2} \\ \theta = 0: \quad & \hat{u}_1 + i\hat{v}_1 = \hat{u}_2 + i\hat{v}_2 \end{aligned} \tag{3.2.10}$$

where u and v are the displacements in the directions r and θ, respectively. The physical meaning of Eq. (3.2.9) is that along the free edges the normal and shear stresses are zero. Equation (3.2.10) means that along the interface the normal and shear stresses, and the displacements u and v are continuous.
In the Mellin domain, stresses can be calculated from the stress function by

$$\begin{aligned} \hat{\sigma}_{rr}(s,\theta) &= (\tfrac{\partial^2}{\partial\theta^2} - s)\hat{\Phi}(s,\theta) \\ \hat{\sigma}_{\theta\theta}(s,\theta) &= (s+1)s\hat{\Phi}(s,\theta) \\ \hat{\tau}_{r\theta}(s,\theta) &= (s+1)\tfrac{\partial\hat{\Phi}(s,\theta)}{\partial\theta}. \end{aligned} \tag{3.2.11}$$

From the relation between the strains, stresses and displacements we obtain for the displacements:

$$\frac{\partial u}{\partial \bar{r}} = \frac{1}{2G}\left\{\frac{\partial\Phi}{\bar{r}\partial\bar{r}} + \frac{\partial^2\Phi}{\bar{r}^2\partial\theta^2} - (1-\frac{m}{4})\nabla^2\Phi\right\} + \frac{q}{E}\kappa T, \tag{3.2.12}$$

$$\frac{\partial u}{\bar{r}\partial\theta} + \frac{\partial v}{\partial\bar{r}} - \frac{v}{\bar{r}} = \frac{1}{G}\left\{\frac{\partial\Phi}{\bar{r}^2\partial\theta} - \frac{\partial^2\Phi}{\bar{r}\partial\bar{r}\partial\theta}\right\} \tag{3.2.13}$$

with

$$m = \begin{cases} \frac{4}{(1+\nu)} & \text{for plane stress} \\ 4(1-\nu) & \text{for plane strain} \end{cases}$$

$$\kappa = \begin{cases} 1 & \text{for plane stress} \\ (1-\nu^2) & \text{for plane strain.} \end{cases}$$

The Mellin transform of the displacement u is calculated from

$$\begin{aligned} \int_0^\infty \bar{r}^2 \frac{\partial u}{\partial\bar{r}}\bar{r}^{(s-1)}d\bar{r} &= -(s+1)\hat{u}(s+1,\theta) \\ &= \frac{1}{2G}\left\{-s + \frac{\partial^2}{\partial\theta^2} - (1-\frac{m}{4})[s(s+1) - s + \frac{\partial^2}{\partial\theta^2}]\right\}\hat{\Phi}(s,\theta) + \frac{\kappa}{E}\hat{T}(s+2). \end{aligned} \tag{3.2.14}$$

For $s \neq -1$

$$2G\hat{u}(s+1,\theta) = \left\{s - \frac{m}{4}\frac{s^2}{(s+1)} - \frac{m}{4(s+1)}\frac{\partial^2}{\partial\theta^2}\right\}\hat{\Phi}(s,\theta) - \frac{m}{4}\frac{\hat{T}(s+2)}{(s+1)}. \tag{3.2.15}$$

The Mellin transform of the displacement v can be obtained from

$$\begin{aligned}\int_0^\infty \bar{r}^2 \left\{ \frac{\partial u}{\bar{r}\partial\theta} + \frac{\partial v}{\partial \bar{r}} - \frac{v}{\bar{r}} \right\} \bar{r}^{(s-1)} d\bar{r} &= \frac{\partial \hat{u}(s+1,\theta)}{\partial\theta} - [(s+1)+1]\hat{v}(s+1,\theta) \\ &= \frac{1}{G}\left\{ \frac{\partial \hat{\Phi}(s,\theta)}{\partial\theta} + s\frac{\partial \hat{\Phi}(s,\theta)}{\partial\theta} \right\}. \end{aligned} \tag{3.2.16}$$

For $s \neq -1, -2$ there is

$$\begin{aligned} & 2G\hat{v}(s+1,\theta) \\ = & -\left[\frac{m}{4}\frac{s^2}{(s+1)(s+2)} + 1 \right] \frac{\partial \hat{\Phi}(s,\theta)}{\partial\theta} - \frac{m}{4}\frac{1}{(s+1)(s+2)}\frac{\partial^3 \hat{\Phi}(s,\theta)}{\partial\theta^3}. \end{aligned} \tag{3.2.17}$$

The complex form of stresses and displacements in the Mellin domain is

$$\hat{\tau}_{r\theta}(s,\theta) + i\hat{\sigma}_{\theta\theta}(s,\theta) = (s+1)(\tfrac{\partial}{\partial\theta} + is)\hat{\Phi}(s,\theta) \tag{3.2.18}$$

and

$$\begin{aligned} 2G\{\hat{u}(s+1,\theta) &+ i\hat{v}(s+1,\theta)\} = -\frac{\kappa\hat{T}(s+2)}{4(s+1)} + \\ &+ (s - i\frac{\partial}{\partial\theta})\{1 + \frac{\kappa(\frac{\partial}{\partial\theta} - is)(\frac{\partial}{\partial\theta} - i(s+2))}{4(s+1)(s+2)}\}\hat{\Phi}(s,\theta). \end{aligned} \tag{3.2.19}$$

Insertion of Eq. (3.2.8) into Eqs. (3.2.18) and (3.2.19) and then into Eqs. (3.2.9) and (3.2.10) for $s \neq -1$ yields

$$sA_1 + (s+1)B_1 e^{i2\theta_1} - \bar{B}_1 e^{-i2(s+1)\theta_1} - \frac{\hat{T}_1(s+2)}{2s} e^{-is\theta_1} = 0 \tag{3.2.20}$$

$$sA_2 + (s+1)B_2 e^{i2\theta_2} - \bar{B}_2 e^{-i2(s+1)\theta_2} - \frac{\hat{T}_2(s+2)}{2s} e^{-is\theta_2} = 0 \tag{3.2.21}$$

$$sA_1 + (s+1)B_1 - \bar{B}_1 - \frac{\hat{T}_1(s+2)}{2s} = sA_2 + (s+1)B_2 - \bar{B}_2 - \frac{\hat{T}_2(s+2)}{2s} \tag{3.2.22}$$

$$\begin{aligned} g\Big\{ sA_1 &+ (s+1)B_1 + \bar{B}_1(m_1 - 1) - \frac{\hat{T}_1(s+2)}{2s} \Big\} \\ &= sA_2 + (s+1)B_2 + \bar{B}_2(m_2 - 1) - \frac{\hat{T}_2(s+2)}{2s} \end{aligned} \tag{3.2.23}$$

with $g = \frac{G_2}{G_1}$. Equations (3.2.20) and (3.2.21) yield

$$sA_1 = \frac{\hat{T}_1(s+2)}{2s} e^{-is\theta_1} - (s+1)B_1 e^{i2\theta_1} + \bar{B}_1 e^{-i2(s+1)\theta_1} \tag{3.2.24}$$

$$sA_2 = \frac{\hat{T}_2(s+2)}{2s} e^{-is\theta_2} - (s+1)B_2 e^{i2\theta_2} + \bar{B}_2 e^{-i2(s+1)\theta_2} \tag{3.2.25}$$

Inserting Eqs. (3.2.24) and (3.2.25) into Eqs. (3.2.22) and (3.2.23) gives:

$$\begin{aligned} B_1(s+1)(1 &- e^{i2\theta_1}) - \bar{B}_1(1 - e^{-i2(s+1)\theta_1}) \\ &- B_2(s+1)(1 - e^{i2\theta_2}) + \bar{B}_2(1 - e^{-i2(s+1)\theta_2}) \\ &= \frac{\hat{T}_1(s+2)}{2s}(1 - e^{-is\theta_1}) - \frac{\hat{T}_2(s+2)}{2s}(1 - e^{-is\theta_2}) \end{aligned} \tag{3.2.26}$$

$$\begin{aligned} gB_1(s+1)(1 &- e^{i2\theta_1}) + g\bar{B}_1(e^{-i2(s+1)\theta_1} + m_1 - 1) \\ &- B_2(s+1)(1 - e^{i2\theta_2}) - \bar{B}_2(e^{-i2(s+1)\theta_2} + m_2 - 1) \\ &= g\frac{\hat{T}_1(s+2)}{2s}(1 - e^{-is\theta_1}) - \frac{\hat{T}_2(s+2)}{2s}(1 - e^{-is\theta_2}). \end{aligned} \tag{3.2.27}$$

To obtain a real expression of the stresses and displacements, the coefficients, A_1, B_1 and A_2, B_2, are separated as

$$\begin{aligned} A_1 &= C_1 + iD_1 \quad , \quad A_2 = C_2 + iD_2 \\ B_1 &= F_1 + iH_1 \quad , \quad B_2 = F_2 + iH_2. \end{aligned} \tag{3.2.28}$$

If s is real, the coefficients C_k, D_k, F_k, H_k can be determined from the following relations by inserting Eq. (3.2.28) into Eqs. (3.2.26) and (3.2.27) and separating their real and imaginary parts:

$$F_1' a_{11} + H_1' a_{12} + F_2' a_{13} + H_2' a_{14} = R_1 \tag{3.2.29}$$

$$F_1' a_{21} + H_1' a_{22} + F_2' a_{23} + H_2' a_{24} = R_2 \tag{3.2.30}$$

$$F_1' a_{31} + H_1' a_{32} + F_2' a_{33} + H_2' a_{34} = R_3 \tag{3.2.31}$$

$$F_1' a_{41} + H_1' a_{42} + F_2' a_{43} + H_2' a_{44} = R_4 \tag{3.2.32}$$

with

$$\begin{aligned} F_1' &= F_1 \frac{2s(s+2)}{T\bar{R}_0{}^{(s+2)}} \\ F_2' &= F_2 \frac{2s(s+2)}{T\bar{R}_0{}^{(s+2)}} \\ H_1' &= H_1 \frac{2s(s+2)}{T\bar{R}_0{}^{(s+2)}} \\ H_2' &= H_2 \frac{2s(s+2)}{T\bar{R}_0{}^{(s+2)}} \end{aligned}$$

and

$$
\begin{aligned}
a_{11} &= (s+1)(1-\cos(2\theta_1)) - 1 + \cos[2(s+1)\theta_1] \\
a_{12} &= (s+1)\sin(2\theta_1) - \sin[2(s+1)\theta_1] \\
a_{13} &= -(s+1)(1-\cos(2\theta_2)) + 1 - \cos[2(s+1)\theta_2] \\
a_{14} &= -(s+1)\sin(2\theta_2) + \sin[2(s+1)\theta_2] \\
a_{21} &= -(s+1)\sin(2\theta_1) - \sin[2(s+1)\theta_1] \\
a_{22} &= (s+1)(1-\cos(2\theta_1)) + 1 - \cos[2(s+1)\theta_1] \\
a_{23} &= (s+1)\sin(2\theta_2) + \sin[2(s+1)\theta_2] \\
a_{24} &= -(s+1)(1-\cos(2\theta_2)) - 1 + \cos[2(s+1)\theta_2] \\
a_{31} &= g(m_1 + a_{11}) \\
a_{32} &= g a_{12} \\
a_{33} &= a_{13} - m_2 \\
a_{34} &= a_{14} \\
a_{41} &= g a_{21} \\
a_{42} &= g(a_{22} - m_1) \\
a_{43} &= a_{23} \\
a_{44} &= a_{24} + m_2
\end{aligned}
$$

$$
\begin{aligned}
R_1 &= (1-\cos(s\theta_1))q_1 - (1-\cos(s\theta_2))q_2 \\
R_2 &= \sin(s\theta_1)q_1 - \sin(s\theta_2)q_2 \\
R_3 &= g(1-\cos(s\theta_1))q_1 - (1-\cos(s\theta_2))q_2 \\
R_4 &= g\sin(s\theta_1)q_1 - \sin(s\theta_2)q_2.
\end{aligned}
$$

Let $\| X \|$ be the determinant of the matrix $(a_{ij})_{4\times 4}$ and Q_l (l=1,2,3,4) the determinant, in which the l-th column of $(a_{ij})_{4\times 4}$ is replaced by $\{R\}_{4\times 1}$. After using Cramer's law, we have the following solution for the coefficients:

$$F_1 = \frac{Q_1}{\| X \|}\frac{T\bar{R}_0{}^{(s+2)}}{2s(s+2)} \equiv \frac{F_1^*}{\| X \|}\frac{T\bar{R}_0{}^{(s+2)}}{2s(s+2)} \tag{3.2.33}$$

$$F_2 = \frac{Q_3}{\| X \|}\frac{T\bar{R}_0{}^{(s+2)}}{2s(s+2)} \equiv \frac{F_2^*}{\| X \|}\frac{T\bar{R}_0{}^{(s+2)}}{2s(s+2)} \tag{3.2.34}$$

$$H_1 = \frac{Q_2}{\| X \|}\frac{T\bar{R}_0{}^{(s+2)}}{2s(s+2)} \equiv \frac{H_1^*}{\| X \|}\frac{T\bar{R}_0{}^{(s+2)}}{2s(s+2)} \tag{3.2.35}$$

$$H_2 = \frac{Q_4}{\| X \|}\frac{T\bar{R}_0{}^{(s+2)}}{2s(s+2)} \equiv \frac{H_2^*}{\| X \|}\frac{T\bar{R}_0{}^{(s+2)}}{2s(s+2)}. \tag{3.2.36}$$

From Eqs. (3.2.24), (3.2.25), (3.2.28), (3.2.33), (3.2.34), (3.2.35), and (3.2.36) the coefficients C_1, C_2, D_1, D_2 can be determined as:

$$\begin{aligned} C_1 &= \frac{1}{\| X \|}\frac{T\bar{R_0}^{(s+2)}}{2s^2(s+2)}\Big\{q_1 \| X \| \cos(s\theta_1) \\ &+ Q_1\cos[2(s+1)\theta_1] - Q_2\sin[2(s+1)\theta_1] - Q_1(s+1)\cos(2\theta_1) + Q_2(s+1)\sin(2\theta_1)\Big\} \\ &\equiv \frac{C_1^*}{\| X \|}\frac{T\bar{R_0}^{(s+2)}}{2s(s+2)}\frac{1}{s} \end{aligned} \tag{3.2.37}$$

$$\begin{aligned} C_2 &= \frac{1}{\| X \|}\frac{T\bar{R_0}^{(s+2)}}{2s^2(s+2)}\Big\{q_2 \| X \| \cos(s\theta_2) \\ &+ Q_3\cos[2(s+1)\theta_2] - Q_4\sin[2(s+1)\theta_2] - Q_3(s+1)\cos(2\theta_2) + Q_4(s+1)\sin(2\theta_2)\Big\} \\ &\equiv \frac{C_2^*}{\| X \|}\frac{T\bar{R_0}^{(s+2)}}{2s(s+2)}\frac{1}{s} \end{aligned} \tag{3.2.38}$$

$$\begin{aligned} D_1 &= \frac{1}{\| X \|}\frac{T\bar{R_0}^{(s+2)}}{2s^2(s+2)}\Big\{ - q_1 \| X \| \sin(s\theta_1) \\ &- Q_1\sin[2(s+1)\theta_1] - Q_2\cos[2(s+1)\theta_1] - Q_1(s+1)\sin(2\theta_1) - Q_2(s+1)\cos(2\theta_1)\Big\} \\ &\equiv \frac{D_1^*}{\| X \|}\frac{T\bar{R_0}^{(s+2)}}{2s(s+2)}\frac{1}{s} \end{aligned} \tag{3.2.39}$$

$$\begin{aligned} D_2 &= \frac{1}{\| X \|}\frac{T\bar{R_0}^{(s+2)}}{2s^2(s+2)}\Big\{ - q_2 \| X \| \sin(s\theta_2) \\ &- Q_3\sin[2(s+1)\theta_2] - Q_4\cos[2(s+1)\theta_2] - Q_3(s+1)\sin(2\theta_2) - Q_4(s+1)\cos(2\theta_2)\Big\} \\ &\equiv \frac{D_2^*}{\| X \|}\frac{T\bar{R_0}^{(s+2)}}{2s(s+2)}\frac{1}{s}. \end{aligned} \tag{3.2.40}$$

Now the coefficients C_k, D_k, F_k, H_k are well-known. Therefore, the Mellin transform of the stress function

$$\begin{aligned} \hat{\Phi}_k(s,\theta) &= 2\{C_k cos(s\theta) - D_k sin(s\theta) + F_k cos((s+2)\theta) \\ &\quad -H_k sin((s+2)\theta)\} - \frac{\hat{T}_k(s+2)}{s^2}, \end{aligned} \tag{3.2.41}$$

is known as well. Finally, the stress components in the Mellin domain can be calculated from

$$\begin{aligned} \hat{\sigma}_{rrk}(s,\theta) &= \frac{1}{\| X \|}\frac{T\bar{R_0}^{(s+2)}}{2s(s+2)}\Big\{2q_k \| X \| - C_k^* 2(s+1)cos(s\theta) + D_k^* 2(s+1)sin(s\theta) \\ &\quad -F_k^* 2(s^2+5s+4)cos((s+2)\theta) + H_k^* 2(s^2+5s+4)sin((s+2)\theta)\Big\} \\ &\equiv \frac{P_{rrk}(s,\theta)}{Q(s)} \end{aligned} \tag{3.2.42}$$

$$\begin{aligned}\hat{\sigma}_{\theta\theta k}(s,\theta) &= \frac{1}{\parallel X \parallel}\frac{T\bar{R_0}^{(s+2)}}{2s(s+2)}(s+1)\Big\{C_k^* 2cos(s\theta) - D_k^* 2sin(s\theta) \\ &\quad + F_k^* 2s\ cos((s+2)\theta) - H_k^* 2s\ sin((s+2)\theta) - 2q_k \parallel X \parallel \Big\} \\ &\equiv \frac{P_{\theta\theta k}(s,\theta)}{Q(s)} \qquad (3.2.43)\end{aligned}$$

$$\begin{aligned}\hat{\sigma}_{r\theta k}(s,\theta) &= -\frac{1}{\parallel X \parallel}\frac{T\bar{R_0}^{(s+2)}}{2s(s+2)}2(s+1)\Big\{C_k^* sin(s\theta) + D_k^* cos(s\theta) \\ &\quad + F_k^*(s+2)sin((s+2)\theta) + H_k^*(s+2)cos((s+2)\theta)\Big\} \\ &\equiv \frac{P_{r\theta k}(s,\theta)}{Q(s)} \qquad (3.2.44)\end{aligned}$$

where

$$\begin{aligned}F_1^* &= Q_1 \\ H_1^* &= Q_2 \\ F_2^* &= Q_3 \\ H_2^* &= Q_4\end{aligned}$$

$$\begin{aligned}C_1^* &= q_1 \parallel X \parallel \cos(s\theta_1) + F_1^* \cos[2(s+1)\theta_1] - H_1^* \sin[2(s+1)\theta_1] \\ &\quad -F_1^*(s+1)\cos(2\theta_1) + H_1^*(s+1)\sin(2\theta_1)\end{aligned}$$

$$\begin{aligned}D_1^* &= -q_1 \parallel X \parallel \sin(s\theta_1) - F_1^* \sin[2(s+1)\theta_1] - H_1^* \cos[2(s+1)\theta_1] \\ &\quad -F_1^*(s+1)\sin(2\theta_1) - H_1^*(s+1)\cos(2\theta_1)\end{aligned}$$

$$\begin{aligned}C_2^* &= q_2 \parallel X \parallel \cos(s\theta_2) + F_2^* \cos[2(s+1)\theta_2] - H_2^* \sin[2(s+1)\theta_2] \\ &\quad -F_2^*(s+1)\cos(2\theta_2) + H_2^*(s+1)\sin(2\theta_2)\end{aligned}$$

$$\begin{aligned}D_2^* &= -q_2 \parallel X \parallel \sin(s\theta_2) - F_2^* \sin[2(s+1)\theta_2] - H_2^* \cos[2(s+1)\theta_2] \\ &\quad -F_2^*(s+1)\sin(2\theta_2) - H_2^*(s+1)\cos(2\theta_2).\end{aligned}$$

In Eqs. (3.2.42 - 3.2.44), Q(s)=$(s+2) \parallel X \parallel$ and $P_{ijk}(s,\theta)$ are the rest terms, i.e.

$$\begin{aligned}P_{ijk}(s,\theta) &= g_{ij}(s)\Big\{A_{1ijk}(s)cos(s\theta) + A_{2ijk}(s)sin(s\theta) + A_{3ijk}(s)cos((s+2)\theta) \\ &\quad + A_{4ijk}(s)sin((s+2)\theta) + A_{5ijk}(s)\Big\} \equiv g_{ij}(s)\mathcal{P}_{\rm ijk}({\rm s},\theta) \qquad (3.2.45)\end{aligned}$$

where

for the component in rr direction,

$$\begin{aligned} g_{rr}(s) &= \frac{T_0 \bar{R}_0^{(s+2)}}{2s}, \\ A_{1rrk} &= -2(s+1)C_k^*, \\ A_{2rrk} &= 2(s+1)D_k^*, \\ A_{3rrk} &= -2(s^2+5s+4)F_k^*, \\ A_{4rrk} &= 2(s^2+5s+4)H_k^*, \\ A_{5rrk} &= 2q_k \parallel X \parallel, \end{aligned}$$

for the component in $\theta\theta$ direction,

$$\begin{aligned} g_{\theta\theta}(s) &= \frac{T_0 \bar{R}_0^{(s+2)}}{2s}(s+1), \\ A_{1\theta\theta k} &= 2C_k^*, \\ A_{2\theta\theta k} &= -2D_k^*, \\ A_{3\theta\theta k} &= 2sF_k^*, \\ A_{4\theta\theta k} &= -2sH_k^*, \\ A_{5\theta\theta k} &= -2q_k \parallel X \parallel, \end{aligned}$$

for the component in $r\theta$ direction,

$$\begin{aligned} g_{r\theta}(s) &= -\frac{T_0 \bar{R}_0^{(s+2)}}{s}(s+1), \\ A_{1r\theta k} &= D_k^*, \\ A_{2r\theta k} &= C_k^*, \\ A_{3r\theta k} &= (s+2)H_k^*, \\ A_{4r\theta k} &= (s+2)F_k^*, \\ A_{5r\theta k} &= 0. \end{aligned}$$

Solution in a Polar Coordinate System

From the definition of the reversion of the Mellin transform, the stresses in a polar coordinate system can be obtained by

$$\sigma_{ijk}(\bar{r},\theta) = \frac{1}{2\pi i}\int_{\gamma-i\infty}^{\gamma+i\infty} \hat{\sigma}_{ijk}(s,\theta)\bar{r}^{-(s+2)}ds \tag{3.2.46}$$

where γ must chosen so that the integration in Eq. (3.2.46) exists. Following the residual principle the stresses can be calculated from

$$\sigma_{ijk}(r,\theta) = \sum_{s_n<\gamma} \mathrm{res}\{\hat{\sigma}_{ijk}(s_n,\theta)\bar{r}^{-(s_n+2)}\}$$

$$
\begin{aligned}
&= \sum_{s_n<\gamma} \frac{1}{(M-1)!} \lim_{s\to s_n} \frac{d^{(M-1)}}{ds^{(M-1)}} \{(s-s_n)^M \hat{\sigma}_{ijk}(s,\theta)\bar{r}^{-(s+2)}\} \\
&= \sum_{s_n<\gamma} \frac{1}{(M-1)!} \lim_{s\to s_n} \frac{d^{(M-1)}}{ds^{(M-1)}} \{(s-s_n)^M \frac{P_{ijk}(s,\theta)}{\parallel X \parallel (s+2)} \bar{r}^{-(s+2)}\}.
\end{aligned} \tag{3.2.47}
$$

where s_n is the M-th order pole of $\hat{\sigma}_{ijk}(s,\theta)$. The definition of the M-th order pole is: if $\lim_{s\to s_n}(s-s_n)^{(M-1)}\hat{\sigma}_{ijk}(s,\theta) \to \infty$ is satisfied, s_n is the M-th order pole of $\hat{\sigma}_{ijk}(s,\theta)$. In this section we are only interested in the regular stress term, which is independent of the distance r. From Eq. (3.2.47) we know that it is the solution according to s=-2 as the first-order pole of $\hat{\sigma}_{ijk}(s,\theta)$.
For s=-2, we always have:

$$
\begin{aligned}
\parallel X \parallel &= 0 \\
C_1^* &= 0 \\
C_2^* &= 0 \\
D_1^* &= 0 \\
D_2^* &= 0 \\
F_1^* &= 0 \\
F_2^* &= 0 \\
H_1^* &= 2m_2(q_1m_1g - q_2m_2)\{\sin[2(\theta_2-\theta_1)] + \sin(2\theta_1) - \sin(2\theta_2)\} \\
H_2^* &= 2m_1g(q_1m_1g - q_2m_2)\{\sin[2(\theta_2-\theta_1)] + \sin(2\theta_1) - \sin(2\theta_2)\}.
\end{aligned}
$$

It can be seen that in general, H_1^* and H_2^* are nonzero for an arbitrary geometry (θ_1, θ_2). However, from Eqs. (3.2.42- 3.2.44) it can be seen that H_1^* and H_2^* always combinate with $\sin[(s+2)\theta]$ or $(s+2)$. Therefore, for s=-2, always $P_{ijk}(s,\theta)$ =0, but $\frac{\partial P_{ijk}(s,\theta)}{\partial s}|_{s=-2} \neq 0$. The condition of s=-2 as the first-order pole of $\hat{\sigma}_{ijk}(s,\theta)$ is that $\parallel X \parallel |_{s=-2} = 0$, but $\frac{\partial \|X\|}{\partial s}|_{s=-2} \neq 0$.
Finally, from Eq. (3.2.47) the regular stress term can be calculated by

$$
\sigma_{ijk0}(\theta) = \frac{\frac{\partial P_{ijk}(s,\theta)}{\partial s}|_{s=-2}}{\frac{\partial \|X\|}{\partial s}|_{s=-2}}. \tag{3.2.48}
$$

After simplifying the equations, we have

$$
\sigma_{rrk0}(\theta) = 2\{A_{k0}\theta + B_{k0} - C_{k0}\sin(2\theta) - D_{k0}\cos(2\theta)\} \tag{3.2.49}
$$

$$
\sigma_{\theta\theta k0}(\theta) = 2\{A_{k0}\theta + B_{k0} + C_{k0}\sin(2\theta) + D_{k0}\cos(2\theta)\} \tag{3.2.50}
$$

$$
\sigma_{r\theta k0}(\theta) = -2\{\frac{1}{2}A_{k0} + C_{k0}\cos(2\theta) - D_{k0}\sin(2\theta)\} \tag{3.2.51}
$$

where the coefficients $A_{k0}, B_{k0}, C_{k0}, D_{k0}$ can be determined analytically from Eq. (3.2.48) and the corresponding equations.
The regular stress term can be rewritten as

$$\sigma_{ijk0}(\theta) = \sigma_0 f_{ijk0}(\theta) \tag{3.2.52}$$

with

$$\sigma_0 = 2(B_{10} + D_{10}) = 2(B_{20} + D_{20}) \tag{3.2.53}$$

and

$$f_{rrk0}(\theta) = \{A_{k0}\theta + B_{k0} - C_{k0}\sin(2\theta) - D_{k0}\cos(2\theta)\}/(B_{10} + D_{10}) \tag{3.2.54}$$

$$f_{\theta\theta k0}(\theta) = \{A_{k0}\theta + B_{k0} + C_{k0}\sin(2\theta) + D_{k0}\cos(2\theta)\}/(B_{10} + D_{10}) \tag{3.2.55}$$

$$f_{r\theta k0}(\theta) = -\{\frac{1}{2}A_{k0} + C_{k0}\cos(2\theta) - D_{k0}\sin(2\theta)\}/(B_{10} + D_{10}) \tag{3.2.56}$$

where always $f_{\theta\theta 10}(0) = f_{\theta\theta 20}(0) = 1$.
In the next sections explicit relations to calculate the coefficients $A_{k0}, B_{k0}, C_{k0}, D_{k0}$ will be given for an arbitrary joint geometry (θ_1, θ_2), and for several special geometries.

3.2.1 Joint with an Arbitrary Geometry θ_1, θ_2

The coefficients $A_{k0}, B_{k0}, C_{k0}, D_{k0}$ can be calculated from

$$A_{k0} = \frac{A^*_{k0}}{Z}, \qquad B_{k0} = \frac{B^*_{k0}}{Z}, \qquad C_{k0} = \frac{C^*_{k0}}{Z}, \qquad D_{k0} = \frac{D^*_{k0}}{Z},$$

with

$$\begin{aligned} Z &= \alpha^2\Big[F_{4s} - (\theta_1 + \theta_2)(F_{12} + F_{21}) - 3F_{4c} + 2F_{1p} - 1\Big] \\ &\quad +2\alpha\beta\Big[(F_{21} - \sin(2\theta_2))\theta_2 + [F_{12} - \sin(2\theta_1)]\theta_1 + 2F_{4c} - 2F_{1p} + 2\Big] \\ &\quad +2\alpha\Big[F_{21}\theta_2 - F_{12}\theta_1 + F_{1n}\Big] \\ &\quad +2\beta\Big[(F_{12} - \sin(2\theta_1))\theta_1 - (F_{21} - \sin(2\theta_2))\theta_2\Big] \\ &\quad +\Big[-F_{4s} + (\theta_1 - \theta_2)(F_{21} - F_{12}) - F_{4c} + 1\Big] \end{aligned} \tag{3.2.57}$$

$$A^*_{10} = \frac{1}{2}(\alpha + 1)\bar{q}\Big\{[F_{21} - \sin(2\theta_2)] - [F_{12} - \sin(2\theta_1)]\Big\} \tag{3.2.58}$$

$$B^*_{10} = \frac{1}{4}\bar{q}\Big\{\alpha[F_{4s} - 2(F_{21} - F_{12} + \sin(2\theta_1))\theta_1 - 2\sin(2\theta_2)\theta_2 + F_{4c} - 2F_{1p} - F_{1n} + 3] + [F_{4s} - 2(F_{21} - F_{12} + \sin(2\theta_1))\theta_1 + 2\sin(2\theta_2)\theta_2 + F_{4c} + F_{1n} - 1]\Big\} \quad (3.2.59)$$

$$C^*_{10} = \frac{1}{4}\bar{q}\Big\{\alpha[2F_{4s}(\theta_1 + \theta_2) + (F_{21} - \sin(2\theta_2)) + 3(F_{12} - \sin(2\theta_1))] + [2F_{4s}(\theta_1 - \theta_2) + (F_{21} - \sin(2\theta_2)) - (F_{12} - \sin(2\theta_1))]\Big\} \quad (3.2.60)$$

$$D^*_{10} = -\frac{1}{4}\bar{q}\Big\{\alpha[F_{4s} - 2F_{21}(\theta_1 + \theta_2) - 3F_{4c} + 2F_{1p} - F_{1n} - 1] + [F_{4s} + 2F_{21}(\theta_2 - \theta_1) + F_{4c} + F_{1n} - 1]\Big\} \quad (3.2.61)$$

$$A^*_{20} = -\frac{1}{2}(\alpha - 1)\bar{q}\Big\{[F_{21} - \sin(2\theta_2)] - [F_{12} - \sin(2\theta_1)]\Big\} \quad (3.2.62)$$

$$B^*_{20} = \frac{1}{4}\bar{q}\Big\{\alpha[F_{4s} + 2(F_{21} - F_{12} + \sin(2\theta_2))\theta_2 - 2\sin(2\theta_1)\theta_1 + F_{4c} - 2F_{1p} - F_{1n} + 3] + [-F_{4s} - 2(F_{21} - F_{12} - \sin(2\theta_2))\theta_2 - 2\sin(2\theta_1)\theta_1 - F_{4c} + F_{1n} + 1]\Big\} \quad (3.2.63)$$

$$C^*_{20} = \frac{1}{4}\bar{q}\Big\{\alpha[2F_{4s}(\theta_1 + \theta_2) + (F_{12} - \sin(2\theta_1)) + 3(F_{21} - \sin(2\theta_2))] + [2F_{4s}(\theta_1 - \theta_2) + (F_{21} - \sin(2\theta_2)) - (F_{12} - \sin(2\theta_1))]\Big\} \quad (3.2.64)$$

$$D^*_{20} = -\frac{1}{4}\bar{q}\Big\{\alpha[F_{4s} - 2F_{12}(\theta_1 + \theta_2) - 3F_{4c} + 2F_{1p} - F_{1n} - 1] + [-F_{4s} + 2F_{12}(\theta_2 - \theta_1) - F_{4c} + F_{1n} + 1]\Big\} \quad (3.2.65)$$

where the quantities $F_{1p}, F_{1n}, F_{12}, F_{21}, F_{4c}, F_{4s}$ are a function of θ_1, θ_2 and s_n, which are given in the Section 3.1 (see Eqs.(3.1.45) - (3.1.56)). The quantity $\bar{q}$ is defined as

$$\bar{q} = T_0 \frac{\alpha_1 - \alpha_2}{\frac{1}{E_1} + \frac{1}{E_2}} = T_0(\alpha_1 - \alpha_2)E_2\frac{\alpha + 1}{2} \quad (3.2.66)$$

for plane stress and

$$\bar{q} = T_0 \frac{(1+\nu_1)\alpha_1 - (1+\nu_2)\alpha_2}{\frac{1-\nu_1^2}{E_1} + \frac{1-\nu_2^2}{E_2}} = T_0\Big[(1+\nu_1)\alpha_1 - (1+\nu_2)\alpha_2\Big]\frac{E_2}{1-\nu_2^2} \quad \frac{\alpha+1}{2} \quad (3.2.67)$$

for plane strain, where α_1 and α_2 are the thermal expansion coefficients in materials 1 and 2, and α and β are the Dundurs parameters.
It should be mentioned that the regular stress term can be determined analytically, whereas the K-factors of the singular terms have to be determined by a numerical method and they are dependent on the overall geometry and the loading conditions.

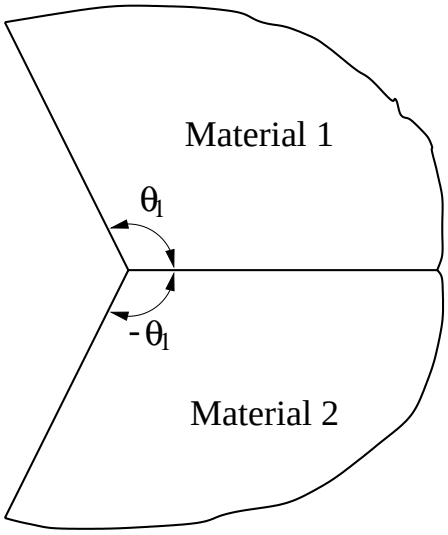

Figure 3.2: Joint with $\theta_1 = -\theta_2$.

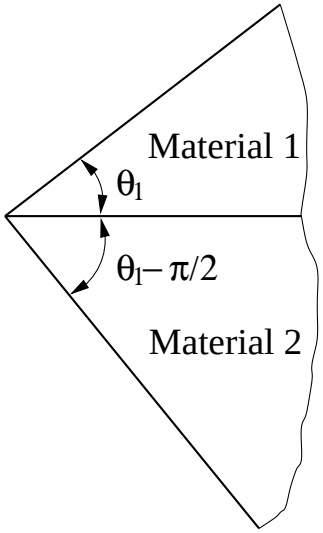

Figure 3.3: Joint with $\theta_1 - \theta_2 = 90°$.

3.2.2 Joint with $\theta_1 = -\theta_2$

For this joint geometry (see Fig. 3.2) the quantities $A^*_{k0}, B^*_{k0}, C^*_{k0}, D^*_{k0}$, and Z can be simplified as

$$\begin{aligned} Z &= -\alpha^2(\cos(2\theta_1)-1)^2 + 2\alpha\beta(\cos(2\theta_1)-1)[\sin(2\theta_1)\theta_1 + \cos(2\theta_1) - 1] \\ &\quad + \sin^2(2\theta_1) - 2\sin(2\theta_1)\cos(2\theta_1)\theta_1 \end{aligned} \tag{3.2.68}$$

$$A^*_{10} = -\frac{1}{2}\bar{q}(\alpha+1)\sin(2\theta_1)[\cos(2\theta_1)-1] \tag{3.2.69}$$

$$\begin{aligned} B^*_{10} &= \frac{1}{4}\bar{q}\Big\{\alpha[\cos(2\theta_1)-1][2\sin(2\theta_1)\theta_1 + (\cos(2\theta_1)-1)] \\ &+ \sin(2\theta_1)[2\cos(2\theta_1)\theta_1 - \sin(2\theta_1)]\Big\} \end{aligned} \tag{3.2.70}$$

$$C^*_{10} = \frac{1}{4}\bar{q}\sin(2\theta_1)\Big\{\alpha[\cos(2\theta_1)-1] - \cos(2\theta_1) + 1 - 2\sin(2\theta_1)\theta_1\Big\} \tag{3.2.71}$$

$$D^*_{10} = -\frac{1}{4}\bar{q}\Big\{-\alpha[\cos(2\theta_1)-1]^2 + 2\sin(2\theta_1)\cos(2\theta_1)\theta_1 + \cos^2(2\theta_1) - 1\Big\} \tag{3.2.72}$$

$$A^*_{20} = \frac{1}{2}\bar{q}(\alpha-1)\sin(2\theta_1)[\cos(2\theta_1)-1]. \tag{3.2.73}$$

$$\begin{aligned} B^*_{20} &= \frac{1}{4}\bar{q}\Big\{\alpha[\cos(2\theta_1)-1][2\sin(2\theta_1)\theta_1 + (\cos(2\theta_1)-1)] \\ &- \sin(2\theta_1)[2\cos(2\theta_1)\theta_1 - \sin(2\theta_1)]\Big\} \end{aligned} \tag{3.2.74}$$

$$C^*_{20} = -\frac{1}{4}\bar{q}\sin(2\theta_1)\Big\{\alpha[\cos(2\theta_1)-1]+\cos(2\theta_1)-1+2\sin(2\theta_1)\theta_1\Big\} \tag{3.2.75}$$

$$D^*_{20} = \frac{1}{4}\bar{q}\Big\{\alpha[\cos(2\theta_1)-1]^2+2\sin(2\theta_1)\cos(2\theta_1)\theta_1+\cos^2(2\theta_1)-1\Big\}. \tag{3.2.76}$$

3.2.3 Joint with $\theta_1 - \theta_2 = \pi/2$

For this joint geometry (see Fig. 3.3) there is:

$$\begin{aligned} Z &= \alpha^2[\cos(2\theta_1)\sin(2\theta_1)(2\theta_1-\pi/2)-2\sin^2(2\theta_1)+1] \\ &\quad +\alpha\beta\sin(2\theta_1)[2\sin(2\theta_1)-\cos(2\theta_1)(2\theta_1-\pi/2)-\pi/2] \\ &\quad +\alpha\cos(2\theta_1)[\sin(2\theta_1)\pi/2-2] \\ &\quad -\beta\sin(2\theta_1)[\cos(2\theta_1)\pi/2+(2\theta_1-\pi/2)]-1 \end{aligned} \tag{3.2.77}$$

$$A^*_{10} = \frac{1}{2}(\alpha+1)\sin(2\theta_1)\bar{q} \tag{3.2.78}$$

$$\begin{aligned} B^*_{10} &= -\frac{1}{4}\bar{q}\Big\{\alpha[-\cos(2\theta_1)+\sin(2\theta_1)\pi/2-1] \\ &\quad +\cos(2\theta_1)+\sin(2\theta_1)(2\theta_1-\pi/2)+1\Big\} \end{aligned} \tag{3.2.79}$$

$$\begin{aligned} C^*_{10} &= -\frac{1}{4}\bar{q}\Big\{\alpha\sin(2\theta_1)[2\cos(2\theta_1)+\sin(2\theta_1)(2\theta_1-\pi/2)+1] \\ &\quad +\sin(2\theta_1)[\sin(2\theta_1)\pi/2-1]\Big\} \end{aligned} \tag{3.2.80}$$

$$\begin{aligned} D^*_{10} &= -\frac{1}{4}\bar{q}\Big\{\alpha[\cos(2\theta_1)+1+\cos(2\theta_1)\sin(2\theta_1)(2\theta_1-\pi/2)-2\sin^2(2\theta_1)] \\ &\quad +\sin(2\theta_1)\cos(2\theta_1)\pi/2-\cos(2\theta_1)-1\Big\} \end{aligned} \tag{3.2.81}$$

$$A^*_{20} = \frac{1}{2}(1-\alpha)\sin(2\theta_1)\bar{q}. \tag{3.2.82}$$

$$\begin{aligned} B^*_{20} &= -\frac{1}{4}\bar{q}\Big\{\alpha[\cos(2\theta_1)+\sin(2\theta_1)\pi/2-1] \\ &\quad +\cos(2\theta_1)+\sin(2\theta_1)(2\theta_1-\pi/2)-1\Big\} \end{aligned} \tag{3.2.83}$$

$$C^*_{20} = -\frac{1}{4}\bar{q}\Big\{\alpha\sin(2\theta_1)[2\cos(2\theta_1)+\sin(2\theta_1)(2\theta_1-\pi/2)-1] + \sin(2\theta_1)[\sin(2\theta_1)\pi/2-1]\Big\} \tag{3.2.84}$$

$$D^*_{20} = -\frac{1}{4}\bar{q}\Big\{\alpha[-\cos(2\theta_1)+1+\cos(2\theta_1)\sin(2\theta_1)(2\theta_1-\pi/2)-2\sin^2(2\theta_1)] + \sin(2\theta_1)\cos(2\theta_1)\pi/2-\cos(2\theta_1)+1\Big\}. \tag{3.2.85}$$

3.2.4 Joint with $\theta_1 - \theta_2 = \pi$

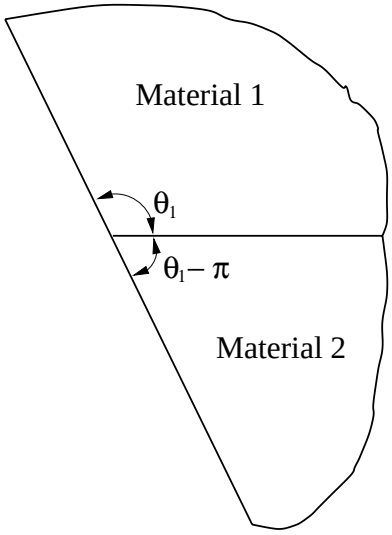

Figure 3.4: Joint with $\theta_1 - \theta_2 = 180°$.

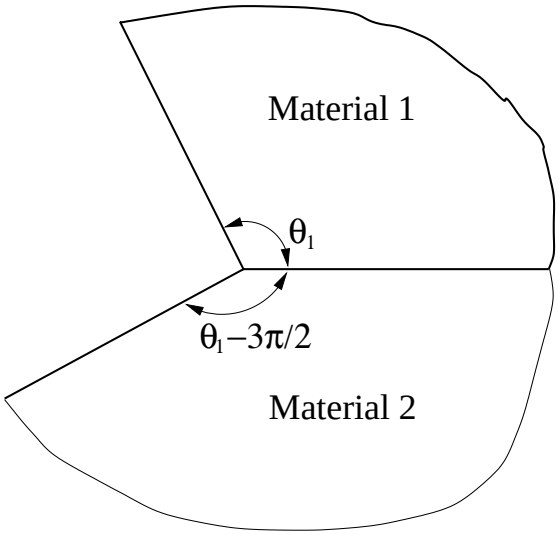

Figure 3.5: Joint with $\theta_1 - \theta_2 = 270°$.

For a joint with $\theta_1 - \theta_2 = \pi$ (see Fig. 3.4), the following relations are valid,

$$A_{10} = A_{20} = 0 \tag{3.2.86}$$

$$B_{10} = -\frac{1}{4}\frac{\bar{q}}{\beta[\cos(2\theta_1)-1]-\alpha\cos(2\theta_1)} \tag{3.2.87}$$

$$C_{10} = -\sin(2\theta_1)B_{10} \tag{3.2.88}$$

$$D_{10} = -\cos(2\theta_1)B_{10} \tag{3.2.89}$$

$$\begin{aligned} B_{20} &= B_{10} \\ C_{20} &= C_{10} \\ D_{20} &= D_{10}. \end{aligned} \tag{3.2.90}$$

The regular stresses in polar coordinates are

$$\begin{aligned} \sigma_{rr0}(\theta) &= 4B_{10}\cos^2(\theta_1-\theta) \\ \sigma_{\theta\theta0}(\theta) &= 4B_{10}\sin^2(\theta_1-\theta) \\ \tau_{r\theta0}(\theta) &= 4B_{10}\sin(\theta_1-\theta)\cos(\theta_1-\theta). \end{aligned} \tag{3.2.91}$$

By using the transformation of the stress component from polar to Cartesian coordinates

$$\sigma_x(x,y) = \sigma_r(r,\theta)\cos^2(\theta) + \sigma_\theta(r,\theta)\sin^2(\theta) - 2\tau_{r\theta}(r,\theta)\sin(\theta)\cos(\theta) \tag{3.2.92}$$

$$\sigma_y(x,y) = \sigma_r(r,\theta)\sin^2(\theta) + \sigma_\theta(r,\theta)\cos^2(\theta) + 2\tau_{r\theta}(r,\theta)\sin(\theta)\cos(\theta) \tag{3.2.93}$$

$$\tau_{xy}(x,y) = [\sigma_r(r,\theta) - \sigma_\theta(r,\theta)]\sin(\theta)\cos(\theta) + \tau_{r\theta}(r,\theta)[\cos^2(\theta) - \sin^2(\theta)] \tag{3.2.94}$$

the regular stresses in Cartesian coordinates can be obtained as

$$\begin{aligned} \sigma_{xx0} &= 4B_{10}\cos^2(\theta_1) \\ \sigma_{yy0} &= 4B_{10}\sin^2(\theta_1) \\ \tau_{xy0} &= 4B_{10}\sin(\theta_1)\cos(\theta_1). \end{aligned} \tag{3.2.95}$$

It can be seen that in Cartesian coordinates the regular stresses are independent of the coordinates, i.e. the regular stress term in Cartesian coordinates is a constant.

3.2.5 Joint with $\theta_1 - \theta_2 = 3\pi/2$

The joint geometry is shown in Fig. 3.5. The simplified relations are:

$$\begin{aligned} Z = {} & \alpha^2[\cos(2\theta_1)\sin(2\theta_1)(2\theta_1 - 3\pi/2) - 2\sin^2(2\theta_1) + 1] \\ & + \alpha\beta\sin(2\theta_1)[2\sin(2\theta_1) - \cos(2\theta_1)(2\theta_1 - 3\pi/2) - 3\pi/2] \\ & + \alpha\cos(2\theta_1)[\sin(2\theta_1)3\pi/2 - 2] \\ & - \beta\sin(2\theta_1)[\cos(2\theta_1)3\pi/2 + (2\theta_1 - 3\pi/2)] - 1 \end{aligned} \tag{3.2.96}$$

$$A^*_{10} = \frac{1}{2}(\alpha+1)\sin(2\theta_1)\bar{q} \tag{3.2.97}$$

$$B^*_{10} = -\frac{1}{4}\bar{q}\Big\{\alpha[-\cos(2\theta_1)+\sin(2\theta_1)3\pi/2-1] + \cos(2\theta_1)+\sin(2\theta_1)(2\theta_1-3\pi/2)+1\Big\} \quad (3.2.98)$$

$$C^*_{10} = -\frac{1}{4}\bar{q}\Big\{\alpha\sin(2\theta_1)[2\cos(2\theta_1)+\sin(2\theta_1)(2\theta_1-3\pi/2)+1] + \sin(2\theta_1)[\sin(2\theta_1)3\pi/2-1]\Big\} \quad (3.2.99)$$

$$D^*_{10} = -\frac{1}{4}\bar{q}\Big\{\alpha[\cos(2\theta_1)+1+\cos(2\theta_1)\sin(2\theta_1)(2\theta_1-3\pi/2)-2\sin^2(2\theta_1)] + \sin(2\theta_1)\cos(2\theta_1)3\pi/2-\cos(2\theta_1)-1\Big\} \quad (3.2.100)$$

$$A^*_{20} = \frac{1}{2}(1-\alpha)\sin(2\theta_1)\bar{q}. \quad (3.2.101)$$

$$B^*_{20} = -\frac{1}{4}\bar{q}\Big\{\alpha[\cos(2\theta_1)+\sin(2\theta_1)3\pi/2-1] + \cos(2\theta_1)+\sin(2\theta_1)(2\theta_1-3\pi/2)-1\Big\} \quad (3.2.102)$$

$$C^*_{20} = -\frac{1}{4}\bar{q}\Big\{\alpha\sin(2\theta_1)[2\cos(2\theta_1)+\sin(2\theta_1)(2\theta_1-3\pi/2)-1] + \sin(2\theta_1)[\sin(2\theta_1)3\pi/2-1]\Big\} \quad (3.2.103)$$

$$D^*_{20} = -\frac{1}{4}\bar{q}\Big\{\alpha[-\cos(2\theta_1)+1+\cos(2\theta_1)\sin(2\theta_1)(2\theta_1-3\pi/2)-2\sin^2(2\theta_1)] + \sin(2\theta_1)\cos(2\theta_1)3\pi/2-\cos(2\theta_1)+1\Big\}. \quad (3.2.104)$$

3.2.6 Joint with $\theta_1 - \theta_2 = 2\pi$

This is the case of a joint with a crack (see Fig. 3.6). It can be shown that the relations to calculate the regular stresses are the same as those of a joint with $\theta_1 - \theta_2 = \pi$ (see Eqs. (3.2.86) to (3.2.95)), except for $\theta_1 = 180°$.

3.2.7 Joint with $\theta_1 = \pi$ and θ_2 being Arbitrary

For this joint geometry (see Fig. 3.7) the regular stress term is very simple. The coefficients $A_{k0}, B_{k0}, C_{k0}, D_{k0}$ take the following values:

$$A_{10} = C_{10} = A_{20} = B_{20} = C_{20} = D_{20} = 0, \quad (3.2.105)$$

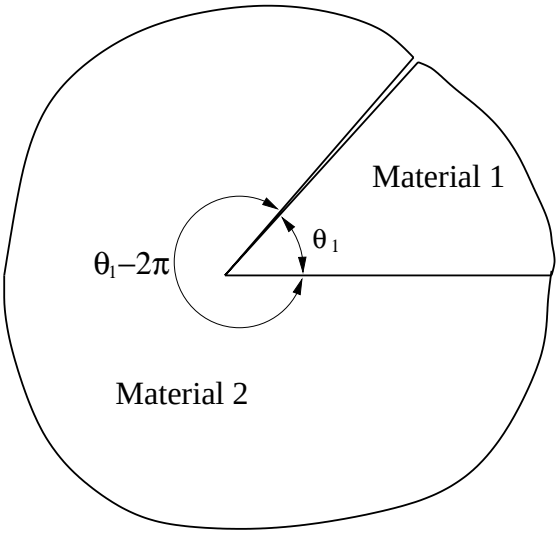

Figure 3.6: Joint with $\theta_1 - \theta_2 = 360°$.

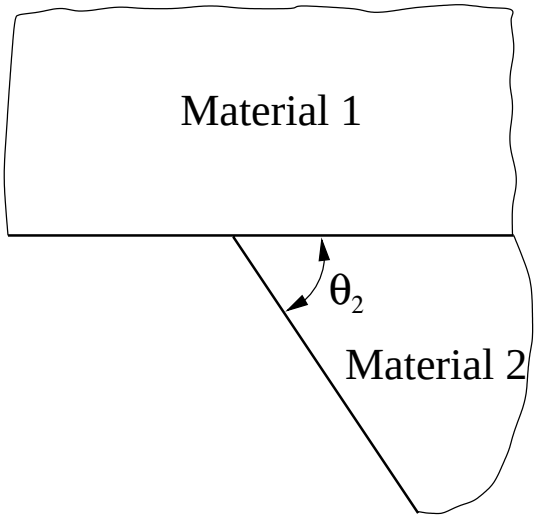

Figure 3.7: Joint with $\theta_1 = 180°$ and θ_2 being arbitrary.

$$B_{10} = -D_{10} \tag{3.2.106}$$

and

$$D_{10} = \frac{1}{2} \frac{\bar{q}}{1-\alpha} \tag{3.2.107}$$

where $\theta_2 \neq -\pi$. The regular stress term in polar coordinates is

$$\begin{aligned} \sigma_{rrk0} &= -4D_{k0}\cos^2(\theta) \\ \sigma_{\theta\theta k0} &= -4D_{k0}\sin^2(\theta) \\ \sigma_{r\theta k0} &= 4D_{k0}\sin(\theta)\cos(\theta), \end{aligned} \tag{3.2.108}$$

and in Cartesian coordinates takes

$$\begin{aligned} \sigma_{xx10} &= -4D_{10} = \frac{2\bar{q}}{\alpha - 1} \\ \sigma_{xx20} &= 0 \\ \sigma_{yy10} &= \sigma_{yy20} = \sigma_{xy10} = \sigma_{xy20} = 0, \end{aligned} \tag{3.2.109}$$

which is independent of the coordinates, i.e. the regular stress term in Cartesian coordinates is a constant.

3.2.8 Joint with $\theta_1 = -\theta_2 = \pi$

This is a special case covered by Section 3.2.2. However, the equations in Section 3.2.2 for calculating the coefficients can not be used directly, because the denominator is zero

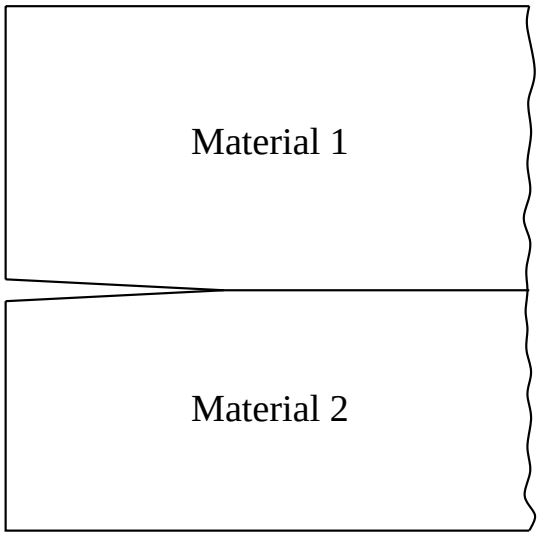

Figure 3.8: Joint with an interface crack.

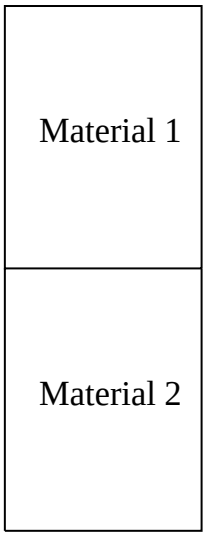

Figure 3.9: A quarter planes joint.

for $\theta_1 = 180°$. A separate treatment has to be applied (see [85]). For this special case (see Fig. 3.8), i.e. a joint with an interface crack, the coefficients $A_{k0}, B_{k0}, C_{k0}, D_{k0}$ are

$$A_{10} = C_{10} = A_{20} = C_{20} = 0 \tag{3.2.110}$$

$$\begin{aligned} B_{10} &= -\frac{\bar{q}}{4} \\ D_{10} &= \frac{\bar{q}}{4} \\ B_{20} &= \frac{\bar{q}}{4} \\ D_{20} &= -\frac{\bar{q}}{4}. \end{aligned} \tag{3.2.111}$$

The regular stress term in a polar coordinate system is

$$\begin{aligned} \sigma_{rrk0} &= -2D_{k0}[\cos(2\theta) + 1] \\ \sigma_{\theta\theta k0} &= 2D_{k0}[\cos(2\theta) - 1] \\ \sigma_{r\theta k0} &= 2D_{k0}\sin(2\theta). \end{aligned} \tag{3.2.112}$$

and in Cartesian coordinates reads

$$\begin{aligned} \sigma_{xx10} &= -4D_{10} = -\bar{q} \\ \sigma_{xx20} &= -4D_{20} = \bar{q} \\ \sigma_{yy10} &= \sigma_{yy20} = \sigma_{xy10} = \sigma_{xy20} = 0. \end{aligned} \tag{3.2.113}$$

From Eq. (3.2.113) it can be seen that for a joint with an interface crack under thermal loading the regular stress term, which is the called T-stress term, can be calculated analytically!

3.2.9 Joint with $\theta_1 = -\theta_2 = \pi/2$

The quarter planes joint (see Fig. 3.9) is a special case covered by Section 3.2.2 or 3.2.4, which is often used in practice. For this joint

$$\begin{aligned} A_{10} &= A_{20} = C_{10} = C_{20} = 0 \\ B_{10} &= B_{20} = D_{10} = D_{20} = \frac{\bar{q}}{4(2\beta - \alpha)}. \end{aligned} \tag{3.2.114}$$

Following the definition of the Dundurs parameters (see Eq. (3.1.86)), the coefficients can be calculated from

$$B_{10} = \frac{1}{4} \frac{T\,(\alpha_1 - \alpha_2)}{\frac{\nu_1}{E_1} - \frac{\nu_2}{E_2}} \tag{3.2.115}$$

for plane stress and

$$B_{10} = \frac{1}{4} \frac{T\,[\alpha_1(1+\nu_1) - \alpha_2(1+\nu_2)]}{\frac{\nu_1(1+\nu_1)}{E_1} - \frac{\nu_2(1+\nu_2)}{E_2}} \tag{3.2.116}$$

for plane strain. The regular stresses in Cartesian coordinates are

$$\begin{aligned} \sigma_{xx0} &= 0 \\ \sigma_{yy0} &= 4B_{10} \\ \tau_{xy0} &= 0. \end{aligned} \tag{3.2.117}$$

This result was also obtained by Mizuno et al. [62].

3.3 Determination of the Regular Stress Term for a Joint under Remote Mechanical Load

For the same joint geometry and material combination, the regular stress term depends strongly on the type of loading. In Section 3.2 the regular stress term for a joint with free edges under thermal loading has been given in an explicit form for an arbitrary geometry (θ_1, θ_2) and for some special geometries. In general, the regular stress term is nonzero for thermal loading. Regarding a joint under remote mechanical loading (see Fig. 3.10), however, the regular stress term is zero for most joint geometries and material combinations. Only for some geometries and material combinations is the regular stress term nonzero. In this section the method and the explicit form to calculate the nonzero regular stress term will be given for a joint with an arbitrary geometry (θ_1, θ_2) under remote mechanical loading and for several special geometries. In this case, the Airy's stress function is used.

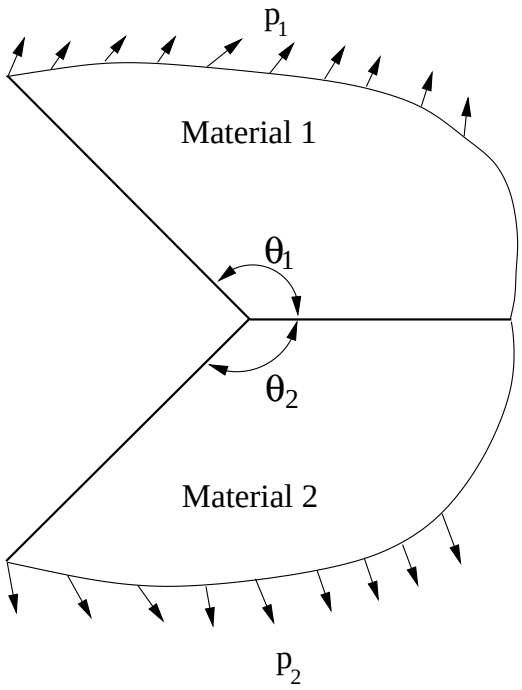

Figure 3.10: A joint under remote mechanical loading.

For the determination of the regular stress term, the following stress function

$$\Phi_0(r,\theta) = r^2[\mathcal{A}_{\mathrm{k}0}\theta + \mathcal{B}_{\mathrm{k}0} + \mathcal{C}_{\mathrm{k}0}\sin(2\theta) + \mathcal{D}_{\mathrm{k}0}\cos(2\theta)] \tag{3.3.1}$$

can be used, where the coefficients $\mathcal{A}_{\mathrm{k}0}, \mathcal{B}_{\mathrm{k}0}, \mathcal{C}_{\mathrm{k}0}, \mathcal{D}_{\mathrm{k}0}$ are real unknowns. The stresses in polar coordinates are

$$\sigma_{rrk0}(r,\theta) = 2[\mathcal{A}_{\mathrm{k}0}\theta + \mathcal{B}_{\mathrm{k}0} - \mathcal{C}_{\mathrm{k}0}\sin(2\theta) - \mathcal{D}_{\mathrm{k}0}\cos(2\theta)] \tag{3.3.2}$$

$$\sigma_{\theta\theta k0}(r,\theta) = 2[\mathcal{A}_{\mathrm{k}0}\theta + \mathcal{B}_{\mathrm{k}0} + \mathcal{C}_{\mathrm{k}0}\sin(2\theta) + \mathcal{D}_{\mathrm{k}0}\cos(2\theta)] \tag{3.3.3}$$

$$\sigma_{r\theta k0}(r,\theta) = -2[\frac{1}{2}\mathcal{A}_{\mathrm{k}0} + \mathcal{C}_{\mathrm{k}0}\cos(2\theta) - \mathcal{D}_{\mathrm{k}0}\sin(2\theta)]. \tag{3.3.4}$$

From the relations between the stresses, strains, and displacements, the following can be obtained (see [86] and [124]):

$$\begin{aligned} u_{k0}(r,\theta) &= \frac{2r}{E_k}[\mathcal{A}_{\mathrm{k}0}\theta(1-\nu_{\mathrm{k}}) + \mathcal{B}_{\mathrm{k}0}(1-\nu_{\mathrm{k}}) \\ &\quad -\mathcal{C}_{\mathrm{k}0}(1+\nu_{\mathrm{k}})\sin(2\theta) - \mathcal{D}_{\mathrm{k}0}(1+\nu_{\mathrm{k}})\cos(2\theta)] \end{aligned} \tag{3.3.5}$$

$$\begin{aligned} v_{k0}(r,\theta) &= \frac{2r}{E_k}[-\mathcal{C}_{\mathrm{k}0}(1+\nu_{\mathrm{k}})\cos(2\theta) + \mathcal{D}_{\mathrm{k}0}(1+\nu_{\mathrm{k}})\sin(2\theta)] \\ &\quad +\mathcal{F}_{\mathrm{k}0}\mathrm{r} - \frac{4\mathcal{A}_{\mathrm{k}0}}{\mathrm{E_k}}\mathrm{rln(r)} \end{aligned} \tag{3.3.6}$$

where, to avoid the rigid body displacements, $u = 0$ and $v = 0$ at r=0 is used, and F_{k0} are real integration constants (see [86]). To determine the coefficients $\mathcal{A}_{\mathrm{k0}}, \mathcal{B}_{\mathrm{k0}}, \mathcal{C}_{\mathrm{k0}}, \mathcal{D}_{\mathrm{k0}}$, and $\mathcal{F}_{\mathrm{k0}}$, boundary conditions have to be used. For a joint with free edges, the regular stress term should also satisfy Eqs. (3.1.18) and (3.1.19), which lead to

$$2\mu[\mathcal{B}_{10}(1-\nu_1) - \mathcal{D}_{10}(1+\nu_1)] - 2[\mathcal{B}_{20}(1-\nu_2) - \mathcal{D}_{20}(1+\nu_2)] = 0, \tag{3.3.7}$$

$$2\mu[-\mathcal{C}_{10}(1+\nu_1)] - 2[-\mathcal{C}_{20}(1+\nu_2)] + \mathrm{E}_2(\mathcal{F}_{10} - \mathcal{F}_{20}) = 0, \tag{3.3.8}$$

$$\mu\mathcal{A}_{10} - \mathcal{A}_{20} = 0, \tag{3.3.9}$$

$$(\mathcal{B}_{10} + \mathcal{D}_{10}) - (\mathcal{B}_{20} + \mathcal{D}_{20}) = 0, \tag{3.3.10}$$

$$(\mathcal{A}_{10} + 2\mathcal{C}_{10}) - (\mathcal{A}_{20} + 2\mathcal{C}_{20}) = 0, \tag{3.3.11}$$

$$\mathcal{A}_{10}\theta_1 + \mathcal{B}_{10} + \mathcal{C}_{10}\sin(2\theta_1) + \mathcal{D}_{10}\cos(2\theta_1) = 0, \tag{3.3.12}$$

$$\mathcal{A}_{20}\theta_2 + \mathcal{B}_{20} + \mathcal{C}_{20}\sin(2\theta_2) + \mathcal{D}_{20}\cos(2\theta_2) = 0, \tag{3.3.13}$$

$$\mathcal{A}_{10} + 2\mathcal{C}_{10}\cos(2\theta_1) - 2\mathcal{D}_{10}\sin(2\theta_1) = 0, \tag{3.3.14}$$

$$\mathcal{A}_{20} + 2\mathcal{C}_{20}\cos(2\theta_2) - 2\mathcal{D}_{20}\sin(2\theta_2) = 0. \tag{3.3.15}$$

From Eqs. (3.3.7, 3.3.9 - 3.3.15) the coefficients $\mathcal{A}_{\mathrm{k0}}, \mathcal{B}_{\mathrm{k0}}, \mathcal{C}_{\mathrm{k0}}, \mathcal{D}_{\mathrm{k0}}$ can be determined, and then from Eqs. (3.3.8) the difference of the coefficients $\mathcal{F}_{10}$ and $\mathcal{F}_{20}$ is known. For the regular stress term only the coefficients $\mathcal{A}_{\mathrm{k0}}, \mathcal{B}_{\mathrm{k0}}, \mathcal{C}_{\mathrm{k0}}, \mathcal{D}_{\mathrm{k0}}$ are of interest. Equations (3.3.7, 3.3.9 - 3.3.15) can be rewritten in a matrix form as

$$[A_0]_{8\times 8}\{X_0\}_{8\times 1} = \{0\}_{8\times 1} \tag{3.3.16}$$

where $\{X_0\}_{8\times 1} = \{\mathcal{A}_{10}, \mathcal{B}_{10}, \mathcal{C}_{10}, \mathcal{D}_{10}, \mathcal{A}_{20}, \mathcal{B}_{20}, \mathcal{C}_{20}, \mathcal{D}_{20}\}^{\mathrm{t}}$, and $[A_0]_{8\times 8}$ is its coefficient matrix, which includes the material properties (E_k, ν_k, k=1,2 for materials 1 and 2) and the geometry angles (θ_1, θ_2). Equation (3.3.16) has a nonzero solution, if and only if

$$\mathrm{Det}([A_0]_{8\times 8}) = 0 \tag{3.3.17}$$

is satisfied. If $\mathrm{Det}([A_0]_{8\times 8}) \neq 0$, the regular stress term is always zero. In the following sections the explicit form of $\mathrm{Det}([A_0]_{8\times 8})$ will be given for an arbitrary geometry and for several special geometries. In case of $\mathrm{Det}([A_0]_{8\times 8}) = 0$, the nonzero coefficients $\mathcal{A}_{\mathrm{k0}}, \mathcal{B}_{\mathrm{k0}}, \mathcal{C}_{\mathrm{k0}}, \mathcal{D}_{\mathrm{k0}}$ can be determined analytically. They are proportional to one arbitrary constant. Relations to calculate these coefficients will be presented below.

3.3.1 Joint with an Arbitrary Geometry θ_1, θ_2

For an arbitrary joint geometry with θ_1, θ_2, there is

$$\begin{aligned}
\mathrm{Det}([A_0]_{8\times 8}) \;=\; & \frac{32}{(1+\alpha)^2}\Big\{1-\alpha^2+4\alpha\beta+2\,\alpha\,\Big[-1+\alpha-2\,\beta\Big]\cos(2\theta_1) \\
& -2\,\Big[1+\alpha\Big]\,\beta\,\theta_1\sin(2\theta_1)+2\,\alpha\,\Big[1+\alpha-2\,\beta\Big]\cos(2\theta_2) \\
& +2\,\Big[1-\alpha\Big]\,\beta\,\theta_2\sin(2\theta_2)+2\,\alpha\,\Big[-\alpha+\beta\Big]\cos\left[2(\theta_1+\theta_2)\right] \\
& +\Big[-1-\alpha^2+2\,\alpha\,\beta\Big]\cos\left[2(\theta_1-\theta_2)\right] \\
& +\Big[-\alpha+\beta\Big]\,\Big[\theta_1(1+\alpha)-\theta_2(1-\alpha)\Big]\sin\left[2(\theta_1+\theta_2)\right] \\
& +\Big[(-1-\alpha+\beta+\alpha\,\beta)\,\theta_1+(1-\alpha+\beta-\alpha\,\beta)\,\theta_2\Big]\sin\left[2(\theta_1-\theta_2)\right]\Big\}
\end{aligned} \tag{3.3.18}$$

or

$$\begin{aligned}
\mathrm{Det}([A_0]_{8\times 8}) \;=\; & \frac{32}{(1+\alpha)^2}\Big\{1-\cos\left[2(\theta_1-\theta_2)\right]+(\theta_2-\theta_1)\sin\left[2(\theta_1-\theta_2)\right] \\
& +\alpha^2\Big[-1+2\,\cos(2\,\theta_1)-\cos[2\,(\theta_1-\theta_2)]+2\,\cos(2\,\theta_2) \\
& \quad -2\,\cos[2\,(\theta_1+\theta_2)]-(\theta_1+\theta_2)\,\sin[2\,(\theta_1+\theta_2)]\Big] \\
& +\alpha\beta\Big[4-4\,\cos(2\,\theta_1)+2\,\cos[2\,(\theta_1-\theta_2)]-4\,\cos(2\,\theta_2) \\
& \quad +2\,\cos[2\,(\theta_1+\theta_2)]-2\,\theta_1\,\sin(2\,\theta_1)+(\theta_1-\theta_2)\,\sin[2\,(\theta_1-\theta_2)] \\
& \quad -2\,\theta_2\,\sin(2\,\theta_2)+(\theta_1+\theta_2)\,\sin[2\,(\theta_1+\theta_2)]\Big] \\
& +\alpha\Big[-2\,\cos(2\,\theta_1)+2\,\cos(2\,\theta_2)-(\theta_1+\theta_2)\,\sin[2\,(\theta_1-\theta_2)] \\
& \quad +(-\theta_1+\theta_2)\,\sin[2\,(\theta_1+\theta_2)]\Big] \\
& +\beta\Big[-2\,\theta_1\,\sin(2\,\theta_1)+(\theta_1+\theta_2)\,\sin[2\,(\theta_1-\theta_2)] \\
& \quad +2\,\theta_2\,\sin(2\,\theta_2)+(\theta_1-\theta_2)\,\sin[2\,(\theta_1+\theta_2)]\Big]\Big\}.
\end{aligned} \tag{3.3.19}$$

From Eqs. (3.3.18) and (3.3.19) we can see that in general $\mathrm{Det}([A_0]_{8\times 8})$ is nonzero, i.e. the regular stress term is zero. However, for a given geometry θ_1, θ_2, material combinations with α, β exist, which lead to $\mathrm{Det}([A_0]_{8\times 8}) = 0$ (using Eq. (3.3.19) makes it easier to find the material combinations). Or, for a given material combination with α, β, a geometry with θ_1, θ_2 exists, which leads to $\mathrm{Det}([A_0]_{8\times 8}) = 0$ (using Eq. (3.3.18) makes it easier to find the joint geometries).
It can be shown that Det $([A_0]_{8\times 8})$ equals to $\mathrm{d}(\det[\mathrm{A}])/\mathrm{d}\omega\,|_{\omega=0}$ (comparing Eq. (3.3.18) and Eq. (3.1.85) in Section 3.1) except of a constant. This means that if $\omega = 0$ is the second order eigenvalue of the problem, for a joint under remote mechanical loading

the regular stress term may be nonzero.

In case of $\mathrm{Det}([A_0]_{8\times 8}) = 0$, the nonzero coefficients $\mathcal{A}_{\mathrm{k0}}, \mathcal{B}_{\mathrm{k0}}, \mathcal{C}_{\mathrm{k0}}, \mathcal{D}_{\mathrm{k0}}$ given as

$$\begin{aligned} A_{k0} &= K_0 A^*_{k0}, \\ B_{k0} &= K_0 B^*_{k0}, \\ C_{k0} &= K_0 C^*_{k0}, \\ D_{k0} &= K_0 D^*_{k0}, \end{aligned}$$

can be determined from

$$\begin{aligned} \mathcal{A}^*_{10} &= 2(1+\alpha)\Big\{1-\alpha+2\beta-2\beta\cos(2\theta_1)+(-1+\beta)\cos[2\,(\theta_1-\theta_2)] \\ &\quad +2\,(\alpha-\beta)\cos(2\theta_2)+(-\alpha+\beta)\cos[2\,(\theta_1+\theta_2)]\Big\} \end{aligned} \tag{3.3.20}$$

$$\begin{aligned} \mathcal{B}^*_{10} &= \Big\{-2(1+\alpha)(1-\alpha+2\beta)\theta_1+2(1-\alpha)(1+\beta)\theta_2\cos[2\,(\theta_1-\theta_2)] \\ &\quad +4(1+\alpha)(\beta-\alpha)\theta_1\cos(2\theta_2)+2(1-\alpha)(\alpha-\beta)\theta_2\cos[2\,(\theta_1+\theta_2)] \\ &\quad +[4\alpha(1-\alpha)-2(1-3\alpha)\beta]\sin(2\theta_1)+\left[1-\alpha+2\alpha^2+(1-3\alpha)\,\beta\right]\sin[2\,(\theta_1-\theta_2)] \\ &\quad +(1-3\alpha)(\beta-\alpha)\sin[2\,(\theta_1+\theta_2)]\Big\} \end{aligned} \tag{3.3.21}$$

$$\begin{aligned} \mathcal{C}^*_{10} &= \Big\{4\alpha(\alpha-1)+2\,(1-3\alpha)\,\beta+\left[1-\alpha^2-2\,(1-3\alpha)\,\beta\right]\cos(2\theta_1) \\ &\quad +[\alpha(1+\alpha)+(1-3\alpha)\,\beta]\cos[2\,(\theta_1-\theta_2)] \\ &\quad +\left[-1+2\alpha-5\alpha^2-2\,(1-3\alpha)\,\beta\right]\cos(2\theta_2) \\ &\quad +[\alpha(1+\alpha)+(1-3\alpha)\,\beta]\cos[2\,(\theta_1+\theta_2)]-2\,(1-\alpha)\,\beta\theta_2\sin[2\,(\theta_1-\theta_2)] \\ &\quad +2(1-\alpha)\left[(1+\alpha)\theta_1-(1-\alpha+2\beta)\,\theta_2\right]\sin(2\theta_2) \\ &\quad +2\,(1-\alpha)\,\beta\theta_2\sin[2\,(\theta_1+\theta_2)]\Big\} \end{aligned} \tag{3.3.22}$$

$$\begin{aligned} \mathcal{D}^*_{10} &= \Big\{4\,(1+\alpha)\,\beta\theta_1-2\,(1-\alpha)\,\beta\theta_2\cos[2\,(\theta_1-\theta_2)] \\ &\quad +2(1+\alpha)\left[\,(1+\alpha-2\beta)\,\theta_1-(1-\alpha)\theta_2\right]\cos(2\theta_2)+2\,(1-\alpha)\,\beta\theta_2\cos[2\,(\theta_1+\theta_2)] \\ &\quad +\left[-1+\alpha^2+2\,(1-3\alpha)\,\beta\right]\sin(2\theta_1)+[-\alpha(1+\alpha)+(-1+3\alpha)\,\beta]\sin[2\,(\theta_1-\theta_2)] \\ &\quad +\left(1-\alpha^2\right)\sin(2\theta_2)+[-\alpha(1+\alpha)+(-1+3\alpha)\,\beta]\sin[2\,(\theta_1+\theta_2)]\Big\} \end{aligned} \tag{3.3.23}$$

$$\mathcal{A}^*_{20} = 2(\alpha-1)\Big\{-1+\alpha-2\beta+2\beta\cos(2\theta_1)+(1-\beta)\cos[2(\theta_1-\theta_2)] \\ +2(-\alpha+\beta)\cos(2\theta_2)+(\alpha-\beta)\cos[2(\theta_1+\theta_2)]\Big\} \tag{3.3.24}$$

$$\mathcal{B}^*_{20} = (1-\alpha)\Big\{-2(1+\alpha)\theta_1+2(1-\beta)\theta_2\cos[2(\theta_1-\theta_2)]+4(-\alpha+\beta)\theta_2\cos(2\theta_2) \\ +2(\alpha-\beta)\theta_2\cos[2(\theta_1+\theta_2)]+2\alpha\sin(2\theta_1)+(1-\beta)\sin[2(\theta_1-\theta_2)] \\ +2(\alpha-\beta)\sin(2\theta_2)+(-\alpha+\beta)\sin[2(\theta_1+\theta_2)]\Big\} \tag{3.3.25}$$

$$\mathcal{C}^*_{20} = (1-\alpha)\Big\{-2\alpha+2\beta+(1+\alpha-2\beta)\cos(2\theta_1)+(-\alpha+\beta)\cos[2(\theta_1-\theta_2)] \\ +(-1+\alpha-2\beta)\cos(2\theta_2)+(\alpha+\beta)\cos[2(\theta_1+\theta_2)]-2\beta\theta_2\sin[2(\theta_1-\theta_2)] \\ +[2(1+\alpha)\theta_1+2(-1+\alpha-2\beta)\theta_2]\sin(2\theta_2)+2\beta\theta_2\sin[2(\theta_1+\theta_2)]\Big\} \tag{3.3.26}$$

$$\mathcal{D}^*_{20} = (\alpha-1)\Big\{-2\beta\theta_2\cos[2(\theta_1-\theta_2)]+[-2(1+\alpha)\theta_1+2(1-\alpha+2\beta)\theta_2]\cos(2\theta_2) \\ -2\beta\theta_2\cos[2(\theta_1+\theta_2)]+(1-\alpha)\sin(2\theta_1)+(\alpha-\beta)\sin[2(\theta_1-\theta_2)] \\ +(-1+\alpha-2\beta)\sin(2\theta_2)+(\alpha+\beta)\sin[2(\theta_1+\theta_2)]\Big\}. \tag{3.3.27}$$

The regular stress term in polar coordinates can be calculated from

$$\sigma_{rrk0}(r,\theta) = K_0[\mathcal{A}^*_{k0}\theta+\mathcal{B}^*_{k0}-\mathcal{C}^*_{k0}\sin(2\theta)-\mathcal{D}^*_{k0}\cos(2\theta)] \tag{3.3.28}$$

$$\sigma_{\theta\theta k0}(r,\theta) = K_0[\mathcal{A}^*_{k0}\theta+\mathcal{B}^*_{k0}+\mathcal{C}^*_{k0}\sin(2\theta)+\mathcal{D}^*_{k0}\cos(2\theta)] \tag{3.3.29}$$

$$\sigma_{r\theta k0}(r,\theta) = -K_0[\frac{1}{2}\mathcal{A}^*_{k0}+\mathcal{C}^*_{k0}\cos(2\theta)-\mathcal{D}^*_{k0}\sin(2\theta)] \tag{3.3.30}$$

where K_0 is an unknown constant, which is proportional to the remote loading and has to be determined from the stress analysis of the total joint, e.g., using the Finite Element Method (FEM). The method to determine K_0 from the stresses calculated from FEM will be explained in Section 3.4.

3.3.2 Joint with $\theta_1 = -\theta_2$

For a joint geometry with $\theta_1 = -\theta_2$ (see Fig. 3.2),

$$\begin{aligned}\mathrm{Det}([A_0]_{8\times 8}) &= \frac{64}{(1+\alpha)^2}\sin(\theta_1)\Big\{\Big[1-3\,\alpha^2+6\,\alpha\,\beta\Big]\sin(\theta_1)-2\theta_1\Big[1+\alpha\,\beta\Big]\,\cos(\theta_1)\\ &\quad -2\,\theta_1\Big[1-\alpha\,\beta\Big]\,\cos(3\,\theta_1)+\Big[1+\alpha^2-2\,\alpha\,\beta\Big]\,\sin(3\,\theta_1)\Big\} \qquad (3.3.31)\end{aligned}$$

or

$$\begin{aligned}\mathrm{Det}([A_0]_{8\times 8}) &= \frac{64}{(1+\alpha)^2}\sin(\theta_1)\Big\{\Big[-2\,\theta_1\,\cos(\theta_1)-2\,\theta_1\,\cos(3\,\theta_1)+\sin(\theta_1)+\sin(3\,\theta_1)\Big]\\ &\quad +\alpha^2\Big[-3\,\sin(\theta_1)+\sin(3\,\theta_1)\Big]\\ &\quad +2\alpha\beta\,\Big[-\theta_1\,\cos(\theta_1)+\theta_1\,\cos(3\,\theta_1)+3\,\sin(\theta_1)-\sin(3\,\theta_1)\Big]\Big\}. \qquad (3.3.32)\end{aligned}$$

For the given joint geometries ($\theta_1 = 45°, 60°, 90°, 120°$ and $135°$), the possible material combinations, which satisfy $\mathrm{Det}([A_0]_{8\times 8}) = 0$, are plotted in a Dundurs diagram in Fig. 3.11. For these joints, the regular stress term is nonzero.

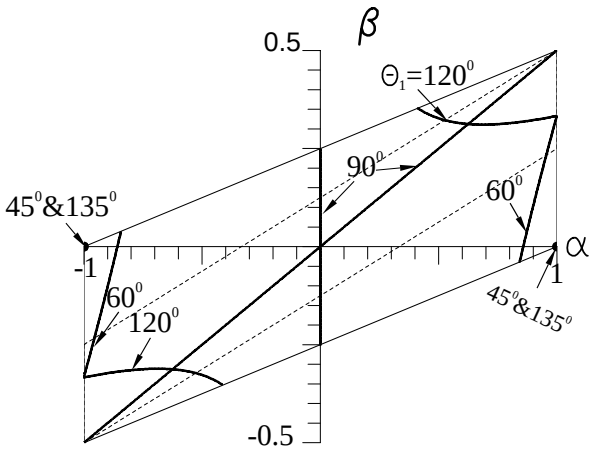

Figure 3.11: Material combinations, for which the regular stress term is nonzero in a joint with $\theta_1 = -\theta_2$.

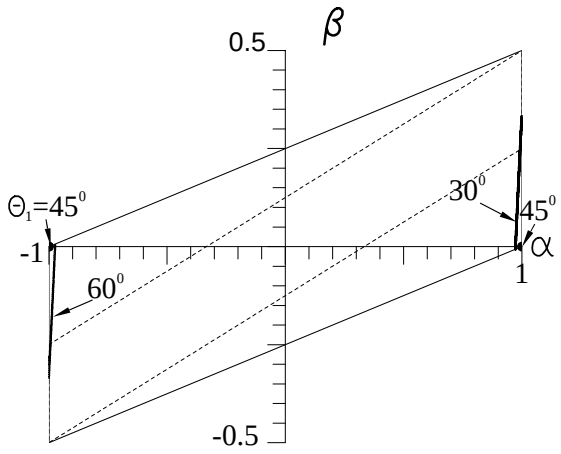

Figure 3.12: Material combinations, for which the regular stress term is nonzero in a joint with $\theta_1 - \theta_2 = 90°$.

In case of $\mathrm{Det}([A_0]_{8\times 8}) = 0$, the nonzero coefficients $\mathcal{A}^*_{k0}, \mathcal{B}^*_{k0}, \mathcal{C}^*_{k0}, \mathcal{D}^*_{k0}$ can be determined from

$$\mathcal{A}^*_{10} = 8(1+\alpha)\sin^2(\theta_1)\Big\{1-\alpha+\beta+(1-\beta)\cos(2\theta_1)\Big\} \qquad (3.3.33)$$

$$\begin{aligned}\mathcal{B}^*_{10} &= \Big\{2\left[-1-\alpha+2\alpha^2-(1+3\alpha)\,\beta\right]\theta_1 \\ &\quad +4(1+\alpha)(\beta-\alpha)\theta_1\cos(2\theta_1)-2(1-\alpha)(1+\beta)\theta_1\cos(4\theta_1) \\ &\quad +2\Big[2\alpha(1-\alpha)+(-1+3\alpha)\,\beta\Big]\sin(2\theta_1) \\ &\quad +\left[1-\alpha+2\alpha^2+(1-3\alpha)\,\beta\right]\sin(4\theta_1)\Big\} \qquad (3.3.34)\end{aligned}$$

$$\begin{aligned}\mathcal{C}^*_{10} &= 2\sin(\theta_1)\Big\{-2(1-\alpha)(2+\beta)\theta_1\cos(\theta_1)+2\,(1-\alpha)\,\beta\theta_1\cos(3\theta_1) \\ &\quad +[\alpha(-3+5\alpha)+3\,(1-3\alpha)\,\beta]\sin(\theta_1) \\ &\quad +[-\alpha(1+\alpha)+(-1+3\alpha)\,\beta]\sin(3\theta_1)\Big\} \qquad (3.3.35)\end{aligned}$$

$$\begin{aligned}\mathcal{D}^*_{10} &= \Big\{2\,(1+3\alpha)\,\beta\theta_1+4(1+\alpha)(1-\beta)\theta_1\cos(2\theta_1) \\ &\quad +2\,(1-\alpha)\,\beta\theta_1\cos(4\theta_1)+2\left[-1+\alpha^2+(1-3\alpha)\,\beta\right]\sin(2\theta_1) \\ &\quad +[-\alpha(1+\alpha)+(-1+3\alpha)\,\beta]\sin(4\theta_1)\Big\} \qquad (3.3.36)\end{aligned}$$

$$\mathcal{A}^*_{20} = 8(1-\alpha)\sin^2(\theta_1)\Big\{1-\alpha+\beta+(1-\beta)\cos(2\theta_1)\Big\} \qquad (3.3.37)$$

$$\begin{aligned}\mathcal{B}^*_{20} &= (1-\alpha)\Big\{2\,(-1-2\alpha+\beta)\,\theta_1+4\,(\alpha-\beta)\,\theta_1\cos(2\theta_1) \\ &\quad +2\,(-1+\beta)\,\theta_1\cos(4\theta_1)+2\beta\sin(2\theta_1)+(1-\beta)\sin(4\theta_1)\Big\} \qquad (3.3.38)\end{aligned}$$

$$\begin{aligned}\mathcal{C}^*_{20} &= 2(1-\alpha)\sin(\theta_1)\Big\{-2\,(2+\beta)\,\theta_1\cos(\theta_1)+2\beta\theta_1\cos(3\theta_1) \\ &\quad +(-\alpha+3\beta)\sin(\theta_1)+(\alpha-\beta)\sin(3\theta_1)\Big\} \qquad (3.3.39)\end{aligned}$$

$$\begin{aligned}\mathcal{D}^*_{20} &= -(1-\alpha)\Big\{2\beta\theta_1-4\,(1+\beta)\,\theta_1\cos(2\theta_1)+2\beta\theta_1\cos(4\theta_1) \\ &\quad +2\,(1-\alpha+\beta)\sin(2\theta_1)+(\alpha-\beta)\sin(4\theta_1)\Big\}. \qquad (3.3.40)\end{aligned}$$

The regular stress term in polar coordinates can be calculated from Eqs. (3.3.28 - 3.3.30).

3.3.3 Joint with $\theta_1 - \theta_2 = \pi/2$

For a joint geometry with $\theta_1 - \theta_2 = \pi/2$ (see Fig. 3.3),

$$\begin{aligned}\mathrm{Det}([A_0]_{8\times 8}) &= \frac{64}{(1+\alpha)^2}\sin(\theta_1)\Big\{-2\theta_1\Big[1+\alpha\beta\Big]\cos(\theta_1)+\Big[1-3\alpha^2+6\alpha\beta\Big]\sin(\theta_1)\\ &\quad +2\theta_1\Big[\alpha\beta-1\Big]\cos(3\theta_1)+\Big[1+\alpha^2-2\alpha\beta\Big]\sin(3\theta_1)\Big\}\end{aligned} \tag{3.3.41}$$

or

$$\begin{aligned}\mathrm{Det}([A_0]_{8\times 8}) &= \frac{64}{(1+\alpha)^2}\sin(\theta_1)\Big\{\Big[-2\theta_1[\cos(3\theta_1)+\cos(\theta_1)]+\sin(3\theta_1)+\sin(\theta_1)\Big]\\ &\quad +\alpha^2\Big[\sin(3\theta_1)-3\sin(\theta_1)\Big]\\ &\quad +2\alpha\beta\Big[\theta_1[\cos(3\theta_1)-\cos(\theta_1)]-\sin(3\theta_1)+3\sin(\theta_1)\Big]\Big\}.\end{aligned} \tag{3.3.42}$$

For the given joint geometries ($\theta_1 = 30°, 45°, 60°$, due to the restriction of $\theta_1 - \theta_2 = \pi/2$ here θ_1 takes different values as in Section 3.3.2), the possible material combinations, which satisfy $\mathrm{Det}([A_0]_{8\times 8}) = 0$, are plotted in Fig. 3.12.
In case of $\mathrm{Det}([A_0]_{8\times 8}) = 0$, the nonzero coefficients $\mathcal{A}^*_{\mathrm{k}0}, \mathcal{B}^*_{\mathrm{k}0}, \mathcal{C}^*_{\mathrm{k}0}, \mathcal{D}^*_{\mathrm{k}0}$ are

$$\mathcal{A}^*_{10} = 2(1+\alpha)\Big\{2-\alpha+\beta-2\alpha\cos(2\theta_1)+(\alpha-\beta)\cos(4\theta_1)\Big\} \tag{3.3.43}$$

$$\begin{aligned}\mathcal{B}^*_{10} &= \Big\{(1-\alpha)(1+\beta)\pi+2\Big[-2+\alpha+\alpha^2-(3+\alpha)\beta\Big]\theta_1\\ &\quad +4(1+\alpha)(\alpha-\beta)\theta_1\cos(2\theta_1)+(\alpha-\beta)(1-\alpha)(\pi-2\theta_1)\cos(4\theta_1)\\ &\quad +2\left[2\alpha(1-\alpha)-(1-3\alpha)\beta\right]\sin(2\theta_1)+(\alpha-\beta)(1-3\alpha)\sin(4\theta_1)\Big\}\end{aligned} \tag{3.3.44}$$

$$\begin{aligned}\mathcal{C}^*_{10} &= \Big\{\alpha(-5+3\alpha)+(1-3\alpha)\beta+2\Big(1-\alpha+2\alpha^2\Big)\cos(2\theta_1)\\ &\quad +\Big[-\alpha(1+\alpha)+(-1+3\alpha)\beta\Big]\cos(4\theta_1)\\ &\quad +(1-\alpha)\Big[(\alpha-1-2\beta)\pi+4(\beta-\alpha)\theta_1\Big]\sin(2\theta_1)\\ &\quad +(1-\alpha)\beta(\pi-2\theta_1)\sin(4\theta_1)\Big\}\end{aligned} \tag{3.3.45}$$

$$\mathcal{D}^*_{10} = \Big\{\Big[(-1+\alpha)\pi + 2(3+\alpha)\theta_1\Big]\beta - (1+\alpha)\Big[(1-\alpha)\pi + 4(\alpha-\beta)\theta_1\Big]\cos(2\theta_1) + (1-\alpha)\beta(\pi-2\theta_1)\cos(4\theta_1) + 2\Big[-1+\alpha^2+(1-3\alpha)\beta\Big]\sin(2\theta_1) + \big[\alpha(1+\alpha)+(1-3\alpha)\,\beta\big]\sin(4\theta_1)\Big\} \quad (3.3.46)$$

$$\mathcal{A}^*_{20} = 2(1-\alpha)\Big\{2-\alpha+\beta-2\alpha\cos(2\theta_1)+(\alpha-\beta)\cos(4\theta_1)\Big\} \quad (3.3.47)$$

$$\mathcal{B}^*_{20} = (1-\alpha)\Big\{(1-\beta)\,\pi + 2\,(-2-\alpha+\beta)\,\theta_1 + 2(\beta-\alpha)(\pi-2\theta_1)\cos(2\theta_1) + (\alpha-\beta)(\pi-2\theta_1)\cos(4\theta_1) + 2\beta\sin(2\theta_1) + (\alpha-\beta)\sin(4\theta_1)\Big\} \quad (3.3.48)$$

$$\mathcal{C}^*_{20} = -(1-\alpha)\Big\{\alpha-\beta-2\cos(2\theta_1)+(\alpha+\beta)\cos(4\theta_1) + \big[(1-\alpha+2\beta)\,\pi + 4\,(\alpha-\beta)\,\theta_1\big]\sin(2\theta_1) - \beta(\pi-2\theta_1)\sin(4\theta_1)\Big\} \quad (3.3.49)$$

$$\mathcal{D}^*_{20} = (1-\alpha)\Big\{(1-\beta)\,\pi - 2\,(2+\alpha-\beta)\,\theta_1 + 2(\beta-\alpha)(\pi-2\theta_1)\cos(2\theta_1) + (\alpha-\beta)(\pi-2\theta_1)\cos(4\theta_1) + 2\beta\sin(2\theta_1) + (\alpha-\beta)\sin(4\theta_1)\Big\}. \quad (3.3.50)$$

3.3.4 Joint with $\theta_1 - \theta_2 = \pi$

For a joint geometry with $\theta_1 - \theta_2 = \pi$ (see Fig. 3.4),

$$\mathrm{Det}([A_0]_{8\times 8}) = \frac{128}{(1+\alpha)^2}\sin(\theta_1)\Big[\beta+\alpha\,\cos(2\,\theta_1)-\beta\,\cos(2\,\theta_1)\Big]\times \times\Big[-\pi\,\cos(\theta_1)+\alpha\,\pi\,\cos(\theta_1)-2\,\alpha\,\theta_1\,\cos(\theta_1)+2\,\alpha\,\sin(\theta_1)\Big] \quad (3.3.51)$$

or

$$\mathrm{Det}([A_0]_{8\times 8}) = \frac{128}{(1+\alpha)^2}\sin(\theta_1)\Big\{\alpha^2\cos(2\,\theta_1)\Big[\pi\,\cos(\theta_1)-2\,\theta_1\,\cos(\theta_1)+2\,\sin(\theta_1)\Big] + \alpha\beta\Big[-1+\cos(2\,\theta_1)\Big]\Big[-\pi\,\cos(\theta_1)+2\,\theta_1\,\cos(\theta_1)-2\,\sin(\theta_1)\Big] - \alpha\Big[\pi\,\cos(\theta_1)\,\cos(2\,\theta_1)\Big]+\beta\pi\,\cos(\theta_1)\Big[-1+\cos(2\,\theta_1)\Big]\Big\}. \quad (3.3.52)$$

For the given joint geometries ($\theta_1 = 30°, 45°, 60°, 90°, 120°, 135°, 150°$), the possible material combinations, which satisfy $\mathrm{Det}([A_0]_{8\times 8}) = 0$, are plotted in Fig. 3.13.

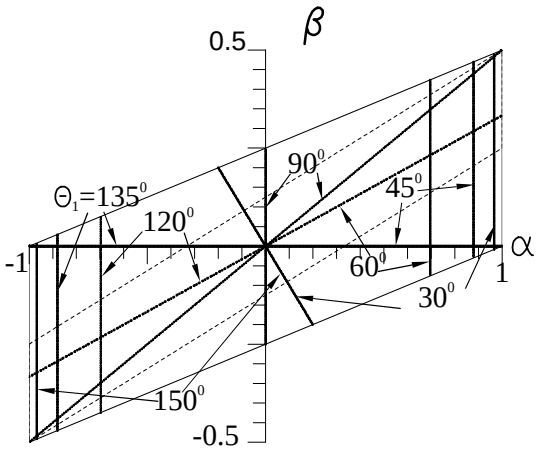

Figure 3.13: Material combinations, for which the regular stress term is nonzero in a joint with $\theta_1 - \theta_2 = 180°$.

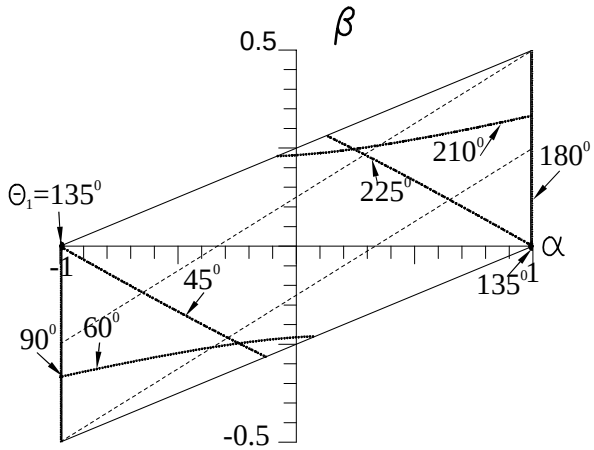

Figure 3.14: Material combinations, for which the regular stress term is nonzero in a joint with $\theta_1 - \theta_2 = 270°$.

In case of $\mathrm{Det}([A_0]_{8\times 8}) = 0$, the nonzero coefficients $\mathcal{A}^*_{k0}, \mathcal{B}^*_{k0}, \mathcal{C}^*_{k0}, \mathcal{D}^*_{k0}$ can be determined from

$$\mathcal{A}^*_{10} = 8(1+\alpha)\sin^2(\theta_1)\Big\{\beta + (\alpha-\beta)\cos(2\theta_1)\Big\} \tag{3.3.53}$$

$$\begin{aligned}\mathcal{B}^*_{10} = \Big\{ & -2(1-\alpha)(1+\beta)\pi - 2\left[\alpha(1-\alpha) + (1+3\alpha)\,\beta\right]\theta_1 \\ & +4(1+\alpha)(\beta-\alpha)\theta_1\cos(2\theta_1) - 2(1-\alpha)(\alpha-\beta)(\pi-\theta_1)\cos(4\theta_1) \\ & +2\left[2\alpha(1-\alpha) - (1-3\alpha)\,\beta\right]\sin(2\theta_1) + (1-3\alpha)(\beta-\alpha)\sin(4\theta_1)\Big\}\end{aligned} \tag{3.3.54}$$

$$\begin{aligned}\mathcal{C}^*_{10} = & \ 2\sin(\theta_1)\Big\{2(1-\alpha)\Big[(1-\alpha+\beta)\pi + (2\alpha-\beta)\theta_1\Big]\cos(\theta_1) \\ & +2(1-\alpha)\beta(-\pi+\theta_1)\cos(3\theta_1) + \left[\alpha(-3+5\alpha) + 3\,(1-3\alpha)\,\beta\right]\sin(\theta_1) \\ & +\left[-\alpha(1+\alpha) + (-1+3\alpha)\,\beta\right]\sin(3\theta_1)\Big\}\end{aligned} \tag{3.3.55}$$

$$\begin{aligned}\mathcal{D}^*_{10} = & \ \Big\{2\,(1-\alpha)\,\beta\pi + 2\,(1+3\alpha)\,\beta\theta_1 + 2(1+\alpha)\ \left[(1-\alpha)\,\pi + 2(\alpha-\beta)\theta_1\right]\cos(2\theta_1) \\ & +2(1-\alpha)\beta(-\pi+\theta_1)\cos(4\theta_1) + 2\,(1-3\alpha)\,\beta\sin(2\theta_1) \\ & +\left[-\alpha(1+\alpha) + (-1+3\alpha)\,\beta\right]\sin(4\theta_1)\Big\}\end{aligned} \tag{3.3.56}$$

$$\mathcal{A}^*_{20} = 8(1-\alpha)\sin^2(\theta_1)\Big\{\beta+(\alpha-\beta)\cos(2\theta_1)\Big\} \tag{3.3.57}$$

$$\begin{aligned}\mathcal{B}^*_{20} = &-(1-\alpha)\Big\{2\,(1-\beta)\,\pi+2\,(\alpha+\beta)\,\theta_1+4(\alpha-\beta)(-\pi+\theta_1)\cos(2\theta_1)\\ &+2(\alpha-\beta)(\pi-\theta_1)\cos(4\theta_1)+2\,(-2\alpha+\beta)\sin(2\theta_1)+(\alpha-\beta)\sin(4\theta_1)\Big\}\end{aligned} \tag{3.3.58}$$

$$\begin{aligned}\mathcal{C}^*_{20} = &-2(1-\alpha)\sin(\theta_1)\Big\{2\,[(-1+\alpha-\beta)\,\pi+(-2\alpha+\beta)\,\theta_1]\cos(\theta_1)\\ &+2\beta\,(\pi-\theta_1)\cos(3\theta_1)+3\,(\alpha-\beta)\sin(\theta_1)+(\alpha+\beta)\sin(3\theta_1)\Big\}\end{aligned} \tag{3.3.59}$$

$$\begin{aligned}\mathcal{D}^*_{20} = &-(1-\alpha)\Big\{2\beta(\pi-\theta_1)+2\,[(-1+\alpha-2\beta)\pi+2\,(-\alpha+\beta)\,\theta_1]\cos(2\theta_1)\\ &+2\beta\,(\pi-\theta_1)\cos(4\theta_1)-2\beta\sin(2\theta_1)+(\alpha+\beta)\sin(4\theta_1)\Big\}.\end{aligned} \tag{3.3.60}$$

From Eq. (3.3.51), it follows that $\mathrm{Det}([A_0]_{8\times 8})=0$ if

$$\alpha=\frac{\beta[\cos(2\theta_1)-1]}{\cos(2\theta_1)} \tag{3.3.61}$$

or

$$\alpha=\frac{\pi\cos(\theta_1)}{\pi\cos(\theta_1)-2\theta_1\cos(\theta_1)+2\sin(\theta_1)}. \tag{3.3.62}$$

For this α, the regular stress term can be simplified. For

$$\alpha=\frac{\beta[\cos(2\theta_1)-1]}{\cos(2\theta_1)} \tag{3.3.63}$$

the regular stress term in Cartesian coordinates is

$$\begin{aligned}\sigma_{xx10} = \sigma_{xx20} = &\frac{64\cos^2(\theta_1)[\beta+\cos(2\theta_1)-\beta\cos(2\theta_1)]}{[\cos(2\theta_1)+\beta\cos(2\theta_1)-\beta]^2}K_0\times\\ &\times\Big\{\beta\theta_1-\pi\cos(2\theta_1)(1+\beta)+\beta\cos(4\theta_1)(\pi-\theta_1)-2\beta\sin(2\theta_1)+\beta\sin(4\theta_1)\Big\}\end{aligned} \tag{3.3.64}$$

$$\sigma_{yy10}=\sigma_{yy20}=\frac{\sin^2(\theta_1)}{\cos^2(\theta_1)}\sigma_{xx10} \tag{3.3.65}$$

$$\tau_{xy10} = \tau_{xy20} = \frac{\sin(\theta_1)}{\cos(\theta_1)}\sigma_{xx10}. \tag{3.3.66}$$

For

$$\alpha = \frac{\pi\cos(\theta_1)}{\pi\cos(\theta_1) - 2\theta_1\cos(\theta_1) + 2\sin(\theta_1)} \tag{3.3.67}$$

it holds

$$\begin{aligned}\sigma_{xx10} = & -\frac{16\sin^2(\theta_1)}{\pi\cos(\theta_1) - \theta_1\cos(\theta_1) + \sin(\theta_1)}K_0 \times \\ & \times \Big\{ 2\left[2\beta + (1-2\beta)\pi\theta_1 + 4\beta\theta_1^2\right]\cos(\theta_1) + 2\left[-2\beta + (1-2\beta)\pi\theta_1 + 4\beta\theta_1^2\right]\cos(3\theta_1) \\ & + \quad 2\beta(\pi + 2\theta_1)\sin(\theta_1) + 2\beta(\pi - 6\theta_1)\sin(3\theta_1) - [2\,\theta + \sin(2\theta)]\Delta_\pi \Big\}\end{aligned} \tag{3.3.68}$$

$$\begin{aligned}\sigma_{yy10} \quad = \quad & \frac{16\sin^2(\theta_1)}{\pi\cos(\theta_1) - \theta_1\cos(\theta_1) + \sin(\theta_1)}K_0 \Big\{ -2\pi\theta_1\cos(\theta_1) - 2\pi\theta_1\cos(3\theta_1) \\ & -2\pi\sin(\theta_1) + 2\pi\sin(3\theta_1) + [2\theta - \sin(2\theta)]\Delta_\pi \Big\}\end{aligned} \tag{3.3.69}$$

$$\begin{aligned}\sigma_{xy10} \quad = \quad & \frac{16\sin^2(\theta_1)}{\pi\cos(\theta_1) - \theta_1\cos(\theta_1) + \sin(\theta_1)}K_0 \Big\{ [(1-\beta)\pi + 6\beta\theta_1]\cos(\theta_1) \\ & + [(1+\beta)\pi - 6\beta\theta_1]\cos(3\theta_1) + 2\left(-3\beta + \beta\pi\theta_1 - 2\beta\theta_1^2\right)\sin(\theta_1) \\ & + 2\beta\left(1 + \pi\theta_1 - 2\theta_1^2\right)\sin(3\theta_1) - \cos(2\theta)\Delta_\pi \Big\}\end{aligned} \tag{3.3.70}$$

$$\begin{aligned}\sigma_{xx20} \quad = \quad & \frac{16\sin^2(\theta_1)[\theta_1\cos(\theta_1) - \sin(\theta_1)]}{[\pi\cos(\theta_1) - \theta_1\cos(\theta_1) + \sin(\theta_1)]^2}K_0 \times \\ & \times \Big\{ 2\left(2\beta - \pi^2 + 2\beta\pi^2 + \pi\theta_1 - 6\beta\pi\theta_1 + 4\beta\theta_1^2\right)\cos(\theta_1) \\ & + 2\left(-2\beta - \pi^2 + 2\beta\pi^2 + \pi\theta_1 - 6\beta\pi\theta_1 + 4\beta\theta_1^2\right)\cos(3\theta_1) \\ & + 2\beta(-3\pi + 2\theta_1)\sin(\theta_1) + 2\beta(5\pi - 6\theta_1)\sin(3\theta_1) - [2\theta + \sin(2\theta)]\Delta_\pi \Big\}\end{aligned} \tag{3.3.71}$$

$$\begin{aligned}\sigma_{yy20} \quad = \quad & \frac{16\sin^2(\theta_1)[\theta_1\cos(\theta_1) - \sin(\theta_1)]}{[\pi\cos(\theta_1) - \theta_1\cos(\theta_1) + \sin(\theta_1)]^2}K_0 \Big\{ 2\pi(-\pi + \theta_1)\cos(\theta_1) \\ & + 2\pi(-\pi + \theta_1)\cos(3\theta_1) + 2\pi\sin(\theta_1) - 2\pi\sin(3\theta_1) - [2\theta - \sin(2\theta)]\Delta_\pi \Big\}\end{aligned} \tag{3.3.72}$$

$$\tau_{xy20} = \frac{16\sin^2(\theta_1)[\theta_1\cos(\theta_1)-\sin(\theta_1)]}{[\pi\cos(\theta_1)-\theta_1\cos(\theta_1)+\sin(\theta_1)]^2}K_0\Big\{(-\pi+5\beta\pi-6\beta\theta_1)\cos(\theta_1) + (-\pi-5\beta\pi+6\beta\theta_1)\cos(3\theta_1)+2\beta\left(3+\pi^2-3\pi\theta_1+2\theta_1^2\right)\sin(\theta_1) +2\beta\left(-1+\pi^2-3\pi\theta_1+2\theta_1^2\right)\sin(3\theta_1)+\cos(2\theta)\Delta_\pi\Big\}, \quad (3.3.73)$$

with

$$\Delta_\pi = [(1+\beta)\,\pi-2\beta\theta_1]\cos(\theta_1)+[(1-\beta)\,\pi+2\beta\theta_1]\cos(3\theta_1)+6\beta\sin(\theta_1)-2\beta\sin(3\theta_1). \quad (3.3.74)$$

3.3.5 Joint with $\theta_1-\theta_2=3\pi/2$

For a joint geometry with $\theta_1-\theta_2=3\pi/2$ (see Fig. 3.5),

$$\mathrm{Det}([A_0]_{8\times8}) = \frac{16}{(1+\alpha)^2}\Big\{4(1+\alpha\beta)-8\,\alpha\cos(2\theta_1)+4\,\alpha\left[\alpha-\beta\right]\cos(4\theta_1) +2\,\beta\left[3\,\pi-3\,\alpha\,\pi-4\,\theta_1\right]\sin(2\theta_1) +(\alpha-\beta)\left[3\,\pi-3\,\alpha\,\pi+4\,\alpha\,\theta_1\right]\sin(4\theta_1)\Big\} \quad (3.3.75)$$

or

$$\mathrm{Det}([A_0]_{8\times8}) = \frac{16}{(1+\alpha)^2}\Big\{4+\alpha^2\left[4\,\cos(4\,\theta_1)-3\,\pi\,\sin(4\,\theta_1)+4\,\theta_1\,\sin(4\,\theta_1)\right] +2\alpha\beta\,\sin(2\theta_1)\left[-3\,\pi+3\,\pi\,\cos(2\,\theta_1)-4\,\theta_1\,\cos(2\,\theta_1)+4\,\sin(2\,\theta_1)\right] +2\,\alpha\,\cos(2\theta_1)\left[-4+3\,\pi\,\sin(2\,\theta_1)\right] +4\,\beta\,\cos(\theta_1)\left[3\,\pi-4\,\theta_1-3\,\pi\,\cos(2\,\theta_1)\right]\sin(\theta_1)\Big\}. \quad (3.3.76)$$

For the given joint geometries ($\theta_1=45°,60°,90°,135°,180°,210°,225°$), the possible material combinations, which satisfy $\mathrm{Det}([A_0]_{8\times8})=0$, are plotted in Fig. 3.14.
In case of $\mathrm{Det}([A_0]_{8\times8})=0$, the nonzero coefficients $\mathcal{A}^*_{k0},\mathcal{B}^*_{k0},\mathcal{C}^*_{k0},\mathcal{D}^*_{k0}$ take

$$\mathcal{A}^*_{10} = 2(1+\alpha)\Big\{2-\alpha+\beta-2\alpha\cos(2\theta_1)+(\alpha-\beta)\cos(4\theta_1)\Big\} \quad (3.3.77)$$

$$\mathcal{B}^*_{10} = \Big\{(1-\alpha)(1+\beta)3\pi+2\left[-2+\alpha+\alpha^2-(3+\alpha)\,\beta\right]\theta_1 +4(1+\alpha)(\alpha-\beta)\theta_1\cos(2\theta_1)+(1-\alpha)(\alpha-\beta)(3\pi-2\theta_1)\cos(4\theta_1) +2\left[2\alpha(1-\alpha)-(1-3\alpha)\,\beta\right]\sin(2\theta_1)+(1-3\alpha)\,(\alpha-\beta)\sin(4\theta_1)\Big\} \quad (3.3.78)$$

$$\mathcal{C}^*_{10} = \Big\{\alpha(-5+3\alpha)+(1-3\alpha)\,\beta+2\left(1-\alpha+2\alpha^2\right)\cos(2\theta_1) + [-\alpha(1+\alpha)+(-1+3\alpha)\,\beta]\cos(4\theta_1) +(1-\alpha)\Big[(\alpha-1-2\beta)3\pi+4(\beta-\alpha)\theta_1\Big]\sin(2\theta_1) +\beta(1-\alpha)(3\pi-2\theta_1)\sin(4\theta_1)\Big\} \tag{3.3.79}$$

$$\mathcal{D}^*_{10} = \Big\{3\,(-1+\alpha)\,\beta\pi+2\,(3+\alpha)\,\beta\theta_1 +(1+\alpha)\Big[3\pi(\alpha-1)+4(\beta-\alpha)\theta_1\Big]\cos(2\theta_1)+(1-\alpha)\,(3\pi-2\theta_1)\beta\cos(4\theta_1) +2\left[-1+\alpha^2+(1-3\alpha)\,\beta\right]\sin(2\theta_1)+\Big[\alpha+\alpha^2+(1-3\alpha)\,\beta\Big]\sin(4\theta_1)\Big\} \tag{3.3.80}$$

$$\mathcal{A}^*_{20} = 2(1-\alpha)\Big\{2-\alpha+\beta-2\alpha\cos(2\theta_1)+(\alpha-\beta)\cos(4\theta_1)\Big\} \tag{3.3.81}$$

$$\mathcal{B}^*_{20} = (1-\alpha)\Big\{3\,(1-\beta)\,\pi+2\,(-2-\alpha+\beta)\,\theta_1 +2(\alpha-\beta)(2\theta_1-3\pi)\cos(2\theta_1)+(\alpha-\beta)(3\pi-2\theta_1)\cos(4\theta_1) +2\beta\sin(2\theta_1)+(\alpha-\beta)\sin(4\theta_1)\Big\} \tag{3.3.82}$$

$$\mathcal{C}^*_{20} = -(1-\alpha)\Big\{\alpha-\beta-2\cos(2\theta_1)+(\alpha+\beta)\cos(4\theta_1) +[(1-\alpha+2\beta)\,3\pi+4\,(\alpha-\beta)\,\theta_1]\sin(2\theta_1) +\beta\,(-3\pi+2\theta_1)\sin(4\theta_1)\Big\} \tag{3.3.83}$$

$$\mathcal{D}^*_{20} = (1-\alpha)\Big\{\beta(3\pi-2\theta_1)+\Big[(-1+\alpha-2\beta)3\pi+4\,(-\alpha+\beta)\,\theta_1\Big]\cos(2\theta_1) +\beta\,(3\pi-2\theta_1)\cos(4\theta_1)+2\,(-1+\alpha-\beta)\sin(2\theta_1) +(\alpha+\beta)\sin(4\theta_1)\Big\}. \tag{3.3.84}$$

3.3.6 Joint with $\theta_1 - \theta_2 = 2\pi$

For a joint geometry with $\theta_1 - \theta_2 = 2\pi$ (see Fig. 3.6),

$$\begin{aligned}\mathrm{Det}([A_0]_{8\times 8}) &= \frac{256}{(1+\alpha)^2}\sin(\theta_1)\Big[\beta+\alpha\,\cos(2\,\theta_1)-\beta\,\cos(2\,\theta_1)\Big]\Big[-\pi\,\cos(\theta_1) \\ &\quad +\alpha\,\pi\,\cos(\theta_1)-\alpha\,\theta_1\,\cos(\theta_1)+\alpha\,\sin(\theta_1)\Big] \end{aligned} \tag{3.3.85}$$

or

$$\begin{aligned}\mathrm{Det}([A_0]_{8\times 8}) &= \frac{256}{(1+\alpha)^2}\sin(\theta_1)\Big\{\alpha^2\cos(2\theta_1)\,[\pi\,\cos(\theta_1)-\theta_1\,\cos(\theta_1)+\sin(\theta_1)] \\ &\quad +2\,\alpha\beta\sin^2(\theta_1)\Big[\pi\,\cos(\theta_1)-\theta_1\,\cos(\theta_1)+\sin(\theta_1)\Big] \\ &\quad -\alpha\Big[\pi\,\cos(\theta_1)\,\cos(2\,\theta_1)\Big]+\beta\pi\cos(\theta_1)\Big[-1+\cos(2\theta_1)\Big]\Big\}. \end{aligned} \tag{3.3.86}$$

For the given joint geometries ($\theta_1 = 45°, 90°, 135°, 225°, 270°, 315°$), the possible material combinations, which satisfy $\mathrm{Det}([A_0]_{8\times 8}) = 0$, are plotted in Fig. 3.15.

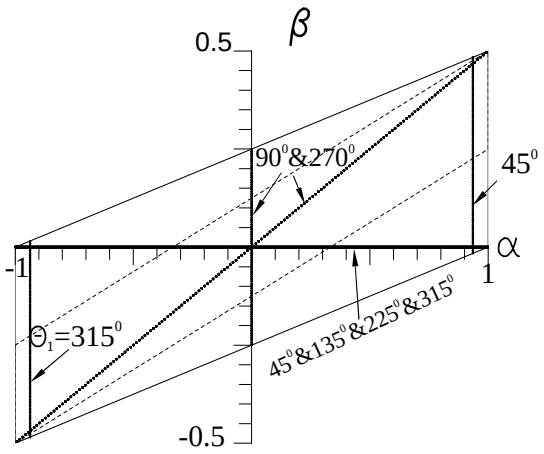

Figure 3.15: Material combinations, for which the regular stress term is nonzero in a joint with $\theta_1 - \theta_2 = 360°$.

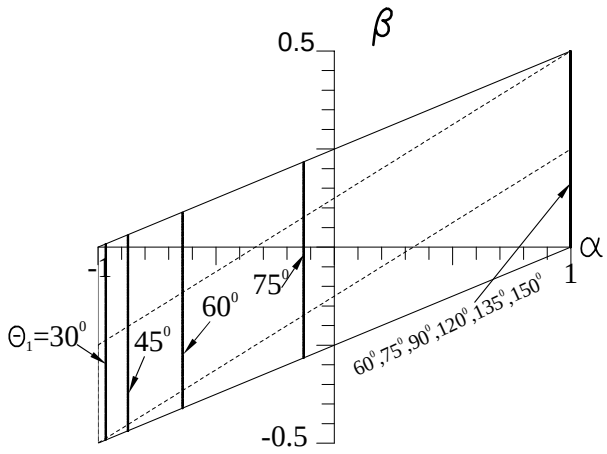

Figure 3.16: Material combinations, for which the regular stress term is nonzero in a joint with $\theta_1 = 180°$ and θ_2 being arbitrary.

In case of $\mathrm{Det}([A_0]_{8\times 8}) = 0$, the nonzero coefficients $\mathcal{A}^*_{k0}, \mathcal{B}^*_{k0}, \mathcal{C}^*_{k0}, \mathcal{D}^*_{k0}$ read

$$\mathcal{A}^*_{10} = 2(1+\alpha)\Big\{2-\alpha+\beta-2\alpha\cos(2\theta_1)+(\alpha-\beta)\cos(4\theta_1)\Big\} \tag{3.3.87}$$

$$\begin{aligned}\mathcal{B}^*_{10} &= \Big\{4(1-\alpha)(1+\beta)\pi + 2\left[-2+\alpha+\alpha^2-(3+\alpha)\,\beta\right]\theta_1 \\ &\quad +4(1+\alpha)(\alpha-\beta)\theta_1\cos(2\theta_1) + 2(1-\alpha)(\alpha-\beta)(2\pi-\theta_1)\cos(4\theta_1) \\ &\quad +2\left[2\alpha(1-\alpha)-(1-3\alpha)\,\beta\right]\sin(2\theta_1) + (1-3\alpha)(\alpha-\beta)\sin(4\theta_1)\Big\}\end{aligned} \tag{3.3.88}$$

$$\begin{aligned}\mathcal{C}^*_{10} &= \Big\{\alpha(-5+3\alpha) + (1-3\alpha)\,\beta + 2\left(1-\alpha+2\alpha^2\right)\cos(2\theta_1) \\ &\quad +\left[-\alpha(1+\alpha)+(-1+3\alpha)\,\beta\right]\cos(4\theta_1) \\ &\quad +4(1-\alpha)\Big[(\alpha-1-2\beta)\pi+(\beta-\alpha)\theta_1\Big]\sin(2\theta_1) \\ &\quad +2\,(1-\alpha)\,\beta(2\pi-\theta_1)\sin(4\theta_1)\Big\}\end{aligned} \tag{3.3.89}$$

$$\begin{aligned}\mathcal{D}^*_{10} &= \Big\{4\,(-1+\alpha)\,\beta\pi + 2\,(3+\alpha)\,\beta\theta_1 + 4(1+\alpha)\Big[(\alpha-1)\pi+(\beta-\alpha)\theta_1\Big]\cos(2\theta_1) \\ &\quad +2\,(1-\alpha)\,\beta(2\pi-\theta_1)\cos(4\theta_1) + 2\left[-1+\alpha^2+(1-3\alpha)\,\beta\right]\sin(2\theta_1) \\ &\quad +\left[\alpha(1+\alpha)+(1-3\alpha)\,\beta\right]\sin(4\theta_1)\Big\}\end{aligned} \tag{3.3.90}$$

$$\mathcal{A}^*_{20} = 2(1-\alpha)\Big\{2-\alpha+\beta-2\alpha\cos(2\theta_1)+(\alpha-\beta)\cos(4\theta_1)\Big\} \tag{3.3.91}$$

$$\begin{aligned}\mathcal{B}^*_{20} &= (1-\alpha)\Big\{4\,(1-\beta)\,\pi + 2\,(-2-\alpha+\beta)\,\theta_1 + 4(\alpha-\beta)(\theta_1-2\pi)\cos(2\theta_1) \\ &\quad +2\,(\alpha-\beta)\,(2\pi-\theta_1)\cos(4\theta_1) + 2\beta\sin(2\theta_1) + (\alpha-\beta)\sin(4\theta_1)\Big\}\end{aligned} \tag{3.3.92}$$

$$\begin{aligned}\mathcal{C}^*_{20} &= -(1-\alpha)\Big\{\alpha-\beta-2\cos(2\theta_1)+(\alpha+\beta)\cos(4\theta_1) \\ &\quad +4\left[(1-\alpha+2\beta)\,\pi+(\alpha-\beta)\,\theta_1\right]\sin(2\theta_1) + 2\beta\,(-2\pi+\theta_1)\sin(4\theta_1)\Big\}\end{aligned} \tag{3.3.93}$$

$$\begin{aligned}\mathcal{D}^*_{20} &= (1-\alpha)\Big\{2\beta(2\pi-\theta_1) + 4\left[(-1+\alpha-2\beta)\,\pi+(-\alpha+\beta)\,\theta_1\right]\cos(2\theta_1) \\ &\quad +2\beta\,(2\pi-\theta_1)\cos(4\theta_1) + 2\,(-1+\alpha-\beta)\sin(2\theta_1) + (\alpha+\beta)\sin(4\theta_1)\Big\}.\end{aligned} \tag{3.3.94}$$

From Eq. (3.3.85), it follows that $\mathrm{Det}([A_0]_{8\times 8}) = 0$ if

$$\alpha = \frac{\beta[\cos(2\theta_1) - 1]}{\cos(2\theta_1)} \tag{3.3.95}$$

or

$$\alpha = \frac{\pi\cos(\theta_1)}{\pi\cos(\theta_1) - \theta_1\cos(\theta_1) + \sin(\theta_1)}. \tag{3.3.96}$$

For

$$\alpha = \frac{\beta[\cos(2\theta_1) - 1]}{\cos(2\theta_1)} \tag{3.3.97}$$

the regular stress term can be simplified as

$$\begin{aligned}\sigma_{xx10} &= \sigma_{xx20} = \frac{64\cos^2(\theta_1)[\beta + \cos(2\theta_1) - \beta\cos(2\theta_1)]}{[\cos(2\theta_1) + \beta\cos(2\theta_1) - \beta]^2}K_0 \times \\ &\times\Big\{\beta\theta_1 - 2\pi\cos(2\theta_1)(1+\beta) + \beta\cos(4\theta_1)(2\pi - \theta_1) \\ &-2\beta\sin(2\theta_1) + \beta\sin(4\theta_1)\Big\}\end{aligned} \tag{3.3.98}$$

$$\sigma_{yy10} = \sigma_{yy20} = \frac{\sin^2(\theta_1)}{\cos^2(\theta_1)}\sigma_{xx10} \tag{3.3.99}$$

$$\tau_{xy10} = \tau_{xy20} = \frac{\sin(\theta_1)}{\cos(\theta_1)}\sigma_{xx10}. \tag{3.3.100}$$

For

$$\alpha = \frac{\pi\cos(\theta_1)}{\pi\cos(\theta_1) - \theta_1\cos(\theta_1) + \sin(\theta_1)} \tag{3.3.101}$$

it holds

$$\begin{aligned}\sigma_{xx10} &= \frac{32\sin^2(\theta_1)}{[2\pi\cos(\theta_1) - \theta_1\cos(\theta_1) + \sin(\theta_1)]}K_0\Big\{2\left(\beta - \pi\theta_1 + 2\beta\pi\theta_1 - 2\beta\theta_1^2\right)\cos(3\theta_1) \\ &-2\left(\beta + \pi\theta_1 - 2\beta\pi\theta_1 + 2\beta\theta_1^2\right)\cos(\theta_1) - 2\beta\left(\pi + \theta_1\right)\sin(\theta_1) \\ &+2\beta\left(-\pi + 3\theta_1\right)\sin(3\theta_1) + [2\theta + \sin(2\theta)]\Delta_{2\pi}\Big\}\end{aligned} \tag{3.3.102}$$

$$\begin{aligned}\sigma_{yy10} &= \frac{32\sin^2(\theta_1)}{[2\pi\cos(\theta_1) - \theta_1\cos(\theta_1) + \sin(\theta_1)]}K_0\Big\{-2\pi\theta_1\cos(\theta_1) - 2\pi\theta_1\cos(3\theta_1) \\ &-2\pi\sin(\theta_1) + 2\pi\sin(3\theta_1) + [2\theta - \sin(2\theta)]\Delta_{2\pi}\Big\}\end{aligned} \tag{3.3.103}$$

$$\tau_{xx10} = \frac{32\sin^2(\theta_1)}{[2\pi\cos(\theta_1)-\theta_1\cos(\theta_1)+\sin(\theta_1)]}K_0\Big\{(\pi-\beta\pi+3\beta\theta_1)\cos(\theta_1) + (\pi+\beta\pi-3\beta\theta_1)\cos(3\theta_1)+\beta\left(-3+2\pi\theta_1-2\theta_1^2\right)\sin(\theta_1) +\beta\left(1+2\pi\theta_1-2\theta_1^2\right)\sin(3\theta_1)-\cos(2\theta)\Delta_{2\pi}\Big\} \quad (3.3.104)$$

$$\sigma_{xx20} = \frac{32\sin^2(\theta_1)[\theta_1\cos(\theta_1)-\sin(\theta_1)]}{[2\pi\cos(\theta_1)-\theta_1\cos(\theta_1)+\sin(\theta_1)]^2}K_0\times \times\Big\{2\left(\beta-2\pi^2+4\beta\pi^2+\pi\theta_1-6\beta\pi\theta_1+2\beta\theta_1^2\right)\cos(\theta_1) +2\left(-\beta-2\pi^2+4\beta\pi^2+\pi\theta_1-6\beta\pi\theta_1+2\beta\theta_1^2\right)\cos(3\theta_1) +2\beta\,(-3\pi+\theta_1)\sin(\theta_1)+2\beta\,(5\pi-3\theta_1)\sin(3\theta_1)-[2\theta+\sin(2\theta)]\Delta_{2\pi}\Big\} \quad (3.3.105)$$

$$\sigma_{yy20} = \frac{32\sin^2(\theta_1)[\theta_1\cos(\theta_1)-\sin(\theta_1)]}{[2\pi\cos(\theta_1)-\theta_1\cos(\theta_1)+\sin(\theta_1)]^2}K_0\Big\{2\pi\,(-2\pi+\theta_1)\cos(\theta_1) +2\pi\,(-2\pi+\theta_1)\cos(3\theta_1)+2\pi\sin(\theta_1)-2\pi\sin(3\theta_1)-[2\theta-\sin(2\theta)]\Delta_{2\pi}\Big\} \quad (3.3.106)$$

$$\tau_{xy20} = \frac{32\sin^2(\theta_1)[\theta_1\cos(\theta_1)-\sin(\theta_1)]}{[2\pi\cos(\theta_1)-\theta_1\cos(\theta_1)+\sin(\theta_1)]^2}K_0\Big\{(-\pi+5\beta\pi-3\beta\theta_1)\cos(\theta_1) + (-\pi-5\beta\pi+3\beta\theta_1)\cos(3\theta_1)+\beta\left(3+4\pi^2-6\pi\theta_1+2\theta_1^2\right)\sin(\theta_1) +\beta\left(-1+4\pi^2-6\pi\theta_1+2\theta_1^2\right)\sin(3\theta_1)+\cos(2\theta)\Delta_{2\pi}\Big\} \quad (3.3.107)$$

with

$$\Delta_{2\pi} = (\pi+\beta\pi-\beta\theta_1)\cos(\theta_1)+(\pi-\beta\pi+\beta\theta_1)\cos(3\theta_1)+3\beta\sin(\theta_1)-\beta\sin(3\theta_1). \quad (3.3.108)$$

3.3.7 Joint with $\theta_1 = \pi$ and θ_2 being Arbitrary

For a joint geometry with $\theta_1 = \pi$ and θ_2 being arbitrary (see Fig. 3.7),

$$\mathrm{Det}([A_0]_{8\times8}) = \frac{64}{(1+\alpha)^2}(1-\alpha)\sin(\theta_2)\Big\{\pi\cos(\theta_2)+\alpha\,\pi\cos(\theta_2)-\theta_2\cos(\theta_2) +\alpha\,\theta_2\cos(\theta_2)+\sin(\theta_2)-\alpha\sin(\theta_2)\Big\} \quad (3.3.109)$$

or

$$\begin{aligned}\mathrm{Det}([A_0]_{8\times 8}) &= \frac{64}{(1+\alpha)^2}\sin(\theta_2)\Big\{\pi\cos(\theta_2)-\theta_2\cos(\theta_2)+\sin(\theta_2)\\ &\quad -\alpha^2\Big[\pi\ \cos(\theta_2)+\theta_2\ \cos(\theta_2)-\sin(\theta_2)\Big]\\ &\quad +2\alpha\ \Big[\theta_2\ \cos(\theta_2)-\sin(\theta_2)\Big]\Big\}. \end{aligned} \tag{3.3.110}$$

For the given joint geometries ($\theta_1 = 30°, 45°, 60°, 75°, 90°, 120°, 135°, 150°$), the possible material combinations, which satisfy $\mathrm{Det}([A_0]_{8\times 8}) = 0$, are plotted in Fig. 3.16.
In case of $\mathrm{Det}([A_0]_{8\times 8}) = 0$, the nonzero coefficients $\mathcal{A}^*_{\mathrm{k}0}, \mathcal{B}^*_{\mathrm{k}0}, \mathcal{C}^*_{\mathrm{k}0}, \mathcal{D}^*_{\mathrm{k}0}$ are

$$\mathcal{A}^*_{10} = 4(1+\alpha)\,(1-\alpha)\sin^2(\theta_2) \tag{3.3.111}$$

$$\begin{aligned}\mathcal{B}^*_{10} &= (1+\alpha)\Big\{2\,(-1+\alpha-2\beta)\,\pi+2\,[2\,(-\alpha+\beta)\,\pi+(1-\alpha)\,\theta_2]\cos(2\theta_2)\\ &\quad -(1-\alpha)\sin(2\theta_2)\Big\}\end{aligned} \tag{3.3.112}$$

$$\mathcal{C}^*_{10} = 2(1-\alpha)\sin(\theta_2)\Big\{2\,[(1+\alpha)\,\pi+(-1+\alpha)\,\theta_2]\cos(\theta_2)+(1-3\alpha)\sin(\theta_2)\Big\} \tag{3.3.113}$$

$$\mathcal{D}^*_{10} = (1+\alpha)\Big\{4\beta\pi+2\,[(1+\alpha-2\beta)\,\pi+(-1+\alpha)\,\theta_2]\cos(2\theta_2)+(1-\alpha)\sin(2\theta_2)\Big\} \tag{3.3.114}$$

$$\mathcal{A}^*_{20} = 4(1-\alpha)^2\sin^2(\theta_2) \tag{3.3.115}$$

$$\mathcal{B}^*_{20} = -(1-\alpha)\Big\{2\,(1+\alpha)\,\pi+2\,(-1+\alpha)\,\theta_2\cos(2\theta_2)+(1-\alpha)\sin(2\theta_2)\Big\} \tag{3.3.116}$$

$$\mathcal{C}^*_{20} = 2(1-\alpha)\sin(\theta_2)\Big\{2\,[(1+\alpha)\,\pi+(-1+\alpha)\,\theta_2]\cos(\theta_2)+(1-\alpha)\sin(\theta_2)\Big\} \tag{3.3.117}$$

$$\mathcal{D}^*_{20} = (1-\alpha)\Big\{2\,[(1+\alpha)\,\pi+(-1+\alpha)\,\theta_2]\cos(2\theta_2)+(1-\alpha)\sin(2\theta_2)\Big\}. \tag{3.3.118}$$

From Eq. (3.3.109) or Eq. (3.3.110), it follows that $\mathrm{Det}([A_0]_{8\times 8}) = 0$ if

$$\alpha = 1 \tag{3.3.119}$$

or

$$\alpha = -\frac{(\pi-\theta_2)\cos(\theta_2)+\sin(\theta_2)}{(\pi+\theta_2)\cos(\theta_2)-\sin(\theta_2)}. \tag{3.3.120}$$

For

$$\alpha = -\frac{(\pi-\theta_2)\cos(\theta_2)+\sin(\theta_2)}{(\pi+\theta_2)\cos(\theta_2)-\sin(\theta_2)}, \tag{3.3.121}$$

the regular stress term in Cartesian coordinates can be simplified as

$$\begin{aligned}\sigma_{xx10} &= \frac{32\pi\sin^2(\theta_2)K_0}{\theta_2\cos(\theta_2)-\sin(\theta_2)}\Big\{2\theta\cos(\theta_2)+\cos(\theta_2)\sin(2\theta)\\ &\quad -2(1-2\beta)\sin(\theta_2)-2(\pi+2\beta\pi+2\beta\theta_2)\cos(\theta_2)\Big\}\end{aligned} \tag{3.3.122}$$

$$\sigma_{yy10} = \frac{32\pi\cos(\theta_2)\sin^2(\theta_2)K_0}{\theta_2\cos(\theta_2)-\sin(\theta_2)}\Big\{-2\pi+2\theta-\sin(2\theta)\Big\} \tag{3.3.123}$$

$$\tau_{xy10} = \frac{64\pi\cos(\theta_2)\sin^2(\theta_2)K_0}{\theta_2\cos(\theta_2)-\sin(\theta_2)}\sin^2(\theta) \tag{3.3.124}$$

$$\sigma_{xx20} = \frac{8\pi^2\sin^2(2\theta_2)K_0}{[\theta_2\cos(\theta_2)-\sin(\theta_2)]^2}\Big\{-2\theta_2+2\theta+\sin(2\theta)\Big\} \tag{3.3.125}$$

$$\begin{aligned}\sigma_{yy20} &= \frac{32\pi^2\cos(\theta_2)\sin^2(\theta_2)K_0}{[\theta_2\cos(\theta_2)-\sin(\theta_2)]^2}\Big\{2\theta\cos(\theta_2)-2\theta_2\cos(\theta_2)\\ &\quad -\cos(\theta_2)\sin(2\theta)+2\sin(\theta_2)\Big\}\end{aligned} \tag{3.3.126}$$

$$\tau_{xx20} = \frac{16\pi^2\sin^2(2\theta_2)K_0}{[\theta_2\cos(\theta_2)-\sin(\theta_2)]^2}\sin^2(\theta) \tag{3.3.127}$$

where $\theta_2\cos(\theta_2)-\sin(\theta_2)\neq 0$, i.e. $\alpha\neq -1$.
For $\alpha = 1$,

$$\begin{aligned}\sigma_{xx10} &= 64\pi K_0[-\beta-\cos(2\theta_2)+\beta\cos(2\theta_2)]\\ \sigma_{xx20} &= 0\\ \sigma_{yy10} &= \sigma_{yy20}=\sigma_{xy10}=\sigma_{xy20}=0.\end{aligned} \tag{3.3.128}$$

3.3.8 Joint with $\theta_1 = -\theta_2 = \pi$

For a joint geometry with $\theta_1 = -\theta_2 = \pi$ (see Fig. 3.8), there is always

$$\mathrm{Det}([A_0]_{8\times 8}) = 0 \tag{3.3.129}$$

according to Eq. (3.3.31) or (3.3.32) or (3.3.85) or (3.3.86). This means that for a joint with an interface crack, in general, the regular stress is nonzero. The nonzero coefficients $\mathcal{A}^*_{\mathrm{k}0}, \mathcal{B}^*_{\mathrm{k}0}, \mathcal{C}^*_{\mathrm{k}0}, \mathcal{D}^*_{\mathrm{k}0}$ are

$$\mathcal{A}^*_{10} = \mathcal{C}^*_{10} = \mathcal{A}^*_{20} = \mathcal{C}^*_{20} = 0 \tag{3.3.130}$$

$$\mathcal{B}^*_{10} = -\mathcal{D}^*_{10} = \frac{1+\alpha}{\alpha - 1} \tag{3.3.131}$$

$$\mathcal{B}^*_{20} = -\mathcal{D}^*_{20} = -1, \tag{3.3.132}$$

for $\alpha \neq 1$.
The regular stress term in Cartesian coordinates is

$$\begin{aligned} \sigma_{xx10} &= 4K_0\mathcal{B}^*_{10} = \frac{4\mathrm{K}_0(1+\alpha)}{\alpha - 1} \\ \sigma_{xx20} &= 4K_0\mathcal{B}^*_{20} = -4\mathrm{K}_0 \\ \sigma_{yy10} &= \sigma_{yy20} = \sigma_{xy10} = \sigma_{xy20} = 0. \end{aligned} \tag{3.3.133}$$

3.3.9 Joint with $\theta_1 = -\theta_2 = \pi/2$

For a joint geometry with $\theta_1 = -\theta_2 = \pi/2$ (see Fig. 3.9),

$$\mathrm{Det}([A_0]_{8\times 8}) = \frac{256\alpha}{(1+\alpha)^2}(2\beta - \alpha) \tag{3.3.134}$$

according to Eq. (3.3.31) or (3.3.32) or (3.3.51) or (3.3.52). It can be seen that if $\alpha = 2\beta$, or $\alpha = 0$ and β is arbitrary (see Fig. 3.13 for $\theta_1 = 90°$), the regular stress is nonzero. The nonzero coefficients $\mathcal{A}^*_{\mathrm{k}0}, \mathcal{B}^*_{\mathrm{k}0}, \mathcal{C}^*_{\mathrm{k}0}$, and $\mathcal{D}^*_{\mathrm{k}0}$ in case of $\alpha = 2\beta$ are:

$$\begin{aligned} \mathcal{A}^*_{10} &= \mathcal{C}^*_{10} = \mathcal{A}^*_{20} = \mathcal{C}^*_{20} = 0 \\ \mathcal{B}^*_{10} &= \mathcal{D}^*_{10} = \mathcal{B}^*_{20} = \mathcal{D}^*_{20} = 1. \end{aligned} \tag{3.3.135}$$

The regular stress term in Cartesian coordinates is

$$\begin{aligned} \sigma_{yy10} &= \sigma_{yy20} = 4K_0 \\ \sigma_{xx10} &= \sigma_{xx20} = \sigma_{xy10} = \sigma_{xy20} = 0. \end{aligned} \tag{3.3.136}$$

For $\alpha = 0$ and β being arbitrary, the coefficients are

$$\begin{aligned} \mathcal{A}^*_{10} &= \mathcal{A}^*_{20} = 16\beta \\ \mathcal{B}^*_{10} &= \mathcal{D}^*_{20} = -2\pi(1+2\beta) \\ \mathcal{C}^*_{10} &= \mathcal{C}^*_{20} = 8\beta \\ \mathcal{D}^*_{10} &= \mathcal{B}^*_{20} = 2\pi(2\beta - 1) \end{aligned} \tag{3.3.137}$$

Short summary: For a joint with free edges under remote mechanical loading, the regular stress term is zero for most joint geometries and material combinations. In case of the regular stress term being nonzero, it can be calculated analytically with one arbitrary constant, which has to be determined from the stress analysis of the total joint, as for the determination of the stress intensity factors.

3.4 Determination of the Stress Intensity Factor

From the earlier sections it is known that in a two dissimilar materials joint the stresses near the singular point can be described analytically by

$$\sigma_{ij}(r,\theta) = \sum_{n=1}^{N} \frac{K_n}{\bar{r}^{\omega_n}} f_{ijn}(\theta) + \sigma_{ij0}(\theta) \tag{3.4.1}$$

for a joint with real eigenvalues and by

$$\begin{aligned} \sigma_{ij}(r,\theta) &= \sum_{n=1}^{N} \frac{K_n}{\bar{r}^{\omega_n}} \Big\{ \cos[p_n ln(\bar{r})] f^c_{ijn}(\theta) \\ &\qquad + \sin[p_n \ln(\bar{r})] f^s_{ijn}(\theta) \Big\} + \sigma_{ij0}(\theta) \end{aligned} \tag{3.4.2}$$

for a joint with complex eigenvalues, where for thermal loading

$$\sigma_{ij0}(\theta) = \sigma_0 f_{ij0}(\theta) \tag{3.4.3}$$

and for remote mechanical loading

$$\sigma_{ij0}(\theta) = K_0 f_{ij0}(\theta) \tag{3.4.4}$$

apply. The quantity σ_0 can be determined analytically, however, K_0 has to be determined by using the stress analysis of the total joint.
In Section 3.1 the singular stress exponent ω_n, the imaginary part p_n and the corresponding angular functions $f_{ijn}(\theta), f^c_{ijn}(\theta), f^s_{ijn}(\theta)$, which are independent of loading, have been studied in details. The regular stress term $\sigma_0 f_{ij0}(\theta)$ for thermal loading has been presented in Section 3.2. In Section 3.3 the regular stress term $K_0 f_{ij0}(\theta)$ for remote mechanical loading has been discussed. All the quantities in Eqs. (3.4.1) and (3.4.2), except the stress intensity factors K_n and K_0 for a remote mechanical loading, can be calculated analytically. To determine the stress intensity factors K_n and K_0,

the stress analysis of the total joint has to be done by using a numerical method, e.g., the Finite Element Method (FEM), the Boundary Element Method (BEM), or the boundary collocation method.

If there is only one unknown in Eq. (3.4.1) or Eq. (3.4.2), it is easy to determine the stress intensity factor K. For each point with (r,θ) near the singular point it holds

$$K = \frac{\sigma_{ij}^{FEM}(r,\theta) - \sigma_0 f_{ij0}(\theta)}{f_{ij}(\theta)} \bar{r}^{\omega} \tag{3.4.5}$$

for a real eigenvalue or

$$K = \frac{\sigma_{ij}^{FEM}(r,\theta) - \sigma_0 f_{ij0}(\theta)}{\cos[p\ln(\bar{r})] f_{ij}^{c}(\theta) + \sin[p\ln(\bar{r})] f_{ij}^{s}(\theta)} \bar{r}^{\omega} \tag{3.4.6}$$

for a complex eigenvalue. The averaged value of M points can be taken as the K-value of the problem.
If there are more than one unknown in Eq. (3.4.1) or Eq. (3.4.2), the least square method has to be used to determine the stress intensity factors at the same time. Methods to determine the unknowns are presented below for different cases.

3.4.1 Joint under Remote Mechanical Loading or after Homogeneous Temperature Change

In Eq. (3.4.1) or Eq. (3.4.2) the left side is known from the FEM. To determine all unknowns at the same time, following the least square method, the quantity Π_{ij} is defined as

$$\Pi_{ij} = \sum_{l=1}^{M} \left\{ \sigma_{ij}^{FEM}(r_l,\theta_l) - \sigma_{ij}^{known}(r_l,\theta_l) - \sum_{n=\xi}^{N} \frac{K_n}{\bar{r}_l^{\omega_n}} f_{ijn}(\theta_l) \right\}^2 \tag{3.4.7}$$

for the real eigenvalue or

$$\begin{aligned} \Pi_{ij} \;=\; & \sum_{l=1}^{M} \Bigg\{ \sigma_{ij}^{FEM}(r_l,\theta_l) - \sigma_{ij}^{known}(r_l,\theta_l) - \\ & - \sum_{n=\xi}^{N} \frac{K_n}{\bar{r}_l^{\omega_n}} \Big\{ \cos[p_n \ln(\bar{r}_l)] f_{ijn}^{c}(\theta_l) + \sin[p_n \ln(\bar{r}_l)] f_{ijn}^{s}(\theta_l) \Big\} \Bigg\}^2 \end{aligned} \tag{3.4.8}$$

for the complex eigenvalue, where ij=rr,$\theta\theta$ and rθ, M is the number of points used for determining K_n. $\sigma_{ij}^{known}(r_l,\theta_l)$ is one term on the righthand side of Eq. (3.4.1) or

Eq.(3.4.2), which can be determined analytically. For example, for a joint under thermal loading, it holds

$$\sigma_{ij}^{known}(r_l, \theta_l) = \sigma_0 f_{ij0}(\theta_l) \tag{3.4.9}$$

and $\xi = 1$. For a joint under remote mechanical loading, the factor K_0 in regular stress term is unknown. Therefore

$$\sigma_{ij}^{known}(r_l, \theta_l) = 0 \tag{3.4.10}$$

$\xi = 0$ and $\omega_0 = 0$.
According to the least square method, the minimum of Π_{ij} with respect to the values of K_n has to be found. It is given by

$$\frac{\partial \Pi_{ij}}{\partial K_n} = 0 \quad (n = \xi, ..., N). \tag{3.4.11}$$

This leads to N (or N+1) equations

$$\sum_{n=\xi}^{N} K_n \sum_{l=1}^{M} \frac{1}{\bar{r}_l^{\omega_n+\omega_q}} f_{ijn}(\theta_l) f_{ijq}(\theta_l) = \sum_{l=1}^{M} \Big[\sigma_{ij}^{FEM}(r_l, \theta_l) - \sigma_{ij}^{known}(r_l, \theta_l)\Big] \frac{1}{\bar{r}_l^{\omega_q}} f_{ijq}(\theta_l)$$
$$(q = \xi, ..., N), \tag{3.4.12}$$

for the real eigenvalue or

$$\begin{aligned}
&\sum_{n=\xi}^{N} K_n \sum_{l=1}^{M} \frac{1}{\bar{r}_l^{\omega_n+\omega_q}} \Big\{ \cos[p_n \ln(\bar{r}_l)] f_{ijn}^{c}(\theta_l) + \sin[p_n \ln(\bar{r}_l)] f_{ijn}^{s}(\theta_l) \Big\} \times \\
&\quad \times \Big\{ \cos[p_q \ln(\bar{r}_l)] f_{ijq}^{c}(\theta_l) + \sin[p_q \ln(\bar{r}_l)] f_{ijq}^{s}(\theta_l) \Big\} \\
&= \sum_{l=1}^{M} \Big[\sigma_{ij}^{FEM}(r_l, \theta_l) - \sigma_{ij}^{known}(r_l, \theta_l)\Big] \frac{1}{\bar{r}_l^{\omega_q}} \times \\
&\quad \times \Big\{ \cos[p_q \ln(\bar{r}_l)] f_{ijq}^{c}(\theta_l) + \sin[p_q \ln(\bar{r}_l)] f_{ijq}^{s}(\theta_l) \Big\} \qquad (q = \xi, ..., N).
\end{aligned} \tag{3.4.13}$$

for the complex eigenvalue. The values of K_n are obtained by solving these equations. For a joint under remote mechanical loading the stress intensity factors K_n are proportional to the remote loading (e.g. σ_∞). For a joint after a homogeneous temperature change, K_n is proportional to the temperature change (T).

3.4.2 Joint after an Inhomogeneous Temperature Change

For a joint after an inhomogeneous temperature change, the stresses near the singular point can also be described by Eq. (3.4.1) or Eq. (3.4.2). However, the regular stress

term $\sigma_0 f_{ij0}(\theta)$ is not the same as that one given in Section 3.2 for a homogeneous temperature change.
In general, the temperature change may be arbitrary. In this section we consider the case in which the temperature change only takes place in the direction perpendicular to the interface of the joint, i.e. $T = f(y)$. The function f(y) may be continuous or non-continuous at the interface. As most functions can be expanded in a polynomial, for convenience, we consider the temperature change in a polynomial as

$$T_k(y) = \sum_{i=0}^{I} \chi_{ik}(y/H_k)^i \tag{3.4.14}$$

where H_k (k=1,2) is the thickness of the k-th material and χ_{ik} is the coefficient of the polynomial (unit in °K) while y denotes the coordinates (see Fig. 3.1). The temperature change at the interface in material 1 is $T_1(y = 0) = \chi_{01}$ and in material 2 $T_2(y = 0) = \chi_{02}$. For $\chi_{01} = \chi_{02}$ a continuous temperature change takes place at the interface.

For the temperature change described in Eq. (3.4.14), the regular stress term can be calculated from the equations given in Section 3.2 by replacing $\bar{q}$ in Eq. (3.2.66) or Eq. (3.2.67) by

$$\bar{q} = \frac{\chi_{01}\alpha_1 - \chi_{02}\alpha_2}{\frac{1}{E_1} + \frac{1}{E_2}} = (\chi_{01}\alpha_1 - \alpha_2\chi_{02})E_2\frac{\alpha + 1}{2} \tag{3.4.15}$$

for plane stress and

$$\bar{q} = \frac{\chi_{01}(1 + \nu_1)\alpha_1 - \chi_{02}(1 + \nu_2)\alpha_2}{\frac{1-\nu_1^2}{E_1} + \frac{1-\nu_2^2}{E_2}} = \left[\chi_{01}(1 + \nu_1)\alpha_1 - \chi_{02}(1 + \nu_2)\alpha_2\right]\frac{E_2}{1 - \nu_2^2}\,\frac{\alpha + 1}{2} \tag{3.4.16}$$

for plane strain [133].
In the following sections, it is assumed that the temperature change is known. By fitting the well-known temperature change in a polynomial, the coefficients χ_{ik} can be determined.

In principle, the stress intensity factor for a given temperature change can also be determined by using the method presented in Section 3.4.1 directly, but the relation between the temperature change and the stress intensity factor is not clear. To obtain a more general relation between the temperature change and the stress intensity factor, we determine the stress intensity factor in another way.

If the temperature change can be described by a linear superposition of different terms, as given in Eq. (3.4.14), in linear elasticity the stresses and the stress intensity factors can be obtained by a linear superposition of the corresponding results. Therefore,

for a given joint geometry and material combination calculations were performed for the case of temperature changes, which are $T = 0$ in one material and a power law (i.e.,$\chi_{ik}(y/H_k)^i$) in another material. These temperature changes are described only by the coefficient χ_{ik}. For each temperature change (i.e., $T_1(y) = 0$ and $T_2(y) = \chi_{i2}(y/H_2)^i$ or $T_2(y) = 0$ and $T_1(y) = \chi_{i1}(y/H_1)^i$) we can use the method given in Section 3.4.1 to determine the corresponding stress intensity factor (i.e., K_{i2} or K_{i1}). The stress intensity factor K_{i2} *or* K_{i1} is proportional to the coefficient χ_{i2} or χ_{i1}. The factor of proportionality is denoted as $\mathcal{K}_{\mathrm{ik}}$, i.e. $K_{ik} = \mathcal{K}_{\mathrm{ik}}\chi_{\mathrm{ik}}$ (k=1,2 and i=0,1,2,...,I). For the temperature change given in Eq. (3.4.14) the total stress intensity factor can be calculated from

$$K = \sum_{k=1}^{2}\sum_{i=0}^{I} \mathcal{K}_{\mathrm{ik}}\chi_{\mathrm{ik}}. \tag{3.4.17}$$

In case of $\chi_{01} = \chi_{02}$ it holds

$$K = K_h T + \sum_{k=1}^{2}\sum_{i=1}^{I} \mathcal{K}_{\mathrm{ik}}\chi_{\mathrm{ik}} \tag{3.4.18}$$

where K_h is the stress intensity factor for a homogeneous temperature change of 1 Kelvin, and T is the temperature change at the interface [133]. In Eq. (3.4.17) or Eq. (3.4.18) the quantities $\mathcal{K}_{\mathrm{ik}}$ are dependent on the material combination and the overall geometry, i.e., $\theta_1, \theta_2, H_1/L, H_2/L$. They have to be determined from FEM for the corresponding temperature change $\chi_{ik}(y/H_k)^i$. As long as the coefficients $\mathcal{K}_{\mathrm{ik}}$ for a given material combination and given geometry have been determined for a given temperature change, the stress intensity factor can be calculated from Eq. (3.4.17) or Eq. (3.4.18) for an arbitrary temperature change as described by Eq. (3.4.14) (i.e. with arbitrary χ_{ik}) without further FEM calculation.

3.5 The Characteristics of the Eigenvalues and the Stress Intensity Factors

To describe the stress field near the singular point, the quantities ω_n, p_n, $f_{ijn}(\theta)$, $f^c_{ijn}(\theta)$, $f^s_{ijn}(\theta)$, $\sigma_0, f_{ij0}(\theta), K_n$ are needed (see Eqs. (3.0.1) and (3.0.2)). The general equation to determine the eigenvalues (ω_n, p_n) of the singularity problem is given in Section 3.1 as a function of the Dundurs parameter α and β. Since Eq. (3.1.37) or Eq. (3.1.38) is a transcendental equation of λ_n or s_n, it has to be solved numerically. In Section 3.5.1 the characteristics of the eigenvalues, e.g. the number of singular terms, the eigenvalues being real or complex, and so on, will be shown for some special geometries.

The angular functions $f_{ijn}(\theta)$, $f^c_{ijn}(\theta)$, $f^s_{ijn}(\theta)$, and $f_{ij0}(\theta)$ have the following mathematical expressions:

$$f_{ij}(\theta) = A\sin(\omega\theta) + B\cos(\omega\theta) + C\sin[(2-\omega)\theta] + D\cos[(2-\omega)\theta] \tag{3.5.1}$$

for real eigenvalues (see Section 3.1.1) and

$$\begin{aligned} f_{ij}^{s}(\theta), f_{ij}^{c}(\theta) &= e^{-p_n\theta}\Big\{A\sin(\omega\theta) + B\cos(\omega\theta) + C\sin[(2-\omega)\theta] + D\cos[(2-\omega)\theta]\Big\} \\ &+ e^{p_n\theta}\Big\{A_p\sin(\omega\theta) + B_p\cos(\omega\theta) + C_p\sin[(2-\omega)\theta] + D_p\cos[(2-\omega)\theta]\Big\} \end{aligned} \tag{3.5.2}$$

for complex eigenvalues (see Section 3.1.2) and

$$f_{ij0}(\theta) = A_0\theta + B_0 + C_0\sin(2\theta) + D_0\cos(2\theta) \tag{3.5.3}$$

for the regular stress term (see Sections 3.2 and 3.3), where the constants A, B, C, D, A_p, B_p, C_p, and D_p are functions of ω, p_n, $\theta_1, \theta_2, \alpha$, and β, but A_0, B_0, C_0, D_0 only depend on $\theta_1, \theta_2, \alpha$, and β. As far as their mathematical expression is concerned, the characteristics of the angular functions are clear.
In the regular stress term $\sigma_0 f_{ij0}(\theta)$, σ_0 can be calculated analytically for thermal loading, whereas for remote mechanical loading σ_0 (in Section 3.3 denoted as K_0) has to be determined numerically by using the stress analysis of the overall joint.
In general, the factors K_n for the singular terms have to be determined numerically from the stress field of the total joint. The characteristics of K_n will be shown in Section 3.5.2. For the joint geometry with $\theta_1 = -\theta_2 = 90°$, in particular, some empirical equations will be given to calculate the K - factor without using FEM.

3.5.1 The Behaviors of the Eigenvalues

For a given joint geometry, if the behavior of the eigenvalue versus the material data is known, the material combination can be found, which produces no stress singularity or the singularity is weaker. The characteristics of the eigenvalues, e.g. with which material combinations and joint geometries the eigenvalues are real only, or complex only, or real and complex; which joint has only one singular stress term and which joint has more than one singular terms; in which case the singular stress exponent is larger than 0.5 (a homogeneous material with a crack having a singular exponent equal to 0.5), and so on, will be shown for 7 joint geometries, which often appear in engineering structures. These informations are useful for the material selection.

For a joint with $\theta_1 = -\theta_2 = 90°$ (see Fig. 3.9), the stress exponent $\omega_n = s_n + 2$ can be determined from (see Section 3.1)

$$\begin{aligned} det[A] &= \Big\{\beta\cos^2(\frac{\pi}{2}s_n) + (\alpha-\beta)(s_n+1)^2\Big\}^2 \\ &+ \sin^2(\frac{\pi}{2}s_n)\cos^2(\frac{\pi}{2}s_n) - \alpha^2(s_n+1)^2 = 0. \end{aligned} \tag{3.5.4}$$

The second-order eigenvalue can be determined from

$$\frac{d(det[A])}{ds_n} = \Big[\Big(-(s_n+1)^2\alpha\beta + (1/2+s_n^2+2s_n)\beta^2\Big)\sin(\pi s_n) + 1/4(1-\beta^2)\sin(2\pi s_n)\Big]\pi$$
$$+ \quad 2(s_n+1)\Big[\beta(\alpha-\beta)\cos(\pi s_n) + (2s_n^2+4s_n+1)\alpha^2 - (2s_n+3)(2s_n+1)\alpha\beta$$
$$+ \quad (2s_n^2+4s_n+1)\beta^2\Big] = 0. \qquad (3.5.5)$$

The isoline of the stress exponent ($-0.5 \leq \omega \leq 1$) is plotted in a Dundurs diagram in Fig. 3.17. It can be seen that: (a) For all material combinations there is only one singular term. (b) Along the lines of $\alpha = 0$ and $\beta = \alpha/2$ (they are plotted in the figure as dotted lines), zero is the second-order eigenvalue. In fact, for $s_n = -2$ (i.e. $\omega_0 = 0$) d(det[A])/d(s_n) $=2\alpha(\alpha - 2\beta)$ (see Eq. (3.5.5)) (c) There are a lot of material combinations, in which the stress exponent is negative, i.e. there is no stress singularity. (d) There is only a very small range in the Dundurs diagram where the eigenvalues are complex, but they are not singular stress term. This means that for this joint geometry the singular stress term is always corresponding to a real eigenvalue.

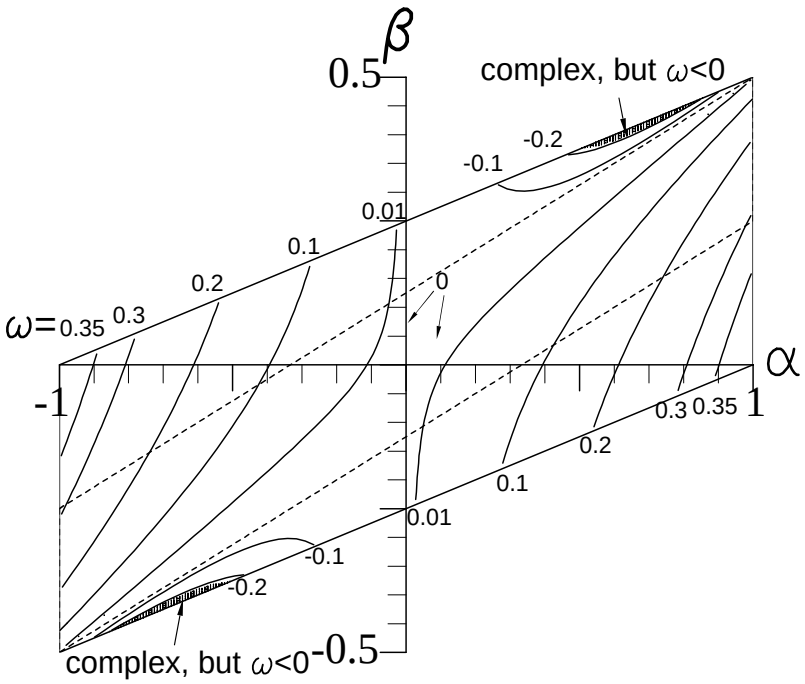

Figure 3.17: Stress exponent distribution in a Dundurs diagram for a joint with $\theta_1 = -\theta_2 = 90°$.

For a joint with $\theta_1 = 120°$ and $\theta_2 = -60°$ (see Fig. 3.18), the isoline of the stress exponent ($-0.5 \leq \omega \leq 1$) is plotted in Fig. 3.19. It is obvious that: (a) For most material combinations there is only one singular term, however, in a small area of α and β there are two singular terms (see Fig. 3.19, where the positive isoline is interest). (b) Along the lines $\beta = \alpha/3$ and $\alpha \approx -0.69638$ (they are plotted in the figure as dotted lines), zero is the second order eigenvalue. (c) There are a lot of material combinations,

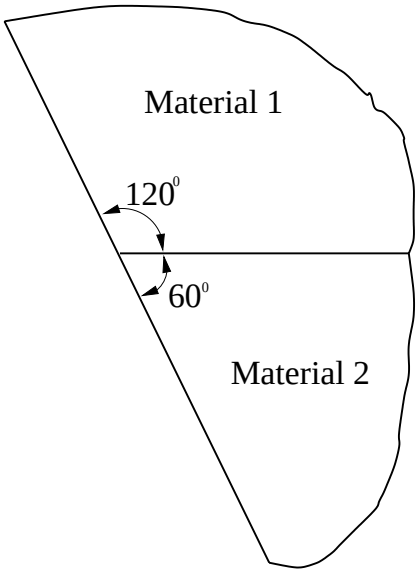

Figure 3.18: A joint with $\theta_1 = 120°$ and $\theta_2 = -60°$.

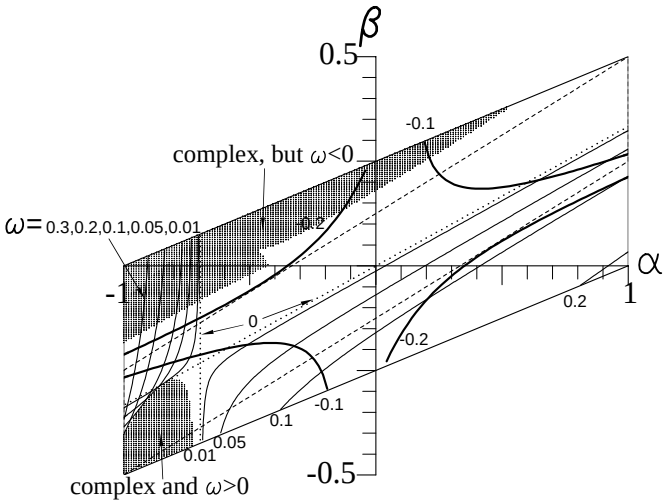

Figure 3.19: Stress exponent distribution in a Dundurs diagram for a joint with $\theta_1 = 120°$ and $\theta_2 = -60°$.

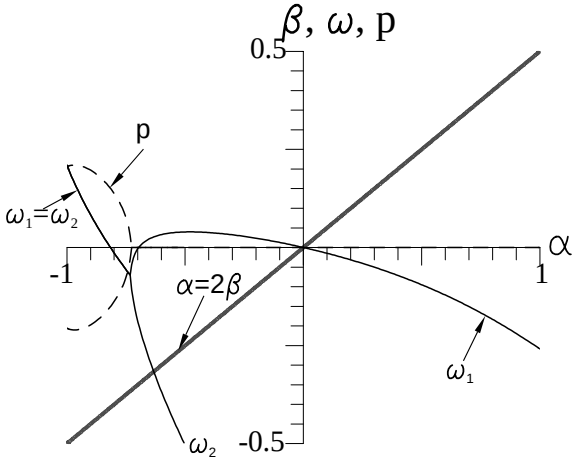

Figure 3.20: Stress exponent distribution for material combinations along the line of $\alpha = 2\beta$ in a joint with $\theta_1 = 120°$ and $\theta_2 = -60°$.

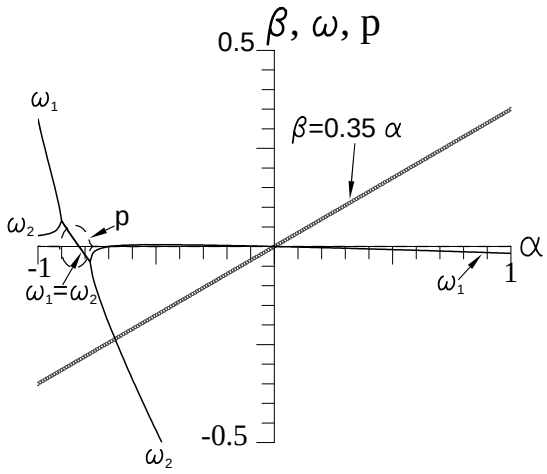

Figure 3.21: Stress exponent distribution for material combinations along the line of $\beta = 0.35\alpha$ in a joint with $\theta_1 = 120°$ and $\theta_2 = -60°$.

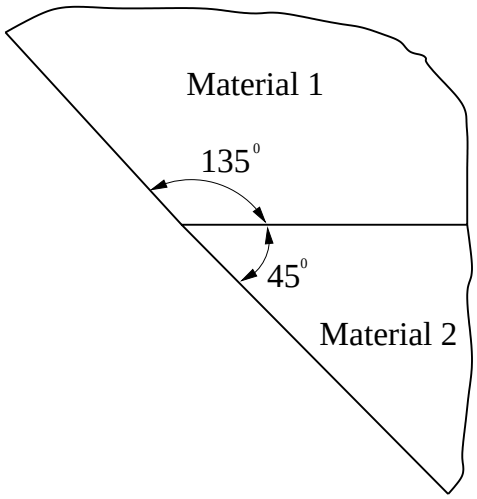

Figure 3.22: A joint with $\theta_1 = 135°$ and $\theta_2 = -45°$.

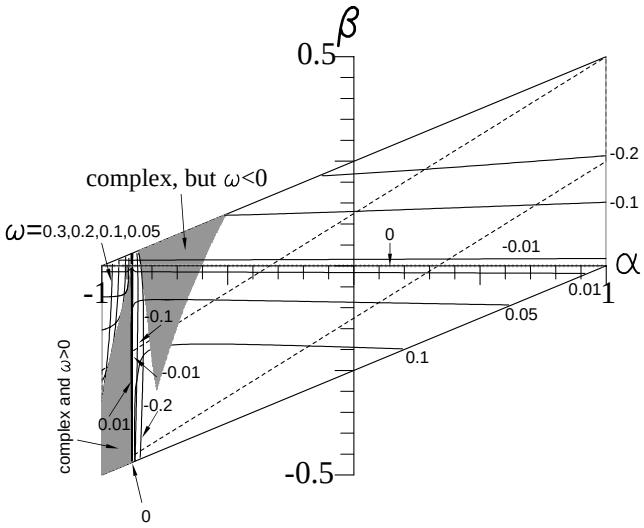

Figure 3.23: Stress exponent distribution in a Dundurs diagram for a joint with $\theta_1 = 135°$ and $\theta_2 = -45°$.

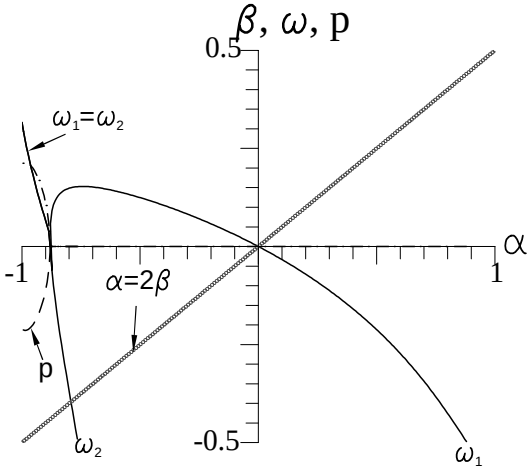

Figure 3.24: Stress exponent distribution for material combinations along the line of $\alpha = 2\beta$ in a joint with $\theta_1 = 135°$ and $\theta_2 = -45°$.

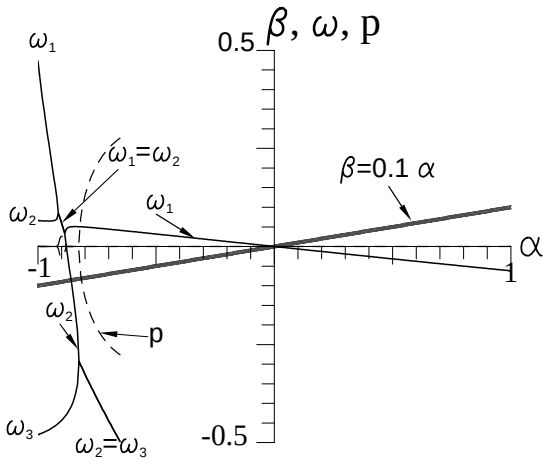

Figure 3.25: Stress exponent distribution for material combinations along the line of $\beta = 0.1\alpha$ in a joint with $\theta_1 = 135°$ and $\theta_2 = -45°$.

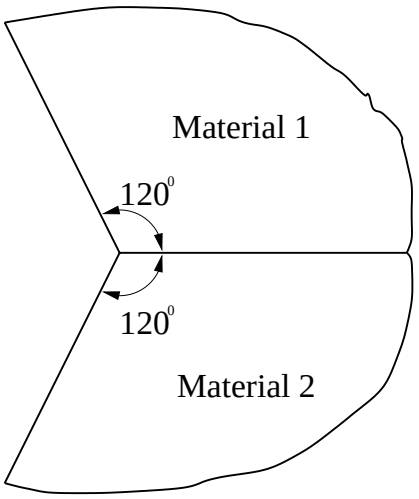

Figure 3.26: A joint with $\theta_1 = 120°$ and $\theta_2 = -120°$.

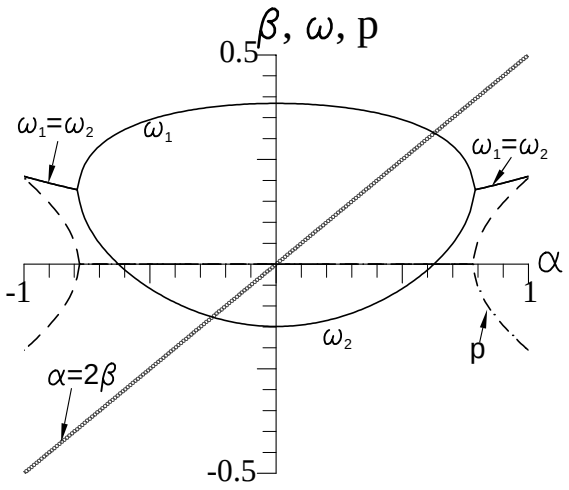

Figure 3.27: Stress exponent distribution for material combinations along the line of $\alpha = 2\beta$ in a joint with $\theta_1 = 120°$ and $\theta_2 = -120°$.

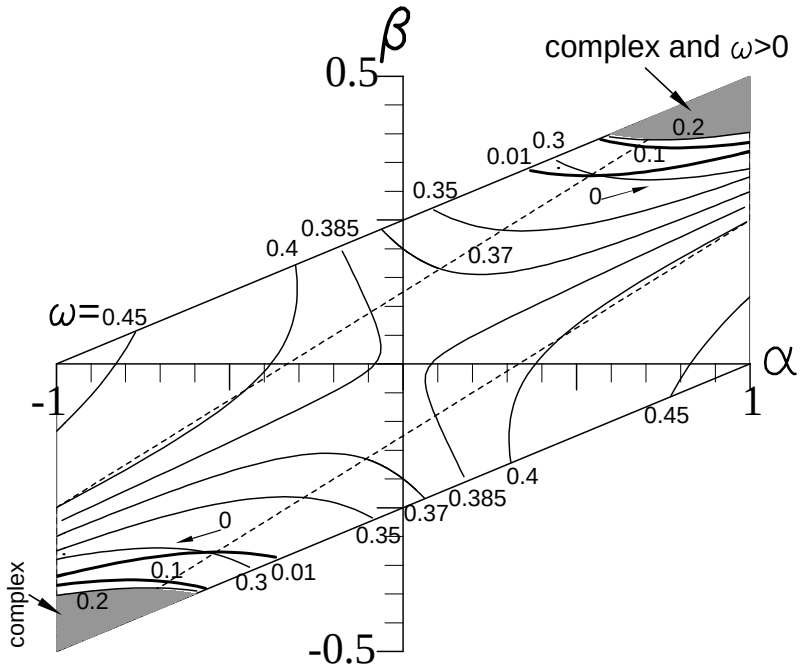

Figure 3.28: Stress exponent distribution in a Dundurs diagram for a joint with $\theta_1 = -\theta_2 = 120°$.

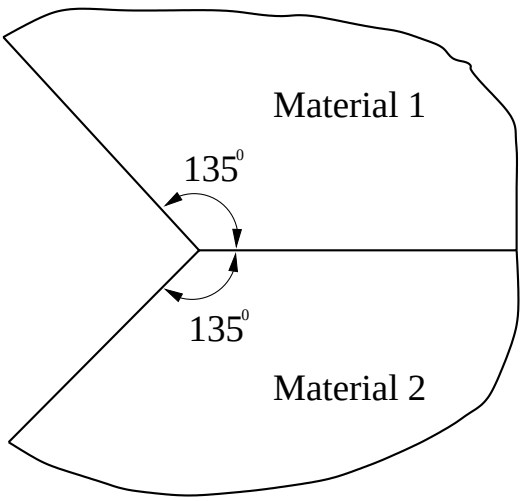

Figure 3.29: A joint with $\theta_1 = 135°$ and $\theta_2 = -135°$.

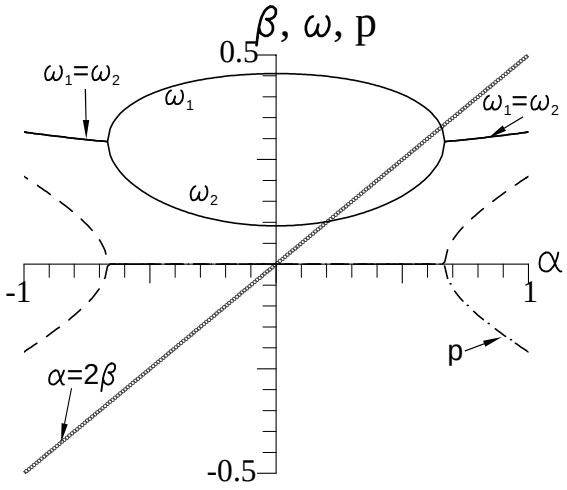

Figure 3.30: Stress exponent distribution for material combinations along the line of $\alpha = 2\beta$ in a joint with $\theta_1 = 135°$ and $\theta_2 = -135°$.

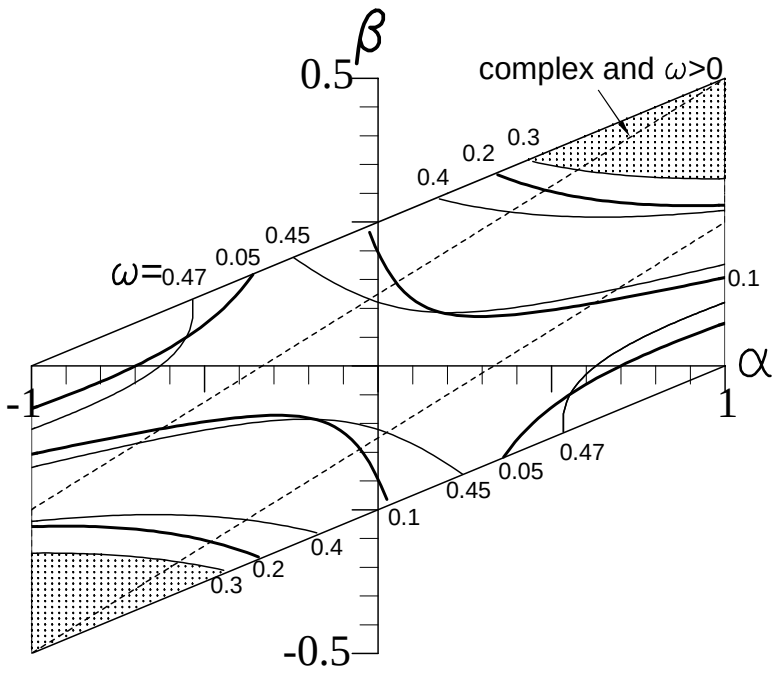

Figure 3.31: Stress exponent distribution in a Dundurs diagram for a joint with $\theta_1 = -\theta_2 = 135°$.

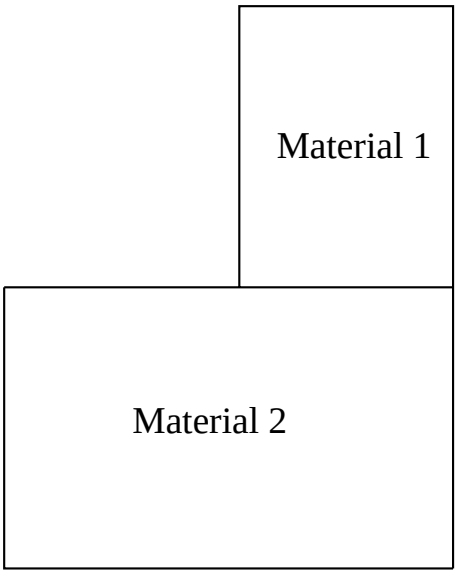

Figure 3.32: A joint with $\theta_1 = 90°$ and $\theta_2 = -180°$.

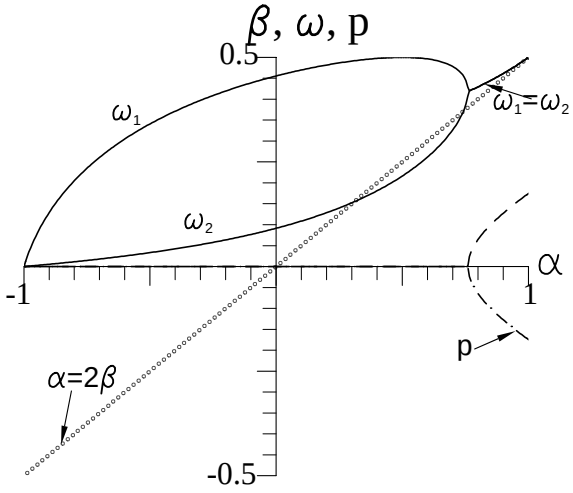

Figure 3.33: Stress exponent distribution for material combinations along the line of $\alpha = 2\beta$ in a joint with $\theta_1 = 90°$ and $\theta_2 = -180°$.

in which the stress exponent is negative, i.e. there is no stress singularity. (d) There are singular terms with complex eigenvalues. To see these clearly, another plot is shown in Fig. 3.20, in which α and β assume values along the line $\alpha = 2\beta$, the corresponding eigenvalues are plotted versus α. In Fig. 3.21 the eigenvalues distribution is along the line of $\beta = 0.35\alpha$. It can be seen that for small α ($\alpha < -0.7$), the eigenvalues may be complex (see Fig. 3.20) or there are two singular exponents (see Fig. 3.21).

For a joint with $\theta_1 = 135°$ and $\theta_2 = -45°$ (see Fig. 3.22), the isoline of the stress exponent ($-0.5 \leq \omega \leq 1$) is plotted in Fig. 3.23. It can be seen that: (a) For most material combinations there is only one singular term, however, in the range of $-1 \leq \alpha \leq -0.85$ there are two singular terms. (b) Along the lines $\beta = 0$ and $\alpha \approx -0.8798$ (they are plotted in the figure as dotted lines), zero is the second order eigenvalue. (c) In the area $\beta \geq 0$ and $\alpha \geq -0.9$, the stress exponent is negative, i.e. there is no stress singularity. (d) There are singular terms with complex eigenvalues ($\alpha \leq -0.85$). These can be seen clearly from Fig. 3.24 along the line of $\beta = \alpha/2$ and Fig. 3.25 along the line of $\beta = 0.1\alpha$. Here, for very small α, the eigenvalues may be complex or two real singular exponents.

For a joint with $\theta_1 = -\theta_2 = 120°$ (see Fig. 3.26), the isoline of the stress exponent ($-0.5 \leq \omega \leq 1$) is plotted in Fig. 3.28. As the geometry is symmetrical, following the definition of α, β given in Eq. (3.1.86), it is known that the isoline of the eigenvalue is point-symmetric to point $\alpha = 0$ and $\beta = 0$, which can be seen in Fig. 3.28. In addition, the following features apply to this joint geometry: (a) For all material combinations,

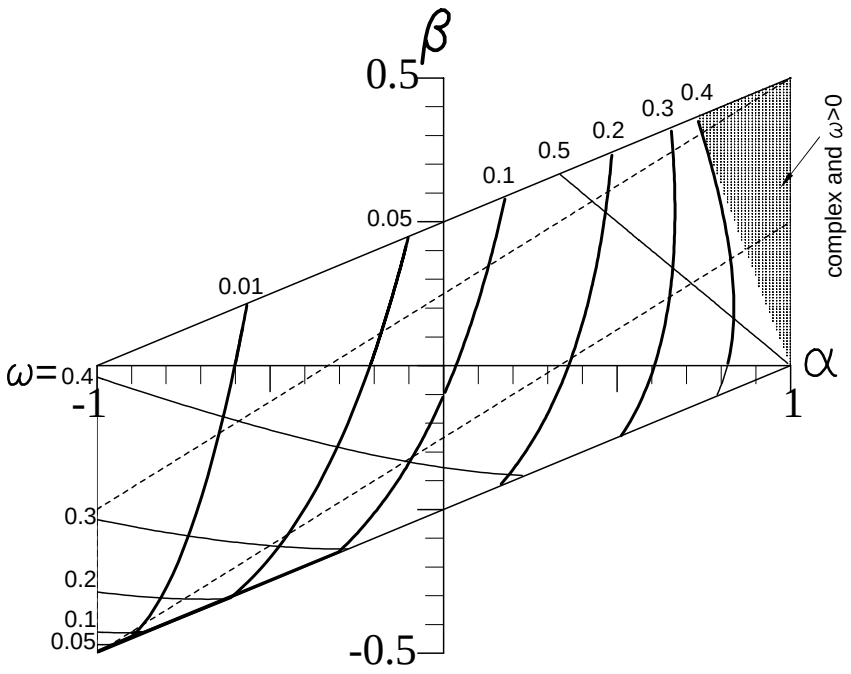

Figure 3.34: Stress exponent distribution in a Dundurs diagram for a joint with $\theta_1 = 90°$ and $\theta_2 = -180°$.

singular stress terms exist (one or two singular terms). (b) Along a curve, which is plotted in the figure as dotted lines and difficult to describe in an equation form, zero is the second order eigenvalue. (c) In the area $\beta > 0.4$ and $\alpha > 0.5$, or $\beta < -0.4$ and $\alpha < -0.5$, the stress exponents are complex. (d) At points $\beta = 0, \alpha = \pm 1$, there is only one singular exponent ($\omega = 0.47525$). Point (c) can be seen clearly from Fig. 3.27, in which for small α ($\alpha < -0.75$) or large α ($\alpha > 0.75$) the eigenvalues are complex.
For a joint with $\theta_1 = -\theta_2 = 135°$ (see Fig. 3.29), the isoline of the stress exponent ($-0.5 \leq \omega \leq 1$) is plotted in Fig. 3.31. It can be seen that the isoline of the eigenvalue is point-symmetric to point $\alpha = 0$ and $\beta = 0$. In addition, the following applies to this joint geometry: (a) For all material combinations two singular terms exist, except for the points $\beta = 0$ and $\alpha = \pm 1$ (at the two points there is $\omega = 0.4899$). (b) Only at points $\beta = 0$ and $\alpha = \pm 1$ zero is the second order eigenvalue. (c) In the area $\beta > 0.35$ and $\alpha > 0.4$, or $\beta < -0.35$ and $\alpha < -0.4$, the stress exponents are complex. This can be seen clearly from Fig. 3.30, in which for small α ($\alpha < -0.6$) or large α ($\alpha > 0.6$), the eigenvalues are complex.

For a joint with $\theta_1 = 90°$ and $\theta_1 = -180°$ (see Fig. 3.32), the isoline of the stress exponent $-0.5 \leq \omega \leq 1$ is plotted in Fig. 3.34. It can be seen that: (a) For most material combinations the eigenvalues are real and always two singular terms exist. (b) Along the line $\alpha = -1$, zero is the second-order eigenvalue. (c) In the area $\beta > 0$ and $\alpha > 0.7$, the stress exponents may be complex. This can be seen clearly from Fig. 3.33, in which for most α the eigenvalues are real and there are two singular terms.

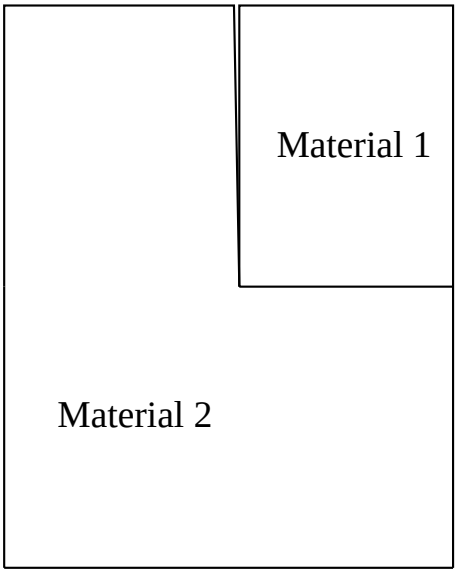

Figure 3.35: A joint with $\theta_1 = 90°$ and $\theta_2 = -270°$.

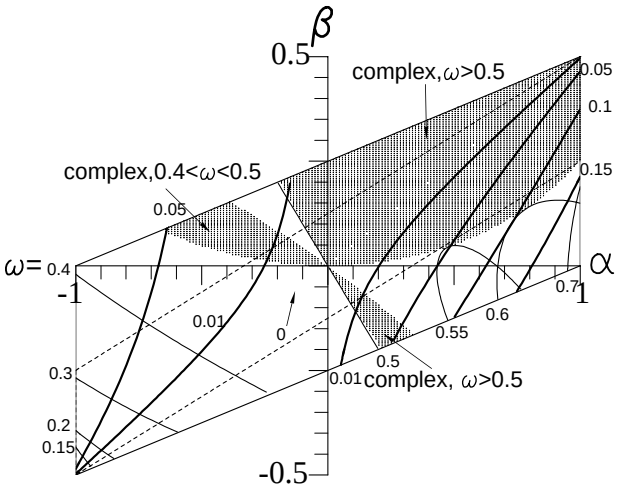

Figure 3.36: Stress exponent distribution in a Dundurs diagram for a joint with $\theta_1 = 90°$ and $\theta_2 = -270°$.

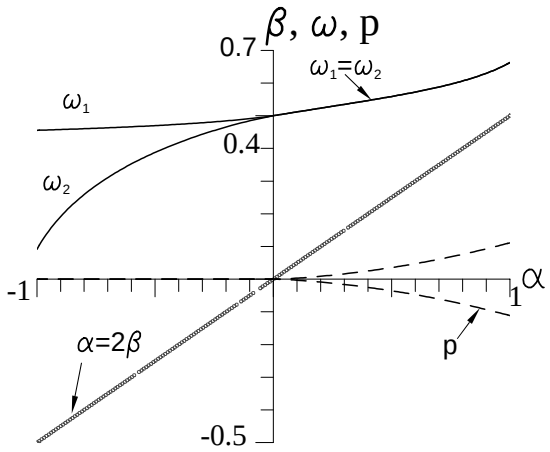

Figure 3.37: Stress exponent distribution for material combinations along the line of $\alpha = 2\beta$ in a joint with $\theta_1 = 90°$ and $\theta_2 = -270°$.

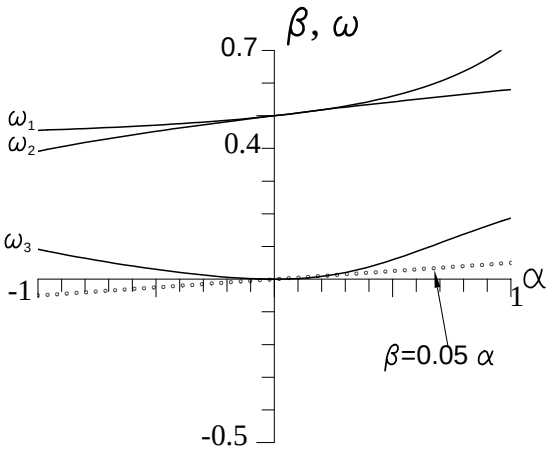

Figure 3.38: Stress exponent distribution for material combinations along the line of $\beta = 0.05\alpha$ in a joint with $\theta_1 = 90°$ and $\theta_2 = -270°$.

For a joint with $\theta_1 = 90°$ and $\theta_1 = -270°$ (see Fig. 3.35), the isoline of the stress exponent is plotted in Fig. 3.36. It can be seen that: (a) For all material combinations two or three singular terms exist, even the singular exponent is larger than 0.5. (b) Along the line $\beta = \alpha/2$ (they are plotted in the figure as dotted lines), zero is the second-order eigenvalue. (c) In the range of $\alpha > 0$, most material combinations yield complex eigenvalues. This can be seen clearly from Fig. 3.37 along the line of $\beta = \alpha/2$ and from Fig. 3.38 along the line of $\beta = 0.05\alpha$. Along the line of $\beta = 0.05\alpha$ there are three singular terms, in the range of $0 < \alpha < 0.25$ two eigenvalues are complex, but the imaginary part is very small (< 0.001, it cannot be seen in the figure). Along the line of $\beta = \alpha/2$, for $\alpha < 0$ there are two real singular stress terms, and for $\alpha > 0$ the eigenvalues are complex and the real part is larger than 0.5.

3.5.2 The Characteristics of the Stress Intensity Factors

A quarter planes joint, i.e. the joint with $\theta_1 = -\theta_2 = 90°$, is the most often used geometry in engineering structures. At first, the behavior of the stress intensity factors for this joint geometry is studied. For a quarter planes joint, only one singular term exists. It is possible to find some empirical relations for calculating the stress intensity factor without using the finite element method.
For other joint geometries, there may be two or three singular terms. It is then very difficult to find some empirical relations for the determination of the stress intensity factor. The general behavior of the stress intensity factor will be shown in some figures only.

The Stress Intensity Factors for a Quarter Planes Joint

The aim of this section is to obtain a general relation between the stress intensity factor, the joint geometry (the ratio of the height and length, $H_1/L, H_2/L$, see Fig. 3.39), and the material data (the Dundurs parameters α and β). At first, the relationship between the K-factor and the ratios of $H_1/L, H_2/L$ is studied for a given material combination. In Eq. (3.0.1) the characteristic length R may be the interface length L or the height of the joint H_1 or H_2. For one singular term case, if the coordinate r is normalized by the interface length L, it holds

$$\sigma_{ij}(r,\theta) = \frac{K}{(r/L)^{\omega}} f_{ij}(\theta) + \sigma_0 f_{ij0}(\theta), \tag{3.5.6}$$

where sometimes K is also denoted as K_L.
For different ratios of $H_1/L, H_2/L$ the K-factor was calculated from FEM and using the equations given in Section 3.4. A plot of K versus H/L (for $H_1 = H_2$=H) is shown in Figs. 3.40 and 3.41 on a linear and semi-logarithmic scale for thermal loading. It can be seen that for H/L > 2 the factor K is a constant. This means that for the

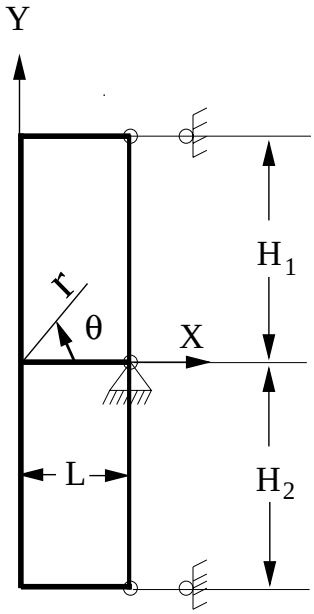

Figure 3.39: A quarter planes joint with the definition of H_1, H_2, and L.

joint geometry with $H_1/L > 2$ and $H_2/L > 2$ (see Fig. 3.42), the stress intensity factor is independent of the overall geometry. Based on this knowledge for a joint with $H_1/L = H_2/L = 2$ under thermal and remote mechanical loading (σ_n), the stress intensity factor are calculated by FEM for material combinations with different ω. The obtained K-factors are plotted in Fig. 3.43 versus the stress singular exponent. An unique curve can be seen for K/σ_0 (σ_0 is the factor of the regular stress term) vs. ω under thermal loading, or for K/σ_n vs. ω under remote mechanical loading, and they are the same. From this unique curve, an empirical equation is found between the K-factor and the stress exponent ω by using the least square method. It is

$$-K/\sigma_0 = K/\sigma_n = 1 - 2.89\,\omega + 11.4\,\omega^2 - 51.9\,\omega^3 + 135.7\,\omega^4 - 135.8\,\omega^5. \qquad (3.5.7)$$

The fitted curve and all FEM points are plotted in Fig. 3.44. It can be seen that Eq. (3.5.7) can describe the FEM results very well. A number of other FE calculations show that for a practically relevant Poisson's ratio, i.e. $0.2 \leq \nu \leq 0.4$, Eq. (3.5.7) can be also used very well for joints with $2 > H_1/L > 1$ and $2 > H_2/L > 1$ (see [84]) and even for joints with a negative stress exponent ($-0.5 \leq \omega \leq 0$, see [79]). For very small ($\nu < 0.1$) or very large ($\nu > 0.45$) Poisson's ratios, the K-factor calculated from Eq. (3.5.7) is not accurate (see [79]).

For joints with $H_1/L < 1$ or $H_2/L < 1$, the coordinate r in Eq. (3.0.1) should be normalized by the height of the joint H_1 or H_2, then the K-factor is denoted as K_{H_1} or K_{H_2}. The factors K, K_{H_1} and K_{H_2} are not independent. The relationship between them is

$$KL^\omega = K_{H_1} H_1^\omega = K_{H_2} H_2^\omega. \qquad (3.5.8)$$

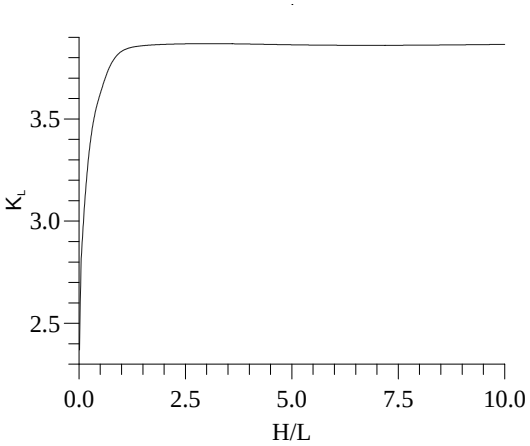

Figure 3.40: The stress intensity factor K_L vs the ratio of H/L for a quarter planes joint with $H_1 = H_2$ on a linear scale ($E_1 = 280$ GPa, $\nu_1 = 0.26$, $\alpha_1 = 2.5 * 10^{-6}/K$, $E_2 = 72$ GPa, $\nu_2 = 0.3$, $\alpha_2 = 18.95 * 10^{-6}/K$).

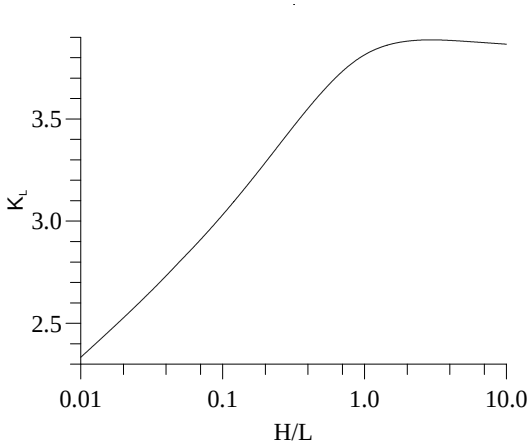

Figure 3.41: The stress intensity factor K_L vs the ratio of H/L for a quarter planes joint with $H_1 = H_2$ on a semi-logarithmic scale.

To show the behavior of the stress intensity factor, the factor K_H is plotted versus L/H on a semi - logarithmic scale for a joint with $H_1/H_2 = 1$ (the material data are $E_1 = 280$ GPa, $\nu_1 = 0.26$, $\alpha_1 = 2.5 * 10^{-6}/K$, $E_2 = 72$ GPa, $\nu_2 = 0.3$, $\alpha_2 = 18.95 * 10^{-6}/K$) in Fig. 3.45. For other ratios of H_1/H_2, K_{H_1} is plotted versus L/H_1 in Fig. 3.46 and K_{H_2} is plotted versus L/H_2 in Fig. 3.47. It is obvious that for very large L/H_1 (or L/H_2, see Fig. 3.48), the K_{H_1} (or K_{H_2}) approach a constant for each ratio of H_1/H_2, denoted as $K_{H_1\infty}$ (or $K_{H_2\infty}$). If the values of $K_{H_2\infty}$ are plotted versus H_1/H_2 (see Fig. 3.49, for $K_{H_1\infty}$ it is similar), $K_{H_2\infty}$ again approach a constant (denoted as $K^*_{H_2\infty}$) at a very large ratio of H_1/H_2 (see Fig. 3.50). Similar to $K^*_{H_2\infty}$, the value of $K^*_{H_1\infty}$ will be obtained at a very large ratios of L/H_1 and H_2/H_1. In summary, there are three stress intensity factors, which describe the stress for limit cases (see [78, 134]):

$$K_{L\infty} = K_L(\frac{H_1}{H_2}, \frac{H_2}{L})\Big|_{min(H_1/L, H_2/L)\geq 2} \tag{3.5.9}$$

$$K^*_{H_1\infty} = K_{H_1}(\frac{H_1}{H_2}, \frac{L}{H_2})\Big|_{H_2/H_1>20, L/H_1>10} \tag{3.5.10}$$

$$K^*_{H_2\infty} = K_{H_2}(\frac{H_1}{H_2}, \frac{L}{H_2})\Big|_{H_1/H_2>20, L/H_2>10}. \tag{3.5.11}$$

Based on the results obtained by FEM for determining the K-factors of different material combinations, an empirical relation between K_{H_2} and the ratios H_2/L and H_1/H_2

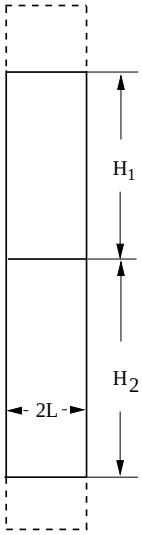

Figure 3.42: A quarter planes joint with $H_1 \gg L$ and $H_2 \gg L$.

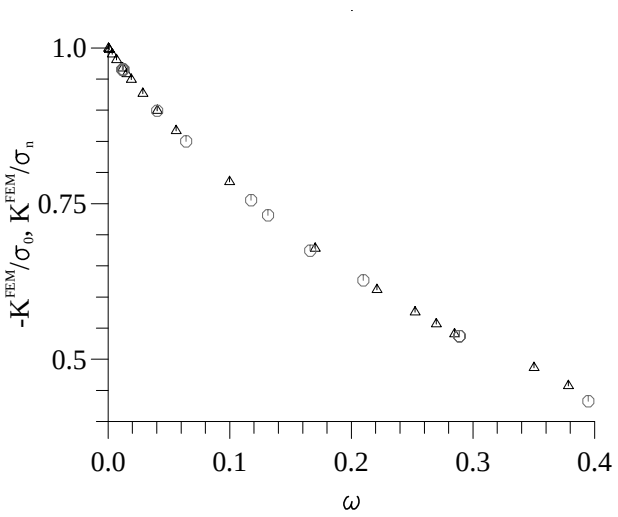

Figure 3.43: The normalized stress intensity factor calculated by FEM for a joint with $H_1/L = H_2/L = 2$ vs. the stress exponent ω.

has been found for joints after a homogeneous temperature change (see [80]):

$$K_{H_2} = A\left[1 - exp\left\{-\left(\frac{K_{L\infty}}{A}\right)^n \left(\frac{L}{H_2}\right)^{n\omega}\right\}\right]^{1/n} \tag{3.5.12}$$

with

$$A = K^*_{H_2\infty}\left[1 - exp\left\{-\left(\frac{K^*_{H_1\infty}}{K^*_{H_2\infty}}\right)^n \left(\frac{H_1}{H_2}\right)^{n\omega}\right\}\right]^{1/n}, \tag{3.5.13}$$

where $K_{L\infty}$ can be determined from Eq. (3.5.7). The parameters $K^*_{H_1\infty}, K^*_{H_2\infty}$, and n can be determined from the following empirical equations:

$$\begin{aligned} -\frac{K^*_{H_1\infty}}{\sigma_0} &= 0.9919 + 0.1523\,\nu_2 - 2.3825\,\omega - 8.0247\,\nu_2\,\omega - 0.5966\,\nu_2^2 \\ &\quad + 14.5589\,\nu_2^2\,\omega + 15.3373\,\omega^2 - 16.7054\,\nu_2\,\omega^2 - 3.5281\,\nu_2^2\,\omega^2 \end{aligned} \tag{3.5.14}$$

$$\begin{aligned} -\frac{K^*_{H_2\infty}}{\sigma_0} &= 1.0137 - 0.1867\,\nu_2 - 2.8641\,\omega + 10.3654\,\nu_2\,\omega + 0.6783\,\nu_2^2 \\ &\quad - 17.5983\,\nu_2^2\,\omega + 2.3556\,\omega^2 - 17.454\,\nu_2\,\omega^2 + 36.2823\,\nu_2^2\,\omega^2 \end{aligned} \tag{3.5.15}$$

$$\begin{aligned} n &= 48.3 - 110.7\,\nu_2 - 479\,\omega + 340.8\,\nu_2\,\omega + 1200.7\,\nu_2^2 \\ &\quad - 3377.9\,\nu_2^2\,\omega + 2056.3\,\omega^2 - 3025.5\,\nu_2\,\omega^2 + 5534.1\,\nu_2^2\,\omega^2 \end{aligned} \tag{3.5.16}$$

where the indication of materials 1 and 2 should satisfy

$$\frac{E_1}{\nu_1} > \frac{E_2}{\nu_2} \tag{3.5.17}$$

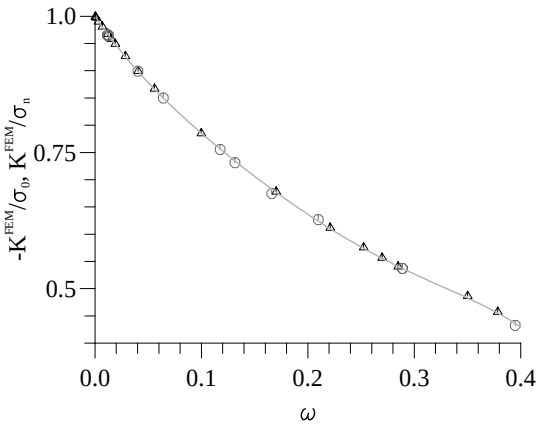

Figure 3.44: The normalized stress intensity factor for a joint with $H_1/L = H_2/L = 2$ vs. the stress exponent ω (the line is obtained from the empirical relation Eq(3.5.7))

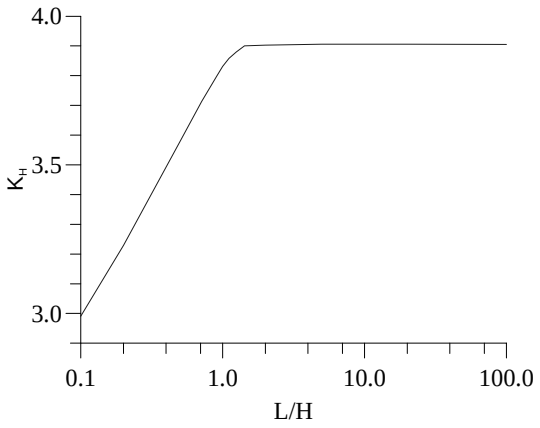

Figure 3.45: Stress intensity factor K_H obtained by FEM vs. L/H for a joint with $H_1/H_2 = 1$.

for plane stress, which corresponds to $\alpha > 2\beta$. If K_{H_2} is known from Eq. (3.5.12), the factors K_{H_1} and K_L can be calculated from Eq. (3.5.8). These empirical equations can be used for joints with $\omega > 0.01$ and with arbitrary ratios of H_1/H_2, H_1/L to calculate the stress intensity factor. In case of $\omega < 0.01$, the values of the singular term and the regular term are in the same order, but with a different sign, except for a very small distance r. In this case, the accuracy of the calculated stresses depends strongly on the accuracy of the determined K-factor. Therefore, the empirical equations should not be used for $\omega < 0.01$.
In summary, the stress field near the singular point can be determined without any FE calculation for a quarter planes joint with arbitrary overall geometry.

The Stress Intensity Factors for an Arbitrary Joint Geometry

For a joint with an arbitrary geometry (θ_1, θ_2), it is impossible to find any empirical relation between the geometry parameters $(\theta_1, \theta_2, H_1, H_2, \mathrm{L})$, the material data (α, β), and the stress intensity factor. The reasons are: (a) There may be more than one singular stress exponent, (b) the ratios of H_1/H_2 and H_1/L cannot determine the overall geometry uniquely (see for example, in Fig. 3.51 the geometry parameters L_1 and L_2 are needed in addition, where L_1 is the upper surface length and L_2 the lower surface length).
The aim of this section is to show some general behavior of the stress intensity factor

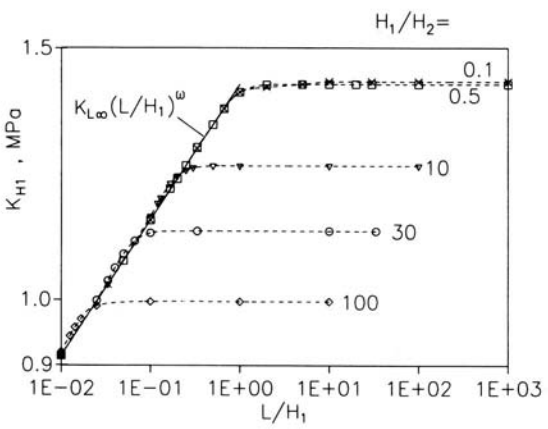

Figure 3.46: $\lg(K_{H_1})$ vs. $lg(L/H_1)$ for different H_1/H_2, $E_1 = 400$ GPa, $\nu_1 = 0.3$, $\alpha_1 = 4 * 10^{-6}/K$, $E_2 = 70$ GPa, $\nu_2 = 0.2$, $\alpha_2 = 8 * 10^{-6}/K$.

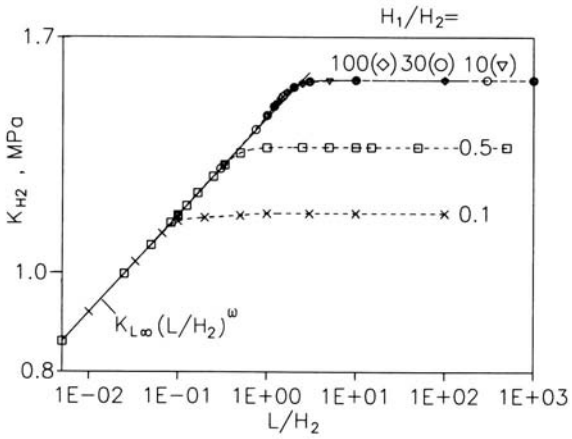

Figure 3.47: $\lg(K_{H_2})$ vs. $lg(L/H_2)$ for different H_1/H_2, $E_1 = 400$ GPa, $\nu_1 = 0.3$, $\alpha_1 = 4 * 10^{-6}/K$, $E_2 = 70$ GPa, $\nu_2 = 0.2$, $\alpha_2 = 8 * 10^{-6}/K$.

for joints with an arbitrary geometry (θ_1, θ_2). As an example, the joint geometry with $\theta_1 = 165°, \theta_2 = -55°$ (see Fig. 3.51) and material data of $E_1 = 280$ GPa, $\nu_1 = 0.26$, $\nu_2 = 0.3$, $\alpha_1 = 2.5 \times 10^{-6}$/K, $\alpha_2 = 18.95 \times 10^{-6}$/K are chosen, where E_2 may vary from $E_2/E_1 = 0.001$ to $E_2/E_1 = 1000$. For this joint, the factors K_1 and K_2 are calculated from the method given in Section 3.4. In Fig. 3.52 the quantities K_1, K_2, σ_0, ω_1, and ω_2 are plotted versus the ratio of E_2/E_1 for thermal loading $\Delta T = 1^0$C. The ratio of K_i/σ_0 (i=1,2) is presented in Fig. 3.53 versus ω_i. From Figs. 3.52 and 3.53 it is obvious that (a) if one stress exponent (e.g. ω_1) goes through zero, the corresponding K-factor (K_1) goes towards infinity and the regular stress constant σ_0 also goes towards infinity with a different sign, (b) the ratio of K_1/σ_0 at $\omega_1 = 0$ or K_2/σ_0 at $\omega_2 = 0$ is finite and equal to -1, (c) the K-factor is not unique function of the stress exponent ω_n. The case of $K_1 = \pm\infty$ and $\sigma_0 = \mp\infty$ at $\omega_1 = 0$ or $K_2 = \pm\infty$ and $\sigma_0 = \mp\infty$ at $\omega_2 = 0$ has no physical meaning. However, the fact that $K_1/\sigma_0 = -1$ at $\omega_1 = 0$ or $K_2/\sigma_0 = -1$ at $\omega_2 = 0$ ensures that the stresses are finite. In fact, in case of $\omega_1 = 0$ or $\omega_2 = 0$ and for thermal loading, Eq. (3.0.1) cannot be used to calculate the stress field near the singular point, the type of log(r) singularity should be considered to describe the singular stress field (see Chapter 7).

For mechanical loading (the load is $\sigma_n = \sigma_\theta = 1$ at the interface) and for the same joint as above, the quantities $K_1, K_2, \omega_1, \omega_2$ are plotted in Fig. 3.54 versus E_2/E_1. It can be seen that the values of K_1 and K_2 are always finite for mechanical loading. By comparing Figs. 3.53 and 3.54, it can be seen that the curves of $K_1/\sigma_0, K_2/\sigma_0$ for thermal loading are not similar to $K_1/\sigma_n, K_2/\sigma_n$ for mechanical loading.

A short summary on the behavior of the K-factor in an arbitrary geometry is: (a) The

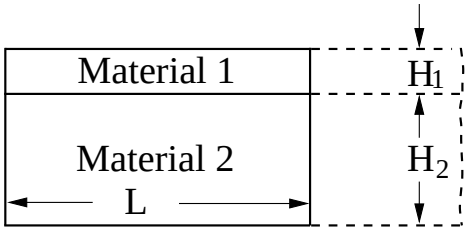

Figure 3.48: A joint with $L \gg H_1$ and $L \gg H_2$.

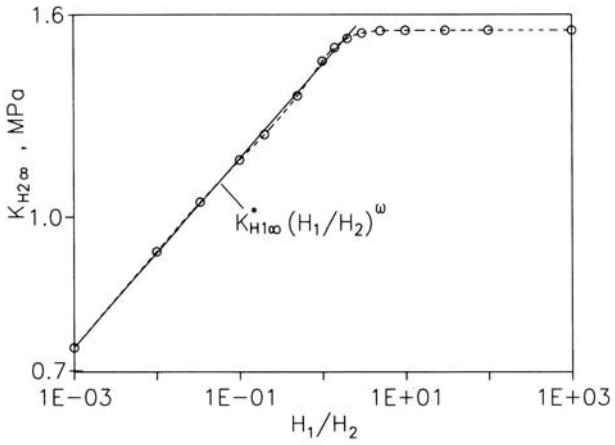

Figure 3.49: $\mathrm{Lg}(K_{H_2\infty})$ vs. $lg(H_1/H_2)$, $E_1 = 400$ GPa, $\nu_1 = 0.3$, $\alpha_1 = 4 * 10^{-6}/K$, $E_2 = 70$ GPa, $\nu_2 = 0.2$, $\alpha_2 = 8 * 10^{-6}/K$

quantity K/σ_0 is not an unique function of the stress exponent ω. (b) The quantity K/σ_0 for thermal loading is not similar to K/σ_n for mechanical loading.

For a joint with arbitrary angles (θ_1, θ_2) and the overall geometry being infinite, a method based on the Mellin transform has been found to determine the factors K_i (i=1,2,3,...,N) analytically (see [135]). Banks-Sills and Sherer have used a conservative integral for the bimaterial notch under mechanical loading to calculate stress intensity factor (see [136]).

3.6 The Displacement Field near the Singular Point

In Sections 3.1 to 3.4 the determination of the stress field near the singular point has been discussed. In the present section the displacement field will be considered.

Joints with real eigenvalues

For joints with real eigenvalues, Eqs. (3.1.16) and (3.1.17) can be used to calculate the displacement. To see the contribution of the singular term and the regular term as it was done for the stresses, the displacement is calculated from

$$u_k(r,\theta) = \tilde{u}_k(r,\theta) + u_{k0}(r,\theta) + r\alpha_k T \tag{3.6.1}$$

$$v_k(r,\theta) = \tilde{v}_k(r,\theta) + v_{k0}(r,\theta) \tag{3.6.2}$$

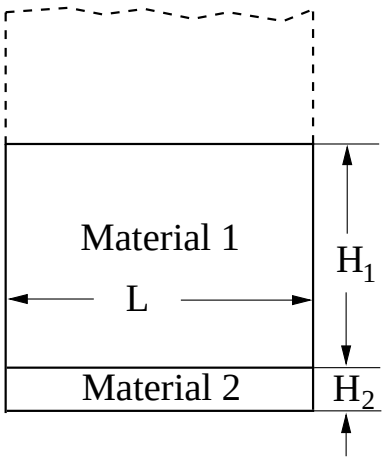

Figure 3.50: A joint with $L \gg H_2$ and $H_1 \gg H_2$.

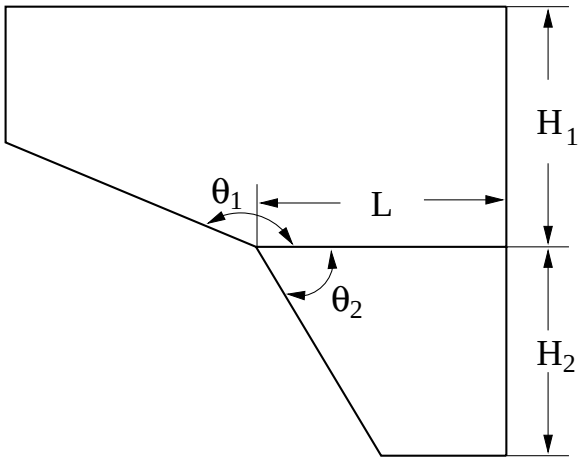

Figure 3.51: A joint with $\theta_1 = 165°$ and $\theta_2 = -55°$ ($H_1/L = 0.984$, $H_2/L = 0.816$, $L_1/L = 2.016$, $L_2/L = 0.432$.)

where for plane stress

$$\tilde{u}_k(r,\theta) = \sum_{n=1}^{N} K_n \frac{r^{(1-\omega_n)}}{E_k} \quad \Big\{ \quad \tilde{A}_{kn}[2(1-\nu_k) + \omega_n(1+\nu_k)]\sin(\omega_n\theta)$$
$$+ \quad \tilde{B}_{kn}[2(1-\nu_k) + \omega_n(1+\nu_k)]\cos(\omega_n\theta)$$
$$- \quad \tilde{C}_{kn}(1+\nu_k)(2-\omega_n)\sin[(2-\omega_n)\theta]$$
$$- \quad \tilde{D}_{kn}(1+\nu_k)(2-\omega_n)\cos[(2-\omega_n)\theta]\Big\} \qquad (3.6.3)$$

$$\tilde{v}_k(r,\theta) = \sum_{n=1}^{N} K_n \frac{r^{(1-\omega_n)}}{E_k} \quad \Big\{ \quad \tilde{A}_{kn}[2(1-\nu_k) + (2-\omega_n)(1+\nu_k)]\cos(\omega_n\theta)$$
$$- \quad \tilde{B}_{kn}[2(1-\nu_k) + (2-\omega_n)(1+\nu_k)]\sin(\omega_n\theta)$$
$$- \quad \tilde{C}_{kn}(1+\nu_k)(2-\omega_n)\cos[(2-\omega_n)\theta]$$
$$+ \quad \tilde{D}_{kn}(1+\nu_k)(2-\omega_n)\sin[(2-\omega_n)\theta]\Big\}, \qquad (3.6.4)$$

with

$$\tilde{A}_{kn} = Y \times A_{kn} \qquad (3.6.5)$$

$$\tilde{B}_{kn} = Y \times B_{kn} \qquad (3.6.6)$$

$$\tilde{C}_{kn} = Y \times C_{kn} \qquad (3.6.7)$$

$$\tilde{D}_{kn} = Y \times D_{kn} \qquad (3.6.8)$$

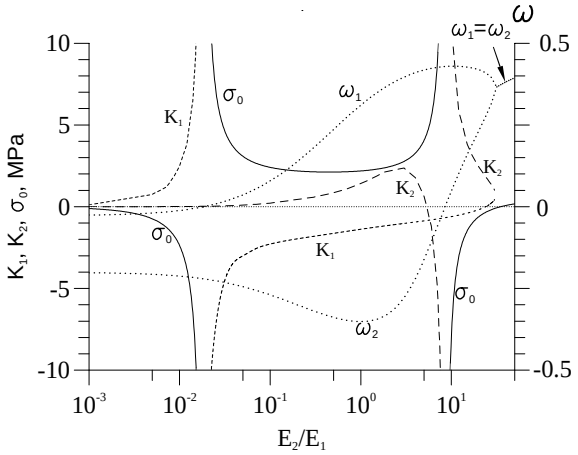

Figure 3.52: Stress intensity factor K, regular stress term σ_0 and the stress exponent ω vs. E_2/E_1 for a joint with $\theta_1 = 165°$ and $\theta_2 = -55°$ under thermal loading.

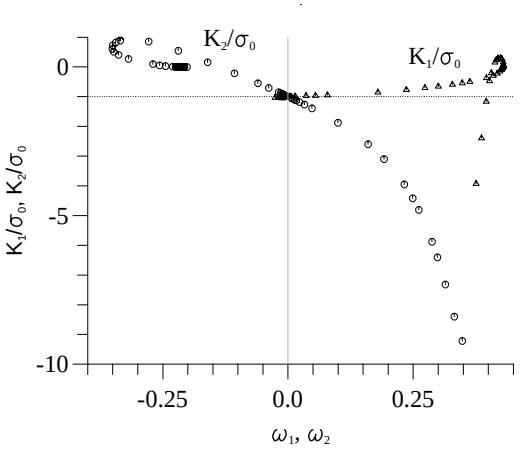

Figure 3.53: Normalized stress intensity K/σ_0 vs. the stress exponent ω for $\theta_1 = 165°$ and $\theta_2 = -55°$ under thermal loading.

and

$$Y = \frac{R^{\omega_n}}{(2-\omega_n)(1-\omega_n)(B_{kn}+D_{kn})} \tag{3.6.9}$$

The coefficients $A_{kn}, B_{kn}, C_{kn}, D_{kn}$, K_n,R and ω_n are the same as those for the calculation of the stresses. The displacements according to the regular stress term are

$$\begin{aligned} u_{k0}(r,\theta) &= \frac{2r}{E_k}[A_{k0}\theta(1-\nu_k) + B_{k0}(1-\nu_k) \\ &\quad -C_{k0}(1+\nu_k)\sin(2\theta) - D_{k0}(1+\nu_k)\cos(2\theta)] \end{aligned} \tag{3.6.10}$$

$$\begin{aligned} v_{k0}(r,\theta) &= \frac{2r}{E_k}[-C_{k0}(1+\nu_k)\cos(2\theta) + D_{k0}(1+\nu_k)\sin(2\theta)] \\ &\quad +F_{k0}r - \frac{4A_{k0}}{E_k}r\ln(r). \end{aligned} \tag{3.6.11}$$

The coefficients A_{k0}, B_{k0}, C_{k0}, D_{k0} are the same as those for the regular stress term and they can be calculated analytically. The constant F_{k0} has to be determined from FEM.

Joints with complex eigenvalues

For joints with complex eigenvalues, Eqs. (3.6.1) and (3.6.2) are valid as well. However, the contribution of the singular terms should be replaced by:

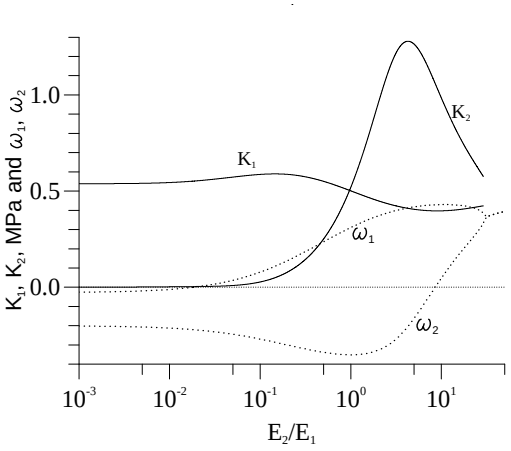

Figure 3.54: Stress intensity factor K and stress exponent ω vs. E_2/E_1 for a joint with $\theta_1 = 165^\circ$ and $\theta_2 = -55^\circ$ under mechanical loading.

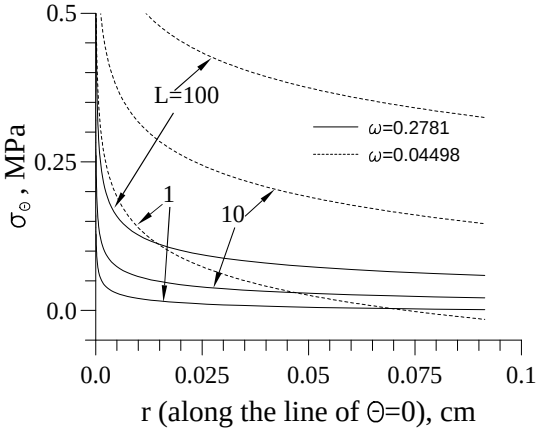

Figure 3.55: Stress component σ_θ along the interface vs. the distance r (not r/L) in a quarter planes joint under thermal loading.

$$
\begin{aligned}
\tilde{u}_k(r,\theta) \;=\; & \sum_{n=1}^{N} \frac{K_n r^{t_n}}{2G_k} \Big\{ \Big\{ (-t_n\, \tilde{\mathcal{A}}^R_{kn} + \xi_k\, \tilde{\mathcal{A}}^R_{kn} + p_n\, \tilde{\mathcal{A}}^I_{kn}) \cos[\ln(\mathrm{r})\, \mathrm{p_n} + \theta\, t_n - \theta] + \\
& + \; (-\xi_k\, \tilde{\mathcal{A}}^I_{kn} + t_n\, \tilde{\mathcal{A}}^I_{kn} + p_n\, \tilde{\mathcal{A}}^R_{kn}) \sin[\ln(\mathrm{r})\, \mathrm{p_n} + \theta\, t_n - \theta] \\
& - \; \tilde{\mathcal{C}}^R_{kn} \cos[\ln(\mathrm{r})\, \mathrm{p_n} + \theta\, t_n + \theta] + \tilde{\mathcal{C}}^I_{kn} \sin[\ln(\mathrm{r})\, \mathrm{p_n} + \theta\, t_n + \theta] \Big\}\, e^{-\theta\, p_n} \\
& + \; \Big\{ (-p_n\, \tilde{\mathcal{B}}^I_{kn} - t_n\, \tilde{\mathcal{B}}^R_{kn} + \xi_k\, \tilde{\mathcal{B}}^R_{kn}) \cos[-\ln(\mathrm{r})\, \mathrm{p_n} + \theta\, t_n - \theta] \\
& + \; (-\xi_k\, \tilde{\mathcal{B}}^I_{kn} + t_n\, \tilde{\mathcal{B}}^I_{kn} - p_n\, \tilde{\mathcal{B}}^R_{kn}) \sin[-\ln(\mathrm{r})\, \mathrm{p_n} + \theta\, t_n - \theta] \\
& - \; \tilde{\mathcal{D}}^R_{kn} \cos[-\ln(\mathrm{r})\, \mathrm{p_n} + \theta\, t_n + \theta] + \tilde{\mathcal{D}}^I_{kn} \sin[-\ln(\mathrm{r})\, \mathrm{p_n} + \theta\, t_n + \theta] \Big\}\, e^{\theta\, p_n} \Big\}
\end{aligned}
\tag{3.6.12}
$$

$$
\begin{aligned}
\tilde{v}_k(r,\theta) \;=\; & \sum_{n=1}^{N} \frac{K_n r^{t_n}}{2G_k} \Big\{ \Big\{ (t_n\, \tilde{\mathcal{A}}^I_{kn} + p_n\, \tilde{\mathcal{A}}^R_{kn} + \xi_k\, \tilde{\mathcal{A}}^I_{kn}) \cos[\ln(\mathrm{r})\, \mathrm{p_n} + \theta\, t_n - \theta] \\
& + \; (t_n\, \tilde{\mathcal{A}}^R_{kn} - p_n\, \tilde{\mathcal{A}}^I_{kn} + \xi_k\, \tilde{\mathcal{A}}^R_{kn}) \sin[\ln(\mathrm{r})\, \mathrm{p_n} + \theta\, t_n - \theta] \\
& + \; \tilde{\mathcal{C}}^I_{kn} \cos[\ln(\mathrm{r})\, \mathrm{p_n} + \theta\, t_n + \theta] + \tilde{\mathcal{C}}^R_{kn} \sin[\ln(\mathrm{r})\, \mathrm{p_n} + \theta\, t_n + \theta] \Big\}\, e^{-\theta\, p_n} \\
& + \; \Big\{ (t_n\, \tilde{\mathcal{B}}^I_{kn} - p_n\, \tilde{\mathcal{B}}^R_{kn} + \xi_k\, \tilde{\mathcal{B}}^I_{kn}) \cos[-\ln(\mathrm{r})\, \mathrm{p_n} + \theta\, t_n - \theta] \\
& + \; (t_n\, \tilde{\mathcal{B}}^R_{kn} + p_n\, \tilde{\mathcal{B}}^I_{kn} + \xi_k\, \tilde{\mathcal{B}}^R_{kn}) \sin[-\ln(\mathrm{r})\, \mathrm{p_n} + \theta\, t_n - \theta] \\
& + \; \tilde{\mathcal{D}}^I_{kn} \cos[-\ln(\mathrm{r})\, \mathrm{p_n} + \theta\, t_n + \theta] + \tilde{\mathcal{D}}^R_{kn} \sin[-\ln(\mathrm{r})\, \mathrm{p_n} + \theta\, t_n + \theta] \Big\}) \, e^{\theta\, p_n} \Big\}
\end{aligned}
\tag{3.6.13}
$$

with $t_n = 1 - \omega_n$ and

$$\tilde{\mathcal{A}}^R_{kn} = Y_{com} \times \mathcal{A}^{\mathrm{R}}_{\mathrm{kn}}$$

$$\tilde{\mathcal{A}}^I_{kn} = Y_{com} \times \mathcal{A}^{\mathrm{I}}_{\mathrm{kn}}$$

$$\tilde{\mathcal{B}}^R_{kn} = Y_{com} \times \mathcal{B}^{\mathrm{R}}_{\mathrm{kn}}$$

$$\tilde{\mathcal{B}}^I_{kn} = Y_{com} \times \mathcal{B}^{\mathrm{I}}_{\mathrm{kn}}$$

$$\tilde{\mathcal{C}}^R_{kn} = Y_{com} \times \mathcal{C}^{\mathrm{R}}_{\mathrm{kn}}$$

$$\tilde{\mathcal{C}}^I_{kn} = Y_{com} \times \mathcal{C}^{\mathrm{I}}_{\mathrm{kn}}$$

$$\tilde{\mathcal{D}}^R_{kn} = Y_{com} \times \mathcal{D}^{\mathrm{R}}_{\mathrm{kn}}$$

$$\tilde{\mathcal{D}}^I_{kn} = Y_{com} \times \mathcal{D}^{\mathrm{I}}_{\mathrm{kn}}$$

and

$$Y_{com} = \frac{-R^{\omega_n}}{(\mathcal{A}^{\mathrm{R}}_{\mathrm{kn}} + \mathcal{B}^{\mathrm{R}}_{\mathrm{kn}})(\mathrm{p_n^2} - \mathrm{t_n^2} - \mathrm{t_n}) + (\mathcal{A}^{\mathrm{I}}_{\mathrm{kn}} - \mathcal{B}^{\mathrm{I}}_{\mathrm{kn}})\mathrm{p_n}(2\mathrm{t_n} + 1) - (\mathcal{C}^{\mathrm{R}}_{\mathrm{kn}} + \mathcal{D}^{\mathrm{R}}_{\mathrm{kn}})\mathrm{t_n} + (\mathcal{C}^{\mathrm{I}}_{\mathrm{kn}} - \mathcal{D}^{\mathrm{I}}_{\mathrm{kn}})\mathrm{p_n}} \tag{3.6.14}$$

where the coefficients $\mathcal{A}^{\mathrm{R}}_{\mathrm{kn}}$, $\mathcal{A}^{\mathrm{I}}_{\mathrm{kn}}$, $\mathcal{B}^{\mathrm{R}}_{\mathrm{kn}}$, $\mathcal{B}^{\mathrm{I}}_{\mathrm{kn}}$, $\mathcal{C}^{\mathrm{R}}_{\mathrm{kn}}$, $\mathcal{C}^{\mathrm{I}}_{\mathrm{kn}}$, $\mathcal{D}^{\mathrm{R}}_{\mathrm{kn}}$, and $\mathcal{D}^{\mathrm{I}}_{\mathrm{kn}}$ are the same as those for the calculations of the stresses.

3.7 The Size Effect on the Stress Distribution

The stress field near the singular point can be described by Eq. (3.0.1) or (3.0.2). The quantities ω_n, p_n, $f_{ijn}(\theta)$, $f^c_{ijn}(\theta)$, and $f^s_{ijn}(\theta)$ are dependent on the material data and the joint geometry. The regular stress term $\sigma_0 f_{ij0}(\theta)$ and the stress intensity factors K_n in addition, depend on the loading, but not on the absolute size of the joint. This is because the distance r is divided by a characteristic length R of the joint. The stress distribution near the singular point is, however, dependent on the absolute size of the joint, i.e. the absolute value of the quantity R. To show this effect, the stress σ_θ along the interface of a joint with $\theta_1 = -\theta_2 = 90^\circ$ and $H_1/L = H_2/L = 2$ (see Fig. 3.39) is plotted vs. the distance r for different interface lengths R (R=L=1cm, 10cm, 100cm) and different material combinations in Figs. 3.55, 3.56 and 3.57.

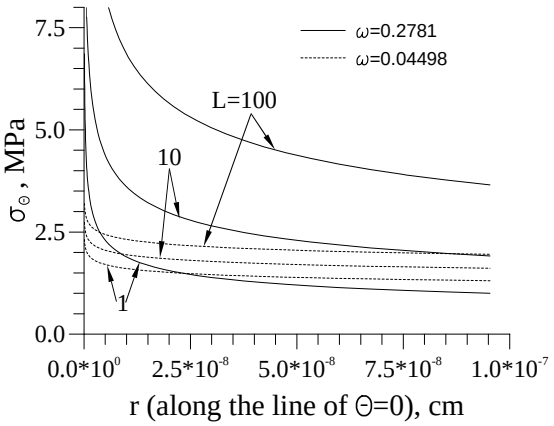

Figure 3.56: Stress component σ_θ along the interface vs. the distance r (not r/L) in a quarter planes joint under thermal loading, in the range very close to the singular point.

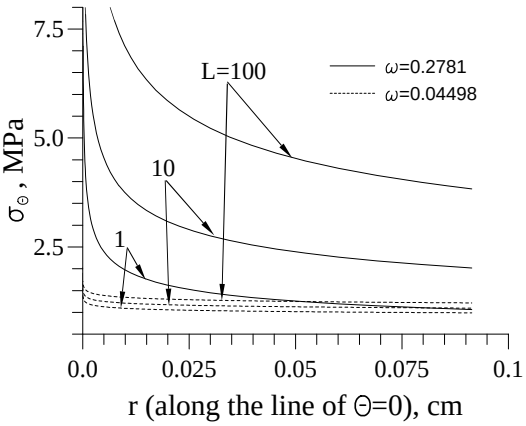

Figure 3.57: Stress component σ_θ along the interface vs. the distance r (not r/L) in a quarter planes joint under mechanical loading.

As the first material combination, the material data are: $E_1 = 100$ GPa, $E_2 = 1$ GPa, $\nu_1 = 0.2, \nu_2 = 0.3, \alpha_1 = 2.5{*}10^{-6}/K$, and $\alpha_2 = 8.5{*}10^{-6}/K$, which leads to ω=0.27805. For thermal loading σ_0=-0.02077 MPa and K=0.0114 MPa. For mechanical loading it follows σ_0=0 and K=0.5475 MPa.

As the second material combination, the material data are: $E_1 = 100$ GPa, $E_2 = 50$ GPa, $\nu_1 = 0.2, \nu_2 = 0.3$, $\alpha_1 = 2.5 * 10^{-6}/K$, and $\alpha_2 = 8.5 * 10^{-6}/K$, which leads to ω=0.04498. For thermal loading σ_0=-1.4907 MPa and K=1.3251 MPa. For mechanical loading it reads σ_0=0 and K=0.8889 MPa.

It should be noted that in the figures the distance r is not normalized by a characteristic length R. Figures 3.55 and 3.56 are for thermal loading ($T = -1^0C$), and Fig. 3.57 corresponds to mechanical loading ($\sigma_n = 1$ MPa at the upper and lower surface). From Figs. 3.55, 3.56, and 3.57, it can be seen that

(a) The absolute value of the quantity R has an obvious effect on the stress distribution near the singular point. The larger the value of ω is, the stronger is the effect of the size on stress.

(b) For thermal loading the stress near the singular point, corresponding to larger value of ω, is not always higher than the stress in a joint with a smaller ω (see Fig. 3.55), except for very small distances r (see Fig. 3.56). However, for mechanical loading the following holds: The larger is the ω, the higher is the stress near the singular point (see Fig. 3.57). (c) For material combinations with small ω, the size effect for thermal loading is larger than that one for mechanical loading (comparing Figs. 3.55 and 3.57). This is due to the existence of the regular stress term (σ_0).

Chapter 4

Notches and Cracks in a Homogeneous Material

A homogeneous material with a notch or crack is the special case of a two dissimilar materials joint. For homogeneous material the Dundurs parameters are zero. In principle, the equations presented in Chapter 3 for the analysis of stress singularity and of the regular stress term are also valid for a homogeneous material with a notch or a crack by putting $\alpha = 0$ and $\beta = 0$. In the following the simplified results will be presented.

In a homogeneous material there is no interface. Therefore, the location of the line $\theta = 0$ can be defined arbitrarily. We define the coordinate system so that both edges have the same angle θ_1 (see Fig. 4.1).

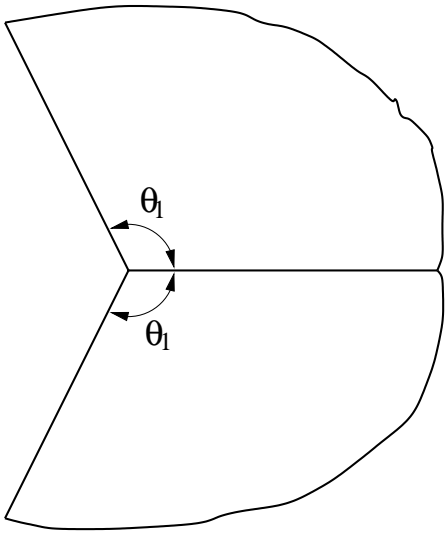

Figure 4.1: Notch in a homogeneous material.

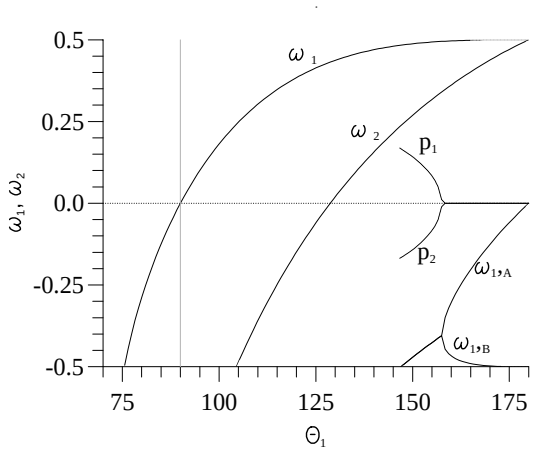

Figure 4.2: Stress exponent ω as a function of the notch angle θ_1.

Now, we can replace the quantities in Chapter 3 by

$$\begin{aligned} A_{1n} &= A_{2n} = A_n, \qquad B_{1n} = B_{2n} = B_n, \\ C_{1n} &= C_{2n} = C_n, \qquad D_{1n} = D_{2n} = D_n, \\ \theta_2 &= -\theta_1. \end{aligned} \tag{4.0.1}$$

The boundary conditions for a notch with free edges are

$$\begin{aligned} \sigma_{\theta\theta}(r, \theta_1) &= 0, \\ \sigma_{\theta\theta}(r, -\theta_1) &= 0, \\ \sigma_{r\theta}(r, \theta_1) &= 0, \\ \sigma_{r\theta}(r, -\theta_1) &= 0. \end{aligned} \tag{4.0.2}$$

4.1 Homogeneous Material with a Notch

Homogeneous material with a notch means that the angle θ_1 is smaller than 180°. The notch with $\theta_1 = 180^\circ$ is called a crack. In this section, the case with $\theta_1 = 180^\circ$ is not considered.

4.1.1 Determination of the Stress Exponent and the Angular Function

From Eqs. (3.1.8), (3.1.9), (4.0.1), and (4.0.2), the following basic equations can be obtained for each n:

$$A_n \sin(\lambda_n\theta_1) + B_n \cos(\lambda_n\theta_1) + C_n \sin[(2-\lambda_n)\theta_1] + D_n \cos[(2-\lambda_n)\theta_1] = 0 \tag{4.1.1}$$

$$-A_n \sin(\lambda_n\theta_1) + B_n \cos(\lambda_n\theta_1) - C_n \sin[(2-\lambda_n)\theta_1] + D_n \cos[(2-\lambda_n)\theta_1] = 0 \tag{4.1.2}$$

$$\begin{aligned} A_n\lambda_n \cos(\lambda_n\theta_1) - B_n\lambda_n \sin(\lambda_n\theta_1) + C_n(2-\lambda_n) \cos[(2-\lambda_n)\theta_1] \\ -D_n(2-\lambda_n) \sin[(2-\lambda_n)\theta_1] = 0 \end{aligned} \tag{4.1.3}$$

$$\begin{aligned} A_n\lambda_n \cos(\lambda_n\theta_1) + B_n\lambda_n \sin(\lambda_n\theta_1) + C_n(2-\lambda_n) \cos[(2-\lambda_n)\theta_1] \\ +D_n(2-\lambda_n) \sin[(2-\lambda_n)\theta_1] = 0. \end{aligned} \tag{4.1.4}$$

Equations (4.1.1 - 4.1.4) are equivalent to

$$B_n \cos(\lambda_n\theta_1) + D_n \cos[(2-\lambda_n)\theta_1] = 0 \tag{4.1.5}$$

$$A_n \sin(\lambda_n\theta_1) + C_n \sin[(2-\lambda_n)\theta_1] = 0 \tag{4.1.6}$$

$$A_n\lambda_n \cos(\lambda_n\theta_1) + C_n(2-\lambda_n) \cos[(2-\lambda_n)\theta_1] = 0 \tag{4.1.7}$$

$$B_n\lambda_n \sin(\lambda_n\theta_1) + D_n(2-\lambda_n) \sin[(2-\lambda_n)\theta_1] = 0. \tag{4.1.8}$$

It is obvious that Eqs. (4.1.5) and (4.1.8) are independent of Eqs. (4.1.6) and (4.1.7). They can be rewritten as

$$\begin{bmatrix} \cos(\lambda_n\theta_1) & \cos[(2-\lambda_n)\theta_1] \\ \lambda_n \sin(\lambda_n\theta_1) & (2-\lambda_n)\sin[(2-\lambda_n)\theta_1] \end{bmatrix} \begin{Bmatrix} B_n \\ D_n \end{Bmatrix} \equiv [\Delta_{BD}]\{X_{BD}\} = 0$$

$$\begin{bmatrix} \sin(\lambda_n\theta_1) & \sin[(2-\lambda_n)\theta_1] \\ \lambda_n \cos(\lambda_n\theta_1) & (2-\lambda_n)\cos[(2-\lambda_n)\theta_1] \end{bmatrix} \begin{Bmatrix} A_n \\ C_n \end{Bmatrix} \equiv [\Delta_{AC}]\{X_{AC}\} = 0.$$

Equations (4.1.5-4.1.8) are a homogeneous linear equations system. The condition of this problem having a nonzero solution is that the determinant of $[\Delta_{BD}]$ or $[\Delta_{AC}]$ is zero. This leads to

$$\mathrm{Det}[\Delta_{BD}] = \cos(\lambda_n\theta_1)(2-\lambda_n)\sin[(2-\lambda_n)\theta_1] - \cos[(2-\lambda_n)\theta_1]\lambda_n \sin(\lambda_n\theta_1) = 0 \tag{4.1.9}$$

or

$$\mathrm{Det}[\Delta_{AC}] = \sin(\lambda_n\theta_1)(2-\lambda_n)\cos[(2-\lambda_n)\theta_1] - \sin[(2-\lambda_n)\theta_1]\lambda_n \cos(\lambda_n\theta_1) = 0. \tag{4.1.10}$$

After simplifying Eq. (4.1.9) and Eq. (4.1.10), it holds

$$\mathrm{Det}[\Delta_{BD}] = \sin[2(1-\lambda_n)\theta_1] + (1-\lambda_n)\sin(2\theta_1) = 0 \tag{4.1.11}$$

or

$$\mathrm{Det}[\Delta_{AC}] = -\sin[2(1-\lambda_n)\theta_1] + (1-\lambda_n)\sin(2\theta_1) = 0. \tag{4.1.12}$$

The solutions λ_n of Eq. (4.1.11) and Eq. (4.1.12) are the eigenvalues of this problem.

For a given eigenvalue, the corresponding eigenvector can be determined. Since the Eqs. (4.1.5) and (4.1.8) are independent of Eqs. (4.1.6) and (4.1.7), the corresponding eigenvectors are independent as well. We will discuss them in two cases.

(I) The case of $\mathrm{Det}[\Delta_{BD}] = 0$

We assume that λ_n' is the solution of $\mathrm{Det}[\Delta_{BD}] = 0$. Then,

$$\sin[2(1-\lambda_n')\theta_1] = -(1-\lambda_n')\sin(2\theta_1) \tag{4.1.13}$$

and

$$\mathrm{Det}[\Delta_{AC}] = 2(1-\lambda'_n)\sin(2\theta_1). \tag{4.1.14}$$

If $\lambda'_n \neq 1$ or $\theta_1 \neq \pi/2$ and π, $\mathrm{Det}[\Delta_{AC}] \neq 0$. This means that for $\lambda'_n \neq 1$ or $\theta_1 \neq \pi/2$ and π, the coefficients A_n and C_n must be zero.
From Section 3.1 we know that the solution with $\lambda'_n = 1$ corresponds to the rigid body displacement, and this is not needed for stress analysis. In this section, we have $\theta_1 \neq \pi$. For $\theta_1 = \pi/2$ (this is a slab without a notch), $\mathrm{Det}[\Delta_{AC}] = 0$, i.e. A_n and C_n may be nonzero. From Eq. (4.1.13) we know that for $\theta_1 = \pi/2$ the eigenvalues are $\lambda'_n = 0, \pm 1, \pm 2, \pm 3, ...$ In the range of $0 \leq \lambda'_n < 1$, the only possible solution is $\lambda'_n = 0$. This means that according to the eigenvalue λ'_n, except for $\lambda'_n = 0$, $A_n = C_n = 0$ is true. The stress term according to $\lambda'_n = 0$ will be discussed in the next section.
For λ'_n, the coefficients B_n and D_n are nonzero. From Eq. (4.1.5) we have

$$B_n = -D_n \frac{\cos[(2-\lambda'_n)\theta_1]}{\cos(\lambda'_n\theta_1)} \tag{4.1.15}$$

for $\cos(\lambda'_n\theta_1) \neq 0$, or from Eq. (4.1.8)

$$B_n = -D_n \frac{(2-\lambda'_n)\sin[(2-\lambda'_n)\theta_1]}{\lambda'_n \sin(\lambda'_n\theta_1)} \tag{4.1.16}$$

for $\lambda'_n \sin(\lambda'_n\theta_1) \neq 0$. For the given λ'_n, the corresponding stress term is

$$\begin{aligned} \sigma_{rrn}(r,\theta) &= r^{-\lambda'_n}(1-\lambda'_n)D_n\Big\{-(2+\lambda'_n)\frac{\cos[(2-\lambda'_n)\theta_1]}{\cos(\lambda'_n\theta_1)}\cos(\lambda'_n\theta) \\ &\quad -(2-\lambda'_n)\cos[(2-\lambda'_n)\theta]\Big\} \end{aligned} \tag{4.1.17}$$

$$\begin{aligned} \sigma_{\theta\theta n}(r,\theta) &= r^{-\lambda'_n}(1-\lambda'_n)(2-\lambda'_n)D_n\Big\{-\frac{\cos[(2-\lambda'_n)\theta_1]}{\cos(\lambda'_n\theta_1)}\cos(\lambda'_n\theta) \\ &\quad +\cos[(2-\lambda'_n)\theta]\Big\} \end{aligned} \tag{4.1.18}$$

$$\begin{aligned} \sigma_{r\theta n}(r,\theta) &= -r^{-\lambda'_n}(1-\lambda'_n)D_n\Big\{\lambda'_n\frac{\cos[(2-\lambda'_n)\theta_1]}{\cos(\lambda'_n\theta_1)}\sin(\lambda'_n\theta) \\ &\quad -(2-\lambda'_n)\sin[(2-\lambda'_n)\theta]\Big\} \end{aligned} \tag{4.1.19}$$

where D_n is an arbitrary constant and we assume $\cos(\lambda'_n\theta_1)$ to be nonzero. If $\cos(\lambda'_n\theta_1) = 0$, there must be $\lambda'_n \sin(\lambda'_n\theta_1) \neq 0$. Therefore, Eq. (4.1.16) should be used instead of Eq. (4.1.15).

The corresponding displacements for plane stress are

$$\begin{aligned} u_n(r,\theta) &= \frac{r^{(1-\lambda'_n)}}{E}\Big\{B_n[2(1-\nu)+\lambda'_n(1+\nu)]\cos(\lambda'_n\theta) \\ &\quad -D_n(1+\nu)(2-\lambda'_n)\cos[(2-\lambda'_n)\theta]\Big\} \\ &= -\frac{r^{(1-\lambda'_n)}}{E}D_n\Big\{\frac{\cos[(2-\lambda'_n)\theta_1]}{\cos(\lambda'_n\theta_1)}\ [2(1-\nu)+\lambda'_n(1+\nu)]\cos(\lambda'_n\theta) \\ &\quad +(1+\nu)(2-\lambda'_n)\cos[(2-\lambda'_n)\theta]\Big\}, \end{aligned} \tag{4.1.20}$$

$$\begin{aligned} v_n(r,\theta) &= \frac{r^{(1-\lambda'_n)}}{E}\Big\{-B_n[2(1-\nu)+(1+\nu)(2-\lambda'_n)]\sin(\lambda'_n\theta) \\ &\quad +D_n(1+\nu)(2-\lambda'_n)\sin[(2-\lambda'_n)\theta]\Big\} \\ &= \frac{r^{(1-\lambda'_n)}}{E}D_n\Big\{\frac{\cos[(2-\lambda'_n)\theta_1]}{\cos(\lambda'_n\theta_1)}\ [2(1-\nu)+(1+\nu)(2-\lambda'_n)]\sin(\lambda'_n\theta) \\ &\quad +(1+\nu)(2-\lambda'_n)\sin[(2-\lambda'_n)\theta]\Big\}. \end{aligned} \tag{4.1.21}$$

(II) The case of $\mathrm{Det}[\Delta_{AC}]=0$

From Eq. (4.1.12) it is known that $\lambda=0$ always is the solution of $\mathrm{Det}[\Delta_{AC}]=0$, which will be discussed in next section. We assume that λ''_n is the solution of $\mathrm{Det}[\Delta_{AC}]=0$. Then,

$$\sin[2(1-\lambda''_n)\theta_1]=(1-\lambda''_n)\sin(2\theta_1) \tag{4.1.22}$$

and

$$\mathrm{Det}[\Delta_{BD}]=2(1-\lambda''_n)\sin(2\theta_1). \tag{4.1.23}$$

If $\lambda''_n\neq 1$ or $\theta_1\neq\pi/2$ and π, there is $\mathrm{Det}[\Delta_{BD}]\neq 0$. This means that for $\lambda''_n\neq 1$ or $\theta_1\neq\pi/2$ and π, the coefficients B_n and D_n must be zero. In analogy to (I), we know that according to the eigenvalue λ''_n, there always is $B_n=D_n=0$, except for $\lambda''_n=0$. Corresponding to λ''_n, the coefficients A_n and C_n are nonzero. From Eq. (4.1.6) we obtain

$$A_n=-C_n\frac{\sin[(2-\lambda''_n)\theta_1]}{\sin(\lambda''_n\theta_1)} \tag{4.1.24}$$

for $\sin(\lambda''_n\theta_1)\neq 0$ or from Eq. (4.1.7),

$$A_n=-C_n\frac{(2-\lambda''_n)\cos[(2-\lambda''_n)\theta_1]}{\lambda''_n\cos(\lambda''_n\theta_1)} \tag{4.1.25}$$

for $\lambda''_n\cos(\lambda''_n\theta_1)\neq 0$. For the given λ''_n, the corresponding stress term is

$$\begin{aligned} \sigma_{rrn}(r,\theta) &= r^{-\lambda''_n}(1-\lambda''_n)C_n\Big\{-(2+\lambda''_n)\frac{\sin[(2-\lambda''_n)\theta_1]}{\sin(\lambda''_n\theta_1)}\sin(\lambda''_n\theta) \\ &\quad -(2-\lambda''_n)\sin[(2-\lambda''_n)\theta]\Big\} \end{aligned} \tag{4.1.26}$$

$$\sigma_{\theta\theta n}(r,\theta) = r^{-\lambda_n''}(1-\lambda_n'')(2-\lambda_n'')C_n\Big\{-\frac{\sin[(2-\lambda_n'')\theta_1]}{\sin(\lambda_n''\theta_1)}\sin(\lambda_n''\theta) + \sin[(2-\lambda_n'')\theta]\Big\} \tag{4.1.27}$$

$$\sigma_{r\theta n}(r,\theta) = -r^{-\lambda_n''}(1-\lambda_n'')C_n\Big\{-\lambda_n''\frac{\sin[(2-\lambda_n'')\theta_1]}{\sin(\lambda_n''\theta_1)}\cos(\lambda_n''\theta) + (2-\lambda_n'')\cos[(2-\lambda_n'')\theta]\Big\} \tag{4.1.28}$$

where C_n is an arbitrary constant and we assume that $\sin(\lambda_n''\theta_1)$ is nonzero. If $\sin(\lambda_n''\theta_1) = 0$, there must be $\lambda_n''\cos(\lambda_n''\theta_1) \neq 0$. Therefore, Eq. (4.1.25) should be used instead of Eq. (4.1.24).

The corresponding displacements for plane stress are

$$\begin{aligned} u_n(r,\theta) &= \frac{r^{(1-\lambda_n'')}}{E}\Big\{A_n[2(1-\nu)+\lambda_n''(1+\nu)]\sin(\lambda_n''\theta) \\ &\quad -C_n(1+\nu)(2-\lambda_n'')\sin[(2-\lambda_n'')\theta]\Big\} \\ &= -\frac{r^{(1-\lambda_n'')}}{E}C_n\Big\{\frac{\sin[(2-\lambda_n'')\theta_1]}{\sin(\lambda_n''\theta_1)}\ [2(1-\nu)+\lambda_n''(1+\nu)]\sin(\lambda_n''\theta) \\ &\quad +(1+\nu)(2-\lambda_n'')\sin[(2-\lambda_n'')\theta]\Big\}, \end{aligned} \tag{4.1.29}$$

$$\begin{aligned} v_n(r,\theta) &= \frac{r^{(1-\lambda_n'')}}{E}\Big\{A_n[2(1-\nu)+(1+\nu)(2-\lambda_n'')]\cos(\lambda_n''\theta) \\ &\quad -C_n(1+\nu)(2-\lambda_n'')\cos[(2-\lambda_n'')\theta]\Big\} \\ &= -\frac{r^{(1-\lambda_n'')}}{E}C_n\Big\{\frac{\sin[(2-\lambda_n'')\theta_1]}{\sin(\lambda_n''\theta_1)}\ [2(1-\nu)+(1+\nu)(2-\lambda_n'')]\cos(\lambda_n''\theta) \\ &\quad +(1+\nu)(2-\lambda_n'')\cos[(2-\lambda_n'')\theta]\Big\}. \end{aligned} \tag{4.1.30}$$

From Chapter 3 it is known that for the singular stress term all eigenvalues in the range of $0 < \lambda_n' < 1$ and $0 < \lambda_n'' < 1$ should be taken into account. Equations (4.1.11) and (4.1.12) only have one solution in this range, respectively. Finally, the singular stress term can be calculated from

$$\begin{aligned} \sigma_{rr}^S(r,\theta) &= \Big(\frac{r}{R}\Big)^{-\lambda'}(1-\lambda')K'\Big\{-(2+\lambda')\frac{\cos[(2-\lambda')\theta_1]}{\cos(\lambda'\theta_1)}\cos(\lambda'\theta) \\ &\quad -(2-\lambda')\cos[(2-\lambda')\theta]\Big\} \\ &+ \Big(\frac{r}{R}\Big)^{-\lambda''}(1-\lambda'')K''\Big\{-(2+\lambda'')\frac{\sin[(2-\lambda'')\theta_1]}{\sin(\lambda''\theta_1)}\sin(\lambda''\theta) \\ &\quad -(2-\lambda'')\sin[(2-\lambda'')\theta]\Big\} \end{aligned} \tag{4.1.31}$$

$$\begin{aligned}\sigma^S_{\theta\theta}(r,\theta) &= \Big(\frac{r}{R}\Big)^{-\lambda'}(1-\lambda')(2-\lambda')K'\Big\{-\frac{\cos[(2-\lambda')\theta_1]}{\cos(\lambda'\theta_1)}\cos(\lambda'\theta)\\ &\quad +\cos[(2-\lambda')\theta]\Big\}\\ &+ \Big(\frac{r}{R}\Big)^{-\lambda''}(1-\lambda'')(2-\lambda'')K''\Big\{-\frac{\sin[(2-\lambda'')\theta_1]}{\sin(\lambda''\theta_1)}\sin(\lambda''\theta)\\ &\quad +\sin[(2-\lambda'')\theta]\Big\} \qquad (4.1.32)\end{aligned}$$

$$\begin{aligned}\sigma^S_{r\theta}(r,\theta) &= -\Big(\frac{r}{R}\Big)^{-\lambda'}(1-\lambda')K'\Big\{\lambda'\frac{\cos[(2-\lambda')\theta_1]}{\cos(\lambda'\theta_1)}\sin(\lambda'\theta)\\ &\quad -(2-\lambda')\sin[(2-\lambda')\theta]\Big\}\\ &- \Big(\frac{r}{R}\Big)^{-\lambda''}(1-\lambda'')K''\Big\{-\lambda''\frac{\sin[(2-\lambda'')\theta_1]}{\sin(\lambda''\theta_1)}\cos(\lambda''\theta)\\ &\quad +(2-\lambda'')\cos[(2-\lambda'')\theta]\Big\} \qquad (4.1.33)\end{aligned}$$

where $K' = D/R^{\lambda'}$ and $K'' = C/R^{\lambda''}$, which have the unit of the stress and should be determined from the stress analysis by FEM.

The corresponding displacements are:

$$\begin{aligned}u^S(r,\theta) &= -\Big\{\Big(\frac{r}{R}\Big)^{(1-\lambda'_n)}K'\Big\{\frac{\cos[(2-\lambda'_n)\theta_1]}{\cos(\lambda'_n\theta_1)}\ [2(1-\nu)+\lambda'_n(1+\nu)]\cos(\lambda'_n\theta)\\ &\quad +(1+\nu)(2-\lambda'_n)\cos[(2-\lambda'_n)\theta]\Big\}\\ &\quad +\Big(\frac{r}{R}\Big)^{(1-\lambda''_n)}K''\Big\{\frac{\sin[(2-\lambda''_n)\theta_1]}{\sin(\lambda''_n\theta_1)}\ [2(1-\nu)+\lambda''_n(1+\nu)]\sin(\lambda''_n\theta)\\ &\quad +(1+\nu)(2-\lambda''_n)\sin[(2-\lambda''_n)\theta]\Big\}\Big\}\ \frac{R}{E}, \qquad (4.1.34)\end{aligned}$$

$$\begin{aligned}v^S(r,\theta) &= \Big\{\Big(\frac{r}{R}\Big)^{(1-\lambda'_n)}K'\Big\{\frac{\cos[(2-\lambda'_n)\theta_1]}{\cos(\lambda'_n\theta_1)}\ [2(1-\nu)+(1+\nu)(2-\lambda'_n)]\sin(\lambda'_n\theta)\\ &\quad +(1+\nu)(2-\lambda'_n)\sin[(2-\lambda'_n)\theta]\Big\}\\ &\quad -\Big(\frac{r}{R}\Big)^{(1-\lambda''_n)}K''\Big\{\frac{\sin[(2-\lambda''_n)\theta_1]}{\sin(\lambda''_n\theta_1)}\ [2(1-\nu)+(1+\nu)(2-\lambda''_n)]\cos(\lambda''_n\theta)\\ &\quad +(1+\nu)(2-\lambda''_n)\cos[(2-\lambda''_n)\theta]\Big\}\Big\}\ \frac{R}{E}. \qquad (4.1.35)\end{aligned}$$

From Eqs. (4.1.17 - 4.1.19) and Eqs. (4.1.26 - 4.1.28) it follows that the stresses corresponding to the eigenvalue λ'_n are symmetric and the stresses corresponding to the eigenvalue λ''_n are antisymmetric to θ. The solutions of Eqs. (4.1.11) and (4.1.12) in the range of $-0.5 \le \lambda \le 1$ are plotted in Fig. 4.2 versus the angle θ_1 (half of angle occupied by the material). The solution of Eq. (4.1.11) is denoted as λ_1,

and as λ_2 if the solution is obtained from Eq. (4.1.12). It can be seen that: (a) In the shown range ($-0.5 < \omega < 1$), Eq. (4.1.11) has three solutions, of which two are always negative and may be complex ($\lambda = \omega + i\ p$), and Eq. (4.1.12) has one solution only. (b) For a notch angle of $\theta_1 \leq 90°$, there is no singular term, for $90° \leq \theta_1 \leq 128.7267°$ there is one singular term only, which corresponds to the symmetric stress term, and for $128.7267° \leq \theta_1 \leq 180°$ there are two singular terms corresponding to both symmetric and antisymmetric stress term. (c) There are only three notch angles, i.e. $\theta_1 = 90°, 128.7267°$, and $180°$, zero being the second-order solution of $\mathrm{Det}[\Delta_{BD}] \times \mathrm{Det}[\Delta_{AC}] = 0$. It should be noted that $\lambda = 0$ always is the first-order solution of $\mathrm{Det}[\Delta_{BD}] \times \mathrm{Det}[\Delta_{AC}] = 0$.

4.1.2 The Regular Stress Term

It is known from Chapter 3 that the regular stress corresponds to the stress term with $\lambda_n = 0$.
For a homogeneous material with a notch, the stresses are always zero for thermal loading. For remote mechanical loading, setting of $\alpha = 0$ and $\beta = 0$ in Eq. (3.3.32) yields

$$\mathrm{Det}([A_0]_{8\times 8}) = 64 \sin(2\theta_1)\Big[-2\theta_1 \cos(2\theta_1) + \sin(2\theta_1)\Big]. \tag{4.1.36}$$

If $\mathrm{Det}([A_0]_{8\times 8}) \neq 0$, the regular stress term is always zero. If $\mathrm{Det}([A_0]_{8\times 8}) = 0$, the regular stress is nonzero. This means that if

$$\sin(2\theta_1) = 0 \tag{4.1.37}$$

or

$$-2\theta_1 \cos(2\theta_1) + \sin(2\theta_1) = 0 \tag{4.1.38}$$

i.e., if

$$\theta_1 = \pi/2 \tag{4.1.39}$$

or

$$\theta_1 = \frac{1}{2}\tan(2\theta_1) \quad (\theta_1 = 128.7267°) \tag{4.1.40}$$

the regular stress term is nonzero.
For $\theta_1 = \pi/2$ (this is a trivial case of a tensile bar),

$$\begin{aligned} \sigma_{yy0} &= 4K_0 \\ \sigma_{xx0} &= \sigma_{xy0} = 0. \end{aligned} \tag{4.1.41}$$

according to Section 3.3.9. The corresponding displacements can be obtained from Eqs. (3.3.135), (3.3.5), and (3.3.6) as

$$u_0 = \frac{2r}{E} K_0 \Big\{ 1 - \nu - (1+\nu)\cos(2\theta) \Big\} \tag{4.1.42}$$

$$v_0 = \frac{2r}{E} K_0 \Big\{ (1+\nu)\sin(2\theta) \Big\}. \tag{4.1.43}$$

It should be noted that for a notch in homogeneous material the quantity $\mathcal{F}$ in Eq. (3.3.6) is equal to zero, because it corresponds to the rigid body rotation. The displacements in polar coordinates (u, v) can be transferred to Cartesian coordinates (u_x, u_y) by using

$$u_x = u\cos(\theta) - v\sin(\theta) \tag{4.1.44}$$

$$u_y = u\sin(\theta) + v\cos(\theta). \tag{4.1.45}$$

In Cartesian coordinates the displacements are

$$u_{x0} = -\nu \frac{4K_0}{E} x \tag{4.1.46}$$

$$u_{y0} = \frac{4K_0}{E} y. \tag{4.1.47}$$

For $\theta_1 = \frac{1}{2}\tan(2\theta_1)$ ($\theta_1 = 128.7267°$), and $\alpha = \beta = 0$, the equations in Section 3.3.2 can be simplified. The regular stress term in polar coordinates is:

$$\sigma_{rr0}(\theta) = 8K_0 \sin(2\theta_1) \Big\{ \sin(2\theta_1)\theta + \sin(2\theta)\ \theta_1 \Big\} \tag{4.1.48}$$

$$\sigma_{\theta\theta 0}(\theta) = 8K_0 \sin(2\theta_1) \Big\{ \sin(2\theta_1)\theta - \sin(2\theta)\ \theta_1 \Big\} \tag{4.1.49}$$

$$\tau_{r\theta 0}(\theta) = -4K_0 \sin(2\theta_1) \Big\{ \sin(2\theta_1) - \cos(2\theta)\ 2\theta_1 \Big\} \tag{4.1.50}$$

and in Cartesian coordinates it is:

$$\begin{aligned} \sigma_{xx0} &= 4K_0 \Big[2\theta + \sin(2\theta) \Big] \sin^2(2\theta_1) \\ \sigma_{yy0} &= 4K_0 \Big[2\theta - \sin(2\theta) \Big] \sin^2(2\theta_1) \\ \sigma_{xy0} &= 4K_0 \Big[2\theta_1 - \cos(2\theta)\sin(2\theta_1) \Big] \sin(2\theta_1) \end{aligned} \tag{4.1.51}$$

The displacements are

$$u_0 = \frac{8r}{E}\ K_0\ \sin(2\theta_1) \Big\{ \theta(1-\nu)\sin(2\theta_1) + (1+\nu)\theta_1 \sin(2\theta) \Big\} \tag{4.1.52}$$

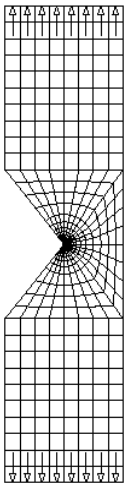

Figure 4.3: Notch with $\theta_1 = 128.7267°$ for a symmetric overall geometry.

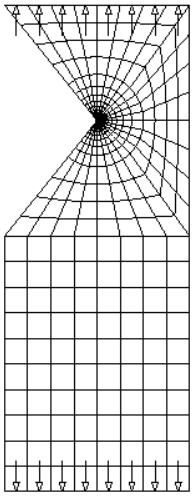

Figure 4.4: Notch with $\theta_1 = 128.7267°$ for an unsymmetric overall geometry.

$$v_0 = \frac{8r}{E} K_0 \ \sin(2\theta_1)\Big\{\theta_1(1+\nu)\cos(2\theta) - 2\sin(2\theta_1)\ln(r)\Big\}. \tag{4.1.53}$$

Finally, the stresses and displacements near the notch tip are calculated from

$$\sigma_{ij}(r,\theta) = \sigma_{ij}^S(r,\theta) + \sigma_{ij0}(\theta), \tag{4.1.54}$$

and

$$u_{ij}(r,\theta) = u_{ij}^S(r,\theta) + u_{ij0}(\theta). \tag{4.1.55}$$

For this special geometry, the regular stress term is nonzero only for unsymmetrical case. To show the effect of the regular stress term on the stresses and displacements, a notch geometry with $\theta_1 = 128.7267°$ and in plane strain will be considered. The material data are E=1 GPa and $\nu = 0.25$. For this notch angle, $\lambda_n' = 0.431886$, $\lambda_n'' = 0$, and the regular stress term is, in general, not zero.
As the first example, a symmetrical overall geometry is used (see Fig. 4.3, here only the left half is shown). The load is $\sigma_y = 1$ MPa. Due to the symmetry of the geometry and the load, the displacement v along the line $\theta = 0$ is always zero. From Eq. (4.1.53), $K_0 = 0$ can be obtained, i.e. for this symmetrical overall geometry the regular stress term is zero. The factor K' has been determined from the stress field near the notch tip, which was obtained by using FEM. The used FE mesh is also shown in Fig. 4.3. From the stresses σ_r and σ_θ along $\theta = 0$ in the range of $10^{-7} \leq r/L \leq 10^{-3}$, the factor K' is calculated and the averaged value is taken as K'. For the given overall geometry as in Fig. 4.3, $K' = 0.4358$ MPa. Using this K-factor, the stresses and displacements along the line of $\theta = -90°$ are calculated analytically from Eqs. (4.1.31-4.1.33) and

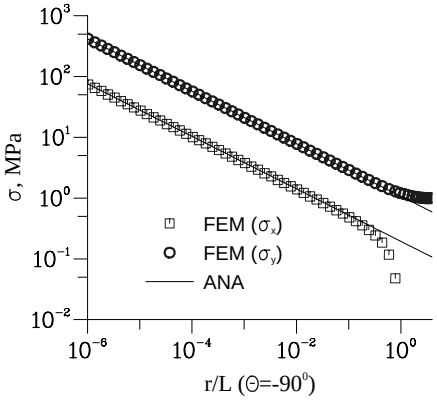

Figure 4.5: Comparison of the stresses calculated from FEM and the asymptotical solution, along the line of $\theta = -90°$.

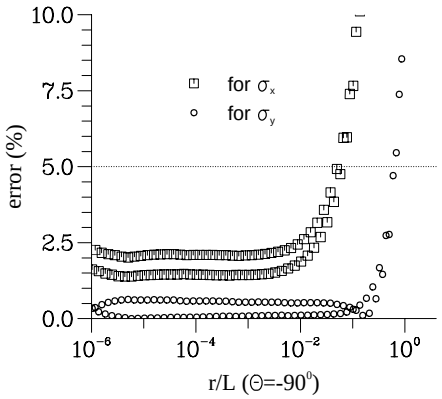

Figure 4.6: Error analysis of the stresses, error $= |\sigma_{\text{FEM}} - \sigma_{\text{Asymp.}}|/\sigma_{\text{FEM}} \times 100$.

(4.1.34-4.1.35) (it should be noted that for this example there is only one singular term and the regular term is zero). A comparison and error analysis of the stresses and displacements obtained from FEM and the analytical calculation are given in Figs. 4.5, 4.6 , 4.7, and 4.8. It can be seen that in the range of $r/L < 10^{-2}$, the stresses and displacements calculated from the analytical equations are in good agreement with those of FEM.

As the second example, an unsymmetrical overall geometry is used (see Fig. 4.4, here only the left half is shown). The load is $\sigma_y = 1$ MPa. Due to the unsymmetry of the geometry, the displacement v along the line $\theta = 0$ is not zero. Therefore, K_0 is not zero (see Eq. (4.1.53)), i.e. the regular stress term is not zero. From Eqs. (4.1.31 - 4.1.33) and (4.1.51) it is known that along the line of $\theta = 0$, the stress components σ_r and σ_θ contain the unknown factor K' only, while the stress component $\sigma_{r\theta}$ includes the unknown K_0 only. For this unsymmetrical overall geometry, the factor K' has therefore been determined from the stress components σ_r, σ_θ along $\theta = 0$ as above, and K_0 has been obtained from the stress component $\sigma_{r\theta}$. The obtained values are: $K' = 0.5707$ MPa, K_0=0.028 MPa. Using these determined K-factors, the stresses and displacements along the line of $\theta = -90°$ are calculated analytically from Eqs. (4.1.54) and (4.1.55) with only one term and with both singular and regular terms. A comparison and error analysis of the stresses and displacements obtained from FEM and the analytical calculation are given in Figs. 4.9, 4.10, , 4.11, and 4.12. From the error analysis it can be seen that if only the singular term is used, the agreement for the stresses and the displacements is good in a very small range ($r/L < 10^{-4}$) only, but if both singular and regular terms are used, the agreement is good in a larger range ($r/L < 10^{-2}$). To describe the stress and displacement field in a practically relevant

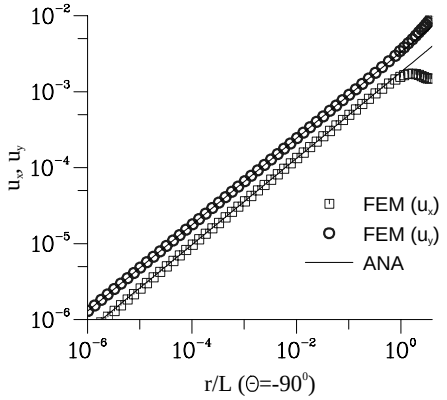

Figure 4.7: Comparison of the displacements calculated from FEM and the asymptotical solution, along the line of $\theta = -90°$.

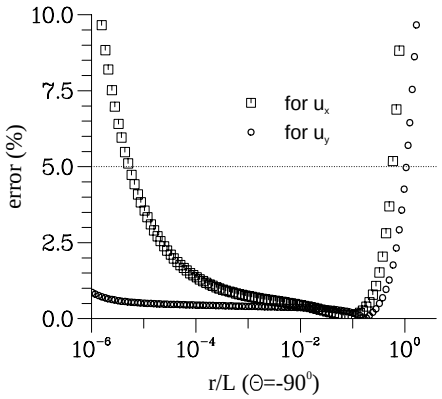

Figure 4.8: Error analysis of displacements, error $=|u_{\mathrm{FEM}} - u_{\mathrm{Asymp.}}|/u_{\mathrm{FEM}} \times 100$.

range of r/L, in the analytical equations the regular stress term should be considered if it is nonzero.
In Fig. 4.6 (also in Fig. 4.10) the fact of the duplicate curves is due to the results from FEM for the nodes at element corner and at the middle have a slight difference.

4.2 Homogeneous Material with a Crack

A homogeneous material with a crack means that the angle θ_1 is equal to 180°.

4.2.1 Determination of the Stress Exponent and the Angular Function

For $\theta_1 = \pi$, Eqs. (4.1.11) and (4.1.12) are valid as well. Therefore

$$\mathrm{Det}[\Delta_{BD}] = \sin[2(1-\lambda_n)\pi] \tag{4.2.1}$$

and

$$\mathrm{Det}[\Delta_{AC}] = -\sin[2(1-\lambda_n)\pi]. \tag{4.2.2}$$

We can see that in the range of $0 < \lambda < 1$ there is only one solution of $\mathrm{Det}[\Delta_{BD}] = 0$ and of $\mathrm{Det}[\Delta_{AC}] = 0$, and they are the same. It is $\lambda = 0.5$.
For $\theta_1 = \pi$ and $\lambda = 1/2$, Eq. (4.1.8) yields

$$B = 3D \tag{4.2.3}$$

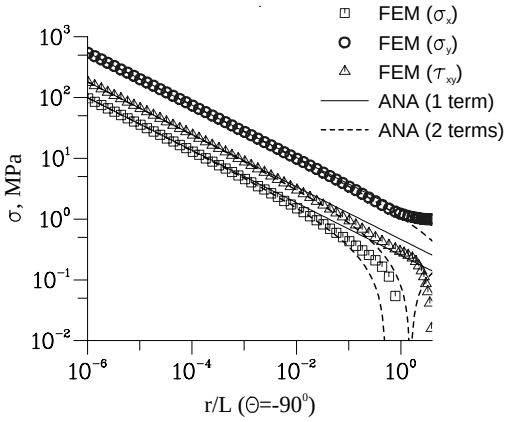

Figure 4.9: Comparison of the stresses calculated from FEM and the asymptotical solution, along the line of $\theta = -90°$, for the unsymmetric case.

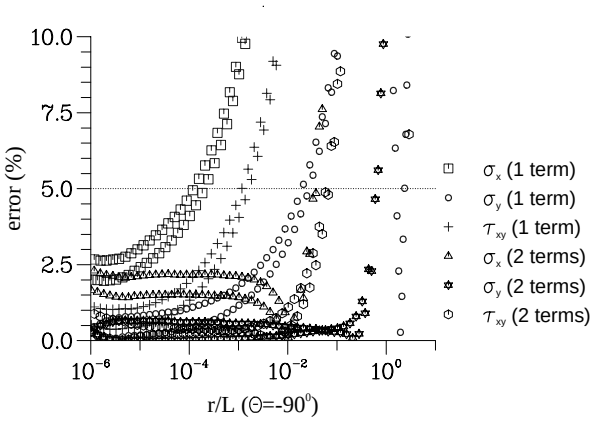

Figure 4.10: Error analysis of the stresses for the unsymmetrical case.

and Eq. (4.1.6) gives

$$A = C, \tag{4.2.4}$$

where Eq. (4.2.3) corresponds to mode I loading (symmetric case) and Eq. (4.2.4) corresponds to mode II loading (antisymmetric case) .
Finally, from Eqs. (3.1.7) to (3.1.9) the singular stress term can be calculated as follows:

$$\sigma^S_{rr}(r,\theta) = \frac{1}{4}(r/R)^{-0.5}\left\{K'\Big[5\cos(\frac{\theta}{2}) - \cos(\frac{3\theta}{2})\Big] + K''\Big[5\sin(\frac{\theta}{2}) - 3\sin(\frac{3\theta}{2})\Big]\right\} \tag{4.2.5}$$

$$\sigma^S_{\theta\theta}(r,\theta) = \frac{1}{4}(r/R)^{-0.5}\left\{K'\Big[3\cos(\frac{\theta}{2}) + \cos(\frac{3\theta}{2})\Big] + 3K''\Big[\sin(\frac{\theta}{2}) + \sin(\frac{3\theta}{2})\Big]\right\} \tag{4.2.6}$$

$$\sigma^S_{r\theta}(r,\theta) = \frac{1}{4}(r/R)^{-0.5}\left\{K'\Big[\sin(\frac{\theta}{2}) + \sin(\frac{3\theta}{2})\Big] - K''\Big[\cos(\frac{\theta}{2}) + 3\cos(\frac{3\theta}{2})\Big]\right\} \tag{4.2.7}$$

where $K' = \frac{3D}{R^{0.5}}$ and $K'' = \frac{C}{R^{0.5}}$, which should be determined from the stress analysis by FEM. From Eqs. (3.1.16) and (3.1.17), the displacements for plane stress are:

$$u^S(r,\theta) \;=\; \frac{1}{2}\,\frac{R}{E}\,\left(\frac{r}{R}\right)^{0.5}\left\{K'\left[(5-3\nu)\cos(\frac{\theta}{2}) - (1+\nu)\cos(\frac{3\theta}{2})\right] +\right.$$

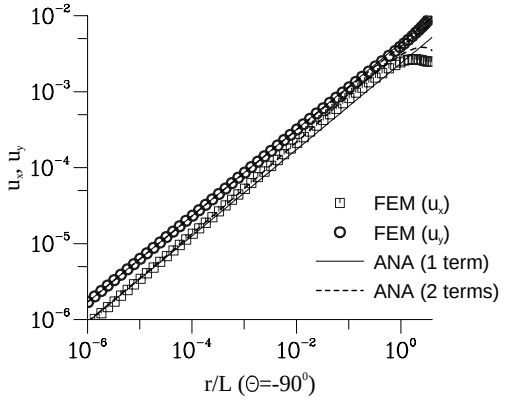

Figure 4.11: Comparison of the displacements calculated from FEM and the asymptotical solution, along the line of $\theta = -90°$, for the unsymmetric case.

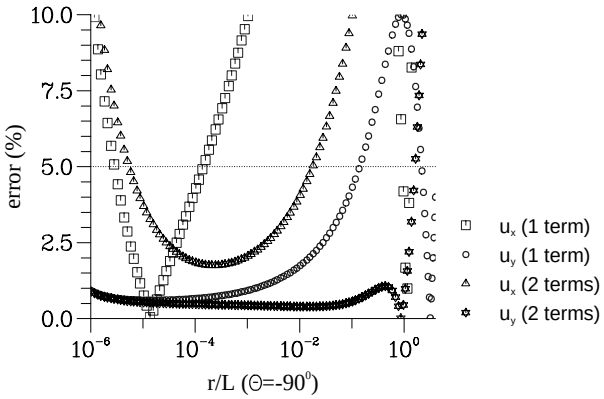

Figure 4.12: Error analysis of the displacements for the unsymmetric case.

$$+K''\left[(5-3\nu)\sin(\frac{\theta}{2}) - 3(1+\nu)\sin(\frac{3\theta}{2})\right]\Bigg\} \tag{4.2.8}$$

$$\begin{aligned} v^S(r,\theta) &= \frac{1}{2}\frac{R}{E}\left(\frac{r}{R}\right)^{0.5}\Bigg\{K'\left[-(7-\nu)\sin(\frac{\theta}{2}) + (1+\nu)\sin(\frac{3\theta}{2})\right] \\ &\quad +K''\left[(7-\nu)\cos(\frac{\theta}{2}) - 3(1+\nu)\cos(\frac{3\theta}{2})\right]\Bigg\}. \end{aligned} \tag{4.2.9}$$

In the following sections, two special cases of load and overall geometry shall be discussed.

(I) Crack under Model I Loading

If the geometry and loading are symmetric to the crack line, the stress tensor in the elasticity is also symmetric to the crack line. This means that

$$\begin{aligned} \sigma_{rr}(r,\theta) &= \sigma_{rr}(r,-\theta) \\ \sigma_{\theta\theta}(r,\theta) &= \sigma_{\theta\theta}(r,-\theta) \\ \sigma_{r\theta}(r,\theta) &= -\sigma_{r\theta}(r,-\theta). \end{aligned} \tag{4.2.10}$$

Model I loading is the type, which is symmetric to the crack line. Therefore, the stress tensor according to mode I loading is symmetric to the crack line. To satisfy Eq. (4.2.10), the factor K'' in Eqs. (4.2.5 - 4.2.7) must be zero.

Finally, for a crack under mode I loading the singular stress term is

$$\sigma^S_{rr}(r,\theta) = \frac{1}{4}(r/R)^{-0.5}K'\Big[5\cos(\frac{\theta}{2}) - \cos(\frac{3\theta}{2})\Big] \tag{4.2.11}$$

$$\sigma^S_{\theta\theta}(r,\theta) = \frac{1}{4}(r/R)^{-0.5}K'\Big[3\cos(\frac{\theta}{2}) + \cos(\frac{3\theta}{2})\Big] \tag{4.2.12}$$

$$\sigma^S_{r\theta}(r,\theta) = \frac{1}{4}(r/R)^{-0.5}K'\Big[\sin(\frac{\theta}{2}) + \sin(\frac{3\theta}{2})\Big]. \tag{4.2.13}$$

Transforming the stress components from polar coordinates into Cartesian coordinates results in:

$$\sigma^S_{xx}(r,\theta) = \frac{K'}{(r/R)^{0.5}}\cos(\frac{\theta}{2})\Big[1 - \sin(\frac{\theta}{2})\sin(\frac{3\theta}{2})\Big] \tag{4.2.14}$$

$$\sigma^S_{yy}(r,\theta) = \frac{K'}{(r/R)^{0.5}}\cos(\frac{\theta}{2})\Big[1 + \sin(\frac{\theta}{2})\sin(\frac{3\theta}{2})\Big] \tag{4.2.15}$$

$$\sigma^S_{xy}(r,\theta) = \frac{K'}{(r/R)^{0.5}}\sin(\frac{\theta}{2})\cos(\frac{\theta}{2})\cos(\frac{3\theta}{2}). \tag{4.2.16}$$

Equations (4.2.14 - 4.2.16) are the same as those in fracture mechanics, but the definition of factor K' is different due to r being normalized by R.

(II) Crack under Model II Loading

If the geometry is symmetric and the loading is antisymmetric to the crack line, the stress tensor in the elasticity is antisymmetric to the crack line. This means that

$$\begin{aligned} \sigma_{rr}(r,\theta) &= - \sigma_{rr}(r,-\theta) \\ \sigma_{\theta\theta}(r,\theta) &= - \sigma_{\theta\theta}(r,-\theta) \\ \sigma_{r\theta}(r,\theta) &= \sigma_{r\theta}(r,-\theta). \end{aligned} \tag{4.2.17}$$

Model II loading is the type, which is antisymmetric to the crack line. Therefore, the stress tensor according to mode II loading is antisymmetric to the crack line. To satisfy Eq. (4.2.17), the factor K' in Eqs. (4.2.5 - 4.2.7) must be zero.
Finally, for a crack under mode II loading the singular stress term is

$$\sigma^S_{rr}(r,\theta) = \frac{1}{4}(r/R)^{-0.5}K''\Big[5\sin(\frac{\theta}{2}) - 3\sin(\frac{3\theta}{2})\Big] \tag{4.2.18}$$

$$\sigma^S_{\theta\theta}(r,\theta) = \frac{3}{4}(r/R)^{-0.5}K''\Big[\sin(\frac{\theta}{2}) + \sin(\frac{3\theta}{2})\Big] \tag{4.2.19}$$

$$\sigma^S_{r\theta}(r,\theta) = -\frac{1}{4}(r/R)^{-0.5}K''\Big[\cos(\frac{\theta}{2}) + 3\cos(\frac{3\theta}{2})\Big]. \tag{4.2.20}$$

Transforming the stress components from polar coordinates into Cartesian coordinates results in:

$$\sigma^S_{xx}(r,\theta) = \frac{K''}{(r/R)^{0.5}}\sin(\frac{\theta}{2})\Big[2 + \cos(\frac{\theta}{2})\cos(\frac{3\theta}{2})\Big] \tag{4.2.21}$$

$$\sigma^S_{yy}(r,\theta) = -\frac{K''}{(r/R)^{0.5}}\sin(\frac{\theta}{2})\cos(\frac{\theta}{2})\cos(\frac{3\theta}{2}) \tag{4.2.22}$$

$$\sigma^S_{xy}(r,\theta) = -\frac{K''}{(r/R)^{0.5}}\cos(\frac{\theta}{2})\Big[1 - \sin(\frac{\theta}{2})\sin(\frac{3\theta}{2})\Big]. \tag{4.2.23}$$

Equations (4.2.21 - 4.2.23) are the same as those in fracture mechanics, but the definition of factor K'' is different.

4.2.2 The Regular Stress Term

For a homogeneous material with a crack under thermal loading the stresses are always zero. For remote mechanical loading, setting of $\alpha = 0$ and $\beta = 0$ in Eq. (3.3.133) yields the regular stress term in Cartesian coordinates:

$$\begin{aligned} \sigma_{xx0} &= -4K_0 \\ \sigma_{yy0} &= \sigma_{xy0} = 0. \end{aligned} \tag{4.2.24}$$

This regular stress term is the called T-stress (see [137]). The displacements for plane stress are:

$$u_0(r,\theta) = \frac{2K_0}{E}\, r\ \{-(1-\nu) + (1+\nu)\cos(2\theta)\} \tag{4.2.25}$$

$$v_0(r,\theta) = -\frac{2K_0}{E}\, r\ \{(1+\nu)\sin(2\theta)\}. \tag{4.2.26}$$

For a crack under mode I loading, the regular stress term satisfies the condition in Eq. (4.2.10). This means that the regular stress term may be nonzero. But for a crack under mode II loading, the regular stress term does not satisfy the condition in Eq. (4.2.17). To satisfy this condition, K_0 must be zero. Therefore, the regular stress term for a crack under mode II loading is zero.

4.2.3 Summary

The stresses and displacements near the crack tip are calculated from

$$\sigma_{ij}(r,\theta) = \sigma_{ij}^{S}(r,\theta) + \sigma_{ij0}(\theta), \tag{4.2.27}$$

$$u_{ij}(r,\theta) = u_{ij}^{S}(r,\theta) + u_{ij0}(\theta). \tag{4.2.28}$$

The relations for determining the stresses and displacements in a homogeneous material with a crack are well known from fracture mechanics. The equations given in this section are identical with those of fracture mechanics, only the definitions of K' and K'' are different due to the coordinate r being normalized by R, where K' and K'' have the unit of the stress. The relationships between K', K'' and K_I, K_{II} (defined in fracture mechanics) are

$$K_I = \sqrt{2\pi R}K', \qquad K_{II} = -\sqrt{2\pi R}K''. \tag{4.2.29}$$

Chapter 5

Dissimilar Materials Joint with Edge Tractions

From Chapter 3 it is known that the singular behavior in a joint is independent of loading. In a dissimilar materials joint with edge tractions, therefore, the singularity behavior corresponds to that one of the same joint with a free edge, i.e. the singular stress exponents and their angular functions in the asymptotic solution of the stresses near the singular point are the same. However, to satisfy the boundary conditions along the edges, higher order regular stress terms have to be considered. Numerical calculations show that the regular stress terms are also important for the stress distribution, even very close to the singular point.

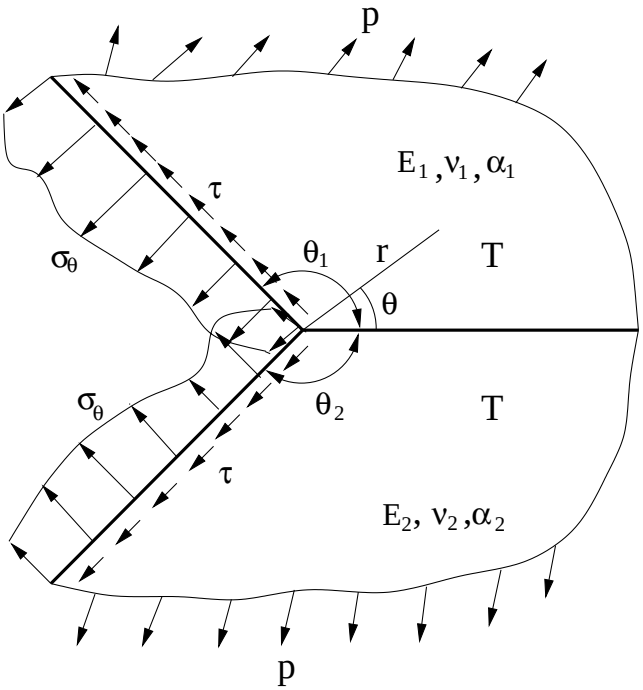

Figure 5.1: An arbitrary joint with edge tractions.

In this section a joint is considered (see Fig. 5.1), which is subjected to three different types of loading:
(a) Remote mechanical loading (RM);
(b) Thermal loading, e.g. a homogeneous temperature change in the joint (TH);
(c) Edge tractions (ET).
For cases (a) and (b) the solutions are known from Chapter 3. Following the superposition principle, only the case (c) is needed to be studied in details for elastic material behavior.
The stress field caused by the edge traction can be described by the superposition of some singular terms with corresponding the stress intensity factors K_i and higher order regular stress terms.
If the edge tractions can be expanded in a polynomial, the higher order regular stress terms can be calculated analytically. In Section 5.1 the equations to calculate these terms will be given in an explicit form. For a quarter planes joint, the behavior of the stress intensity factor (K) and some empirical relations to calculate K will be given in Section 5.2 for a normal edge traction and in 5.3 for a shear edge traction.

5.1 Basic Equations for Determination of the Higher-order Regular Stress Terms

In this section it is assumed that the tractions on the edges can be described by a polynomial. They have the following form:
at $\theta = \theta_1$

$$\sigma_{\theta\theta 1} = p_1 + \sum_{i=1}^{N_1} \bar{A}_i r^i \tag{5.1.1}$$

$$\tau_{r\theta 1} = t_1 + \sum_{j=1}^{N_2} \bar{B}_j r^j \tag{5.1.2}$$

at $\theta = \theta_2$

$$\sigma_{\theta\theta 2} = p_2 + \sum_{k=1}^{M_1} \bar{C}_k r^k \tag{5.1.3}$$

$$\tau_{r\theta 2} = t_2 + \sum_{l=1}^{M_2} \bar{D}_l r^l. \tag{5.1.4}$$

This means that the tractions $\sigma_{\theta\theta}, \tau_{r\theta}$ at $\theta = \theta_1$ and $\theta = \theta_2$ may be described by polynoms of different order. We take $M = max\Big\{N_1, N_2, M_1, M_2\Big\}$, then the boundary conditions for this problem are:

for $\theta = \theta_1$:

$$\sigma_{\theta\theta 1}(r,\theta_1) = p_1 + \sum_{l=1}^{M} \bar{A}_l r^l \tag{5.1.5}$$

$$\tau_{r\theta 1}(r,\theta_1) = t_1 + \sum_{l=1}^{M} \bar{B}_l r^l \tag{5.1.6}$$

for $\theta = \theta_2$:

$$\sigma_{\theta\theta 2}(r,\theta_2) = p_2 + \sum_{l=1}^{M} \bar{C}_l r^l \tag{5.1.7}$$

$$\tau_{r\theta 2}(r,\theta_2) = t_2 + \sum_{l=1}^{M} \bar{D}_l r^l \tag{5.1.8}$$

for $\theta = 0^\circ$:

$$\sigma_{\theta\theta 1}(r,0) = \sigma_{\theta\theta 2}(r,0), \qquad \tau_{r\theta 1}(r,0) = \tau_{r\theta 2}(r,0) \tag{5.1.9}$$

$$u_1(r,0) = u_2(r,0), \qquad v_1(r,0) = v_2(r,0), \tag{5.1.10}$$

where $\bar{A}_l = 0$ (for $l = N_1 + 1$ *to* M), $\bar{B}_l = 0$ (for $l = N_2 + 1$ *to* M), $\bar{C}_l = 0$ (for $l = M_1 + 1$ *to* M), $\bar{D}_l = 0$ (for $l = M_2 + 1$ *to* M). The stresses and the displacements near the singular point can be described by Eqs. (3.1.7) to (3.1.9) and Eqs. (3.1.16) to (3.1.17), considering the regular term as given in Eqs. (3.3.2) to (3.3.6). The boundary conditions lead to the following eight equations for plane stress:

$$\begin{aligned} \sum_n r^{-\omega_n}(2-\omega_n)(1-\omega_n) \quad \Big\{ \quad & A_{1n}\sin(\omega_n\theta_1) + B_{1n}\cos(\omega_n\theta_1) \\ + \quad & C_{1n}\sin\left[(2-\omega_n)\theta_1\right] + D_{1n}\cos\left[(2-\omega_n)\theta_1\right] \Big\} \\ + \quad & \sigma_{\theta\theta 10}(\theta_1) = p_1 + \sum_{l=1}^{M} \bar{A}_l r^l \end{aligned} \tag{5.1.11}$$

$$\begin{aligned} \sum_n r^{-\omega_n}(\omega_n - 1) \quad \Big\{ \quad & A_{1n}\omega_n\cos(\omega_n\theta_1) - B_{1n}\omega_n\sin(\omega_n\theta_1) \\ + \quad & C_{1n}(2-\omega_n)\cos\left[(2-\omega_n)\theta_1\right] - D_{1n}(2-\omega_n)\sin\left[(2-\omega_n)\theta_1\right] \Big\} \\ + \quad & \tau_{r\theta 10}(\theta_1) = t_1 + \sum_{l=1}^{M} \bar{B}_l r^l \end{aligned} \tag{5.1.12}$$

$$\sum_n r^{-\omega_n}(2-\omega_n)(1-\omega_n) \quad \Big\{ \quad A_{2n}\sin(\omega_n\theta_2) + B_{2n}\cos(\omega_n\theta_2)$$
$$+ \quad C_{2n}\sin\left[(2-\omega_n)\theta_2\right] + D_{2n}\cos\left[(2-\omega_n)\theta_2\right]\Big\}$$
$$+ \quad \sigma_{\theta\theta 20}(\theta_2) = p_2 + \sum_{l=1}^{M}\bar{C}_l r^l \tag{5.1.13}$$

$$\sum_n r^{-\omega_n}(\omega_n-1) \quad \Big\{ \quad A_{2n}\omega_n\cos(\omega_n\theta_2) - B_{2n}\omega_n\sin(\omega_n\theta_2)$$
$$+ \quad C_{2n}(2-\omega_n)\cos\left[(2-\omega_n)\theta_2\right] - D_{2n}(2-\omega_n)\sin\left[(2-\omega_n)\theta_2\right]\Big\}$$
$$+ \quad \tau_{r\theta 20}(\theta_2) = t_2 + \sum_{l=1}^{M}\bar{D}_l r^l \tag{5.1.14}$$

$$\sum_n r^{-\omega_n}(2-\omega_n)(1-\omega_n)\Big\{(B_{1n}+D_{1n}) - (B_{2n}+D_{2n})\Big\} + \sigma_{\theta\theta 10}(0) - \sigma_{\theta\theta 20}(0) = 0 \tag{5.1.15}$$

$$-\sum_n r^{-\omega_n}(1-\omega_n)\Big\{A_{1n}\omega_n + C_{1n}(2-\omega_n) \quad - \quad A_{2n}\omega_n - C_{2n}(2-\omega_n)\Big\} + \tau_{r\theta 10}(0)$$
$$- \quad \tau_{r\theta 20}(0) = 0 \tag{5.1.16}$$

$$\sum_n r^{1-\omega_n} \quad \Big\{ \quad B_{1n}\mu\Big[2(1-\nu_1) + \omega_n(1+\nu_1)\Big] - D_{1n}\mu(1+\nu_1)(2-\omega_n)$$
$$- \quad B_{2n}\Big[2(1-\nu_2) + \omega_n(1+\nu_2)\Big] + D_{2n}(1+\nu_2)(2-\omega_n)\Big\}$$
$$+ \quad u_{10}(r,0) - u_{20}(r,0) = rT \times E_2(\alpha_2 - \alpha_1) \tag{5.1.17}$$

$$\sum_n r^{1-\omega_n} \quad \Big\{ \quad A_{1n}\mu\Big[2(1-\nu_1) + (2-\omega_n)(1+\nu_1)\Big] - C_{1n}\mu(1+\nu_1)(2-\omega_n)$$
$$- \quad A_{2n}\Big[2(1-\nu_2) + (2-\omega_n)(1+\nu_2)\Big] + C_{2n}(1+\nu_2)(2-\omega_n)\Big\}$$
$$+ \quad \upsilon_{10}(r,0) - \upsilon_{20}(r,0) = 0 \tag{5.1.18}$$

where $\mu = E_2/E_1$ and $\omega_n \neq 0$ ($\omega_n = 0$ is concluded in the terms with σ_{ij0}). The quantities corresponding to the regular term, $\sigma_{ij10}, \sigma_{ij20}, u_{10}, u_{20}, \upsilon_{10}, \upsilon_{20}$, have the same form as those given in Eqs. (3.3.2) to (3.3.6).
To solve Eqs. (5.1.11 - 5.1.18) different cases should be considered:
(I) r-independent stress term;
(II) r-dependent stress terms: (a) $\omega_n = -1, -2, ... - l, ..., -M$; (b) $0 < \omega_n < 1$.

(I) The r-independent stress term.
From Eqs. (5.1.11 - 5.1.18) and Eqs. (3.3.2) to (3.3.6), the r-independent stress term has to fulfill the following boundary conditions:

$$\sigma_{\theta\theta 10}(\theta_1) = p_1 \tag{5.1.19}$$

$$\tau_{r\theta 10}(\theta_1) = t_1 \tag{5.1.20}$$

$$\sigma_{\theta\theta 20}(\theta_2) = p_2 \tag{5.1.21}$$

$$\tau_{r\theta 20}(\theta_2) = t_2 \tag{5.1.22}$$

$$\sigma_{\theta\theta 10}(0) - \sigma_{\theta\theta 20}(0) = 0 \tag{5.1.23}$$

$$\tau_{r\theta 10}(0) - \tau_{r\theta 20}(0) = 0 \tag{5.1.24}$$

$$u_{10}(r,0) - u_{20}(r,0) = rT \times E_2(\alpha_2 - \alpha_1) \tag{5.1.25}$$

$$\upsilon_{10}(r,0) - \upsilon_{20}(r,0) = 0. \tag{5.1.26}$$

Solving Eqs. (5.1.19 - 5.1.26), the coefficients $A_{k0}, B_{k0}, C_{k0}, D_{k0}$ in Eqs. (3.3.2) to (3.3.4) can be determined analytically. From Eqs. (5.1.19 - 5.1.26), we can see that the solution is made up of two parts; one is the contribution of the constant mechanical tractions p_1, t_1, p_2, and t_2. The other is the contribution of thermal loading with the temperature difference T. The solution according to the constant mechanical edge traction is denoted as $\sigma^{ET}_{ijk0}(\theta)$ and according to thermal loading as $\sigma^{TH}_{ijk0}(\theta)$. The term $\sigma^{TH}_{ijk0}(\theta)$ is known from Section 3.2. Here, only the solution for the constant mechanical traction will be given, i.e. in Eqs. (5.1.19 - 5.1.26) let T = 0.
To determine the coefficients A_{k0}, B_{k0},C_{k0}, and D_{k0} for an arbitrary joint geometry with θ_1 and θ_2, generally, an 8×8 linear equations system has to be solved directly. The disadvantage of directly solving an 8×8 linear equations system is that the relationship between the coefficients, the material properties (e.g. the Dundurs parameters), the joint angles θ_1, θ_2 and the loading are not clear. For some special geometries, e.g. $\theta_1 = -\theta_2$ or $\theta_1 - \theta_2 = 180°$ ($\theta_2 < 0$), the solution of Eqs. (5.1.19 - 5.1.26) can be simplified. As an example, the solution of Eqs. (5.1.19 - 5.1.26) will be given explicitly below for a joint with $\theta_1 = -\theta_2 = 90°$.
The coefficients in Eqs. (3.3.2 -3.3.4) can be calculated from $A_{k0} = A^*_{k0}/Z$, $B_{k0} = B^*_{k0}/Z$, $C_{k0} = C^*_{k0}/Z$, and $D_{k0} = D^*_{k0}/Z$ with

$$Z = 4(\mu - 1)\Big[(\mu - 1) - 2\beta(\mu + 1)\Big] \tag{5.1.27}$$

$$A^*_{10} = 2(t_1 - t_2)\Big[(\mu - 1) - 2\beta(\mu + 1)\Big] \tag{5.1.28}$$

$$B^*_{10} = (1 - \mu)\Big\{p_1\Big[2\beta(\mu + 1) - (2\mu - 1)\Big] + p_2\Big\} + \frac{\pi}{2}(t_1 - t_2)(2\beta\mu + 2\beta - 3\mu + 1) \tag{5.1.29}$$

$$C^*_{10} = \Big[t_1(2\mu-1) - t_2\Big]\Big[(\mu-1) - 2\beta(\mu+1)\Big] \tag{5.1.30}$$

$$D^*_{10} = (1-\mu)\Big\{p_2 - p_1\Big[2\beta(\mu+1)+1\Big]\Big\} + \frac{\pi}{2}(t_2-t_1)(\mu+1)(2\beta+1) \tag{5.1.31}$$

$$A^*_{20} = 2\mu(t_1-t_2)\Big[(\mu-1) - 2\beta(\mu+1)\Big] \tag{5.1.32}$$

$$B^*_{20} = (1-\mu)\Big\{-\mu p_1 + p_2\Big[2\beta(\mu+1)+2-\mu\Big]\Big\} + \frac{\pi}{2}\mu(t_2-t_1)(2\beta\mu-\mu+2\beta+3) \tag{5.1.33}$$

$$C^*_{20} = \Big[t_1\mu + t_2(\mu-2)\Big]\Big[(\mu-1) - 2\beta(\mu+1)\Big] \tag{5.1.34}$$

$$D^*_{20} = (\mu-1)\Big\{p_1\mu + p_2\Big[2\beta(\mu+1)-\mu\Big]\Big\} + \frac{\pi}{2}\mu(t_1-t_2)(\mu+1)(2\beta-1) \tag{5.1.35}$$

where $Z \neq 0$ and β is the Dundurs parameter. The relation between μ and α is

$$\mu = \frac{1+\alpha}{1-\alpha}.$$

Using the coefficients calculated with Eqs. (5.1.27 - 5.1.35), the stress term $\sigma^{ET}_{ijk0}(\theta)$ can be obtained from Eqs. (3.3.2 -3.3.4). In case of $Z = 0$ and $A_{k0} \neq 0$ or $B_{k0} \neq 0$ or $C_{k0} \neq 0$ or $D_{k0} \neq 0$, there is a logarithmic singularity.

(II) The case of $\omega_n = -1, -2, ... - l, ..., -M$.
Following Eqs. (5.1.11 - 5.1.18), to fulfill the r-dependent edge tractions for each $\omega_n = -l$ the boundary conditions lead to:

$$\begin{aligned} -A_{1l}sin(l\theta_1) \;&+\; B_{1l}cos(l\theta_1) + C_{1l}sin\Big[(2+l)\theta_1\Big] \\ &+\; D_{1l}cos\Big[(2+l)\theta_1\Big] = \frac{\bar{A}_l}{(2+l)(1+l)} \end{aligned} \tag{5.1.36}$$

$$\begin{aligned} A_{1l}lcos(l\theta_1) \;&+\; B_{1l}lsin(l\theta_1) - C_{1l}(2+l)cos\Big[(2+l)\theta_1\Big] \\ &+\; D_{1l}(2+l)sin\Big[(2+l)\theta_1\Big] = \frac{\bar{B}_l}{l+1} \end{aligned} \tag{5.1.37}$$

$$\begin{aligned} -A_{2l}sin(l\theta_2) \;&+\; B_{2l}cos(l\theta_2) + C_{2l}sin\Big[(2+l)\theta_2\Big] \\ &+\; D_{2l}cos\Big[(2+l)\theta_2\Big] = \frac{\bar{C}_l}{(2+l)(1+l)} \end{aligned} \tag{5.1.38}$$

$$A_{2l}lcos(l\theta_2) + B_{2l}lsin(l\theta_2) - C_{2l}(2+l)cos\Big[(2+l)\theta_2\Big] + D_{2l}(2+l)sin\Big[(2+l)\theta_2\Big] = \frac{\bar{D}_l}{1+l} \tag{5.1.39}$$

$$(B_{1l} + D_{1l}) - (B_{2l} + D_{2l}) = 0 \tag{5.1.40}$$

$$-A_{1l}l + C_{1l}(2+l) + A_{2l}l - C_{2l}(2+l) = 0 \tag{5.1.41}$$

$$B_{1l}\mu\Big[2(1-\nu_1) - l(1+\nu_1)\Big] - D_{1l}\mu(1+\nu_1)(2+l) - B_{2l}\Big[2(1-\nu_2) - l(1+\nu_2)\Big] + D_{2l}(1+\nu_2)(2+l) = 0 \tag{5.1.42}$$

$$A_{1l}\mu\Big[2(1-\nu_1) + (2+l)(1+\nu_1)\Big] - C_{1l}\mu(1+\nu_1)(2+l) - A_{2l}\Big[2(1-\nu_2) + (2+l)(1+\nu_2)\Big] + C_{2l}(1+\nu_2)(2+l) = 0 \tag{5.1.43}$$

By solving Eqs. (5.1.36 - 5.1.43), the coefficients $A_{kl}, B_{kl}, C_{kl}, D_{kl}$ (k=1,2) can be determined analytically. Generally, an 8×8 linear equations system has to be solved directly for an arbitrary joint geometry with θ_1 and θ_2. To see the relationship between the solution and the Dundurs parameters α and β, we need to describe the solution in an explicit form. For an arbitrary joint geometry the explicit form is very long and complicated. The coefficients for a joint with $\theta_1 = -\theta_2 = 90^\circ$ will be given below. We take

$$A_{kl} = \frac{A^*_{kl}}{Z_l},\ B_{kl} = \frac{B^*_{kl}}{Z_l},\ C_{kl} = \frac{C^*_{kl}}{Z_l},\ D_{kl} = \frac{D^*_{kl}}{Z_l} \tag{5.1.44}$$

with l = $2\mathcal{N}$ - 1 for odd numbers of l and l = $2\mathcal{N}$ for even numbers of l. They can be calculated from

$$Z_l = 256\mathcal{N}^2(2\mathcal{N}+1)\Big\{4\mathcal{N}^2\mu^2\beta^2 - 8\mathcal{N}^2\mu^2\beta + (4\mathcal{N}^2-1)\mu^2 + 8\mathcal{N}^2\mu\beta^2 - (8\mathcal{N}^2-2)\mu + 4\mathcal{N}^2\beta^2 + 8\mathcal{N}^2\beta + 4\mathcal{N}^2 - 1\Big\} \tag{5.1.45}$$

$$A^*_{1l} = 32(2\mathcal{N}+1)(-1)^{\mathcal{N}}\Big\{4\mathcal{N}^2\mu^2\beta^2\bar{\mathrm{A}} - (4\mathcal{N}-1)2\mathcal{N}\mu^2\beta\bar{\mathrm{A}} + (2\mathcal{N}-1)2\mathcal{N}\mu^2\bar{\mathrm{A}} + 8\mathcal{N}^2\mu\beta^2\bar{\mathrm{A}} + 2\mathcal{N}\mu\beta\bar{\mathrm{A}} - (4\mathcal{N}+1)(2\mathcal{N}-1)\mu\bar{\mathrm{A}} + 2\mathcal{N}\mu\beta\bar{\mathrm{C}} - (2\mathcal{N}-1)\mu\bar{\mathrm{C}} + 4\mathcal{N}^2\beta^2\bar{\mathrm{A}} + 8\mathcal{N}^2\beta\bar{\mathrm{A}} + (4\mathcal{N}^2-1)\bar{\mathrm{A}} + 2\mathcal{N}\beta\bar{\mathrm{C}} + (2\mathcal{N}-1)\bar{\mathrm{C}}\Big\} \tag{5.1.46}$$

$$B^*_{1l} = 32(2\mathcal{N}+1)(-1)^{(\mathcal{N}-1)}\Big\{4\mathcal{N}^2\mu^2\beta^2\bar{\mathrm{B}} - (4\mathcal{N}+1)2\mathcal{N}\mu^2\beta\bar{\mathrm{B}} + (2\mathcal{N}+1)2\mathcal{N}\mu^2\bar{\mathrm{B}} + 8\mathcal{N}^2\mu\beta^2\bar{\mathrm{B}} - 2\mathcal{N}\mu\beta\bar{\mathrm{B}} - (4\mathcal{N}-1)(2\mathcal{N}+1)\mu\bar{\mathrm{B}} - 2\mathcal{N}\mu\beta\bar{\mathrm{D}} + (2\mathcal{N}+1)\mu\bar{\mathrm{D}} + 4\mathcal{N}^2\beta^2\bar{\mathrm{B}} + 8\mathcal{N}^2\beta\bar{\mathrm{B}} + (4\mathcal{N}^2-1)\bar{\mathrm{B}} - 2\mathcal{N}\beta\bar{\mathrm{D}} - (2\mathcal{N}+1)\bar{\mathrm{D}}\Big\} \tag{5.1.47}$$

$$
\begin{aligned}
C^*_{1l} &= 32(-1)^{\mathcal{N}}\Big\{4\mathcal{N}^2(2\mathcal{N}-1)\mu^2\beta^2\bar{\mathrm{A}} - 2\Big[(4\mathcal{N}^2-3\mathcal{N}+2)(2\mathcal{N}+1)-2\Big]\mu^2\beta\bar{\mathrm{A}} \\
&+ (4\mathcal{N}^2-1)2\mathcal{N}\mu^2\bar{\mathrm{A}} + 8\mathcal{N}^2(2\mathcal{N}-1)\mu\beta^2\bar{\mathrm{A}} \\
&- 2\mathcal{N}(2\mathcal{N}+1)\mu\beta\bar{\mathrm{A}} - (4\mathcal{N}^2-1)(4\mathcal{N}-1)\mu\bar{\mathrm{A}} \\
&- 2\mathcal{N}(2\mathcal{N}+1)\mu\beta\bar{\mathrm{C}} + (4\mathcal{N}^2-1)\mu\bar{\mathrm{C}} + (2\mathcal{N}-1)4\mathcal{N}^2\beta^2\bar{\mathrm{A}} + 8\mathcal{N}^2(2\mathcal{N}-1)\beta\bar{\mathrm{A}} \\
&+ (2\mathcal{N}-1)^2(2\mathcal{N}+1)\bar{\mathrm{A}} - 2\mathcal{N}(2\mathcal{N}+1)\beta\bar{\mathrm{C}} - (4\mathcal{N}^2-1)\bar{\mathrm{C}}\Big\} \qquad (5.1.48)
\end{aligned}
$$

$$
\begin{aligned}
D^*_{1l} &= 32(-1)^{\mathcal{N}}\Big\{4\mathcal{N}^2(2\mathcal{N}+1)\mu^2\beta^2\bar{\mathrm{B}} - 2\Big[(2\mathcal{N}+1)(4\mathcal{N}^2-3\mathcal{N}+2)+4\mathcal{N}^2-2\Big]\mu^2\beta\bar{\mathrm{B}} \\
&+ (4\mathcal{N}^2-1)2\mathcal{N}\mu^2\bar{\mathrm{B}} + 8\mathcal{N}^2(2\mathcal{N}+1)\mu\beta^2\bar{\mathrm{B}} \\
&+ 2\mathcal{N}(2\mathcal{N}-1)\mu\beta\bar{\mathrm{B}} - (4\mathcal{N}^2-1)(4\mathcal{N}+1)\mu\bar{\mathrm{B}} \\
&+ 2\mathcal{N}(2\mathcal{N}-1)\mu\beta\bar{\mathrm{D}} - (4\mathcal{N}^2-1)\mu\bar{\mathrm{D}} + 4\mathcal{N}^2(2\mathcal{N}+1)\beta^2\bar{\mathrm{B}} + 8\mathcal{N}^2(2\mathcal{N}+1)\beta\bar{\mathrm{B}} \\
&+ (2\mathcal{N}-1)(2\mathcal{N}+1)^2\bar{\mathrm{B}} + 2\mathcal{N}(2\mathcal{N}-1)\beta\bar{\mathrm{D}} + (4\mathcal{N}^2-1)\bar{\mathrm{D}}\Big\} \qquad (5.1.49)
\end{aligned}
$$

$$
\begin{aligned}
A^*_{2l} &= 32(2\mathcal{N}+1)(-1)^{\mathcal{N}}\Big\{2\mathcal{N}\mu^2\beta\bar{\mathrm{A}} - (2\mathcal{N}-1)\mu^2\bar{\mathrm{A}} - 4\mathcal{N}^2\mu^2\beta^2\bar{\mathrm{C}} \\
&+ 8\mathcal{N}^2\mu^2\beta\bar{\mathrm{C}} - (4\mathcal{N}^2-1)\mu^2\bar{\mathrm{C}} + 2\mathcal{N}\mu\beta\bar{\mathrm{A}} + (2\mathcal{N}-1)\mu\bar{\mathrm{A}} - 8\mathcal{N}^2\mu\beta^2\bar{\mathrm{C}} \\
&+ 2\mathcal{N}\mu\beta\bar{\mathrm{C}} + (4\mathcal{N}+1)(2\mathcal{N}-1)\mu\bar{\mathrm{C}} - 4\mathcal{N}^2\beta^2\bar{\mathrm{C}} - 2\mathcal{N}(4\mathcal{N}-1)\beta\bar{\mathrm{C}} \\
&- 2\mathcal{N}(2\mathcal{N}-1)\bar{\mathrm{C}}\Big\} \qquad (5.1.50)
\end{aligned}
$$

$$
\begin{aligned}
B^*_{2l} &= 32(2\mathcal{N}+1)(-1)^{\mathcal{N}}\Big\{2\mathcal{N}\mu^2\beta\bar{\mathrm{B}} - (2\mathcal{N}+1)\mu^2\bar{\mathrm{B}} + 4\mathcal{N}^2\mu^2\beta^2\bar{\mathrm{D}} \\
&- 8\mathcal{N}^2\mu^2\beta\bar{\mathrm{D}} + (4\mathcal{N}^2-1)\mu^2\bar{\mathrm{D}} + 2\mathcal{N}\mu\beta\bar{\mathrm{B}} + (2\mathcal{N}+1)\mu\bar{\mathrm{B}} + 8\mathcal{N}^2\mu\beta^2\bar{\mathrm{D}} \\
&+ 2\mathcal{N}\mu\beta\bar{\mathrm{D}} - (4\mathcal{N}-1)(2\mathcal{N}+1)\mu\bar{\mathrm{D}} + 4\mathcal{N}^2\beta^2\bar{\mathrm{D}} + 2\mathcal{N}(4\mathcal{N}+1)\beta\bar{\mathrm{D}} \\
&+ 2\mathcal{N}(2\mathcal{N}+1)\bar{\mathrm{D}}\Big\} \qquad (5.1.51)
\end{aligned}
$$

$$
\begin{aligned}
C^*_{2l} &= 32(-1)^{(\mathcal{N}-1)}\Big\{2\mathcal{N}(2\mathcal{N}+1)\mu^2\beta\bar{\mathrm{A}} - (4\mathcal{N}^2-1)\mu^2\bar{\mathrm{A}} + 4\mathcal{N}^2(2\mathcal{N}-1)\mu^2\beta^2\bar{\mathrm{C}} - \\
&- 8\mathcal{N}^2(2\mathcal{N}-1)\mu^2\beta\bar{\mathrm{C}} + (2\mathcal{N}-1)^2(2\mathcal{N}+1)\mu^2\bar{\mathrm{C}} + 2\mathcal{N}(2\mathcal{N}+1)\mu\beta\bar{\mathrm{A}} \\
&+ (4\mathcal{N}^2-1)\mu\bar{\mathrm{A}} + 8\mathcal{N}^2(2\mathcal{N}-1)\mu\beta^2\bar{\mathrm{C}} + 2\mathcal{N}(2\mathcal{N}+1)\mu\beta\bar{\mathrm{C}} \\
&- (4\mathcal{N}-1)(4\mathcal{N}^2-1)\mu\bar{\mathrm{C}} + 4\mathcal{N}^2(2\mathcal{N}-1)\beta^2\bar{\mathrm{C}} \\
&+ 2\Big[(2\mathcal{N}+1)(4\mathcal{N}^2-3\mathcal{N}+2)-2\Big]\beta\bar{\mathrm{C}} + 2\mathcal{N}(4\mathcal{N}^2-1)\bar{\mathrm{C}}\Big\} \qquad (5.1.52)
\end{aligned}
$$

$$
\begin{aligned}
D^*_{2l} &= 32(-1)^{\mathcal{N}}\Big\{2\mathcal{N}(2\mathcal{N}-1)\mu^2\beta\bar{\mathrm{B}} - (4\mathcal{N}^2-1)\mu^2\bar{\mathrm{B}} - 4\mathcal{N}^2(2\mathcal{N}+1)\mu^2\beta^2\bar{\mathrm{D}} \\
&+ 8\mathcal{N}^2(2\mathcal{N}+1)\mu^2\beta\bar{\mathrm{D}} - (2\mathcal{N}-1)(2\mathcal{N}+1)^2\mu^2\bar{\mathrm{D}} + 2\mathcal{N}(2\mathcal{N}-1)\mu\beta\bar{\mathrm{B}} \\
&+ (4\mathcal{N}^2-1)\mu\bar{\mathrm{B}} - 8\mathcal{N}^2(2\mathcal{N}+1)\mu\beta^2\bar{\mathrm{D}} + 2\mathcal{N}(2\mathcal{N}-1)\mu\beta\bar{\mathrm{D}} \\
&+ (4\mathcal{N}^2-1)(4\mathcal{N}+1)\mu\bar{\mathrm{D}} - 4\mathcal{N}^2(2\mathcal{N}+1)\beta^2\bar{\mathrm{D}} \\
&- 2\Big[(2\mathcal{N}+1)(4\mathcal{N}^2-3\mathcal{N}+2)+4\mathcal{N}^2-2\Big]\beta\bar{\mathrm{D}} - 2\mathcal{N}(4\mathcal{N}^2-1)\bar{\mathrm{D}}\Big\} \qquad (5.1.53)
\end{aligned}
$$

for the odd numbers of l and

$$\begin{aligned} Z_l &= 256(\mathcal{N}+1)^2 2\mathcal{N}\Big\{4\mathcal{N}(\mathcal{N}+1)\mu^2\beta^2 - 2(2\mathcal{N}+1)^2\mu^2\beta + (4\mathcal{N}(\mathcal{N}+1)+1)\mu^2 \\ &+ 2((2\mathcal{N}+1)^2-1)\mu\beta^2 - 2(2\mathcal{N}+1)^2\mu + 4\mathcal{N}(\mathcal{N}+1)\beta^2 \\ &+ 2(2\mathcal{N}+1)^2\beta + 4\mathcal{N}(\mathcal{N}+1)+1\Big\} \end{aligned} \tag{5.1.54}$$

$$\begin{aligned} A^*_{1l} &= 128\frac{(\mathcal{N}+1)^2}{(2\mathcal{N}+1)}(-1)^{\mathcal{N}}\Big\{4\mathcal{N}(\mathcal{N}+1)\mu^2\beta^2\bar{\mathrm{A}} - 2\mathcal{N}(4\mathcal{N}+3)\mu^2\beta\bar{\mathrm{A}} + (2\mathcal{N}+1)2\mathcal{N}\mu^2\bar{\mathrm{A}} \\ &+ 8\mathcal{N}(\mathcal{N}+1)\mu\beta^2\bar{\mathrm{A}} + 2(\mathcal{N}+1)\mu\beta\bar{\mathrm{A}} - (4\mathcal{N}+1)(2\mathcal{N}+1)\mu\bar{\mathrm{A}} - 2(\mathcal{N}+1)\mu\beta\bar{\mathrm{C}} \\ &+ (2\mathcal{N}+1)\mu\bar{\mathrm{C}} + 4\mathcal{N}(\mathcal{N}+1)\beta^2\bar{\mathrm{A}} + 2(2\mathcal{N}+1)^2\beta\bar{\mathrm{A}} \\ &+ (4\mathcal{N}(\mathcal{N}+1)+1)\bar{\mathrm{A}} - 2(\mathcal{N}+1)\beta\bar{\mathrm{C}} - (2\mathcal{N}+1)\bar{\mathrm{C}}\Big\} \end{aligned} \tag{5.1.55}$$

$$\begin{aligned} B^*_{1l} &= 128\frac{(\mathcal{N}+1)\mathcal{N}}{(2\mathcal{N}+1)}(-1)^{\mathcal{N}}\Big\{4\mathcal{N}(\mathcal{N}+1)\mu^2\beta^2\bar{\mathrm{B}} - 2\Big[\mathcal{N}(4\mathcal{N}+5)+1\Big]\mu^2\beta\bar{\mathrm{B}} \\ &+ (2\mathcal{N}+1)2(\mathcal{N}+1)\mu^2\bar{\mathrm{B}} + 8\mathcal{N}(\mathcal{N}+1)\mu\beta^2\bar{\mathrm{B}} - 2\mathcal{N}\mu\beta\bar{\mathrm{B}} - (4\mathcal{N}+3)(2\mathcal{N}+1)\mu\bar{\mathrm{B}} \\ &+ 2\mathcal{N}\mu\beta\bar{\mathrm{D}} - (2\mathcal{N}+1)\mu\bar{\mathrm{D}} + 4\mathcal{N}(\mathcal{N}+1)\beta^2\bar{\mathrm{B}} + 2(2\mathcal{N}+1)^2\beta\bar{\mathrm{B}} \\ &+ (4\mathcal{N}(\mathcal{N}+1)+1)\bar{\mathrm{B}} + 2\mathcal{N}\beta\bar{\mathrm{D}} + (2\mathcal{N}+1)\bar{\mathrm{D}}\Big\} \end{aligned} \tag{5.1.56}$$

$$\begin{aligned} C^*_{1l} &= 128\frac{(\mathcal{N}+1)\mathcal{N}}{(2\mathcal{N}+1)}(-1)^{\mathcal{N}}\Big\{4\mathcal{N}(\mathcal{N}+1)\mu^2\beta^2\bar{\mathrm{A}} - 2\Big[\mathcal{N}(4\mathcal{N}+5)+2\Big]\mu^2\beta\bar{\mathrm{A}} \\ &+ 2(\mathcal{N}+1)(2\mathcal{N}+1)\mu^2\bar{\mathrm{A}} + 8\mathcal{N}(\mathcal{N}+1)\mu\beta^2\bar{\mathrm{A}} \\ &- 2(\mathcal{N}+1)\mu\beta\bar{\mathrm{A}} - (4\mathcal{N}+3)(2\mathcal{N}+1)\mu\bar{\mathrm{A}} \\ &+ 2(\mathcal{N}+1)\mu\beta\bar{\mathrm{C}} - (2\mathcal{N}+1)\mu\bar{\mathrm{C}} + (\mathcal{N}+1)4\mathcal{N}\beta^2\bar{\mathrm{A}} + 2(4\mathcal{N}(\mathcal{N}+1)+1)\beta\bar{\mathrm{A}} \\ &+ (4\mathcal{N}(\mathcal{N}+1)+1)\bar{\mathrm{A}} + 2(\mathcal{N}+1)\beta\bar{\mathrm{C}} + (2\mathcal{N}+1)\bar{\mathrm{C}}\Big\} \end{aligned} \tag{5.1.57}$$

$$\begin{aligned} D^*_{1l} &= 128\frac{(\mathcal{N}+1)\mathcal{N}}{(2\mathcal{N}+1)}(-1)^{(\mathcal{N}-1)}\Big\{4\mathcal{N}(\mathcal{N}+1)\mu^2\beta^2\bar{\mathrm{B}} - 2(4\mathcal{N}^2+3\mathcal{N}+1)\mu^2\beta\bar{\mathrm{B}} + \\ &+ (2\mathcal{N}+1)2\mathcal{N}\mu^2\bar{\mathrm{B}} + 8\mathcal{N}(\mathcal{N}+1)\mu\beta^2\bar{\mathrm{B}} + 2\mathcal{N}\mu\beta\bar{\mathrm{B}} - (2\mathcal{N}+1)(4\mathcal{N}+1)\mu\bar{\mathrm{B}} \\ &- 2\mathcal{N}\mu\beta\bar{\mathrm{D}} + (2\mathcal{N}+1)\mu\bar{\mathrm{D}} + 4\mathcal{N}(\mathcal{N}+1)\beta^2\bar{\mathrm{B}} + 2(4\mathcal{N}(\mathcal{N}+1)+1)\beta\bar{\mathrm{B}} \\ &+ (4\mathcal{N}(\mathcal{N}+1)+1)\bar{\mathrm{B}} - 2\mathcal{N}\beta\bar{\mathrm{D}} - (2\mathcal{N}+1)\bar{\mathrm{D}}\Big\} \end{aligned} \tag{5.1.58}$$

$$\begin{aligned} A^*_{2l} &= 128\frac{(\mathcal{N}+1)^2}{(2\mathcal{N}+1)}(-1)^{\mathcal{N}}\Big\{2(\mathcal{N}+1)\mu^2\beta\bar{\mathrm{A}} - (2\mathcal{N}+1)\mu^2\bar{\mathrm{A}} + 4\mathcal{N}(\mathcal{N}+1)\mu^2\beta^2\bar{\mathrm{C}} \\ &- 2(4\mathcal{N}(\mathcal{N}+1)+1)\mu^2\beta\bar{\mathrm{C}} + (4\mathcal{N}(\mathcal{N}+1)+1)\mu^2\bar{\mathrm{C}} \\ &+ 2(\mathcal{N}+1)\mu\beta\bar{\mathrm{A}} + (2\mathcal{N}+1)\mu\bar{\mathrm{A}} \\ &+ 8\mathcal{N}(\mathcal{N}+1)\mu\beta^2\bar{\mathrm{C}} - 2(\mathcal{N}+1)\mu\beta\bar{\mathrm{C}} - (4\mathcal{N}+1)(2\mathcal{N}+1)\mu\bar{\mathrm{C}} \\ &+ 4\mathcal{N}(\mathcal{N}+1)\beta^2\bar{\mathrm{C}} + 2\mathcal{N}(4\mathcal{N}+3)\beta\bar{\mathrm{C}} + 2\mathcal{N}(2\mathcal{N}+1)\bar{\mathrm{C}}\Big\} \end{aligned} \tag{5.1.59}$$

$$
\begin{aligned}
B^{*}_{2l} &= 128\frac{\mathcal{N}(\mathcal{N}+1)}{(2\mathcal{N}+1)}(-1)^{\mathcal{N}}\Big\{-2\mathcal{N}\mu^2\beta\bar{\mathrm{B}}+(2\mathcal{N}+1)\mu^2\bar{\mathrm{B}}+4\mathcal{N}(\mathcal{N}+1)\mu^2\beta^2\bar{\mathrm{D}}\\
&- 2(2\mathcal{N}+1)^2\mu^2\beta\bar{\mathrm{D}}+(4\mathcal{N}(\mathcal{N}+1)+1)\mu^2\bar{\mathrm{D}}-2\mathcal{N}\mu\beta\bar{\mathrm{B}}-(2\mathcal{N}+1)\mu\bar{\mathrm{B}}\\
&+ 8\mathcal{N}(\mathcal{N}+1)\mu\beta^2\bar{\mathrm{D}}+2\mathcal{N}\mu\beta\bar{\mathrm{D}}-(4\mathcal{N}+3)(2\mathcal{N}+1)\mu\bar{\mathrm{D}}\\
&+ 4\mathcal{N}(\mathcal{N}+1)\beta^2\bar{\mathrm{D}}+2(\mathcal{N}(4\mathcal{N}+5)+1)\beta\bar{\mathrm{D}}+2(\mathcal{N}+1)(2\mathcal{N}+1)\bar{\mathrm{D}}\Big\}
\end{aligned}
\tag{5.1.60}
$$

$$
\begin{aligned}
C^{*}_{2l} &= 128\frac{\mathcal{N}(\mathcal{N}+1)}{(2\mathcal{N}+1)}(-1)^{\mathcal{N}}\Big\{-2(\mathcal{N}+1)\mu^2\beta\bar{\mathrm{A}}+(2\mathcal{N}+1)\mu^2\bar{\mathrm{A}}+4\mathcal{N}(\mathcal{N}+1)\mu^2\beta^2\bar{\mathrm{C}}\\
&- 2(4\mathcal{N}(\mathcal{N}+1)+1)\mu^2\beta\bar{\mathrm{C}}+(4\mathcal{N}(\mathcal{N}+1)+1)\mu^2\bar{\mathrm{C}}-2(\mathcal{N}+1)\mu\beta\bar{\mathrm{A}}-(2\mathcal{N}+1)\mu\bar{\mathrm{A}}\\
&+ 8\mathcal{N}(\mathcal{N}+1)\mu\beta^2\bar{\mathrm{C}}+2(\mathcal{N}+1)\mu\beta\bar{\mathrm{C}}-(4\mathcal{N}+3)(2\mathcal{N}+1)\mu\bar{\mathrm{C}}+4\mathcal{N}(\mathcal{N}+1)\beta^2\bar{\mathrm{C}}\\
&+ 2\Big[\mathcal{N}(4\mathcal{N}+5)+2\Big]\beta\bar{\mathrm{C}}+2(\mathcal{N}+1)(2\mathcal{N}+1)\bar{\mathrm{C}}\Big\}
\end{aligned}
\tag{5.1.61}
$$

$$
\begin{aligned}
D^{*}_{2l} &= 128\frac{\mathcal{N}(\mathcal{N}+1)}{(2\mathcal{N}+1)}(-1)^{(\mathcal{N}-1)}\Big\{2\mathcal{N}\mu^2\beta\bar{\mathrm{B}}-(2\mathcal{N}+1)\mu^2\bar{\mathrm{B}}+4\mathcal{N}(\mathcal{N}+1)\mu^2\beta^2\bar{\mathrm{D}}\\
&- 2(4\mathcal{N}(\mathcal{N}+1)+1)\mu^2\beta\bar{\mathrm{D}}+(4\mathcal{N}(\mathcal{N}+1)+1)\mu^2\bar{\mathrm{D}}+2\mathcal{N}\mu\beta\bar{\mathrm{B}}+(2\mathcal{N}+1)\mu\bar{\mathrm{B}}\\
&+ 8\mathcal{N}(\mathcal{N}+1)\mu\beta^2\bar{\mathrm{D}}-2\mathcal{N}\mu\beta\bar{\mathrm{D}}-(2\mathcal{N}+1)(4\mathcal{N}+1)\mu\bar{\mathrm{D}}+4\mathcal{N}(\mathcal{N}+1)\beta^2\bar{\mathrm{D}}\\
&+ 2\Big[4\mathcal{N}^2+3\mathcal{N}+1\Big]\beta\bar{\mathrm{D}}+2\mathcal{N}(2\mathcal{N}+1)\bar{\mathrm{D}}\Big\}
\end{aligned}
\tag{5.1.62}
$$

for the even numbers of l. In Eqs. (5.1.45 - 5.1.62), there is a logarithmic singularity if $Z_l = 0$ and $A^{*}_{kl} \neq 0$ or $B^{*}_{kl} \neq 0$ or $C^{*}_{kl} \neq 0$ or $D^{*}_{kl} \neq 0$.
The stress term according to $\omega_n = -l$ is $r^l\,\tilde{\sigma}^{ET}_{ijkl}(\theta)$ with

$$
\begin{aligned}
\tilde{\sigma}^{ET}_{rrkl}(\theta) &= (1+l)\Big\{-A_{kl}(2-l)sin(l\theta)+B_{kl}(2-l)cos(l\theta)-\\
&- C_{kl}(2+l)sin\Big[(2+l)\theta\Big]-D_{kl}(2+l)cos\Big[(2+l)\theta\Big]\Big\}
\end{aligned}
\tag{5.1.63}
$$

$$
\begin{aligned}
\tilde{\sigma}^{ET}_{\theta\theta kl}(\theta) &= (2+l)(1+l)\Big\{-A_{kl}sin(l\theta)+B_{kl}cos(l\theta)\\
&+ C_{kl}sin\Big[(2+l)\theta\Big]+D_{kl}cos\Big[(2+l)\theta\Big]\Big\}
\end{aligned}
\tag{5.1.64}
$$

$$
\begin{aligned}
\tilde{\tau}^{ET}_{r\theta kl}(\theta) &= (1+l)\Big\{A_{kl}lcos(l\theta)+B_{kl}lsin(l\theta)\\
&- C_{kl}(2+l)cos\Big[(2+l)\theta\Big]+D_{kl}(2+l)sin\Big[(2+l)\theta\Big]\Big\}.
\end{aligned}
\tag{5.1.65}
$$

It should be noted that $\tilde{\sigma}^{ET}_{ijkl}(\theta)$ do not have the unit of stress, the total $r^l\,\tilde{\sigma}^{ET}_{ijkl}(\theta)$ has a unit of a stress. Therefore, a normalized definition

$$
\sigma^{ET}_{ijkl}(\theta) = R^l\,\tilde{\sigma}^{ET}_{ijkl}(\theta) \tag{5.1.66}
$$

is used. Where R is a characteristic length of the joint. Finally, the higher-order regular stress term according to $\omega_n = -l$ is $(r/R)^l\,\sigma^{ET}_{ijkl}(\theta)$, where $\sigma^{ET}_{ijkl}(\theta)$ has a unit of a

stress.

(III) The case of $0 < \omega_n < 1$.
For this case the stress term is denoted as $\sigma_{ij}^S(r,\theta)$, because for this ω_n stress singularity exists. The stress term according to $0 < \omega_n < 1$ has the same expression as that one for the same joint with a free edge (see Section 3.1), i.e.

$$\sigma_{ijk}^S(r,\theta) = \sum_{n=1}^{N} \frac{K_n}{(r/R)^{\omega_n}} f_{ijkn}(\theta) \tag{5.1.67}$$

for the real eigenvalue and

$$\sigma_{ijk}^S(r,\theta) = \sum_{n=1}^{N} \frac{K_n}{(r/R)^{\omega_n}} \Big\{ cos\Big[p_n ln(r/R)\Big] f_{ijkn}{}^c(\theta) + sin\Big[p_n ln(r/R)\Big] f_{ijkn}{}^s(\theta) \Big\} \tag{5.1.68}$$

for the complex eigenvalue. In Eqs. (5.1.67) and (5.1.68) ω_n corresponds to the real part of the eigenvalue, p_n is the imaginary part of the eigenvalue, $f_{ijkn}(\theta)$, $f_{ijkn}^c(\theta)$, *and* $f_{ijkn}^s(\theta)$ are angular functions, N is the number of the singular terms. All parameters in Eqs. (5.1.67) and (5.1.68), except for the factor K_n, can be determined analytically and are the same as those in a joint with a traction free edge (see Section 3.1), which are independent of the loading. Only the stress intensity factor K_n depends on the applied loading. Generally, the stress intensity factor should be determined by a numerical method, e.g the Finite Element Method (FEM) (see Section 3.4). For elastic behavior, the factor K_n in Eqs. (5.1.67) and (5.1.68) can be separated as

$$K_n = K_n^{RM} + K_n^{ET} + K_n^{TH}, \tag{5.1.69}$$

where $K_n^{\mathrm{RM}}, K_n^{\mathrm{ET}}$, and K_n^{TH} correspond to the remote mechanical loading, the edge tractions, and the thermal loading, respectively.

Finally, in a two dissimilar materials joint under the three types of loading, the stresses near the singular point can be calculated from

$$\begin{aligned} \sigma_{ijk}(r,\theta) &= \sigma_{ijk}^S(r,\theta) + \sigma_{ijk0}^{TH}(\theta) + \sigma_{ijk0}^{RM}(\theta) + \sigma_{ijk0}^{ET}(\theta) + \sum_{l=1}^{M} (r/R)^l \sigma_{ijkl}^{ET}(\theta) \\ &= \sum_{n=1}^{N} \frac{K_n}{(r/R)^{\omega_n}} f_{ijkn}(\theta) + \sigma_{ijk0}^{TH}(\theta) + \sigma_{ijk0}^{RM}(\theta) + \sigma_{ijk0}^{ET}(\theta) + \sum_{l=1}^{M} (r/R)^l \sigma_{ijkl}^{ET}(\theta) \end{aligned} \tag{5.1.70}$$

for the real eigenvalue. In Eq. (5.1.70) the terms $\sigma_{ijk0}^{TH}(\theta)$, $\sigma_{ijk0}^{RM}(\theta)$, and components of $\sigma_{ijk}^S(r,\theta)$ are the same as those for the same joint with a free edge, except for the K-factor. The term $\sigma_{ijk0}^{ET}(\theta)$ can be calculated from Eqs. (3.3.2 -3.3.4) with the coefficients given in Eqs. (5.1.27 - 5.1.35). The quantities $\sigma_{ijkl}^{ET}(r,\theta)$ can be obtained from

Eqs. (5.1.63 - 5.1.66) using the coefficients given in Eqs. (5.1.45 - 5.1.62) for a joint with $\theta_1 = -\theta_2 = 90°$. It should be noted that for most joint geometries and material combinations, the term $\sigma_{ijk0}^{RM}(\theta)$ is zero, as shown in Section 3.3.

Now, all the regular stress terms, constant and higher-order, are well-known. In the next sections the behavior of the stress intensity factor will be studied in details by using the method given in Section 3.4.

5.2 Empirical Relations of the Stress Intensity Factor in a Joint under Tension Edge Traction

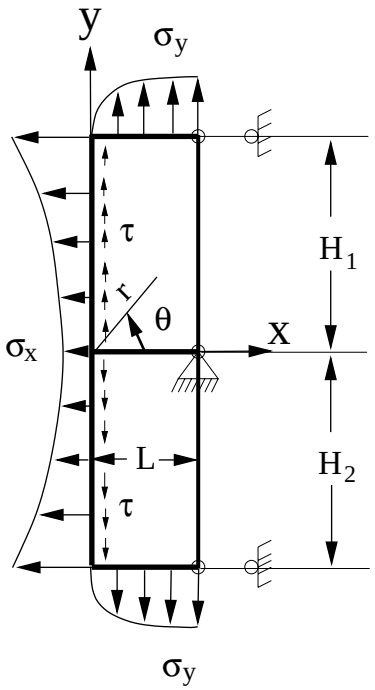

Figure 5.2: A quarter planes joint with edge tractions.

From the results of a joint with a free edge, it is known that for an arbitrary geometry (θ_1, θ_2) the relationship between the K-factors and the stress exponents is very complicated, and it is impossible to find an empirical relation for the stress intensity factor in a finite joint geometry. However, for a quarter planes joint ($\theta_1 = -\theta_2 = 90°$), empirical relations have been found to determine the K-factors (see Section 3.5.2). Therefore, in this section only quarter planes joints are considered.
The polynomial of the tension edge traction is

$$\sigma_x(y) = \sum_{l=1}^{M} A_l y^l + A_0, \tag{5.2.1}$$

where A_0 is introduced for the convenience of mathematical description, A_0 may be p_1 in Eq. (5.1.1) or p_2 in Eq. (5.1.3) (the coordinate see Fig. 5.2). For linear elasticity the stress field under the loading given in Eq. (5.2.1) is the same as that obtained from the sum of each loading $\sigma_x^l(y) = A_l y^l$ (l=0,1,2,...,M). Therefore, we will focus on the loading $\sigma_x^l(y) = A_l y^l$ below and study the corresponding characteristics of the K-factor.

If the geometry is $L > H$, the coordinate r in Eq. (3.0.1) is normalized by H (K is denoted as K_H); if the geometry is $H > L$, the coordinate r in Eq. (3.0.1) is normalized by L (K is denoted as K_L or K). The relation between K_L and K_H is given in Eq. (3.5.8). It is known from Section 3.5.2 that for a quarter planes joint with a free edge and under thermal loading, the factor K_L is a constant (i.e. K_L is independent of H/L) if $H/L \geq 2$; if $H_1/L \leq 0.1$ (or $H_2/L \leq 0.1$), the factor K_{H_1} (or K_{H_2}) is a constant (i.e. $K_{H_1}(K_{H_2})$ is independent of H_1/L (H_2/L)). To see whether this is also true for a joint under a tension edge traction, the stress intensity factors are calculated from FEM for different ratios of H/L $(H_1 = H_2)$ under $\sigma_x^l(y) =\mid y/H \mid^l$ (l=0, 1, 2, 3, 4, 5) (i.e. the loading is symmetrical to the interface for all values of l).

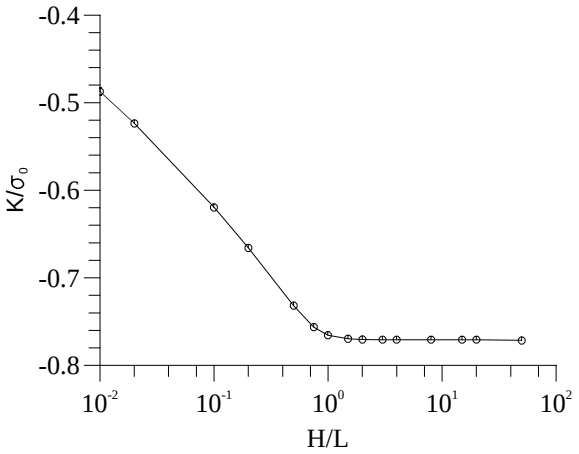

Figure 5.3: Normalized stress intensity factor K_L/σ_0 at the edge traction of σ_x = constant vs. H/L.

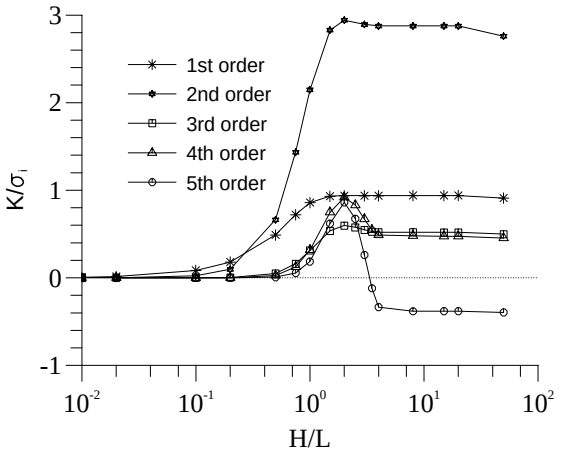

Figure 5.4: Normalized stress intensity factor K_L/σ_i at the edge traction of $\sigma_x^l(y) =\mid y/H \mid^l$ (l=1,2,3,4,5) vs. H/L.

As an example, the material data E_1 = 1GPa, E_2 = 7GPa, $\nu_1 = 0.2$, and $\nu_2 = 0.4$ are chosen. For this material combination, the stress exponent of the singular term is $\omega = 0.104$. It should be noted that the values of the K-factor in Eq. (3.0.1) and of $\sigma_{ijkl}^{ET}(\theta)$ in Eq. (5.1.66) are dependent on the absolute size of R, because the loading $\sigma_x^l(y) = (y/H)^l$ is dependent on the absolute size of H (here R=H). They also depend on the overall geometry form, e.g. the ratio of $H_1/L, H_2/L$. However, the ratio of $K/\sigma_{ijkl}^{ET}(\theta)$ is independent of the absolute size of R. In Fig. 5.3 the ratio of K_L/σ_0 is plotted versus H/L for the case of σ_x = constant, where $\sigma_0 = \sigma_{\theta\theta 10}(0) = \sigma_{\theta\theta 20}(0)$ is calculated from Eqs. (3.3.2 - 3.3.4) with the coefficients from Eqs. (5.1.27 - 5.1.35). In Fig. 5.4 the ratio of K_L/σ_l is plotted versus H/L for the case of $\sigma_x^l(y) =\mid y/H \mid^l$

(l=1,2,3,4,5), where $\sigma_l = \sigma_{r1l}^{ET}(\theta = 90°)$ and is calculated from Eqs. (5.1.66) and (5.1.63) with the coefficients from Eqs. (5.1.45 - 5.1.62) (here R=L). On the other hand, in Fig. 5.5 the ratio of K_H/σ_0 is plotted versus L/H for the case of σ_x = constant. The ratio of K_H/σ_l is plotted versus L/H in Fig. 5.6 for the case of $\sigma_x^l(y) =\mid y/H \mid^l$ (l=1,2,3,4,5), where R=H is used for the calculation of σ_l in Eq. (5.1.66). From Figs. 5.3, 5.4, 5.5, and 5.6 it can be seen that if $H/L > 10$, the ratio of K_L/σ_l (l=0,1,2,3,4,5) is a constant and if $L/H > 10$, the ratio of K_H/σ_l (l=0,1,2,3,4,5) is a constant. In fact, for small l (l=0,1,2) the ratio of K_L/σ_l always is a constant like that one in a joint with a free edge, if $H/L \geq 2$.

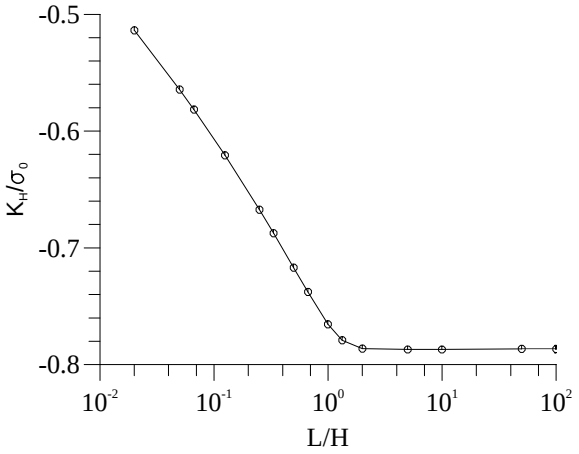

Figure 5.5: Normalized stress intensity factor K_H/σ_0 at the edge traction of σ_x = constant vs. L/H.

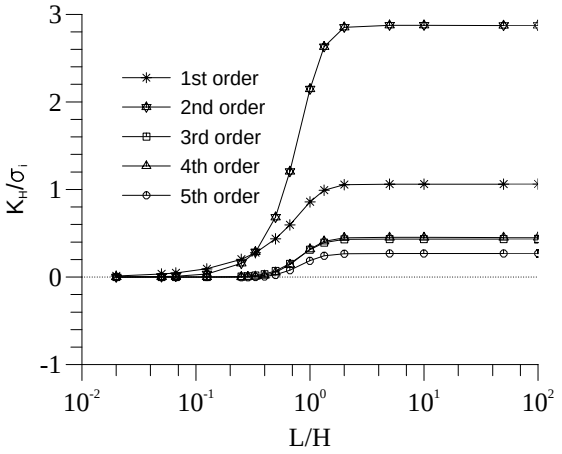

Figure 5.6: Normalized stress intensity factor K_H/σ_i at the edge traction of $\sigma_x^l(y) =\mid y/H \mid^l$ (l=1,2,3,4,5) vs. L/H.

By using the finite element method (FEM), the stress intensity factors K_L and K_H are calculated for different material combinations (various ratios of E_2/E_1 and ν_2/ν_1), different geometries (various H/L), and different loadings ($\sigma_x(y) = A_l y^l$ (l=0,1,2,3,4,5)). As an example, the normalized stress intensity factors K_L/σ_0 and K_L/σ_1 are plotted vs. ω for σ_x = constant and $\sigma_x =\mid y/H \mid$ in Figs. 5.7 and 5.8. It can be seen that for σ_x = constant a unique relation exists between K_L/σ_0 and ω, and for $\sigma_x =\mid y/H \mid$ there is no direct unique relation between K_L/σ_1 and ω. However, between the quantity $(K_L/\sigma_1)\omega^x\nu^y$ and ω there is a unique relation, see Fig. 5.9, where the fitting parameters are x=1.1 and y=1/1.45. Analogously to σ_x = constant and $\sigma_x =\mid y/H \mid$, some empirical relations to calculate the stress intensity factor for $\sigma_x(y) = A_l y^l$ (l=2,3,4,5) have been obtained for the joint geometry with H/L = 0.1, 2, and 8.
Below the notations of

$$\begin{aligned} \nu &= \nu_1 \qquad \text{for } E_2/E_1 > 1, \\ \nu &= \nu_2 \qquad \text{for } E_2/E_1 < 1, \end{aligned} \tag{5.2.2}$$

if $\nu_1 \neq \nu_2$, and

$$\text{sign} = 1 \qquad \text{for } E_2/E_1 < 1$$

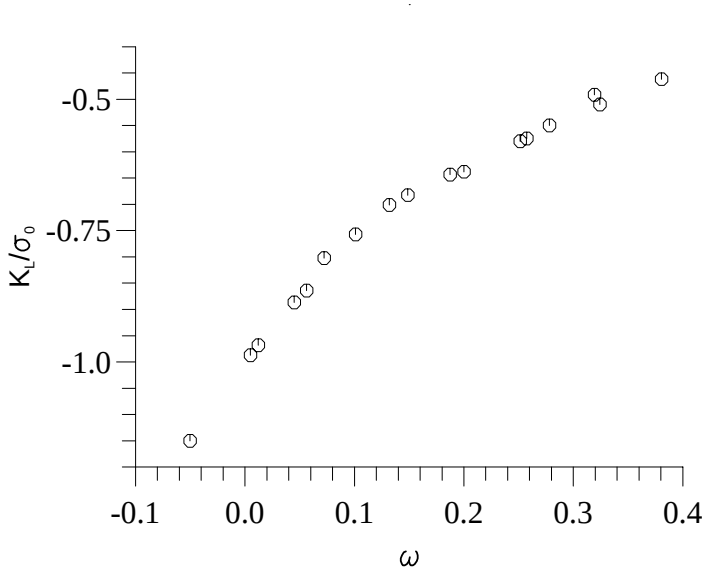

Figure 5.7: The normalized stress intensity factor K_L/σ_0 vs. the singular stress exponent ω for H/L=2 and $\sigma_x(y)$ = constant.

$$\text{sign} \quad = \quad -1 \qquad \text{for } E_2/E_1 > 1. \tag{5.2.3}$$

are used.
(I) Empirical relations for the joint geometry with $H/L = 2$.

(a) If the loading $\sigma_x(y)$ is constant, the stress intensity factor K_L can be calculated from

$$K_L^{(0)} = \sigma_0 \left(-0.9850 + 2.2212\,\omega - 2.297\,\omega^2\right) \tag{5.2.4}$$

(b) For the loading $\sigma_x(y) =\mid y/H \mid$ (i.e. the loading is symmetrical to the interface), the stress intensity factor K_L can be calculated from

$$K_L^{(1)} = - \mid \sigma_1 \, \frac{f_{n1}}{\omega^{1.1}\nu^{(1.0/1.45)}} \mid \tag{5.2.5}$$

with

$$f_{n1} = 0.5 \, \left(0.08164\,\omega + 1.872\,\omega^2 - 6.312\,\omega^3 + 6.784\,\omega^4\right) \tag{5.2.6}$$

(c) For the loading $\sigma_x(y)$ = (y/H) (i.e. the loading is antisymmetric to the interface), the stress intensity factor K_L can be calculated from

$$K_L^{(1)} = \text{ sign } \; 10^{f_{n1}/(\omega^{0.9499}\nu^{-0.5481})} \tag{5.2.7}$$

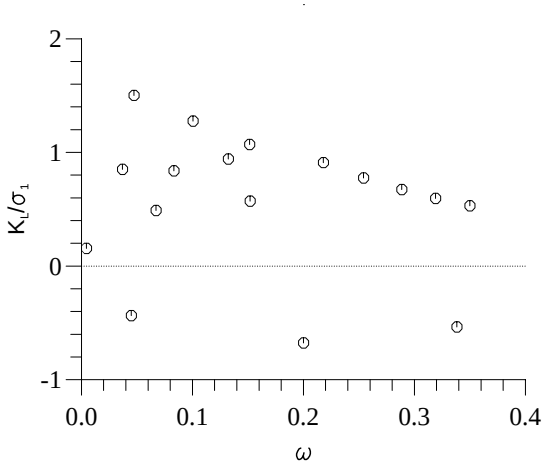

Figure 5.8: The normalized stress intensity factor K_L/σ_1 vs. the singular stress exponent ω for H/L=2 and $\sigma_x(y) = \mid y/H \mid$.

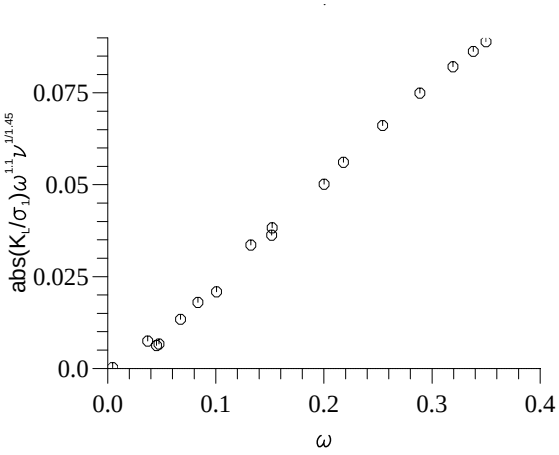

Figure 5.9: The modified stress intensity factor $K_L/\sigma_1\omega^x\nu^y$ vs. the singular stress exponent ω for $\sigma_x(y) =\mid y/H \mid$ and H/L=2.

with

$$\begin{aligned} f_{n1} &= -0.009705 - 2.423\,\omega + 9.741\,\omega^2 \\ &\quad -54.25\,\omega^3 + 140.3\,\omega^4 - 138.4\,\omega^5 \end{aligned} \tag{5.2.8}$$

(d) For the loading $\sigma_x(y) = (y/H)^2$, the stress intensity factor K_L can be calculated from

$$K_L^{(2)} = -10^{f_{n2}} \tag{5.2.9}$$

with

$$f_{n2} = -0.7906 - 1.933\,\omega \tag{5.2.10}$$

(e) For the loading $\sigma_x(y) =\mid y/H \mid^3$, the stress intensity factor K_L can be calculated from

$$K_L^{(3)} = -10^{f_{n3}/(\omega^{-0.003209}\nu^{0.05761})} \tag{5.2.11}$$

with

$$f_{n3} = -0.9430 - 2.109\,\omega \tag{5.2.12}$$

(f) For the loading $\sigma_x(y) = (y/H)^3$, the stress intensity factor K_L can be calculated from

$$K_L^{(3)} = \text{ sign } 10^{f_{n3}/(\omega^{1.022}\nu^{-0.2724})} \tag{5.2.13}$$

with

$$\begin{aligned} f_{n3} &= -0.002966 - 2.963\,\omega + 4.156\,\omega^2 \\ &\quad -5.982\,\omega^3 - 0.05717\,\omega^4 + 2.036\,\omega^5 \end{aligned} \tag{5.2.14}$$

(g) For the loading $\sigma_x(y) = (y/H)^4$, the stress intensity factor K_L can be calculated from

$$K_L^{(4)} = -10^{f_{n4}/(\omega^{0.4784}\nu^{0.1806})} \tag{5.2.15}$$

with

$$f_{n4} = -0.09568 - 2.70\,\omega \tag{5.2.16}$$

(h) For the loading $\sigma_x(y) = \mid y/H \mid^5$, the stress intensity factor K_L can be calculated from

$$K_L^{(5)} = -10^{f_{n5}/(\omega^{0.6536}\nu^{0.2859})} \tag{5.2.17}$$

with

$$f_{n5} = -0.01177 - 2.318\,\omega \tag{5.2.18}$$

(i) For the loading $\sigma_x(y) = (y/H)^5$, the stress intensity factor K_L can be calculated from

$$K_L^{(5)} = -\ln\left(f_{n5}/\omega\right) \tag{5.2.19}$$

with

$$f_{n5} = -0.0003693 + 1.006\,\omega. \tag{5.2.20}$$

(II) Empirical relations for the joint geometry with $H/L = 0.1$.

(a) If the loading $\sigma_x(y)$ is constant, the stress intensity factor K_H can be calculated from

$$K_H^{(0)} = \sigma_0(-0.9983 + 2.719\omega - 6.985\omega^2 + 6.090\omega^3) \tag{5.2.21}$$

(b) For the loading $\sigma_x(y) = \mid y/H \mid$, the stress intensity factor K_H can be calculated from

$$K_H^{(1)} = -\mid \sigma_1 \frac{f_{n1}}{\omega^{0.4562}\nu^{0.9976}} \mid \tag{5.2.22}$$

with

$$\begin{aligned} f_{n1} &= -0.0002005 + 1.040\,\omega - 7.633\,\omega^2 \\ &\quad +53.96\,\omega^3 - 169.7\,\omega^4 + 195.7\,\omega^5 \end{aligned} \tag{5.2.23}$$

(c) For the loading $\sigma_x(y) = (\mathrm{y/H})$, the stress intensity factor K_H can be calculated from

$$K_H^{(1)} = \text{ sign } \ln\left(f_{n1}/(\omega^{0.7844}\nu^{0.5222})\right) \tag{5.2.24}$$

with

$$\begin{aligned} f_{n1} &= 0.004572 + 1.058\,\omega + 1.641\,\omega^2 \\ &\quad -16.20\,\omega^3 + 51.77\,\omega^4 - 52.97\,\omega^5 \end{aligned} \tag{5.2.25}$$

(d) For the loading $\sigma_x(y) = (y/H)^2$, the stress intensity factor K_H can be calculated from

$$K_H^{(2)} = \frac{f_{n2}}{\omega^{1.498}\nu^{0.6323}} \tag{5.2.26}$$

with

$$\begin{aligned} f_{n2} &= 0.00008791 - 0.02705\,\omega - 0.2085\,\omega^2 \\ &\quad -0.06308\,\omega^3 + 2.271\,\omega^4 - 4.151\,\omega^5 \end{aligned} \tag{5.2.27}$$

(e) For the loading $\sigma_x(y) = \mid y/H \mid^3$, the stress intensity factor K_H can be calculated from

$$K_H^{(3)} = -10^{f_{n3}/(\omega^{0.7880}\nu^{-0.3815})} \tag{5.2.28}$$

with

$$\begin{aligned} f_{n3} &= -0.002264 - 1.843\,\omega + 5.948\,\omega^2 \\ &\quad -35.63\,\omega^3 + 93.70\,\omega^4 - 85.34\,\omega^5 \end{aligned} \tag{5.2.29}$$

(f) For the loading $\sigma_x(y) = (y/H)^3$, the stress intensity factor K_H can be calculated from

$$K_H^{(3)} = \text{ sign } 10^{f_{n3}/(\omega^{1.436}\nu^{-0.7922})} \tag{5.2.30}$$

with

$$\begin{aligned} f_{n3} &= 0.003659 - 0.9672\,\omega - 2.416\,\omega^2 \\ &\quad +16.83\,\omega^3 - 53.74\,\omega^4 + 67.77\,\omega^5 \end{aligned} \tag{5.2.31}$$

(g) For the loading $\sigma_x(y) = (y/H)^4$, the stress intensity factor K_H can be calculated from

$$K_H^{(4)} = -10^{f_{n4}/(\omega^{0.9267}\nu^{-0.3069})} \tag{5.2.32}$$

with

$$f_{n4} = 0.0003382 - 1.127\,\omega - 0.2943\,\omega^2 - 1.998\,\omega^3 + 3.681\,\omega^4 + 3.658\,\omega^5 \quad (5.2.33)$$

(h) For the loading $\sigma_x(y) = |\ y/H\ |^5$, the stress intensity factor K_H can be calculated from

$$K_H^{(5)} = -10^{f_{n5}/(\omega^{0.8535}\nu^{-0.2650})} \quad (5.2.34)$$

with

$$f_{n5} = -0.001671 - 1.519\,\omega + 1.455\,\omega^2 - 7.438\,\omega^3 + 11.73\,\omega^4 + 0.1310\,\omega^5 \quad (5.2.35)$$

(i) For the loading $\sigma_x(y) = (y/H)^5$, the stress intensity factor K_H can be calculated from

$$K_H^{(5)} = \text{sign}\ \ 10^{f_{n5}/(\omega^{1.343}\nu^{-0.6651})} \quad (5.2.36)$$

$$f_{n5} = 0.003666 - 1.283\,\omega - 3.344\,\omega^2 + 29.26\,\omega^3 - 94.73\,\omega^4 + 112.6\,\omega^5 \quad (5.2.37)$$

(III) Empirical relations for the joint geometry with $H/L = 8$.

For the edge traction of $\sigma_x(y) = (y/H)^l$ with l=0,1,2, the ratio of K_L/σ_l for H/L=8 is the same as for $H/L = 2$ (see Fig. 5.4). Therefore, the empirical equations given in section (I) can be used here. For a higher-order edge traction of $\sigma_x(y) = (y/H)^l$ with l=3,4,5, the ratio of K_L/σ_l for H/L=8 differs from that one for $H/L = 2$. Some approximate relations will be presented below.

(a) If the loading is $\sigma_x(y) = (y/H)^3$, the stress intensity factor K_L can be calculated from

$$K_L^{(3)} = \text{sign}\ \ \frac{f_{n3}}{\omega^{0.2692}\nu^{0.7403}} 10^{-6} \quad (5.2.38)$$

with

$$f_{n3} = -0.3592 + 170.9\omega + 664.3\omega^2 - 572.8\omega^3 - 5397\omega^4 + 9162\omega^5 \quad (5.2.39)$$

(b) If the loading is $\sigma_x(y) = (y/H)^4$, the stress intensity factor K_L can be calculated from

$$K_L^{(4)} = \text{sign}\ \ \frac{f_{n4}}{\omega^{-0.2562}\nu^{-0.2989}} 10^{-6} \quad (5.2.40)$$

with

$$\begin{aligned} f_{n4} &= -1240 + 10872\omega - 19693\omega^2 \\ &\quad -9583\omega^3 - 3558\omega^4 - 1232\omega^5 \end{aligned} \tag{5.2.41}$$

(c) If the loading is $\sigma_x(y) = (y/H)^5$, the stress intensity factor K_L can be calculated from

$$K_L^{(5)} = \text{sign} \ \frac{f_{n5}}{\omega^{1.239}\nu^{1.120}} 10^{-8} \tag{5.2.42}$$

with

$$\begin{aligned} f_{n5} &= 0.5579 - 164.2\omega - 1003\omega^2 \\ &\quad +3165\omega^3 - 845.8\omega^4 - 131\omega^5. \end{aligned} \tag{5.2.43}$$

For an arbitrary tension edge traction of

$$\sigma_x(y) = A_0 + \sum_{l=1}^{M} A_l \left(\frac{y}{H}\right)^l \tag{5.2.44}$$

where A_0 and A_l (l=1, 2, 3, 4, 5) are known constants, according to the superposition principle, the stress intensity factor can be calculated from

$$K_L = A_0 K_L^{(0)} + \sum_{l=1}^{M} A_l K_L^{(l)} \tag{5.2.45}$$

in case of $H/L \geq 2$, where $K_L^{(l)}$ (l=0, 1, 2, 3, 4, 5) can be determined from Eqs. (5.2.4 - 5.2.20) or Eqs. (5.2.38 - 5.2.43), and from

$$K_H = A_0 K_H^{(0)} + \sum_{l=1}^{M} A_l K_H^{(l)} \tag{5.2.46}$$

in case of $H/L \leq 0.1$, where $K_H^{(l)}$ are given in Eqs. (5.2.21 - 5.2.37). In Eqs. (5.2.44), (5.2.45), and (5.2.46) the max M is 5.

For joints with $H/L > 2$, the K_L value obtained from the empirical equations given in sections (I) and (III) are almost the same if the edge traction is $\sigma_x(y) = (y/H)^l$ (l=0,1,2,3) because $K_L^{(l)}/\sigma_l$ with l=0, 1, 2, 3 is almost constant; but for the edge traction $\sigma_x(y) = (y/H)^l$ (l=4, 5), the K_L value calculated from the empirical equations given in sections (I) and (III) are different. Due to the fact that the absolute values of $K_L^{(l)}$ for l=4 and 5 are much smaller than those for l=0, 1, 2, 3, the values calculated from the empirical equations for H/L=2 in section (I) (i.e. from Eqs. (5.2.4 - 5.2.20)) can be used approximately for joints of $8 > H/L > 2$, as long as the absolute values of A_4 and A_5 in Eq. (5.2.44) are not much larger than A_0. Examples will be given below

to show this.

Many test calculations, in which the stresses obtained from FEM and from Eq. (5.1.70) with the K factor value from the empirical equations are compared, have shown that if the Poisson's ratio is in the range of $0.2 \leq \nu \leq 0.4$, the stress exponent $\omega \geq 0.05$ and the absolute values of A_4 and A_5 in Eq. (5.2.44) are not much larger than A_0, the empirical equations given above can be used to calculate the stress distribution near the singular point in the range of $r/R \leq 0.01$ (R is H or L). The general situation is:
(a) The larger the stress exponent ω is, the more accurate is the K factor obtained from the empirical equations.
(b) The smaller the value of M in Eq. (5.2.44) is, the more accurate is the K factor obtained from the empirical equations.
(c) In Eq. (5.2.44), the smaller the absolute value of A_4 and A_5 compared to A_0 is, the more accurate is the K factor obtained from the empirical equations.
(d) For an antisymmetric loading, the value of the K-factor obtained from the empirical equations is more accurate than that for a symmetrical loading.
(e) Under the same loading, the value of the K-factor obtained from the empirical equations for a joint with $H/L \geq 2$ is more accurate than that for a joint with $H/L \leq 0.1$, especially if the absolute values of A_4 and A_5 in Eq. (5.2.44) are not smaller than A_0.

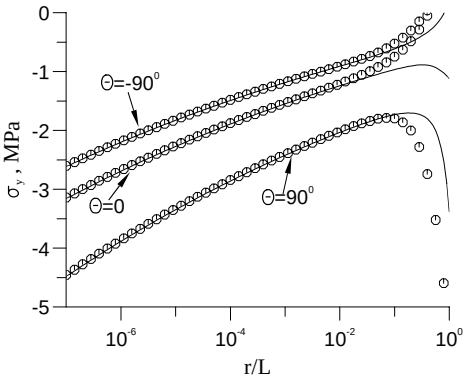

Figure 5.10: Comparison of the stresses obtained from FEM and the asymptotical equation using the K-factor from the empirical relations, for example 1 and H/L=2.

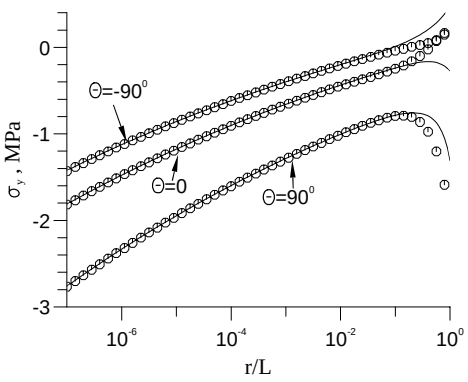

Figure 5.11: Comparison of the stresses obtained from FEM and the asymptotical equation using the K-factor from the empirical relations, for example 1 and H/L=3.

Below, two examples will be given to show the agreement of the stresses calculated from the FEM and from Eq. (5.1.70) by using the empirical equations for the K-factor. The material data of the joint are $E_1 = 10$ GPa, $\nu_1 = 0.2$, $E_2 = 5$ GPa, $\nu_2 = 0.3$ and the corresponding stress exponent is $\omega = 0.0449768$.

As Example 1 the edge traction is

$$\sigma_x(y) = 1 + 3\left(\frac{y}{H}\right) + 5\left(\frac{y}{H}\right)^2 + 7\left(\frac{y}{H}\right)^3 + 9\left(\frac{y}{H}\right)^4 + 11\left(\frac{y}{H}\right)^5 . \text{ MPa} \quad (5.2.47)$$

For H/L=2, the K-factor obtained from the empirical equations is K_L =-2.302 GPa. Using this K-factor value, the stresses near the singular point are calculated from Eq. (5.1.70), and they are compared with those obtained from FEM in Fig. 5.10 along different directions. It can be seen that they are in good agreement in the range of $r/L < 0.01$ (the relative error is smaller than 5%). For a joint with H/L=0.1 and the loading corresponding to that one given in Eq. (5.2.47), the K-factor obtained is K_H =-4.352 GPa. The agreement of the stresses is a little worse (the relative error is about 5%). For a joint with H/L=3 and the loading corresponding to that one given in Eq. (5.2.47), the K-factor obtained is K_L =-1.649 GPa by using Eqs. (5.2.38 - 5.2.43). The stresses are compared in Fig. 5.11. It can be seen that they also agree very well in the range of $r/L < 0.01$ (the relative error is smaller than 5%). This shows that the empirical equations for H/L=2 and H/L=8 can be used for a joint with $H/L > 2$.

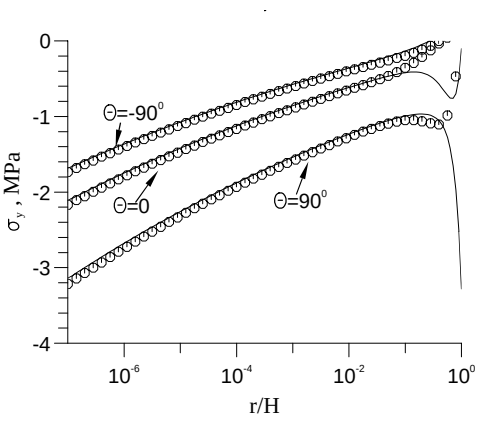

Figure 5.12: Comparison of the stresses obtained from FEM and the asymptotical equation using the K-factor from the empirical relations, for example 2 and H/L=0.1.

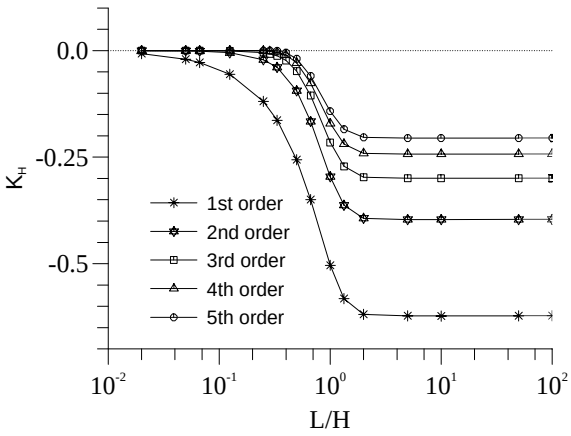

Figure 5.13: The stress intensity factor K_H (not K_H/σ_i) at the edge traction of $\sigma_x^l(y) =\mid y/H \mid^l$ (l=1,2,3,4,5) vs. L/H.

The edge traction for Example 2 reads

$$\sigma_x(y) = 1 + \left(\frac{y}{H}\right) + \left(\frac{y}{H}\right)^2 + \left(\frac{y}{H}\right)^3 + \left(\frac{y}{H}\right)^4 + \left(\frac{y}{H}\right)^5 . \text{ MPa} \quad (5.2.48)$$

For H/L=0.1, the K-factor obtained is K_H =-1.795 GPa. Using this K-factor value, the stresses near the singular point are calculated from Eq. (5.1.70), and compared with those from FEM in Fig. 5.12. It can be seen that they are in very good agreement in the range of $r/L < 0.01$ (the relative error is smaller than 5%). Under this loading and for H/L=2, the agreement of the stresses also is very good.

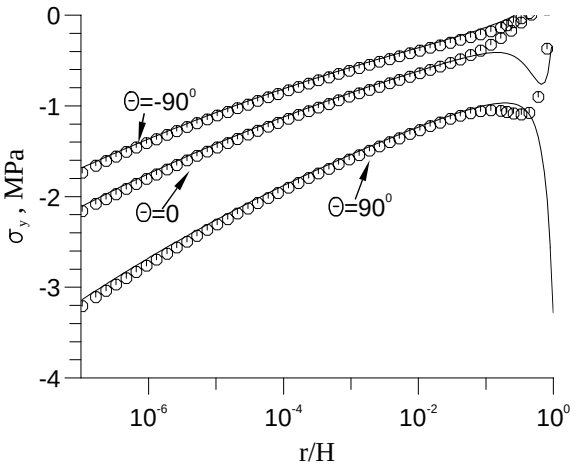

Figure 5.14: Comparison of the stresses obtained from FEM and the asymptotical equation using the K-factor from the empirical relations, for example 2 and H/L=0.06.

The only difference between this and the last example is that in this example the values of A_4 and A_5 in Eq. (5.2.44) is not larger than A_0, whereas in the last example they are much larger than A_0.
The same results as in Fig. 5.6, but only K_H (not K_H/σ_l), is plotted vs. L/H in Fig. 5.13. It can be seen that for joints of L/H> 2 (i.e. $H/L < 0.5$) the factors $K_H^{(l)}$ are constant. Therefore, the empirical equations for H/L=0.1 can also be used for a joint with $H/L < 0.5$. As an example, a joint with H/L=0.06 under the edge traction as given in Eq. (5.2.48) is considered. The K_H factor is the same as that one for the joint with H/L=0.1. The stresses obtained from FEM and Eq. (5.1.70) are compared in Fig. 5.14. For H/L=0.06, the agreement also is very good.
The short summary is that the empirical relations for H/L=2 can be used approximately for joints with H/L> 2 to calculate the factor K_L and the empirical equations for H/L=0.1 can be applied for joints with H/L< 0.5 to evaluate the factor K_H.

5.3 The Behavior of the Stress Intensity Factor in a Joint under Shear Edge Traction

From the results of Section 5.2 it is known that for a joint under tension edge traction $\sigma_x(y) = (y/H)^i$ (i=0, 1, 2, 3, 4, 5), the normalized stress intensity factor K_L/σ_i is constant, if the ratio of H/L is very large (e.g. for l=0, 1, 2, H/L > 2 and for l=3, 4, 5, H/L> 8) and the normalized stress intensity factor K_H/σ_i is constant for very large

L/H (e.g. $L/H > 2$). For a joint with shear edge traction, the question is whether the factors K_L and K_H have the same behavior as that one in a joint with a tension edge traction.

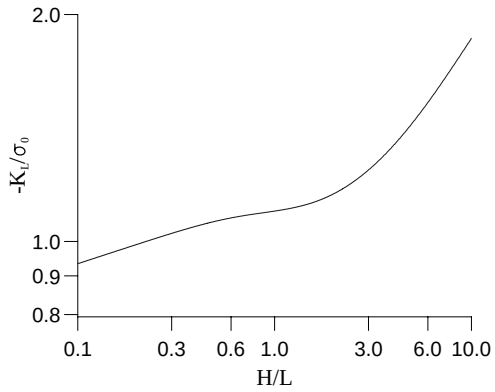

Figure 5.15: Normalized stress intensity factor K_L/σ_0 at the edge traction of $\tau_1 = -1$ and $\tau_2 = 1$ vs. H/L.

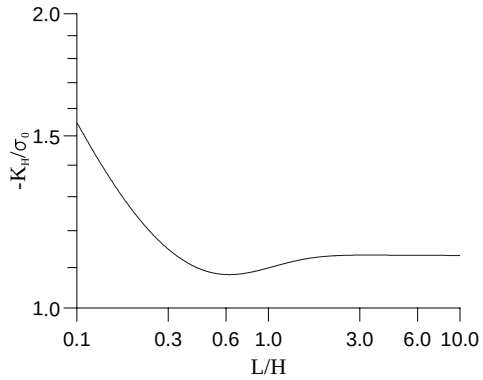

Figure 5.16: Normalized stress intensity factor K_H/σ_0 at the edge traction of $\tau_1 = -1$ and $\tau_2 = 1$ vs. L/H.

Below, it is assumed that the shear edge traction can be expanded in a polynomial, i.e.

$$\tau(y) = \sum_{n=1}^{N} B_n y^n + B_0. \tag{5.3.1}$$

where $B_0 = t_1$ in Eq. (5.1.2) or t_2 in Eq. (5.1.4).
To answer the question, the stress intensity factors are calculated from FEM for different ratios of H/L ($H_1 = H_2$) under the edge traction $\tau(y) = \pm B_0$ and $\tau(y) = \pm y/H$. The material data are $E_1 = 1$GPa, $E_2 = 5$GPa, $\nu_1 = 0.2$, and $\nu_2 = 0.3$. For this material combination, the stress exponent is $\omega = 0.0834$.
As for the tension edge traction, the values of K-factor in Eq. (3.0.1) and $\sigma^{ET}_{ijkl}(\theta)$ in Eq. (5.1.66) are dependent on the absolute size of R, because the loading $\tau^{(n)}(y) = (y/H)^n$ is dependent on the absolute size of H (here R=H).
For the edge traction $\tau_1 = -1$ MPa and $\tau_2 = 1$ MPa (in polar coordinates) the normalized stress intensity factor K_L/σ_0 (where $\sigma_0 = \sigma^{ET}_{\theta 0}(\theta = 0)$, see Section 5.1) is plotted vs H/L in Fig. 5.15 and the normalized stress intensity factor K_H/σ_0 is plotted vs L/H in Fig. 5.16. It can be seen that under shear edge traction, at a very large ratio of H/L, the normalized factor K_L/σ_0 is not constant, and with increasing of H/L the absolute value of K_L/σ_0 increases. However, for very large ratio of L/H the normalized factor K_H/σ_0 is constant.
For the edge traction $\tau_1 = \tau_{r\theta}(\theta = \theta_1) = -1$ MPa and $\tau_2 = \tau_{r\theta}(\theta = \theta_2) = -1$ MPa the normalized stress intensity factor K_L/σ_0 (because of $\sigma^{ET}_{\theta\theta 0}(\theta = 0) = 0$, see Section 5.1, here σ_0 is defined as $\sigma_0 = \tau^{ET}_{r\theta 0}(\theta = 0)$) is plotted vs H/L in Fig. 5.17, and the normalized stress intensity factor K_H/σ_0 is plotted vs L/H in Fig. 5.18. Again,

at a very large ratio of H/L, the normalized factor K_L/σ_0 is not constant, and with increasing H/L the absolute value of K_L/σ_0 increases, whereas for a very large ratio of L/H the normalized factor K_H/σ_0 is constant.

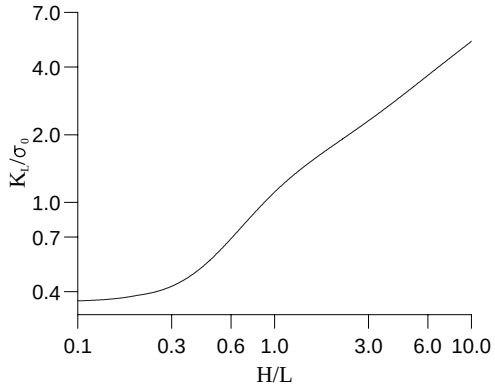

Figure 5.17: Normalized stress intensity factor K_L/σ_0 at the edge traction of $\tau_1 = -1$ and $\tau_2 = -1$ vs. H/L.

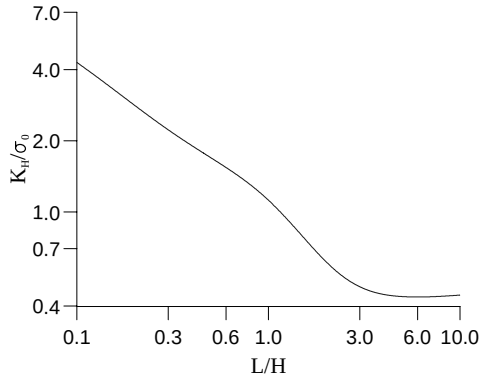

Figure 5.18: Normalized stress intensity factor K_H/σ_0 at the edge traction of $\tau_1 = -1$ and $\tau_2 = -1$ vs. L/H.

For a shear edge traction of linear function $\tau_1 = r/H$ MPa and $\tau_2 = -r/H$ MPa (in polar coordinates) the normalized stress intensity factor K_L/σ_1 ($\sigma_1 = \sigma^{ET}_{\theta\theta 1}(\theta = 0)$ and R=L) is plotted vs H/L in Fig. 5.19, and the normalized stress intensity factor K_H/σ_1 ($\sigma_1 = \sigma^{ET}_{\theta 1}(\theta = 0)$ and R=H) is plotted vs L/H in Fig. 5.20. It can be seen that under a shear edge traction of linear function, at a very large ratio of H/L, the normalized factor K_L/σ_1 is not constant, and with increasing H/L the absolute value of K_L/σ_1 increases, whereas the quantity $K_L(L/H)$ is constant for a large ratio of H/L (see Fig. 5.19). For very large ratio of L/H the normalized factor K_H/σ_1 is constant.
For an edge traction of linear function $\tau_1 = -r/H$ MPa and $\tau_2 = -r/H$ MPa, the normalized stress intensity factor K_L/σ_1 is plotted vs H/L in Fig. 5.21. The normalized stress intensity factor K_H/σ_1 is plotted vs L/H in Fig. 5.22. Here, due to the K-factor value being negative, only K_L (or K_H), not $\log(K_L)$, is plotted in the figures. Again, at a very large ratio of H/L, the normalized factor K_L/σ_1 is not constant, and with increasing H/L the absolute value of K_L/σ_1 increases, whereas the quantity $K_L(L/H)$ is constant for a large ratio of H/L (see Fig. 5.21). At a very large ratio of L/H, the normalized factor K_H/σ_1 is constant.
Now, we have seen that the behavior of the stress intensity factors for a shear and for a tension edge traction is different, especially for the factor K_L. Due to the fact that the factor K_L is not constant at a large ratio of H/L, finding the empirical relation for the calculation of the factors K_L and K_H under shear edge traction will not be studied any more.

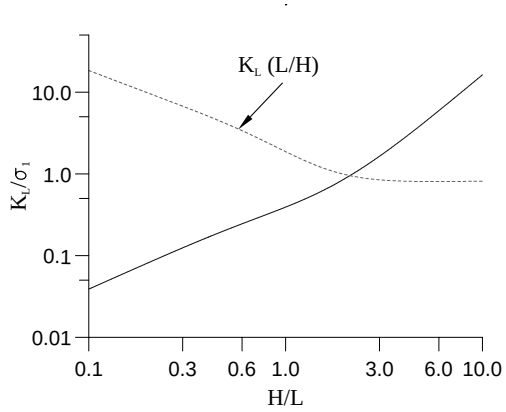

Figure 5.19: Normalized stress intensity factor K_L/σ_1 at the edge traction of $\tau_1 = r/H$ and $\tau_2 = -r/H$ vs. H/L.

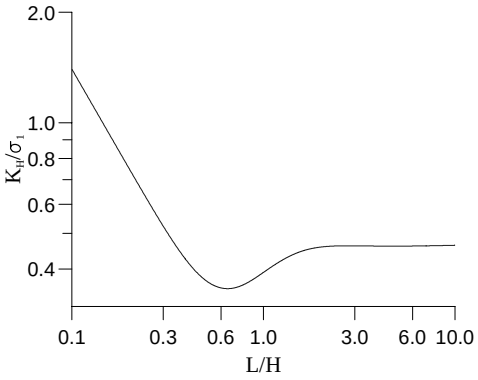

Figure 5.20: Normalized stress intensity factor K_H/σ_1 at the edge traction of $\tau_1 = r/H$ and $\tau_2 = -r/H$ vs. L/H.

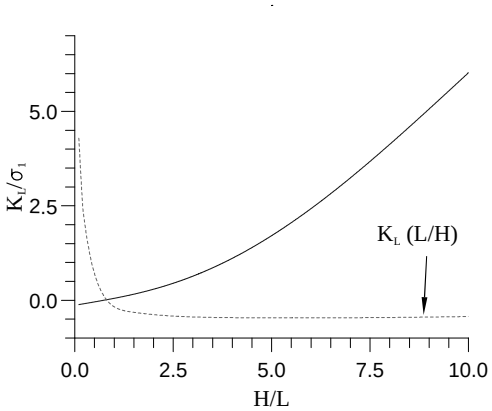

Figure 5.21: Normalized stress intensity factor K_L/σ_1 at the edge traction of $\tau_1 = -r/H$ and $\tau_2 = -r/H$ vs. H/L.

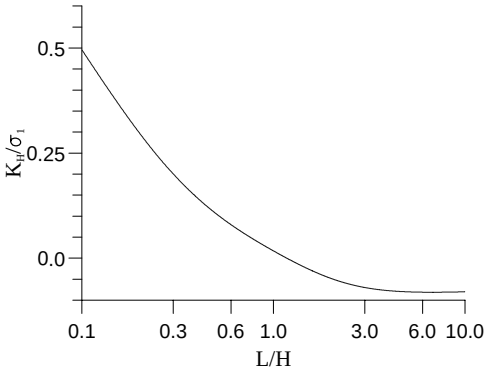

Figure 5.22: Normalized stress intensity factor K_H/σ_1 at the edge traction of $\tau_1 = -r/H$ and $\tau_2 = -r/H$ vs. L/H.

Chapter 6

Joint with Interface Corner

In a dissimilar materials joint with an internal interface corner (see Fig. 6.1), which is made of two interfaces, singular stresses near the intersection of the two interfaces may also occur for mechanical or thermal loading. The stresses near the corner can be described by an analytical form with one, two or three singular terms and a regular stress term. The stress exponents, the angular functions, and the regular stress term can be determined analytically. They will be given in Sections 6.1 and 6.2. For various geometries and material combinations, the general behavior of the stress exponents is shown in Section 6.3. The corresponding stress intensity factors have to be determined by means of the stress analysis of the whole joint using the Finite Element Method (FEM). The characteristics of the stress intensity factors are presented in Section 6.4. It can be seen that the behavior of the stress intensity factor for a joint under mechanical loading is much simpler than that one under thermal loading. The stresses near the corner calculated from FEM and the analytical description are compared in Section 6.5. It is shown that for most joint geometries and material combinations more than one singular term exists, and all of them are important to the contribution to the stresses near the singular point, even close to the singular point.

6.1 Determination of the Stress Exponents and the Angular Functions

For a joint with an interface corner the boundary conditions are

at the interface $\theta = 0$

$$\begin{aligned} u_1(r,0) &= u_2(r,0), \\ v_1(r,0) &= v_2(r,0), \\ \sigma_{\theta\theta 1}(r,0) &= \sigma_{\theta\theta 2}(r,0), \\ \sigma_{r\theta 1}(r,0) &= \sigma_{r\theta 2}(r,0), \end{aligned} \tag{6.1.1}$$

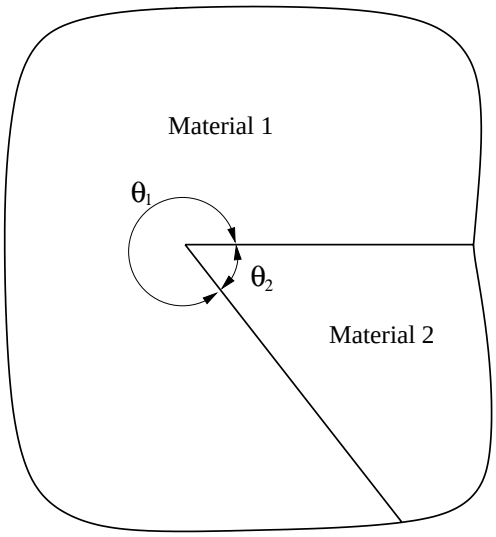

Figure 6.1: A joint with an interface corner.

and at the interface $\theta = \theta_1$

$$\begin{aligned} u_1(r,\theta_1) &= u_2(r,\theta_2), \\ v_1(r,\theta_1) &= v_2(r,\theta_2), \\ \sigma_{\theta\theta 1}(r,\theta_1) &= \sigma_{\theta\theta 2}(r,\theta_2), \\ \sigma_{r\theta 1}(r,\theta_1) &= \sigma_{r\theta 2}(r,\theta_2), \end{aligned} \tag{6.1.2}$$

where $\theta_2 = -(2\pi - \theta_1)$ and $\theta < 0$ in material 2.
For plane stress and thermal loading, insertion of Eqs. (3.1.7-3.1.9) and (3.1.16-3.1.17) into Eqs. (6.1.1) and (6.1.2) yields

$$\begin{aligned} &\sum_n r^{(1-\lambda_n)} \Big\{ B_{1n}\mu[2(1-\nu_1) + \lambda_n(1+\nu_1)] - D_{1n}\mu(1+\nu_1)(2-\lambda_n) \\ - \quad & B_{2n}[2(1-\nu_2) + \lambda_n(1+\nu_2)] + D_{2n}(1+\nu_2)(2-\lambda_n) \Big\} = rTE_2(\alpha_2 - \alpha_1) \end{aligned} \tag{6.1.3}$$

$$\begin{aligned} &\sum_n r^{(1-\lambda_n)} \Big\{ A_{1n}\mu[2(1-\nu_1) + (2-\lambda_n)(1+\nu_1)] - C_{1n}\mu(1+\nu_1)(2-\lambda_n) \\ - \quad & A_{2n}[2(1-\nu_2) + (2-\lambda_n)(1+\nu_2)] + C_{2n}(1+\nu_2)(2-\lambda_n) \Big\} = 0 \end{aligned} \tag{6.1.4}$$

$$\sum_n r^{-\lambda_n} \Big\{ B_{1n} + D_{1n} - B_{2n} - D_{2n} \Big\} = 0 \tag{6.1.5}$$

$$\sum_n r^{-\lambda_n} \Big\{ A_{1n}\lambda_n + C_{1n}(2-\lambda_n) - A_{2n}\lambda_n - C_{2n}(2-\lambda_n) \Big\} = 0 \tag{6.1.6}$$

$$\sum_n r^{-\lambda_n}\Big\{A_{1n}\sin(\lambda_n\theta_1)+B_{1n}\cos(\lambda_n\theta_1)+C_{1n}\sin[(2-\lambda_n)\theta_1]$$
$$+\quad D_{1n}\cos[(2-\lambda_n)\theta_1]-\Big\{A_{2n}\sin(\lambda_n\theta_2)+B_{2n}\cos(\lambda_n\theta_2)$$
$$+\quad C_{2n}\sin[(2-\lambda_n)\theta_2]+D_{2n}\cos[(2-\lambda_n)\theta_2]\Big\}\Big\}=0 \tag{6.1.7}$$

$$\sum_n r^{-\lambda_n}\Big\{A_{1n}\lambda_n\cos(\lambda_n\theta_1)-B_{1n}\lambda_n\sin(\lambda_n\theta_1)$$
$$+\quad C_{1n}(2-\lambda_n)\cos[(2-\lambda_n)\theta_1]-D_{1n}(2-\lambda_n)\sin[(2-\lambda_n)\theta_1]$$
$$-\quad \Big\{A_{2n}\lambda_n\cos(\lambda_n\theta_2)-B_{2n}\lambda_n\sin(\lambda_n\theta_2)+C_{2n}(2-\lambda_n)\cos[(2-\lambda_n)\theta_2]$$
$$-\quad D_{2n}(2-\lambda_n)\sin[(2-\lambda_n)\theta_2]\Big\}\Big\}=0. \tag{6.1.8}$$

$$\sum_n r^{(1-\lambda_n)}\Big\{\mu\Big\{A_{1n}[2(1-\nu_1)+\lambda_n(1+\nu_1)]sin(\lambda_n\theta_1)$$
$$+\quad B_{1n}[2(1-\nu_1)+\lambda_n(1+\nu_1)]cos(\lambda_n\theta_1)$$
$$-\quad C_{1n}(1+\nu_1)(2-\lambda_n)sin[(2-\lambda_n)\theta_1]-D_{1n}(1+\nu_1)(2-\lambda_n)cos[(2-\lambda_n)\theta_1]\Big\}$$
$$-\quad \Big\{A_{2n}[2(1-\nu_2)+\lambda_n(1+\nu_2)]sin(\lambda_n\theta_2)+B_{2n}[2(1-\nu_2)+\lambda_n(1+\nu_2)]cos(\lambda_n\theta_2)$$
$$-\quad C_{2n}(1+\nu_2)(2-\lambda_n)sin[(2-\lambda_n)\theta_2]-D_{2n}(1+\nu_2)(2-\lambda_n)cos[(2-\lambda_n)\theta_2]\Big\}\Big\}$$
$$=\quad rTE_2(\alpha_2-\alpha_1) \tag{6.1.9}$$

$$\sum_n r^{(1-\lambda_n)}\Big\{\mu\Big\{A_{1n}[2(1-\nu_1)+(2-\lambda_n)(1+\nu_1)]cos(\lambda_n\theta_1)$$
$$-\quad B_{1n}[2(1-\nu_1)+(2-\lambda_n)(1+\nu_1)]sin(\lambda_n\theta_1)$$
$$-\quad C_{1n}(1+\nu_1)(2-\lambda_n)cos[(2-\lambda_n)\theta_1]+D_{1n}(1+\nu_1)(2-\lambda_n)sin[(2-\lambda_n)\theta_1]\Big\}$$
$$-\quad \Big\{A_{2n}[2(1-\nu_2)+(2-\lambda_n)(1+\nu_2)]cos(\lambda_n\theta_2)$$
$$-\quad B_{2n}[2(1-\nu_2)+(2-\lambda_n)(1+\nu_2)]sin(\lambda_n\theta_2)-C_{2n}(1+\nu_2)(2-\lambda_n)cos[(2-\lambda_n)\theta_2]$$
$$+\quad D_{2n}(1+\nu_2)(2-\lambda_n)sin[(2-\lambda_n)\theta_2]\Big\}\Big\}=0. \tag{6.1.10}$$

For mechanical loading, Eqs. (6.1.3) through (6.1.10) are also valid by setting T=0 in Eqs. (6.1.3) and (6.1.9). This means that the right hand side of Eqs. (6.1.3) through (6.1.10) is zero.

Because r in Eqs. (6.1.3- 6.1.10) is arbitrary, for each n and $\lambda_n \neq 0$ this equation system can be rewritten in a matrix form as

$$[A]_{8\times 8}\{X\}_{8\times 1}=\{0\}_{8\times 1} \tag{6.1.11}$$

where $\{X\}_{8\times1} = \{A_{1n}, B_{1n}, C_{1n}, D_{1n}, A_{2n}, B_{2n}, C_{2n}, D_{2n}\}^t$ and $[A]_{8\times8}$ denotes its coefficient matrix. $\{X\}_{8\times1}$ is unknown and $[A]_{8\times8}$ includes the unknown exponent λ_n, the material properties (E_k, ν_k, k=1,2 for materials 1 and 2), and the geometry angle (θ_1). For $\lambda_n = 0$,

$$[A_0]_{8\times8}\{X_0\}_{8\times1} = \{S_0\}_{8\times1} \tag{6.1.12}$$

where $\{X_0\}_{8\times1} = \{A_{10}, B_{10}, C_{10}, D_{10}, A_{20}, B_{20}, C_{20}, D_{20}\}^t$, $[A_0]_{8\times8}$ is its coefficient matrix, and $\{S_0\}_{8\times1} = \{TE_2(\alpha_2 - \alpha_1), 0, 0, 0, 0, 0, TE_2(\alpha_2 - \alpha_1), 0\}$ is the right hand side of Eqs. (6.1.3) to (6.1.10). This case will be discussed in Section 6.2.

Equation (6.1.11) has a nonzero solution, if and only if

$$\mathrm{Det}([A]_{8\times8}) = 0 \tag{6.1.13}$$

is satisfied. In Eq. (6.1.13) the only unknown is the exponent λ_n. Its solutions are the eigenvalues of this problem. Because this is a transcendental equation, there are infinite solutions of λ_n (n=1,2,3,...) and they may be real and complex. If the eigenvalues are complex, the stress function Eq. (3.1.3) cannot be used directly. The relations given in Section 3.1.2 for complex eigenvalues should be applied. In this section, the real solutions are considered only.
For an arbitrary joint geometry with θ_1 the expansion of Eq. (6.1.13) is

$$\begin{aligned}\mathrm{Det}([A]_{8\times8}) &= \frac{512(1+t_n)^2}{(1+\alpha)^4}\Big\{\alpha^4 Y_1 + \beta^4 Y_2 + \alpha^2\beta^2 Y_3 + \alpha\beta^3 Y_4 + \alpha^3\beta Y_5 \\ &+ \beta^3 Y_6 + \alpha^2\beta Y_7 + \alpha\beta^2 Y_8 + \alpha^2 Y_9 + \beta^2 Y_{10} + \alpha\beta Y_{11} + Y_{12}\Big\}\end{aligned} \tag{6.1.14}$$

with

$$Y_1 = 8\Big\{\sin^2[t_n(\pi-\theta_1)] - t_n^2\sin^2(\theta_1)\Big\}^2 \tag{6.1.15}$$

$$Y_2 = 8[\sin^2(t_n\theta_1) - t_n^2\sin^2(\theta_1)]\Big[\sin^2[t_n(2\pi-\theta_1)] - t_n^2\sin^2(\theta_1)\Big] \tag{6.1.16}$$

$$\begin{aligned}Y_3 &= -16\sin^2[t_n(\pi-\theta_1)]\cos^2(t_n\pi)(1+2t_n^2\sin^2(\theta_1)) \\ &+ 4\sin^2[2t_n(\pi-\theta_1)] + 16t_n^2\sin^2(\theta_1)[3t_n^2\sin^2(\theta_1) - \sin^2(t_n\pi)]\end{aligned} \tag{6.1.17}$$

$$Y_4 = 16t_n^2\sin^2(\theta_1)\Big[\sin^2[t_n(2\pi-\theta_1)] + \sin^2(t_n\theta_1) - 2t_n^2\sin^2(\theta_1)\Big] \tag{6.1.18}$$

$$Y_5 = 32t_n^2\sin^2(\theta_1)\Big[\sin^2[t_n(\pi-\theta_1)] - t_n^2\sin^2(\theta_1)\Big] \tag{6.1.19}$$

$$Y_6 = -16t_n^2 \sin(2t_n\pi)\sin[2t_n(\pi-\theta_1)]\sin^2(\theta_1) \tag{6.1.20}$$

$$Y_7 = Y_6 \tag{6.1.21}$$

$$Y_8 = -2Y_6 \tag{6.1.22}$$

$$Y_9 = -16\left[\sin^2[t_n(\pi-\theta_1)] + t_n^2\cos[2t_n(\pi-\theta_1)]\sin^2(\theta_1)\right]\sin^2(t_n\pi) \tag{6.1.23}$$

$$Y_{10} = -16\left[\sin[t_n(2\pi-\theta_1)]\sin(t_n\theta_1) + t_n^2\cos[2t_n(\pi-\theta_1)]\sin^2(\theta_1)\right]\sin^2(t_n\pi) \tag{6.1.24}$$

$$Y_{11} = 32t_n^2\cos[2t_n(\pi-\theta_1)]\sin^2(t_n\pi)sin^2(\theta_1) \tag{6.1.25}$$

$$Y_{12} = 8\sin^4(t_n\pi) \tag{6.1.26}$$

where $t_n = 1-\lambda_n$. From Eqs. (6.1.14) through (6.1.26) it can be seen that if t_n ($t_n \neq -1$) is the solution of Eq. (6.1.14), -t_n is also. This means that if λ_n is the eigenvalue of the problem, 2-λ_n is as well. If λ_n is in the range of $0 < \lambda_n < 1$, however, $2-\lambda_n$ is not. Therefore, only the eigenvalue λ_n is used to describe the singular stress field.

For a special case of $\theta_1 = 90°$, Eq. (6.1.14) can be simplified as

$$\begin{aligned}
\mathrm{Det}([A]_{8\times8}) &= \frac{512(1+t_n)^2}{(1+\alpha)^4}\Big\{3-4\alpha^2+3\alpha^4-2\beta^2-2\alpha^2\beta^2+2\beta^4 \\
&- 8t_n^2(\beta-\alpha)^2(\alpha^2+\beta^2)+8t_n^4(\beta-\alpha)^4 \\
&- 2(\alpha-\beta)\Big[(\alpha+\beta)(-1+2\alpha^2-\beta^2) \\
&+ 2t_n^2(\beta-\alpha)\left(-1+2\alpha^2-2\beta+\beta^2\right)\Big]\cos(t_n\pi) \\
&+ \left[(\alpha^2-\beta^2)^2+4(1-\alpha^2)(\beta^2-1)\right]\cos(2t_n\pi) \\
&- 2(\alpha-\beta)(1+\beta)\left[(\alpha+\beta)(1-\beta)+2(1+\beta)(\beta-\alpha)t_n^2\right]\cos(3t_n\pi) \\
&+ (\beta^2-1)^2\cos(4t_n\pi)\Big\},
\end{aligned} \tag{6.1.27}$$

and the coefficients of the angular functions can be calculated from

$$A_{1n} = (1+t_n)\cos(\frac{\pi}{2}t_n)\Big\{2\beta t_n - 2 - \beta^2\left(1+6t_n+4{t_n}^2\right)+\alpha^3\left(3+2t_n-4{t_n}^2-4{t_n}^3\right)+$$

$$
\begin{aligned}
&+ \quad 2\beta^3\left(2{t_n}^2-1\right)t_n+\alpha^2\left(3-2t_n-4{t_n}^2+8\beta{t_n}^2+12\beta{t_n}^3\right)+\\
&+ \quad \alpha\left(-2-2t_n+8\beta t_n\left(1+t_n\right)-\beta^2\left(1+4{t_n}^2+12{t_n}^3\right)\right)+\left(1+\alpha\right)\\
&+ \quad \Big[1-4\alpha^2+3\beta^2+2\alpha t_n-2\alpha^2 t_n-2\beta t_n-2\alpha\beta t_n+4\beta^2 t_n+\\
&+ \quad 4\alpha^2{t_n}^2-8\alpha\beta{t_n}^2+4\beta^2{t_n}^2\Big]\cos(\pi t_n)+\\
&+ \quad \left(1+\alpha\right)\Big[2+\alpha^2-3\beta^2+2\alpha t_n-2\beta t_n+2\alpha\beta t_n-2\beta^2 t_n\Big]\cos(2\pi t_n)+\\
&+ \quad \left(1+\beta\right)\Big[-1-\alpha+\beta+\alpha\beta-2\alpha t_n+2\beta t_n-2\alpha\beta t_n+2\beta^2 t_n\Big]\cos(3\pi t_n)\Bigg\}
\end{aligned}
\tag{6.1.28}
$$

$$
\begin{aligned}
B_{1n} \;=\; &\left(1+t_n\right)\sin(\frac{\pi}{2}t_n)\Bigg\{-2-2\beta\left(1+t_n\right)+\beta^2\left(1-2t_n+4{t_n}^2\right)+\alpha^3\left(1+2t_n-4{t_n}^3\right)\\
&+ \quad 2\beta^3\left(1-t_n-2{t_n}^2+2{t_n}^3\right)+\alpha^2\left(1+2t_n+4{t_n}^2+4\beta t_n\left(-1-t_n+3{t_n}^2\right)\right)\\
&+ \quad \alpha\left(2t_n-8\beta{t_n}^2+\beta^2\left(-1+4t_n+8{t_n}^2-12{t_n}^3\right)\right)+\\
&+ \quad \left(1+\alpha\right)\Bigg[-1+2\alpha-2\alpha^2-2\beta+2\alpha\beta+\beta^2+2\alpha t_n-2\alpha^2 t_n-2\beta t_n+\\
&+ \quad 6\alpha\beta t_n-4\beta^2 t_n+4\alpha^2{t_n}^2-8\alpha\beta{t_n}^2+4\beta^2{t_n}^2\Bigg]\cos(\pi t_n)+\\
&+\left(1+\alpha\right)\Big[2-2\alpha+\alpha^2+2\beta-2\alpha\beta-\beta^2-2\alpha t_n+2\beta t_n-2\alpha\beta t_n+2\beta^2 t_n\Big]\cos(2\pi t_n)\\
&+ \quad \left(1+\beta\right)\Big[1-\alpha+\beta+\alpha\beta-2\beta^2-2\alpha t_n+2\beta t_n-2\alpha\beta t_n+2\beta^2 t_n\Big]\cos(3\pi t_n)\Bigg\}
\end{aligned}
\tag{6.1.29}
$$

$$
\begin{aligned}
C_{1n} \;=\; &\cos(\frac{\pi}{2}t_n)\Bigg\{2+2t_n+2\beta\left(-1+t_n\right)t_n+2\beta^3 t_n\left(1-t_n-2{t_n}^2+2{t_n}^3\right)+\\
&+ \quad \beta^2\left(1-t_n-2{t_n}^2+4{t_n}^3\right)+\alpha^3\left(-3-t_n+6{t_n}^2-4{t_n}^4\right)+\\
&+ \quad \alpha^2\left(-3-5t_n+2{t_n}^2+4{t_n}^3+4\beta t_n\left(1-2t_n-{t_n}^2+3{t_n}^3\right)\right)\\
&+ \quad \alpha\left(2-2{t_n}^2+4t_n\beta\left(1-2{t_n}^2\right)+\beta^2\left(1-3t_n+4{t_n}^2+8{t_n}^3-12{t_n}^4\right)\right)+\\
&+ \quad \left(1+\alpha\right)\Bigg[-1+4\alpha^2-3\beta^2-t_n+2\alpha t_n+2\alpha^2 t_n-2\beta t_n-6\alpha\beta t_n+5\beta^2 t_n\\
&+ \quad 2\alpha{t_n}^2-6\alpha^2{t_n}^2-2\beta{t_n}^2+6\alpha\beta{t_n}^2-4\alpha^2{t_n}^3+8\alpha\beta{t_n}^3-4\beta^2{t_n}^3\Bigg]\cos(\pi t_n)+\\
&+ \quad \left(1+\alpha\right)\Bigg[-2-\alpha^2+3\beta^2-2t_n+2\alpha t_n-\alpha^2 t_n+2\beta t_n+2\alpha\beta t_n-\\
&- \quad 3\beta^2 t_n+2\alpha{t_n}^2-2\beta{t_n}^2+2\alpha\beta{t_n}^2-2\beta^2{t_n}^2\Bigg]\cos(2\pi t_n)+\\
&+ \quad \left(1+\beta\right)\Big[1+\alpha-\beta-\alpha\beta+t_n-\alpha t_n+\beta t_n+\alpha\beta t_n-
\end{aligned}
$$

$$- \quad 2\beta^2 t_n - 2\alpha {t_n}^2 + 2\beta {t_n}^2 - 2\alpha\beta {t_n}^2 + 2\beta^2 {t_n}^2 \Big] \cos(3\pi t_n) \Big\} \tag{6.1.30}$$

$$\begin{aligned}
D_{1n} \;=\; & \sin(\frac{\pi}{2} t_n) \Big\{ -2 - 2t_n + 2\beta(1+t_n)^2 + \beta^2 \left(1 - t_n - 10{t_n}^2 + 4{t_n}^3\right) - \\
- \quad & 2\beta^3 \left(1 - 3{t_n}^2 + 2{t_n}^4\right) + \alpha^3 \left(1 - t_n - 2{t_n}^2 + 4{t_n}^3 + 4{t_n}^4\right) + \\
+ \quad & \alpha^2 \left(1 - t_n + 2{t_n}^2 + 4{t_n}^3 + 4\beta {t_n}^2 \left(2 - 2t_n - 3{t_n}^2\right)\right) + \\
+ \quad & \alpha \left(-2t_n - 2{t_n}^2 + 4\beta t_n \left(1 + 2t_n - 2{t_n}^2\right) + \beta^2 \left(-1 - t_n - 12{t_n}^2 + 4{t_n}^3 + 12{t_n}^4\right)\right) \\
+ \quad & (1+\alpha) \Big[-1 + 2\alpha - 2\alpha^2 + 2\beta - 2\alpha\beta + \beta^2 - t_n + \beta^2 t_n - 2\alpha {t_n}^2 + \\
+ \quad & 6\alpha^2 {t_n}^2 + 2\beta {t_n}^2 + 2\alpha\beta {t_n}^2 - 8\beta^2 {t_n}^2 + 4\alpha^2 {t_n}^3 - 8\alpha\beta {t_n}^3 + 4\beta^2 {t_n}^3 \Big] \cos(\pi t_n) + \\
+ \quad & (1+\alpha) \Big[2 - 2\alpha + \alpha^2 - 2\beta + 2\alpha\beta - \beta^2 + 2t_n + \alpha^2 t_n - 4\beta t_n + \\
+ \quad & \beta^2 t_n + 2\alpha {t_n}^2 - 2\beta {t_n}^2 + 2\alpha\beta {t_n}^2 - 2\beta^2 {t_n}^2 \Big] \cos(2\pi t_n) + \\
+ \quad & (1+\beta) \Big[1 - \alpha - 3\beta + \alpha\beta + 2\beta^2 + t_n + \alpha t_n - \beta t_n - \alpha\beta t_n + 2\alpha {t_n}^2 - \\
- \quad & 2\beta {t_n}^2 + 2\alpha\beta {t_n}^2 - 2\beta^2 {t_n}^2 \Big] \cos(3\pi t_n) \Big\}
\end{aligned} \tag{6.1.31}$$

$$\begin{aligned}
A_{2n} \;=\; & (1+t_n) \cos(\frac{\pi}{2} t_n) \Big\{ -2 - 2\beta t_n - \beta^2 \left(1 + 6t_n + 4{t_n}^2\right) + 4t_n \beta^3 \left(1 - {t_n}^2\right) + \\
+ \quad & \alpha^3 \left(-3 - 4t_n + 4{t_n}^2 + 4{t_n}^3\right) + \alpha^2 \left(3 - 2t_n - 4{t_n}^2 + 2\beta t_n \left(3 - 4t_n - 6{t_n}^2\right)\right) \\
+ \quad & \alpha \left(2 + 2t_n + 8\beta t_n \left(1 + t_n\right) + \beta^2 \left(1 - 6t_n + 4{t_n}^2 + 12{t_n}^3\right)\right) + \\
+ \quad & \Big[1 + \beta^2 \left(3 + 8t_n + 4{t_n}^2\right) + \alpha^3 \left(4 + 6t_n - 4{t_n}^2 - 8{t_n}^3\right) + 2t_n \beta^3 \left(-3 + 4{t_n}^2\right) + \\
+ \quad & 2\alpha^2 \left(-2 + 2{t_n}^2 + \beta t_n \left(-5 + 4t_n + 12{t_n}^2\right)\right) + \\
+ \quad & \alpha \left(-1 - 8\beta t_n \left(1 + t_n\right) + \beta^2 \left(-3 + 10t_n - 4{t_n}^2 - 24{t_n}^3\right)\right) \Big] \cos(\pi t_n) + \\
+ \quad & \Big[2 - 2\alpha + \alpha^2 - \alpha^3 - 3\beta^2 + 3\alpha\beta^2 - 2\alpha t_n + 2\alpha^2 t_n - 2\alpha^3 t_n + 2\beta t_n + \\
+ \quad & 4\alpha^2 \beta t_n - 2\beta^2 t_n - 4\alpha\beta^2 t_n + 2\beta^3 t_n \Big] \cos(2\pi t_n) \\
+ \quad & \left(-1 + \alpha + \beta^2 - \alpha\beta^2\right) \cos(3\pi t_n) \Big\}
\end{aligned} \tag{6.1.32}$$

$$B_{2n} \;=\; (1+t_n) \sin(\frac{\pi}{2} t_n) \Big\{ -2 + 4\beta^3 \left(1 - t_n\right) {t_n}^2 + 2\beta \left(1 + t_n\right) + \beta^2 \left(1 - 2t_n + 4{t_n}^2\right) +$$

$$
\begin{aligned}
&+ \quad \alpha^3\left(1+4{t_n}^3\right)+\alpha^2\left(1+2t_n+4{t_n}^2-2\beta\left(1+t_n-2{t_n}^2+6{t_n}^3\right)\right)+\\
&+ \quad \alpha\left(-2t_n-8\beta{t_n}^2+\beta^2\left(-1+2t_n-8{t_n}^2+12{t_n}^3\right)\right)+\\
&+ \quad \Bigg[-1+\beta^2\left(1+4{t_n}^2\right)+2\beta^3\left(-1+t_n+4{t_n}^2-4{t_n}^3\right)+\\
&+ \quad 2\alpha^3\left(-1-t_n+2{t_n}^2+4{t_n}^3\right)+2\alpha^2\left(2{t_n}^2+\beta\left(1+3t_n-12{t_n}^3\right)\right)\\
&+ \quad \alpha\left(1-8\beta{t_n}^2+\beta^2\left(1-6t_n-12{t_n}^2+24{t_n}^3\right)\right)\Bigg]\cos(\pi t_n)+\Bigg[2-\alpha^2+\alpha^3\\
&- \quad 2\beta-\beta^2-\alpha\beta^2+2\beta^3+2\alpha t_n-2\alpha^2t_n+2\alpha^3t_n-2\beta t_n-4\alpha^2\beta t_n+\\
&+ \quad 2\beta^2t_n+4\alpha\beta^2t_n-2\beta^3t_n\Bigg]\cos(2\pi t_n)+\left(1-\alpha-\beta^2+\alpha\beta^2\right)\cos(3\pi t_n)\Bigg\} \qquad (6.1.33)
\end{aligned}
$$

$$
\begin{aligned}
C_{2n} \;=\; &\cos(\frac{\pi}{2}t_n)\Bigg\{2+2t_n+2\beta\left(1-t_n\right)t_n-4\beta^3(-1+t_n)^2t_n\left(1+t_n\right)+\\
&+ \quad \beta^2\left(1-t_n-2{t_n}^2+4{t_n}^3\right)+\alpha^2\left(1+t_n\right)\times\\
&\times \quad \left(-3-2t_n-2\beta t_n+4{t_n}^2+16\beta{t_n}^2-12\beta{t_n}^3\right)+\alpha^3\left(3-t_n-8{t_n}^2+4{t_n}^4\right)+\\
&+ \quad \alpha\left(-2+2{t_n}^2+4t_n\beta\left(1-2{t_n}^2\right)+\beta^2\left(-1+5t_n-10{t_n}^2-8{t_n}^3+12{t_n}^4\right)\right)+\\
&+\Bigg[-1-t_n-4\beta t_n+\beta^2\left(-3+t_n+4{t_n}^2-4{t_n}^3\right)+2\beta^3t_n\left(3-3t_n-4{t_n}^2+4{t_n}^3\right)\\
&+ \quad 2\alpha^3\left(-2+t_n+5{t_n}^2-2{t_n}^3-4{t_n}^4\right)+\\
&+ \quad \alpha\left(1+t_n-4t_n\beta\left(1-2{t_n}^2\right)+\beta^2\left(3-7t_n+14{t_n}^2+12{t_n}^3-24{t_n}^4\right)\right)+\\
&+ \quad \alpha^2\left(4+4t_n-4{t_n}^2-4{t_n}^3+2t_n\beta\left(1-9t_n+12{t_n}^3\right)\right)\Bigg]\cos(\pi t_n)+\\
&+ \quad \Bigg[-2-2t_n+2\beta\left(-1+t_n\right)t_n+2\beta^3\left(-1+t_n\right)t_n+\beta^2\left(3-3t_n-2{t_n}^2\right)+\\
&+ \quad \alpha^3\left(1-t_n-2{t_n}^2\right)+\alpha^2\left(-1+t_n+2{t_n}^2+4\beta{t_n}^2\right)+\\
&+ \quad \alpha\left(2+4\beta t_n-2{t_n}^2+\beta^2\left(-3+5t_n-4{t_n}^2\right)\right)\Bigg]\cos(2\pi t_n)+\\
&+ \quad \left(1-\alpha\right)\left(1+\beta\right)\left(1-\beta+t_n+3\beta t_n\right)\cos(3\pi t_n)\Bigg\} \qquad (6.1.34)
\end{aligned}
$$

$$
\begin{aligned}
D_{2n} \;=\; &\sin(\frac{\pi}{2}t_n)\Bigg\{-2-2t_n-2\beta(1+t_n)^2+\beta^2\left(1-t_n-10{t_n}^2+4{t_n}^3\right)+\\
&+ \quad \alpha^3\left(1+t_n-4{t_n}^3-4{t_n}^4\right)-4{t_n}^2\beta^3\left(1-{t_n}^2\right)+\\
&+ \quad \alpha\left(2t_n+2{t_n}^2+4\beta t_n\left(1+2t_n-2{t_n}^2\right)+\beta^2\left(-1+t_n+6{t_n}^2-4{t_n}^3-12{t_n}^4\right)\right)+\\
&+ \quad \alpha^2\left(1-t_n+2{t_n}^2+4{t_n}^3+2\beta\left(1-{t_n}^2+4{t_n}^3+6{t_n}^4\right)\right)+\\
&+ \quad \Bigg[-1-t_n-4\beta t_n+\beta^2\left(1-3t_n-12{t_n}^2+4{t_n}^3\right)-
\end{aligned}
$$

$$
\begin{aligned}
&- \quad 2\alpha^3\left(1-3{t_n}^2+2{t_n}^3+4{t_n}^4\right)+2\beta^3\left(1-5{t_n}^2+4{t_n}^4\right)\\
&+ \quad \alpha\left(1+t_n+4\beta t_n\left(1+2t_n-2{t_n}^2\right)+\beta^2\left(1+3t_n+10{t_n}^2-4{t_n}^3-24{t_n}^4\right)\right)+\\
&+ \quad \alpha^2\left(4{t_n}^2+4{t_n}^3-2\beta\left(1+3{t_n}^2-4{t_n}^3-12{t_n}^4\right)\right)\Bigg]\cos(\pi t_n)+\\
&+ \quad \Bigg[2+2t_n+2\beta(1+t_n)^2+\alpha^3\left(1-t_n-2{t_n}^2\right)+\beta^2\left(-1+t_n-2{t_n}^2\right)-\\
&- \quad 2\beta^3\left(1-{t_n}^2\right)+\alpha^2\left(-1+t_n+2{t_n}^2+4\beta{t_n}^2\right)-\\
&- \quad \alpha\left(2t_n+4\beta t_n+2{t_n}^2+\beta^2\left(1+t_n+4{t_n}^2\right)\right)\Bigg]\cos(2\pi t_n)+\\
&+ \quad (1-\alpha)(1+\beta)(1-\beta+t_n+3\beta t_n)\cos(3\pi t_n)\Bigg\} \qquad (6.1.35)
\end{aligned}
$$

where $t_n = 1-\lambda_n$. The angular functions can be calculated from Eqs. (3.1.97- 3.1.99).

6.2 Determination of the Regular Stress Term

6.2.1 Joint under Thermal Loading

To determine the regular stress term, corresponding to the solution of $\lambda_n = 0$ in the last section, the stress function Eq. (3.3.1) given in Section 3.3 will be used. The stresses and the displacement v have the same relations as in Section 3.3. Only for thermal loading, the displacement u is given by

$$
\begin{aligned}
u_{k0}(r,\theta) &= \frac{2r}{E_k}[\mathcal{A}_{\mathrm{k0}}\theta(1-\nu_{\mathrm{k}})+\mathcal{B}_{\mathrm{k0}}(1-\nu_{\mathrm{k}})-\mathcal{C}_{\mathrm{k0}}(1+\nu_{\mathrm{k}})\sin(2\theta)\\
&- \mathcal{D}_{\mathrm{k0}}(1+\nu_{\mathrm{k}})\cos(2\theta)]+\mathrm{r}\alpha_{\mathrm{k}}\mathrm{T}. \qquad (6.2.1)
\end{aligned}
$$

Converting Eqs(3.3.3, 3.3.4, 3.3.6, 6.2.1) into Eqs. (6.1.1-6.1.2) yields

$$-2C_{10}\mu(1+\nu_1)+F_{10}E_2+2C_{20}(1+\nu_2)-F_{20}E_2=0 \qquad (6.2.2)$$

$$\mu A_{10}-A_{20}=0 \qquad (6.2.3)$$

$$
\begin{aligned}
B_{10}\mu(1-\nu_1) &- D_{10}\mu(1+\nu_1)-B_{20}(1-\nu_2)+D_{20}(1+\nu_2)\\
&= E_2/2T(\alpha_2-\alpha_1) \qquad (6.2.4)
\end{aligned}
$$

$$B_{10}+D_{10}-B_{20}-D_{20}=0 \qquad (6.2.5)$$

$$A_{10}+2C_{10}-A_{20}-2C_{20}=0 \qquad (6.2.6)$$

$$\begin{aligned} A_{10}\mu\theta_1(1 &- \nu_1) + B_{10}\mu(1-\nu_1) - \mu C_{10}(1+\nu_1)\sin(2\theta_1) - \mu D_{10}(1+\nu_1)\cos(2\theta_1) \\ &- A_{20}\theta_2(1-\nu_2) - B_{20}(1-\nu_2) + C_{20}(1+\nu_2)\sin(2\theta_2) + D_{20}(1+\nu_2)\cos(2\theta_2) \\ &= E_2/2T(\alpha_2-\alpha_1) \end{aligned} \tag{6.2.7}$$

$$\begin{aligned} -2C_{10}\mu(1 &+ \nu_1)\cos(2\theta_1) + 2D_{10}\mu(1+\nu_1)\sin(2\theta_1) + F_{10}E_2 \\ &+ 2C_{20}(1+\nu_2)\cos(2\theta_2) - 2D_{20}(1+\nu_2)\sin(2\theta_2) - F_{20}E_2 = 0 \end{aligned} \tag{6.2.8}$$

$$\begin{aligned} A_{10}\theta_1 &+ B_{10} + C_{10}\sin(2\theta_1) + D_{10}\cos(2\theta_1) \\ &- A_{20}\theta_2 - B_{20} - C_{20}\sin(2\theta_2) - D_{20}\cos(2\theta_2) = 0 \end{aligned} \tag{6.2.9}$$

$$\begin{aligned} A_{10} &+ 2C_{10}\cos(2\theta_1) - 2D_{10}\sin(2\theta_1) \\ &- A_{20} - 2C_{20}\cos(2\theta_2) + 2D_{20}\sin(2\theta_2) = 0 \end{aligned} \tag{6.2.10}$$

for plane stress with $\mu = E_2/E_1$. The regular stress term is independent of the coefficients F_{k0}. Therefore, the coefficient F_{k0} is not considered any more.
Solving the Eqs. (6.2.4-6.2.10) yields

$$A_{10} = A_{20} = C_{10} = C_{20} = D_{10} = D_{20} = 0 \tag{6.2.11}$$

$$B_{10} = B_{20} = -\frac{E_2^*}{2}T(\alpha_2^* - \alpha_1^*)\frac{1+\alpha}{4\beta} \tag{6.2.12}$$

with $E_k^* = E_k$ and $\alpha_k^* = \alpha_k$ for plane stress and $E_k^* = E_k/(1-\nu_k^2)$ and $\alpha_k^* = (1+\nu_k)\alpha_k$ for plane strain. From Eqs. (3.3.2-3.3.4) the regular stress term in polar coordinates reads

$$\sigma_{r0} = \sigma_{\theta 0} = -E_2^* T(\alpha_2^* - \alpha_1^*)\frac{1+\alpha}{4\beta} \tag{6.2.13}$$

$$\tau_{r\theta} = 0 \tag{6.2.14}$$

and in Cartesian coordinates is

$$\sigma_{x0} = \sigma_{y0} = -E_2^* T(\alpha_2^* - \alpha_1^*)\frac{1+\alpha}{4\beta} \tag{6.2.15}$$

$$\tau_{xy} = 0, \tag{6.2.16}$$

which is independent of the joint geometry θ_1.

6.2.2 Joint under Mechanical Loading

For joints under mechanical loading Eqs. (6.2.2-6.2.10) are still valid, in which T should be replaced by zero. From Eqs. (6.2.15-6.2.16) it follows that in the general cases the regular stresses are zero for $T = 0$. However, for some special material combinations and geometries the regular stress term is nonzero.
Equation system Eqs. (6.2.4-6.2.10) is homogeneous for $T = 0$. The condition of it having a non-zero solution is that the determinant of its coefficient matrix is zero, it is

$$\frac{(\alpha-\beta)^2\beta\sin^3(\theta_1)}{(1+\alpha)^4}\Big\{-\pi\cos(\theta_1)+\alpha\big[(\pi-\theta_1)\cos(\theta_1)+\sin(\theta_1)\big]\Big\}=0 \tag{6.2.17}$$

This means that if

$$\alpha=\beta \tag{6.2.18}$$

or

$$\beta=0 \text{ and } \alpha \text{ arbitrary} \tag{6.2.19}$$

or

$$\theta_1=\pi \text{ (no corner)} \tag{6.2.20}$$

or

$$\alpha=\frac{\pi\cos(\theta_1)}{(\pi-\theta_1)\cos(\theta_1)+\sin(\theta_1)} \text{ and } \beta \text{ arbitrary} \tag{6.2.21}$$

the regular stress term is non-zero.
The case of $\beta = 0$ corresponds to

$$\frac{E_2}{E_1}=\frac{1-\nu_2}{1-\nu_1} \tag{6.2.22}$$

for plane stress and

$$\frac{E_2}{E_1}=\frac{(1-2\nu_2)(1+\nu_2)}{(1-2\nu_1)(1+\nu_1)} \tag{6.2.23}$$

for plane strain.
The case of $\alpha = \beta$ is identical to $G_1 = G_2$ for plane stress and plane strain.

In case of $\alpha = \beta$, the coefficients of the regular stress term are

$$A_{10}=A_{20}=B_{10}=B_{20}=0 \tag{6.2.24}$$

$$C_{10}=C_{20}=K_0^1/2 \tag{6.2.25}$$

$$D_{10} = D_{20} = K_0^2/2. \tag{6.2.26}$$

From Eqs. (3.3.2-3.3.4) the regular stress term is

$$\begin{aligned} \sigma_{r0} &= -K_0^1 \sin(2\theta) - K_0^2 \cos(2\theta) \\ \sigma_{\theta 0} &= K_0^1 \sin(2\theta) + K_0^2 \cos(2\theta) \\ \sigma_{r\theta 0} &= -K_0^1 \cos(2\theta) + K_0^2 \sin(2\theta) \end{aligned} \tag{6.2.27}$$

where there are two arbitrary constants K_0^1 and K_0^2.

In case of $\beta = 0$ and α arbitrary, the coefficients of the regular stress term are

$$A_{10} = A_{20} = C_{10} = C_{20} = D_{10} = D_{20} = 0 \tag{6.2.28}$$

$$B_{10} = B_{20} = K_0/2. \tag{6.2.29}$$

The regular stress term reads

$$\sigma_{r0} = \sigma_{\theta 0} = K_0, \qquad \tau_{r\theta 0} = 0, \tag{6.2.30}$$

or

$$\sigma_{x0} = \sigma_{y0} = K_0, \qquad \tau_{r\theta 0} = 0. \tag{6.2.31}$$

For $\alpha = \frac{\pi \cos(\theta_1)}{(\pi - \theta_1)\cos(\theta_1) + \sin(\theta_1)}$ the coefficients of the regular stress term are

$$A_{10} = K_0 \tag{6.2.32}$$

$$B_{10} = K_0 \frac{-\theta_1}{2} \tag{6.2.33}$$

$$C_{10} = K_0 \frac{\cot(\theta_1)\left(\beta\pi\theta_1 \cos(\theta_1) - \beta {\theta_1}^2 \cos(\theta_1) - \pi \sin(\theta_1) + \beta\theta_1 \sin(\theta_1)\right)}{2\left(\pi \cos(\theta_1) - \beta\pi \cos(\theta_1) + \beta\theta_1 \cos(\theta_1) - \beta \sin(\theta_1)\right)} \tag{6.2.34}$$

$$D_{10} = -K_0 \frac{\sin(\theta_1)}{\cos(\theta_1)} C_{10} \tag{6.2.35}$$

$$A_{20} = K_0 \frac{\theta_1 \cos(\theta_1) - \sin(\theta_1)}{-2\pi \cos(\theta_1) + \theta_1 \cos(\theta_1) - \sin(\theta_1)} \tag{6.2.36}$$

$$B_{20} = K_0 \frac{2\pi - \theta_1}{2} A_{20} \tag{6.2.37}$$

$$
\begin{aligned}
C_{20} &= K_0 \cot(\theta_1) \left[\theta_1 \cos(\theta_1) - \sin(\theta_1)\right] \Big\{ 2\beta\pi^2 \cos(\theta_1) - 3\beta\pi\theta_1 \cos(\theta_1) + \beta {\theta_1}^2 \cos(\theta_1) + \\
&+ \pi \sin(\theta_1) + 2\beta\pi \sin(\theta_1) - \beta\theta_1 \sin(\theta_1) \Big\} / \Big\{ 2 \left(2\pi \cos(\theta_1) - \theta_1 \cos(\theta_1) + \sin(\theta_1)\right) \\
&\times \left(\pi \cos(\theta_1) - \beta\pi \cos(\theta_1) + \beta\theta_1 \cos(\theta_1) - \beta \sin(\theta_1)\right) \Big\} \qquad (6.2.38)
\end{aligned}
$$

$$
D_{20} = -K_0 \frac{\sin(\theta_1)}{\cos(\theta_1)} C_{20} \qquad (6.2.39)
$$

The regular stress term can be calculated from Eqs. (3.3.2-3.3.4).

For the special joint geometry with $\theta_1 = 90°$ the regular stress term is nonzero, if $\alpha = \beta$, or $\beta = 0$ and arbitrary α, or $\alpha = 0$ and arbitrary β (see Eq. (6.2.17)). In case of $\alpha = \beta$, or $\beta = 0$ and arbitrary α, the regular stress term is independent of the joint geometry, which can be calculated from Eqs. (6.2.27), (6.2.30), and (6.2.31). In case of $\alpha = 0$ and arbitrary β, the coefficients of the regular stress term can be simplified as

$$
A_{10} = K_0 \qquad (6.2.40)
$$

$$
B_{10} = -K_0 \pi / 4 \qquad (6.2.41)
$$

$$
C_{10} = 0 \qquad (6.2.42)
$$

$$
D_{10} = K_0 \frac{\pi}{4} (1 - 2/\beta) \qquad (6.2.43)
$$

$$
A_{20} = K_0 \qquad (6.2.44)
$$

$$
B_{20} = 3\pi / 4 K_0 \qquad (6.2.45)
$$

$$
C_{20} = 0 \qquad (6.2.46)
$$

$$
D_{20} = -K_0 \frac{\pi}{4\beta} (2 + 3\beta). \qquad (6.2.47)
$$

In general, for a joint under thermal loading, the regular stress term always is nonzero and it can be determined analytically. The regular stress term is independent of the joint geometry. However, for a joint under mechanical loading the regular stress term for most joint geometries and material combinations is zero. In some special cases, the regular stress term is non-zero. It can be determined analytically with one or two arbitrary constants, which have to be determined from the stress analysis of the total joint.

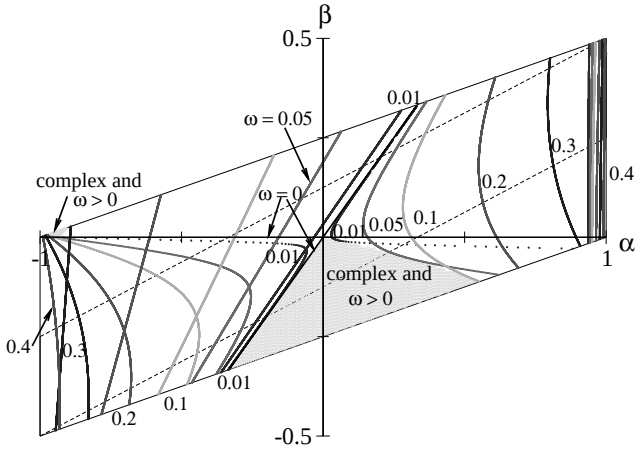

Figure 6.2: Stress exponent distribution in a Dundurs diagram for a joint with $\theta_1 = 45°$.

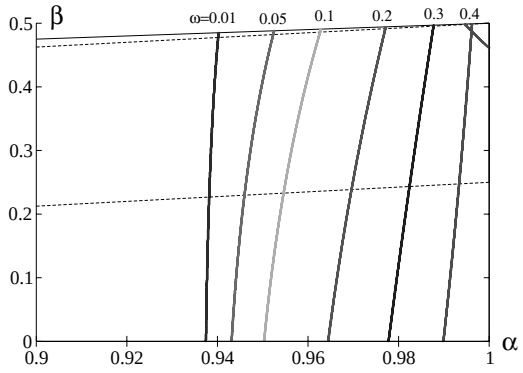

Figure 6.3: Enlargement of Fig. 6.2.

6.3 The Characteristics of the Eigenvalues

From Eqs. (6.1.14) through (6.1.26) it follows that $\lambda_n = 0$ (i.e. $t_n = 1$) always is the first-order solution of $\mathrm{Det}([A]_{8\times 8}) = 0$, which corresponds to the regular stress term (see Section 6.2). For some joints, $\lambda_n = 0$ may be the second or higher-order solution of $\mathrm{Det}([A]_{8\times 8}) = 0$. For a joint with interface corner, it is easy to find the condition when $\lambda_n = 0$ is the second or higher-order solution of $\mathrm{Det}([A]_{8\times 8}) = 0$. The differential of Eq. (6.1.14) at $\lambda_n = 0$ is

$$\begin{aligned} \frac{\mathrm{Det}([A]_{8\times 8})}{d\lambda_n}\Big|_{\lambda_n=0} &= \frac{2048}{(1+\alpha)^4}(\alpha-\beta)^2\beta\sin^3(\theta_1)\{-\pi\cos(\theta_1) \\ &+ \alpha[\pi\cos(\theta_1) - \theta_1\cos(\theta_1) + \sin(\theta_1)]\}. \end{aligned} \tag{6.3.1}$$

From Eq. (6.3.1) it can be seen that if:
(a) $\alpha = \beta$ or
(b) $\beta = 0$ or
(c) $\sin(\theta_1) = 0$, i.e. $\theta_1 = 0$ or π or 2π (no corner) or
(d) $\alpha = \frac{\pi\cos(\theta_1)}{(\pi-\theta_1)\cos(\theta_1)+\sin(\theta_1)}$,

yields $\frac{\mathrm{Det}([A]_{8\times 8})}{d\lambda_n}\Big|_{\lambda_n=0} = 0$, i.e. $\lambda_n = 0$ is the second or higher-order solution of $\mathrm{Det}([A]_{8\times 8}) = 0$. Its physical meaning is that if one of the above conditions (a) - (d) is satisfied, (i) the eigenvalue curve goes through zero in the Dundurs diagram (see the following figures), (ii) for thermal loading, the stress field is described by the type of ln(r) singularity (see Chapter 7), not the type of $r^{-\omega}$ singularity; (iii) for mechanical

loading, the regular stress term is nonzero.

In Figs.6.2 through 6.14 the distributions of the eigenvalues are shown in the Dundurs diagram for some special value of θ_1. From these figures, the range of Dundurs parameters with complex eigenvalues or with more than one singular terms or with no singular term can be seen clearly.

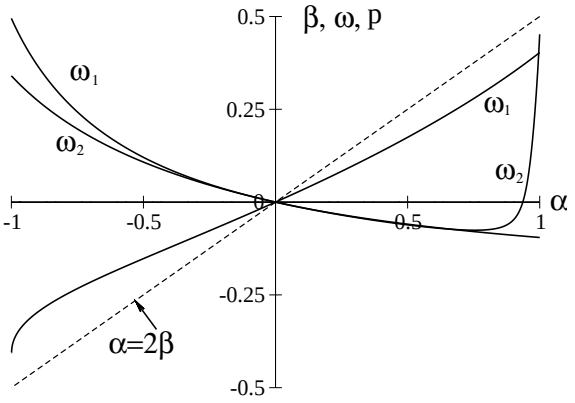

Figure 6.4: Stress exponent distribution for material combinations along the line of $\alpha = 2\beta$ in a joint with $\theta_1 = 45°$.

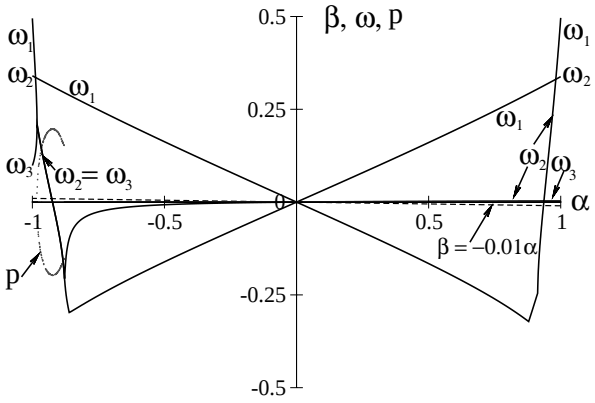

Figure 6.5: Stress exponent distribution for material combinations along the line of $\beta = -0.01\alpha$ in a joint with $\theta_1 = 45°$.

For the joint geometry with $\theta_1 = 45°$, the eigenvalues distribution in the Dundurs diagram is shown in Figs. 6.2 and 6.3. For this joint geometry, the material combinations corresponding to $\beta > 0$ almost always have real singular terms, except for a very small range near $\alpha = -1$. However, for $\beta < 0$ and $\alpha > \beta$, a lot of material combinations have complex singular terms. To illustrate this, another plots of the eigenvalues are shown in Figs. 6.4 and 6.5, in which the eigenvalues are given continuously for the material combinations along the lines of $\alpha = 2\beta$ and of $\beta = -0.01\alpha$. From Figs. 6.2 and 6.5 it can be seen that (a) For $\beta < 0$ there are at least two singular terms. If $\alpha > 0$, one singular term is very weak (see Fig. 6.5). (b) For $\beta > 0$, the most material combinations have only one singular term. (c) For $\alpha < -0.9$ and $\alpha > 0.9$ there may be three singular terms, which may be three real singular terms or one real and two complex singular terms (see Fig. 6.5).
For the joint geometry with $\theta_1 = 60°$, the eigenvalues distribution in the Dundurs diagram is shown in Figs. 6.6 and 6.7. For this joint geometry, the material combinations corresponding to $\beta > 0$ almost always have real singular terms, except for the range with $\alpha < -0.75$. However, for $\beta < 0$ and $\alpha > \beta$, a lot of material combinations have complex singular terms. To illustrate this, another plots of the eigenvalues are shown in Figs. 6.8 and 6.9, in which the eigenvalues are given continuously for the material combinations along the lines of $\alpha = 2\beta$ and of $\beta = -0.01\alpha$. From Figs. 6.6 and 6.9 it can be seen that (a) For $\beta < 0$ there are at least two singular terms. According to $\alpha > 0$, one singular term is very weak (see Fig. 6.9). (b) For $\beta > 0$, the most material

combinations have only one singular term. (c) For $\alpha < -0.8$ and $\alpha > 0.8$ there may be three singular terms, which may be three real singular terms or one real and two complex singular terms (see Fig. 6.9).

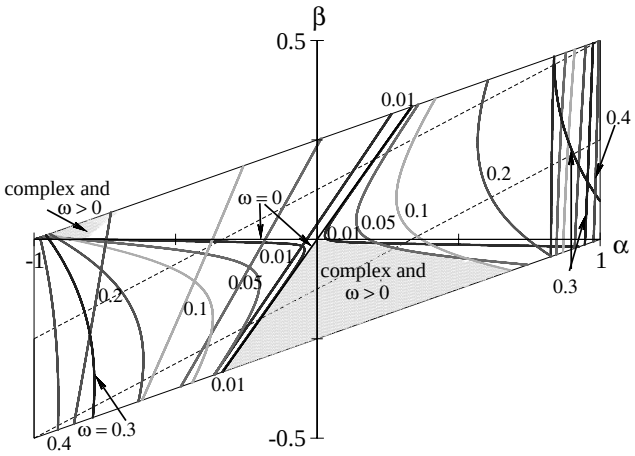

Figure 6.6: Stress exponent distribution in a Dundurs diagram for a joint with $\theta_1 = 60°$.

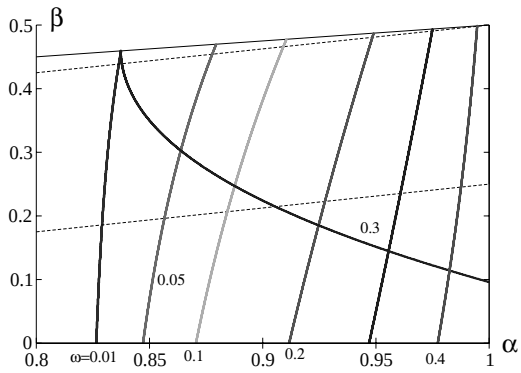

Figure 6.7: Enlargement of Fig. 6.6.

For the joint geometry of $\theta_1 = 90°$, the eigenvalues distribution in the Dundurs diagram is shown in Fig. 6.10. For this joint geometry, the material combinations corresponding to $\alpha > \beta$ for $\beta > 0$, and $\alpha < \beta$ for $\beta < 0$ always have real singular terms. However, the material combinations corresponding to $\alpha < \beta$ for $\beta > 0$, and $\alpha > \beta$ for $\beta < 0$ almost always have complex singular terms. To see this clearly, another plot of the eigenvalues is shown in Fig. 6.11, in which the eigenvalues are given continuously for the material combinations along the line of $\alpha = 2\beta$. From Fig. 6.11 it can be seen that along the line of $\alpha = 2\beta$ there are always two real singular terms. Along another line of $\alpha = -100\beta$, the distribution of the eigenvalues is plotted in Fig. 6.12. It can be seen that the material combinations with a small and large value of α correspond to three real singular terms, those combinations with the values of α lying in-between also have three singular terms, but one pair is complex.
For the joint geometry of $\theta_1 = 135°$, the eigenvalues distribution in the Dundurs diagram is shown in Fig. 6.13. For this joint geometry, the material combinations corresponding to $\beta < 0$ always have a real singular term. For $\beta > 0$ and $\alpha < \beta$, there is a range where the singular terms are complex. To see this clearly, another plot of the eigenvalues is shown in Fig. 6.14, in which the eigenvalues are given continuously for the material combinations along the line of $\alpha = 2\beta$. From Fig. 6.14 it can be seen that along the line of $\alpha = 2\beta$, for $\alpha < 0$ there is only one real singular term, for $\alpha > 0$ there are two singular terms. In fact, for $\beta > 0$ two singular terms always exist.

Conclusions: For a joint with an interface corner, there may be three singular terms, which are three real terms or one pair is complex. For most material combinations there

are two singular terms. The maximum value of the singular stress exponent is 0.5. In comparing to a joint with a free edge, the solution for a joint with interface corner is more complicated.

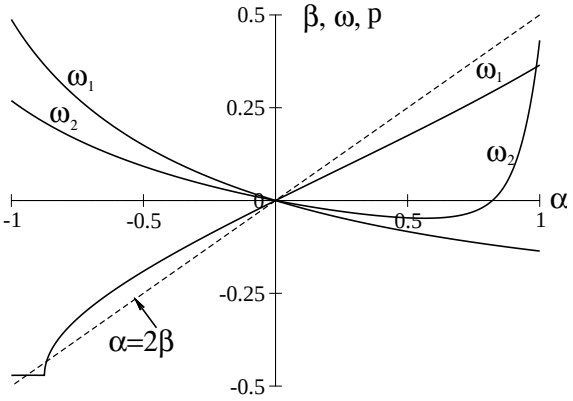

Figure 6.8: Stress exponent distribution for material combinations along the line of $\alpha = 2\beta$ in a joint with $\theta_1 = 60°$.

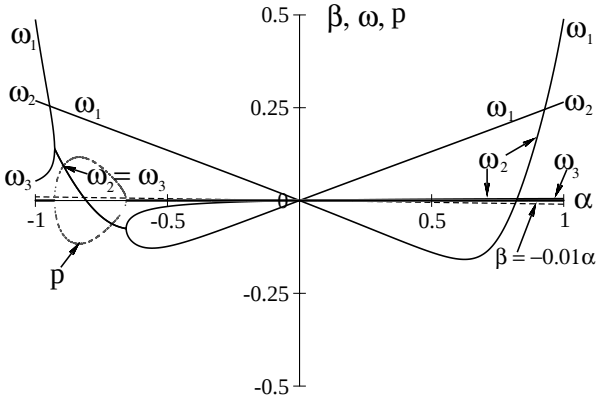

Figure 6.9: Stress exponent distribution for material combinations along the line of $\beta = -0.01\alpha$ in a joint with $\theta_1 = 60°$.

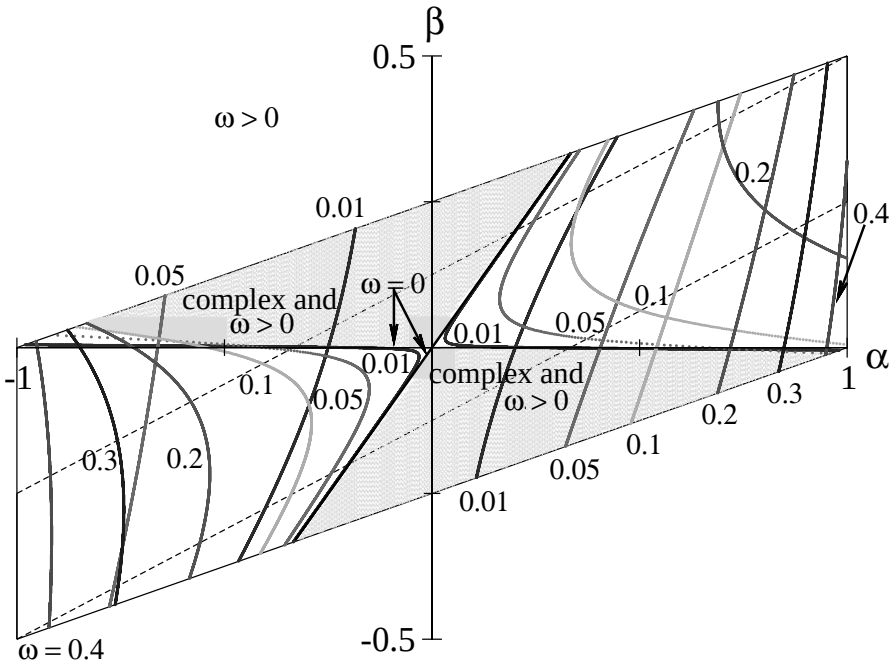

Figure 6.10: Stress exponent distribution in a Dundurs diagram for a joint with $\theta_1 = 90°$.

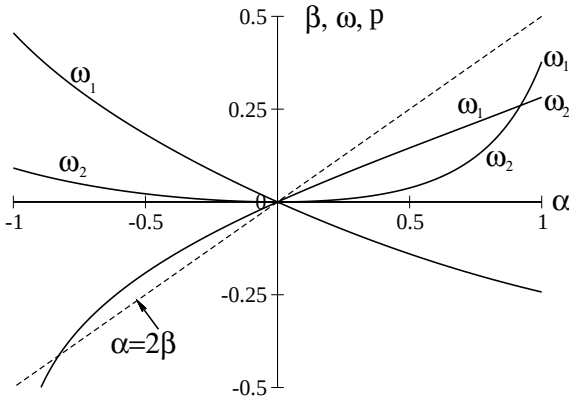

Figure 6.11: Stress exponent distribution for material combinations along the line of $\alpha = 2\beta$ in a joint with $\theta_1 = 90°$.

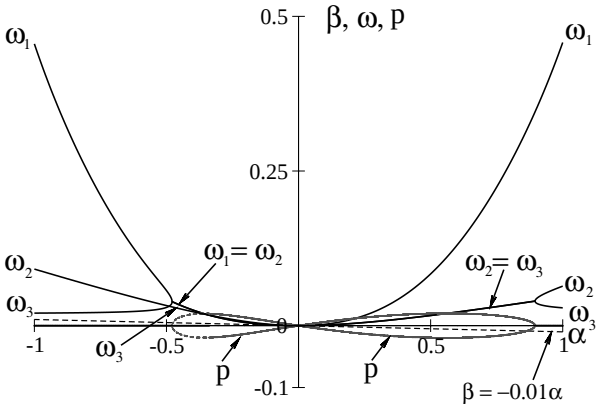

Figure 6.12: Stress exponent distribution for material combinations along the line of $\beta = -0.01\alpha$ in a joint with $\theta_1 = 90°$.

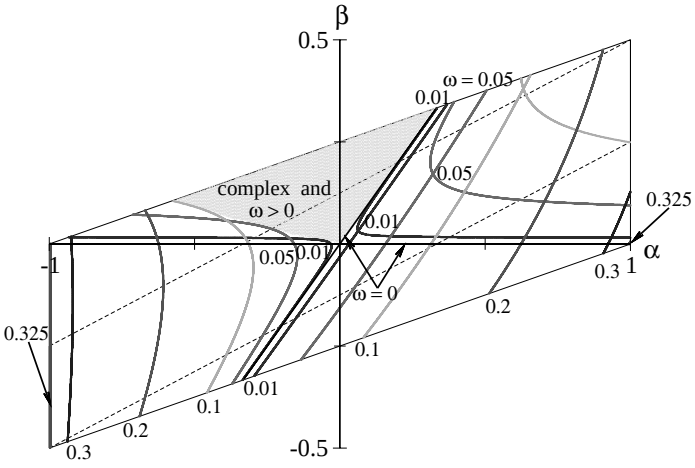

Figure 6.13: Stress exponent distribution in a Dundurs diagram for a joint with $\theta_1 = 135°$.

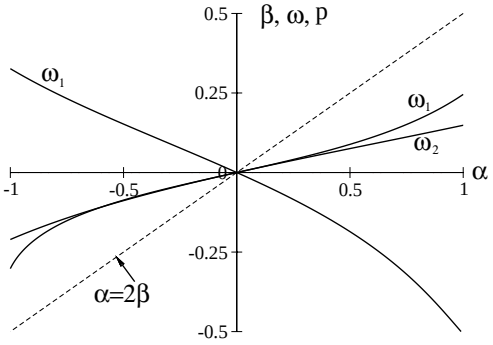

Figure 6.14: Stress exponent distribution for material combinations along the line of $\alpha = 2\beta$ in a joint with $\theta_1 = 135°$.

6.4 The Behavior of the Stress Intensity Factors

It is obvious from Section 6.3 that for most material combinations and joint geometries there are two or three singular terms. Therefore, to find an empirical relationship between the stress intensity factor and the stress exponent (as for a joint with free edge) is almost impossible, even for a special joint geometry (e.g. $\theta_1 = 90°$). Below an example will be presented to show the behaviors of the stress intensity factor for a joint with an interface corner.

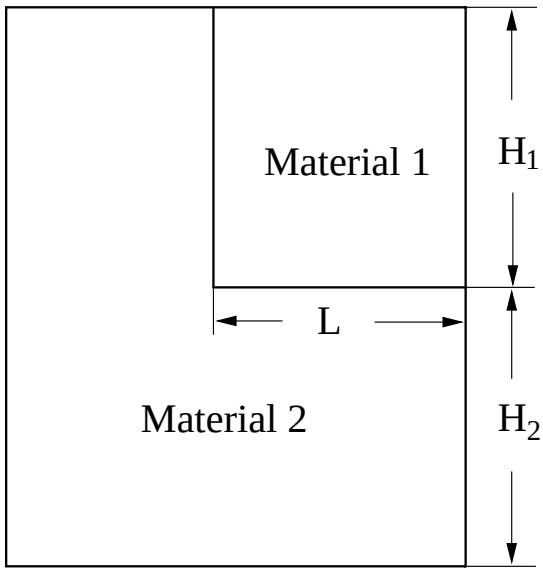

Figure 6.15: A joint with an interface corner and $\theta_1 = 90°$.

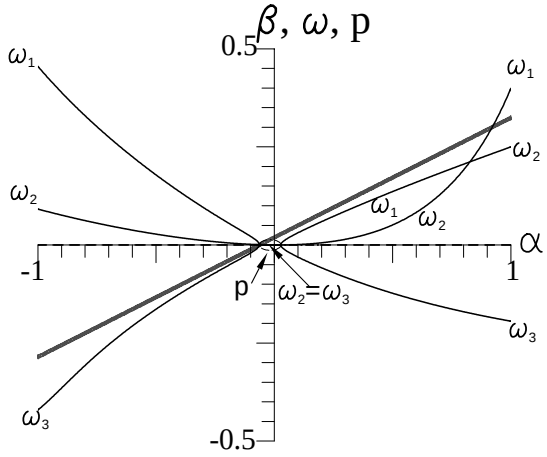

Figure 6.16: Stress exponent in a Dundurs diagram for $\nu_1 = 0.3$, $\nu_2 = 0.26$, and varying E_2/E_1 ($\theta_1 = 90°$).

The joint geometry of the example is $\theta_1 = 90°$ (see Fig. 6.15). The used Poisson's ratios are $\nu_1 = 0.3$ and $\nu_2 = 0.26$, the ratio of the Young's modulus varies. For these given Poisson's ratios and for plane strain the possible material combinations correspond to the line of $\beta = 0.019305 + 0.30502\ \alpha$ in the Dundurs diagram (see Fig. 6.16). In Fig. 6.16 the distribution of the stress exponents is plotted for all possible material combinations. It can be seen that for most cases there are two real singular terms and there is a small range (α is near zero) where the singular terms are complex, but their real part is very small (see Fig. 6.18). The same stress exponents are plotted versus the ratio of Young's modulus in Figs. 6.17, 6.18, and 6.19 to see the relationship between the stress exponents and the material data. It can be seen that if $\alpha = \beta$ or $\beta = 0$, one or more of the stress exponents go through zero (as explained in Section 6.3).
For this example the stress intensity factors are calculated using FEM. The thermal loading is $T = -100^0$C and $\alpha_1 = 18.95 * 10^{-6}, \alpha_2 = 2.5 * 10^{-6}$. The distribution of the regular stress term is shown in Fig. 6.20. Because the definitions of the stress intensity factors for real and complex stress exponents are different (see Chapter 3),

the distribution of the stress intensity factors versus the ratio of the Young's modulus is not continuous. On the other hand, if the stress exponent goes through zero, the type of ln(r) singularity appears (as mentioned in Section 6.3), then the definition of the stress intensity factor is different from that one of the type of $r^{-\omega}$ singularity. Therefore, the distribution of the stress intensity factors is plotted in 4 figures (Figs. 6.21, 6.22, 6.23, and 6.24) for 4 ranges. Comparing Figs. 6.17, 6.18, and 6.19, and Figs. 6.21, 6.22, 6.23, and 6.24 it can be seen that (a) at $\alpha = \beta$ the stress exponents ω_1, ω_2 and ω_3 go through zero (see Fig. 6.18), the value of the regular stress is very large, the factors K_2 and K_3, too. They are, however, finite (see Fig. 6.21), (b) at $\beta = 0$ the stress exponent ω_2 goes through zero (see Fig. 6.19), the corresponding factor K_2 and the regular stress term σ_0 go to infinity, but with different signs (see Fig. 6.22). This is clearly from Eq. (6.2.15) that the regular stress term $\sigma_0 = \sigma_{x0} = \sigma_{y0}$ approaches infinity for $\beta \to 0$. The stresses are finite. Therefore, the stress intensity factor has to approach infinity with an opposite sign. (c) near $\beta = 0$, at the point of ending the complex stress exponents (see Fig. 6.19, it should be noted that at this point $\beta \neq 0$), two stress exponents ($\omega_2 = \omega_3$) are the same, the corresponding K-factors (K_2 and K_3) go to infinity, but with different signs (see Fig. 6.23). Here, the regular stress term is finite. In fact, at this point the stress field should be described by the type of $r^{-\omega}\ln(r)$ singularity (see Chapter 7).

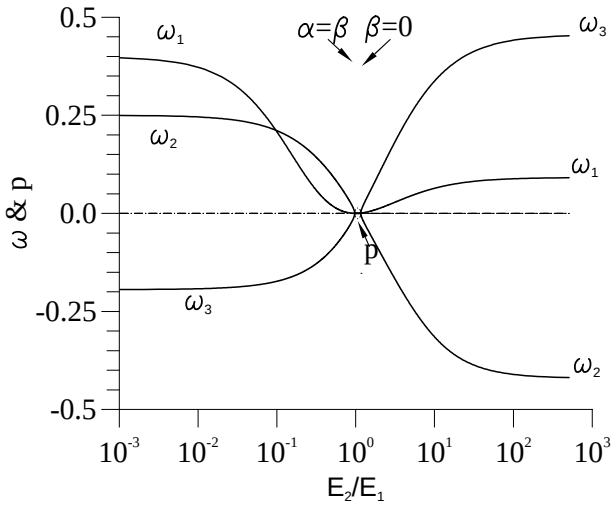

Figure 6.17: Stress exponent ω vs. E_2/E_1 for $\nu_1 = 0.3$ and $\nu_2 = 0.26$ ($\theta_1 = 90°$).

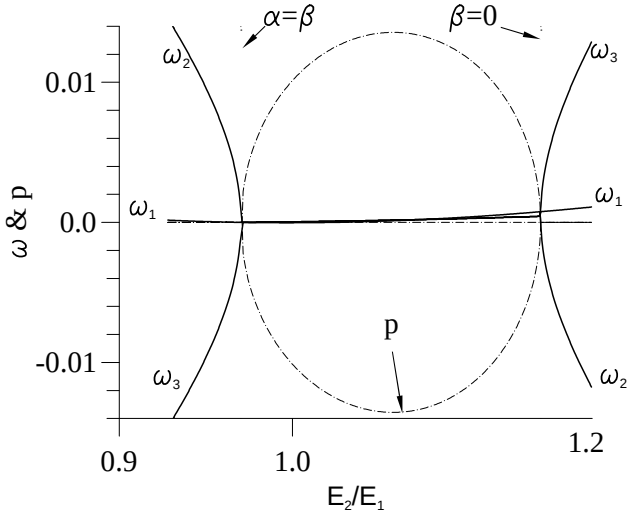

Figure 6.18: Extended range of Fig. 6.17, in which the eigenvalues are complex.

As the distribution of ω_1 is continuous, its K-factor is also continuous (see Fig. 6.25). A plot of $(K_2 + K_3)/\sigma_0$ is shown in Fig. 6.26. It can be seen that (a) at the points of $\alpha = \beta$ and $\beta = 0$, the ratio of $(K_2 + K_3)/\sigma_0$ is always finites. Therefore, the stresses at these points are finite as well. (b) At the point of $\beta = 0$, only one stress exponent (ω_2) goes through zero, the ratio of $(K_2 + K_3)/\sigma_0$ is equal to -1; However, at the point $\alpha = \beta$,

more than one stress exponent $(\omega_1, \omega_2, \omega_3)$ go through zero, the ratio of $(K_2 + K_3)/\sigma_0$ is not equal to -1.

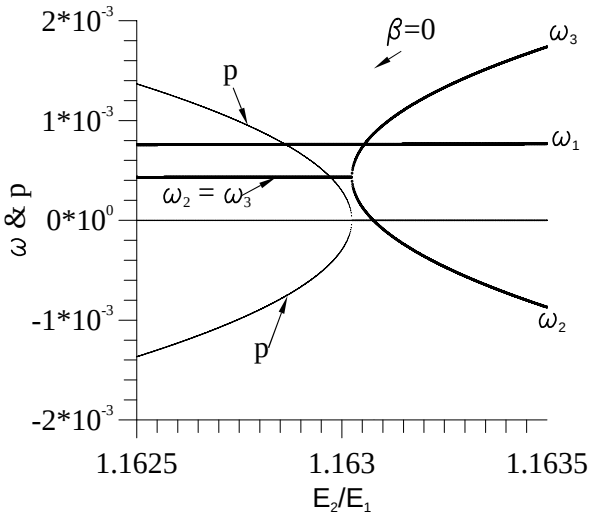

Figure 6.19: Extended range of Fig. 6.17 near $\beta = 0$.

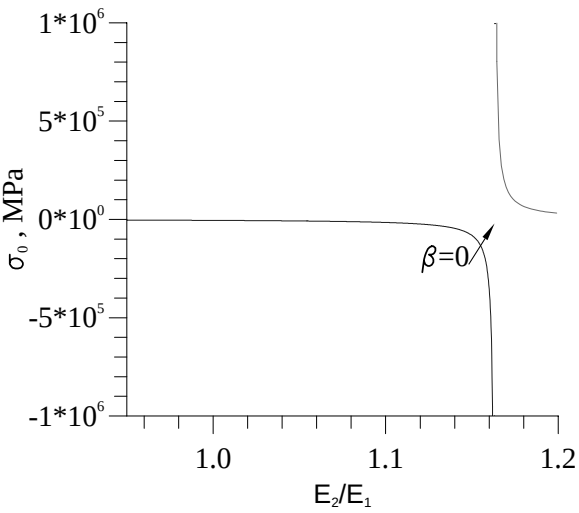

Figure 6.20: Distribution of the regular stress term.

In general, it applies to a joint with an interface corner under thermal loading that if $\beta \to 0$ and ω_i goes through zero, its corresponding K-factor (K_i) and the regular stress term σ_0 go to infinity with a different sign. If ω_i goes towards ω_j and it is the point of ending complex eigenvalues, the corresponding K-factors K_i and K_j go towards infinity with different signs, but the regular stress term is finite.
For the same joint under mechanical loading (see Fig. 6.27, at the upper and the lower surface homogeneous loads (σ_n) are applied), the regular stress term for most cases is zero and for the cases of $\alpha = \beta$ and $\beta = 0$, the regular stress term is finite (see Section 6.2), the distribution of the stress intensity factors is continuous, which is plotted in Fig. 6.28.
We can conclude that for the same joint under different loading the behavior of the stress intensity factor is strongly different.

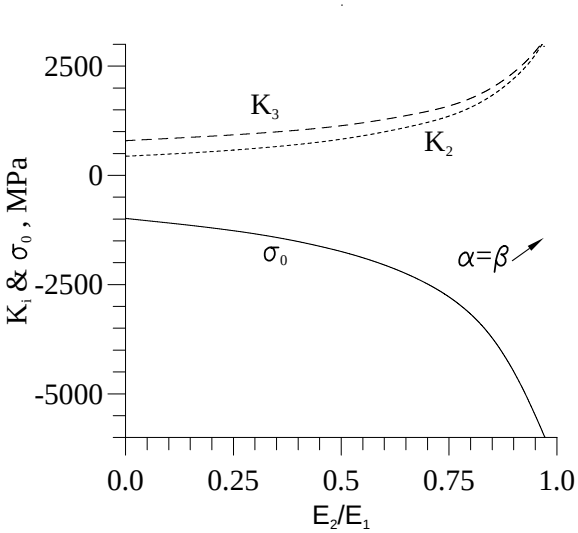

Figure 6.21: Stress intensity factors (K_2, K_3) and the regular stress σ_0 near $\alpha = \beta$, where $\omega_2 = \omega_3 = 0$.

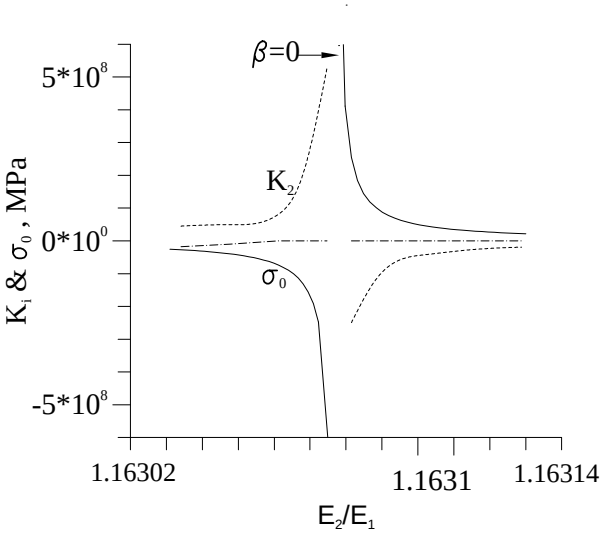

Figure 6.22: Stress intensity factor (K_2) and the regular stress σ_0 very near $\beta = 0$, where $\omega_2 = 0$.

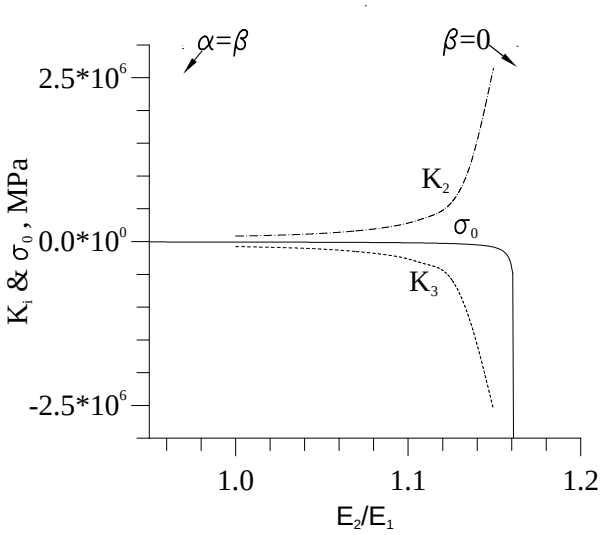

Figure 6.23: Stress intensity factors (K_2, K_3) and the regular stress σ_0 near the point of ending complex stress exponents.

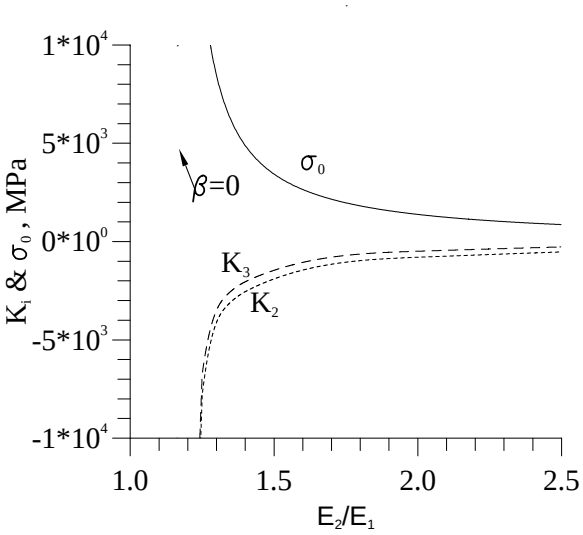

Figure 6.24: Stress intensity factors (K_2, K_3) and the regular stress σ_0 on the right hand side of $\beta = 0$.

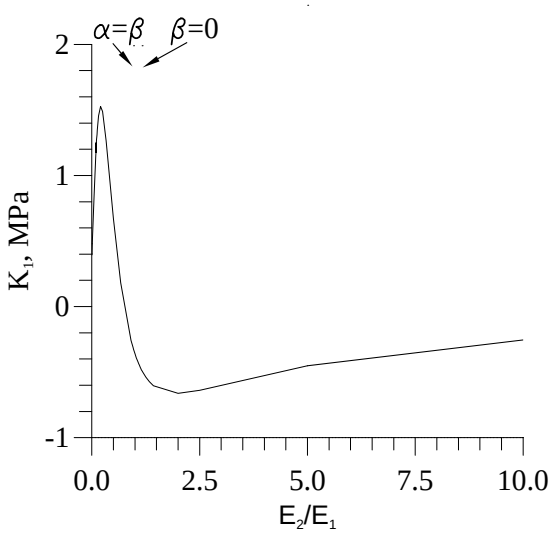

Figure 6.25: The distribution of the stress intensity factor K_1 vs. E_2/E_1.

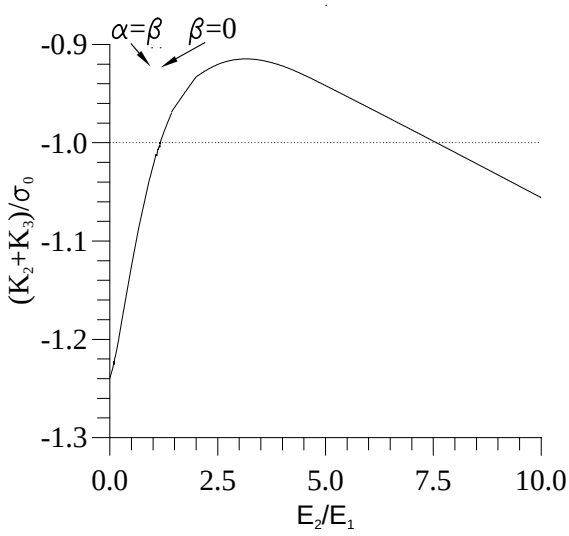

Figure 6.26: The curve of $(K_2 + K_3)/\sigma_0$ vs. E_2/E_1 is continuous.

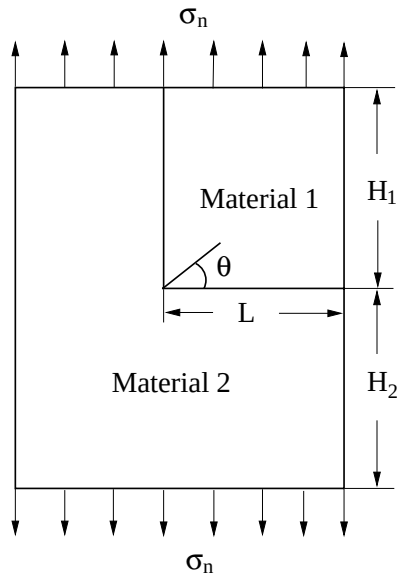

Figure 6.27: Joint with an interface corner under mechanical loading.

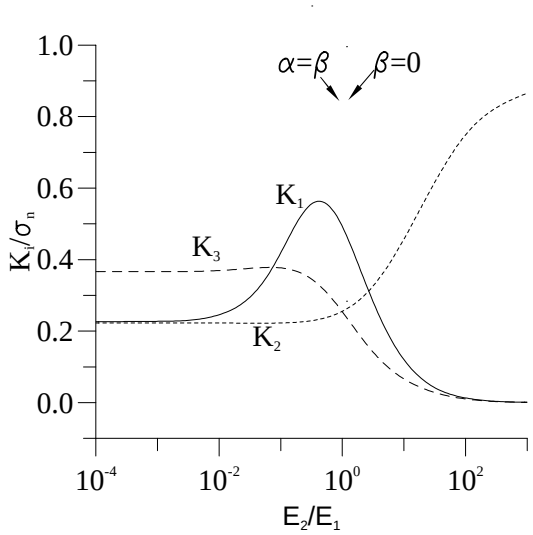

Figure 6.28: Stress intensity factors (K_1, K_2, K_3) for mechanical loading.

6.5 Stress Distribution near the Singular Point

In Section 6.3 it was mentioned that for a joint with an interface corner, in general, there are two or even three singular terms and the singularity is strong, i.e. one of the stress exponents is large. In the following section, an example will be given to show how many terms should be used to describe the singular stress field and whether the so-called dominant singular term is enough to determine the stress field near the singular point.
The geometry, the material data, and the loading for the example are:
$\theta_1 = 90°$, $T = 100°\mathrm{C}$
$E_1 = 100\mathrm{GPa}$, $\nu_1 = 0.05$, $\alpha_1 = 5 * 10^{-6}/\mathrm{K}$
$E_2 = 1.93\mathrm{GPa}$, $\nu_2 = 0.4988$, $\alpha_2 = 10 * 10^{-6}/\mathrm{K}$.
For plane strain the stress exponents are

$$\omega_1 = 0.40104, \quad \omega_2 = 0.05534, \quad \omega_3 = 0.03099, \tag{6.5.1}$$

i.e. there are three real singular terms, but two of them are very weak. The regular stress term for this example is

$$\sigma_{x0} = \sigma_{y0} = 128.4\mathrm{MPa}, \quad \tau_{xy0} = 0 \tag{6.5.2}$$

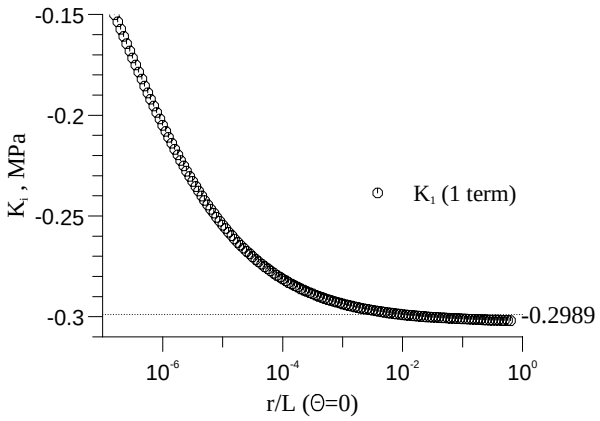

Figure 6.29: The determined stress intensity factor K_1, if the so-called dominant term ω_1 is considered only.

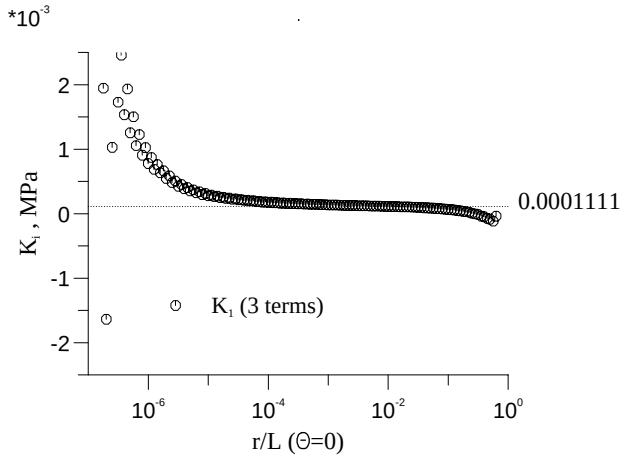

Figure 6.30: The stress intensity factor K_1 determined with all three singular terms.

To determine the stress intensity factors, the method and equations given in Section 3.4 are used. If the dominant singular term (i.e. ω_1) and the regular term are considered only, no constant value of K_1 can be obtained when different numbers of points are used to determine the factor K_1 in the range of $r/L > 10^{-7}$ (see Fig. 6.29, in which the value of r/L means that to obtain its corresponding K-factor, the stresses calculated from FEM at the points with r between 10^{-7} and r/L are used). Therefore, three

singular terms should be used. When three singular and the regular terms are used, a relatively constant value of K-factor can be obtained (see Figs. 6.30 and 6.31). The values at $r/L = 10^{-2}$ are used as the determined K-factors. They are:

$$K_1 = 0.0001111\text{MPa}, \quad K_2 = 156.2\text{MPa}, \quad K_3 = -284\text{MPa}, \tag{6.5.3}$$

where the stress component σ_y along the line $\theta = 0$ is used.
Using the K-factors determined, stresses along different lines (with different values of θ) are calculated from Eq. (3.0.1) analytically, where the angular functions are obtained from the equations given in Section 6.1 (for the coefficients Eqs. (6.1.28) to (6.1.35) are used). A comparison of the stresses obtained from FEM and Eq. (3.0.1) is presented in Figs. 6.32 and 6.33 for $\theta = 90°$ and $\theta = -90°$. Along the line of $\theta = 90°$, it is not plotted in the figure as the stress component σ_y is not continuous. From the figures it can be seen that using three singular and one regular terms, the analytical equation may describe the stresses very well in the range of $r/L < 10^{-2}$. However, using the so-called dominant singular term only, the analytical equation cannot describe the stresses near the singular point well, even in the range of $r/L < 10^{-4}$.

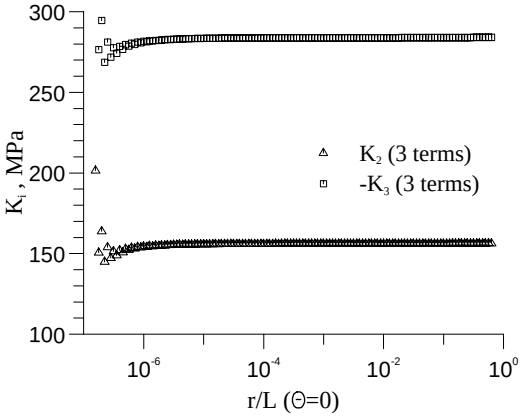

Figure 6.31: The stress intensity factors K_2, K_3 determined with all three singular terms.

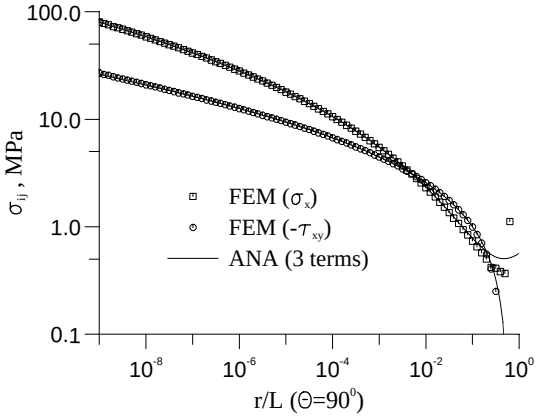

Figure 6.32: Comparison of the stresses calculated from FEM and Eq. (3.0.1) along the line of $\theta = 90°$.

6.6 The Interface Condition Effect on the Singular Stress Field

To see the effect of interface conditions on the stresses near the singular point, another case is considered, in which the joint also has $|\theta_1| + |\theta_2| = 360°$, but one interface ($\theta_1 = 90°$) is stress free (see Fig. 6.34). This is the case of a joint with a delamination crack. The material data and loading are the same as those used in Section 6.5. From the equations given in Section 3.1 (for $\theta_1 = 90°$, $\theta_2 = -270°$), the corresponding stress

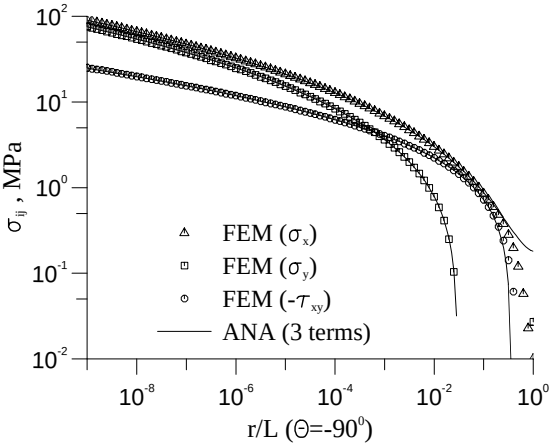

Figure 6.33: Comparison of the stresses calculated from FEM and Eq. (3.0.1) along the line of $\theta = -90°$.

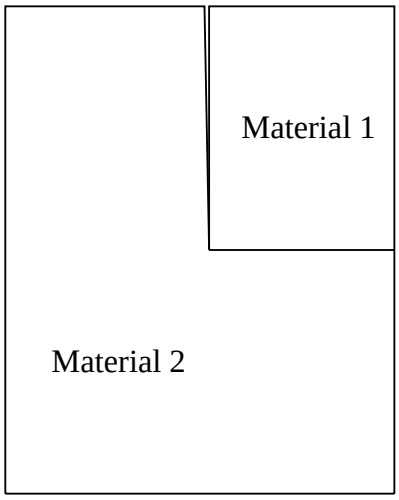

Figure 6.34: A joint with a free edge and $\theta_1 = 90°, \theta_2 = -270°$.

singular exponents can be obtained. For plane strain they are:

$$\omega_1 = 0.69986, \quad \omega_2 = 0.56839, \quad \omega_3 = 0.18800, \tag{6.6.1}$$

i.e. there are three real singular terms, which are much stronger than those of a joint with an interface corner. The regular stress term for this case is

$$\sigma_y = 2.5174 \text{ MPa}, \quad \sigma_x = \tau_{xy} = 0 \tag{6.6.2}$$

The distributions of the stress intensity factors determined using one, two or three singular terms plus the regular term are shown in Figs. 6.35, 6.36, and 6.37. It can be seen that for this case with only one so-called dominant singular term one range with a constant value of the K-factor exists. In the following sections, the values at $r/L = 10^{-2}$ are used as the determined K-factors. They are:

$$K_1 = -0.05452 \text{ MPa} \tag{6.6.3}$$

if only one dominant singular and the regular stress term are used,

$$K_1 = -0.07761 \text{ MPa}, \quad K_2 = 0.17541 \text{ MPa} \tag{6.6.4}$$

when two singular and the regular stress terms are considered,

$$K_1 = -0.08022 \text{ MPa}, \quad K_2 = 0.1993 \text{ MPa}, \quad K_3 = -1.3422 \text{ MPa}, \tag{6.6.5}$$

for including three singular and the regular stress terms, where the stress component σ_y along the line $\theta = 0$ is used.

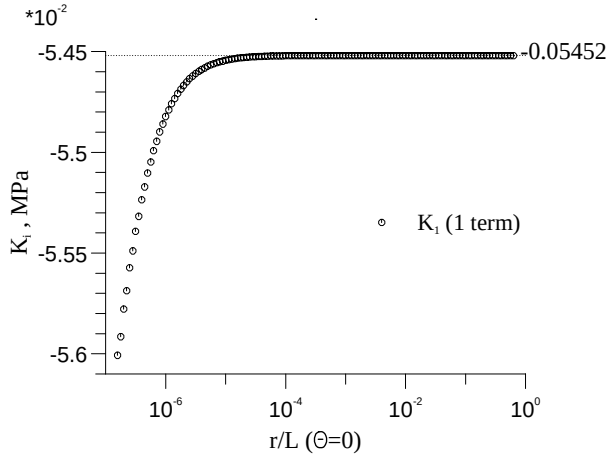

Figure 6.35: The stress intensity factor K_1 determined with the so-called dominant term ω_1 only for a joint with a delamination crack.

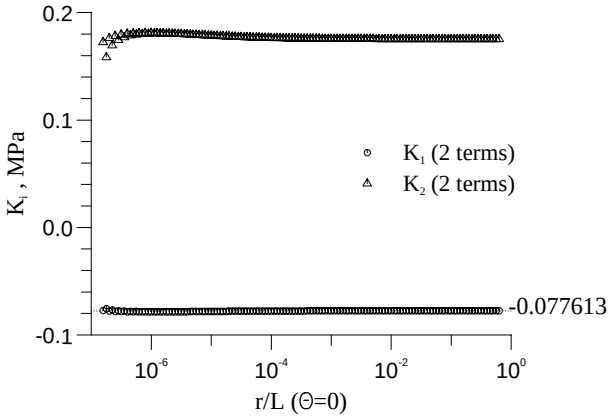

Figure 6.36: The stress intensity factors K_1, K_2 determined with two singular terms for a joint with a delamination crack.

Using the K-factors determined, stresses along different lines are calculated analytically from Eq. (3.0.1), where the angular functions are obtained from the equations given in Chapter 3. A comparison of the stresses obtained from FEM and Eq. (3.0.1) with one, two or three singular terms plus the regular stress term is presented in Figs. 6.38 through 6.43 for $\theta = 0°$, $\theta = 90°$, and $\theta = -90°$. From the figures it can be seen that using three singular and one regular terms, the analytical equation may describe the stresses very well in the range of $r/L < 10^{-2}$. If two singular terms are used, the analytical equation may describe the stresses well only in the range of $r/L < 10^{-4}$. However, when using the so-called dominant singular term only, the analytical equation may describe only some stress components well, even in the range of $r/L < 10^{-4}$.
To sum up, it may be states that (a) for joints with the same material combination, loading, and geometry, but with different interface conditions, the joint with a delamination crack (i.e. the interface being stress free) has much stronger singular stress exponents than a joint with an interface corner (interface being perfectly joined), it is even larger than 0.5. (b) To describe the stress field near the singular point in a larger range, all singular terms plus the regular stress term should be used. Use of the so-called dominant singular term only is not sufficient to describe the singular stress field in the range of $r/L > 10^{-7}$.

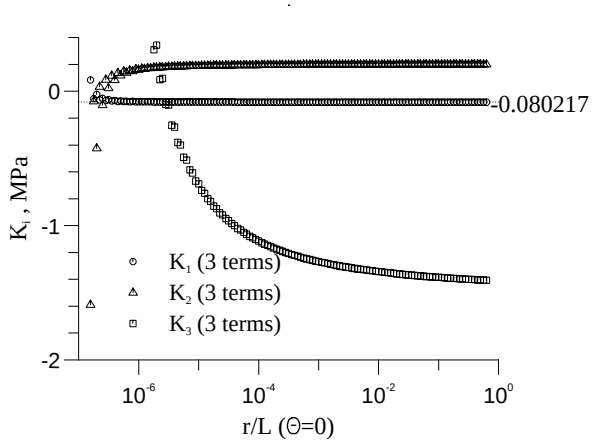

Figure 6.37: The stress intensity factors K_1, K_2, K_3 determined with all three singular terms.

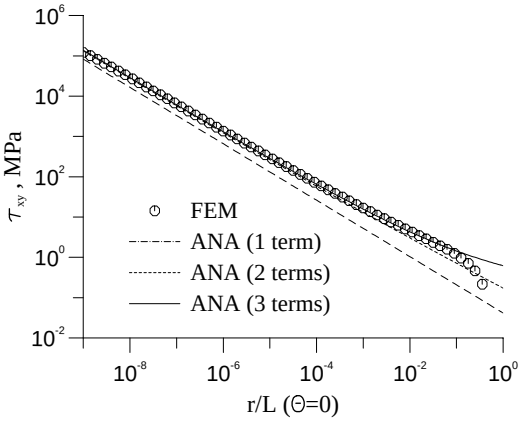

Figure 6.38: Comparison of the stresses calculated from FEM and Eq. (3.0.1) with one or two or three singular terms along the line of $\theta = 0^\circ$ for stress component τ_{xy}.

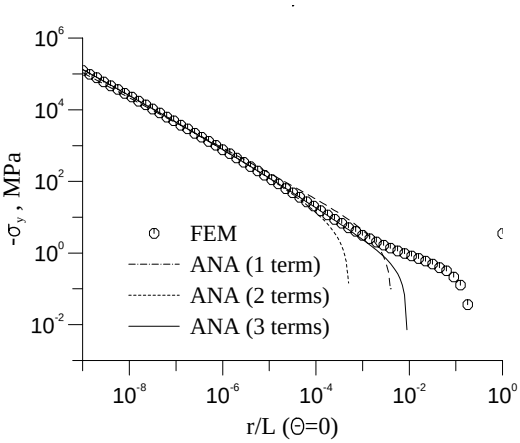

Figure 6.39: Comparison of the stresses calculated from FEM and Eq. (3.0.1) with one or two or three singular terms along the line of $\theta = 0^\circ$ for stress component σ_y.

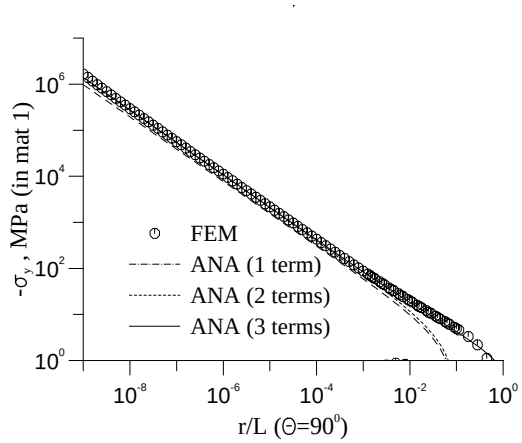

Figure 6.40: Comparison of the stresses calculated from FEM and Eq. (3.0.1) with one or two or three singular terms along the line of $\theta = 90^\circ$ for stress component σ_y.

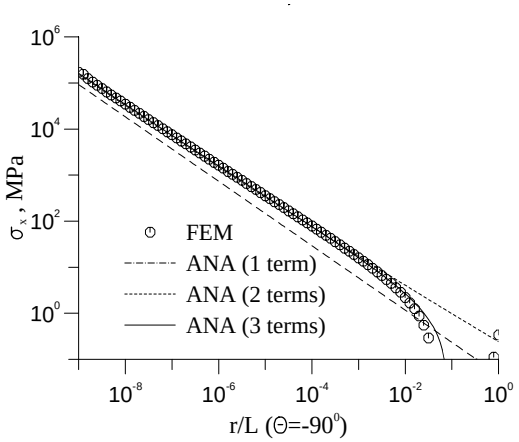

Figure 6.41: Comparison of the stresses calculated from FEM and Eq. (3.0.1) with one or two or three singular terms along the line of $\theta = -90°$ for stress component σ_x.

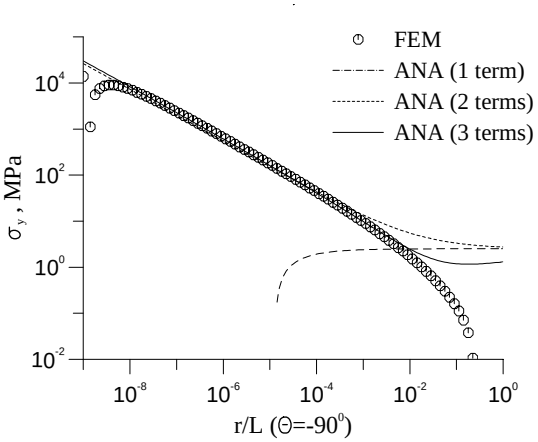

Figure 6.42: Comparison of the stresses calculated from FEM and the Eq. (3.0.1) with one or two or three singular terms, along the line of $\theta = -90°$ for stress component σ_y.

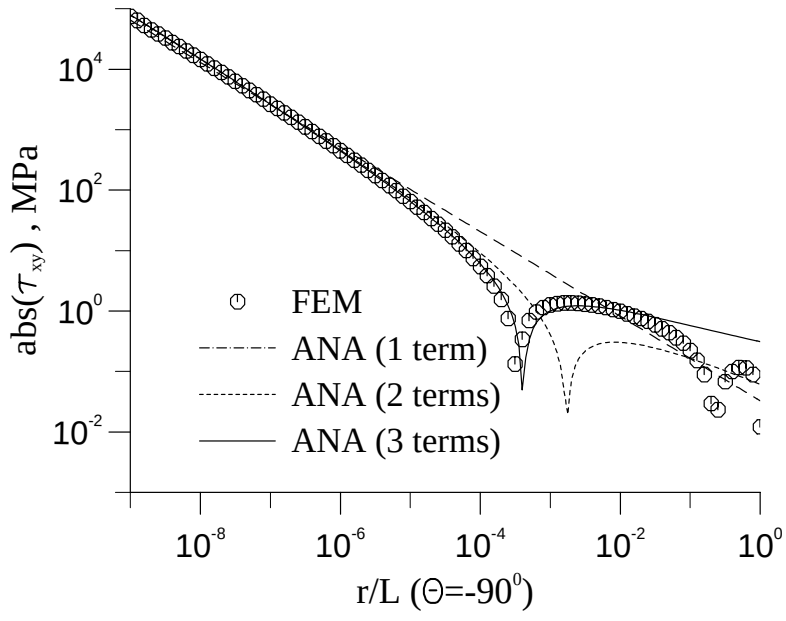

Figure 6.43: Comparison of the stresses calculated from FEM and the Eq. (3.0.1) with one or two or three singular terms, along the line of $\theta = -90°$ for stress component τ_{xy}.

Chapter 7

Logarithmic Stress Singularities in a Joint under Thermal Loading

In Chapters 3 through 6 the type of $r^{-\omega}$ singularities have been studied. However, there is also another type of stress singularity. Bogy and Dempsey [see [109], [35], [111], [46]) described the conditions of a two dissimilar materials joint having the type of ln(r) and $r^{-\omega}$ln(r) singularity. Bogy (see [109]) studied the type of ln(r) singularity in a quarter-planes joint under edge tractions. Dempsey (see [121]) examined special cases with an $r^{-\omega}$ln(r) singularity. The asymptotical description of the stress distribution for the type of ln(r) and $r^{-\omega}$ln(r) singularity are investigated in [122, 123] for a two dissimilar materials joint under thermal loading. Further, in Section 7.1 the type of ln(r) stress singularity and in Section 7.2 the type of $r^{-\omega}$ln(r) stress singularity shall be treated by the Mellin transform method for a joint with free edges under thermal loading. For an arbitrary joint angular functions are given. In a special case, i.e. for a quarter-planes joint, angular functions are presented even in an explicit form. The angular functions for a joint under thermal loading are different from those shown by Bogy for a quarter planes joint under edge tractions. As example, the unknown factor K used to describe the stress in a finite joint is determined numerically.

Although the type of ln(r) or $r^{-\omega}$ln(r) singularity is on rare occasions in a real joint, the intention of this study is to complete the solution of the singularity problems. On the other hand, the most important application of the solution for the type of ln(r) singularity is that it can be used to describe approximately the singular stress field for material combinations with very small stress exponent ω of $r^{-\omega}$ singularity, which will be illustrated by the examples given in Section 7.3. For joints under thermal loading this is useful, because for material combinations with very small stress exponents ω ($\omega \to 0$) the solution based on the type of $r^{-\omega}$ singularity is numerically not stable.
The solution for the type of $r^{-\omega}$ln(r) singularity can be used to describe approximately the singular stress field for material combinations with two almost the same stress exponents ω (i.e. $\omega_i = \omega_j = \omega$) of $r^{-\omega}$ singularity.
For a joint with an interface corner or a joint with edge tractions, the method used in

the following sections is the same. Only the boundary conditions are different.

7.1 Asymptotic Description of ln(r) Singular Stress Field

In this section the type of ln(r) singularity is studied. The asymptotic description of the singular stress field will be presented.

7.1.1 Determination of Angular Functions and Asymptotic Description of the Stresses

In case of a semi-infinite joint with the temperature change

$$T = \begin{cases} T_0 & \text{for r} \leq R_0 \\ 0 & \text{for r} > R_0, \end{cases}$$

the following relations for stresses in the Mellin domain were given in Section 3.2:

$$\hat{\sigma}_{ijk}(s,\theta) = \frac{\mathcal{P}_{\text{ijk}}(\text{s},\theta)\text{g}_{\text{ij}}(\text{s})}{\parallel X \parallel (s+2)} \tag{7.1.1}$$

with

$$\begin{aligned} \mathcal{P}_{\text{ijk}}(\text{s},\theta) \;=\; & \Big\{A_{1ijk}(s)cos(s\theta) + A_{2ijk}(s)sin(s\theta) + A_{3ijk}(s)cos((s+2)\theta) \\ & + A_{4ijk}(s)sin((s+2)\theta) + A_{5ijk}(s)\Big\} \end{aligned} \tag{7.1.2}$$

where all quantities and their coefficients are given in Section 3.2 and k=1 for $\theta > 0$ and k=2 for $\theta < 0$. Our aim is to calculate the stresses in a polar coordinate system, i.e. $\sigma_{ij}(r,\theta)$, which is the reversal transform of $\hat{\sigma}_{ij}(s,\theta)$. For the calculation of the reversal of $\hat{\sigma}_{ij}(s,\theta)$ we need the poles of $\hat{\sigma}_{ij}(s,\theta)$, which are defined as follows: If $\lim_{s\to s_n} \hat{\sigma}_{ij}(s,\theta) \to \infty$, s_n is the pole of $\hat{\sigma}_{ij}(s,\theta)$. From Eq. (7.1.1) it can be seen that the possible poles of $\hat{\sigma}_{ij}(s,\theta)$ are the solutions of $\parallel X \parallel = 0$ and s=-2.
According to the residual principle, the stresses in a polar coordinate system can be obtained from (see Eq. (3.2.47))

$$\sigma_{ijk}(r,\theta) = \sum_{s_n<\gamma} \frac{1}{(M-1)!} \lim_{s\to s_n} \frac{d^{(M-1)}}{ds^{(M-1)}} \{(s-s_n)^M \frac{\mathcal{P}_{\text{ijk}}(\text{s},\theta)\text{g}_{\text{ij}}(\text{s})}{\parallel X \parallel (s+2)} \bar{r}^{-(s+2)}\} \tag{7.1.3}$$

where s_n is the M-th order pole of $\hat{\sigma}_{ij}(s,\theta)$. In this section, we only consider the case with M=2 and $s_n = -2$, i.e. s=-2 is the second order pole of $\hat{\sigma}_{ij}(s,\theta)$, which corresponds to the type of ln(r) singularity. From Eq. (7.1.3) and the equations given in Section 3.2 for $\mathcal{P}_{\text{ij}}(\text{s},\theta)$ and $g_{ij}(s)$, we know that this is the case with $\parallel X \parallel|_{s=-2} = \frac{d\parallel X\parallel}{ds}|_{s=-2}$=0, $\frac{d^2\parallel X\parallel}{ds^2}|_{s=-2} \neq 0$ and $\mathcal{P}_{\text{ij}}(\text{s},\theta)|_{\text{s}=-2} = 0$, $\frac{\partial \mathcal{P}_{\text{ij}}(\text{s},\theta)}{\partial s}|_{s=-2} \neq 0$, because for s=-2 there always is $g_{ij}(s) \neq 0$ for $T_0 \neq 0$. For the case with M > 2, the calculation of stress

reversal $\hat{\sigma}_{ij}(s,\theta)$ is more complicated, but the procedure is similar to that one given here for M=2. For $M > 2$, the stress field has the type of $\ln^N(r)$ (where N=M-1 >1) singularity.
For M=2 and s=-2, the stresses in polar coordinates can be calculated from

$$\begin{aligned}
\sigma_{ij}(r,\theta) &= \lim_{s\to -2}\frac{d}{ds}\{(s+2)^2\bar{r}^{-(s+2)}\frac{\mathcal{P}_{\rm ij}({\rm s},\theta){\rm g_{ij}(s)}}{\parallel X \parallel (s+2)}\} \\
&= -g_{ij}(s)\Big|_{s=-2} ln(\bar{r}) \lim_{s\to -2}\frac{\mathcal{P}_{\rm ij}({\rm s},\theta)({\rm s}+2)}{\parallel X \parallel} \\
&+ g_{ij}(s)\Big|_{s=-2} \lim_{s\to -2}\frac{\frac{\partial \mathcal{P}_{\rm ij}({\rm s},\theta)}{\partial s}(s+2)\parallel X \parallel + \parallel X \parallel \mathcal{P}_{\rm ij}({\rm s},\theta) - \frac{{\rm d}\parallel {\rm X}\parallel}{{\rm ds}}({\rm s}+2)\mathcal{P}_{\rm ij}({\rm s},\theta)}{\parallel X \parallel^2} \\
&+ \frac{dg_{ij}(s)}{ds}\Big|_{s=-2} \lim_{s\to -2}\frac{\mathcal{P}_{\rm ij}({\rm s},\theta)({\rm s}+2)}{\parallel X \parallel}. \qquad (7.1.4)
\end{aligned}$$

In the following sections, the definitions of

$$\begin{aligned}
f_{ij}(\theta) &= \frac{1}{2}\lim_{s\to -2}\frac{\mathcal{P}_{\rm ij}({\rm s},\theta)({\rm s}+2)}{\parallel X \parallel} \\
&= \frac{\frac{\partial \mathcal{P}_{\rm ij}({\rm s},\theta)}{\partial s}}{\frac{d^2\parallel X \parallel}{ds^2}}\Big|_{s=-2}, \qquad (7.1.5)
\end{aligned}$$

$$\begin{aligned}
t_{ij}(\theta) &= \lim_{s\to -2}\frac{\frac{\partial \mathcal{P}_{\rm ij}({\rm s},\theta)}{\partial s}(s+2)\parallel X \parallel + \parallel X \parallel \mathcal{P}_{\rm ij}({\rm s},\theta) - \frac{{\rm d}\parallel {\rm X}\parallel}{{\rm ds}}({\rm s}+2)\mathcal{P}_{\rm ij}({\rm s},\theta)}{\parallel X \parallel^2} \\
&= \frac{\frac{d^2\parallel X \parallel}{ds^2}\frac{\partial^2 \mathcal{P}_{\rm ij}({\rm s},\theta)}{\partial s^2} - \frac{2}{3}\frac{d^3\parallel X \parallel}{ds^3}\frac{\partial \mathcal{P}_{\rm ij}({\rm s},\theta)}{\partial s}}{\left(\frac{d^2\parallel X \parallel}{ds^2}\right)^2}\Big|_{s=-2} \qquad (7.1.6)
\end{aligned}$$

and

$$l_{ij} = g_{ij}(s)\Big|_{s=-2} \qquad (7.1.7)$$

will be used, where $l_{rr} = -\frac{T_0}{4}$, $l_{\theta\theta} = \frac{T_0}{4}$ and $l_{r\theta} = -\frac{T_0}{2}$. From Eq. (3.2.45) we have

$$\frac{dg_{ij}(s)}{ds}\Big|_{s=-2} = \frac{1}{2}l_{ij}(K + I_{ij}) \qquad (7.1.8)$$

with $K = 2ln(\bar{R}_0)$ and $I_{rr} = 1, I_{\theta\theta} = -1, I_{r\theta} = -1$. Finally, the stresses near the singular point in polar coordinates can be rewritten as

$$\sigma_{ij}(r,\theta) = l_{ij}\{-2ln(r/L)f_{ij}(\theta) + t_{ij}(\theta) + (K + I_{ij})f_{ij}(\theta)\}. \qquad (7.1.9)$$

In Eq. (7.1.9) K is dimensionless, $f_{ij}(\theta)$ and $t_{ij}(\theta)$ have the unit of $E_k \times \alpha_k$, and l_{ij} has the unit of temperature. The quantities $f_{ij}(\theta)$ and $t_{ij}(\theta)$ can be calculated analytically from Eqs. (7.1.5) and (7.1.6), because $\mathcal{P}_{\rm ij}({\rm s},\theta)$ and $\parallel X \parallel$ are known from Section 3.2. They depend on the material parameters $(E_1, E_2, \nu_1, \nu_2, \alpha_1, \alpha_2)$ and the angles θ_1 and θ_2. l_{ij} is proportional to the temperature change. For a semi-infinite joint the factor K is known, because R_0 is well known (see Section 3.2).
Generally, the quantities $f_{ijk}(\theta)$ and $t_{ijk}(\theta)$ (k=1,2 for material 1 and 2) have the following form:

$$f_{ijk}(\theta) = F_{1ijk}cos(2\theta) + F_{2ijk}sin(2\theta) + F_{3ijk} + F_{4ijk}\theta \tag{7.1.10}$$

$$\begin{aligned} t_{ijk}(\theta) &= T_{1ijk}cos(2\theta) + T_{2ijk}sin(2\theta) + T_{3ijk} \\ &\quad + T_{4ijk}cos(2\theta)\theta + T_{5ijk}sin(2\theta)\theta + T_{6ijk}\theta. \end{aligned} \tag{7.1.11}$$

The coefficients F_{lijk} and T_{nijk} with $ij = rr, \theta\theta, r\theta$; l=1,2,3,4, and n=1,2,3,4,5,6, can be calculated analytically by inserting Eq. (3.2.45) into Eqs. (7.1.5) and (7.1.6). For an arbitrary joint geometry with θ_1, θ_2, the relations between the coefficients F_{lijk}, T_{nijk}, the material properties $(E_1, E_2, \nu_1, \nu_2, \alpha_1, \alpha_2)$, and the geometry θ_1, θ_2 have a very long form. However, for a quarter-planes joint (i.e., $\theta_1 = -\theta_2 = 90°$) they are simple and given below in an explicit form by using the REDUCE code. For the coefficients F_{lijk} it holds:

$$F_{4ijk} = 0 \tag{7.1.12}$$

$$F_{Lij1} = F_{Lij2} \quad \text{for L=1,2,3} \tag{7.1.13}$$

$$F_{1rr1} = -F_{3rr1} = F_{1\theta\theta1} = F_{3\theta\theta1} = -2F_{2r\theta1} = \frac{16Q\alpha}{Z} \tag{7.1.14}$$

$$F_{Lr\theta k} = 0, \quad \text{for L=1,3} \tag{7.1.15}$$

$$F_{2IJk} = 0, \quad \text{for IJ=}rr, \theta\theta. \tag{7.1.16}$$

For the coefficients T_{nijk} there is:

$$T_{1rr1} = -\frac{16Q}{Z^2}\left(Z(\alpha + 2\beta - \theta_1^2) + 32(\alpha - \beta)[(3\alpha - 2\beta)(\alpha - 2\beta) + \theta_1^2]\right) \tag{7.1.17}$$

$$T_{1rr2} = -\frac{16Q}{Z^2}\left(Z(\alpha + 2\beta + \theta_1^2) + 32(\alpha - \beta)[(3\alpha - 2\beta)(\alpha - 2\beta) + \theta_1^2]\right) \tag{7.1.18}$$

$$T_{2rr1} = -\frac{16Q}{Z}(\alpha - 1)\theta_1 \tag{7.1.19}$$

$$T_{2rr2} = \frac{16Q}{Z}(\alpha + 1)\theta_1 \tag{7.1.20}$$

$$T_{4IJk} = 0 \quad \text{for IJ=}rr, \theta\theta \tag{7.1.21}$$

$$T_{5rr1} = T_{5rr2} = \frac{32Q}{Z}\alpha \tag{7.1.22}$$

$$T_{3rr1} = \frac{16Q}{Z^2}\left(Z[(2\alpha+1)\theta_1^2 - (\alpha - 2\beta)] + 32(\alpha-\beta)[(3\alpha-2\beta)(\alpha-2\beta) + \theta_1^2]\right) \tag{7.1.23}$$

$$T_{3rr2} = \frac{16Q}{Z^2}\left(Z[(2\alpha-1)\theta_1^2 - (\alpha - 2\beta)] + 32(\alpha-\beta)[(3\alpha-2\beta)(\alpha-2\beta) + \theta_1^2]\right) \tag{7.1.24}$$

$$T_{6rr1} = -\frac{32Q}{Z}(\alpha+1)\theta_1 \tag{7.1.25}$$

$$T_{6rr2} = \frac{32Q}{Z}(\alpha-1)\theta_1 \tag{7.1.26}$$

$$T_{1\theta\theta1} = \frac{16Q}{Z^2}\left(Z(\alpha - 2\beta + \theta_1^2) - 32(\alpha-\beta)[(3\alpha-2\beta)(\alpha-2\beta) + \theta_1^2]\right) \tag{7.1.27}$$

$$T_{1\theta\theta2} = \frac{16Q}{Z^2}\left(Z(\alpha - 2\beta - \theta_1^2) - 32(\alpha-\beta)[(3\alpha-2\beta)(\alpha-2\beta) + \theta_1^2]\right) \tag{7.1.28}$$

$$T_{N\theta\theta k} = T_{Nrrk} \quad \text{for N=2,5} \tag{7.1.29}$$

$$T_{N\theta\theta k} = -T_{Nrrk} \quad \text{for N=3,6} \tag{7.1.30}$$

$$T_{1r\theta1} = -T_{6rr2}/4 \tag{7.1.31}$$

$$T_{1r\theta2} = T_{2rr2}/2 \tag{7.1.32}$$

$$T_{2r\theta k} = -T_{1\theta\theta k}/2 \tag{7.1.33}$$

$$T_{4r\theta k} = T_{5rrk}/2 \tag{7.1.34}$$

$$T_{3r\theta1} = T_{2rr2}/2 \tag{7.1.35}$$

$$T_{3r\theta2} = T_{2rr1}/2 \tag{7.1.36}$$

$$T_{Nr\theta k} = 0 \quad \text{for N=5,6} \tag{7.1.37}$$

with

$$Z = 8(-2\alpha\beta\theta_1^2 + \theta_1^2 + 5\alpha^2 - 10\alpha\beta + 4\beta^2) \tag{7.1.38}$$

$$Q = \frac{\Delta\alpha}{\frac{1}{E_1^{'}} + \frac{1}{E_2^{'}}} \tag{7.1.39}$$

$$E_k^{'} = \begin{cases} E_k & \text{for plane stress} \\ \dfrac{E_k}{1-\nu_k^2} & \text{for plane strain} \end{cases},$$

where α, β are the Dundurs parameters.

For a quarter-planes joint transforming $f_{ij}l_{ij}$ from polar coordinates to Cartesian coordinates yields

$$\begin{aligned} f_x l_x &= 0 \\ f_y l_y &= \frac{T_0}{2} F_{1\theta\theta 1} = \frac{T_0}{2} F_{1\theta\theta 2} \\ f_{xy} l_{xy} &= 0. \end{aligned} \tag{7.1.40}$$

From Eqs. (7.1.9) and (7.1.40) we know that in Cartesian coordinates the stress components σ_x and τ_{xy} are independent of r. Therefore, σ_x and τ_{xy} are not singular. Only the stress component σ_y is singular.

7.1.2 Example of Use of the Asymptotic Description

In this section an example will be presented to show the use of the asymptotic solution for the logarithmic singular stress field in a quarter-planes joint. The stresses calculated from FEM and the analytical description as given in Eq. (7.1.9) are compared.

Although Eq. (7.1.9) is deduced in case of a semi-infinite joint, it can be used in a finite joint with a homogeneous temperature change to calculate the stresses near the singular point (it should be noted that this solution can be used only in the area near the singular point). This means that the angular functions are the same for a finite joint as for a semi-infinite joint. However, for a finite joint the quantity R_0 is unknown and hence, the factor K in Eq. (7.1.9) is unknown. It has to be determined from the stresses calculated by FEM.
To determine the factor K in a finite joint, we can define one quantity Π:

$$\Pi_{ij} = \sum_{l=1}^{M} \left\{ \sigma_{ij}^{FEM}(r_l, \theta_l) - l_{ij} \Big\{ -2ln(r_l/L) f_{ij}(\theta_l) + t_{ij}(\theta_l) + (K + I_{ij}) f_{ij}(\theta_l) \Big\} \right\}^2 \tag{7.1.41}$$

where ij=xx, yy, xy, or rr, $\theta\theta$, $r\theta$, M is the number of points used for the determination of the K factor. In principle, any stress component at any point (r_l, θ_l) near the singular point can be used. In general, we use the points along a line, i.e. θ_l is a constant. According to the least square method, the factor K can be determined from

$$\frac{\partial \Pi_{ij}}{\partial K} = 0. \tag{7.1.42}$$

The results given below apply to plane strain. The geometry is $H_1/L = H_2/L$=2 (see Fig. 7.1). Thermal loading is a temperature change of $-100°C$.

The material data used in this example are

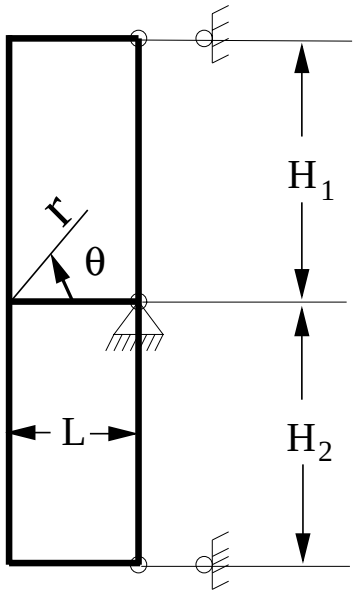

Figure 7.1: A quarter planes joint with $H_1/L = H_2/L$=2.

$$\begin{aligned} E_1 &= 100 \text{ GPa}, \quad \nu_1 = \tfrac{1}{3}, \quad \alpha_1 = 2.5 * 10^{-6}/\text{K}, \\ E_2 &= 54 \text{ GPa }, \quad \nu_2 = 0.2, \quad \alpha_2 = 8.5 * 10^{-6}/\text{K}. \end{aligned}$$

For this joint the stress exponent is

$$\omega = 0,$$

and

$$\begin{aligned} \left.\frac{d \parallel X \parallel}{ds}\right|_{s=-2} &= 0, \\ \left.\frac{d^2 \parallel X \parallel}{ds^2}\right|_{s=-2} &\neq 0. \end{aligned}$$

This corresponds to the case of $\alpha = 2\beta$ for a quarter-planes joint.
The factor K in Eq. (7.1.9) was determined using Eq. (7.1.42) and FEM. For this example

$$K = 0.4424,$$

which is the averaged value of those calculated from Eq. (7.1.42) with $\theta_l = -90°$, $90°$, $-45°$, $45°$, and 0. Using the K-factor as determined, we can calculate the stresses analytically at an arbitrary point with Eq. (7.1.9). Comparison of the stresses obtained from FEM and Eq. (7.1.9) along $\theta = 0$ is shown in Fig. 7.2. The quantities used to calculate the stresses with Eq. (7.1.9) in the Cartesian coordinate system are

$\theta°$	σ_{ij}	f_{ij} ,GPa/K	t_{ij},GPa/K
0	σ_x	0	$-2.1863 * 10^{-4}$
0	σ_y	$-1.4899 * 10^{-4}$	$6.8670 * 10^{-4}$
0	τ_{xy}	0	$-3.5106 * 10^{-4}$.

The results show that the stresses calculated by FEM and Eq. (7.1.9) are in excellent agreement in the range near the singular point. It can therefore be concluded that for thermal loading Eq. (7.1.9) can describe very well the stresses near the singular point analytically for the type of ln(r) singularity.

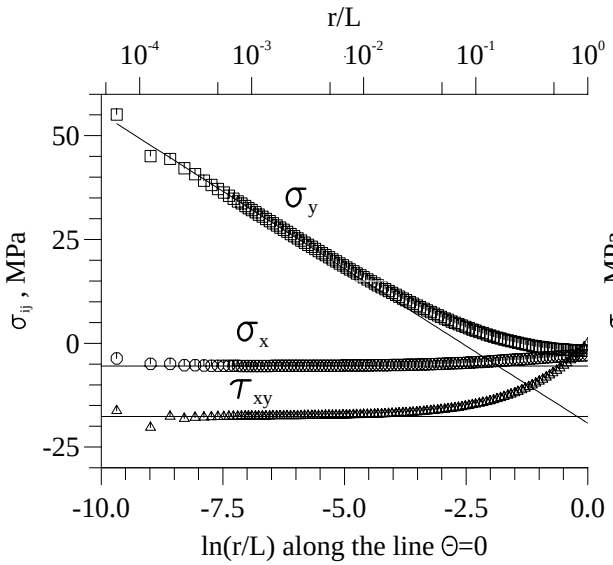

Figure 7.2: Comparison of the stresses obtained from FEM and Eq. (7.1.9) along $\theta = 0$ for thermal loading.

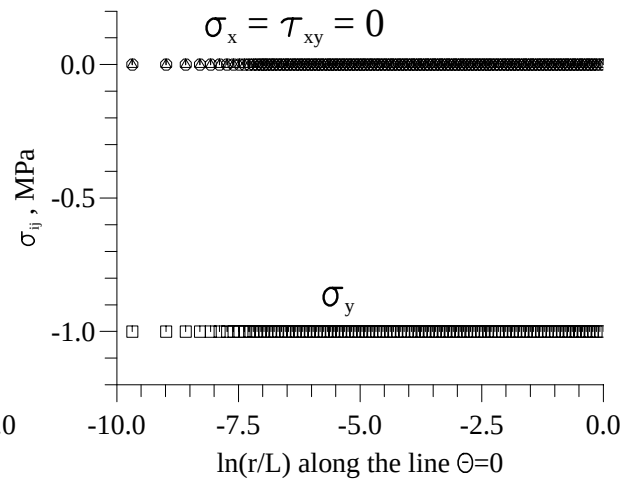

Figure 7.3: Stresses obtained from FEM along $\theta = 0$ for mechanical loading, the same joint as in Fig. 7.2.

For the same joint, but with remote mechanical loading, i.e. the upper and lower surfaces of the joint are subjected to homogeneous stress (e.g., $\sigma_y = -1$ MPa), the stress distribution in the joint was calculated by FEM. The stress distribution along θ=0 is plotted in Fig. 7.3. It can be seen that there is no stress singularity in the same joint under remote mechanical loading.
Therefore, we can say that $\| X \| |_{s=-2} = 0$, $\frac{d\|X\|}{ds}|_{s=-2} = 0$, and $\frac{d^2\|X\|}{ds^2}|_{s=-2} \neq 0$ are not all conditions for the type of ln(r) singularity. It also depends on the loading.

A short summary: In general, if s=-2 (i.e. ω_n=0) is the second-order pole of $\hat{\sigma}_{ij}(s,\theta) = \frac{\mathcal{P}_{ij}(s,\theta)g_{ij}(s)}{\|X\|(s+2)}$ in the Mellin domain, ln(r) singularity appears. This is the case with $\| X \| |_{s=-2} = 0$, $\frac{d\|X\|}{ds}|_{s=-2}$=0, $\frac{d^2\|X\|}{ds^2}|_{s=-2} \neq 0$ and $\mathcal{P}_{ij}(s,\theta)|_{s=-2} = 0$, $\frac{\partial \mathcal{P}_{ij}(s,\theta)}{\partial s}|_{s=-2} \neq 0$.
In an arbitrary finite joint under thermal loading, stresses near the singular point can be calculated from Eq. (7.1.9). The angular functions $f_{ij}(\theta)$ and $t_{ij}(\theta)$ can be calculated analytically, but in a longer form. However, for a quarter-planes joint ($\theta_1 = -\theta_2 = 90°$) the angular functions $f_{ij}(\theta)$ and $t_{ij}(\theta)$ in polar coordinates are simple and given in an explicit form (see Eqs(7.1.10) through (7.1.39)). The K factor has to be determined using the stresses calculated from FEM and the least squares method.

So far, the equations to determine the quantities in the asymptotic description of the

type of ln(r) singular stress field has been given for a joint with free edges under thermal loading. For a joint with an interface corner under thermal loading or a joint with edge tractions the method shown in this section to determine the asymptotic description of the type of ln(r) singular stress field is the same, only the boundary conditions are different. For a joint with edge tractions, constant and the higher order regular stress terms should be added.

7.2 The Type of $r^{-\omega}$ln(r) Stress Singularities in a Joint with Free Edges

In this section the type of $r^{-\omega}$ln(r) is treated. Emphasis is placed on the analytical description of the stress distribution near the singular point in a finite joint under thermal loading. The angular functions and the K factors used to describe the stress distribution near the singular point are given.

7.2.1 Angular Functions in the Asymptotic Description

From Section 7.1 it is known that the stresses in a polar coordinate system can be calculated from

$$\sigma_{ijk}(r,\theta) = \sum_{s_n<\gamma} \frac{1}{(M-1)!} \lim_{s\to s_n} \frac{d^{(M-1)}}{ds^{(M-1)}} \{(s-s_n)^M \frac{\mathcal{P}_{\mathrm{ijk}}(\mathrm{s},\theta)\mathrm{g_{ij}(s)}}{\parallel X \parallel (s+2)} \bar{r}^{-(s+2)}\} \tag{7.2.1}$$

where s_n is the M-th-order pole of $\hat{\sigma}_{ij}(s,\theta)$. The case of a joint with s=-2 as a second-order pole of $\hat{\sigma}_{ij}(s,\theta)$ was studied. In this section, we consider the case of M=2 and $s_n \neq -2$. It generally is the case with $\parallel X \parallel |_{s=s_n} = 0$, $\frac{d\parallel X\parallel}{ds}|_{s=s_n}$=0, $\frac{d^2\parallel X\parallel}{ds^2}|_{s=s_n} \neq 0$, and $\mathcal{P}_{\mathrm{ij}}(\mathrm{s},\theta)|_{\mathrm{s=s_n}} \neq 0$. In case of M > 2, calculation of stress reversal $\hat{\sigma}_{ij}(s,\theta)$ is more complicated, but the procedure is similar to that one for M=2. The case of M> 2 corresponds to the type of $r^{-\omega}\ln^N(r)$ stress singularity (with N=M-1 >1).
For $s = s_n$ and M=2, the stresses in polar coordinates can be calculated from

$$\begin{aligned}
\sigma_{ijn}(r,\theta) &= \lim_{s\to s_n} \frac{d}{ds}\{(s-s_n)^2 \bar{r}^{-(s+2)} \frac{\mathcal{P}_{\mathrm{ij}}(\mathrm{s},\theta)\mathrm{g_{ij}(s)}}{\parallel X \parallel (s+2)}\} \\
&= \frac{1}{\omega_n^2}\bar{r}^{-\omega_n} \lim_{s\to s_n} \Big\{ \Big\{ -ln(\bar{r})g_{ij}(s)\mathcal{P}_{\mathrm{ij}}(\mathrm{s},\theta) \parallel \mathrm{X} \parallel (\mathrm{s}-\mathrm{s_n})^2(\mathrm{s}+2) \\
&\quad +[\frac{dg_{ij}(s)}{ds}\mathcal{P}_{\mathrm{ij}}(\mathrm{s},\theta) + \frac{\mathrm{d}\mathcal{P}_{\mathrm{ij}}(\mathrm{s},\theta)}{\mathrm{ds}}\mathrm{g_{ij}(s)}](\mathrm{s}-\mathrm{s_n})^2(\mathrm{s}+2) \parallel \mathrm{X} \parallel \\
&\quad -\frac{d \parallel X \parallel}{ds} g_{ij}(s)\mathcal{P}_{\mathrm{ij}}(\mathrm{s},\theta)(\mathrm{s}-\mathrm{s_n})^2(\mathrm{s}+2) \\
&\quad +(s+s_n+4)g_{ij}(s)\mathcal{P}_{\mathrm{ij}}(\mathrm{s},\theta) \parallel \mathrm{X} \parallel (\mathrm{s}-\mathrm{s_n})\Big\} / \parallel \mathrm{X} \parallel^2 \Big\}
\end{aligned} \tag{7.2.2}$$

with $\omega_n = 2 + s_n$.
After using l'Hopital's rule,

$$\begin{aligned}\sigma_{ijn}(r,\theta) &= \frac{2}{\omega_n}\frac{\bar{r}^{-\omega_n}}{(\frac{d^2\|X\|}{ds^2})|_{s=s_n}}\Big\{ - ln(\bar{r})g_{ij}(s)\mathcal{P}_{\rm ij}({\rm s},\theta) + \frac{{\rm dg_{ij}(s)}}{\rm ds}\mathcal{P}_{\rm ij}({\rm s},\theta) + \frac{{\rm d}\mathcal{P}_{\rm ij}({\rm s},\theta)}{\rm ds}{\rm g_{ij}(s)} \\ &\quad -\frac{1}{3}\frac{\frac{d^3\|X\|}{ds^3}}{\frac{d^2\|X\|}{ds^2}}g_{ij}(s)\mathcal{P}_{\rm ij}({\rm s},\theta) - \frac{1}{\omega_{\rm n}}{\rm g_{ij}(s)}\mathcal{P}_{\rm ij}({\rm s},\theta)\Big\}\Big|_{s=s_n}. \qquad (7.2.3)\end{aligned}$$

From Eq. (3.2.45) we have

$$g_{ij}|_{s=s_n} = \bar{R}_0^{\omega_n} l_{ijn}, \qquad (7.2.4)$$

$$\begin{aligned}\frac{dg_r}{ds} &= \frac{\bar{R}_0^{(s+2)}T_0}{2s^2}\Big(ln(\bar{R}_0)\ s - 1\Big), \\ \frac{dg_\theta}{ds} &= \frac{\bar{R}_0^{(s+2)}T_0}{2s^2}\Big(ln(\bar{R}_0)\ (1+s)s - 1)\Big), \\ \frac{dg_{r\theta}}{ds} &= -\frac{\bar{R}_0^{(s+2)}T_0}{s^2}\Big(ln(\bar{R}_0)\ s(1+s) - 1\Big). \qquad (7.2.5)\end{aligned}$$

Taking

$$\begin{aligned}K_{1n} &= \bar{R}_0^{\omega_n}, \\ K_{2n} &= \bar{R}_0^{\omega_n} ln(\bar{R}_0), \\ l_{rrn} &= \frac{T_0}{2s_n}, \\ l_{\theta\theta n} &= \frac{T_0(s_n+1)}{2s_n}, \\ l_{r\theta n} &= -\frac{T_0(s_n+1)}{s_n}, \\ I_{rrn} &= -l_{rrn}/s_n, \\ I_{\theta\theta n} &= -l_{rrn}/s_n, \\ I_{r\theta n} &= 2l_{rrn}/s_n, \qquad (7.2.6)\end{aligned}$$

Eqs. (7.2.4) and (7.2.5) can be rewritten as

$$g_{ij}|_{s=s_n} = K_{1n} l_{ijn}, \qquad (7.2.7)$$

$$\frac{dg_{ij}}{ds}|_{s=s_n} = K_{1n} I_{ijn} + K_{2n} l_{ijn}. \qquad (7.2.8)$$

By using the definitions of

$$X_{2n} = \frac{d^2 \parallel X \parallel}{ds^2}\Big|_{s=s_n}, \qquad (7.2.9)$$

$$X_{3n} = \frac{d^3 \parallel X \parallel}{ds^3}\Big|_{s=s_n}, \tag{7.2.10}$$

and

$$\begin{aligned} f_{ijn}(\theta) &= \frac{2}{\omega_n X_{2n}} \mathcal{P}_{\mathrm{ij}}(\mathrm{s},\theta)\Big|_{s=s_n} \\ &= \frac{2}{\omega_n X_{2n}} \Big\{ A_{1ijk}(s_n)\cos\Big((\omega_n-2)\theta\Big) + A_{2ijk}(s_n)\sin\Big((\omega_n-2)\theta\Big) \\ &\quad + A_{3ijk}(s_n)\cos(\omega_n\theta) + A_{4ijk}(s_n)\sin(\omega_n\theta) + A_{5ijk}(s_n)\Big\}, \end{aligned} \tag{7.2.11}$$

$$\begin{aligned} t_{ijn}(\theta) &= \frac{2}{\omega_n X_{2n}} \frac{d\mathcal{P}_{\mathrm{ij}}(\mathrm{s},\theta)}{ds}\Big|_{s=s_n} \\ &= \frac{2}{\omega_n X_{2n}} \Big\{ \frac{dA_{1ijk}(s)}{ds}|_{s=s_n}\cos\Big((\omega_n-2)\theta\Big) + \frac{dA_{2ijk}(s)}{ds}|_{s=s_n}\sin\Big((\omega_n-2)\theta\Big) \\ &\quad + \frac{dA_{3ijk}(s)}{ds}|_{s=s_n}\cos(\omega_n\theta) + \frac{dA_{4ijk}(s)}{ds}|_{s=s_n}\sin(\omega_n\theta) + \frac{dA_{5ijk}(s)}{ds}|_{s=s_n} \\ &\quad - A_{1ijk}(s_n)\theta\sin\Big((\omega_n-2)\theta\Big) + A_{2ijk}(s_n)\theta\cos\Big((\omega_n-2)\theta\Big) \\ &\quad - A_{3ijk}(s_n)\theta\sin\Big(\omega_n\theta\Big) + A_{4ijk}(s_n)\theta\cos\Big(\omega_n\theta\Big)\Big\}, \end{aligned} \tag{7.2.12}$$

with k=1 for $\theta > 0$ and k=2 for $\theta < 0$, finally corresponding to s_n ($\omega_n = s_n + 2$), the stresses near the singular point can be calculated from the relation of

$$\begin{aligned} \sigma_{ijn}(r,\theta) &= -\bar{r}^{-\omega_n} ln(\bar{r}) K_{1n} l_{ijn} f_{ijn}(\theta) + \bar{r}^{-\omega_n}\Big\{ K_{2n} l_{ijn} f_{ijn}(\theta) \\ &\quad + K_{1n}\Big\{ I_{ijn} f_{ijn}(\theta) + l_{ijn}\Big[t_{ijn}(\theta) - \frac{X_{3n}}{3X_{2n}} f_{ijn}(\theta) - \frac{1}{\omega_n} f_{ijn}(\theta)\Big]\Big\}\Big\}. \end{aligned} \tag{7.2.13}$$

In Eq. (7.2.13) K_{1n} and K_{2n} are dimensionless, $f_{ijn}(\theta)$ and $t_{ijn}(\theta)$ have the unit of $E_k \times \alpha_k$, and l_{ijn} and I_{ijn} have the unit of temperature. The coefficients A_{lijk} (l=1,2,3,4,5) are given in Section 3.2. They depend on the material properties (E_1, ν_1, E_2, ν_2), the angles θ_1, θ_2, and s_n. For each given s_n the functions $f_{ijn}(\theta)$ and $t_{ijn}(\theta)$ can thus be calculated analytically from Eqs. (7.2.11) and (7.2.12). The quantities l_{ijn} and I_{ijn} are proportional to the loading and well known. The quantities $f_{ijn}(\theta), t_{ijn}(\theta), l_{ijn}, I_{ijn}$ are independent of the overall geometry of the joint; only the factors K_{1n} and K_{2n} depend on the overall geometry, i.e., R_0. For a semi-infinite joint under thermal loading the factors K_{1n} and K_{2n} are well known. For a finite joint the quantity R_0 is unknown. Therefore, the factors K_{1n} and K_{2n} in Eq. (7.2.13) are unknown. They should be

determined by a numerical method, such as the finite element method. They are a function of the material properties $(E_1, \nu_1, E_2, \nu_2, \alpha_1, \alpha_2)$, the angles θ_1, θ_2, the overall geometry, and the loading.

For any two dissimilar materials joint under thermal loading, s=-2 (i.e. $\omega = 0$) always is the first-order pole of $\hat{\sigma}_{ij}(s,\theta)$ (the case with s=-2 as a second-order pole of $\hat{\sigma}_{ij}(s,\theta)$ is not considered; it was presented in Section 7.1). For a given geometry and material combination, there may be more than one s_n (n=1,2,...,N) as a second-order pole of $\hat{\sigma}_{ij}(s,\theta)$. Therefore, the stresses near the singular point for the case of more than one s_n (n=1,2,...,N) as a second-order pole of $\hat{\sigma}_{ij}(s,\theta)$ can be described by

$$\begin{aligned}\sigma_{ij}(r,\theta) &= \sum_{n=1}^{N} \sigma_{ijn}(r,\theta) + \sigma_{ij0}(\theta) \\ &= \sum_{n=1}^{N} \Big\{ -\bar{r}^{-\omega_n} ln(\bar{r}) K_{1n} l_{ijn} f_{ijn}(\theta) + \bar{r}^{-\omega_n} \Big\{ K_{2n} l_{ijn} f_{ijn}(\theta) \\ &+ K_{1n} \Big\{ I_{ijn} f_{ijn}(\theta) + l_{ijn} \Big[t_{ijn}(\theta) - \frac{X_{3n}}{3X_{2n}} f_{ijn}(\theta) - \frac{1}{\omega_n} f_{ijn}(\theta) \Big] \Big\} \Big\} \Big\} + \sigma_{ij0}(\theta)\end{aligned} \tag{7.2.14}$$

where the regular stress term $\sigma_{ij0}(\theta)$ is independent of the distance r.

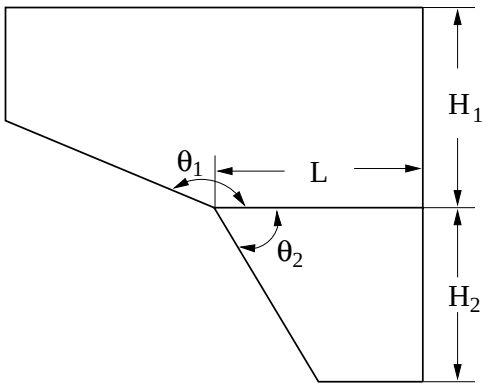

Figure 7.4: A joint with $\theta_1 = 165°$ and $\theta_2 = -55°$ ($H_1/L = 0.984$, $H_2/L = 0.816$, $L_1/L = 2.016$, $L_2/L = 0.432$.)

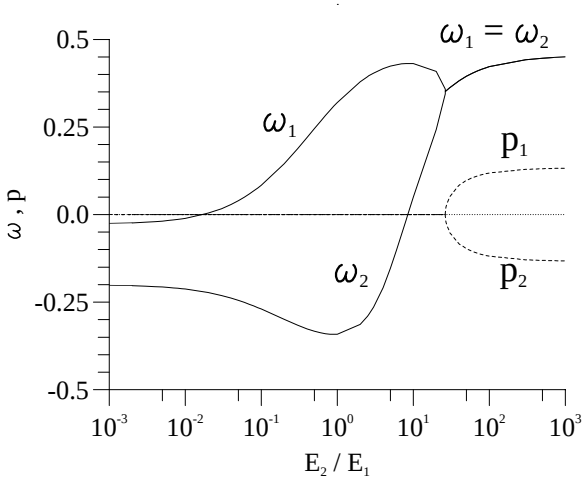

Figure 7.5: The stress exponent (real and imaginary part) vs. the ratio of Young's modulus for the joint with $\theta_1 = 165°$ and $\theta_2 = -55°$, $\nu_1 = 0.2, \nu_2 = 0.3$.

Generally, the functions $f_{ijn}(\theta)$, $t_{ijn}(\theta)$ and $\sigma_{ij0}(\theta)$ have the following expression:

$$f_{ijn}(\theta) = F_{1ijn} cos[(\omega_n - 2)\theta] + F_{2ijn} sin[(\omega_n - 2)\theta] + F_{3ijn} cos(\omega_n \theta) + F_{4ijn} sin(\omega_n \theta) + F_{5ij}$$

$$\begin{aligned}t_{ijn}(\theta) = {} & T_{1ijn} cos[(\omega_n - 2)\theta] + T_{2ijn} sin[(\omega_n - 2)\theta] + T_{3ijn} cos(\omega_n \theta) + T_{4ijn} sin(\omega_n \theta) + T_{5ij} \\ & + T_{6ijn} \theta cos[(\omega_n - 2)\theta] + T_{7ijn} \theta sin[(\omega_n - 2)\theta] + T_{8ijn} \theta cos(\omega_n \theta) + T_{9ijn} \theta sin(\omega_n \theta)\end{aligned}$$

$$\sigma_{ij0}(\theta) = S_{1ij}cos(2\theta) + S_{2ij}sin(2\theta) + S_{3ij}\theta + S_{4ij}.$$

In this section, the determination of the coefficients F_{lijn} and T_{Lijn} is given. They can be calculated analytically from Eqs. (7.2.11) and (7.2.12). Calculation of σ_{ij0} is well known from Section 3.2. Only the factors K_{1n} and K_{2n} cannot be calculated analytically for a finite joint.

7.2.2 Examples and Discussions

Two examples will be given to show the agreement of the stresses near the singular point calculated by FEM and from Eq. (7.2.14). The loading is a homogeneous temperature change of $T_0 = -100$ K. For convenience the components rr and $\theta\theta$ are replaced below by r and θ.

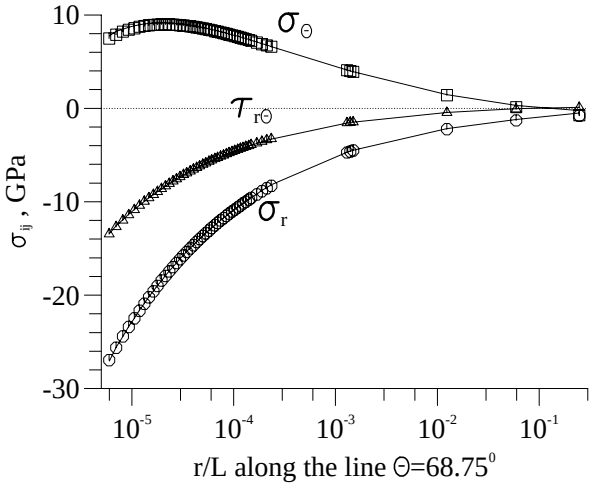

Figure 7.6: Comparison of the stresses obtained by FEM and Eq. (7.2.14) along the line of $\theta = 68.75°$ for the joint with $\theta_1 = 165°$ and $\theta_2 = -55°$.

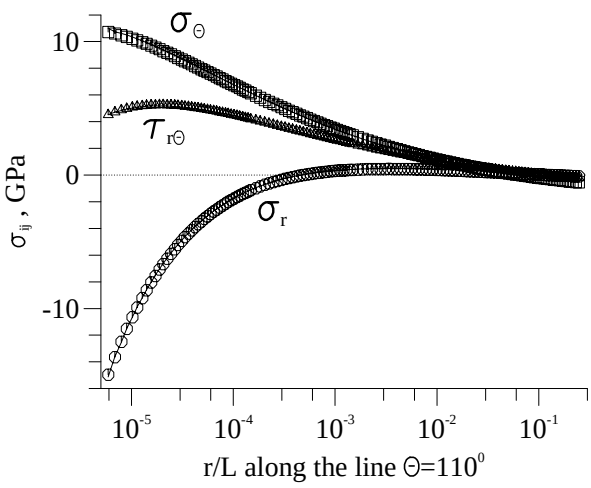

Figure 7.7: Comparison of the stresses obtained by FEM and Eq. (7.2.14) along the line of $\theta = 110°$ for the joint with $\theta_1 = 165°$ and $\theta_2 = -55°$.

Example 1

The geometry (see Fig. 7.4) and the material data for Example 1 are

$$\begin{array}{lll} \theta_1 = 165°, & \theta_2 = -55°, & \\ E_1 = 1000 \text{ GPa}, & \nu_1 = 0.2, & \alpha_1 = 2.5 * 10^{-6}/\text{K}, \\ E_2 = 26359.8973406 \text{ GPa}, & \nu_2 = 0.3\ , & \alpha_2 = 18.95 * 10^{-6}/\text{K}. \end{array}$$

For this joint, the stress exponent is

$$\omega_n = 0.35140544186$$

and N=1 in Eq. (7.2.14). For this ω_n ($s_n = \omega_n - 2$), there is $\| X \| < 10^{-10}$ and $\frac{d\|X\|}{ds}|_{s=s_n} < 10^{-8}$. As the relation between the material data, the angles θ_1, θ_2, and ω_n is very complicated, it is difficult to find a material combination and an ω_n so that $\| X \|_{s=s_n} = 0$ and $\frac{d\|X\|}{ds}|_{s=s_n} = 0$ are satisfied exactly. It can be said that example 1 nearly is the case, in which s_n is a second-order pole of $\hat{\sigma}_{ij}(s, \theta)$. This ω_n is very close to the transient point from a real eigenvalue to a complex eigenvalue for these angles θ_1, θ_2 and ν_1, ν_2, and for various ratios of E_2/E_1 (see Fig. 7.5).
FEM has been used to determine the two unknown factors K_1 and K_2 in Eq. (7.2.14). The method for determining K_1 and K_2 from the stresses calculated by FEM is similar to that one given in Section 3.4. The factors obtained for this example are

$$K_1 = -2.4229 \quad , \quad K_2 = 133.38.$$

Using the K-factors as determined, we can calculate the stresses analytically with Eq. (7.2.14). The quantities used to calculate the stresses with Eq. (7.2.14) are

$$X_{2n} = 25358 \quad , \quad X_{3n} = -860$$

θ°	σ_{ij}	f_{ij}, GPa/K	t_{ij}, GPa/K	σ_{ij0},GPa
68.75	σ_r	-0.0001803	-0.002781	0.09460
68.75	σ_θ	-0.001929	-0.08719	-2.5504
68.75	$\sigma_{r\theta}$	0.00002715	0.003391	0.3792
110	σ_r	0.0008027	0.03912	-0.7817
110	σ_θ	-0.001144	-0.04970	-1.7903
110	$\sigma_{r\theta}$	0.0005258	0.02372	-1.2271
165	σ_r	0.002019	0.08671	-2.7271
-55	σ_r	-0.003834	-0.1311	1.7446 .

Comparisons of the stresses obtained by FEM and from Eq. (7.2.14) are shown in Figs. 7.6, 7.7, 7.8, and 7.9 along different directions and for different components. The results show that they have very good agreement, except for a very small distance r. The stresses for a very small distance r as obtained by FEM are not accurate because of the stress singularity.

Example 2

The geometry (see Fig. 7.10) and the material data for Example 2 are

$$\begin{aligned} &\theta_1 = 120^\circ, && \theta_2 = -120^\circ, \\ &E_1 = 1000 \text{ GPa}, && \nu_1 = 0.1, \qquad \alpha_1 = 2.5 * 10^{-6}/\text{K}, \\ &E_2 = 9141.3623351 \text{ GPa} , && \nu_2 = 0.4, \qquad \alpha_2 = 18.95 * 10^{-6}/\text{K}. \end{aligned}$$

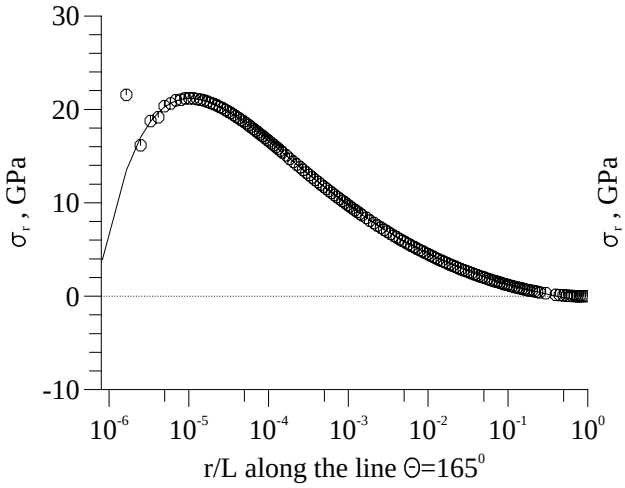

Figure 7.8: Comparison of the stresses obtained by FEM and Eq. (7.2.14) along the line of $\theta = 165°$ for the joint with $\theta_1 = 165°$ and $\theta_2 = -55°$.

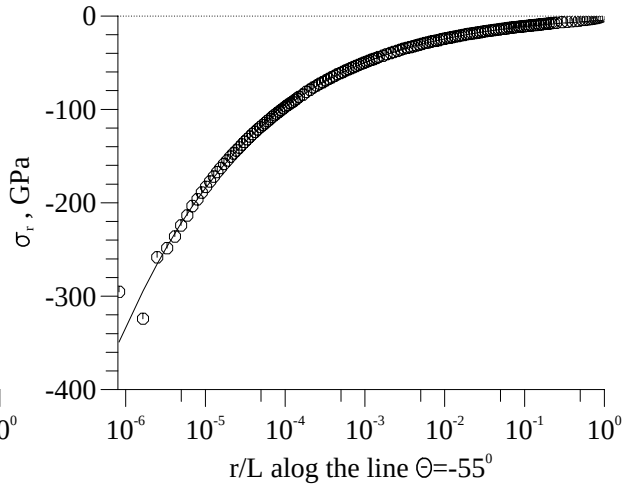

Figure 7.9: Comparison of the stresses obtained by FEM and Eq. (7.2.14) along the line of $\theta = -55°$ for the joint with $\theta_1 = 165°$ and $\theta_2 = -55°$.

For this joint, the stress exponent is

$$\omega_n = 0.17998265382$$

and N=1. For this ω_n, there is $\| X \| < 10^{-7}$ and $\frac{d\|X\|}{ds}|_{s=s_n} < 10^{-6}$. We can say this nearly is the case, in which s_n is a second-order pole of $\hat{\sigma}_{ij}(s,\theta)$. This ω_n is very close to the transient point from a real eigenvalue to a complex eigenvalue for these angles θ_1, θ_2 and ν_1, ν_2, and various ratios of E_2/E_1 (see Fig. 7.11).
The K-factors obtained for this example are

$$K_1 = 1.1029 \quad , \quad K_2 = 1.1266.$$

Using the K-factors as determined, we can calculate the stresses analytically with Eq. (7.2.14). The quantities used to calculate the stresses with Eq. (7.2.14) are:

$$X_{2n} = 10038 \quad , \quad X_{3n} = 129024$$

$\theta°$	σ_{ij}	f_{ij}, GPa/K	t_{ij}, GPa/K	σ_{ij0}, GPa
0	σ_θ	0.08579	0.2478	-14.5072
0	$\sigma_{r\theta}$	0.01921	-0.02237	10.0897
120	σ_r	-0.0977	-0.0755	-21.9573
-120	σ_r	0.006196	-0.2597	8.8239

Comparisons of the stresses obtained by FEM and from Eq. (7.2.14) are shown in Figs. 7.12, 7.13, and 7.14 along different directions and for different components. The results show that they have very good agreement, except for a very small distance r. So we can say that in a joint with $r^{-\omega}\ln(r)$ singularity under thermal loading Eq. (7.2.14) can analytically describe the stresses near the singular point very well.

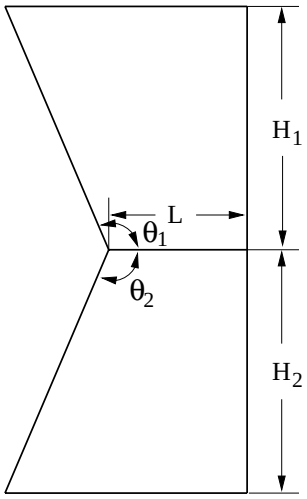

Figure 7.10: A joint with $\theta_1 = 120°$ and $\theta_2 = -120°$, and $H_1/L = H_2/L = 1.732$.

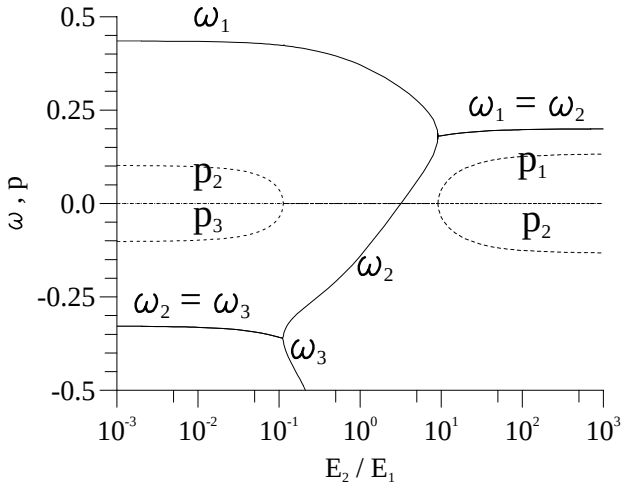

Figure 7.11: The stress exponent (real and imaginary part) vs. the ratio of Young's modulus for the joint with $\theta_1 = 120°$ and $\theta_2 = -120°$, $\nu_1 = 0.1, \nu_2 = 0.4$.

Both examples have demonstrated that near the singular point of a joint with the type of $r^{-\omega}\ln(r)$ singularity under thermal loading the stresses calculated by FEM and the analytical description based on Eq. (7.2.14) are in excellent agreement.

7.3 Application of the Asymptotic Description of ln(r) Singularity

In this section, use of the asymptotic description of ln(r) singularity to evaluate analytically the singular stresses without using any numerical method will be presented for joints with very small ω in the type of $r^{-\omega}$ singularity.

Theoretically, if the stress exponent ω_n ($\omega_n = 2 + s_n$, and s_n is the solution of $\| X \| = 0$) is nonzero (may be very small), the stresses near the singular point in a joint under thermal loading should be described by

$$\sigma_{ij}(r,\theta) = \sum_{n=1}^{N} \frac{K_n}{(r/L)^{\omega_n}} h_{ijn}(\theta) + \sigma_{ij0}(\theta), \tag{7.3.1}$$

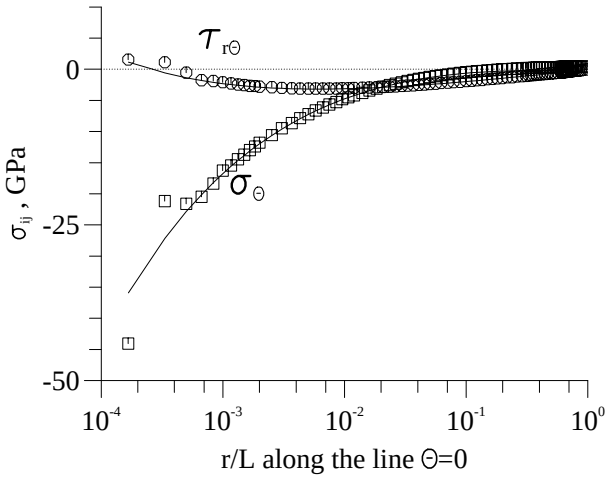

Figure 7.12: Comparison of the stresses obtained by FEM and Eq. (7.2.14) along the line of $\theta = 0°$ for the joint with $\theta_1 = 120°$ and $\theta_2 = -120°$.

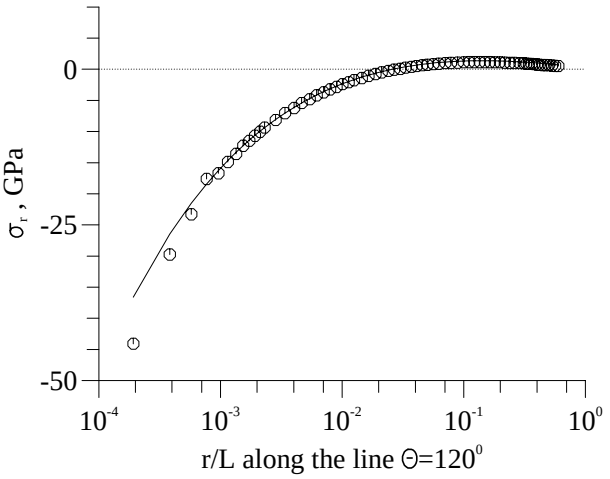

Figure 7.13: Comparison of the stresses obtained by FEM and Eq. (7.2.14) along the line of $\theta = 120°$ for the joint with $\theta_1 = 120°$ and $\theta_2 = -120°$.

where $\sigma_{ij0}(\theta)$ is the regular stress term (see Sections 3.2 and 3.3), ω_n is the singular stress exponent (see Section 3.1), $h_{ijn}(\theta)$ are the angular functions for non-logarithmic stress singularity (here, the angular functions $h_{ijn}(\theta)$ are the same as those given in Section 3.1 for $f_{ijn}(\theta)$). They can be determined analytically. The factors K_n should be determined from the stress analysis using FEM.

If the value of ω_n is very small, however, use of Eq. (7.3.1) is questionable. As the equation $\| X \| = 0$ is a transcendental equation, a numerical method has to be used to solve it. For very, very small ω ($\omega < 10^{-6}$), the solution is sensitive to the explicit form of $\| X \|$. If for the same $\| X \|$ explicit form different numerical methods are used to solve $\| X \| = 0$, the solution is different as well. This means that it is difficult to determine the accurate value of ω for a material combination with a very, very small ω. Use of Eq. (7.3.1) to describe stresses near the singular point in a joint under thermal loading is difficult as well. In practice and from the physical point of view, the exact value of ω is not important to a joint with very, very small ω. On the other hand, due to the effect of the regular term $\sigma_{ij0}(\theta)$, for a two dissimilar materials joint under thermal loading the case of $\omega \to 0$ does not mean that the stress singularity disappears. However, this cannot be seen from Eq. (7.3.1).

From mathematics it is known that if $\omega_n \to 0$, there is also $\frac{d\|X\|}{ds}|_{s=s_n} \to 0$ ($s_n = \omega_n - 2$). Now, the question arises whether Eq. (7.1.9) can be used to calculate the stresses near the singular point in a joint with very small ω_n for thermal loading. If so, how small may ω_n be? Examples will be given to answer these questions. The results given below are for a quarter planes joint with $H_1/L = H_2/L = 2$ and for plane strain. The loading

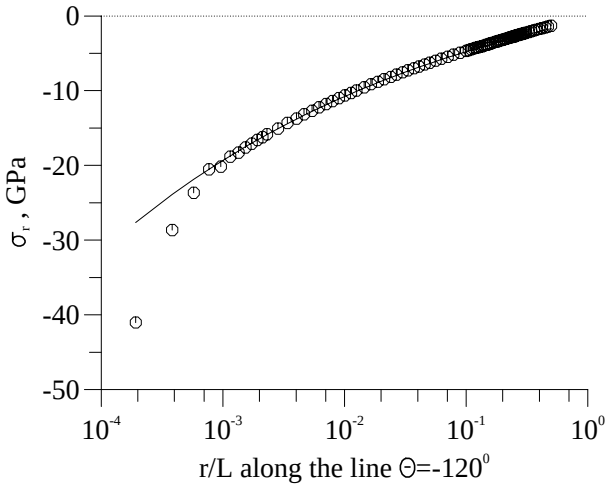

Figure 7.14: Comparison of the stresses obtained by FEM and Eq. (7.2.14) along the line of $\theta = -120°$ for the joint with $\theta_1 = 120°$ and $\theta_2 = -120°$.

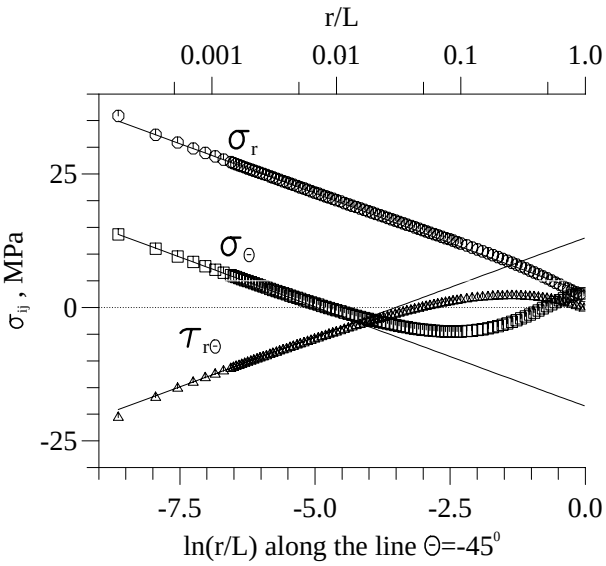

Figure 7.15: A comparison of the stresses obtained from FEM and Eq. (7.1.9) along $\theta = -45°$ for example 1.

is a temperature change of $-100°$C.

The material data for Example 1 are

$$E_1 = 100 \text{ GPa}, \quad \nu_1 = 0.333, \quad \alpha_1 = 2.5 * 10^{-6}/\text{K},$$
$$E_2 = 54 \text{ GPa} , \quad \nu_2 = 0.2, \quad \alpha_2 = 8.5 * 10^{-6}/\text{K} .$$

For this joint, the stress exponent is

$$\omega = 6.0222 * 10^{-5}$$

and

$$\frac{d \parallel X \parallel}{ds}|_{s=s_n} = 1.3880 * 10^{-4}.$$

Although the conditions for the type of ln(r) singularity are not satisfied exactly, Eq. (7.1.9) is used to calculate the stresses near the singular point. The K factor obtained in Eq. (7.1.9) is

$$K = 0.3856.$$

The quantities used to calculate the stresses with Eq. (7.1.9) are

$\theta°$	σ_{ij}	f_{ij},GPa/K	t_{ij} ,GPa/K
$-45°$	σ_r	$7.44588 * 10^{-5}$	$7.79347 * 10^{-6}$
$-45°$	σ_θ	$-7.44588 * 10^{-5}$	$6.94198 * 10^{-4}$
$-45°$	$\tau_{r\theta}$	$-3.72294 * 10^{-5}$	$2.38395 * 10^{-4}$.

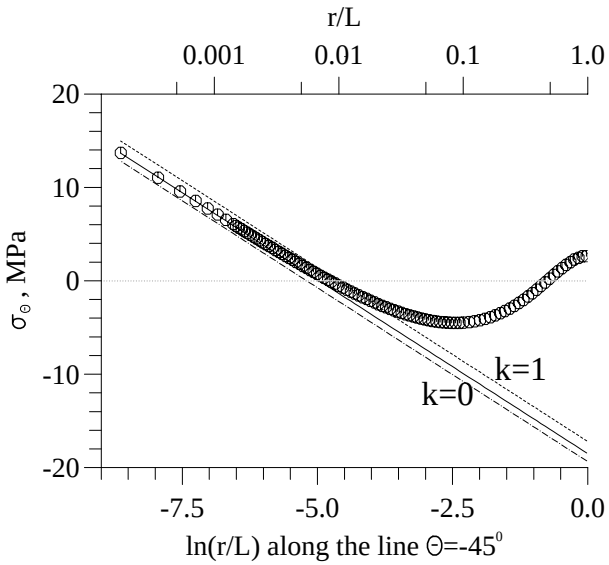

Figure 7.16: A comparison of the stresses obtained from FEM and Eq. (7.1.9) along $\theta = -45°$ for example 1, K=0, K=0.3865 (solid line), and K=1.

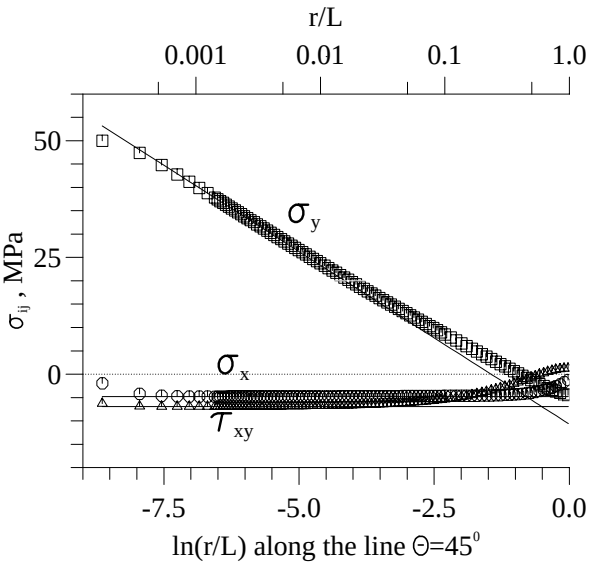

Figure 7.17: A comparison of the stresses obtained from FEM and Eq. (7.1.9) along $\theta = 45°$ for example 2.

A comparison of the stresses obtained from FEM and Eq. (7.1.9) along $\theta = -45°$ is given in Fig. 7.15. The results show that for this material combination (i.e. the stress exponent ω approximately is $6 * 10^{-5}$) Eq. (7.1.9) can be also used to describe the stresses near the singular point very well, and that the stress singularity is obvious, although the stress exponent ω is very small.
Since the absolute value of the term K $f_{ij}l_{ij}$ is relatively smaller than that one of the term $\ln(r)f_{ij}l_{ij}$ for a very small distance r, from Eq. (7.1.9) we know that the stresses calculated from Eq. (7.1.9) are not sensitive to the accuracy of the determined K factor value. Figure 7.16 shows an example. In Fig. 7.16 the solid line indicates the results with K=0.3856, the dashed line is that one with K=1, and the dotted line is for K=0. It can be seen that the effect of the K value on stress is not strong. If the absolute value of K is lower, the effect of the accuracy of K on stress is smaller.

Another two examples will show that Eq. (7.1.9) can be also used to calculate the stresses for a larger singular stress exponent.

The material data for Example 2 are

$$E_1 = 100 \text{ GPa}, \quad \nu_1 = 0.328, \quad \alpha_1 = 2.5 * 10^{-6}/\text{K},$$
$$E_2 = 54 \text{ GPa} , \quad \nu_2 = 0.2, \quad \alpha_2 = 8.5 * 10^{-6}/\text{K} .$$

For this joint, the stress exponent is

$$\omega = 9.5167076 * 10^{-4}.$$

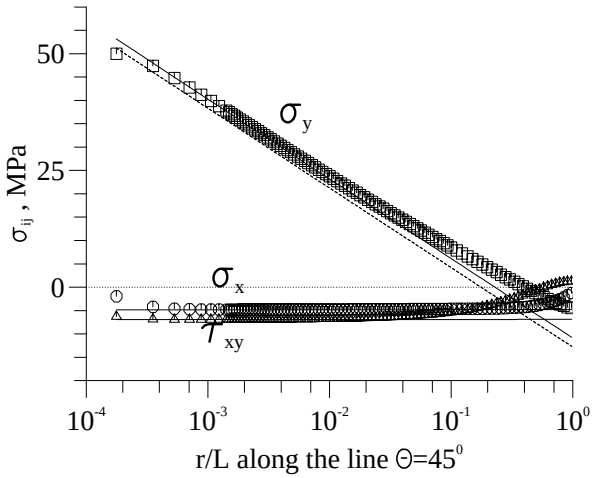

Figure 7.18: A comparison of the stresses obtained from FEM and Eq. (7.3.1) along $\theta = 45°$ for example 2, the dashed line represents the results from Eq. (7.3.1) with K=7.7436, solid lines indicate the results with 1.00025 K.

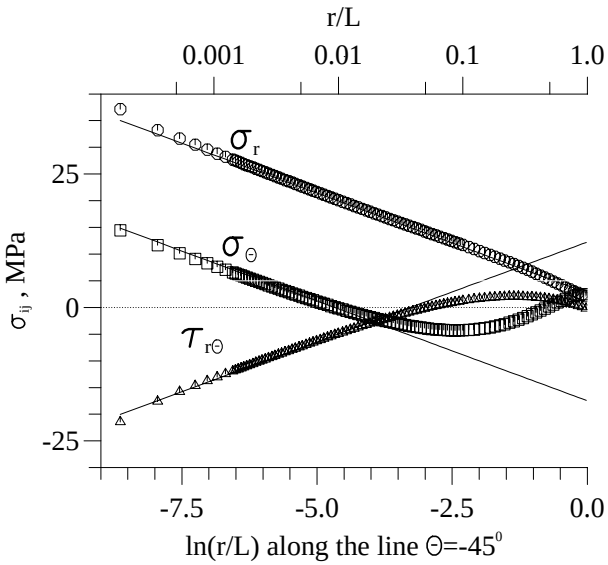

Figure 7.19: A comparison of the stresses obtained from FEM and Eq. (7.1.9) along $\theta = -45°$ for example 3.

A comparison of the stresses obtained from FEM and Eq. (7.1.9) in Cartesian coordinates is shown in Fig. 7.17, where K=0.0525. The results show that for this material combination (i.e. the stress exponent ω approximately is 10^{-3}) Eq. (7.1.9) may well be used to describe the stresses near the singular point.
On the other hand, a comparison of the stresses calculated from FEM (as symbol) and from Eq. (7.3.1) with K=7.7436 (K was calculated from Eq. (3.5.7), as dashed lines) is plotted in Fig. 7.18, in which the solid lines are the results from Eq. (7.3.1) with 1.00025 K. It can be seen that for very small ω, the stresses calculated from the equations for the type of $r^{-\omega}$ are affected strongly by the accuracy of the K-factor value determined.

The material data for Example 3 are

$$E_1 = 100 \text{ GPa}, \quad \nu_1 = 0.3, \quad \alpha_1 = 2.5 * 10^{-6}/\text{K},$$
$$E_2 = 50 \text{ GPa}, \quad \nu_2 = 0.2, \quad \alpha_2 = 8.5 * 10^{-6}/\text{K}.$$

For this joint, the stress exponent is

$$\omega = 9.6826076 * 10^{-3}.$$

For this material combination stresses were calculated by FEM and from Eq. (7.1.9). The K factor obtained in Eq. (7.1.9) for this example is

$$K = 0.094.$$

The quantities used to calculate the stresses with Eq. (7.1.9) are

θ°	σ_{ij}	f_{ij},GPa/K	t_{ij} ,GPa/K
-45°	σ_r	$7.4797 * 10^{-5}$	$-2.1864 * 10^{-5}$
-45°	σ_θ	$-7.4797 * 10^{-5}$	$6.8028 * 10^{-4}$
-45°	$\tau_{r\theta}$	$-3.7399 * 10^{-5}$	$2.3596 * 10^{-4}$.

A comparison of the stresses obtained from FEM and Eq. (7.1.9) along $\theta = -45^\circ$ is given in Fig. 7.19. The results show that for this material combination (i.e. the stress exponent ω approximately is 10^{-2}), Eq. (7.1.9) can be used to describe the stresses near the singular point well, although the condition $\frac{d\|X\|}{ds}|_{s=s_n} = 0$ is not satisfied.

Other comparisons of the stresses calculated from FEM and Eq. (7.3.1) show that for ω being about 0.01, the stresses calculated from the equations for the type of $r^{-\omega}$ are also affected strongly by the accuracy of the K-factor value determined.

Below two examples will be given to show for which material combination Eq. (7.1.9) with K=0 can be used to calculate the stress distribution near the singular point.

As example 4 a real material combination is chosen, which is a Si_3N_4/W joint. The material data are

$$E_1 = 314 \text{ GPa}, \quad \nu_1 = 0.28, \quad \alpha_1 = 2.7 * 10^{-6}/\text{K},$$
$$E_2 = 411 \text{ GPa} , \quad \nu_2 = 0.28, \quad \alpha_2 = 4.5 * 10^{-6}/\text{K} .$$

For this joint, the stress exponent is

$$\omega = 0.0056.$$

The stresses were calculated by FEM and from Eq. (7.1.9) with K=0. The quantities used to calculate the stresses with Eq. (7.1.9) are

θ°	σ_{ij}	f_{ij},GPa/K	t_{ij} ,GPa/K
-45°	σ_r	$-4.7979 * 10^{-5}$	$7.9641 * 10^{-4}$
-45°	σ_θ	$4.7979 * 10^{-5}$	$3.3018 * 10^{-4}$
-45°	$\tau_{r\theta}$	$-2.3990 * 10^{-5}$	$6.5716 * 10^{-5}$.

A comparison of the stresses obtained from FEM and from Eq. (7.1.9) with K=0 along $\theta = -45^\circ$ is shown in Fig. 7.20. The results show that for this material combination (i.e. the stress exponent ω approximately is 0.006) Eq. (7.1.9) with K=0 can be used to describe the stresses near the singular point well (with an error of $< 6\%$ for r/L< 0.01).

For the same joint as used in example 3, i.e. the stress exponent is $\omega = 9.6826 * 10^{-3}$, a comparison of the stresses obtained from FEM and Eq. (7.1.9) with K=0 along

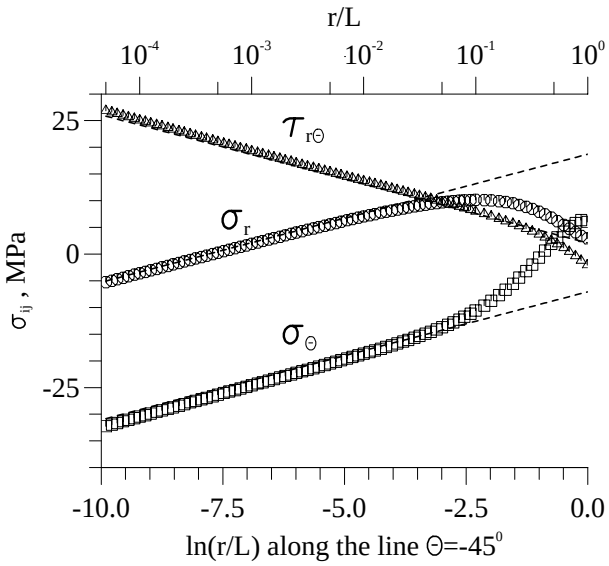

Figure 7.20: A comparison of the stresses obtained from FEM and Eq. (7.1.9) with K=0 along $\theta = -45°$ for example 4.

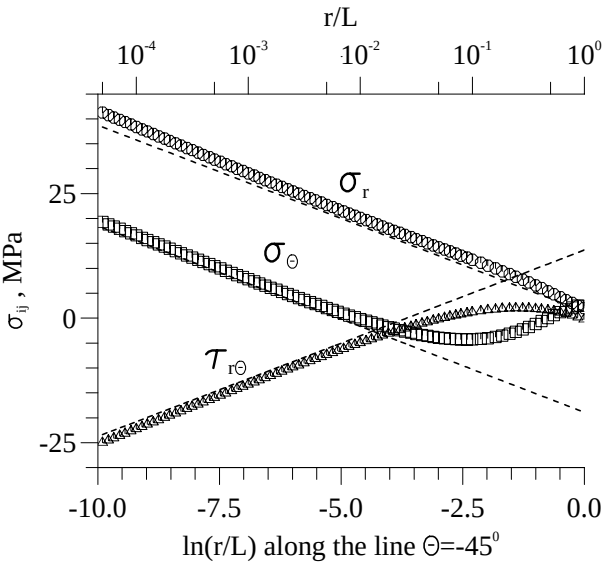

Figure 7.21: A comparison of the stresses obtained from FEM and Eq. (7.1.9) with K=0 along $\theta = -45°$ for example 3.

$\theta = -45°$ is shown in Fig. 7.21. The results demonstrate that for this material combination (i.e. the stress exponent ω approximately is 10^{-2}) Eq. (7.1.9) with K=0 can be used to describe the stresses near the singular point with an error smaller than 10% for r/L< 0.01.

From Figs. 7.20 and 7.21, it can be seen that the equations for the type of ln(r) singularity with K=0 can be used to calculate stresses near the singular point, if the stress exponent ω in the type of $r^{-\omega}$ is very small (say $\omega < 0.01$). The advantage is that for a joint with very small ω, FEM is not needed to calculate the stresses near the singular point when Eq. (7.1.9) with K=0 is applied.
For practically relevant materials, i.e. $0.2 < \nu_1 < 0.4$ and $0.2 < \nu_2 < 0.4$, material combinations with $0.6 < E_2/E_1 < 2$ usually have a very small stress exponent ω, see Fig. 7.22 (curve 1 is for $\nu_1 = 0.2, \nu_2 = 0.3$; curve 2 for $\nu_1 = \nu_2 = 0.2$; curve 3 for $\nu_1 = \nu_2 = 0.3$; curve 4 for $\nu_1 = 0.25, \nu_2 = 0.35$). Therefore, application of the asymptotic description of the logarithmic singular stress field is of interest. Numerical calculations show that if ω is negative and its absolute value very small, Eq. (7.1.9) with K=0 can be used to calculate stresses near the "singular point" as well.
We can conclude: (a) The case of $\omega \to 0$ does not mean that the stress singularity disappears for a joint with a free edge under thermal loading. (b) For joints with very small ω ($\omega < 10^{-2}$) in the type of $r^{-\omega}$ singularity, stresses near the singular point can also be described by the equations for the type of ln(r) stress singularity. (c) The equations for the type of ln(r) stress singularity with K=0 can be applied to calculate stresses near the singular point for joints with $\omega < 0.01$ and $H_1/L > 1$, and $H_2/L > 1$.

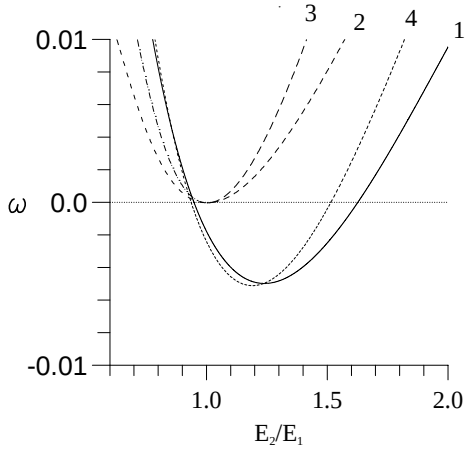

Figure 7.22: Stress exponent for real material combinations (curve 1 is for $\nu_1 = 0.2, \nu_2 = 0.3$; curve 2 for $\nu_1 = \nu_2 = 0.2$; curve 3 for $\nu_1 = \nu_2 = 0.3$; curve 4 for $\nu_1 = 0.25, \nu_2 = 0.35$).

This means that the stresses near the singular point can be calculated without using any FEM. The error is less than 10% for $\omega < 0.01$ and r/L< 0.01. For $\omega < 0.005$ the error is less than 5%. If the corresponding value of K in Eq. (7.1.9) is used, the error is even smaller.

7.4 Displacement Field Corresponding to the Logarithmic Stress Singularity

The analytical description of the logarithmic singular stress field is known from Sections 7.1 and 7.2 (see Eqs. (7.1.9) and (7.2.14)). By inserting Eq. (7.1.9) or Eq. (7.2.14) into Eqs.(3.1.10), (3.1.11), and (3.1.12) the strains $\varepsilon_{rr}, \varepsilon_{\theta\theta}$, and $\varepsilon_{r\theta}$ can be calculated as a function of the polar coordinates r and θ. For the type of ln(r) stress singularity,

$$\varepsilon_{rr}(r,\theta) = y_1\Big(ln(r), sin(2\theta), cos(2\theta), \theta\Big) \tag{7.4.1}$$

$$\varepsilon_{\theta\theta}(r,\theta) = y_2\Big(ln(r), sin(2\theta), cos(2\theta), \theta\Big) \tag{7.4.2}$$

$$\varepsilon_{r\theta}(r,\theta) = y_3\Big(ln(r), sin(2\theta), cos(2\theta), \theta\Big) \tag{7.4.3}$$

are true. From Eq. (3.1.13) the displacement u in r direction can be obtained:

$$\begin{aligned} u(r,\theta) &= \int y_1\Big(ln(r), sin(2\theta), cos(2\theta), \theta\Big)dr + h(\theta) \\ &\equiv rY_1\Big(ln(r), sin(2\theta), cos(2\theta), \theta\Big) + h(\theta) \end{aligned} \tag{7.4.4}$$

and from Eq. (3.1.14) the displacement v in θ direction is

$$\begin{aligned} v(r,\theta) &= \int \Big[y_2\Big(ln(r), sin(2\theta), cos(2\theta), \theta\Big)\, r - u(r,\theta) \Big]\, d\theta + f(r) \\ &\equiv rY_2\Big(ln(r), sin(2\theta), cos(2\theta), \theta\Big) + f(r). \end{aligned} \tag{7.4.5}$$

Due to the requirement of $u = v = 0$ at r=0, there must be $h(\theta) = 0$. The unknown function f(r) should be determined from Eq. (3.1.15), i.e.

$$\begin{aligned} y_3\Big(ln(r), sin(2\theta), cos(2\theta), \theta\Big) &= \frac{1}{2}\left(\frac{\partial Y_1}{\partial \theta} + \frac{\partial (rY_2)}{\partial r} - Y_2 + \frac{\partial f(r)}{\partial r} - \frac{f(r)}{r} \right) \\ &= \frac{1}{2}\left(\frac{\partial Y_1}{\partial \theta} + r\frac{\partial (Y_2)}{\partial r} + \frac{\partial f(r)}{\partial r} - \frac{f(r)}{r} \right). \end{aligned} \tag{7.4.6}$$

After simplifying, Eq. (7.4.6) yields

$$\frac{df(r)}{dr} - \frac{f(r)}{r} + H = 0. \tag{7.4.7}$$

The general solution of Eq. (7.4.7) is

$$f(r) = Cr - rln(r)H, \tag{7.4.8}$$

where C is an unknown constant. Finally, the displacements can be calculated from

$$u(r,\theta) = rY_1\Big(ln(r), sin(2\theta), cos(2\theta), \theta\Big) \tag{7.4.9}$$

$$v(r,\theta) = rY_2\Big(ln(r), sin(2\theta), cos(2\theta), \theta\Big) + Cr - rln(r)H. \tag{7.4.10}$$

For the type of $r^{-\omega}ln(r)$ stress singularity, there is

$$\varepsilon_{rr}(r,\theta) = \bar{y}_1\Big(r^{-\omega}, r^{-\omega}\, ln(r), sin[(\omega-2)\theta], cos[(\omega-2)\theta], sin(\omega\theta), cos(\omega\theta), \theta\Big) \tag{7.4.11}$$

$$\varepsilon_{\theta\theta}(r,\theta) = \bar{y}_2\Big(r^{-\omega}, r^{-\omega}\, ln(r), sin[(\omega-2)\theta], cos[(\omega-2)\theta], sin(\omega\theta), cos(\omega\theta), \theta\Big) \tag{7.4.12}$$

$$\varepsilon_{r\theta}(r,\theta) = \bar{y}_3\Big(r^{-\omega}, r^{-\omega}\, ln(r), sin[(\omega-2)\theta], cos[(\omega-2)\theta], sin(\omega\theta), cos(\omega\theta), \theta\Big) \tag{7.4.13}$$

In analogy,

$$u(r,\theta) = r^{1-\omega}\bar{Y}_1\Big(ln(r), sin[(\omega-2)\theta], cos[(\omega-2)\theta], sin(\omega\theta), cos(\omega\theta), \theta\Big) \tag{7.4.14}$$

$$v(r,\theta) = r^{1-\omega}\bar{Y}_2\Big(ln(r), sin[(\omega-2)\theta], cos[(\omega-2)\theta], sin(\omega\theta), cos(\omega\theta), \theta\Big) + \bar{f}(r), \tag{7.4.15}$$

where the determination of $\bar{f}(r)$ is the same as for f(r) in Eq. (7.4.7), but H should be replaced by $\bar{H}$.

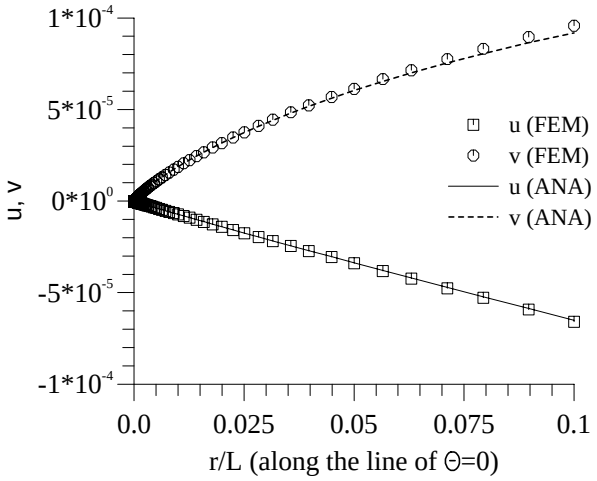

Figure 7.23: A comparison of the displacements calculated from FEM and Eqs. (7.4.16) through (7.4.19) for example 1 in Section 7.1 along the line of $\theta = 0°$.

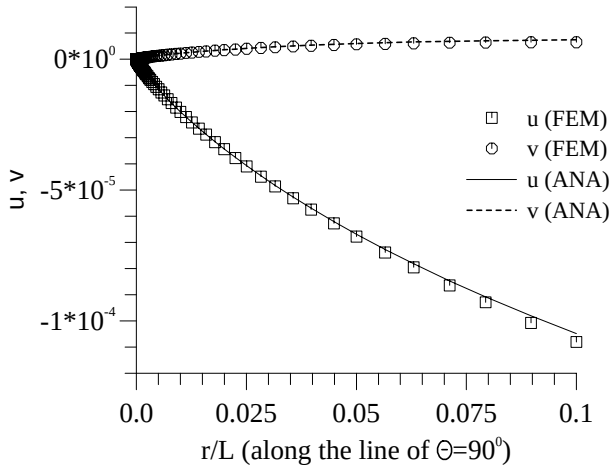

Figure 7.24: A comparison of the displacements calculated from FEM and Eqs. (7.4.16) through (7.4.19) for example 1 in Section 7.1 along the line of $\theta = 90°$.

For an arbitrary geometry the function Y_1, Y_2, and the constant H or $\bar{Y}_1, \bar{Y}_2$, and the constant $\bar{H}$ can be determined analytically, but in a very long form. As an example, the displacements will be given below for a joint with $\theta_1 = -\theta_2 = 90°$ and for the type of ln(r) stress singularity. For plane stress the displacements in materials 1 and 2 are:

$$
\begin{aligned}
u^{(1)} = \frac{TQ}{E_1 Z^2}(r/L)\Big\{ & 8\,[(\nu_1+1)\cos(2\theta)+\nu_1-1]\,Z\alpha\,\ln(r/L) \\
& + 2\,(\alpha-1)\pi Z(\nu_1+1)\sin(2\theta) - 8\,Z\alpha\,(\nu_1+1)\sin(2\theta)\theta + 4\,(\alpha+1)\pi Z(1-\nu_1)\theta \\
& + \Big[-256\,\alpha^3 + 64\left(\pi^2+8\right)\beta\,\alpha^2 + \left(-64(4+\pi^2)\beta^2 + 8\,Z - 4\,ZK\right)\alpha \\
& \quad -Z\pi^2 - 8\,Z\beta\Big](\nu_1+1)\cos(2\theta) \\
& + 256\,\alpha^3 - 64(\pi^2+8)\beta\,\alpha^2 + \left(64(\pi^2+4)\beta^2 - 2\,Z\pi^2 + 4\,ZK - 8\,\frac{\nu_1 Z}{\nu_1-1}\right)\alpha \\
& + 8\,Z\beta - Z\pi^2\Big\} + \alpha_1 T(r/L)
\end{aligned}
\tag{7.4.16}
$$

$$
\begin{aligned}
v^{(1)} = \frac{TQ}{2E_1 Z^2}(r/L)\Big\{ & -16\,\sin(2\theta)Z\alpha\,\ln(r/L)\,(\nu_1+1) + \Big\{\Big[128\alpha\left(4+\pi^2\right)\beta^2 \\
& + 16\left(-64\,\alpha^2 + Z - 8\,\alpha^2\pi^2\right)\beta + 2\left(4\,\alpha\,K - 8\,\alpha + \pi^2\right)Z + 512\,\alpha^3\Big]\sin(2\theta) \\
& + 4\,(\alpha-1)\pi Z\cos(2\theta) - 16\,\alpha\,\cos(2\theta)\theta\,Z\Big\}(\nu_1+1) - 32\,\alpha\,\theta\,Z\Big\} -
\end{aligned}
$$

$$- \quad \frac{8\pi QT(\alpha+1)}{E_1 Z}\,(r/L)\ln(r/L) + C_1\,(r/L) \tag{7.4.17}$$

$$\begin{aligned} u^{(2)} = {} & \frac{T\,Q}{E_2 Z^2}\,(r/L)\Big\{8\,\Big((\nu_2+1)\cos(2\,\theta) - 1 + \nu_2\Big)\,Z\,\alpha\,\ln(r/L) \\ & - 2\,(1+\alpha)\,\pi\,Z\sin(2\,\theta)\,(\nu_2+1) - 8\,Z\alpha\,\sin(2\,\theta)\theta\,\,(\nu_2+1) - 4\,\,(\alpha-1)\,\pi\,Z\theta\,\,(1-\nu_2) \\ & + \quad \Big[-256\,\alpha^3 + 64\,\Big(\pi^2+8\Big)\,\beta\,\alpha^2 + \Big(-64(4+\,\pi^2)\beta^2 + 4\,(2-\,K)\,Z\Big)\,\alpha \\ & + \quad Z\pi^2 - 8\,Z\beta\Big]\,(\nu_2+1)\cos(2\,\theta) + 256\,\alpha^3 - 64\,\Big(\pi^2+8\,\Big)\,\beta\alpha^2 \\ & - \quad \Big(2(\,\pi^2 - 2\,K + 4\,\frac{\nu_2}{-1+\nu_2})Z - 64\,\pi^2\beta^2 - 256\,\beta^2\Big)\,\alpha \\ & + \quad \Big(\pi^2+8\,\beta\Big)\,Z\Big\} + \alpha_2 T(r/L) \end{aligned} \tag{7.4.18}$$

$$\begin{aligned} v^{(2)} = {} & \frac{T\,Q}{2E_2 Z^2}\,(r/L)\Big\{-16\,(1+\,\nu_2)\,\alpha\,Z\sin(2\,\theta)\ln(r/L) + \Big\{[512\,\alpha^3 - 128\,\Big(\pi^2+8\Big)\,\beta\,\alpha^2 \\ & + \quad \Big(128(4+\,\pi^2)\beta^2 + 8\,(\,K-2)\,Z\Big)\,\alpha - 2\,Z\pi^2 + 16\,Z\beta]\sin(2\,\theta) \\ & - \quad 4\,\,(1+\alpha)\,\pi\,Z\cos(2\,\theta) - 16\,\alpha\,\cos(2\,\theta)\theta\,Z\Big\}\,(\nu_2+1) - 32\,\alpha\,\theta\,Z\Big\} \\ & + \quad \frac{8\pi QT(\alpha-1)}{E_2 Z}(r/L)ln(r/L) + \Big\{\frac{2\,(\,\nu_2+1)\,\pi\,qT\,(\alpha+1)}{E_2 Z} \\ & + \quad \frac{2\,(1+\,\nu_1)\,\pi\,qT\,(\alpha-1)}{E_1 Z} + C_1\Big\}(r/L) \end{aligned} \tag{7.4.19}$$

where Q and Z result from Eqs.(7.1.38) and (7.1.39). The quantity C_1 should be determined from the numerical stress analysis, as it was done for the K-factor. For this joint geometry the constant H in material 1 is

$$H = \frac{8\pi QT(\alpha+1)}{E_1 Z} \tag{7.4.20}$$

and in material 2 reads

$$H = -\frac{8\pi QT(\alpha-1)}{E_2 Z}. \tag{7.4.21}$$

For the example given in Section 7.1 the displacements have been calculated from FEM and Eqs.(7.4.16) through (7.4.19). Here, the unknown constant C_1 is determined from the displacement v at $\theta = 0$ and r/L=0.01, which gives $C_1 = 3.8499 \times 10^{-5}$. In Figs. 7.23, 7.24, and 7.25 the results along $\theta = 0, \theta = 90°$, and $\theta = -90°$ are compared. It can be seen that they are in good agreement in the range of $r/L < 0.1$. Especially for a very small value of r/L, the analytical equations may describe the displacements very well. To see this clearly, the absolute values of the displacements, which are the same as those in Figs. 7.23, 7.24, and 7.25 are plotted vs. r/L on a double logarithmic scale in Figs. 7.26, 7.27 and 7.28.

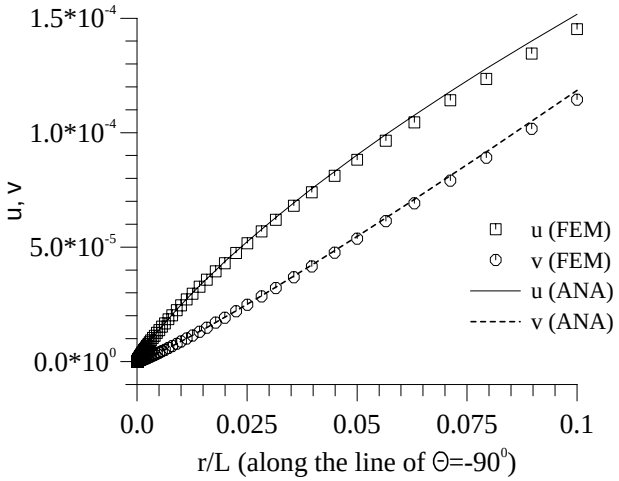

Figure 7.25: A comparison of the displacements calculated from FEM and Eqs. (7.4.16) through (7.4.19) for example 1 in Section 7.1 along the line of $\theta = -90°$.

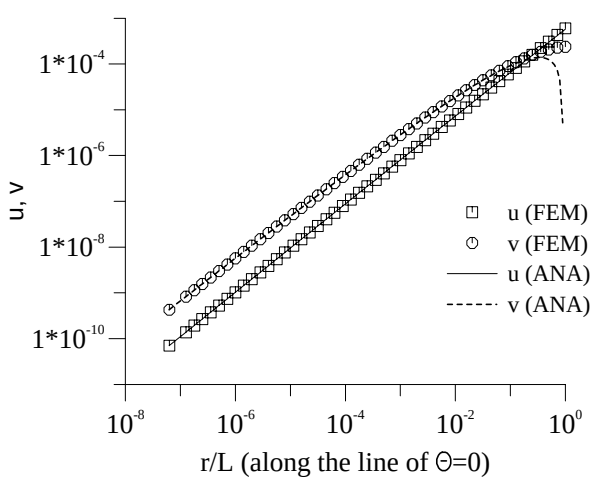

Figure 7.26: The same as in Fig. 7.23, but on a double-logarithmic scale.

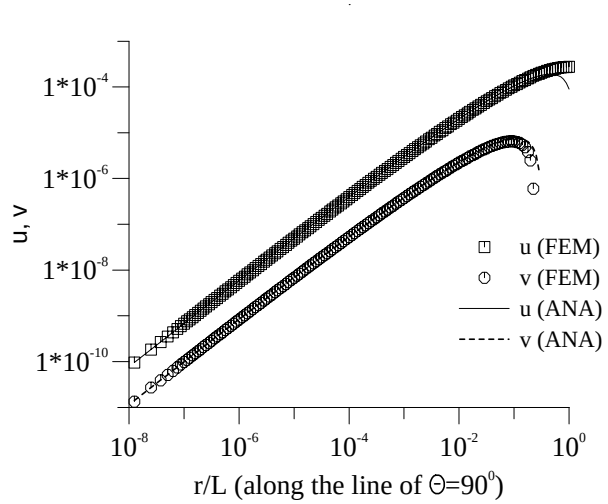

Figure 7.27: The same as in Fig. 7.24, but on a double-logarithmic scale.

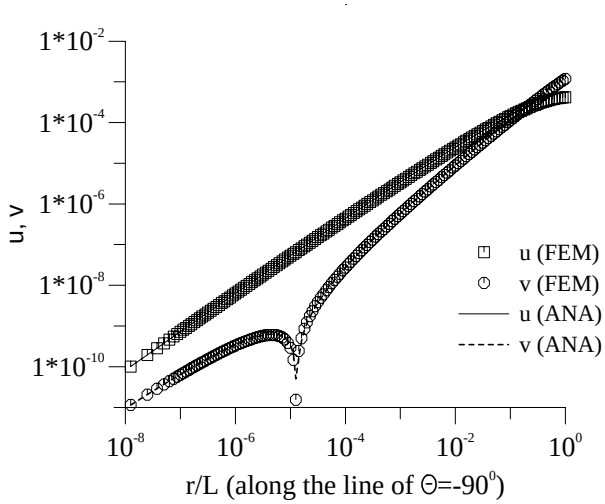

Figure 7.28: The same as in Fig. 7.25, but on a double-logarithmic scale.

Chapter 8

Joint with a Given Displacement at One Edge

In this Section a joint with a free edge and a given displacement edge will be considered. The analytical description of the stress field near the singular point will be studied in details. In Sections 8.1 and 8.2 the determination of the stress exponent, angular functions, and regular stress term will be given. The general behavior of the stress exponents is shown in Section 8.3 for various geometries and material combinations. It will be shown that for the same joint geometry and material combination the singularity of a joint with a given displacement at one edge is much stronger than that one of a joint with free edges. For a joint with a given displacement at one edge the stress exponent may take the value about 1 and there may be three strong singular terms.

8.1 Determination of the Stress Exponents and the Angular Functions

For a joint with a free edge and a given displacement edge (see Fig. 8.1) the boundary conditions are:

at the interface

$$\begin{aligned} u_1(r,0) &= u_2(r,0), \\ v_1(r,0) &= v_2(r,0), \\ \sigma_{\theta\theta 1}(r,0) &= \sigma_{\theta\theta 2}(r,0), \\ \sigma_{r\theta 1}(r,0) &= \sigma_{r\theta 2}(r,0), \end{aligned} \tag{8.1.1}$$

for the free edge

$$\begin{aligned} \sigma_{\theta\theta 1}(r,\theta_1) = 0, \\ \sigma_{r\theta 1}(r,\theta_1) = 0, \end{aligned} \tag{8.1.2}$$

for the given displacement edge

$$\begin{aligned} \sigma_{r\theta 2}(r,\theta_2) &= 0, \\ v_2(r,\theta_2) &= 0. \end{aligned} \tag{8.1.3}$$

This also represents the case of a symmetrical problem as shown in Fig. 8.2.

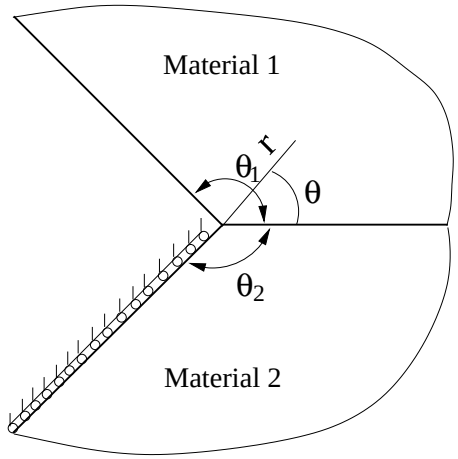

Figure 8.1: A joint with a free edge and a given displacement edge.

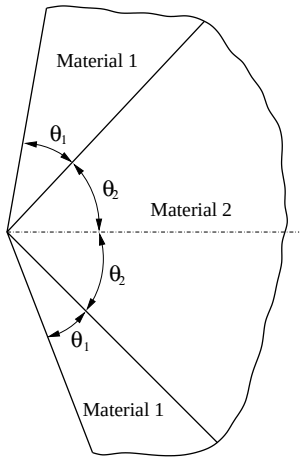

Figure 8.2: A symmetric joint geometry.

To solve this problem, the stress function as given in Eq. (3.1.3) will be used. From these eight conditions, the following equations hold for $\lambda_n \neq 0, 1, 2$ (n=1,2,3,...)

$$\begin{aligned} B_{1n}\mu[2(1-\nu_1) &+ \lambda_n(1+\nu_1)] - D_{1n}\mu(1+\nu_1)(2-\lambda_n) \\ &- B_{2n}[2(1-\nu_2) + \lambda_n(1+\nu_2)] + D_{2n}(1+\nu_2)(2-\lambda_n) = 0 \end{aligned} \tag{8.1.4}$$

$$\begin{aligned} A_{1n}\mu[2(1-\nu_1) &+ (2-\lambda_n)(1+\nu_1)] - C_{1n}\mu(1+\nu_1)(2-\lambda_n) \\ &- A_{2n}[2(1-\nu_2) + (2-\lambda_n)(1+\nu_2)] + C_{2n}(1+\nu_2)(2-\lambda_n) = 0 \end{aligned} \tag{8.1.5}$$

$$B_{1n} + D_{1n} - B_{2n} - D_{2n} = 0 \tag{8.1.6}$$

$$A_{1n}\lambda_n + C_{1n}(2-\lambda_n) - A_{2n}\lambda_n - C_{2n}(2-\lambda_n) = 0 \tag{8.1.7}$$

$$\begin{aligned} A_{1n}\sin(\lambda_n\theta_1) &+ B_{1n}\cos(\lambda_n\theta_1) \\ &+ C_{1n}\sin[(2-\lambda_n)\theta_1] + D_{1n}\cos[(2-\lambda_n)\theta_1] = 0 \end{aligned} \tag{8.1.8}$$

$$A_{1n}\lambda_n\cos(\lambda_n\theta_1) - B_{1n}\lambda_n\sin(\lambda_n\theta_1) + C_{1n}(2-\lambda_n)\cos[(2-\lambda_n)\theta_1] - D_{1n}(2-\lambda_n)\sin[(2-\lambda_n)\theta_1] = 0 \tag{8.1.9}$$

$$A_{2n}\lambda_n\cos(\lambda_n\theta_2) - B_{2n}\lambda_n\sin(\lambda_n\theta_2) + C_{2n}(2-\lambda_n)\cos[(2-\lambda_n)\theta_2] - D_{2n}(2-\lambda_n)\sin[(2-\lambda_n)\theta_2] = 0 \tag{8.1.10}$$

$$\begin{aligned} A_{2n}[2(1-\nu_2) &+ (2-\lambda_n)(1+\nu_2)]cos(\lambda_n\theta_2) - \\ &- B_{2n}[2(1-\nu_2)+(2-\lambda_n)(1+\nu_2)]sin(\lambda_n\theta_2) \\ &- C_{2n}(1+\nu_2)(2-\lambda_n)cos[(2-\lambda_n)\theta_2] + \\ &+ D_{2n}(1+\nu_2)(2-\lambda_n)sin[(2-\lambda_n)\theta_2] = 0. \end{aligned} \tag{8.1.11}$$

They are the same for mechanical loading and thermal loading. This equation system can be rewritten in a matrix form as

$$[A]_{8\times8}\{X\}_{8\times1} = \{0\}_{8\times1} \tag{8.1.12}$$

where $\{X\}_{8\times1} = \{A_{1n}, B_{1n}, C_{1n}, D_{1n}, A_{2n}, B_{2n}, C_{2n}, D_{2n}\}^t$ and $[A]_{8\times8}$ is its coefficient matrix. $\{X\}_{8\times1}$ is unknown and $[A]_{8\times8}$ includes the unknown exponent λ_n, the material properties (E_k, ν_k, k=1,2 for materials 1 and 2), and the geometry angles (θ_1, θ_2). Equation (8.1.12) has a nonzero solution, if and only if

$$\mathrm{Det}([A]_{8\times8}) = 0 \tag{8.1.13}$$

is satisfied. In Eq. (8.1.13) the only unknown is the exponent λ_n. Its solutions are the eigenvalues of this problem.
The expansion of Eq. (8.1.13) for an arbitrary joint geometry with θ_1, θ_2 is

$$\begin{aligned} \mathrm{Det}([A]_{8\times8}) &= -\frac{64(1+t_n)^2}{(1+\alpha)^2}\Big\{t_n\cos(2\theta_2)\sin(2\theta_1) + \cos(2t_n\theta_2)\sin(2t_n\theta_1) - \\ &- t_n\cos(2\theta_1)\sin(2\theta_2) - \cos(2t_n\theta_1)\sin(2t_n\theta_2) + \\ &+ 2\beta^2\Big[-1+{t_n}^2-{t_n}^2\cos(2\theta_1)+\cos(2t_n\theta_1)\Big](t_n\sin(2\theta_2)+\sin(2t_n\theta_2)) + \\ &+ \beta\Big[2t_n\sin(2\theta_2) - 2t_n\cos(2t_n\theta_1)\sin(2\theta_2) + 2{t_n}^2\sin(2t_n\theta_2) - \\ &- 2{t_n}^2\cos(2\theta_1)\sin(2t_n\theta_2)\Big] + \alpha\Big[2t_n\cos(2t_n\theta_1)\sin(2\theta_2) + 2\sin(2t_n\theta_2) - \\ &- 2{t_n}^2\sin(2t_n\theta_2) + 2{t_n}^2\cos(2\theta_1)\sin(2t_n\theta_2)\Big] + \\ &+ \alpha\beta\Big[2t_n\sin(2\theta_2) - 4{t_n}^3\sin(2\theta_2) + 4{t_n}^3\cos(2\theta_1)\sin(2\theta_2) - \\ &- 2t_n\cos(2t_n\theta_1)\sin(2\theta_2) - 2{t_n}^2\sin(2t_n\theta_2) + 2{t_n}^2\cos(2\theta_1)\sin(2t_n\theta_2)\Big] + \\ &+ \alpha^2\Big[-t_n\sin[2(\theta_1-\theta_2)] + {t_n}^3\sin[2(\theta_1-\theta_2)] - 2t_n\sin(2\theta_2) + \\ &+ 2{t_n}^3\sin(2\theta_2) - {t_n}^3\sin[2(\theta_1+\theta_2)] - \sin[2t_n(\theta_1+\theta_2)]\Big]\Big\}, \end{aligned} \tag{8.1.14}$$

where α, β are the Dundurs parameters and t_n=1-λ_n. The expansion of Eq. (8.1.13) in λ_n form (not in t_n) follows

$$\begin{aligned}\mathrm{Det}([A]_{8\times 8}) &= -\frac{64(2-\lambda_n)^2}{(1+\alpha)^2}\Big\{Y_1 sin[2\theta_2] + Y_2 sin[2(\theta_1-\theta_2)] \\ &+ Y_3 sin[2(\theta_1+\theta_2)] + Y_4 sin[2(1-\lambda_n)\theta_2] \\ &+ Y_5 sin[2(1-\lambda_n)(\theta_1-\theta_2)] + Y_6 sin[2(1-\lambda_n)(\theta_1+\theta_2)] \\ &+ Y_7 sin[2((1-\lambda_n)\theta_1-\theta_2)] + Y_8 sin[2((1-\lambda_n)\theta_1+\theta_2)] \\ &+ Y_9 sin[2(\theta_1-(1-\lambda_n)\theta_2)] + Y_{10} sin[2(\theta_1+(1-\lambda_n)\theta_2)]\Big\}\end{aligned} \tag{8.1.15}$$

with

$$Y_1 = (1-\lambda_n)\{2\beta - 2\alpha\beta[2(1-\lambda_n)^2-1] + \alpha^2 2\lambda_n(\lambda_n-2) + \beta^2 2\lambda_n(\lambda_n-2)\} \tag{8.1.16}$$

$$Y_2 = (1-\lambda_n)\{1 - 2\alpha\beta(1-\lambda_n)^2 + \alpha^2\lambda_n(\lambda_n-2) + \beta^2(1-\lambda_n)^2\} \tag{8.1.17}$$

$$Y_3 = (\alpha-\beta)^2(\lambda_n-1)^3 \tag{8.1.18}$$

$$Y_4 = 2\Big\{\beta^2\lambda_n(\lambda_n-2) + \beta(1-\lambda_n) + \alpha\lambda_n(2-\lambda_n) - \alpha\beta(1-\lambda_n)^2\Big\} \tag{8.1.19}$$

$$Y_5 = 1-\beta^2 \tag{8.1.20}$$

$$Y_6 = \beta^2 - \alpha^2 \tag{8.1.21}$$

$$Y_7 = (\alpha-\beta)(\beta-1)(1-\lambda_n) \tag{8.1.22}$$

$$Y_8 = -Y_7 \tag{8.1.23}$$

$$Y_9 = -(\alpha-\beta)(\beta+1)(1-\lambda_n)^2 \tag{8.1.24}$$

$$Y_{10} = -Y_9. \tag{8.1.25}$$

The stress exponent ω_n is equal to λ_n.

For the special case of $\theta_1 = -\theta_2$, there is

$$\begin{aligned}
\mathrm{Det}([A]_{8\times 8}) &= -\frac{64(1+t_n)^2}{(1+\alpha)^2}\Big\{8\alpha^2 t_n\left(1-{t_n}^2\right)\cos(\theta_1)\sin(\theta_1)^3 + \\
&+ \beta\Big[-2t_n\sin(2\theta_1) + 2t_n\cos(2t_n\theta_1)\sin(2\theta_1) - 2{t_n}^2\sin(2t_n\theta_1) + \\
&+ 2{t_n}^2\cos(2\theta_1)\sin(2t_n\theta_1)\Big] + \alpha\Big[-2t_n\cos(2t_n\theta_1)\sin(2\theta_1) \\
&- 2\sin(2t_n\theta_1) + 2{t_n}^2\sin(2t_n\theta_1) - 2{t_n}^2\cos(2\theta_1)\sin(2t_n\theta_1)\Big] + \\
&+ \alpha\beta\Big[-2t_n\sin(2\theta_1) + 4{t_n}^3\sin(2\theta_1) + 2t_n\cos(2t_n\theta_1)\sin(2\theta_1) - \\
&- 2{t_n}^3\sin(4\theta_1) + 2{t_n}^2\sin(2t_n\theta_1) - 2{t_n}^2\cos(2\theta_1)\sin(2t_n\theta_1)\Big] + \\
&+ \beta^2\Big[2t_n\sin(2\theta_1) - 2{t_n}^3\sin(2\theta_1) - 2t_n\cos(2t_n\theta_1)\sin(2\theta_1) + \\
&+ {t_n}^3\sin(4\theta_1) + 2\sin(2t_n\theta_1) - 2{t_n}^2\sin(2t_n\theta_1) - \sin(4t_n\theta_1) \\
&+ 2{t_n}^2\cos(2\theta_1)\sin(2t_n\theta_1)\Big] + t_n\sin(4\theta_1) + \sin(4t_n\theta_1)\Big\}. \qquad (8.1.26)
\end{aligned}$$

At $\theta_1 = -\theta_2 = \pi/4$, the determinant is

$$\begin{aligned}
\mathrm{Det}([A]_{8\times 8}) = &-\frac{64(1+t_n)^2}{(1+\alpha)^2}\Big\{2\alpha^2 t_n\left(1-{t_n}^2\right) + \sin(\pi t_n) \\
&+ \beta\Big[-2t_n + 2t_n\cos(\frac{\pi t_n}{2}) - 2{t_n}^2\sin(\frac{\pi t_n}{2})\Big] + \\
&+ \alpha\Big[-2t_n\cos(\frac{\pi t_n}{2}) - 2\sin(\frac{\pi t_n}{2}) + 2{t_n}^2\sin(\frac{\pi t_n}{2})\Big] + \\
&+ 2\alpha\beta t_n\Big[-1 + 2{t_n}^2 + \cos(\frac{\pi t_n}{2}) + t_n\sin(\frac{\pi t_n}{2})\Big] + \\
&+ \beta^2\Big[2t_n - 2{t_n}^3 - 2t_n\cos(\frac{\pi t_n}{2}) + 2\sin(\frac{\pi t_n}{2}) - 2{t_n}^2\sin(\frac{\pi t_n}{2}) - \sin(\pi t_n)\Big]\Big\}. \\
& \qquad (8.1.27)
\end{aligned}$$

For $\theta_1 = -\theta_2 = \pi/2$ the determinant can be simplified as

$$\mathrm{Det}([A]_{8\times 8}) = \frac{128(1+t_n)^2\sin(t_n\pi)}{(1+\alpha)^2}(1-\beta^2)\Big\{\frac{2t_n^2}{1-\beta}(\beta-\alpha) - \frac{\beta^2-\alpha}{1-\beta^2} - cos(\pi t_n)\Big\}. \qquad (8.1.28)$$

For $\theta_1 = -\theta_2 = \pi$, i.e. a joint with an interface crack, in which one crack surface has a given displacement, the determinant can be simplified as

$$\mathrm{Det}([A]_{8\times 8}) = \frac{128(1+t_n)^2\sin(2t_n\pi)\Big(\alpha-\beta^2-(1-\beta^2)\cos(2t_n\pi)\Big)}{(1+\alpha)^2}. \qquad (8.1.29)$$

It follows from Eq. (8.1.29) that $t_n = 0.5$, i.e. $\lambda_n = 0.5$ always is the solution of $\mathrm{Det}([A]_{8\times 8}) = 0$ irrespective of the material data. In addition, eigenvalues exist, which do not equal 0.5, and they depend on the material combination (see figures in Section 8.3).

From Eqs.(8.1.14-8.1.29) it can see that if t_n ($t_n \neq -1$) is the solution of $\mathrm{Det}([A]_{8\times 8}) = 0$, $-t_n$ is also. This means that if λ_n is the eigenvalue of the problem, $2-\lambda_n$ is also.

Now the eigenvalues λ_n ($\lambda_n = 1 - t_n$) are known. The stress exponent ω_n and the angular functions $f_{ijn}(\theta)$ can then be calculated. The stress exponent is

$$\omega_n = \lambda_n \qquad (-0.5 \leq \lambda_n < 1). \tag{8.1.30}$$

The coefficients of the angular functions for $\theta_1 = -\theta_2 = \pi/2$ are

$$\begin{aligned} A_1 &= (2-\lambda_n)\Big\{ -1 + \beta\left(-3 + 4\lambda_n - 2\lambda_n^2\right) + \\ &+ \alpha 2\lambda_n\left(-1+\lambda_n\right) - (1+\beta)\cos(\pi\lambda_n)\Big\}\sin(\frac{\pi\lambda_n}{2}) \end{aligned} \tag{8.1.31}$$

$$\begin{aligned} B_1 &= (2-\lambda_n)\cos(\frac{\pi\lambda_n}{2})\Big\{1 + \beta\left(1-2\lambda_n^2\right) - 2\lambda_n\alpha\left(1-\lambda_n\right) + \\ &- (1+\beta)\cos(\pi\lambda_n)\Big\} \end{aligned} \tag{8.1.32}$$

$$\begin{aligned} C_1 &= \Big\{ -\lambda_n + \beta\left(2 - 7\lambda_n + 8\lambda_n^2 - 2\lambda_n^3\right) + \alpha 2\lambda_n\left(2 - 3\lambda_n + \lambda_n^2\right) + \\ &+ \left[-\lambda_n + \beta\left(-2+3\lambda_n\right)\right]\cos(\pi\lambda_n)\Big\}\sin(\frac{\pi\lambda_n}{2}) \end{aligned} \tag{8.1.33}$$

$$\begin{aligned} D_1 &= -\cos(\frac{\pi\lambda_n}{2})\Big\{\lambda_n + \beta\left(2 - 3\lambda_n + 4\lambda_n^2 - 2\lambda_n^3\right) + \\ &+ \alpha 2\lambda_n\left(2 - 3\lambda_n + \lambda_n^2\right) + \left[-\lambda_n + \beta\left(-2+3\lambda_n\right)\right]\cos(\pi\lambda_n)\Big\} \end{aligned} \tag{8.1.34}$$

$$\begin{aligned} A_2 &= \frac{(2-\lambda_n)}{(1+\alpha)}\Big\{ -1 - \beta\left(3 - 6\lambda_n + 2\lambda_n^2\right) + 2\beta^2\left(-1 + 5\lambda_n - 6\lambda_n^2 + 2\lambda_n^3\right) + \\ &+ \alpha^2 2\lambda_n\left(3 - 5\lambda_n + 2\lambda_n^2\right) + \alpha\left[1 - 4\lambda_n + 2\lambda_n^2 + \beta\left(5 - 18\lambda_n + 22\lambda_n^2 - 8\lambda_n^3\right)\right] \\ &+ \Big[-1 + 2\beta^2\left(1-\lambda_n\right) + \beta\left(-1+2\lambda_n\right) + \\ &+ \alpha\left[1 - 2\lambda_n + \beta\left(-1+2\lambda_n\right)\right]\Big]\cos(\pi\lambda_n)\Big\}\sin(\frac{\pi\lambda_n}{2}) \end{aligned} \tag{8.1.35}$$

$$\begin{aligned} B_2 = \frac{(2-\lambda_n)\cos(\frac{\pi\lambda_n}{2})}{(1+\alpha)}\Big\{1 - \beta\left(1 - 2\lambda_n + 2\lambda_n^2\right) - \beta^2 2\lambda_n\left(1 - 4\lambda_n + 2\lambda_n^2\right) - \\ - \alpha^2 2\lambda_n\left(3 - 5\lambda_n + 2\lambda_n^2\right) + \alpha\Big[1 - 4\lambda_n + 2\lambda_n^2 + \beta\left(-1 + 10\lambda_n - 18\lambda_n^2 + 8\lambda_n^3\right)\Big] \\ + \Big[-1 + \beta\left(1-2\lambda_n\right) + 2\beta^2\lambda_n + \alpha\left(-1 + \beta\left(1-2\lambda_n\right) + 2\lambda_n\right)\Big]\cos(\pi\lambda_n)\Big\} \end{aligned} \tag{8.1.36}$$

$$
\begin{aligned}
C_2 &= \frac{1}{(1+\alpha)}\Big\{ -\lambda_n + \beta\left(2 - 7\lambda_n + 6\lambda_n^2 - 2\lambda_n^3\right) + \\
&+ \beta^2 2\lambda_n\left(1 - 5\lambda_n + 6\lambda_n^2 - 2\lambda_n^3\right) + \alpha^2 2\lambda_n\left(2 - 7\lambda_n + 7\lambda_n^2 - 2\lambda_n^3\right) + \\
&+ \alpha\Big[\lambda_n - 4\lambda_n^2 + 2\lambda_n^3 + \beta\left(2 - 15\lambda_n + 30\lambda_n^2 - 26\lambda_n^3 + 8\lambda_n^4\right)\Big] + \\
&+ \Big[-\lambda_n + \beta\left(-2 + 3\lambda_n - 2\lambda_n^2\right) - \beta^2 2\lambda_n\left(1 - \lambda_n\right) + \\
&+ \alpha[-3\lambda_n + 2\lambda_n^2 + \beta\left(-2 + 3\lambda_n - 2\lambda_n^2\right)]\Big]\cos(\pi\lambda_n)\Big\}\sin(\frac{\pi\lambda_n}{2}) \qquad (8.1.37)
\end{aligned}
$$

$$
\begin{aligned}
D_2 &= \frac{\cos(\frac{\pi\lambda_n}{2})}{(1+\alpha)}\Big\{ -\lambda_n + \beta\left(2 - 3\lambda_n - 2\lambda_n^2 + 2\lambda_n^3\right) + \\
&+ \alpha^2 2\lambda_n\left(2 - 7\lambda_n + 7\lambda_n^2 - 2\lambda_n^3\right) + \beta^2 2\lambda_n\left(2 - 9\lambda_n + 8\lambda_n^2 - 2\lambda_n^3\right) + \\
&+ \alpha\Big[-\lambda_n + 4\lambda_n^2 - 2\lambda_n^3 + \beta\left(2 - 19\lambda_n + 38\lambda_n^2 - 30\lambda_n^3 + 8\lambda_n^4\right)\Big] + \\
&+ \Big[\lambda_n + \beta\left(-2 + 3\lambda_n - 2\lambda_n^2\right) - \beta^2 2\lambda_n\left(2 - \lambda_n\right) + \\
&+ \alpha[-3\lambda_n + 2\lambda_n^2 + \beta\left(-2 + 3\lambda_n - 2\lambda_n^2\right)]\Big]\cos(\pi\lambda_n)\Big\}. \qquad (8.1.38)
\end{aligned}
$$

The angular functions can be calculated from Eqs. (3.1.97- 3.1.99).

8.2 Determination of the Regular Stress Term

8.2.1 Joint under Thermal Loading

To determine the regular stress term, which corresponds to the solution of $\lambda_n = 0$ in the last section, the stress function given in Section 3.3 (see Eq. (3.3.1)) is used. The stresses and the displacement v have the same relations as in Section 3.3 (see Eqs. (3.3.2, 3.3.3,3.3.4,3.3.6)). Only for thermal loading the displacement u (see Eq. (3.3.5)) should be replaced by

$$
\begin{aligned}
u_{k0}(r,\theta) &= \frac{2r}{E_k}[\mathcal{A}_{\mathrm{k0}}\theta(1-\nu_{\mathrm{k}}) + \mathcal{B}_{\mathrm{k0}}(1-\nu_{\mathrm{k}}) - \mathcal{C}_{\mathrm{k0}}(1+\nu_{\mathrm{k}})\sin(2\theta) \\
&- \mathcal{D}_{\mathrm{k0}}(1+\nu_{\mathrm{k}})\cos(2\theta)] + \mathrm{r}\alpha_{\mathrm{k}}\mathrm{T}, \qquad (8.2.1)
\end{aligned}
$$

where the thermal strain $\alpha_k T$ (for plane stress) has been considered.
Insertion of Eqs. (3.3.3, 3.3.4, 3.3.6, 8.2.1) into Eqs. (8.1.1-8.1.3) gives

$$
\begin{aligned}
B_{10}\mu(1-\nu_1) &- D_{10}\mu(1+\nu_1) - B_{20}(1-\nu_2) + D_{20}(1+\nu_2) \\
&= E_2/2T(\alpha_2 - \alpha_1) \qquad (8.2.2)
\end{aligned}
$$

$$
-2C_{10}\mu(1+\nu_1) + F_{10}E_2 + 2C_{20}(1+\nu_2) - F_{20}E_2 = 0 \qquad (8.2.3)
$$

$$
\mu A_{10} - A_{20} = 0 \qquad (8.2.4)
$$

$$B_{10} + D_{10} - B_{20} - D_{20} = 0 \tag{8.2.5}$$

$$A_{10} + 2C_{10} - A_{20} - 2C_{20} = 0 \tag{8.2.6}$$

$$A_{10}\theta_1 + B_{10} + C_{10}\sin(2\theta_1) + D_{10}\cos(2\theta_1) = 0 \tag{8.2.7}$$

$$A_{10} + 2C_{10}\cos(2\theta_1) - 2D_{10}\sin(2\theta_1) = 0 \tag{8.2.8}$$

$$A_{20} + 2C_{20}\cos(2\theta_2) - 2D_{20}\sin(2\theta_2) = 0 \tag{8.2.9}$$

$$2[-C_{20}(1+\nu_2)\cos(2\theta_2) + D_{20}(1+\nu_2)\sin(2\theta_2)] + F_{20}E_2 = 0 \tag{8.2.10}$$

$$A_{20} = 0 \tag{8.2.11}$$

for plane stress with $\mu = E_2/E_1$. The regular stress term is independent of the coefficients F_{k0}. From Eqs. (8.2.4) and (8.2.11) it follows

$$A_{10} = A_{20} = 0. \tag{8.2.12}$$

Solving the Eqs. (8.2.2, 8.2.5 - 8.2.9) yields

$$B_{10} = \frac{Q\sin(2\theta_2)}{\Delta_{TH}} \tag{8.2.13}$$

$$C_{10} = -\frac{Q\sin(2\theta_1)\sin(2\theta_2)}{\Delta_{TH}} \tag{8.2.14}$$

$$D_{10} = -\frac{Q\cos(2\theta_1)\sin(2\theta_2)}{\Delta_{TH}} \tag{8.2.15}$$

$$B_{20} = \frac{Q\{\sin[2(\theta_1 - \theta_2)] + \sin(2\theta_2)\}}{\Delta_{TH}} \tag{8.2.16}$$

$$C_{20} = C_{10} \tag{8.2.17}$$

$$D_{20} = -\frac{Q\cos(2\theta_2)\sin(2\theta_1)}{\Delta_{TH}} \tag{8.2.18}$$

where

$$\Delta_{TH} = -\frac{2}{1+\alpha}\Big\{(1+\beta)\sin[2(\theta_1-\theta_2)] + 2\beta\sin(2\theta_2) + (\alpha-\beta)\sin[2(\theta_1+\theta_2)]\Big\} \tag{8.2.19}$$

$$Q = \frac{E_2}{2}T[\alpha_2 - \alpha_1] \tag{8.2.20}$$

for plane stress and

$$Q = \frac{E_2}{2(1-\nu_2^2)}T[\alpha_2(1+\nu_2) - \alpha_1(1+\nu_1)] \tag{8.2.21}$$

for plane strain.
For the special case of $\theta_2 = -\theta_1$, there is

$$B_{10} = -\frac{2Q\sin(2\theta_1)}{\Delta_{TH}} \tag{8.2.22}$$

$$C_{10} = \frac{2Q\sin^2(2\theta_1)}{\Delta_{TH}} \tag{8.2.23}$$

$$D_{10} = \frac{Q\sin(4\theta_1)}{\Delta_{TH}} \tag{8.2.24}$$

$$B_{20} = \frac{2Q[-\sin(2\theta_1) + \sin(4\theta_1)]}{\Delta_{TH}} \tag{8.2.25}$$

$$C_{20} = C_{10} \tag{8.2.26}$$

$$D_{20} = -D_{10} \tag{8.2.27}$$

with

$$\Delta_{TH} = \frac{8\sin(2\theta_1)}{1+\alpha}\{\beta - \cos(2\theta_1) - \beta\cos(2\theta_1)\}. \tag{8.2.28}$$

The regular stress term can be determined analytically from Eqs. (3.3.2- 3.3.4).
If $\theta_2 = -\theta_1 = \pi/2$ or π, it can be seen from Eq. (8.2.28) that Δ_{TH} is always zero for $\alpha \neq -1$. Therefore, the regular stress term cannot be determined directly from Eqs. (8.2.22-8.2.27). By using the l'Hospital principle at the points of $\theta_2 = -\theta_1 = \pi/2$ and π, the six coefficients $B_{10}, C_{10}, D_{10}\ B_{20}, C_{20}, D_{20}$ can be determined. They are

$$B_{10} = -Q\frac{1+\alpha}{4(1+2\beta)} \tag{8.2.29}$$

$$C_{10} = C_{20} = 0 \tag{8.2.30}$$

$$D_{10} = B_{10} \tag{8.2.31}$$

$$B_{20} = 3B_{10} \tag{8.2.32}$$

$$D_{20} = -B_{10}, \tag{8.2.33}$$

for $\theta_1 = -\theta_2 = \pi/2$ and

$$B_{10} = \frac{Q(1+\alpha)}{4} \tag{8.2.34}$$

$$C_{10} = C_{20} = 0 \tag{8.2.35}$$

$$D_{10} = -B_{10} \tag{8.2.36}$$

$$B_{20} = -B_{10} \tag{8.2.37}$$

$$D_{20} = B_{10} \tag{8.2.38}$$

for $\theta_1 = -\theta_2 = \pi$. The regular stress term in polar coordinates can be calculated from Eqs. (3.3.2- 3.3.4). In Cartesian coordinates the regular stress term can be simplified as

$$\begin{aligned} \sigma_{xx10} &= \tau_{xy10} = 0 \\ \sigma_{yy10} &= -Q\frac{1+\alpha}{1+2\beta} \\ \sigma_{xx20} &= 2\sigma_{yy10} \\ \sigma_{yy20} &= \sigma_{yy10} \\ \tau_{xy20} &= 0. \end{aligned} \tag{8.2.39}$$

for $\theta_1 = -\theta_2 = \pi/2$ and

$$\begin{aligned} \sigma_{yy10} &= \tau_{xy10} = \sigma_{yy20} = \tau_{xy20} = 0 \\ \sigma_{xx10} &= -\sigma_{xx20} = Q(1+\alpha) \end{aligned} \tag{8.2.40}$$

for $\theta_1 = -\theta_2 = \pi$. This means that for a joint with $\theta_1 = -\theta_2 = 90^0$ the shear stress component of the regular stress term and the stress component parallel to the interface in material 1 are always zero in Cartesian coordinates. For a joint with an interface crack, only the stress component parallel to the interface is nonzero.

8.2.2 Joint under Mechanical Loading

For joints under mechanical loading Eqs. (8.2.2-8.2.11) are still valid, in which T should be replaced by zero. From Eqs. (8.2.13-8.2.18) it is known that for $T = 0$ (i.e. Q=0) the coefficients and hence the regular stress term are zero in the general cases. However, for some special material combinations and geometries the regular stress term is nonzero. Equation system (8.2.2 - 8.2.11) is a homogeneous one for $\Delta T = 0$. The condition of it having a non-zero solution is that the determinant of its coefficient matrix is zero,

$$\frac{16}{1+\alpha}\Big\{(1+\beta)\sin[2(\theta_1-\theta_2)] + 2\beta\sin(2\theta_2) + (\alpha-\beta)\sin[2(\theta_1+\theta_2)]\Big\} = 0. \tag{8.2.41}$$

This means that if

$$\alpha = \beta - \frac{(1+\beta)\sin[2(\theta_1-\theta_2)] + 2\beta\sin(2\theta_2)}{\sin[2(\theta_1+\theta_2)]} \tag{8.2.42}$$

with $\theta_2 \neq -\theta_1$, the regular stress term may be non-zero.
For $\alpha = \beta - \frac{(1+\beta)\sin[2(\theta_1-\theta_2)]+2\beta\sin(2\theta_2)}{\sin[2(\theta_1+\theta_2)]}$ and $\theta_2 \neq -\theta_1$, in case of an arbitrary geometry the coefficients of the regular stress term in Eqs. (3.3.28-3.3.30) are

$$A^*_{10} = A^*_{20} = 0 \tag{8.2.43}$$

$$B^*_{10} = 1 \tag{8.2.44}$$

$$C^*_{10} = -\sin(2\theta_1) \tag{8.2.45}$$

$$D^*_{10} = -\cos(2\theta_1) \tag{8.2.46}$$

$$B^*_{20} = \frac{2\cos(\theta_1-2\theta_2)\sin(\theta_1)}{\sin(2\theta_2)} \tag{8.2.47}$$

$$C^*_{20} = C^*_{10} \tag{8.2.48}$$

$$D^*_{20} = -\frac{\cos(2\theta_2)\sin(2\theta_1)}{\sin(2\theta_2)}, \tag{8.2.49}$$

with $\sin(2\theta_2) \neq 0$, i.e. $\theta_2 \neq -\pi/2$ or $-\pi$.
In case of $\theta_2 = -\pi/2$ or $\theta_2 = -\pi$ (i.e. $\sin(2\theta_2) = 0$), Eq. (8.2.41) is true only, if $\sin(2\theta_1) = 0$, i.e $\theta_1 = \pi/2$ or $\theta_1 = \pi$, where α and β are arbitrary. This may be true in four cases, (a) $\theta_1 = \pi/2$, $\theta_2 = -\pi/2$, (b) $\theta_1 = \pi/2$, $\theta_2 = -\pi$, (c) $\theta_1 = \pi$, $\theta_2 = -\pi/2$,

(d) $\theta_1 = \pi,\ \theta_2 = -\pi$. Cases (a) and (d) correspond to the joint with $\theta_2 = -\theta_1$, which will be discussed later on.
For the case (b) (i.e. $\theta_1 = \pi/2, \theta_2 = -\pi$) the regular stress term always is non-zero and

$$B^*_{10} = \frac{1+\alpha}{1-\alpha+4\beta} \tag{8.2.50}$$

$$C^*_{10} = C^*_{20} = 0 \tag{8.2.51}$$

$$D^*_{10} = B^*_{10} \tag{8.2.52}$$

$$B^*_{20} = \frac{1+3\alpha-4\beta}{1-\alpha+4\beta} \tag{8.2.53}$$

$$D^*_{20} = 1. \tag{8.2.54}$$

In Cartesian coordinates the regular stress term can be simplified as

$$\begin{aligned}
\sigma_{xx10} &= \tau_{xy10} = 0 \\
\sigma_{yy10} &= 4K_0\frac{1+\alpha}{1-\alpha+4\beta} \\
\sigma_{xx20} &= 8K_0\frac{\alpha-2\beta}{1-\alpha+4\beta} \\
\sigma_{yy20} &= \sigma_{yy10} \\
\tau_{xy20} &= 0.
\end{aligned} \tag{8.2.55}$$

For the case (c) (i.e. $\theta_1 = \pi, \theta_2 = -\pi/2$) the regular stress term always is non-zero and

$$B^*_{10} = -\frac{1+\alpha}{1-\alpha} \tag{8.2.56}$$

$$C^*_{10} = C^*_{20} = 0 \tag{8.2.57}$$

$$D^*_{10} = -B^*_{10} \tag{8.2.58}$$

$$B^*_{20} = -1 \tag{8.2.59}$$

$$D^*_{20} = 1. \tag{8.2.60}$$

The regular stress term in Cartesian coordinates is:

$$\sigma_{xx10} = -4K_0\frac{1+\alpha}{1-\alpha} \tag{8.2.61}$$

$$\sigma_{yy10} = \tau_{xy10} = 0 \tag{8.2.62}$$

and

$$\sigma_{xx20} = -4K_0 \tag{8.2.63}$$

$$\sigma_{yy20} = \tau_{xy20} = 0. \tag{8.2.64}$$

In case of $\theta_2 = -\theta_1$ Eq. (8.2.41) is simplified as

$$\sin(2\theta_1)[(1+\beta)\cos(2\theta_1) - \beta] = 0. \tag{8.2.65}$$

This means that if $\theta_1 = \pi/2$, or $\theta_1 = \pi$ and α, β arbitrary, or $\beta = \frac{\cos(2\theta_1)}{1-\cos(2\theta_1)}$ the regular stress term may be non-zero.

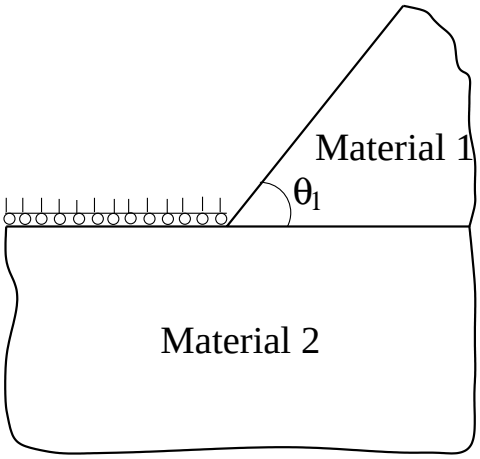

Figure 8.3: A joint: One material occupies the angle of 180°, the other is arbitrary.

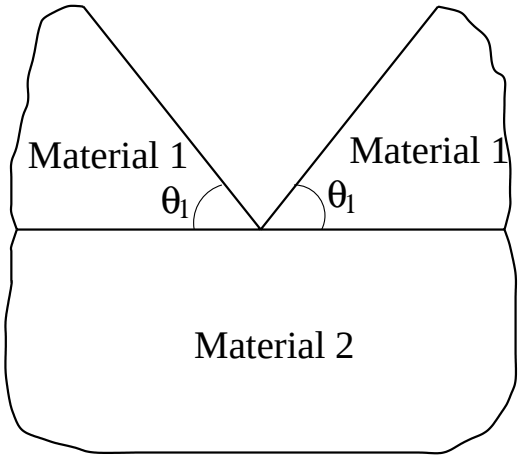

Figure 8.4: The joint is symmetric to the line of $\theta = 90°$ and material 2 occupies the angle of 180°.

In case of $\theta_2 = -\theta_1 = 90°$ (this is case (a)), the regular stress term always is non-zero, which is the same as that one of a joint with $\theta_1 = \pi/2, \theta_2 = -\pi$ (i.e. case (b)). It can be calculated from Eqs. (8.2.50-8.2.55).
In case of $\theta_2 = -\theta_1 = 180°$ (this is case (d)), the regular stress term always is non-zero, which is the same as that one of a joint with $\theta_1 = \pi, \theta_2 = -\pi/2$ (i.e. case (c)), and can be calculated from Eqs. (8.2.56-8.2.64).
In case of $\beta = \frac{\cos(2\theta_1)}{1-\cos(2\theta_1)}$ ($\theta_1 \neq 180°$) the coefficients of the regular stress term are

$$B^*_{10} = \frac{1}{\cos(2\theta_1)} \tag{8.2.66}$$

$$C^*_{10} = -\frac{\sin(2\theta_1)}{\cos(2\theta_1)} \tag{8.2.67}$$

$$D_{10}^{*} = -1 \tag{8.2.68}$$

$$B_{20}^{*} = -2 + \frac{1}{\cos(2\theta_1)} \tag{8.2.69}$$

$$C_{20}^{*} = C_{10}^{*} \tag{8.2.70}$$

$$D_{10}^{*} = 1. \tag{8.2.71}$$

In general, the regular stress term always is non-zero and can be determined analytically for a joint under thermal loading. However, for a joint under mechanical loading the regular stress term of most joint geometries and material combinations is zero. In some special cases, the regular stress term is non-zero. It can be determined analytically with an arbitrary constant K_0 to be determined from the stress analysis of the total joint.

8.3 The Characteristics of the Eigenvalues in a Joint with a Given Displacement Edge

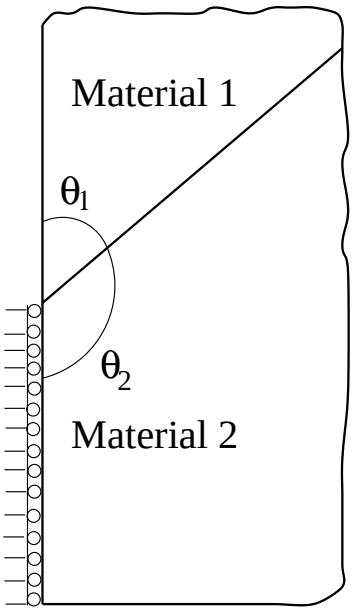

Figure 8.5: A joint with $\mid \theta_1 \mid + \mid \theta_2 \mid = 180°$.

The equation to determine the eigenvalues of the problem (i.e. the stress exponents) is given in Section 8.1. Since Det([A]) =0 in Eq. (8.1.14) is a transcendental equation of t_n or $\lambda_n = 1 - t_n$, the characteristics of the eigenvalues is not obvious. In this section the behaviors of the eigenvalues will be discussed for three types of geometry. The first type of geometry is that one material has the angle of 180°, while the other is arbitrary

(see Fig. 8.3). The second type of geometry is that the joint is symmetrical to the line of $\theta = 90°$ (see Fig. 8.4, this corresponds to θ_1 being arbitrary and $\theta_2 = -90°$). The third type of geometry is that the materials occupy the angle 180° (see Fig. 8.5).
For a joint with $\theta_1 = 45°$ and $\theta_2 = -180°$ the isoline of the stress exponent $0 \leq \omega \leq 1$ is plotted in a Dundurs diagram in Fig. 8.6. It can be seen that for this joint geometry: (a) Two singular terms exist for all material combinations. To see this clearly, another plot is shown in Fig. 8.7, in which the singular stress exponents are plotted along a line of $\alpha = 2\beta$ as a dotted line. (b) For all material combinations there are only real singular terms. (c) For a large value of α ($\alpha > 0.95$, i.e. $E_1 \gg E_2$) the singular stress exponent is very large ($\omega \geq 0.8$).
For a joint with $\theta_1 = 60°$ and $\theta_2 = -180°$ and a joint with $\theta_1 = 90°$ and $\theta_2 = -180°$, the isoline of the stress exponent $0 \leq \omega \leq 1$ is plotted in Figs. 8.8 and 8.9, for clarity also in Figs. 8.10 and 8.11. The behavior of the stress exponents is similar to that one of the joint with $\theta_1 = 45°$. For the same material combination the singularity of the joint with $\theta_1 = 90°$ is slightly larger than that one of the joint with $\theta_1 = 60°$ and with $\theta_1 = 45°$. Singularity of the joint with $\theta_1 = 60°$ is larger than that one of the joint with $\theta_1 = 45°$.

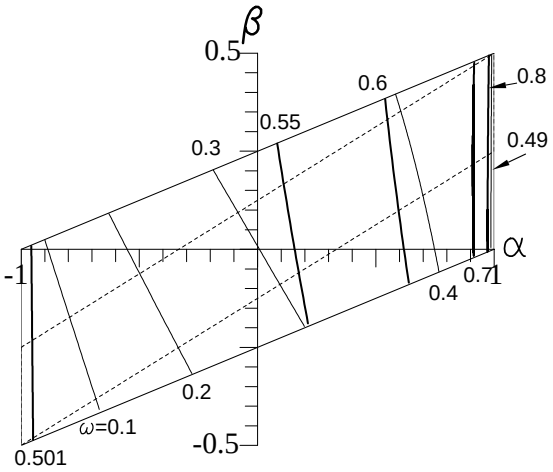

Figure 8.6: The isoline of the stress exponent in a Dundurs diagram for a joint with $\theta_1 = 45°$ and $\theta_2 = -180°$.

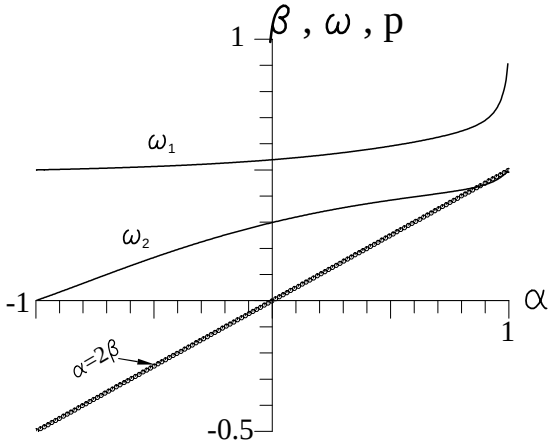

Figure 8.7: The singular stress exponents along the line of $\alpha = 2\beta$ for a joint with $\theta_1 = 45°$ and $\theta_2 = -180°$.

For a joint with $\theta_1 = 135°$ and $\theta_2 = -180°$ the isoline of the stress exponent is plotted in Figs. 8.12 and 8.13. In this case with $\theta_1 > 90°$, there is a large range where the eigenvalues are complex, and there are almost always three singular terms (see Fig. 8.13).
In case of a joint with an interface crack, i.e. $\theta_1 = -\theta_2 = 180°$, the isoline of the stress exponent is plotted in Figs. 8.14 and 8.15. It can be seen that: (a) For this joint there are always three singular terms, in which $\omega = 0.5$ is true for all material combinations, the other two singular exponents may be real or complex (see Fig. 8.15). (b) The real

part of the eigenvalue may be smaller or larger than 0.5. (c) If one singular exponent is real and $\omega_1 = c \neq 0.5$, then 1-c is the other real singular stress exponent. (d) If one crack surface has a given displacement in the direction perpendicular to the crack, there is only a small range in the Dundurs diagram, in which the eigenvalues are complex. This is very different from a joint with an interface crack having free edges. There, the eigenvalues are always complex as long as $\beta \neq 0$.

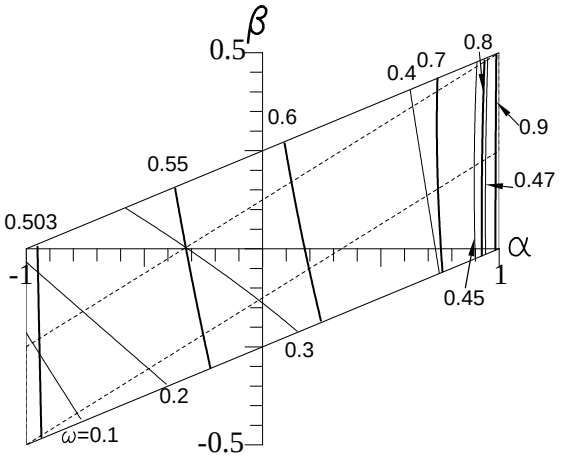

Figure 8.8: The isoline of the stress exponent in a Dundurs diagram for a joint with $\theta_1 = 60°$ and $\theta_2 = -180°$.

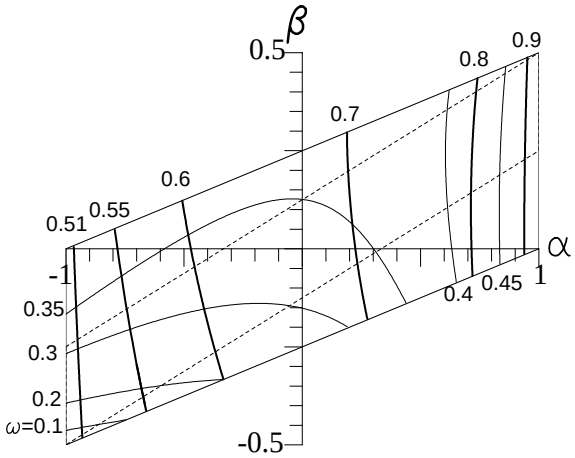

Figure 8.9: The isoline of the stress exponent in a Dundurs diagram for a joint with $\theta_1 = 90°$ and $\theta_2 = -180°$.

For a joint with $\theta_1 = 45°$ and $\theta_2 = -90°$ the isoline of the stress exponent $0 \leq \omega \leq 1$ is plotted in Figs. 8.16. It can be seen that for this joint geometry: (a) For all material combinations only one real singular term exists. To see this clearly, another plot is shown in Fig. 8.17, in which the singular stress exponents are plotted along a line of $\alpha = 2\beta$, as indicated by the dotted line. (b) For large value of α ($\alpha > 0.9$, i.e. $E_1 \gg E_2$) the singular stress exponent is very large ($\omega \geq 0.8$).

For a joint with $\theta_1 = 60°$ and $\theta_2 = -90°$ and a joint with $\theta_1 = 90°$ and $\theta_2 = -90°$, the isoline of the stress exponent $0 \leq \omega \leq 1$ is plotted in Figs. 8.18 and 8.19, for clarity see also Figs. 8.20 and 8.21. The behavior of the stress exponents is similar to that one of the joint with $\theta_1 = 45°$. For the same material combination singularity of the joint with $\theta_1 = 90°$ is slightly larger than that one of the joint with $\theta_1 = 60°$ and with $\theta_1 = 45°$. Singularity of the joint with $\theta_1 = 60°$ is slightly larger than that one of the joint with $\theta_1 = 45°$.

For a joint with $\theta_1 = 45°$ and $\theta_2 = -135°$ the isoline of the stress exponent $0 \leq \omega \leq 1$ is plotted in Figs. 8.22. It can be seen that for this joint geometry: (a) If $\beta > 0$, there are two singular terms. If $\beta < 0$, there exists only one singular term. To see this clearly, another plot is shown in Fig. 8.23. (b) There is a very small range in the Dundurs diagram ($\alpha > 0.95, \mid \beta \mid < 0.05$), where the eigenvalues are complex. Its real part is very small (< 0.05). (c) For a large value of α ($\alpha > 0.95$, i.e. $E_1 \gg E_2$) the singular stress exponent is very large ($\omega \geq 0.8$).

For a joint with $\theta_1 = 60°$ and $\theta_2 = -120°$ and a joint with $\theta_1 = 135°$ and $\theta_2 = -45°$, the isoline of the stress exponent is plotted in Figs. 8.24 and 8.28, for clarity see also Figs. 8.25, 8.26, and 8.27. It can be seen that with an increasing absolute value of θ_1, the range of complex eigenvalues is larger. For the joint with $\theta_1 = 60°$ and $\theta_2 = -120°$ there may be three singular terms for $\alpha > 0.9$ (see Fig. 8.26).

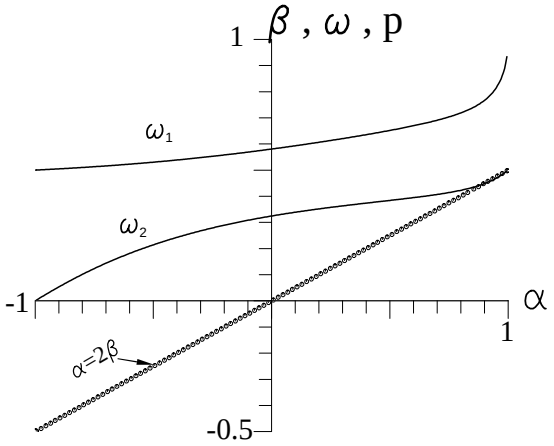

Figure 8.10: The singular stress exponents along the line of $\alpha = 2\beta$ for a joint with $\theta_1 = 60°$ and $\theta_2 = -180°$.

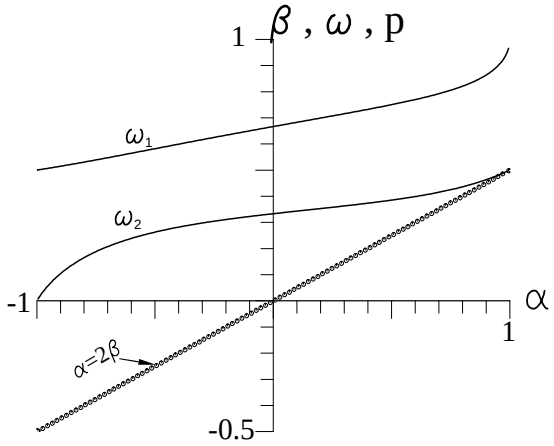

Figure 8.11: The singular stress exponents along the line of $\alpha = 2\beta$ for a joint with $\theta_1 = 90°$ and $\theta_2 = -180°$.

The results may be summed up as follows:
(a) For the type of joint with one material having the angle 180° and the other being arbitrary, there are at least two singular terms. When $\theta_1 \leq 90°$ all singular terms correspond to real eigenvalues. On the contrary, if $\theta_1 > 90°$, there is a range of α, β, where the eigenvalues are complex. For the joint with $\theta_1 = 180°$ and $\theta_2 = -180°$ there are three singular terms, in which one singular exponent is equal to 0.5. If the other two exponents are real, one is smaller than 0.5, the other larger than 0.5. The sum of them is equal to 1. If the other two exponents are complex, the real part is equal to 0.5.
(b) For the type of joint with a symmetrical line of $\theta = 90°$ (i.e. θ_1 arbitrary and $\theta_2 = -90°$), there is only one singular term and it corresponds to a real eigenvalue.
(c) For the joints, where the materials occupy the angle of 180°, there always is a range of α, β, in which the eigenvalues are complex, except for the case of $\theta_1 = -\theta_2 = 90°$. There may be one or two real singular terms. If the eigenvalues are complex, there are even three singular terms. For this type of joint, if $\alpha = \beta = 0$ (i.e. for homogenous material), always $\omega = 0.5$.

Comparing the eigenvalue behaviour of a joint with free edges and a joint with a given displacement edge (see Figs. 3.17 and 8.19, Figs. 3.23 and 8.28, Figs. 3.34 and 8.9) it follows that: (i) For the same material combination the singular stress exponent of a joint having a given displacement at one edge is larger than that one of a joint with free edges. (ii) For a joint with free edges, in Dundurs diagram there is an area

where there is no singular stress exponent (i.e. $\omega < 0$), however, in a joint with a given displacement at one edge, there exists at least one singular stress exponent. (iii) In a joint with a given displacement edge the maximum singular exponent is close to 1.

The stress field near the singular point can also be calculated from:

$$\sigma_{ij}(r,\theta) = \sum_{n=1}^{N} \frac{K_n}{\bar{r}^{\omega_n}} f_{ijn}(\theta) + \sigma_0 f_{ij0}(\theta) \tag{8.3.1}$$

for real eigenvalues, and from

$$\sigma_{ij}(r,\theta) = \sum_{n=1}^{N} \frac{K_n}{\bar{r}^{\omega_n}} \quad \Big\{ \quad \cos[p_n ln\bar{r}] f^c_{ijn}(\theta) + \sin[p_n ln\bar{r}] f^s_{ijn}(\theta) \Big\} + \sigma_0 f_{ij0}(\theta) \tag{8.3.2}$$

for complex eigenvalues. It should be noted that if ω is very large and $N \neq 1$, it is difficult to obtain a constant K-factor value by using the method presented in Section 3.4, because the mesh has a strong effect on the stresses very close to the singular point. To obtain the correct K-factor value, the FE mesh and the FE stress used should be chosen carefully.

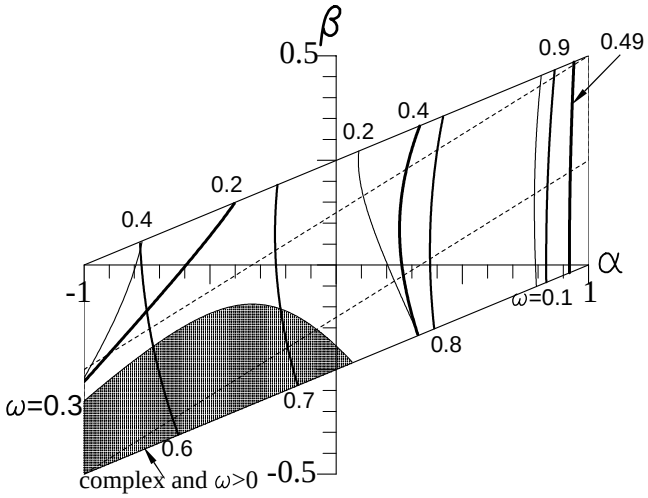

Figure 8.12: The isoline of the stress exponent in a Dundurs diagram for a joint with $\theta_1 = 135°$ and $\theta_2 = -180°$.

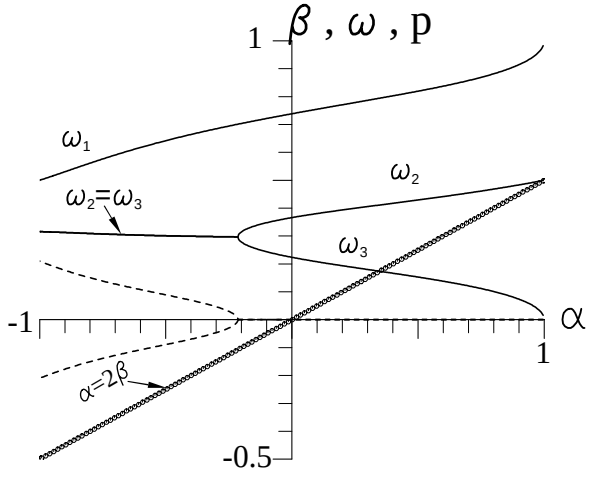

Figure 8.13: The singular stress exponents along the line of $\alpha = 2\beta$ for a joint with $\theta_1 = 135°$ and $\theta_2 = -180°$.

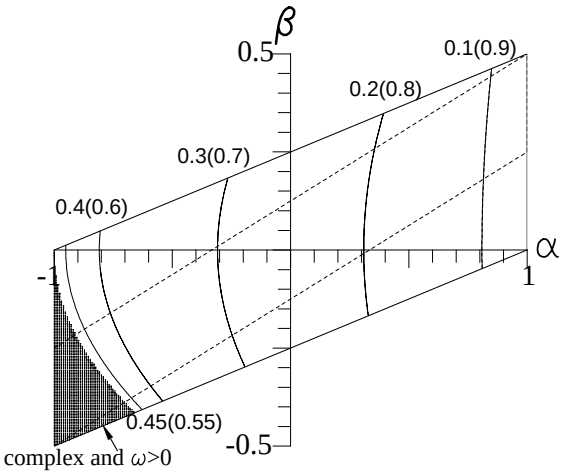

Figure 8.14: The isoline of the stress exponent in a Dundurs diagram for a joint with $\theta_1 = 180°$ and $\theta_2 = -180°$.

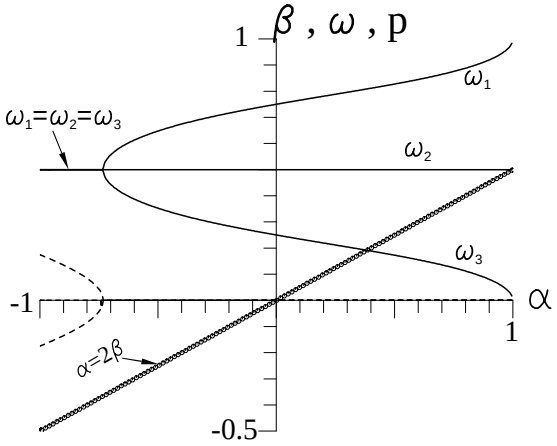

Figure 8.15: The singular stress exponents along the line of $\alpha = 2\beta$ for a joint with $\theta_1 = 180°$ and $\theta_2 = -180°$.

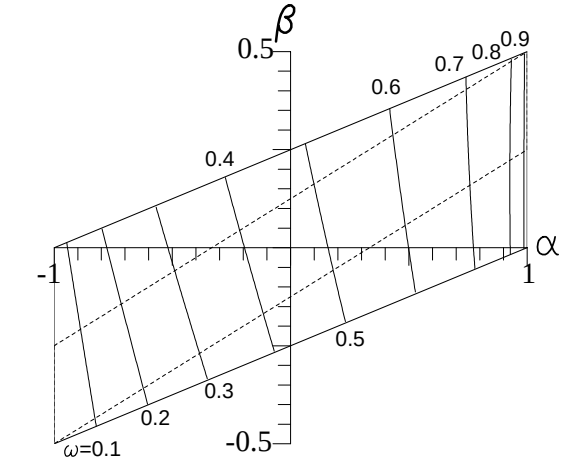

Figure 8.16: The isoline of the stress exponent in a Dundurs diagram for a joint with $\theta_1 = 45°$ and $\theta_2 = -90°$.

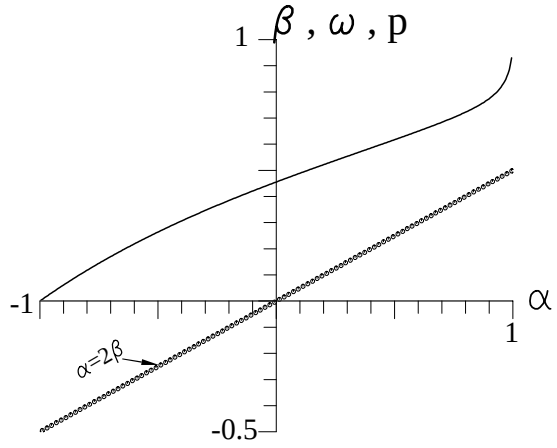

Figure 8.17: The singular stress exponents along the line of $\alpha = 2\beta$ for a joint with $\theta_1 = 45°$ and $\theta_2 = -90°$.

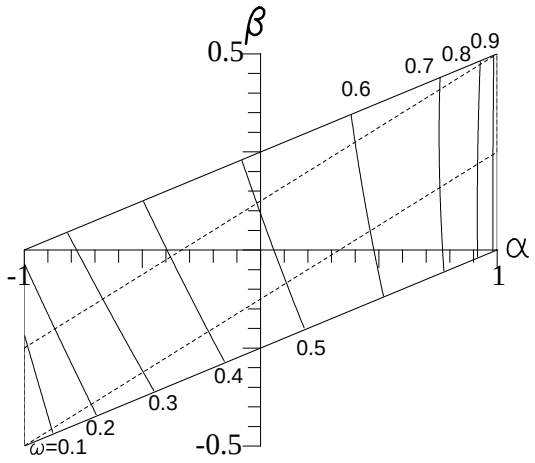

Figure 8.18: The isoline of the stress exponent in a Dundurs diagram for a joint with $\theta_1 = 60°$ and $\theta_2 = -90°$.

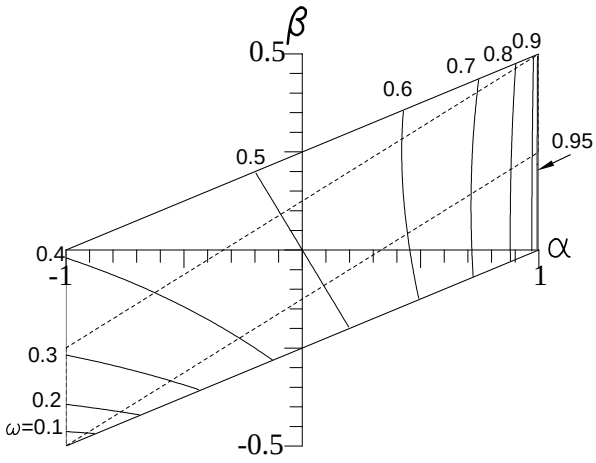

Figure 8.19: The isoline of the stress exponent in a Dundurs diagram for a joint with $\theta_1 = 90°$ and $\theta_2 = -90°$.

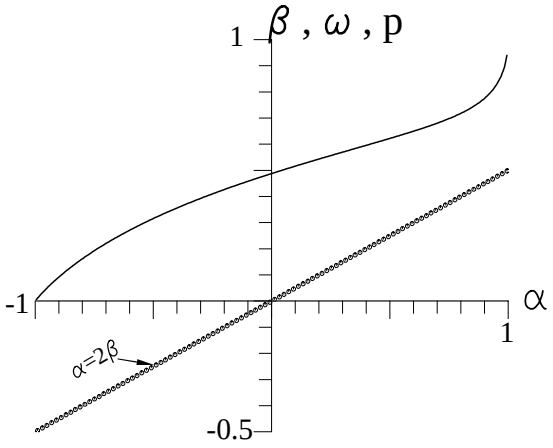

Figure 8.20: The singular stress exponents along the line of $\alpha = 2\beta$ for a joint with $\theta_1 = 60°$ and $\theta_2 = -90°$.

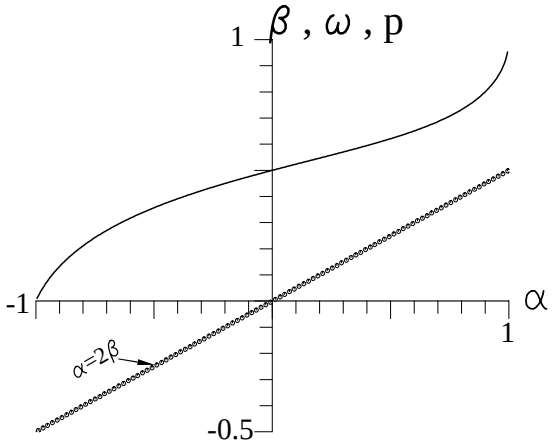

Figure 8.21: The singular stress exponents along the line of $\alpha = 2\beta$ for a joint with $\theta_1 = 90°$ and $\theta_2 = -90°$.

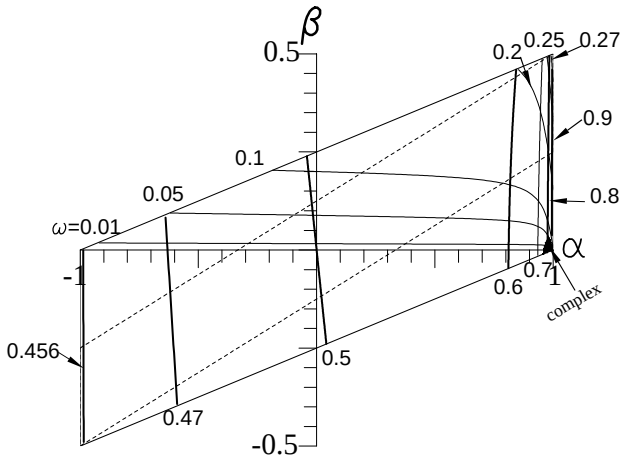

Figure 8.22: The isoline of the stress exponent in a Dundurs diagram for a joint with $\theta_1 = 45°$ and $\theta_2 = -135°$.

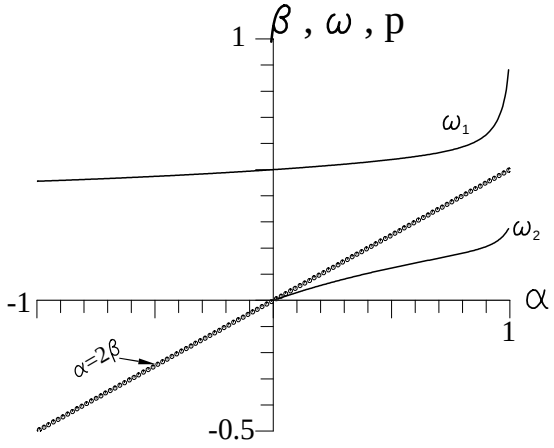

Figure 8.23: The singular stress exponents along the line of $\alpha = 2\beta$ for a joint with $\theta_1 = 45°$ and $\theta_2 = -135°$.

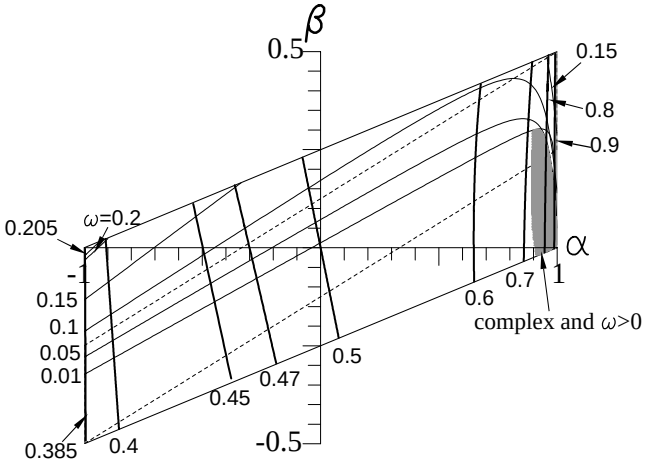

Figure 8.24: The isoline of the stress exponent in a Dundurs diagram for a joint with $\theta_1 = 60°$ and $\theta_2 = -120°$.

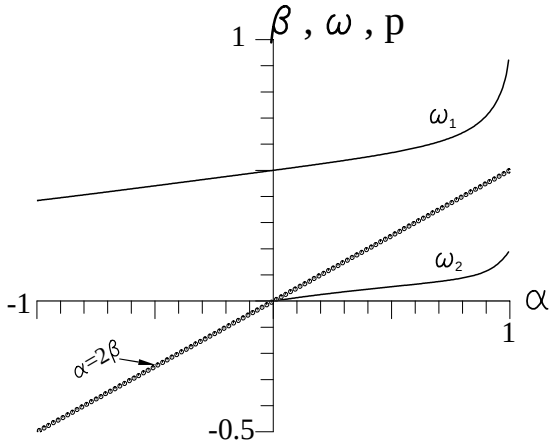

Figure 8.25: The singular stress exponents along the line of $\alpha = 2\beta$ for a joint with $\theta_1 = 60°$ and $\theta_2 = -120°$.

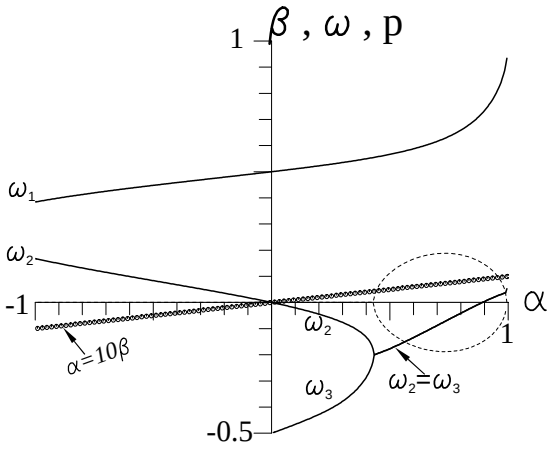

Figure 8.26: The singular stress exponents along the line of $\alpha = 10\beta$ for a joint with $\theta_1 = 60°$ and $\theta_2 = -120°$.

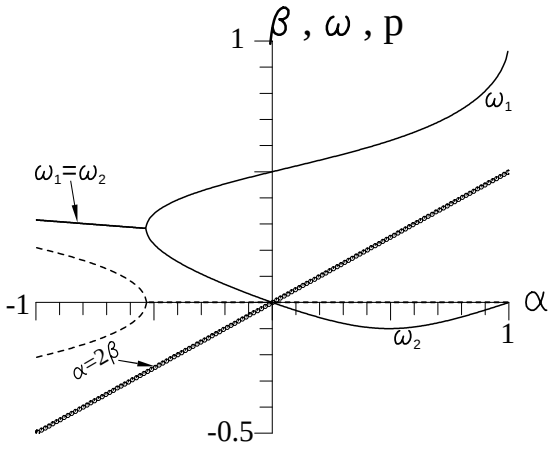

Figure 8.27: The singular stress exponents along the line of $\alpha = 2\beta$ for a joint with $\theta_1 = 135°$ and $\theta_2 = -45°$.

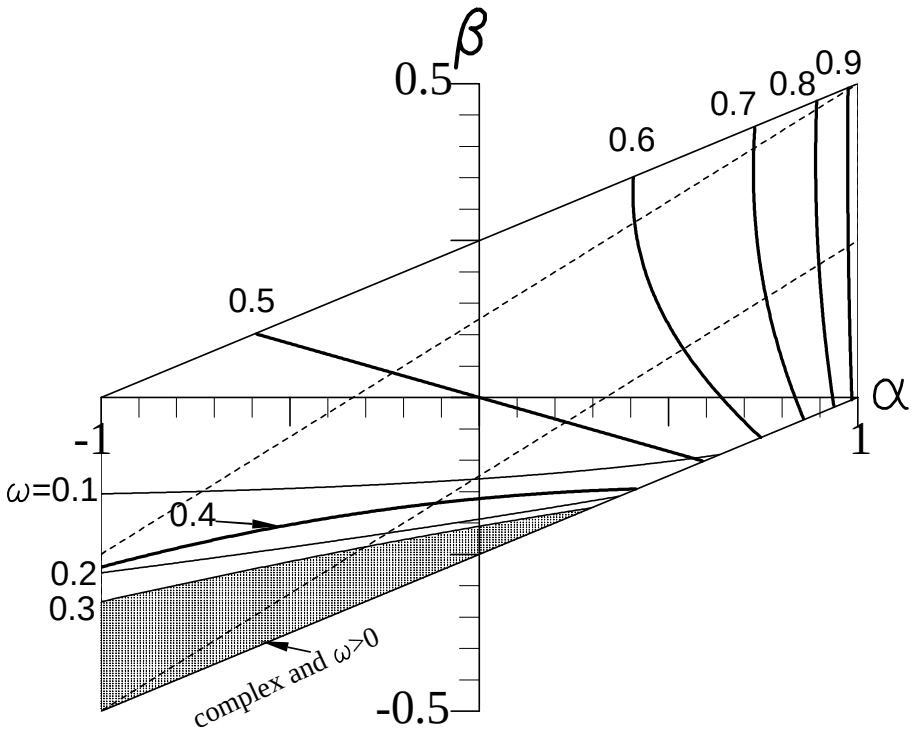

Figure 8.28: The isoline of the stress exponent in a Dundurs diagram for a joint with $\theta_1 = 135°$ and $\theta_2 = -45°$.

Chapter 9

Cracks in a Dissimilar Materials Joint

In a dissimilar materials joint adhesion at the interface mostly is the weaker position due to the different expansion coefficients of the joined components. In practice, cracks exist or are initiated near or at the interface. Different cracks can be considered in a dissimilar materials joint (see e.g. [90], [99], [138] - [142]). Of special interest are interface cracks or cracks terminating at the interface. For cracks with crack tips near the interface, the stress singularity is the same as in a homogeneous material [99]. This means that the singular stress exponent still is 0.5 (i.e. $\sigma_{ij}(r,\theta) \sim \sqrt{r}$, see Chapter 4). The effect of the existence of the other joined component on the stresses is included in the stress intensity factor.

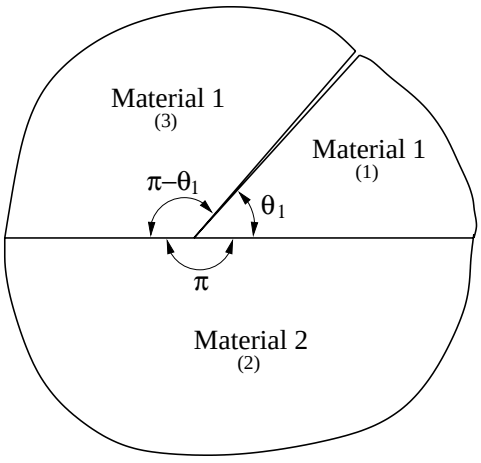

Figure 9.1: A joint with a crack terminating at the interface under an arbitrary angle.

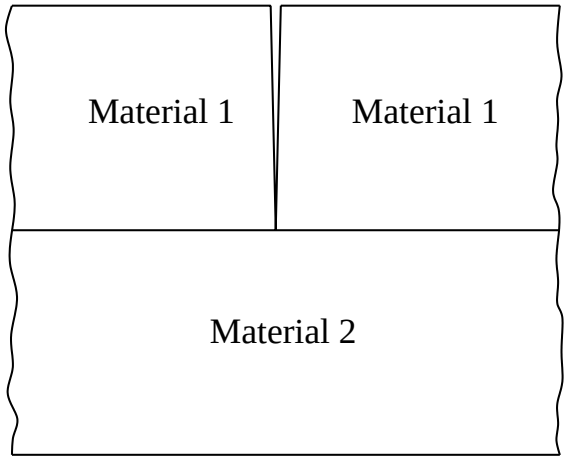

Figure 9.2: A joint with a crack perpendicular to the interface.

In this section cracks terminating at the interface are considered. Four types of cracks are considered: (a) Cracks with an arbitrary angle terminating at the interface (see

Fig. 9.1), (b) cracks perpendicular to the interface (see Fig. 9.2), (c) interface cracks (see Fig. 9.3), (d) delamination cracks or interface corner cracks (see Fig. 9.4), which are under thermal and mechanical loading. Determination of the stress exponent, the angular functions, and the regular stress term will be discussed in Section 9.1 for type (a), in Section 9.2 for type (b), in Section 9.3 for type (c), and in Section 9.4 for type (d). Some examples will be given to show the agreement of stresses calculated from the analytical description and FEM.

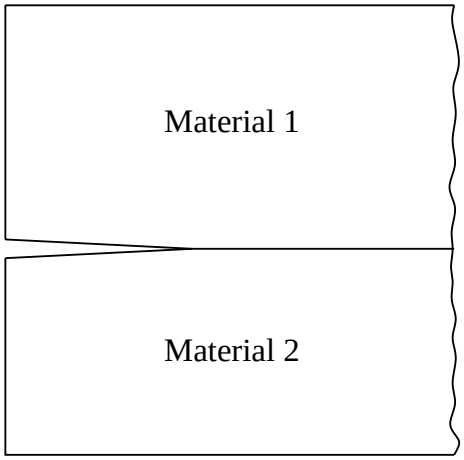

Figure 9.3: A joint with an interface crack.

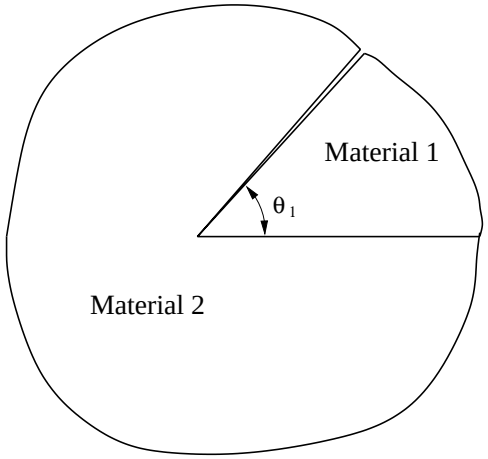

Figure 9.4: A joint with a delamination crack.

9.1 Crack Terminating at the Interface

In this section a joint with a crack terminating at the interface under an arbitrary angle θ_1 will be studied. The stress distribution near the crack tip will be described analytically. The analytical solution can be used on the scale of practical interest. The quantities used to calculate the stresses, like the stress exponent, the angular functions, the regular stress term, and stress intensity factors will be presented analytically and numerically.

9.1.1 Determination of the Stress Exponent

For a two dissimilar materials joint with a crack terminating at the interface (see Fig. 9.1), there are three material ranges. The boundary conditions for this problem are:

at the interface $\theta = 0$

$$u_r^{(1)}(r,0) \quad = \quad u_r^{(2)}(r,0),$$

$$
\begin{aligned}
v_\theta^{(1)}(r,0) &= v_\theta^{(2)}(r,0), \\
\sigma_{\theta\theta}^{(1)}(r,0) &= \sigma_{\theta\theta}^{(2)}(r,0), \\
\sigma_{r\theta}^{(1)}(r,0) &= \sigma_{r\theta}^{(2)}(r,0),
\end{aligned} \tag{9.1.1}
$$

at the free edge $\theta = \theta_1$

$$
\begin{aligned}
\sigma_{\theta\theta}^{(1)} &= 0, \\
\sigma_{r\theta}^{(1)} &= 0,
\end{aligned} \tag{9.1.2}
$$

at the free edge $\theta = -(2\pi - \theta_1)$

$$
\begin{aligned}
\sigma_{\theta\theta}^{(3)} &= 0, \\
\sigma_{r\theta}^{(3)} &= 0,
\end{aligned} \tag{9.1.3}
$$

and at the interface $\theta = -\pi$

$$
\begin{aligned}
u_r^{(3)}(r,-\pi) &= u_r^{(2)}(r,-\pi), \\
v_\theta^{(3)}(r,-\pi) &= v_\theta^{(2)}(r,-\pi), \\
\sigma_{\theta\theta}^{(3)}(r,-\pi) &= \sigma_{\theta\theta}^{(2)}(r,-\pi), \\
\sigma_{r\theta}^{(3)}(r,-\pi) &= \sigma_{r\theta}^{(2)}(r,-\pi),
\end{aligned} \tag{9.1.4}
$$

where the superscripts (1), (2), and (3) denote the ranges 1, 2, and 3, respectively. Airy's stress function given in Eq. (3.1.3) is used here. By inserting Eqs. (3.1.7-3.1.9, 3.1.16-3.1.17) into Eqs. (9.1.1-9.1.4) for thermal loading and for plane stress, the following 12 equations are obtained:

$$
\begin{aligned}
&\sum_n r^{(1-\lambda_n)} \Big\{ B_{1n}\mu[2(1-\nu_1) + \lambda_n(1+\nu_1)] - D_{1n}\mu(1+\nu_1)(2-\lambda_n) \\
- \;& B_{2n}[2(1-\nu_2) + \lambda_n(1+\nu_2)] + D_{2n}(1+\nu_2)(2-\lambda_n) \Big\} = rTE_2(\alpha_2 - \alpha_1)
\end{aligned} \tag{9.1.5}
$$

$$
\begin{aligned}
&\sum_n r^{(1-\lambda_n)} \Big\{ A_{1n}\mu[2(1-\nu_1) + (2-\lambda_n)(1+\nu_1)] - C_{1n}\mu(1+\nu_1)(2-\lambda_n) \\
- \;& A_{2n}[2(1-\nu_2) + (2-\lambda_n)(1+\nu_2)] + C_{2n}(1+\nu_2)(2-\lambda_n) \Big\} = 0
\end{aligned} \tag{9.1.6}
$$

$$
\sum_n r^{-\lambda_n}(1-\lambda_n)(2-\lambda_n)\Big\{ B_{1n} + D_{1n} - B_{2n} - D_{2n} \Big\} = 0 \tag{9.1.7}
$$

$$
\sum_n r^{-\lambda_n}(1-\lambda_n)\Big\{ A_{1n}\lambda_n + C_{1n}(2-\lambda_n) - A_{2n}\lambda_n - C_{2n}(2-\lambda_n) \Big\} = 0 \tag{9.1.8}
$$

$$\sum_n r^{-\lambda_n}(1-\lambda_n)(2-\lambda_n)\Big\{A_{1n}\sin(\lambda_n\theta_1) \quad + \quad B_{1n}\cos(\lambda_n\theta_1) + C_{1n}\sin[(2-\lambda_n)\theta_1] + \\ + \quad D_{1n}\cos[(2-\lambda_n)\theta_1]\Big\} = 0 \tag{9.1.9}$$

$$\sum_n r^{-\lambda_n}(1-\lambda_n)\Big\{A_{1n}\lambda_n\cos(\lambda_n\theta_1) \quad - \quad B_{1n}\lambda_n\sin(\lambda_n\theta_1) + C_{1n}(2-\lambda_n)\cos[(2-\lambda_n)\theta_1] \\ - \quad D_{1n}(2-\lambda_n)\sin[(2-\lambda_n)\theta_1]\Big\} = 0 \tag{9.1.10}$$

$$\sum_n r^{-\lambda_n}(1-\lambda_n)(2-\lambda_n)\Big\{ - A_{3n}\sin[\lambda_n(2\pi-\theta_1)] + B_{3n}\cos[\lambda_n(2\pi-\theta_1)] - \\ - \quad C_{3n}\sin[(2-\lambda_n)(2\pi-\theta_1)] + D_{3n}\cos[(2-\lambda_n)(2\pi-\theta_1)]\Big\} = 0 \tag{9.1.11}$$

$$\sum_n r^{-\lambda_n}(1-\lambda_n)\Big\{A_{3n}\lambda_n\cos[\lambda_n(2\pi-\theta_1)] + B_{3n}\lambda_n\sin[\lambda_n(2\pi-\theta_1)] + \\ + \quad C_{3n}(2-\lambda_n)\cos[(2-\lambda_n)(2\pi-\theta_1)] + D_{3n}(2-\lambda_n)\sin[(2-\lambda_n)(2\pi-\theta_1)]\Big\} = 0 \tag{9.1.12}$$

$$\sum_n r^{-\lambda_n}(1-\lambda_n)(2-\lambda_n)\Big\{ - A_{3n}\sin(\lambda_n\pi) + B_{3n}\cos(\lambda_n\pi) + C_{3n}\sin(\lambda_n\pi) + D_{3n}\cos(\lambda_n\pi) \\ + \quad A_{2n}\sin(\lambda_n\pi) - B_{2n}\cos(\lambda_n\pi) - C_{2n}\sin(\lambda_n\pi) - D_{2n}\cos(\lambda_n\pi)\Big\} = 0 \tag{9.1.13}$$

$$\sum_n r^{-\lambda_n}(1-\lambda_n)\Big\{A_{3n}\lambda_n\cos(\lambda_n\pi) + B_{3n}\lambda_n\sin(\lambda_n\pi) + C_{3n}(2-\lambda_n)\cos(\lambda_n\pi) \\ - \quad D_{3n}(2-\lambda_n)\sin(\lambda_n\pi) - A_{2n}\lambda_n\cos(\lambda_n\pi) - B_{2n}\lambda_n\sin(\lambda_n\pi) \\ - \quad C_{2n}(2-\lambda_n)\cos(\lambda_n\pi) + D_{2n}(2-\lambda_n)\sin(\lambda_n\pi)\Big\} = 0 \tag{9.1.14}$$

$$\sum_n r^{(1-\lambda_n)}\Big\{ - A_{3n}\mu[2(1-\nu_1) + \lambda_n(1+\nu_1)]\sin(\lambda_n\pi) \\ + \quad B_{3n}\mu[2(1-\nu_1) + \lambda_n(1+\nu_1)]\cos(\lambda_n\pi) - C_{3n}\mu(1+\nu_1)(2-\lambda_n)\sin(\lambda_n\pi) \\ - \quad D_{3n}\mu(1+\nu_1)(2-\lambda_n)\cos(\lambda_n\pi) + A_{2n}[2(1-\nu_2) + \lambda_n(1+\nu_2)]\sin(\lambda_n\pi) \\ - \quad B_{2n}[2(1-\nu_2) + \lambda_n(1+\nu_2)]\cos(\lambda_n\pi) + C_{2n}(1+\nu_2)(2-\lambda_n)\sin(\lambda_n\pi) \\ + \quad D_{2n}(1+\nu_2)(2-\lambda_n)\cos(\lambda_n\pi)\Big\} = rTE_2(\alpha_2-\alpha_1) \tag{9.1.15}$$

$$
\begin{aligned}
&\sum_n r^{(1-\lambda_n)}\Big\{A_{3n}\mu[2(1-\nu_1)+(2-\lambda_n)(1+\nu_1)]\cos(\lambda_n\pi)\\
+\;& B_{3n}\mu[2(1-\nu_1)+(2-\lambda_n)(1+\nu_1)]\sin(\lambda_n\pi)-C_{3n}\mu(1+\nu_1)(2-\lambda_n)\cos(\lambda_n\pi)\\
+\;& D_{3n}\mu(1+\nu_1)(2-\lambda_n)\sin(\lambda_n\pi)-A_{2n}[2(1-\nu_2)+(2-\lambda_n)(1+\nu_2)]\cos(\lambda_n\pi)\\
-\;& B_{2n}[2(1-\nu_2)+(2-\lambda_n)(1+\nu_2)]\sin(\lambda_n\pi)+C_{2n}(1+\nu_2)(2-\lambda_n)\cos(\lambda_n\pi)\\
-\;& D_{2n}(1+\nu_2)(2-\lambda_n)\sin(\lambda_n\pi)\Big\}=0 \qquad (9.1.16)
\end{aligned}
$$

As r in Eqs. (9.1.5- 9.1.16) is arbitrary, this equation system can be rewritten in the following matrix form for each n and $\lambda_n \neq 0, 1, 2$:

$$[A]_{12\times12}\{X\}_{12\times1}=\{0\}_{12\times1} \qquad (9.1.17)$$

where $\{X\}_{12\times1}=\{A_{1n},B_{1n},C_{1n},D_{1n},A_{2n},B_{2n},C_{2n},D_{2n},A_{3n},B_{3n},C_{3n},D_{3n}\}^t$ and $[A]_{12\times12}$ is its coefficient matrix. $\{X\}_{12\times1}$ is unknown and $[A]_{12\times12}$ includes the unknown exponent λ_n, the material properties (E_k, ν_k, k=1,2 for materials 1 and 2), and the geometry angles θ_1.
For $\lambda_n = 0$,

$$[A_0]_{12\times12}\{X_0\}_{12\times1}=\{S_0\}_{12\times1} \qquad (9.1.18)$$

where $\{X_0\}_{12\times1}=\{A_{10},B_{10},C_{10},D_{10},A_{20},B_{20},C_{20},D_{20},A_{30},B_{30},C_{30},D_{30}\}^t$, $[A_0]_{12\times12}$ is its coefficient matrix, and $\{S_0\}_{12\times1}=\{TE_2(\alpha_2-\alpha_1),0,0,0,0,0,0,0,0,0,0,TE_2(\alpha_2-\alpha_1),0\}$ is the right hand side of Eqs. (9.1.5) through (9.1.16). This case will be discussed in next section.

Equation (9.1.17) has a nonzero solution, if and only if

$$\mathrm{Det}([A]_{12\times12})=0 \qquad (9.1.19)$$

is satisfied. In Eq. (9.1.19) the only unknown is the exponent λ_n. Its solutions are the eigenvalues of this problem. As it is a transcendental equation, there are infinite solutions λ_n (n=1,2,3,...) and they may be real or complex. If the eigenvalues are complex the stress function of Eq. (3.1.3) cannot be used directly and Eqs. (3.1.115-3.1.119) should be used.
For an arbitrary joint geometry with θ_1 the expansion of Eq. (9.1.19) is

$$
\begin{aligned}
\mathrm{Det}([A])=\frac{512(1+t_n)^2}{(1+\alpha)^4}\Big\{&2\sin^2(2\pi t_n)-\\
&-\beta\ 32\ {t_n}^2\cos(\pi t_n)\cos[t_n(\pi-2\theta_1)]\sin^2(\pi t_n)\sin^2(\theta_1)+\\
&+\alpha\ 16\ \cos(\pi t_n)\cos[t_n(\pi-2\theta_1)]\sin^2(\pi t_n)\Big[2{t_n}^2\sin^2(\theta_1)-1\Big]+\\
&+\alpha\beta^2\ 8\ \sin^2(\pi t_n)\Big[-2+\cos[2t_n(\pi-\theta_1)]+\cos(2t_n\theta_1)+\\
&\quad+2{t_n}^2\Big(4-\cos[2t_n(\pi-\theta_1)]-\cos(2t_n\theta_1)\Big)\sin^2(\theta_1)-16{t_n}^4\sin^4(\theta_1)\Big]+
\end{aligned}
$$

$$
\begin{aligned}
&+\alpha\beta^3\ 16\ {t_n}^2\sin^2(\pi t_n)\sin^2(\theta_1)\Big[2-\cos[2t_n\,(\pi-\theta_1)]-\cos(2t_n\theta_1)-4t_n^2\sin^2(\theta_1)\Big]\\
&+\alpha\beta\ 16\ {t_n}^2\sin^2(\pi t_n)\sin^2(\theta_1)\Big[2+\cos[2t_n\,(\pi-\theta_1)]+\cos(2t_n\theta_1)-4{t_n}^2\sin^2(\theta_1)\Big]\\
&+\alpha^2\beta^2\Big[2-2\cos(2\pi t_n)-2\cos[2t_n\,(\pi-2\theta_1)]+\cos[4t_n\,(\pi-\theta_1)]\\
&\qquad+\cos(4t_n\theta_1)+32{t_n}^4\sin^2(\pi t_n)\sin^4(\theta_1)\Big]\\
&+\alpha^2\Big[2-2\cos(2\pi t_n)+2\cos[2t_n\,(\pi-2\theta_1)]-\cos[4t_n\,(\pi-\theta_1)]\\
&\qquad-\cos(4t_n\theta_1)-32{t_n}^2\sin^2(\pi t_n)\sin^2(\theta_1)+32{t_n}^4\sin^2(\pi t_n)\sin^4(\theta_1)\Big]\\
&+\beta^2\ 4\ \sin^2(\pi t_n)\Big[-1-2\cos(2\pi t_n)-\cos[2t_n\,(\pi-2\theta_1)]+2\cos[2t_n\,(\pi-\theta_1)]\\
&\qquad+2\cos(2t_n\theta_1)-8{t_n}^2\cos(\pi t_n)\cos[t_n\,(\pi-2\theta_1)]\sin^2(\theta_1)+8{t_n}^4\sin^4(\theta_1)\Big]\\
&+\alpha^2\beta\ 32\ {t_n}^2\sin^2(\pi t_n)\sin^2(\theta_1)\Big[2{t_n}^2\sin^2(\theta_1)-1\Big]\\
&+\beta^3 16\ {t_n}^2\sin^2(\pi t_n)\sin^2(\theta_1)\Big[-2+\cos[2t_n\,(\pi-\theta_1)]+\cos(2t_n\theta_1)+4{t_n}^2\sin^2(\theta_1)\Big]\\
&+\beta^4\Big[16{t_n}^2\Big(-2+\cos[2t_n\,(\pi-\theta_1)]+\cos(2t_n\theta_1)\Big)\sin^2(\pi t_n)\sin^2(\theta_1)\\
&\qquad+32{t_n}^4\sin^2(\pi t_n)\sin^4(\theta_1)+8\Big(\cos[t_n\,(2\pi-\theta_1)]-\cos(t_n\theta_1)\Big)^2\sin^2(t_n\theta_1)\Big]\Big\},
\end{aligned}
\tag{9.1.20}
$$

where $t_n = 1-\lambda_n$. From Eq. (9.1.20) it can be seen that if t_n is the solution of Eq. (9.1.20), -t_n is also. Therefore, if λ_n is the eigenvalue of the problem, 2-λ_n is as well, but only one corresponds to the singular term.
For a special case with $\theta_1 = \pi/4$,

$$
\begin{aligned}
\mathrm{Det}([A]) &= \frac{512(1+t_n)^2}{(1+\alpha)^4}\Big\{16\ \alpha^2\beta{t_n}^2\left[-1+{t_n}^2\right]+4\ \alpha^2\beta^2\left[1+2{t_n}^4-\cos(\pi t_n)\right]-\\
&- 16\ \beta{t_n}^2\cos(\pi t_n/2)\cos(\pi t_n)+16\alpha\left[-1+{t_n}^2\right]\cos(\pi t_n/2)\cos(\pi t_n)+\\
&+ 8\cos^2(\pi t_n)+4\ \alpha^2\left[1-4{t_n}^2+2{t_n}^4+\cos(\pi t_n)\right]+\\
&+ 8\ \alpha\beta^3{t_n}^2\left[2-2{t_n}^2-\cos(\pi t_n/2)-\cos(3\pi t_n/2)\right]+\\
&+ 8\ \alpha\beta{t_n}^2\left[2-2{t_n}^2+\cos(\pi t_n/2)+\cos(3\pi t_n/2)\right]+\\
&+ 8\ \beta^3{t_n}^2\left[-2+2{t_n}^2+\cos(\pi t_n/2)+\cos(3\pi t_n/2)\right]+\\
&+ 8\ \alpha\beta^2\Big[-2+4{t_n}^2-4{t_n}^4+\cos(\pi t_n/2)-{t_n}^2\cos(\pi t_n/2)+\\
&\quad+\cos(3\pi t_n/2)-{t_n}^2\cos(3\pi t_n/2)\Big]+\\
&+ 4\ \beta^2\Big[-1+2{t_n}^4+2\cos(\pi t_n/2)-2{t_n}^2\cos(\pi t_n/2)-\\
&\quad-\cos(\pi t_n)+2\cos(3\pi t_n/2)-2{t_n}^2\cos(3\pi t_n/2)-2\cos(2\pi t_n)\Big]+\\
&+ 4\ \beta^4\Big[2-4{t_n}^2+2{t_n}^4-2\cos(\pi t_n/2)+2{t_n}^2\cos(\pi t_n/2)+\cos(\pi t_n)-\\
&\quad-2\cos(3\pi t_n/2)+2{t_n}^2\cos(3\pi t_n/2)+\cos(2\pi t_n)\Big]\Big\}\sin^2(\pi t_n).
\end{aligned}
\tag{9.1.21}
$$

For each given eigenvalue $\lambda_n = 1-t_n$, the coefficient $A_{kn}, B_{kn}, C_{kn}, D_{kn}$ (k=1,2,3) of

the angular function can be determined with one arbitrary constant from Eqs. (9.1.5-9.1.16). Then the normalized angular functions are known. For an arbitrary angle θ_1 the equations to calculate the coefficient $A_{kn}, B_{kn}, C_{kn}, D_{kn}$ (k=1,2,3) are very long and, hence, not given here. For some special cases, e.g. $\theta_1 = 90^0$ and $\theta_1 = 180^0$, the angular functions will be given in Sections 9.2 and 9.3.

9.1.2 The Regular Stress Term

For Thermal Loading

For the determination of the regular stress term, the following equations should be solved:

$$\begin{aligned} B_{10}\mu(1-\nu_1) &- D_{10}\mu(1+\nu_1) - B_{20}(1-\nu_2) + D_{20}(1+\nu_2) \\ &= E_2/2T(\alpha_2 - \alpha_1) \end{aligned} \tag{9.1.22}$$

$$-2C_{10}\mu(1+\nu_1) + F_{10}E_2 + 2C_{20}(1+\nu_2) - F_{20}E_2 = 0 \tag{9.1.23}$$

$$\mu A_{10} - A_{20} = 0 \tag{9.1.24}$$

$$B_{10} + D_{10} - B_{20} - D_{20} = 0 \tag{9.1.25}$$

$$A_{10} + 2C_{10} - A_{20} - 2C_{20} = 0 \tag{9.1.26}$$

$$A_{10}\theta_1 + B_{10} + C_{10}\sin(2\theta_1) + D_{10}\cos(2\theta_1) = 0 \tag{9.1.27}$$

$$A_{10} + 2C_{10}\cos(2\theta_1) - 2D_{10}\sin(2\theta_1) = 0 \tag{9.1.28}$$

$$-A_{30}(2\pi - \theta_1) + B_{30} + C_{30}\sin(2\theta_1) + D_{30}\cos(2\theta_1) = 0 \tag{9.1.29}$$

$$A_{30} + 2C_{30}\cos(2\theta_1) - 2D_{30}\sin(2\theta_1) = 0 \tag{9.1.30}$$

$$\begin{aligned} &-A_{30}\mu(1-\nu_1)\pi + B_{30}\mu(1-\nu_1) - D_{30}\mu(1+\nu_1) + A_{20}(1-\nu_2)\pi \\ &-B_{20}(1-\nu_2) + D_{20}(1+\nu_2) = E_2/2T(\alpha_2 - \alpha_1) \end{aligned} \tag{9.1.31}$$

$$-2C_{30}\mu(1+\nu_1) + F_{30}E_2 + 2C_{20}(1+\nu_2) - F_{20}E_2 = 0 \tag{9.1.32}$$

$$\mu A_{30} - A_{20} = 0 \tag{9.1.33}$$

$$-A_{30}\pi + B_{30} + D_{30} + A_{20}\pi - B_{20} - D_{20} = 0 \tag{9.1.34}$$

$$A_{30} + 2C_{30} - A_{20} - 2C_{20} = 0, \tag{9.1.35}$$

with $\mu = E_2/E_1$ and for plane stress. The regular stress term depends only on the coefficients $A_{k0}, B_{k0}, C_{k0}, D_{k0}$ (k=1,2,3). Equations (9.1.24) and (9.1.33) yields

$$A_{30} = A_{10}. \tag{9.1.36}$$

From Eqs. (9.1.26), (9.1.35), and (9.1.36),

$$C_{30} = C_{10}. \tag{9.1.37}$$

Following Eqs. (9.1.28), (9.1.30), (9.1.36), and (9.1.37) we have

$$D_{30} = D_{10}. \tag{9.1.38}$$

From Eqs. (9.1.25), (9.1.34), (9.1.27), (9.1.29), (9.1.26), (9.1.36), (9.1.37), and (9.1.38)

$$\begin{aligned} A_{30} = A_{10} &= A_{20} = 0 \\ B_{30} &= B_{10} \\ C_{10} = C_{20} &= C_{30} \end{aligned} \tag{9.1.39}$$

can be obtained. Now, only five coefficients $B_{10}, C_{10}, D_{10}, B_{20}, D_{20}$ are independent. To determine them, four independent equations, i.e. Eqs. (9.1.22), (9.1.25), (9.1.27), (9.1.28) exist. Therefore, one coefficient is arbitrary. If D_{20} is assumed to be the arbitrary constant and takes the value of K_0, the solution for the coefficients is:

$$B_{10} = -\frac{Q}{2\Delta}(1+\alpha) + \frac{K_0}{\Delta}(1+\alpha) \tag{9.1.40}$$

$$C_{10} = \frac{Q}{2\Delta}(1+\alpha)\sin(2\theta_1) - \frac{K_0}{\Delta}(1+\alpha)\sin(2\theta_1) \tag{9.1.41}$$

$$D_{10} = \frac{Q}{2\Delta}(1+\alpha)\cos(2\theta_1) - \frac{K_0}{\Delta}(1+\alpha)\cos(2\theta_1) \tag{9.1.42}$$

$$B_{20} = -\frac{Q}{\Delta}(1+\alpha)\sin^2(\theta_1) + \frac{K_0}{\Delta}[1+\alpha-2\beta-2\alpha\cos(2\theta_1)+2\beta\cos(2\theta_1)] \tag{9.1.43}$$

$$D_{20} = K_0 \tag{9.1.44}$$

with

$$\Delta = 2\beta - \cos(2\theta_1)[1 - \alpha + 2\beta], \tag{9.1.45}$$

and Q from Eq. (8.2.20) for plane stress and Eq. (8.2.21) for plane strain. The quantity Q is proportional to the thermal loading ΔT. The quantity K_0 depends, however, on the total loading. If there is no mechanical loading, K_0 is also proportional to the thermal loading ΔT. Otherwise, K_0 is not proportional to ΔT. Using the coefficients determined the regular stress term in a polar coordinate system can be calculated from Eqs. (3.3.2-3.3.4).
As in this case there always is $A_{10} = A_{20} = A_{30} = 0$, the regular stress term in Cartesian coordinates is very simple and is a constant in each material, i.e.

$$\begin{aligned} \sigma_{xxi0} &= 2(B_{i0} - D_{i0}) \\ \sigma_{yyi0} &= 2(B_{i0} + D_{i0}) \\ \tau_{xyi0} &= -2C_{i0}, \end{aligned} \tag{9.1.46}$$

where i=1 and 2.
For displacement the coefficients F_{10}, F_{20}, F_{30} are needed. From Eqs. (9.1.23), (9.1.32), and (9.1.39) $F_{10} = F_{30}$ can be obtained. The difference $F_{10} - F_{20}$ can be determined from Eq. (9.1.23). For the determination of K_0 and the separated values of F_{10} and F_{20}, stress analysis of the total joint is required.
In case of $\Delta = 0$ in Eq. (9.1.45), i.e. $\alpha = 1 + 2\beta - 2\beta/\cos(2\theta_1)$, the solution is

$$B_{10} = -\frac{K_0}{\sin(2\theta_1)} \tag{9.1.47}$$

$$C_{10} = K_0 \tag{9.1.48}$$

$$D_{10} = K_0 \frac{\cos(2\theta_1)}{\sin(2\theta_1)} \tag{9.1.49}$$

$$B_{20} = K_0 \frac{\cos(2\theta_1) - 1}{\sin(2\theta_1)} - \frac{Q}{2} \tag{9.1.50}$$

$$D_{20} = \frac{Q}{2} \tag{9.1.51}$$

for $\cos(2\theta_1) \neq 0$ and $\sin(2\theta_1) \neq 0$. The cases of $\cos(2\theta_1) = 0$ and $\sin(2\theta_1) = 0$, i.e. $\theta_1 = \pi/4$ or $\theta_1 = \pi/2$ or $\theta_1 = \pi$, will be treated below.

If $\theta_1 = \pi/4$, the coefficients can be simplified as follows based on Eqs. (9.1.40) through (9.1.45):

$$B_{10} = K_0 \frac{1 + \alpha}{2\beta} - Q \frac{1 + \alpha}{4\beta} \tag{9.1.52}$$

$$C_{10} = -B_{10} \tag{9.1.53}$$

$$D_{10} = 0 \tag{9.1.54}$$

$$B_{20} = K_0 \frac{1+\alpha-2\beta}{2\beta} - Q\frac{1+\alpha}{4\beta} \tag{9.1.55}$$

$$D_{20} = K_0 \tag{9.1.56}$$

for $\beta \neq 0$. For $\beta = 0$ the coefficients are:

$$B_{10} = K_0 + \frac{Q}{2} \tag{9.1.57}$$

$$C_{10} = -K_0 - \frac{Q}{2} \tag{9.1.58}$$

$$D_{10} = 0 \tag{9.1.59}$$

$$B_{20} = K_0 \tag{9.1.60}$$

$$D_{20} = \frac{Q}{2}. \tag{9.1.61}$$

For joints with $\theta_1 = \pi/2$ and $\theta_1 = \pi$ (i.e. $\sin(2\theta_1) = 0$) and for thermal loading the solutions cannot be obtained directly from Eqs. (9.1.22-9.1.35). Special additional conditions have to be used (see Sections 9.2 and 9.3).

For Mechanical Loading

For a joint under mechanical loading the solutions of the coefficients given in Eqs. (9.1.36) - (9.1.61) are still valid by setting Q=0 (due to $\Delta T = 0$). It can be seen that for a joint with a crack terminating at the interface, the regular stress term always is non-zero for mechanical loading. The regular stress term in Cartesian coordinates can be simplified as:

$$\sigma_{xx10} = K_0 \frac{4(1+\alpha)\cos^2(\theta_1)}{\Delta} \tag{9.1.62}$$

$$\sigma_{xx20} = K_0 \frac{2\{1+\alpha-4\beta-\cos(2\theta_1)[1-3\alpha+4\beta]\}}{\Delta} \tag{9.1.63}$$

$$\sigma_{yy10} = \sigma_{yy20} = K_0 \frac{4(1+\alpha)\sin^2(\theta_1)}{\Delta} \tag{9.1.64}$$

$$\tau_{xy10} = \tau_{xy20} = K_0 \frac{2(1+\alpha)\sin(2\theta_1)}{\Delta} \tag{9.1.65}$$

for $\Delta \neq 0$. For $\Delta = 0$ there is

$$\sigma_{xx10} = -2K_0 \frac{\cos(\theta_1)}{\sin(\theta_1)} \tag{9.1.66}$$

$$\sigma_{xx20} = -2K_0 \frac{\sin(\theta_1)}{\cos(\theta_1)} \tag{9.1.67}$$

$$\sigma_{yy10} = \sigma_{yy20} = \sigma_{xx20} \tag{9.1.68}$$

$$\tau_{xy10} = \tau_{xy20} = -2K_0, \tag{9.1.69}$$

with $\sin(\theta_1) \neq 0$ and $\cos(\theta_1) \neq 0$, i.e. $\theta_1 \neq \pi/2$ and $\theta_1 \neq \pi$. For $\theta_1 = \pi/4$ and $\beta = 0$, the results are

$$\sigma_{xx10} = \sigma_{xx20} = \sigma_{yy10} = \sigma_{yy20} = \tau_{xy10} = \tau_{xy20} = 2K_0. \tag{9.1.70}$$

In Section 9.2 the case of $\theta_1 = \pi/2$ and in Section 9.3 the case of $\theta_1 = \pi$ will be discussed.
The stress field near the singular point can be calculated from Eqs. (3.0.1) and (3.0.2) for real and complex eigenvalues with the quantities given in this section. For the displacements the equations given in Section 3.6 should be used.

9.2 Crack Perpendicular to the Interface

In this section an important special case in practice will be considered. It is a joint with a crack perpendicular to the interface (see Fig. 9.2). In a coated structure this kind of crack usually occurs when the coating is made of ceramic or brittle material. The stress distribution near the crack tip will be described analytically on the practically interesting scale. The quantities used to calculate the stresses, like the stress exponent, the angular functions, the regular stress term, and stress intensity factors will be presented.

9.2.1 The Singular Stress Exponent

A joint with a crack perpendicular to the interface is a special case of Chapter 8 with $\theta_1 = -\theta_2 = 90°$ (because at $\theta_2 = -90°$ the conditions $v = 0$ and $\tau_{r\theta} = 0$ satisfy if a

semi-infinite joint is considered) or Section 9.1 with $\theta_1 = 90°$. In this case, the equation to determine the eigenvalue is

$$\frac{128(2-\lambda_n)^2\sin(\lambda_n\pi)}{(1+\alpha)^2}(1-\beta^2)\Big\{\frac{2(1-\lambda_n)^2}{1-\beta}(\beta-\alpha)-\frac{\beta^2-\alpha}{1-\beta^2}+cos(\pi\lambda_n)\Big\}=0, \tag{9.2.1}$$

from Chapter 8 or

$$\frac{4096(2-\lambda_n)^2\sin^2(\lambda_n\pi)}{(1+\alpha)^4}(1-\beta^2)^2\Big\{\frac{2(1-\lambda_n)^2}{1-\beta}(\beta-\alpha)-\frac{\beta^2-\alpha}{1-\beta^2}+cos(\pi\lambda_n)\Big\}^2=0, \tag{9.2.2}$$

from Section 9.1. From Eq. (9.2.1) or Eq. (9.2.2) it is known that $\lambda_n = 2$ and $\lambda_n = 0, \pm1, \pm2, ..., \pm n$ are always the eigenvalue of this problem. However, as the displacements at the singular point (i.e. r=0) are finite, only the eigenvalues $\lambda_n \leq 1$ have a physical meaning (see Eqs. (3.1.16-3.1.17)). Only eigenvalues $0 < \lambda_n \leq 1$ are responsible for the singular stress term. The case of $\lambda_n = 1$ corresponds to a rigid body displacement. Therefore, the equation for determining the stress exponent of the singular term is

$$2(1-\lambda_n)^2(1+\beta)(\beta-\alpha)-(\beta^2-\alpha)+cos(\pi\lambda_n)(1-\beta^2)=0, \tag{9.2.3}$$

for $\alpha \neq -1$ (Eqs. (9.2.1) and (9.2.2) offer the same singular stress exponents).

For a given eigenvalue λ_n the angular function can be determined. The coefficients of the angular functions can be determined from Eqs. (8.1.31) through (8.1.38). The angular functions can be calculated from Eqs. (3.1.97- 3.1.99). It should be noted that in terms of geometry and material, this problem is symmetric to the crack surface. Therefore, the solutions in Section 9.1 are the same for material ranges 1 and 3.

9.2.2 The Regular Stress Term

In case of a joint with a crack perpendicular to the interface, which is the case of $\theta_1 = -\theta_2 = \pi/2$ in Section 8.2, the regular stress term in Cartesian coordinates is

$$\sigma_{xx10} = \tau_{xy10} = 0 \tag{9.2.4}$$

$$\sigma_{yy10} = -Q\frac{(1+\alpha)}{1+2\beta} \tag{9.2.5}$$

$$\sigma_{xx20} = 2\sigma_{yy10} \tag{9.2.6}$$

$$\sigma_{yy20} = \sigma_{yy10} \tag{9.2.7}$$

$$\tau_{xy20} = 0, \tag{9.2.8}$$

for thermal loading and

$$\sigma_{xx10} = \tau_{xy10} = 0 \tag{9.2.9}$$

$$\sigma_{yy10} = 4K_0 \frac{1+\alpha}{1-\alpha+4\beta} \tag{9.2.10}$$

$$\sigma_{xx20} = 8K_0 \frac{\alpha-2\beta}{1-\alpha+4\beta} \tag{9.2.11}$$

$$\sigma_{yy20} = \sigma_{yy10} \tag{9.2.12}$$

$$\tau_{xy20} = 0, \tag{9.2.13}$$

for mechanical loading, where K_0 has to be determined by the stress analysis of the total joint, e.g. using FEM. It can be seen that in Cartesian coordinates the shear stress component of the regular stress term and the stress component parallel to the interface in material 1 always are zero for thermal and mechanical loading.

9.3 Joint with Interface Crack

Now an important special case in the practice will be considered. It is a joint with an interface crack (see Fig. 9.3).

9.3.1 The Singular Stress Exponent

A joint with an interface crack is a special case of Chapter 3 with $\theta_1 = 180°$ and $\theta_2 = -180°$ or Section 9.1 with $\theta_1 = \pi$. From Section 9.1 it is known that

$$\mathrm{Det}[A] = \frac{2048(2-\lambda_n)^2 \sin^2(\lambda_n\pi)(1-\alpha)^2}{(1+\alpha)^4}\Big\{1+\beta^2+\cos(2\pi\lambda_n)(1-\beta^2)\Big\}, \tag{9.3.1}$$

with $\lambda_n = t_n + ip_n$. From Chapter 3 the eigenvalues $t + ip$ can also be obtained by setting $\theta_1 = 180°$ and $\theta_2 = -180°$ in equations (3.1.127-3.1.134) and (3.1.136). For this case Eq. (3.1.136) can be simplified as

$$Z_1 * Z_2 = 0 \tag{9.3.2}$$

with

$$Z_1 = [cos(t_n\pi)(e^{2p_n\pi} - 1) - i\ sin(t_n\pi)(1 + e^{2p_n\pi})]^2 \tag{9.3.3}$$

and

$$\begin{aligned} Z_2 &= 2e^{2p_n\pi}(1+\beta^2) + cos(2t_n\pi)[1 - \beta^2 + e^{4p_n\pi} - \beta^2 e^{4p_n\pi}] \\ &+ i\ sin(2t_n\pi)[1 - \beta^2 - e^{4p_n\pi} + \beta^2 e^{4p_n\pi}]. \end{aligned} \tag{9.3.4}$$

By expanding Eq. (9.3.1) in a real and an imaginary part, it can be shown that in the range of $0 < t_n < 1$, the solutions of Det[A] = 0 in Eq. (9.3.1) are the same as those of $Z_2 = 0$ in Eq. (9.3.4).
The solution of $Z_1 = 0$ is

$$p_n = 0, \quad t_n = 0, \pm 1, \pm 2, \pm 3, ..., \pm n \tag{9.3.5}$$

The solutions of $Z_2 = 0$ are

$$t_n = 0, \pm 1/2, \pm 3/2, \pm 5/2, \pm 7/2, ..., \tag{9.3.6}$$

while p_n satisfies

$$2e^{2p_n\pi}(1+\beta^2) + cos(2t_n\pi)[1 - \beta^2 + e^{4p_n\pi} - \beta^2 e^{4p_n\pi}] = 0. \tag{9.3.7}$$

The displacement at the singular point must be finite. From Eqs. (3.1.113) through (3.1.116) and (3.1.137) it is known that the displacement is proportional to r^{t_n}. Therefore, the value of t_n cannot be negative. This means that only t_n=0, 1/2, 3/2, 5/2, 7/2, ..., n/2 should be considered. From Eq. (3.1.111) and Eq. (3.1.112) it can be seen that the stresses are proportional to $r^{t_n - 1}$. As singular stress terms, only t_n=0 and t_n=1/2 are possible. If t_n=0, Eq. (9.3.7) reads

$$2e^{2p_n\pi}(1+\beta^2) + (1-\beta^2)(1+e^{4p_n\pi}) = 0. \tag{9.3.8}$$

Due to $\beta < 1/2$, $e^{2p_n\pi} > 0$ and $e^{4p_n\pi} > 0$, there is no solution of p_n (p_n is a real value), so that Eq. (9.3.8) is satisfied. Therefore, the only singular term corresponds to t_n=1/2. For t=1/2 the solution of Eq. (9.3.7) is

$$p = \pm\frac{1}{2\pi} ln\left[\frac{1+\beta}{1-\beta}\right], \tag{9.3.9}$$

where β is the second Dundurs parameter.

9.3.2 The Angular Functions of the Singular Terms

At the eigenvalues determined, Eqs. (3.1.127-3.1.134) can be solved for the coefficients $\mathcal{A}_{1n}$, $\mathcal{B}_{1n}$, $\mathcal{C}_{1n}$, $\mathcal{D}_{1n}$ and $\mathcal{A}_{2n}$, $\mathcal{B}_{2n}$, $\mathcal{C}_{2n}$, $\mathcal{D}_{2n}$ including one arbitrary complex constant. For the eigenvalue $t + ip = 1/2 + i\frac{1}{2\pi} ln\left[\frac{1+\beta}{1-\beta}\right]$ the solution is

$$\mathcal{A}_1 = -\frac{1+\beta}{1-\beta}\frac{0.5 - \mathrm{ip}}{0.25 + \mathrm{p}^2} \tag{9.3.10}$$

$$\bar{\mathcal{B}}_1 = 0 \tag{9.3.11}$$

$$\mathcal{C}_1 = \frac{1+\beta}{1-\beta} \tag{9.3.12}$$

$$\bar{\mathcal{D}}_1 = -\frac{0.5 - ip}{0.25 + p^2} \tag{9.3.13}$$

$$\mathcal{A}_2 = \bar{\mathcal{D}}_1 \tag{9.3.14}$$

$$\bar{\mathcal{B}}_2 = 0 \tag{9.3.15}$$

$$\mathcal{C}_2 = 1 \tag{9.3.16}$$

$$\bar{\mathcal{D}}_2 = \mathcal{A}_1 \tag{9.3.17}$$

For the eigenvalue $t + ip = 1/2 - i\frac{1}{2\pi} ln\left[\frac{1+\beta}{1-\beta}\right]$ the solution is

$$\mathcal{A}_1 = 0 \tag{9.3.18}$$

$$\bar{\mathcal{B}}_1 = -\frac{1+\beta}{1-\beta}\frac{0.5 - ip}{0.25 + p^2} \tag{9.3.19}$$

$$\mathcal{C}_1 = -\frac{0.5 - \mathrm{ip}}{0.25 + \mathrm{p}^2} \tag{9.3.20}$$

$$\bar{\mathcal{D}}_1 = \frac{1+\beta}{1-\beta} \tag{9.3.21}$$

$$\mathcal{A}_2 = 0 \tag{9.3.22}$$

$$\bar{\mathcal{B}}_2 = \mathcal{C}_1 \tag{9.3.23}$$

$$\mathcal{C}_2 = \bar{\mathcal{B}}_1 \tag{9.3.24}$$

$$\bar{\mathcal{D}}_2 = 1. \tag{9.3.25}$$

In this special case with $\theta_1 = 180°$, $\theta_2 = -180°$ and $t = 0.5$, the angular functions defined in Eqs. (3.1.144-3.1.150) for $\pm p$ (p is given in Eq. (9.3.9)) have the relationship of

$$f^c_{ijk}(\theta, p) = f^c_{ijk}(\theta, -p) \tag{9.3.26}$$

and

$$f^s_{ijk}(\theta,p) = -f^s_{ijk}(\theta,-p). \tag{9.3.27}$$

From Eqs. (3.1.151-3.1.153) it can be seen that both eigenvalues $t \pm ip$ give the same information concerning the stresses, but have only one independent undetermined stress intensity factor K. Therefore, the definition given in Section 3.1.2, Eqs. (3.1.144) through (3.1.153), cannot be used for the angular functions and the K-factors in case of an interface crack. Now, we have to use another definition for the angular functions and the K-factors. If in Eqs. (3.1.117-3.1.119) the coefficients $\mathcal{A}_{\rm k}, \mathcal{B}_{\rm k}, \mathcal{C}_{\rm k}, \mathcal{D}_{\rm k}$ are formally normalized by a complex constant $K = K_I + iK_{II}$, i.e.

$$\begin{aligned} \tilde{\mathcal{A}}_k &= \mathcal{A}_{\rm k}/{\rm K} \qquad \tilde{\mathcal{B}}_{\rm k} = \mathcal{B}_{\rm k}/{\rm K} \\ \tilde{\mathcal{C}}_k &= \mathcal{C}_{\rm k}/{\rm K} \qquad \tilde{\mathcal{D}}_{\rm k} = \mathcal{D}_{\rm k}/{\rm K} \end{aligned} \tag{9.3.28}$$

the singular stress terms are

$$\begin{aligned} \sigma_{ijk}(r,\theta) &= \frac{K_I}{(r/L)^\omega}\left\{\cos\left[p\ln\left(\frac{r}{L}\right)\right] f^{cI}_{ijk}(\theta) + \sin\left[p\ln\left(\frac{r}{L}\right)\right] f^{sI}_{ijk}(\theta)\right\} \\ &+ \frac{K_{II}}{(r/L)^\omega}\left\{\cos\left[p\ln\left(\frac{r}{L}\right)\right] f^{cII}_{ijk}(\theta) + \sin\left[p\ln\left(\frac{r}{L}\right)\right] f^{sII}_{ijk}(\theta)\right\} \end{aligned} \tag{9.3.29}$$

where $\omega = 1 - t$.
The angular functions in Eq. (9.3.29) can be calculated from

$$\begin{aligned} F^{sI}_{rr}(\theta) = e^{-p\theta}\Big\{ &\left(-1.25\,a_i + 1.25\,b_i\,e^{2p\theta} - 2\,a_r\,p - 2\,b_r\,e^{2p\theta}\,p - a_i\,p^2 + b_i\,e^{2p\theta}\,p^2\right)\cos(0.5\,\theta) \\ &+ \left(0.5\,c_i - 0.5\,d_i\,e^{2p\theta} + c_r\,p + d_r\,e^{2p\theta}\,p\right)\cos(1.5\,\theta) \\ &+ \left(1.25\,a_r - 1.25\,b_r\,e^{2p\theta} - 2\,a_i\,p - 2\,b_i\,e^{2p\theta}\,p + a_r\,p^2 - b_r\,e^{2p\theta}\,p^2\right)\sin(0.5\,\theta) \\ &+ \left(0.5\,c_r - 0.5\,d_r\,e^{2p\theta} - c_i\,p - d_i\,e^{2p\theta}\,p\right)\sin(1.5\,\theta)\Big\} \end{aligned} \tag{9.3.30}$$

$$\begin{aligned} F^{cI}_{rr}(\theta) = e^{-p\theta}\Big\{ &\left(1.25\,a_r + 1.25\,b_r\,e^{2p\theta} - 2\,a_i\,p + 2\,b_i\,e^{2p\theta}\,p + a_r\,p^2 + b_r\,e^{2p\theta}\,p^2\right)\cos(0.5\,\theta) \\ &+ \left(-0.5\,c_r - 0.5\,d_r\,e^{2p\theta} + c_i\,p - d_i\,e^{2p\theta}\,p\right)\cos(1.5\,\theta) \\ &+ \left(1.25\,a_i + 1.25\,b_i\,e^{2p\theta} + 2\,a_r\,p - 2\,b_r\,e^{2p\theta}\,p + a_i\,p^2 + b_i\,e^{2p\theta}\,p^2\right)\sin(0.5\,\theta) \\ &+ \left(0.5\,c_i + 0.5\,d_i\,e^{2p\theta} + c_r\,p - d_r\,e^{2p\theta}\,p\right)\sin(1.5\,\theta)\Big\} \end{aligned} \tag{9.3.31}$$

$$F^{sI}_{\theta\theta}(\theta) = e^{-p\theta}\Big\{ \left(-0.75\,a_i + 0.75\,b_i\,e^{2p\theta} - 2\,a_r\,p - 2\,b_r\,e^{2p\theta}\,p + a_i\,p^2 - b_i\,e^{2p\theta}\,p^2\right)\cos(0.5\,\theta)$$

$$+ \quad \left(-0.5\, c_i + 0.5\, d_i\, e^{2\,p\,\theta} - c_r\, p - d_r\, e^{2\,p\,\theta}\, p\right) \cos(1.5\,\theta)$$
$$+ \quad \left(0.75\, a_r - 0.75\, b_r\, e^{2\,p\,\theta} - 2\, a_i\, p - 2\, b_i\, e^{2\,p\,\theta}\, p - a_r\, p^2 + b_r\, e^{2\,p\,\theta}\, p^2\right) \sin(0.5\,\theta)$$
$$+ \quad \left(-0.5\, c_r + 0.5\, d_r\, e^{2\,p\,\theta} + c_i\, p + d_i\, e^{2\,p\,\theta}\, p\right) \sin(1.5\,\theta)\Bigg\} \tag{9.3.32}$$

$$F_{\theta\theta}^{cI}(\theta) = e^{-p\theta}\Bigg\{ \left(0.75\, a_r + 0.75\, b_r\, e^{2\,p\,\theta} - 2\, a_i\, p + 2\, b_i\, e^{2\,p\,\theta}\, p - a_r\, p^2 - b_r\, e^{2\,p\,\theta}\, p^2\right) \cos(0.5\,\theta)$$
$$+ \quad \left(0.5\, c_r + 0.5\, d_r\, e^{2\,p\,\theta} - c_i\, p + d_i\, e^{2\,p\,\theta}\, p\right) \cos(1.5\,\theta)$$
$$+ \quad \left(0.75\, a_i + 0.75\, b_i\, e^{2\,p\,\theta} + 2\, a_r\, p - 2\, b_r\, e^{2\,p\,\theta}\, p - a_i\, p^2 - b_i\, e^{2\,p\,\theta}\, p^2\right) \sin(0.5\,\theta)$$
$$+ \quad \left(-0.5\, c_i - 0.5\, d_i\, e^{2\,p\,\theta} - c_r\, p + d_r\, e^{2\,p\,\theta}\, p\right) \sin(1.5\,\theta)\Bigg\} \tag{9.3.33}$$

$$\begin{aligned} F_{r\theta}^{sI}(\theta) &= e^{-p\theta}\Bigg\{ \left(-0.25\, a_r + 0.25\, b_r\, e^{2\,p\,\theta} - a_r\, p^2 + b_r\, e^{2\,p\,\theta}\, p^2\right) \cos(0.5\,\theta) \\ &+ \left(0.5\, c_r - 0.5\, d_r\, e^{2\,p\,\theta} - c_i\, p - d_i\, e^{2\,p\,\theta}\, p\right) \cos(1.5\,\theta) \\ &+ \left(-0.25\, a_i + 0.25\, b_i\, e^{2\,p\,\theta} - a_i\, p^2 + b_i\, e^{2\,p\,\theta}\, p^2\right) \sin(0.5\,\theta) \\ &+ \left(-0.5\, c_i + 0.5\, d_i\, e^{2\,p\,\theta} - c_r\, p - d_r\, e^{2\,p\,\theta}\, p\right) \sin(1.5\,\theta)\Bigg\} \end{aligned} \tag{9.3.34}$$

$$\begin{aligned} F_{r\theta}^{cI}(\theta) &= e^{-p\theta}\Bigg\{ \left(-0.25\, a_i - 0.25\, b_i\, e^{2\,p\,\theta} - a_i\, p^2 - b_i\, e^{2\,p\,\theta}\, p^2\right) \cos(0.5\,\theta) \\ &+ \left(0.5\, c_i + 0.5\, d_i\, e^{2\,p\,\theta} + c_r\, p - d_r\, e^{2\,p\,\theta}\, p\right) \cos(1.5\,\theta) \\ &+ \left(0.25\, a_r + 0.25\, b_r\, e^{2\,p\,\theta} + a_r\, p^2 + b_r\, e^{2\,p\,\theta}\, p^2\right) \sin(0.5\,\theta) \\ &+ \left(0.5\, c_r + 0.5\, d_r\, e^{2\,p\,\theta} - c_i\, p + d_i\, e^{2\,p\,\theta}\, p\right) \sin(1.5\,\theta)\Bigg\} \end{aligned} \tag{9.3.35}$$

and

$$F_{rr}^{sII}(\theta) = e^{-p\theta}\Bigg\{ \left(-1.25\, a_r + 1.25\, b_r\, e^{2\,p\,\theta} + 2\, a_i\, p + 2\, b_i\, e^{2\,p\,\theta}\, p - a_r\, p^2 + b_r\, e^{2\,p\,\theta}\, p^2\right) \cos(0.5\,\theta)$$
$$+ \quad \left(0.5\, c_r - 0.5\, d_r\, e^{2\,p\,\theta} - c_i\, p - d_i\, e^{2\,p\,\theta}\, p\right) \cos(1.5\,\theta)$$
$$+ \quad \left(-1.25\, a_i + 1.25\, b_i\, e^{2\,p\,\theta} - 2\, a_r\, p - 2\, b_r\, e^{2\,p\,\theta}\, p - a_i\, p^2 + b_i\, e^{2\,p\,\theta}\, p^2\right) \sin(0.5\,\theta)$$
$$+ \quad \left(-0.5\, c_i + 0.5\, d_i\, e^{2\,p\,\theta} - c_r\, p - d_r\, e^{2\,p\,\theta}\, p\right) \sin(1.5\,\theta)\Bigg\} \tag{9.3.36}$$

$$F_{rr}^{cII}(\theta) = e^{-p\theta}\Bigg\{ \left(-1.25\, a_i - 1.25\, b_i\, e^{2\,p\,\theta} - 2\, a_r\, p + 2\, b_r\, e^{2\,p\,\theta}\, p - a_i\, p^2 - b_i\, e^{2\,p\,\theta}\, p^2\right) \cos(0.5\,\theta)$$

$$
\begin{aligned}
&+ \quad \left(0.5\, c_i + 0.5\, d_i\, e^{2\,p\,\theta} + c_r\, p - d_r\, e^{2\,p\,\theta}\, p\right) \cos(1.5\,\theta) \\
&+ \quad \left(1.25\, a_r + 1.25\, b_r\, e^{2\,p\,\theta} - 2\, a_i\, p + 2\, b_i\, e^{2\,p\,\theta}\, p + a_r\, p^2 + b_r\, e^{2\,p\,\theta}\, p^2\right) \sin(0.5\,\theta) \\
&+ \quad \left(0.5\, c_r + 0.5\, d_r\, e^{2\,p\,\theta} - c_i\, p + d_i\, e^{2\,p\,\theta}\, p\right) \sin(1.5\,\theta)\Bigg\} \qquad (9.3.37)
\end{aligned}
$$

$$
\begin{aligned}
F_{\theta\theta}^{sII}(\theta) = e^{-p\theta}\Bigg\{ & \left(-0.75\, a_r + 0.75\, b_r\, e^{2\,p\,\theta} + 2\, a_i\, p + 2\, b_i\, e^{2\,p\,\theta}\, p + a_r\, p^2 - b_r\, e^{2\,p\,\theta}\, p^2\right) \cos(0.5\,\theta) \\
&+ \quad \left(-0.5\, c_r + 0.5\, d_r\, e^{2\,p\,\theta} + c_i\, p + d_i\, e^{2\,p\,\theta}\, p\right) \cos(1.5\,\theta) \\
&+ \quad \left(-0.75\, a_i + 0.75\, b_i\, e^{2\,p\,\theta} - 2\, a_r\, p - 2\, b_r\, e^{2\,p\,\theta}\, p + a_i\, p^2 - b_i\, e^{2\,p\,\theta}\, p^2\right) \sin(0.5\,\theta) \\
&+ \quad \left(0.5\, c_i - 0.5\, d_i\, e^{2\,p\,\theta} + c_r\, p + d_r\, e^{2\,p\,\theta}\, p\right) \sin(1.5\,\theta)\Bigg\} \qquad (9.3.38)
\end{aligned}
$$

$$
\begin{aligned}
F_{\theta\theta}^{cII}(\theta) = e^{-p\theta}\Bigg\{ & \left(-0.75\, a_i - 0.75\, b_i\, e^{2\,p\,\theta} - 2\, a_r\, p + 2\, b_r\, e^{2\,p\,\theta}\, p + a_i\, p^2 + b_i\, e^{2\,p\,\theta}\, p^2\right) \cos(0.5\,\theta) \\
&+ \quad \left(-0.5\, c_i - 0.5\, d_i\, e^{2\,p\,\theta} - c_r\, p + d_r\, e^{2\,p\,\theta}\, p\right) \cos(1.5\,\theta) \\
&+ \quad \left(0.75\, a_r + 0.75\, b_r\, e^{2\,p\,\theta} - 2\, a_i\, p + 2\, b_i\, e^{2\,p\,\theta}\, p - a_r\, p^2 - b_r\, e^{2\,p\,\theta}\, p^2\right) \sin(0.5\,\theta) \\
&+ \quad \left(-0.5\, c_r - 0.5\, d_r\, e^{2\,p\,\theta} + c_i\, p - d_i\, e^{2\,p\,\theta}\, p\right) \sin(1.5\,\theta)\Bigg\} \qquad (9.3.39)
\end{aligned}
$$

$$
\begin{aligned}
F_{r\theta}^{sII}(\theta) &= e^{-p\theta}\Bigg\{ \left(0.25\, a_i - 0.25\, b_i\, e^{2\,p\,\theta} + a_i\, p^2 - b_i\, e^{2\,p\,\theta}\, p^2\right) \cos(0.5\,\theta) \\
&+ \quad \left(-0.5\, c_i + 0.5\, d_i\, e^{2\,p\,\theta} - c_r\, p - d_r\, e^{2\,p\,\theta}\, p\right) \cos(1.5\,\theta) \\
&+ \quad \left(-0.25\, a_r + 0.25\, b_r\, e^{2\,p\,\theta} - a_r\, p^2 + b_r\, e^{2\,p\,\theta}\, p^2\right) \sin(0.5\,\theta) \\
&+ \quad \left(-0.5\, c_r + 0.5\, d_r\, e^{2\,p\,\theta} + c_i\, p + d_i\, e^{2\,p\,\theta}\, p\right) \sin(1.5\,\theta)\Bigg\} \qquad (9.3.40)
\end{aligned}
$$

$$
\begin{aligned}
F_{r\theta}^{cII}(\theta) &= e^{-p\theta}\Bigg\{ \left(-0.25\, a_r - 0.25\, b_r\, e^{2\,p\,\theta} - a_r\, p^2 - b_r\, e^{2\,p\,\theta}\, p^2\right) \cos(0.5\,\theta) \\
&+ \quad \left(0.5\, c_r + 0.5\, d_r\, e^{2\,p\,\theta} - c_i\, p + d_i\, e^{2\,p\,\theta}\, p\right) \cos(1.5\,\theta) \\
&+ \quad \left(-0.25\, a_i - 0.25\, b_i\, e^{2\,p\,\theta} - a_i\, p^2 - b_i\, e^{2\,p\,\theta}\, p^2\right) \sin(0.5\,\theta) \\
&+ \quad \left(-0.5\, c_i - 0.5\, d_i\, e^{2\,p\,\theta} - c_r\, p + d_r\, e^{2\,p\,\theta}\, p\right) \sin(1.5\,\theta)\Bigg\} \qquad (9.3.41)
\end{aligned}
$$

where

$$
\begin{aligned}
a_r = Re[\tilde{\mathcal{A}}_k], \qquad & a_i = Im[\tilde{\mathcal{A}}_k] \\
b_r = Re[\tilde{\mathcal{B}}_k], \qquad & b_i = Im[\tilde{\mathcal{B}}_k] \\
c_r = Re[\tilde{\mathcal{C}}_k], \qquad & c_i = Im[\tilde{\mathcal{C}}_k] \\
d_r = Re[\tilde{\mathcal{D}}_k], \qquad & d_i = Im[\tilde{\mathcal{D}}_k]. \qquad (9.3.42)
\end{aligned}
$$

for the angular functions of K_I and

$$\begin{aligned} a_r &= Re[\tilde{\mathcal{A}}_k], \qquad a_i = Im[\tilde{\mathcal{A}}_k] \\ b_r &= -Re[\tilde{\mathcal{B}}_k], \qquad b_i = -Im[\tilde{\mathcal{B}}_k] \\ c_r &= Re[\tilde{\mathcal{C}}_k], \qquad c_i = Im[\tilde{\mathcal{C}}_k] \\ d_r &= -Re[\tilde{\mathcal{D}}_k], \qquad d_i = -Im[\tilde{\mathcal{D}}_k] \end{aligned} \tag{9.3.43}$$

for the angular functions of K_{II}. The values of $\tilde{\mathcal{A}}_k, \tilde{\mathcal{B}}_k, \tilde{\mathcal{C}}_k, \tilde{\mathcal{D}}_k$ can take those of Eqs. (9.3.10-9.3.17) or Eqs. (9.3.18-9.3.25). For example, for the eigenvalue $t + ip = 1/2 + i\frac{1}{2\pi} ln\left[\frac{1+\beta}{1-\beta}\right]$

$$\tilde{\mathcal{A}}_1 = -\frac{1+\beta}{1-\beta}\frac{0.5-ip}{0.25+p^2} \tag{9.3.44}$$

$$\tilde{\mathcal{B}}_1 = 0 \tag{9.3.45}$$

$$\tilde{\mathcal{C}}_1 = \frac{1+\beta}{1-\beta} \tag{9.3.46}$$

$$\tilde{\bar{\mathcal{D}}}_1 = -\frac{0.5-ip}{0.25+p^2} \tag{9.3.47}$$

$$\tilde{\mathcal{A}}_2 = -\frac{0.5-ip}{0.25+p^2} \tag{9.3.48}$$

$$\tilde{\mathcal{B}}_2 = 0 \tag{9.3.49}$$

$$\tilde{\mathcal{C}}_2 = 1 \tag{9.3.50}$$

$$\tilde{\bar{\mathcal{D}}}_2 = -\frac{1+\beta}{1-\beta}\frac{0.5-ip}{0.25+p^2}, \tag{9.3.51}$$

are true. The angular functions are normalized as

$$\begin{aligned} f^{sI}_{rr}(\theta) &= \frac{F^{sI}_{rr}(\theta)}{F^{cI}_{\theta\theta}(0)} \\ f^{cI}_{rr}(\theta) &= \frac{F^{cI}_{rr}(\theta)}{F^{cI}_{\theta\theta}(0)} \\ f^{sI}_{\theta\theta}(\theta) &= \frac{F^{sI}_{\theta\theta}(\theta)}{F^{cI}_{\theta\theta}(0)} \\ f^{cI}_{\theta\theta}(\theta) &= \frac{F^{cI}_{\theta\theta}(\theta)}{F^{cI}_{\theta\theta}(0)} \\ f^{sI}_{r\theta}(\theta) &= \frac{F^{sI}_{r\theta}(\theta)}{F^{cI}_{\theta\theta}(0)} \\ f^{cI}_{r\theta}(\theta) &= \frac{F^{cI}_{r\theta}(\theta)}{F^{cI}_{\theta\theta}(0)} \end{aligned} \tag{9.3.52}$$

i.e. $f_{\theta\theta}^{cI} = 1$ at $\theta = 0$. According to the definition of the angular functions in Eq. (9.3.29), both eigenvalues $t \pm ip$ with two independent stress intensity factors give the same information for the stresses and

$$f_{ijk}^{sII}(\theta) = -f_{ijk}^{cI}(\theta) \tag{9.3.53}$$

and

$$f_{ijk}^{cII}(\theta) = f_{ijk}^{sI}(\theta). \tag{9.3.54}$$

This definition of the angular functions is identical to that one used in fracture mechanics.

9.3.3 The Stress Intensity Factors and the Stress Distribution near the Singular Point

In order to describe the stresses near the singular point over a larger range, which is of practical relevance, both singular stress terms and the regular stress term have to be used in the asymptotic solution. The stresses near the singular point can be calculated by

$$\begin{aligned}
\sigma_{ijk}(r,\theta) &= \frac{K_I}{(r/L)^{0.5}} \left\{ \cos\left[p \ln\left(\frac{r}{L}\right)\right] f_{ijk}^{cI}(\theta) + \sin\left[p \ln\left(\frac{r}{L}\right)\right] f_{ijk}^{sI}(\theta) \right\} \\
&+ \frac{K_{II}}{(r/L)^{0.5}} \left\{ \cos\left[p \ln\left(\frac{r}{L}\right)\right] f_{ijk}^{cII}(\theta) + \sin\left[p \ln\left(\frac{r}{L}\right)\right] f_{ijk}^{sII}(\theta) \right\} \\
&+ \sigma_{ij0}(\theta).
\end{aligned} \tag{9.3.55}$$

In Eq. (9.3.55) the quantities $p, f_{ijk}^{cI}(\theta), f_{ijk}^{sI}(\theta), f_{ijk}^{cII}(\theta), f_{ijk}^{sII}(\theta)$, the regular stress term $\sigma_{ij0}(\theta)$ (which is called T - stress term, see Eq. (3.3.133) for mechanical loading, and Eq. (3.2.113) for thermal loading) are known.
The regular stress term is

$$\sigma_{xx10} = Q(1+\alpha) \tag{9.3.56}$$

$$\sigma_{xx20} = -\sigma_{xx10} \tag{9.3.57}$$

$$\sigma_{yy10} = \sigma_{yy20} = \tau_{xy10} = \tau_{xy20} = 0 \tag{9.3.58}$$

for thermal loading and

$$\sigma_{xx10} = K_0 \frac{4(1+\alpha)}{\alpha - 1} \tag{9.3.59}$$

$$\sigma_{xx20} = -4K_0 \tag{9.3.60}$$

$$\sigma_{yy10} = \sigma_{yy20} = \tau_{xy10} = \tau_{xy20} = 0 \tag{9.3.61}$$

for mechanical loading.
By using the method given in Section 3.4, the unknown factors K_0, K_I, K_{II} can be determined. Now, two examples shall be given to illustrate the agreement of the stresses from FEM and Eq. (9.3.55), and the effect of the T - stress term on the stresses close to the singular point.
The material data of example 1 are chosen as

$$E_1 = 1000 \text{ GPa}, \quad \nu_1 = 0.3$$
$$E_2 = 100 \text{ GPa} , \quad \nu_2 = 0.2$$

which gives $\alpha = 0.826872$, $\beta = 0.317793$, and p=0.1048. Loading is a remote tensile stress perpendicular to the interface, σ_∞ =1 MPa. The regular stress term is

$$\begin{aligned} \sigma_{xx10} = -42.20K_0, \quad & \sigma_{xx20} = -4K_0 \\ \sigma_{yy10} = 0, \quad & \sigma_{yy20} = 0 \\ \sigma_{xy10} = 0, \quad & \sigma_{xy20} = 0. \end{aligned} \tag{9.3.62}$$

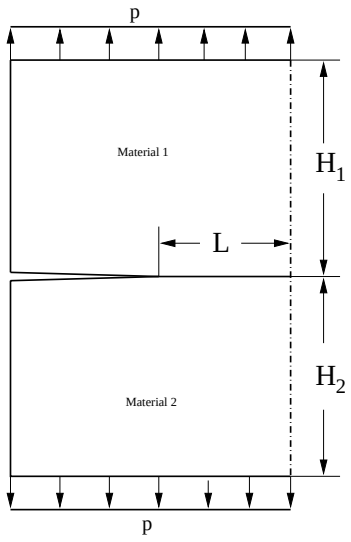

Figure 9.5: A finite joint with an interface crack, $H_1/L = H_2$=2. The geometry is symmetric, here only the left half joint is shown.

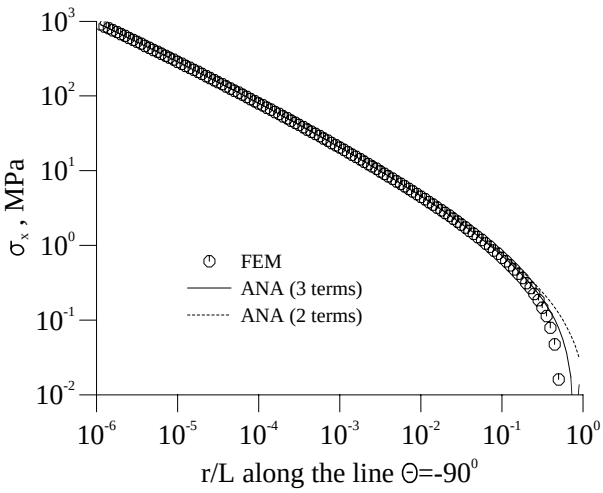

Figure 9.6: Comparison of the stresses obtained from FEM and Eq. (9.3.55) with two (dashed line) or three (solid line) terms along the line of $\theta = -90°$ for the component σ_x of example 1.

The results given below hold for plane strain. For the FEM calculation the ABAQUS code was used with an 8-nodes standard element. The mesh near the singular point is fine. The smallest length in the element is about 10^{-6}L (L see Fig. 9.5).

To determine the unknown K-factors and in particular the T - stress term (here K_0), points in the range of $10^{-6} < r/L < 10^{-3}$ are used. The K-values obtained are those calculated from $\theta_l = 90°$ applying the stress exponent σ_x.
The K-factors determined are

$$K_1 = 9.2858 \text{ MPa} , \quad K_2 = 0.8540 \text{ MPa}$$

when only two terms are used and

$$K_0 = 0.1004 \text{ MPa} , \quad K_1 = 9.3189 \text{ MPa} , \quad K_2 = 0.8992 \text{ MPa}$$

when the T - stress term is considered.

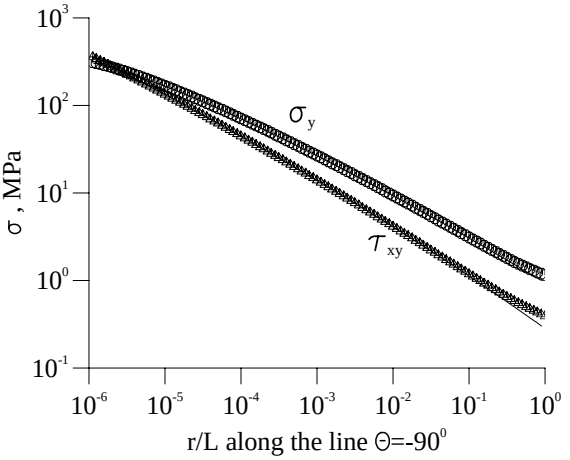

Figure 9.7: Comparison of the stresses obtained from FEM and Eq. (9.3.55) (with 3 terms) along the line of $\theta = -90°$ for the components σ_y and τ_{xy} of example 1.

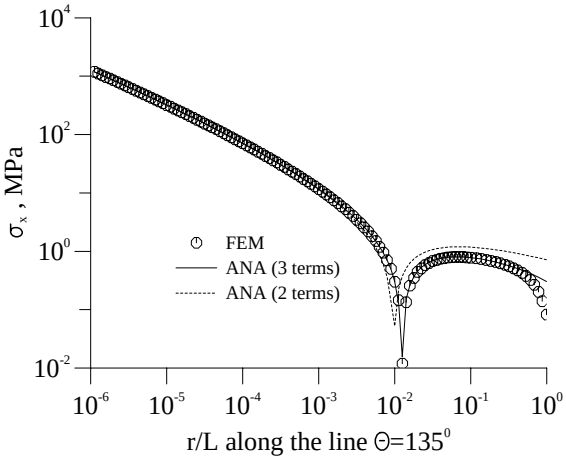

Figure 9.8: Comparison of the stresses obtained from FEM and Eq. (9.3.55) with two (dashed line) or three (solid line) terms along the line of $\theta = 135°$ for the component σ_x of example 1.

Using the K-factors as determined, stresses have been calculated from Eq. (9.3.55) with only two singular terms and all three terms. Comparisons of the stresses obtained from FEM and Eq. (9.3.55) along $\theta = -90°$ and $\theta = 135°$ are shown in Figs. 9.6, 9.7, 9.8, and 9.9. It can be seen that if the singular terms are used only, they are in good agreement in the range of $r/L < 10^{-3}$ only (see Fig. 9.8). But if the regular stress term is considered, they are in good agreement in a very large range near the singular point ($r/L < 10^{-1}$, see Figs. 9.6, 9.7, 9.8, and 9.9).
The material data of the example 2 are chosen as

$$E_1 = 100 \text{ GPa}, \quad \nu_1 = 0.2$$
$$E_2 = 200 \text{ GPa} , \quad \nu_2 = 0.3$$

which gives $\alpha = -0.35689, \beta = -0.163544$, and p=-0.052202. The regular stress term is

$$\begin{aligned} \sigma_{xx10} &= -1.8958K_0, \qquad \sigma_{xx20} = -4K_0 \\ \sigma_{yy10} &= 0, \qquad \sigma_{yy20} = 0 \\ \sigma_{xy10} &= 0, \qquad \sigma_{xy20} = 0 \end{aligned} \tag{9.3.63}$$

To determine the unknown K-factors and in particular the T - stress term, points in the range of $10^{-6} < r/L < 10^{-2}$ are used. The K-values are those obtained from $\theta_l = 90^\circ$ applying the stress exponent σ_x.

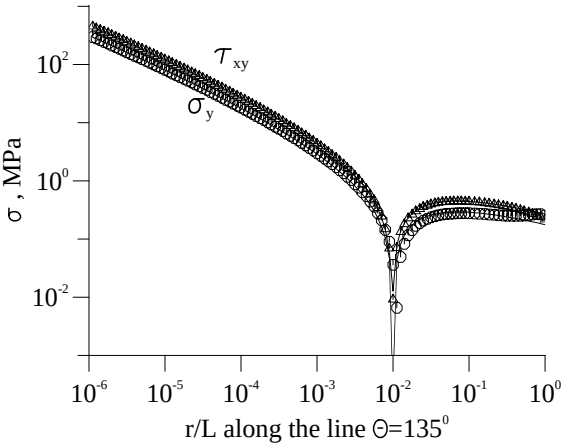

Figure 9.9: Comparison of the stresses obtained from FEM and Eq. (9.3.55) (with 3 terms) along the line of $\theta = 135^\circ$ for the components σ_y and τ_{xy} of example 1.

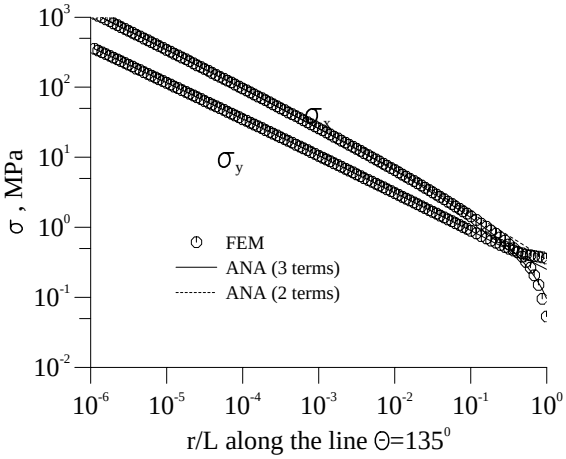

Figure 9.10: Comparison of the stresses obtained from FEM and Eq. (9.3.55) with two (dashed line) or three (solid line) terms along the line of $\theta = 135^\circ$ for the components σ_x, σ_y of example 2.

The K-factors obtained are

$$K_1 = 9.4224 \text{ MPa} , \quad K_2 = -0.5059 \text{ MPa}$$

when only two terms are used and

$$K_0 = 1.3447 \text{ MPa} , \quad K_1 = 9.3752 \text{ MPa} , \quad K_2 = -0.4408 \text{ MPa}$$

when the T - stress term is considered. Using the K-factors as determined, stresses have been calculated with Eq. (9.3.55) using two terms only and all three terms. Comparisons of the stresses obtained from FEM and Eq. (9.3.55) along $\theta = 135^\circ$ and $\theta = -90^\circ$ are shown in Figs. 9.10, 9.11, and 9.12. It can be seen that if the singular terms are used only, they are in good agreement in the range of $r/L < 10^{-3}$ or smaller only (see Fig. 9.11). But if the regular stress term is considered, they are in good

agreement over a very large range near the singular point ($r/L < 10^{-1}$, see Fig. 9.10, 9.11, and 9.12).
The results have demonstrated that to obtain a good description of the stresses near the singular point over a large range from Eq. (9.3.55), the regular stress term should be considered, also for the joint with a large singular stress exponent.

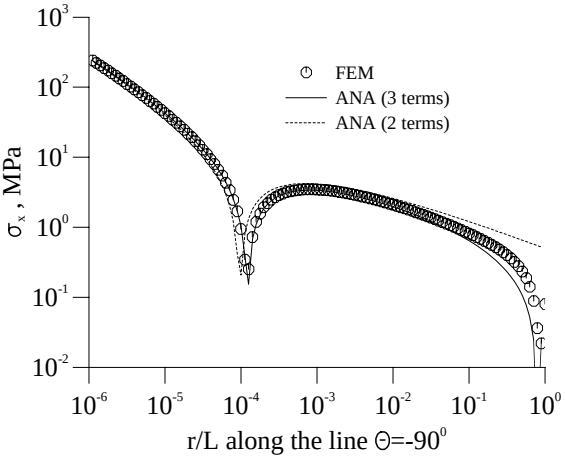

Figure 9.11: Comparison of the stresses obtained from FEM and Eq. (9.3.55) with two (dashed line) or three (solid line) terms along the line of $\theta = -90°$ for the component σ_x of example 2.

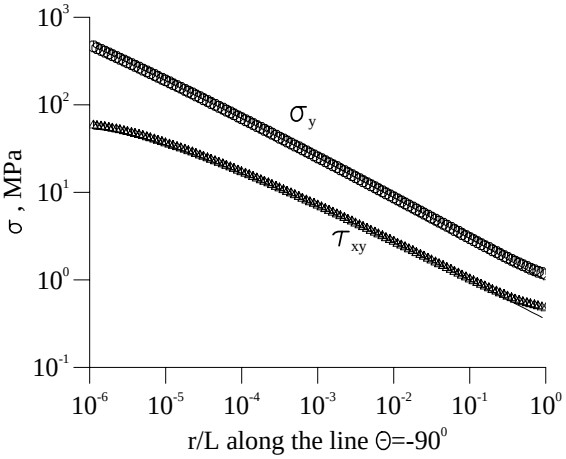

Figure 9.12: Comparison of the stresses obtained from FEM and Eq. (9.3.55) along the line of $\theta = -90°$ for the components σ_y and τ_{xy} of example 2.

9.4 Joint with Delamination Crack

In a two dissimilar materials joint with free edges, a special case is $\mid \theta_1 \mid + \mid \theta_2 \mid = 2\pi$ (see Fig. 9.4). This case is called delamination crack, because it corresponds to a joint with an interface corner (see Chapter 6) and one interface delaminated. The stress distribution near the crack tip will be described analytically on the practically interesting scale.

9.4.1 The Singular Stress Exponent

A joint with a delamination crack is a special case of Chapter 3 with $\theta_2 = -(2\pi - \theta_1)$. For this case Eq. (3.1.37) can be simplified as

$$\mathrm{Det}[A] \;=\; -\frac{64(t_n+1)}{(1+\alpha)^2}\Big\{\sin^2(2\pi t_n) + \beta {t_n}^2\big[-\cos[2t_n\,(2\pi-\theta_1)]\cos(2\theta_1) +$$

$$
\begin{aligned}
& + \cos(2\theta_1)\cos(2t_n\theta_1) - 2\sin(2\pi t_n)\sin[2t_n\,(\pi-\theta_1)]\Big] + \\
+ \;& \alpha\Big[-2\sin(2\pi t_n)\sin[2t_n\,(\pi-\theta_1)] + {t_n}^2\Big(\cos[2t_n\,(2\pi-\theta_1)]\cos(2\theta_1) - \\
& - \cos(2\theta_1)\cos(2t_n\theta_1) + 2\sin(2\pi t_n)\sin[2t_n\,(\pi-\theta_1)]\Big)\Big] + \\
+ \;& \alpha^2\Big[\sin^2[2t_n\,(\pi-\theta_1)] - 4{t_n}^2\sin^2(\theta_1) + 4{t_n}^4\sin^4(\theta_1)\Big] + \\
+ \;& \beta^2\Big[1 - 2\cos(2\pi t_n)\cos[2t_n\,(\pi-\theta_1)] + \cos[2t_n\,(2\pi-\theta_1)]\cos(2t_n\theta_1) + \\
& + 4{t_n}^4\sin^4(\theta_1) + {t_n}^2\Big(2\cos(2\pi t_n)\cos[2t_n\,(\pi-\theta_1)] - \\
& - \cos[2t_n\,(2\pi-\theta_1)]\cos(2\theta_1) - \cos(2\theta_1)\cos(2t_n\theta_1) - 4\sin^2(\theta_1)\Big)\Big] + \\
+ \;& \alpha\beta\Big[-8{t_n}^4\sin^4(\theta_1) + {t_n}^2\Big(-2\cos(2\pi t_n)\cos[2t_n\,(\pi-\theta_1)] + \\
& + \cos[2t_n\,(2\pi-\theta_1)]\cos(2\theta_1) + \cos(2\theta_1)\cos(2t_n\theta_1) + 4\sin^2(\theta_1)\Big)\Big]\Bigg\},
\end{aligned}
\tag{9.4.1}
$$

or simplified as

$$
\begin{aligned}
det[A] \;=\; & \frac{64(1+t_n)}{(1+\alpha)^2}\Bigg\{ -\sin^2(2\pi t_n) + 2\beta{t_n}^2\Big[1-\cos(2\theta_1)\Big]\sin(2\pi t_n)\sin[2t_n\,(\pi-\theta_1)] \\
+ \;& 2\alpha\Big[1 - {t_n}^2 + {t_n}^2\cos(2\theta_1)\Big]\sin(2\pi t_n)\sin[2t_n\,(\pi-\theta_1)] + \\
+ \;& 4\alpha\beta{t_n}^2\sin^2(\theta_1)\Big[-1 + \cos(2\pi t_n)\cos[2t_n\,(\pi-\theta_1)] + 2{t_n}^2\sin^2(\theta_1)\Big] + \\
+ \;& \alpha^2\Big[-\sin^2[2t_n\,(\pi-\theta_1)] + 4{t_n}^2\sin^2(\theta_1) - 4{t_n}^4\sin^4(\theta_1)\Big] + \\
+ \;& 4\beta^2\Big[-{t_n}^4\sin^4(\theta_1) + {t_n}^2\sin^2(\theta_1)\Big(1 - \cos(2\pi t_n)\cos[2t_n\,(\pi-\theta_1)]\Big) - \\
& - \sin^2[t_n\,(2\pi-\theta_1)]\sin^2(t_n\theta_1)\Big]\Bigg\}
\end{aligned}
\tag{9.4.2}
$$

with $t_n = 1 - \lambda_n$, where λ_n is the eigenvalue of the problem, which may be complex. In the special case of $\theta_1 = 90^\circ$, there is

$$
\begin{aligned}
\mathrm{Det}[A] \;=\; & -\frac{64(t_n+1)}{(1+\alpha)^2}\Bigg\{ \sin^2(2\pi t_n) - \beta\Big[8t_n^2\cos(\pi t_n)\sin^2(\pi t_n)\Big] \\
- \;& \alpha\Big[2(1-2t_n^2)\sin(\pi t_n)\sin(2\pi t_n)\Big] + \alpha^2\Big[\sin^2(\pi t_n) + 4t_n^2(t_n^2-1)\Big] \\
+ \;& \beta^2\Big[1 - 4t_n^2 + 4t_n^4 + \cos(3\pi t_n)\cos(\pi t_n) + 2(2t_n^2-1)\cos(2\pi t_n)\cos(\pi t_n)\Big] \\
+ \;& \alpha\beta 4t_n^2\Big[1 - 2t_n^2 - \cos(2\pi t_n)\cos(\pi t_n)\Big]\Bigg\}
\end{aligned}
\tag{9.4.3}
$$

and for $\theta_1 = 180^\circ$

$$
\mathrm{Det}[A] \;=\; -\frac{256(t_n+1)}{(1+\alpha)^2}\sin^2(\pi t_n)\Big\{\beta^2\sin^2(\pi t_n) + \cos^2(\pi t_n)\Big\}. \tag{9.4.4}
$$

By expanding Eq. (9.4.4) in a real and an imaginary part, it can be shown that Eqs. (9.3.1), (9.3.2), and (9.4.4) have the same eigenvalues for the singular stress terms.

9.4.2 The Angular Functions of the Singular Terms

For a given real eigenvalue λ_n the normalized angular functions can be determined from Eqs. (3.1.97) through (3.1.99). If the eigenvalues are complex, the angular functions should be calculated from Eqs. (3.1.144-3.1.150). The coefficients of the angular functions under an arbitrary joint geometry θ_1 with real eigenvalues are:

$$\begin{aligned}
A_{1n} &= \frac{16(1+t_n)^2}{(1+\alpha)}\Big\{2\cos[(1-t_n)\,\theta_1]\sin(2\pi t_n) + \\
&+ 4\beta\Big[-t_n\sin[2t_n\,(\pi-\theta_1)]\sin(\theta_1)\sin(t_n\theta_1) + \\
&+ \sin[t_n\,(2\pi-\theta_1)]\sin[(1-t_n)\,\theta_1]\sin(t_n\theta_1) - {t_n}^2\sin^2(\theta_1)\sin[2\pi t_n-\theta_1-t_n\theta_1]\Big] \\
&- 2\alpha\Big[\cos[(1-t_n)\,\theta_1]\sin[2t_n\,(\pi-\theta_1)] - 2t_n\cos[2t_n\,(\pi-\theta_1)]\cos(t_n\theta_1)\sin(\theta_1) - \\
&\quad -2{t_n}^2\sin^2(\theta_1)\sin[2\pi t_n-\theta_1-t_n\theta_1]\Big]\Big\} \qquad (9.4.5)
\end{aligned}$$

$$\begin{aligned}
B_{1n} &= \frac{16(1+t_n)^2}{(1+\alpha)}\Big\{-2\sin(2\pi t_n)\sin[(1-t_n)\,\theta_1] + \\
&+ \beta\Big[2t_n\Big(\sin[t_n\,(2\pi-3\theta_1)] - 3\sin[t_n\,(2\pi-\theta_1)]\Big)\sin(\theta_1) + \\
&+ 4{t_n}^2\cos[2\pi t_n-\theta_1-t_n\theta_1]\sin^2(\theta_1) + 4\cos[(1-t_n)\,\theta_1]\sin[t_n\,(2\pi-\theta_1)]\sin(t_n\theta_1)\Big] \\
&+ \alpha\Big[-4{t_n}^2\cos[2\pi t_n-\theta_1-t_n\theta_1]\sin^2(\theta_1) + 2\sin[2t_n\,(\pi-\theta_1)]\sin[(1-t_n)\,\theta_1] + \\
&\quad +4t_n\cos[2t_n\,(\pi-\theta_1)]\sin(\theta_1)\sin(t_n\theta_1)\Big]\Big\} \qquad (9.4.6)
\end{aligned}$$

$$\begin{aligned}
C_{1n} &= \frac{16(1+t_n)}{(1+\alpha)}\Big\{2\,(-1+t_n)\cos[(1+t_n)\,\theta_1]\sin(2\pi t_n) + \\
&+ 4\beta\Big[t_n\Big(\sin(2\pi t_n)\sin(\theta_1) + \sin[t_n\,(2\pi-\theta_1)]\sin[(1-t_n)\,\theta_1]\Big)\sin(t_n\theta_1) + \\
&+ {t_n}^2\sin(\theta_1)\Big(\sin[t_n\,(2\pi-\theta_1)]\sin(2\theta_1) - \sin[(-1+t_n)\,\theta_1]\sin[2\pi t_n-\theta_1-2t_n\theta_1]\Big) \\
&- {t_n}^3\sin^2(\theta_1)\sin[2\pi t_n+\theta_1-t_n\theta_1] - \sin[t_n\,(2\pi-\theta_1)]\sin(t_n\theta_1)\sin[(1+t_n)\,\theta_1]\Big] + \\
&+ 2\alpha\Big[\cos[(1+t_n)\,\theta_1]\sin[2t_n\,(\pi-\theta_1)] + 2{t_n}^3\sin^2(\theta_1)\sin[2\pi t_n+\theta_1-t_n\theta_1] \\
&\quad +2{t_n}^2\cos[(1+t_n)\,\theta_1]\cos[2\pi t_n+\theta_1-2t_n\theta_1]\sin(\theta_1) + \\
&\quad +t_n\Big(-\cos[t_n\,(2\pi-\theta_1)]\sin(\theta_1) - \cos(t_n\theta_1)\sin[2\pi t_n+\theta_1-2t_n\theta_1]\Big)\Big]\Big\} \qquad (9.4.7)
\end{aligned}$$

$$\begin{aligned}
D_{1n} &= \frac{16(1+t_n)}{(1+\alpha)}\Big\{2\,(1-t_n)\sin(2\pi t_n)\sin[(1+t_n)\,\theta_1] - \\
&- 4\beta\Big[{t_n}^3\cos[2\pi t_n+\theta_1-t_n\theta_1]\sin^2(\theta_1) + \cos[(1+t_n)\,\theta_1]\sin[t_n\,(2\pi-\theta_1)]\sin(t_n\theta_1)
\end{aligned}$$

$$
\begin{aligned}
&- \; {t_n}^2 \sin(\theta_1)\Big(\cos(2\theta_1)\sin[t_n\,(2\pi-\theta_1)] + \cos[2\pi t_n - \theta_1 - 2t_n\theta_1]\sin[(t_n-1)\,\theta_1]\Big)\\
&- \; t_n/2\Big(\sin[t_n\,(2\pi-\theta_1)]\sin[(1-2t_n)\,\theta_1] + \sin(\theta_1)\sin[t_n\,(2\pi+\theta_1)]\Big)\Big]\\
&+ \; 2\alpha\Big[2{t_n}^3\cos[2\pi t_n + \theta_1 - t_n\theta_1]\sin^2(\theta_1) - \sin[2t_n\,(\pi-\theta_1)]\sin[(1+t_n)\,\theta_1] -\\
&\quad -2{t_n}^2\cos[2\pi t_n + \theta_1 - 2t_n\theta_1]\sin(\theta_1)\sin[(1+t_n)\,\theta_1] +\\
&\quad +t_n\Big(\sin[t_n\,(2\pi-\theta_1)]\sin(\theta_1) + \sin(t_n\theta_1)\sin[2\pi t_n + \theta_1 - 2t_n\theta_1]\Big)\Big]\Big\} \qquad (9.4.8)
\end{aligned}
$$

$$
\begin{aligned}
A_{2n} \;=\; & -\frac{16(1+t_n)^2}{(1+\alpha)^2}\Big\{ -2\cos[(1-t_n)\,\theta_1]\sin(2\pi t_n) - 8\beta^2\Big[\cos(\theta_1)\sin[t_n\,(2\pi-\theta_1)] -\\
&\quad -t_n\cos[t_n\,(2\pi-\theta_1)]\sin(\theta_1)\Big]\Big(\sin^2(t_n\theta_1) - {t_n}^2\sin^2(\theta_1)\Big) +\\
&+ \; 2\alpha\Big[\cos[(1+t_n)\,\theta_1]\sin(2\pi t_n) + \cos[(1-t_n)\,\theta_1]\sin[2t_n\,(\pi-\theta_1)] -\\
&\quad -2t_n\cos[t_n\,(2\pi-\theta_1)]\cos(2t_n\theta_1)\sin(\theta_1) - 2{t_n}^2\sin^2(\theta_1)\sin[2\pi t_n - \theta_1 - t_n\theta_1]\Big] +\\
&+ \; 2\alpha^2\Big[-\cos[(1+t_n)\,\theta_1]\sin[2t_n\,(\pi-\theta_1)] + 2t_n\cos[t_n\,(2\pi-\theta_1)]\sin(\theta_1) -\\
&\quad -4{t_n}^3\cos[t_n\,(2\pi-\theta_1)]\sin^3(\theta_1) + 2{t_n}^2\sin^2(\theta_1)\sin[2\pi t_n + \theta_1 - t_n\theta_1]\Big] +\\
&+ \; 4\beta\Big[-2t_n\cos[t_n\,(2\pi-\theta_1)]\sin(\theta_1)\sin^2(t_n\theta_1) + {t_n}^2\sin^2(\theta_1)\sin[2\pi t_n - \theta_1 - t_n\theta_1]\\
&\quad +\sin^2(t_n\theta_1)\sin[2\pi t_n + \theta_1 - t_n\theta_1]\Big] +\\
&+ \; 4\alpha\beta\Big[-2t_n\cos[t_n\,(2\pi-\theta_1)]\sin(\theta_1)\sin^2(t_n\theta_1) + \sin^2(t_n\theta_1)\sin[2\pi t_n + \theta_1 - t_n\theta_1]\\
&\quad +{t_n}^2\Big(-\sin^2(\theta_1)\sin[2\pi t_n - \theta_1 - t_n\theta_1] - 2\sin^2(\theta_1)\sin[2\pi t_n + \theta_1 - t_n\theta_1]\Big) +\\
&\quad +4{t_n}^3\cos[t_n\,(2\pi-\theta_1)]\sin^3(\theta_1)\Big]\Big\} \qquad (9.4.9)
\end{aligned}
$$

$$
\begin{aligned}
B_{2n} \;=\; & \frac{16(1+t_n)^2}{(1+\alpha)^2}\Big\{ -2\sin(2\pi t_n)\sin[(1-t_n)\,\theta_1] +\\
&+ \; 8\beta^2\Big[-1+t_n\Big]\sin[t_n\,(2\pi-\theta_1)]\sin(\theta_1)\Big(\sin^2(t_n\theta_1) - {t_n}^2\sin^2(\theta_1)\Big) +\\
&+ \; 4\beta\Big[{t_n}^2\cos[2\pi t_n - \theta_1 - t_n\theta_1]\sin^2(\theta_1) - \cos[2\pi t_n + \theta_1 - t_n\theta_1]\sin^2(t_n\theta_1) -\\
&\quad -2t_n\sin[t_n\,(2\pi-\theta_1)]\sin(\theta_1)\sin^2(t_n\theta_1)\Big] +\\
&+ \; 2\alpha\Big[-2t_n\cos(2t_n\theta_1)\sin[t_n\,(2\pi-\theta_1)]\sin(\theta_1) - 2{t_n}^2\cos[2\pi t_n - \theta_1 - t_n\theta_1]\sin^2(\theta_1)\\
&\quad +\sin[2t_n\,(\pi-\theta_1)]\sin[(1-t_n)\,\theta_1] + \sin(2\pi t_n)\sin[(1+t_n)\,\theta_1]\Big] +\\
&+ \; 2\alpha^2\Big[2t_n\sin[t_n\,(2\pi-\theta_1)]\sin(\theta_1) - 2{t_n}^2\cos[2\pi t_n + \theta_1 - t_n\theta_1]\sin^2(\theta_1) -\\
&\quad -4{t_n}^3\sin[t_n\,(2\pi-\theta_1)]\sin^3(\theta_1) - \sin[2t_n\,(\pi-\theta_1)]\sin[(1+t_n)\,\theta_1]\Big] +\\
&+ \; 2\alpha\beta\Big[8{t_n}^3\sin[t_n\,(2\pi-\theta_1)]\sin^3(\theta_1) - 4t_n\sin[t_n\,(2\pi-\theta_1)]\sin(\theta_1)\sin^2(t_n\theta_1) +\\
&\quad +{t_n}^2\Big(-2\cos[2\pi t_n - \theta_1 - t_n\theta_1]\sin^2(\theta_1) + 4\cos[2\pi t_n + \theta_1 - t_n\theta_1]\sin^2(\theta_1)\Big) -\\
&\quad -\sin(t_n\theta_1)\sin[2\pi t_n + \theta_1] + \sin(t_n\theta_1)\sin[2\pi t_n + \theta_1 - 2t_n\theta_1]\Big]\Big\} \qquad (9.4.10)
\end{aligned}
$$

$$
\begin{aligned}
C_{2n} &= -\frac{16(1+t_n)}{(1+\alpha)^2}\Big\{2\,(1-t_n)\cos[(1+t_n)\,\theta_1]\sin(2\pi t_n) + \\
&+ 2\alpha\Big[-\cos[(1-t_n)\,\theta_1]\sin(2\pi t_n) - \cos[(1+t_n)\,\theta_1]\sin[2t_n\,(\pi-\theta_1)] + \\
&\quad + {t_n}^2\sin(\theta_1)\Big(-2\cos[(1+t_n)\,\theta_1]\cos[2\pi t_n+\theta_1-2t_n\theta_1] + 2\sin(2\pi t_n)\sin(t_n\theta_1)\Big) \\
&\quad + 2t_n\cos^2(t_n\theta_1)\sin[2\pi t_n+\theta_1-t_n\theta_1] - 2{t_n}^3\sin^2(\theta_1)\sin[2\pi t_n+\theta_1-t_n\theta_1]\Big] + \\
&+ 2\alpha^2\Big[\cos[(1-t_n)\,\theta_1]\sin[2t_n\,(\pi-\theta_1)] - 4{t_n}^4\cos[t_n\,(2\pi-\theta_1)]\sin^3(\theta_1) + \\
&\quad + {t_n}^2\Big(3\cos[t_n\,(2\pi-\theta_1)] - \cos[2\pi t_n - 2\theta_1 - t_n\theta_1]\Big)\sin(\theta_1) + \\
&\quad + t_n\Big(-\cos[t_n\,(2\pi-\theta_1)]\sin(\theta_1) - \cos(t_n\theta_1)\sin[2\pi t_n+\theta_1-2t_n\theta_1]\Big) \\
&\quad + 2{t_n}^3\sin^2(\theta_1)\sin[2\pi t_n+\theta_1-t_n\theta_1]\Big] + \\
&+ 4\beta^2\Big[-2{t_n}^4\cos[t_n\,(2\pi-\theta_1)]\sin^3(\theta_1) + 2\cos(\theta_1)\sin[t_n\,(2\pi-\theta_1)]\sin^2(t_n\theta_1) + \\
&\quad + {t_n}^2\sin(\theta_1)\Big(-\sin[t_n\,(2\pi-\theta_1)]\sin(2\theta_1) + 2\cos[t_n\,(2\pi-\theta_1)]\sin^2(t_n\theta_1)\Big) + \\
&\quad + 2{t_n}^3\sin^2(\theta_1)\sin[2\pi t_n+\theta_1-t_n\theta_1] - 2t_n\sin^2(t_n\theta_1)\sin[2\pi t_n+\theta_1-t_n\theta_1]\Big] + \\
&+ 4\alpha\beta\Big[4{t_n}^4\cos[t_n\,(2\pi-\theta_1)]\sin^3(\theta_1) + t_n\sin^2(t_n\theta_1)\sin[2\pi t_n+\theta_1-t_n\theta_1] \\
&\quad + {t_n}^2\sin(\theta_1)\Big(-\sin(2\pi t_n)\sin(t_n\theta_1) + \sin[(1+t_n)\,\theta_1]\sin[2\pi t_n+\theta_1-2t_n\theta_1]\Big) + \\
&\quad + \sin^2(t_n\theta_1)\sin[2\pi t_n-\theta_1-t_n\theta_1] - 3{t_n}^3\sin^2(\theta_1)\sin[2\pi t_n+\theta_1-t_n\theta_1]\Big] + \\
&+ 4\beta\Big[{t_n}^2\sin(\theta_1)\Big(-\sin[t_n\,(2\pi-\theta_1)]\sin(2\theta_1) - \sin(2\pi t_n)\sin(t_n\theta_1) + \\
&\quad + \sin[(-1+t_n)\,\theta_1]\sin[2\pi t_n-\theta_1-2t_n\theta_1]\Big) + \sin^2(t_n\theta_1)\sin[2\pi t_n-\theta_1-t_n\theta_1] \\
&\quad + {t_n}^3\sin^2(\theta_1)\sin[2\pi t_n+\theta_1-t_n\theta_1] + t_n\sin^2(t_n\theta_1)\sin[2\pi t_n+\theta_1-t_n\theta_1]\Big]\Big\} \quad (9.4.11)
\end{aligned}
$$

$$
\begin{aligned}
D_{2n} &= \frac{16(1+t_n)}{(1+\alpha)^2}\Big\{8\beta^2\Big[-1+{t_n}^2\Big]\sin[t_n\,(2\pi-\theta_1)]\sin(\theta_1)\Big({t_n}^2\sin^2(\theta_1) - \sin^2(t_n\theta_1)\Big) + \\
&+ 4\beta\Big[-{t_n}^3\cos[2\pi t_n+\theta_1-t_n\theta_1]\sin^2(\theta_1) + {t_n}^2\sin(\theta_1)\Big(-\cos(t_n\theta_1)\sin(2\pi t_n) + \\
&\quad + \cos(2\theta_1)\sin[t_n\,(2\pi-\theta_1)] + \cos[2\pi t_n-\theta_1-2t_n\theta_1]\sin[(-1+t_n)\,\theta_1]\Big) + \\
&\quad + \cos[2\pi t_n-\theta_1-t_n\theta_1]\sin^2(t_n\theta_1) + t_n\cos[2\pi t_n+\theta_1-t_n\theta_1]\sin^2(t_n\theta_1)\Big] + \\
&+ 4\alpha\beta\Big[-{t_n}^3\cos[2\pi t_n+\theta_1-t_n\theta_1]\sin^2(\theta_1) - 4{t_n}^4\sin[t_n\,(2\pi-\theta_1)]\sin^3(\theta_1) + \\
&\quad + \cos[2\pi t_n-\theta_1-t_n\theta_1]\sin^2(t_n\theta_1) + t_n\cos[2\pi t_n+\theta_1-t_n\theta_1]\sin^2(t_n\theta_1) + \\
&\quad + {t_n}^2\Big(-\cos[2\pi t_n+\theta_1-t_n\theta_1]\sin^2(\theta_1) + 2\sin[t_n\,(2\pi-\theta_1)]\sin(\theta_1)\sin^2(t_n\theta_1)\Big)\Big] + \\
&+ 2\alpha\Big[2{t_n}^3\cos[2\pi t_n+\theta_1-t_n\theta_1]\sin^2(\theta_1) - \sin(2\pi t_n)\sin[(1-t_n)\,\theta_1] - \\
&\quad - 2t_n\cos[2\pi t_n+\theta_1-t_n\theta_1]\sin^2(t_n\theta_1) - \sin[2t_n\,(\pi-\theta_1)]\sin[(1+t_n)\,\theta_1] + \\
&\quad + {t_n}^2\sin(\theta_1)\Big(2\cos(t_n\theta_1)\sin(2\pi t_n) - 2\cos[2\pi t_n+\theta_1-2t_n\theta_1]\sin[(1+t_n)\,\theta_1]\Big)\Big] + \\
&+ 2\alpha^2\Big[2{t_n}^3\cos[2\pi t_n+\theta_1-t_n\theta_1]\sin^2(\theta_1) + 4{t_n}^4\sin[t_n\,(2\pi-\theta_1)]\sin^3(\theta_1) + \\
&\quad + t_n\Big(\sin[t_n\,(2\pi-\theta_1)]\sin(\theta_1) + \sin(t_n\theta_1)\sin[2\pi t_n+\theta_1-2t_n\theta_1]\Big) +
\end{aligned}
$$

$$+{t_n}^2\sin(\theta_1)\Big(-3\sin[t_n\,(2\pi-\theta_1)]+\sin(2\pi t_n-2\theta_1-t_n\theta_1)\Big)+$$
$$+\sin[2t_n\,(\pi-\theta_1)]\sin[(1-t_n)\,\theta_1]\Big]+2\,(1-t_n)\sin(2\pi t_n)\sin[(1+t_n)\,\theta_1]\Bigg\} \tag{9.4.12}$$

where $t_n = 1-\lambda_n$ and λ_n is the eigenvalue of the problem. The singular stress exponent ω_n is equal to λ_n. The angular functions can be calculated from Eqs. (3.1.97-3.1.99) with the coefficients given above.
For the special case with $\theta_1 = 90^\circ$, the coefficients are simplified as

$$\begin{aligned} A_{1n} &= \frac{32(2-\lambda_n)^2}{1+\alpha}\sin(\frac{\pi\lambda_n}{2})\Bigg\{-4\cos^2(\frac{\pi\lambda_n}{2})\cos(\pi\lambda_n)+ \\ &+ \beta\Big[-4+6\lambda_n-2\lambda_n^2-7\cos(\pi\lambda_n)+10\lambda_n\cos(\pi\lambda_n)-4\lambda_n^2\cos(\pi\lambda_n)-\cos(2\pi\lambda_n)\Big] \\ &+ \alpha\Big[1-4\lambda_n+2\lambda_n^2+\cos(\pi\lambda_n)-6\lambda_n\cos(\pi\lambda_n)+4\lambda_n^2\cos(\pi\lambda_n)\Big]\Bigg\} \end{aligned} \tag{9.4.13}$$

$$\begin{aligned} B_{1n} &= \frac{32(2-\lambda_n)^2}{1+\alpha}\cos(\frac{\pi\lambda_n}{2})\Bigg\{4\sin^2(\frac{\pi\lambda_n}{2})\cos(\pi\lambda_n)+ \\ &+ \beta\Big[-2\lambda_n+2\lambda_n^2+\cos(\pi\lambda_n)+2\lambda_n\cos(\pi\lambda_n)-4\lambda_n^2\cos(\pi\lambda_n)-\cos(2\pi\lambda_n)\Big]+ \\ &+ \alpha\Big[-1+4\lambda_n-2\lambda_n^2+\cos(\pi\lambda_n)-6\lambda_n\cos(\pi\lambda_n)+4\lambda_n^2\cos(\pi\lambda_n)\Big]\Bigg\} \end{aligned} \tag{9.4.14}$$

$$\begin{aligned} C_{1n} &= \frac{32\,(2-\lambda_n)}{1+\alpha}\Bigg\{-4\lambda_n\cos^2(\frac{\pi\lambda_n}{2})\cos(\pi\lambda_n)+\beta\Big[-4\lambda_n+6\lambda_n^2-2\lambda_n^3+2\cos(\pi\lambda_n) \\ &- 11\lambda_n\cos(\pi\lambda_n)+14\lambda_n^2\cos(\pi\lambda_n)-4\lambda_n^3\cos(\pi\lambda_n)-2\cos(2\pi\lambda_n)+3\lambda_n\cos(2\pi\lambda_n)\Big] \\ &+ \alpha\lambda_n\Big[1-4\lambda_n+2\lambda_n^2+5\cos(\pi\lambda_n)-10\lambda_n\cos(\pi\lambda_n)+4\lambda_n^2\cos(\pi\lambda_n)\Big]\Bigg\}\sin(\frac{\pi\lambda_n}{2}) \end{aligned} \tag{9.4.15}$$

$$\begin{aligned} D_{1n} &= \frac{32\,(2-\lambda_n)}{1+\alpha}\Bigg\{\alpha\lambda_n\Big[1-4\lambda_n+2\lambda_n^2-5\cos(\pi\lambda_n)+10\lambda_n\cos(\pi\lambda_n)-4\lambda_n^2\cos(\pi\lambda_n)\Big] \\ &+ \beta\Big[2\lambda_n^2-2\lambda_n^3-2\cos(\pi\lambda_n)+3\lambda_n\cos(\pi\lambda_n)-6\lambda_n^2\cos(\pi\lambda_n)+4\lambda_n^3\cos(\pi\lambda_n)+ \\ &+ 2\cos(2\pi\lambda_n)-3\lambda_n\cos(2\pi\lambda_n)\Big]-4\lambda_n\sin^2(\frac{\pi\lambda_n}{2})\cos(\pi\lambda_n)\Bigg\}\cos(\frac{\pi\lambda_n}{2}) \end{aligned} \tag{9.4.16}$$

$$\begin{aligned} A_{2n} &= -\frac{16(2-\lambda_n)^2}{(1+\alpha)^2}\Bigg\{8\beta^2\Big[-1+\lambda_n\Big]\left(-(1-\lambda_n)^2+\cos^2(\frac{\pi\lambda_n}{2})\right)\sin(\frac{3\pi\lambda_n}{2})+ \\ &+ 2\beta\Big[3-6\lambda_n+2\lambda_n^2+\cos(\pi\lambda_n)-2\lambda_n\cos(\pi\lambda_n)\Big]\sin(\frac{3\pi\lambda_n}{2})+ \end{aligned}$$

$$
\begin{aligned}
&+ \quad 2\alpha\beta\Big[-5+18\lambda_n-22\lambda_n^2+8\lambda_n^3+\cos(\pi\lambda_n)-2\lambda_n\cos(\pi\lambda_n)\Big]\sin(\frac{3\pi\lambda_n}{2})+\\
&+ \quad 2\alpha\Big[-1+4\lambda_n-2\lambda_n^2-\cos(\pi\lambda_n)+2\lambda_n\cos(\pi\lambda_n)\Big]\sin(\frac{3\pi\lambda_n}{2})+\\
&+ \quad \alpha^2\Big[\sin(\frac{\pi\lambda_n}{2})+\sin(\frac{3\pi\lambda_n}{2})-12\lambda_n\sin(\frac{3\pi\lambda_n}{2})+20\lambda_n^2\sin(\frac{3\pi\lambda_n}{2})-\\
&\quad -8\lambda_n^3\sin(\frac{3\pi\lambda_n}{2})\Big]+2\cos(\frac{\pi\lambda_n}{2})\sin(2\pi\lambda_n)\Big\} \qquad (9.4.17)
\end{aligned}
$$

$$
\begin{aligned}
B_{2n} \quad &= \quad \frac{16(2-\lambda_n)^2}{(1+\alpha)^2}\Big\{8\beta^2\lambda_n\Big[-(1-\lambda_n)^2+\cos^2(\frac{\pi\lambda_n}{2})\Big]\cos(\frac{3\pi\lambda_n}{2})+\\
&+ \quad 2\beta\Big[-1+2\lambda_n-2\lambda_n^2+\cos(\pi\lambda_n)-2\lambda_n\cos(\pi\lambda_n)\Big]\cos(\frac{3\pi\lambda_n}{2})+\\
&+ \quad 2\alpha\beta\Big[-1+10\lambda_n-18\lambda_n^2+8\lambda_n^3+\cos(\pi\lambda_n)-2\lambda_n\cos(\pi\lambda_n)\Big]\cos(\frac{3\pi\lambda_n}{2})+\\
&+ \quad 2\alpha\Big[1-4\lambda_n+2\lambda_n^2-\cos(\pi\lambda_n)+2\lambda_n\cos(\pi\lambda_n)\Big]\cos(\frac{3\pi\lambda_n}{2})+\\
&- \quad \alpha^2\Big[\cos(\frac{\pi\lambda_n}{2})-\cos(\frac{3\pi\lambda_n}{2})+12\lambda_n\cos(\frac{3\pi\lambda_n}{2})-20\lambda_n^2\cos(\frac{3\pi\lambda_n}{2})+\\
&\quad +8\lambda_n^3\cos(\frac{3\pi\lambda_n}{2})\Big]+2\sin(\frac{\pi\lambda_n}{2})\sin(2\pi\lambda_n)\Big\} \qquad (9.4.18)
\end{aligned}
$$

$$
\begin{aligned}
C_{2n}= &-\frac{16\,(2-\lambda_n)}{(1+\alpha)^2}\Big\{2\alpha^2\lambda_n\Big[-3+14\lambda_n-14\lambda_n^2+4\lambda_n^3-7\cos(\pi\lambda_n)+\\
&\quad +28\lambda_n\cos(\pi\lambda_n)-28\lambda_n^2\cos(\pi\lambda_n)+8\lambda_n^3\cos(\pi\lambda_n)\Big]\sin(\frac{\pi\lambda_n}{2})+\\
&+ \quad 4\beta^2\Big(-1+\lambda_n\Big)\lambda_n\Big[1-4\lambda_n+2\lambda_n^2-\cos(\pi\lambda_n)\Big]\sin(\frac{3\pi\lambda_n}{2})+\\
&+ \quad 2\alpha\lambda_n\Big[-1+4\lambda_n-2\lambda_n^2+3\cos(\pi\lambda_n)-2\lambda_n\cos(\pi\lambda_n)\Big]\sin(\frac{3\pi\lambda_n}{2})-\\
&- \quad 2\beta\Big[2-7\lambda_n+6\lambda_n^2-2\lambda_n^3-2\cos(\pi\lambda_n)+3\lambda_n\cos(\pi\lambda_n)-2\lambda_n^2\cos(\pi\lambda_n)\Big]\sin(\frac{3\pi\lambda_n}{2})\\
&+ \quad 2\alpha\beta\Big[-2+15\lambda_n-30\lambda_n^2+26\lambda_n^3-8\lambda_n^4+2\cos(\pi\lambda_n)-3\lambda_n\cos(\pi\lambda_n)+\\
&\quad +2\lambda_n^2\cos(\pi\lambda_n)\Big]\sin(\frac{3\pi\lambda_n}{2})+2\lambda_n\cos(\frac{\pi\lambda_n}{2})\sin(2\pi\lambda_n)\Big\} \qquad (9.4.19)
\end{aligned}
$$

$$
\begin{aligned}
D_{2n}= &\frac{16\,(2-\lambda_n)}{(1+\alpha)^2}\Big\{2\alpha^2\lambda_n\cos(\frac{\pi\lambda_n}{2})\Big[-3+14\lambda_n-14\lambda_n^2+4\lambda_n^3+7\cos(\pi\lambda_n)-\\
&\quad -28\lambda_n\cos(\pi\lambda_n)+28\lambda_n^2\cos(\pi\lambda_n)-8\lambda_n^3\cos(\pi\lambda_n)\Big]+\\
&+ \quad 8\beta^2\,(2-\lambda_n)\,\lambda_n\Big[(-1+\lambda_n)^2-\cos^2(\frac{\pi\lambda_n}{2})\Big]\cos(\frac{3\pi\lambda_n}{2})+\\
&+ \quad 2\alpha\lambda_n\Big[-1+4\lambda_n-2\lambda_n^2-3\cos(\pi\lambda_n)+2\lambda_n\cos(\pi\lambda_n)\Big]\cos(\frac{3\pi\lambda_n}{2})+
\end{aligned}
$$

$$+ \quad 2\beta\Big[2-3\lambda_n-2\lambda_n^2+2\lambda_n^3-2\cos(\pi\lambda_n)+3\lambda_n\cos(\pi\lambda_n)-2\lambda_n^2\cos(\pi\lambda_n)\Big]\cos(\frac{3\pi\lambda_n}{2})$$

$$+ \quad 2\alpha\beta\Big[2-19\lambda_n+38\lambda_n^2-30\lambda_n^3+8\lambda_n^4-2\cos(\pi\lambda_n)+3\lambda_n\cos(\pi\lambda_n)-$$

$$-2\lambda_n^2\cos(\pi\lambda_n)\Big]\cos(\frac{3\pi\lambda_n}{2})-2\lambda_n\sin(\frac{\pi\lambda_n}{2})\sin(2\pi\lambda_n)\Big\}. \qquad (9.4.20)$$

The regular stress term was given in Sections 3.2 for thermal loading (see Section 3.2.6) and in 3.3 for remote mechanical loading (see Section 3.3.6) . For thermal loading the regular stresses in Cartesian coordinates are the same in materials 1 and 2, and in general, they are non-zero. Under remote mechanical loading, the regular stress term is zero in most cases. When the regular stress term is non-zero (conditions see Section 3.3), the regular stresses in materials 1 and 2 in Cartesian coordinates may be the same or not, depending on the Dundurs parameters.

For a joint with a delamination crack the value of the singular stress exponent may be larger than 0.5, and there may be three real singular terms. Although the dominant singular stress exponent is very large, the other singular terms and the regular stress term should be considered for stress calculation, even very close to the singular point. An example was presented in Section 6.6 (see Figs. 6.38 through 6.43).

Chapter 10

Contact Problem in Dissimilar Materials

So far, a dissimilar materials joint with a perfect interface was assumed. This means that at the interface both displacement components, the stress component perpendicular to the interface and the shear stress, are continuous. In real situation, the interface may be imperfect. In this section a two dissimilar materials contact problem will be considered, in which the interface may be friction free or with friction (see Fig.10.1). The determination of the stress exponent and the angular functions for a friction free interface and an interface with friction will be given in Sections 10.1 and 10.2. The regular stress term will be discussed in Section 10.3. For various geometries and material combinations the general behavior of the stress exponents is presented in Section 10.4.

10.1 Determination of Stress Exponents and Angular Functions for a Friction Free Interface

For a joint with free edges and a friction free interface the boundary conditions are:

at the interface

$$\begin{aligned} v_1(r,0) &= v_2(r,0), \\ \sigma_{\theta\theta 1}(r,0) &= \sigma_{\theta\theta 2}(r,0), \\ \sigma_{r\theta 1}(r,0) &= 0 \\ \sigma_{r\theta 2}(r,0) &= 0 \end{aligned} \tag{10.1.1}$$

for the free edges

$$\begin{aligned} \sigma_{\theta\theta 1}(r,\theta_1) = 0, \\ \sigma_{r\theta 1}(r,\theta_1) = 0, \end{aligned} \tag{10.1.2}$$

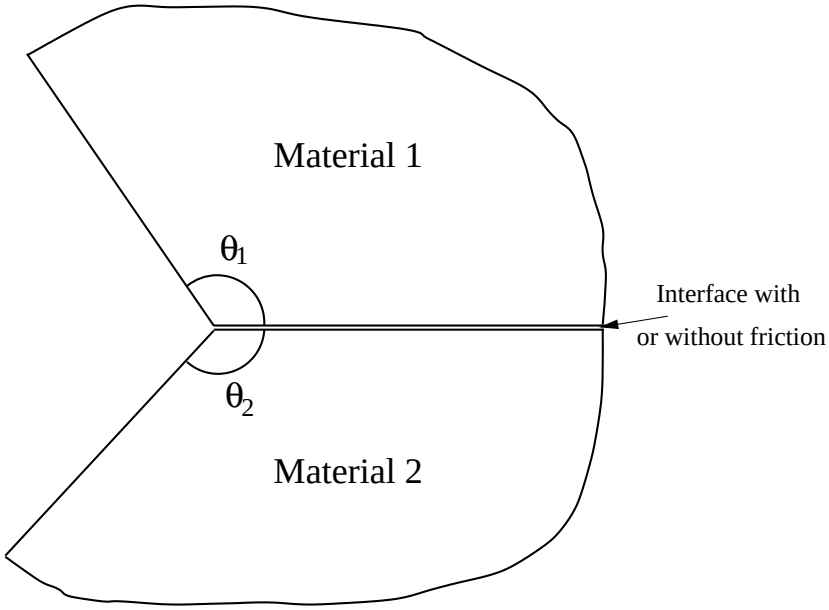

Figure 10.1: Two dissimilar materials contact problem with or without friction.

$$\sigma_{\theta\theta 2}(r,\theta_2) = 0,$$
$$\sigma_{r\theta 2}(r,\theta_2) = 0. \tag{10.1.3}$$

The stress function as given in Eq. (3.1.3) will be used. From these eight conditions the following equations hold for $\lambda_n \neq 0, 1, 2$ (n=1,2,3,...):

$$A_{1n}\mu[2(1-\nu_1)+(2-\lambda_n)(1+\nu_1)] - A_{2n}[2(1-\nu_2)+(2-\lambda_n)(1+\nu_2)] - \\ -C_{1n}\mu(1+\nu_1)(2-\lambda_n) + C_{2n}(1+\nu_2)(2-\lambda_n) = 0 \tag{10.1.4}$$

$$B_{1n} + D_{1n} - B_{2n} - D_{2n} = 0 \tag{10.1.5}$$

$$A_{1n}\lambda_n + C_{1n}(2-\lambda_n) = 0 \tag{10.1.6}$$

$$A_{2n}\lambda_n + C_{2n}(2-\lambda_n) = 0 \tag{10.1.7}$$

$$A_{1n}\sin(\lambda_n\theta_1) + B_{1n}\cos(\lambda_n\theta_1) + C_{1n}\sin[(2-\lambda_n)\theta_1] + \\ +D_{1n}\cos[(2-\lambda_n)\theta_1] = 0 \tag{10.1.8}$$

$$A_{1n}\lambda_n\cos(\lambda_n\theta_1) - B_{1n}\lambda_n\sin(\lambda_n\theta_1) + C_{1n}(2-\lambda_n)\cos[(2-\lambda_n)\theta_1] - \\ -D_{1n}(2-\lambda_n)\sin[(2-\lambda_n)\theta_1] = 0 \tag{10.1.9}$$

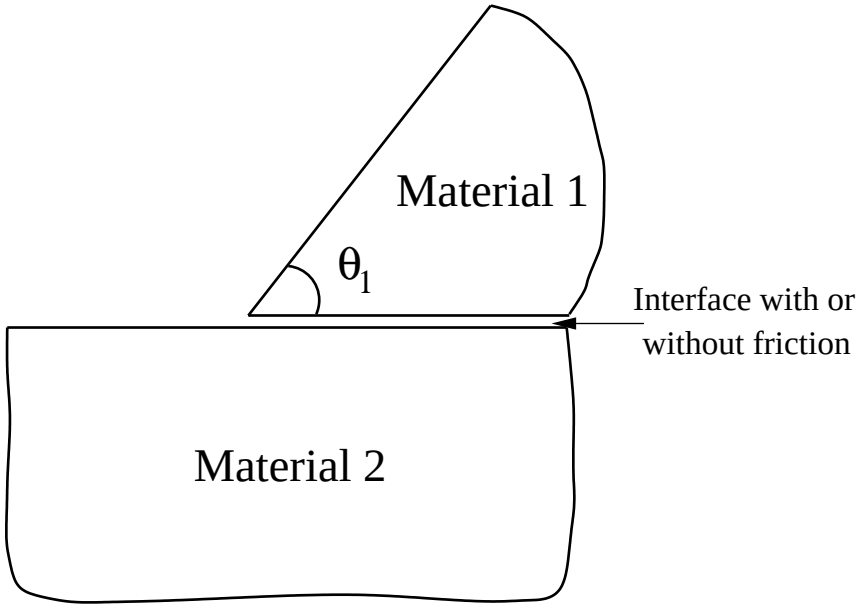

Figure 10.2: Two dissimilar materials contact: One material occupies the angle of 180° and the other is arbitrary.

$$A_{2n}\sin(\lambda_n\theta_2) + B_{2n}\cos(\lambda_n\theta_2) + C_{2n}\sin[(2-\lambda_n)\theta_2] + \\ +D_{2n}\cos[(2-\lambda_n)\theta_2] = 0 \tag{10.1.10}$$

$$A_{2n}\lambda_n\cos(\lambda_n\theta_2) - B_{2n}\lambda_n\sin(\lambda_n\theta_2) + C_{2n}(2-\lambda_n)\cos[(2-\lambda_n)\theta_2] - \\ -D_{2n}(2-\lambda_n)\sin[(2-\lambda_n)\theta_2] = 0. \tag{10.1.11}$$

This equation system can be rewritten in a matrix form as

$$[A]_{8\times8}\{X\}_{8\times1} = \{0\}_{8\times1} \tag{10.1.12}$$

where $\{X\}_{8\times1} = \{A_{1n}, B_{1n}, C_{1n}, D_{1n}, A_{2n}, B_{2n}, C_{2n}, D_{2n}\}^t$ and $[A]_{8\times8}$ is its coefficient matrix. $\{X\}_{8\times1}$ is unknown and $[A]_{8\times8}$ includes the unknown exponent λ_n, the material properties (E_k, ν_k, k=1,2 for materials 1 and 2), and the geometry angles (θ_1, θ_2).

Determination of the Stress Exponent

Equation (10.1.12) has a nonzero solution, if and only if

$$\mathrm{Det}([A]_{8\times8}) = 0 \tag{10.1.13}$$

is satisfied. In Eq. (10.1.13) the only unknown is the exponent λ_n. Its solutions are the eigenvalues of this problem.

The expansion of Eq. (10.1.13) for an arbitrary joint geometry with θ_1, θ_2 is

$$\begin{aligned}
\mathrm{Det}([A]) &= -\frac{16(1+t_n)}{1+\alpha}\Big\{ -2{t_n}^3 \sin(\theta_1)\sin(\theta_1-\theta_2)\sin(\theta_2) + \\
&\quad +2\sin(t_n\theta_1)\sin[t_n(\theta_1-\theta_2)]\sin(t_n\theta_2) + \\
&\quad +t_n\Big(\sin^2(t_n\theta_1)\sin(2\theta_2) - \sin(2\theta_1)\sin^2(t_n\theta_2)\Big) + \\
&\quad +{t_n}^2\Big(\sin(2t_n\theta_1)\sin^2(\theta_2) - \sin^2(\theta_1)\sin(2t_n\theta_2)\Big) + \\
&+ \quad \alpha\Big[t_n\Big(\sin^2(t_n\theta_1)\sin(2\theta_2) + \sin(2\theta_1)\sin^2(t_n\theta_2)\Big) - \\
&\quad -{t_n}^2\Big(\sin(2t_n\theta_1)\sin^2(\theta_2) + \sin^2(\theta_1)\sin(2t_n\theta_2)\Big) - \\
&\quad -2{t_n}^3\sin(\theta_1)\sin(\theta_2)\sin(\theta_1+\theta_2) + \\
&\quad +2\sin(t_n\theta_1)\sin(t_n\theta_2)\sin[t_n(\theta_1+\theta_2)]\Big]\Big\} \qquad (10.1.14)
\end{aligned}$$

with $t_n = 1-\lambda_n$. From Eq. (10.1.14) it can be seen that if t_n is the solution of Eq. (10.1.13), -t_n is also. Therefore, if λ_n is the eigenvalue, 2-λ_n is as well for a friction free contact problem. In addition, the eigenvalue is independent of the Dundurs parameter β.

For the special case of $\theta_1 = -\theta_2$ there is

$$\begin{aligned}
\mathrm{Det}([A]) &= -\frac{16(1+t_n)}{1+\alpha}\Big\{\Big[-1+{t_n}^2-{t_n}^2\cos(2\theta_1)+\cos(2t_n\theta_1)\Big]\times \\
&\quad \times\Big[t_n\sin(2\theta_1)+\sin(2t_n\theta_1)\Big]\Big\}. \qquad (10.1.15)
\end{aligned}$$

It can be seen that for these geometries the eigenvalues are independent of the material data, i.e. λ_n is independent of the Dundurs parameters α and β.
$\theta_2 = -\theta_1 = \pi/2$ yields

$$\mathrm{Det}([A]) = -\frac{16(1+t_n)}{1+\alpha}\Big\{-1+2t_n^2+\cos(\pi t_n)\Big\}\sin(\pi t_n). \qquad (10.1.16)$$

In the considered range (i.e. $0<\lambda_n<1$) Eq. (10.1.16) equaling zero has no solution.
For $\theta_2 = -\theta_1 = \pi$

$$\mathrm{Det}([A]) = -\frac{64(1+t_n)}{1+\alpha}\cos(\pi t_n)\sin^3(\pi t_n). \qquad (10.1.17)$$

In the range of $0<\lambda_n<1$, the solution of $\mathrm{Det}([A])=0$ is $\lambda = 0.5$.
If the joint geometry is $\theta_2 = -\pi$ and θ_1 arbitrary, which is the general case of a contact problem, the eigenvalue should be determined from

$$\begin{aligned}
\mathrm{Det}([A]) &= -\frac{16(1+t_n)}{1+\alpha}\Big\{{t_n}^2\sin(2\pi t_n)\sin^2(\theta_1) - t_n\sin^2(\pi t_n)\sin(2\theta_1) -
\end{aligned}$$

$$
\begin{aligned}
& -2\sin(\pi t_n)\sin(t_n\theta_1)\sin[t_n\,(\pi+\theta_1)] \\
+ \;& \alpha\Big[{t_n}^2\sin(2\pi t_n)\sin^2(\theta_1)+t_n\sin^2(\pi t_n)\sin(2\theta_1)- \\
& -2\sin(\pi t_n)\sin(t_n\theta_1)\sin[t_n\,(-\pi+\theta_1)]\Big]\Big\}. \qquad (10.1.18)
\end{aligned}
$$

In case of $\theta_1=\pi/2$ and $\theta_2=-\pi$

$$
\begin{aligned}
\mathrm{Det}([A]_{8\times 8}) \;=\; & -\frac{16(1+t_n)}{1+\alpha}\Big\{-\cos(\pi t_n)+2{t_n}^2\cos(\pi t_n)+\cos(2\pi t_n)+ \\
& +\alpha\Big[1-\cos(\pi t_n)+2{t_n}^2\cos(\pi t_n)\Big]\Big\}\sin(\pi t_n). \qquad (10.1.19)
\end{aligned}
$$

Determination of the Angular Functions

For a given eigenvalue λ_n the coefficients of the angular functions under an arbitrary geometry with θ_1,θ_2 can be determined from

$$
A_{1n}=8(1+t_n)^2\left[t_n\sin(2\theta_1)+\sin(2t_n\theta_1)\right]\left[t_n\cos(t_n\theta_2)\sin(\theta_2)+\cos(\theta_2)\sin(t_n\theta_2)\right] \qquad (10.1.20)
$$

$$
\begin{aligned}
B_{1n} \;=\; & 8(1+t_n)^2\left[1-t_n+t_n\cos(2\theta_1)-\cos(2t_n\theta_1)\right]\times \\
& \times\left[t_n\cos(t_n\theta_2)\sin(\theta_2)+\cos(\theta_2)\sin(t_n\theta_2)\right] \qquad (10.1.21)
\end{aligned}
$$

$$
C_{1n}=8\left({t_n}^2-1\right)\left[t_n\sin(2\theta_1)+\sin(2t_n\theta_1)\right]\left[t_n\cos(t_n\theta_2)\sin(\theta_2)+\cos(\theta_2)\sin(t_n\theta_2)\right] \qquad (10.1.22)
$$

$$
\begin{aligned}
D_{1n} \;=\; & 8\left(-1+{t_n}^2\right)\left[-1-t_n+t_n\cos(2\theta_1)+\cos(2t_n\theta_1)\right]\times \\
& \times\left[t_n\cos(t_n\theta_2)\sin(\theta_2)+\cos(\theta_2)\sin(t_n\theta_2)\right] \qquad (10.1.23)
\end{aligned}
$$

$$
\begin{aligned}
A_{2n} \;=\; & \frac{8\,(1-\alpha)\,(1+t_n)^2}{1+\alpha}\left[t_n\sin(2\theta_1)+\sin(2t_n\theta_1)\right]\Big[t_n\cos(t_n\theta_2)\sin(\theta_2) \\
+ \;& \cos(\theta_2)\sin(t_n\theta_2)\Big] \qquad (10.1.24)
\end{aligned}
$$

$$
\begin{aligned}
B_{2n} \;=\; & \frac{8(1+t_n)^2}{1+\alpha}\Big\{{t_n}^2\Big[-2\cos[\theta_1-\theta_2-t_n\theta_2]\sin(\theta_1)+\cos(\theta_2)\cos(t_n\theta_2)\sin(2\theta_1)+ \\
& +\alpha\Big(2\cos[\theta_1+\theta_2+t_n\theta_2]\sin(\theta_1)-\cos(\theta_2)\cos(t_n\theta_2)\sin(2\theta_1)\Big)\Big]+ \\
+ \;& 2\cos[t_n\theta_1-\theta_2-t_n\theta_2]\sin(t_n\theta_1)-2\alpha\cos[t_n\theta_1+\theta_2+t_n\theta_2]\sin(t_n\theta_1)- \\
& -\cos(\theta_2)\cos(t_n\theta_2)\sin(2t_n\theta_1)+\alpha\cos(\theta_2)\cos(t_n\theta_2)\sin(2t_n\theta_1)+ \\
+ \;& 2\,(\alpha-1)\,t_n\cos[(1+t_n)\,\theta_1]\sin[(1-t_n)\,\theta_1]\sin(\theta_2)\sin(t_n\theta_2)\Big\} \qquad (10.1.25)
\end{aligned}
$$

$$
\begin{aligned}
C_{2n} &= \frac{8\,(1-\alpha)\,({t_n}^2-1)}{1+\alpha}\,[t_n\sin(2\theta_1)+\sin(2t_n\theta_1)]\,\Big[t_n\cos(t_n\theta_2)\sin(\theta_2) \\
&+ \cos(\theta_2)\sin(t_n\theta_2)\Big] \qquad (10.1.26)
\end{aligned}
$$

$$
\begin{aligned}
D_{2n} &= \frac{8\,(-1+{t_n}^2)}{1+\alpha}\Big\{{t_n}^2\Big[-2\cos[\theta_1-\theta_2+t_n\theta_2]\sin(\theta_1)+\cos(\theta_2)\cos(t_n\theta_2)\sin(2\theta_1)+ \\
&+\alpha\Big(2\cos[\theta_1+\theta_2-t_n\theta_2]\sin(\theta_1)-\cos(\theta_2)\cos(t_n\theta_2)\sin(2\theta_1)\Big)\Big]- \\
&- 2\cos[t_n\theta_1+\theta_2-t_n\theta_2]\sin(t_n\theta_1)-\alpha\cos(\theta_2)\cos(t_n\theta_2)\sin(2t_n\theta_1)+ \\
&+ 2\,(\alpha-1)\,t_n\cos[(1-t_n)\,\theta_1]\sin[(1+t_n)\,\theta_1]\sin(\theta_2)\sin(t_n\theta_2)+ \\
&+ 2\alpha\cos[t_n\theta_1-\theta_2+t_n\theta_2]\sin(t_n\theta_1)+\cos(\theta_2)\cos(t_n\theta_2)\sin(2t_n\theta_1)\Big\}, \qquad (10.1.27)
\end{aligned}
$$

with $t_n = 1-\lambda_n$ and $A_{1n} \neq 0$. The angular functions can be calculated from Eqs. (3.1.97- 3.1.99).
In case of $\theta_2 = -\theta_1$ the coefficients can be simplified as

$$
A_{1n} = -8(1+t_n)^2\,[t_n\cos(t_n\theta_1)\sin(\theta_1)+\cos(\theta_1)\sin(t_n\theta_1)]\,[t_n\sin(2\theta_1)+\sin(2t_n\theta_1)] \qquad (10.1.28)
$$

$$
\begin{aligned}
B_{1n} &= -8(1+t_n)^2\,[1-t_n+t_n\cos(2\theta_1)-\cos(2t_n\theta_1)]\times \\
&\times[t_n\cos(t_n\theta_1)\sin(\theta_1)+\cos(\theta_1)\sin(t_n\theta_1)] \qquad (10.1.29)
\end{aligned}
$$

$$
C_{1n} = -8\left({t_n}^2-1\right)[t_n\cos(t_n\theta_1)\sin(\theta_1)+\cos(\theta_1)\sin(t_n\theta_1)]\,[t_n\sin(2\theta_1)+\sin(2t_n\theta_1)] \qquad (10.1.30)
$$

$$
\begin{aligned}
D_{1n} &= -8\left({t_n}^2-1\right)[-1-t_n+t_n\cos(2\theta_1)+\cos(2t_n\theta_1)]\times \\
&\times[t_n\cos(t_n\theta_1)\sin(\theta_1)+\cos(\theta_1)\sin(t_n\theta_1)] \qquad (10.1.31)
\end{aligned}
$$

$$
\begin{aligned}
A_{2n} &= -\frac{8\,(1-\alpha)\,(1+t_n)^2}{1+\alpha}\,[t_n\cos(t_n\theta_1)\sin(\theta_1)+\cos(\theta_1)\sin(t_n\theta_1)]\times \\
&\times[t_n\sin(2\theta_1)+\sin(2t_n\theta_1)] \qquad (10.1.32)
\end{aligned}
$$

$$
\begin{aligned}
B_{2n} &= \frac{8(1+t_n)^2}{1+\alpha}\Big\{{t_n}^2\Big[-2\cos[(2+t_n)\,\theta_1]\sin(\theta_1)+2\alpha\cos(t_n\theta_1)\sin^3(\theta_1)+ \\
&+ \cos(\theta_1)\cos(t_n\theta_1)\sin(2\theta_1)\Big]-2\alpha\cos(\theta_1)\sin(t_n\theta_1)+2\cos[(1+2t_n)\,\theta_1]\sin(t_n\theta_1) \\
&+ 2\,(\alpha-1)\,t_n\cos[(1+t_n)\,\theta_1]\sin(\theta_1)\sin[(1-t_n)\,\theta_1]\sin(t_n\theta_1)- \\
&- \cos(\theta_1)\cos(t_n\theta_1)\sin(2t_n\theta_1)+\alpha\cos(\theta_1)\cos(t_n\theta_1)\sin(2t_n\theta_1)\Big\} \qquad (10.1.33)
\end{aligned}
$$

$$C_{2n} = -\frac{8\,(1-\alpha)\,({t_n}^2-1)}{1+\alpha}\,[t_n\cos(t_n\theta_1)\sin(\theta_1)+\cos(\theta_1)\sin(t_n\theta_1)]\times$$
$$\times\,[t_n\sin(2\theta_1)+\sin(2t_n\theta_1)] \qquad (10.1.34)$$

$$\begin{aligned} D_{2n} &= \frac{8\,(-1+{t_n}^2)}{1+\alpha}\Big\{{t_n}^2\big[-2\cos[(2-t_n)\,\theta_1]\sin(\theta_1)+2\alpha\cos(t_n\theta_1)\sin^3(\theta_1)\\ &+ \cos(\theta_1)\cos(t_n\theta_1)\sin(2\theta_1)\big]+2\alpha\cos(\theta_1)\sin(t_n\theta_1)-2\cos[(1-2t_n)\,\theta_1]\sin(t_n\theta_1)\\ &+ \cos(\theta_1)\cos(t_n\theta_1)\sin(2t_n\theta_1)-\alpha\cos(\theta_1)\cos(t_n\theta_1)\sin(2t_n\theta_1)+\\ &+ 2\,(-1+\alpha)\,t_n\cos[(1-t_n)\,\theta_1]\sin(\theta_1)\sin(t_n\theta_1)\sin[(1+t_n)\,\theta_1]\Big\}. \qquad (10.1.35)\end{aligned}$$

For $\theta_2=-\theta_1=\pi/2$ there is

$$A_{1n} = -8t_n(1+t_n)^2\cos(\frac{\pi t_n}{2})\sin(\pi t_n) \qquad (10.1.36)$$

$$B_{1n} = 8t_n(1+t_n)^2\cos(\frac{\pi t_n}{2})\,[-1+2t_n+\cos(\pi t_n)] \qquad (10.1.37)$$

$$C_{1n} = -8\left({t_n}^2-1\right)t_n\cos(\frac{\pi t_n}{2})\sin(\pi t_n) \qquad (10.1.38)$$

$$D_{1n} = 8\left({t_n}^2-1\right)t_n\cos(\frac{\pi t_n}{2})\,[1+2t_n-\cos(\pi t_n)] \qquad (10.1.39)$$

$$A_{2n} = -\frac{8\,(1-\alpha)}{1+\alpha}t_n(1+t_n)^2\cos(\frac{\pi t_n}{2})\sin(\pi t_n) \qquad (10.1.40)$$

$$\begin{aligned} B_{2n} &= \frac{8(1+t_n)^2}{1+\alpha}\cos(\frac{\pi t_n}{2})\big[-2+t_n-\alpha t_n+2{t_n}^2+2\alpha{t_n}^2+2\cos(\pi t_n)-\\ &-t_n\cos(\pi t_n)+\alpha t_n\cos(\pi t_n)\big] \qquad (10.1.41)\end{aligned}$$

$$C_{2n} = -\frac{8\,(1-\alpha)}{1+\alpha}\left({t_n}^2-1\right)t_n\cos(\frac{\pi t_n}{2})\sin(\pi t_n) \qquad (10.1.42)$$

$$\begin{aligned} D_{2n} &= \frac{8\,(1-{t_n}^2)}{1+\alpha}\cos(\frac{\pi t_n}{2})\big[2+t_n-\alpha t_n-2{t_n}^2-2\alpha{t_n}^2-2\cos(\pi t_n)-\\ &-t_n\cos(\pi t_n)+\alpha t_n\cos(\pi t_n)\big] \qquad (10.1.43)\end{aligned}$$

and for $\theta_2=-\theta_1=\pi$

$$A_{1n} = -8t_n(1+t_n)^2\cos(\frac{\pi t_n}{2})\sin(2\pi t_n) \qquad (10.1.44)$$

$$B_{1n} = -16t_n(1+t_n)^2\cos(\frac{\pi t_n}{2})\sin^2(\pi t_n) \tag{10.1.45}$$

$$C_{1n} = -8\left({t_n}^2-1\right)t_n\cos(\frac{\pi t_n}{2})\sin(2\pi t_n) \tag{10.1.46}$$

$$D_{1n} = 16\left({t_n}^2-1\right)t_n\cos(\frac{\pi t_n}{2})\sin^2(\pi t_n) \tag{10.1.47}$$

$$A_{2n} = -\frac{8\,(1-\alpha)}{1+\alpha}t_n(1+t_n)^2\cos(\frac{\pi t_n}{2})\sin(2\pi t_n) \tag{10.1.48}$$

$$\begin{aligned} B_{2n} &= \frac{32(1+t_n)^2}{1+\alpha}\cos(\frac{\pi t_n}{2})\Big[-1-\alpha-2\cos(\pi t_n)+t_n\cos(\pi t_n)- \\ &\quad -\alpha t_n\cos(\pi t_n)\Big]\sin^2(\frac{\pi t_n}{2}) \end{aligned} \tag{10.1.49}$$

$$C_{2n} = -\frac{8\,(1-\alpha)}{1+\alpha}\left({t_n}^2-1\right)t_n\cos(\frac{\pi t_n}{2})\sin(2\pi t_n) \tag{10.1.50}$$

$$\begin{aligned} D_{2n} &= \frac{32\,({t_n}^2-1)}{1+\alpha}\cos(\frac{\pi t_n}{2})\Big[-1-\alpha-2\cos(\pi t_n)-t_n\cos(\pi t_n)+ \\ &\quad +\alpha t_n\cos(\pi t_n)\Big]\sin^2(\frac{\pi t_n}{2}) \end{aligned} \tag{10.1.51}$$

If $\theta_2 = -\pi$ and θ_1 arbitrary, the coefficients read

$$A_{1n} = 8(1+t_n)^2\sin(\pi t_n)\left[t_n\sin(2\theta_1)+\sin(2t_n\theta_1)\right] \tag{10.1.52}$$

$$B_{1n} = 8(1+t_n)^2\Big[1-t_n+t_n\cos(2\theta_1)-\cos(2t_n\theta_1)\Big]\sin(\pi t_n) \tag{10.1.53}$$

$$C_{1n} = 8\left({t_n}^2-1\right)\sin(\pi t_n)\left[t_n\sin(2\theta_1)+\sin(2t_n\theta_1)\right] \tag{10.1.54}$$

$$D_{1n} = 8\left({t_n}^2-1\right)\Big[-1-t_n+t_n\cos(2\theta_1)+\cos(2t_n\theta_1)\Big]\sin(\pi t_n) \tag{10.1.55}$$

$$A_{2n} = \frac{8\,(1-\alpha)}{1+\alpha}(1+t_n)^2\sin(\pi t_n)\left[t_n\sin(2\theta_1)+\sin(2t_n\theta_1)\right] \tag{10.1.56}$$

$$\begin{aligned} B_{2n} &= \frac{8(1+t_n)^2}{1+\alpha}\Big\{-2\,(1+\alpha)\,{t_n}^2\sin(\pi t_n)\sin^2(\theta_1)+ \\ &+ \quad 2\alpha\cos[t_n\,(\pi-\theta_1)]\sin(t_n\theta_1)-2\cos[t_n\,(\pi+\theta_1)]\sin(t_n\theta_1)+ \\ &\quad +\cos(\pi t_n)\sin(2t_n\theta_1)-\alpha\cos(\pi t_n)\sin(2t_n\theta_1)\Big\} \end{aligned} \tag{10.1.57}$$

$$C_{2n} = \frac{8\,(1-\alpha)}{1+\alpha}\left({t_n}^2-1\right)\sin(\pi t_n)\,[t_n\sin(2\theta_1)+\sin(2t_n\theta_1)] \tag{10.1.58}$$

$$\begin{aligned} D_{2n} \;=\; & \frac{8\,(-1+{t_n}^2)}{1+\alpha}\Big\{2\,(1+\alpha)\,{t_n}^2\sin(\pi t_n)\sin^2(\theta_1) - \\ & -2\alpha\cos[t_n\,(\pi-\theta_1)]\sin(t_n\theta_1)+2\cos[t_n\,(\pi+\theta_1)]\sin(t_n\theta_1) - \\ & -\cos(\pi t_n)\sin(2t_n\theta_1)+\alpha\cos(\pi t_n)\sin(2t_n\theta_1)\Big\} \end{aligned} \tag{10.1.59}$$

For $\theta_1 = \pi/2$ and $\theta_2 = -\pi$, which usually occurs in practice, the coefficients are

$$A_{1n} = 8(1+t_n)^2\sin^2(\pi t_n) \tag{10.1.60}$$

$$B_{1n} = 8(1+t_n)^2\,[1-2t_n-\cos(\pi t_n)]\sin(\pi t_n) \tag{10.1.61}$$

$$C_{1n} = 8\left({t_n}^2-1\right)\sin^2(\pi t_n) \tag{10.1.62}$$

$$D_{1n} = 8\left({t_n}^2-1\right)[-1-2t_n+\cos(\pi t_n)]\sin(\pi t_n) \tag{10.1.63}$$

$$A_{2n} = \frac{8\,(1-\alpha)\,(1+t_n)^2\sin^2(\pi t_n)}{1+\alpha} \tag{10.1.64}$$

$$B_{2n} = 8(1+t_n)^2\left[1-2{t_n}^2-\cos(\pi t_n)\right]\sin(\pi t_n) \tag{10.1.65}$$

$$C_{2n} = \frac{8\,(1-\alpha)\,({t_n}^2-1)\sin^2(\pi t_n)}{1+\alpha} \tag{10.1.66}$$

$$D_{2n} = 8\left({t_n}^2-1\right)\left[-1+2{t_n}^2+\cos(\pi t_n)\right]\sin(\pi t_n) \tag{10.1.67}$$

It should be mentioned that the equations to calculate the angular functions are also valid for non-singular eigenvalues (i.e. $t_n > 1$).

10.2 Determination of Stress Exponents and Angular Functions for an Interface with Friction

For a contact problem with friction, at the interface the relationship between the normal and shear stress is

$$\mid \sigma_{r\theta}(r,0) \mid \leq \eta \;\mid \sigma_{\theta\theta}(r,0) \mid . \tag{10.2.1}$$

In the following only the limit case

$$\mid \sigma_{r\theta}(r,0) \mid = \eta \ \mid \sigma_{\theta\theta}(r,0) \mid \tag{10.2.2}$$

is considered.
For an interface with friction contact problem, the boundary conditions are:

at the interface

$$\begin{aligned} v_1(r,0) &= v_2(r,0), \\ \sigma_{\theta\theta 1}(r,0) &= \sigma_{\theta\theta 2}(r,0), \\ \sigma_{r\theta 1}(r,0) &= \sigma_{r\theta 2}(r,0) \\ \mid \sigma_{r\theta 1}(r,0) \mid &= \eta \ \mid \sigma_{\theta\theta 1}(r,0) \mid \end{aligned} \tag{10.2.3}$$

for the free edges

$$\begin{aligned} \sigma_{\theta\theta 1}(r,\theta_1) &= 0, \\ \sigma_{r\theta 1}(r,\theta_1) &= 0, \end{aligned} \tag{10.2.4}$$

$$\begin{aligned} \sigma_{\theta\theta 2}(r,\theta_2) &= 0, \\ \sigma_{r\theta 2}(r,\theta_2) &= 0, \end{aligned} \tag{10.2.5}$$

where η is the friction coefficient. The case of $\eta = 0$ corresponds to a friction free contact problem.
The stress function as given in Eq. (3.1.3) is used. From these eight conditions, the following equations hold for $\lambda_n \neq 0, 1, 2$ (n=1,2,3,...)

$$\begin{aligned} &A_{1n}\mu[2(1-\nu_1)+(2-\lambda_n)(1+\nu_1)] - A_{2n}[2(1-\nu_2)+(2-\lambda_n)(1+\nu_2)] - \\ &-C_{1n}\mu(1+\nu_1)(2-\lambda_n) + C_{2n}(1+\nu_2)(2-\lambda_n) = 0 \end{aligned} \tag{10.2.6}$$

$$B_{1n} + D_{1n} - B_{2n} - D_{2n} = 0 \tag{10.2.7}$$

$$A_{1n}\lambda_n + C_{1n}(2-\lambda_n) - A_{2n}\lambda_n - C_{2n}(2-\lambda_n) = 0 \tag{10.2.8}$$

$$\mid A_{1n}\lambda_n + C_{1n}(2-\lambda_n) \mid -\eta \ \mid (2-\lambda_n)(B_{1n}+D_{1n}) \mid = 0 \tag{10.2.9}$$

(this equation is equivalent to

$$A_{1n}\lambda_n + C_{1n}(2-\lambda_n) \pm \eta\,(2-\lambda_n)(B_{1n}+D_{1n}) = 0 \tag{10.2.10}$$

where it is assumed that the sign of the stress $\sigma_{r\theta}$ and $\sigma_{\theta\theta}$ does change vs. the distance r.)

$$\begin{aligned} &A_{1n}\sin(\lambda_n\theta_1) + B_{1n}\cos(\lambda_n\theta_1) + C_{1n}\sin[(2-\lambda_n)\theta_1] + \\ &+D_{1n}\cos[(2-\lambda_n)\theta_1] = 0 \end{aligned} \tag{10.2.11}$$

$$A_{1n}\lambda_n \cos(\lambda_n\theta_1) - B_{1n}\lambda_n \sin(\lambda_n\theta_1) + C_{1n}(2-\lambda_n)\cos[(2-\lambda_n)\theta_1] - \\ -D_{1n}(2-\lambda_n)\sin[(2-\lambda_n)\theta_1] = 0 \tag{10.2.12}$$

$$A_{2n}\sin(\lambda_n\theta_2) + B_{2n}\cos(\lambda_n\theta_2) + C_{2n}\sin[(2-\lambda_n)\theta_2] + \\ +D_{2n}\cos[(2-\lambda_n)\theta_2] = 0 \tag{10.2.13}$$

$$A_{2n}\lambda_n \cos(\lambda_n\theta_2) - B_{2n}\lambda_n \sin(\lambda_n\theta_2) + C_{2n}(2-\lambda_n)\cos[(2-\lambda_n)\theta_2] - \\ -D_{2n}(2-\lambda_n)\sin[(2-\lambda_n)\theta_2] = 0. \tag{10.2.14}$$

This equations system can be rewritten in a matrix form as

$$[A]_{8\times 8}\{X\}_{8\times 1} = \{0\}_{8\times 1} \tag{10.2.15}$$

where there is $\{X\}_{8\times 1} = \{A_{1n}, B_{1n}, C_{1n}, D_{1n}, A_{2n}, B_{2n}, C_{2n}, D_{2n}\}^t$, and $[A]_{8\times 8}$ is its coefficients matrix. $\{X\}_{8\times 1}$ is unknown and $[A]_{8\times 8}$ includes the unknown exponent λ_n, the material properties (E_k, ν_k, k=1,2 for materials 1 and 2) and the geometry angles (θ_1, θ_2).

Determination of the Stress Exponent

Equation (10.2.15) has a nonzero solution, if and only if

$$\mathrm{Det}([A]_{8\times 8}) = 0 \tag{10.2.16}$$

is satisfied. In Eq. (10.2.16) the only unknown is the exponent λ_n. Its solutions are the eigenvalues of this problem.
The expansion of Eq. (10.2.16) for an arbitrary joint geometry with θ_1, θ_2 is

$$\begin{aligned} det[A] = &-\frac{16(1+t_n)}{1+\alpha}\Big\{ -2{t_n}^3 \sin(\theta_1)\sin(\theta_1-\theta_2)\sin(\theta_2) + \\ &+2\sin(t_n\theta_1)\sin[t_n\,(\theta_1-\theta_2)]\sin(t_n\theta_2) + t_n\Big(\sin^2(t_n\theta_1)\sin(2\theta_2) - \\ &-\sin(2\theta_1)\sin^2(t_n\theta_2)\Big) + {t_n}^2\Big(\sin(2t_n\theta_1)\sin^2(\theta_2) - \sin^2(\theta_1)\sin(2t_n\theta_2)\Big) + \\ + \;&\alpha\Big[t_n\Big(\sin^2(t_n\theta_1)\sin(2\theta_2) + \sin(2\theta_1)\sin^2(t_n\theta_2)\Big) - \\ &-{t_n}^2\Big(\sin(2t_n\theta_1)\sin^2(\theta_2) + \sin^2(\theta_1)\sin(2t_n\theta_2)\Big) - \\ &-2{t_n}^3\sin(\theta_1)\sin(\theta_2)\sin(\theta_1+\theta_2) + 2\sin(t_n\theta_1)\sin(t_n\theta_2)\sin[t_n\,(\theta_1+\theta_2)]\Big]\Big\} \\ \pm \;&\eta\,\frac{8(1+t_n)}{1+\alpha}\Big\{8\beta\Big[-{t_n}^2\sin^2(\theta_1) + \sin^2(t_n\theta_1)\Big]\Big(-{t_n}^2\sin^2(\theta_2) + \sin^2(t_n\theta_2)\Big) + \\ + \;&4\alpha t_n\,(1+t_n)\Big[-2{t_n}^2\sin^2(\theta_1)\sin^2(\theta_2) + \sin^2(t_n\theta_1)\sin^2(\theta_2) + \sin^2(\theta_1)\sin^2(t_n\theta_2)\Big] \\ + \;&t_n(1+t_n)\Big[\cos(2\theta_1) - \cos(2\theta_2) + 2\cos(2t_n\theta_2)\sin^2(\theta_1) - 2\cos(2t_n\theta_1)\sin^2(\theta_2)\Big]\Big\} \end{aligned} \tag{10.2.17}$$

with $t_n = 1 - \lambda_n$. From Eq. (10.2.17) it can be seen that if t_n is the solution of Det(A)=0, -t_n is not for $\eta \neq 0$. This means that if λ_n is the eigenvalue, 2-λ_n is not for a contact problem with friction.
For the special case with $\theta_1 = -\theta_2$ there is

$$\begin{aligned} det[A] &= -\frac{32(1+t_n)}{1+\alpha}\Big\{2{t_n}^3\cos(\theta_1)\sin^3(\theta_1) - t_n\sin(2\theta_1)\sin^2(t_n\theta_1) - \\ &- 2\cos(t_n\theta_1)\sin^3(t_n\theta_1) + {t_n}^2\sin^2(\theta_1)\sin(2t_n\theta_1)\Big\} \\ &\pm \eta\,\frac{64(1+t_n)}{1+\alpha}\Big\{\beta\Big[-{t_n}^2\sin^2(\theta_1) + \sin^2(t_n\theta_1)\Big]^2 \\ &+ \alpha t_n(1+t_n)\Big[-{t_n}^2\sin^4(\theta_1) + \sin^2(\theta_1)\sin^2(t_n\theta_1)\Big]\Big\}. \end{aligned} \tag{10.2.18}$$

For $\theta_2 = -\theta_1 = \pi/2$ yields

$$\begin{aligned} det[A] &= -\frac{16(1+t_n)}{1+\alpha}\Big(-1 + 2{t_n}^2 + \cos(\pi t_n)\Big)\sin(\pi t_n) \\ &\pm \eta\,\frac{16(1+t_n)}{1+\alpha}\Big\{\Big(1 - 2{t_n}^2 - \cos(\pi t_n)\Big)\times \\ &\quad \times\Big[\beta + 2\alpha t_n + 2\alpha{t_n}^2 - 2\beta{t_n}^2 - \beta\cos(\pi t_n)\Big]\Big\}, \end{aligned} \tag{10.2.19}$$

and for $\theta_2 = -\theta_1 = \pi$

$$det[A] = \frac{64(1+t_n)}{1+\alpha}\sin^3(\pi t_n)\Big\{\cos(\pi t_n) \pm \eta\,\beta\sin(\pi t_n)\Big\}. \tag{10.2.20}$$

If the joint geometry is $\theta_2 = -\pi$ and θ_1 arbitrary, which is the general case of a contact problem, the eigenvalue should be determined from

$$\begin{aligned} det[A] &= -\frac{16(1+t_n)}{1+\alpha}\Big\{{t_n}^2\sin(2\pi t_n)\sin^2(\theta_1) - t_n\sin^2(\pi t_n)\sin(2\theta_1) + \\ &+ \alpha\Big[{t_n}^2\sin(2\pi t_n)\sin^2(\theta_1) + t_n\sin^2(\pi t_n)\sin(2\theta_1) - \\ &\quad -2\sin(\pi t_n)\sin(t_n\theta_1)\sin[t_n(-\pi+\theta_1)]\Big] - \\ &- 2\sin(\pi t_n)\sin(t_n\theta_1)\sin[t_n(\pi+\theta_1)]\Big\} \\ &\pm \eta\,\frac{8(1+t_n)}{1+\alpha}\Big\{4\alpha t_n(1+t_n)\sin^2(\pi t_n)\sin^2(\theta_1) + \\ &+ t_n(1+t_n)\Big[-1 + \cos(2\theta_1) + 2\cos(2\pi t_n)\sin^2(\theta_1)\Big] + \\ &+ 8\beta\sin^2(\pi t_n)\Big[-{t_n}^2\sin^2(\theta_1) + \sin^2(t_n\theta_1)\Big]\Big\}. \end{aligned} \tag{10.2.21}$$

In case of $\theta_1 = \pi/2$ and $\theta_2 = -\pi$ there is

$$\begin{aligned} det[A] &= -\frac{16(1+t_n)}{1+\alpha}\Big\{\alpha\Big[1-\cos(\pi t_n)+2{t_n}^2\cos(\pi t_n)\Big]+ \\ &+ \Big[-\cos(\pi t_n)+2{t_n}^2\cos(\pi t_n)+\cos(2\pi t_n)\Big]\Big\}\sin(\pi t_n) \\ &\pm \eta\,\frac{32(1+t_n)}{1+\alpha}\Big\{\beta - t_n + \alpha t_n - {t_n}^2 + \alpha {t_n}^2 - 2\beta {t_n}^2 - \beta\cos(\pi t_n)\Big\}\sin^2(\pi t_n). \end{aligned} \tag{10.2.22}$$

Friction free is a special case of a contact problem with friction. Therefore, the equations given in this section should be the same as those in Section 10.1 by setting $\eta = 0$.

Determination of the Angular Functions

In case of $A_{1n} \neq 0$ and θ_1, θ_2 being arbitrary, the coefficients in Eqs.(3.1.97 - 3.1.99) can be determined from

$$\begin{aligned} A_{1n} &= 8(1+t_n)^2\Big[t_n\sin(2\theta_1)+\sin(2t_n\theta_1)-2\eta\,\Big(t_n\sin^2(\theta_1)+\sin^2(t_n\theta_1)\Big)\Big]\times \\ &\quad\times\Big[t_n\cos(t_n\theta_2)\sin(\theta_2)+\cos(\theta_2)\sin(t_n\theta_2)\Big] \end{aligned} \tag{10.2.23}$$

$$\begin{aligned} B_{1n} &= 8(1+t_n)^2\Big[1-\cos(2t_n\theta_1)-2t_n\sin^2(\theta_1)+\eta\,\Big(-t_n\sin(2\theta_1)+\sin(2t_n\theta_1)\Big)\Big]\times \\ &\quad\times\Big[t_n\cos(t_n\theta_2)\sin(\theta_2)+\cos(\theta_2)\sin(t_n\theta_2)\Big] \end{aligned} \tag{10.2.24}$$

$$\begin{aligned} C_{1n} &= 8\,(1+t_n)\Big[\eta\,\Big(\cos(2t_n\theta_1)-1+t_n[\cos(2t_n\theta_1)-\cos(2\theta_1)]+2t_n{}^2\sin^2(\theta_1)\Big)+ \\ &+ t_n{}^2\sin(2\theta_1)-\sin(2t_n\theta_1)+t_n\Big(-\sin(2\theta_1)+\sin(2t_n\theta_1)\Big)\Big]\times \\ &\quad\times\Big[t_n\cos(t_n\theta_2)\sin(\theta_2)+\cos(\theta_2)\sin(t_n\theta_2)\Big] \end{aligned} \tag{10.2.25}$$

$$\begin{aligned} D_{1n} &= 8\,(1+t_n)\Big[(-1+t_n)\Big(-1+\cos(2t_n\theta_1)-2t_n\sin^2(\theta_1)\Big)+ \\ &+ \eta\,\Big(t_n{}^2\sin(2\theta_1)+t_n\,[\sin(2\theta_1)-\sin(2t_n\theta_1)]-\sin(2t_n\theta_1)\Big)\Big]\times \\ &\quad\times\Big[t_n\cos(t_n\theta_2)\sin(\theta_2)+\cos(\theta_2)\sin(t_n\theta_2)\Big] \end{aligned} \tag{10.2.26}$$

$$\begin{aligned} A_{2n} &= Eq.(10.1.24)+ \\ &+ \eta\;\;\frac{8(1+t_n)^2}{1+\alpha}\Big\{-2t_n{}^2\cos(t_n\theta_2)\sin^2(\theta_1)\sin(\theta_2)-2\cos(\theta_2)\sin^2(t_n\theta_1)\sin(t_n\theta_2) \\ &+ t_n\Big[\sin[(1-t_n)\,\theta_1]\sin[(1+t_n)\,\theta_1]\sin[(1-t_n)\,\theta_2]-\sin[(1+t_n)\,\theta_2]+ \\ &\quad+\cos[(1-t_n)\,\theta_1]\cos[(1+t_n)\,\theta_1]\sin[(1+t_n)\,\theta_2]\Big]+ \end{aligned}$$

$$
\begin{aligned}
&+ \quad 4\beta\Big[\sin^2(t_n\theta_1) - {t_n}^2\sin^2(\theta_1)\Big]\left[t_n\cos(t_n\theta_2)\sin(\theta_2) + \cos(\theta_2)\sin(t_n\theta_2)\right] + \\
&+ \quad \alpha\Big\{4{t_n}^3\cos(t_n\theta_2)\sin^2(\theta_1)\sin(\theta_2) - 2\cos(\theta_2)\sin^2(t_n\theta_1)\sin(t_n\theta_2) - \\
&\quad -{t_n}^2\sin^2(\theta_1)\Big[\sin[(1-t_n)\,\theta_2] - 3\sin[(1+t_n)\,\theta_2]\Big] + \\
&\quad +t_n\Big[-\sin[(1-t_n)\,\theta_2] + \cos[(1-t_n)\,\theta_1]\cos[(1+t_n)\,\theta_1]\sin[(1-t_n)\,\theta_2] + \\
&\quad +\sin[(1-t_n)\,\theta_1]\sin[(1+t_n)\,\theta_1]\sin[(1+t_n)\,\theta_2]\Big]\Big\}\Big\} \qquad (10.2.27)
\end{aligned}
$$

$$
\begin{aligned}
B_{2n} \quad &= \quad Eq.(10.1.25) + \\
&+ \quad \eta \quad \frac{8(1+t_n)^2}{1+\alpha}\Big\{4\beta\,(-1+t_n)\Big[\sin^2(t_n\theta_1) - {t_n}^2\sin^2(\theta_1)\Big]\sin(\theta_2)\sin(t_n\theta_2) + \\
&+ \quad \Big[-2{t_n}^2\cos(\theta_2)\cos(t_n\theta_2)\sin^2(\theta_1) + 2\cos(\theta_2)\cos(t_n\theta_2)\sin^2(t_n\theta_1) + \\
&\quad +t_n\left[-\cos(2\theta_1) + \cos(2t_n\theta_1)\right]\sin(\theta_2)\sin(t_n\theta_2)\Big] + \\
&+ \quad \alpha\Big[-2{t_n}^2\cos(\theta_2)\cos(t_n\theta_2)\sin^2(\theta_1) + 2\cos(\theta_2)\cos(t_n\theta_2)\sin^2(t_n\theta_1) + \\
&+ \quad t_n\left[-2 + \cos(2\theta_1) + \cos(2t_n\theta_1)\right]\sin(\theta_2)\sin(t_n\theta_2) + 4{t_n}^3\sin^2(\theta_1)\sin(\theta_2)\sin(t_n\theta_2)\Big]\Big\}
\end{aligned}
\qquad (10.2.28)
$$

$$
\begin{aligned}
C_{2n} \quad &= \quad Eq.(10.1.26) + \\
&+ \quad \eta \quad \frac{8\,(1+t_n)}{1+\alpha}\Big\{2{t_n}^3\cos(t_n\theta_2)\sin^2(\theta_1)\sin(\theta_2) - 2\cos(\theta_2)\sin^2(t_n\theta_1)\sin(t_n\theta_2) + \\
&+{t_n}^2\Big(\cos(2t_n\theta_1)\cos(t_n\theta_2)\sin(\theta_2) + \cos(\theta_2)\sin(t_n\theta_2) - \cos(2\theta_1)\sin[(1+t_n)\,\theta_2]\Big) - \\
&-t_n\Big(\cos(t_n\theta_2)\sin(\theta_2) + \cos(2\theta_1)\cos(\theta_2)\sin(t_n\theta_2) - \cos(2t_n\theta_1)\sin[(1+t_n)\,\theta_2]\Big) + \\
&+ \quad 2\beta\Big[-2{t_n}^4\cos(t_n\theta_2)\sin^2(\theta_1)\sin(\theta_2) + 2{t_n}^3\sin^2(\theta_1)\sin[(1-t_n)\,\theta_2] - \\
&-2t_n\sin^2(t_n\theta_1)\sin[(1-t_n)\,\theta_2] - 2\cos(\theta_2)\sin^2(t_n\theta_1)\sin(t_n\theta_2) + \\
&+{t_n}^2\Big(-\sin[(1-t_n)\,\theta_1]\sin[(1+t_n)\,\theta_1]\sin[(1-t_n)\,\theta_2] + \\
&+\sin[(1+t_n)\,\theta_2] - \cos[(1-t_n)\,\theta_1]\cos[(1+t_n)\,\theta_1]\sin[(1+t_n)\,\theta_2]\Big)\Big] + \\
&+ \quad \alpha\Big[4{t_n}^4\cos(t_n\theta_2)\sin^2(\theta_1)\sin(\theta_2) + {t_n}^2\Big(-\cos(t_n\theta_2)\sin(\theta_2) + \\
&+\cos(2t_n\theta_1)\cos(t_n\theta_2)\sin(\theta_2) - 2\sin^2(\theta_1)\sin[(1-t_n)\,\theta_2]\Big) - \\
&-2\cos(\theta_2)\sin^2(t_n\theta_1)\sin(t_n\theta_2) - {t_n}^3\sin^2(\theta_1)\Big(\sin[(1-t_n)\,\theta_2] - 3\sin[(1+t_n)\,\theta_2]\Big) + \\
&+t_n\Big(-\cos(\theta_2)\sin(t_n\theta_2) + \cos(2\theta_1)\cos(\theta_2)\sin(t_n\theta_2) - 2\sin^2(t_n\theta_1)\sin[(1+t_n)\,\theta_2]\Big)\Big]\Big\}
\end{aligned}
\qquad (10.2.29)
$$

$$
D_{2n} \quad = \quad Eq.(10.1.27) +
$$

$$
\begin{aligned}
&+ \quad \eta \quad \frac{16(1+t_n)^2}{1+\alpha}\Big\{ {t_n}^2 \cos(\theta_2)\cos(t_n\theta_2)\sin^2(\theta_1) - \cos(\theta_2)\cos(t_n\theta_2)\sin^2(t_n\theta_1) - \\
&- \quad t_n \sin[(1-t_n)\,\theta_1]\sin[(1+t_n)\,\theta_1]\sin(\theta_2)\sin(t_n\theta_2) + \\
&+ \quad 2\beta\,(-1+t_n)\left[{t_n}^2\sin^2(\theta_1) - \sin^2(t_n\theta_1)\right]\sin(\theta_2)\sin(t_n\theta_2) + \\
&+ \quad \alpha\Big[{t_n}^2\cos(\theta_2)\cos(t_n\theta_2)\sin^2(\theta_1) - \cos(\theta_2)\cos(t_n\theta_2)\sin^2(t_n\theta_1) + \\
&\qquad +t_n\sin(\theta_2)\sin(t_n\theta_2) - t_n\cos[(1-t_n)\,\theta_1]\cos[(1+t_n)\,\theta_1]\sin(\theta_2)\sin(t_n\theta_2) - \\
&\qquad -2{t_n}^3\sin^2(\theta_1)\sin(\theta_2)\sin(t_n\theta_2)\Big]\Big\}. \qquad (10.2.30)
\end{aligned}
$$

In case of $\theta_1 = -\theta_2$

$$
\begin{aligned}
A_{1n} &= 8(1+t_n)^2\left[-t_n\cos(t_n\theta_1)\sin(\theta_1) - \cos(\theta_1)\sin(t_n\theta_1)\right]\times \\
&\times \quad \left[t_n\sin(2\theta_1) + \sin(2t_n\theta_1) - 2\eta\,\left(t_n\sin^2(\theta_1) + \sin^2(t_n\theta_1)\right)\right] \qquad (10.2.31)
\end{aligned}
$$

$$
\begin{aligned}
B_{1n} &= -8(1+t_n)^2\left[1 - t_n + t_n\cos(2\theta_1) - \cos(2t_n\theta_1) - \eta\left(t_n\sin(2\theta_1) - \sin(2t_n\theta_1)\right)\right]\times \\
&\times\left[t_n\cos(t_n\theta_1)\sin(\theta_1) + \cos(\theta_1)\sin(t_n\theta_1)\right] \qquad (10.2.32)
\end{aligned}
$$

$$
\begin{aligned}
C_{1n} &= -8\,(1+t_n)\left[t_n\cos(t_n\theta_1)\sin(\theta_1) + \cos(\theta_1)\sin(t_n\theta_1)\right]\times \\
&\times\Big\{\eta\Big[-1 + \cos(2t_n\theta_1) + t_n\left[-\cos(2\theta_1) + \cos(2t_n\theta_1)\right] + 2{t_n}^2\sin^2(\theta_1)\Big] + \\
&+{t_n}^2\sin(2\theta_1) - \sin(2t_n\theta_1) + t_n\left[-\sin(2\theta_1) + \sin(2t_n\theta_1)\right]\Big\} \qquad (10.2.33)
\end{aligned}
$$

$$
\begin{aligned}
D_{1n} &= -8\,(1+t_n)\left[t_n\cos(t_n\theta_1)\sin(\theta_1) + \cos(\theta_1)\sin(t_n\theta_1)\right]\times \\
&\times\Big\{\,(-1+t_n)\left[-1 + \cos(2t_n\theta_1) - 2t_n\sin^2(\theta_1)\right] + \\
&+\eta\left[t_n\sin(2\theta_1) + {t_n}^2\sin(2\theta_1) - \sin(2t_n\theta_1) - t_n\sin(2t_n\theta_1)\right]\Big\} \qquad (10.2.34)
\end{aligned}
$$

$$
\begin{aligned}
A_{2n} &= Eq.(10.1.32) + \\
&+ \quad \eta \quad \frac{8(1+t_n)^2}{1+\alpha}\Big\{2{t_n}^2\cos(t_n\theta_1)\sin^3(\theta_1) + 2\cos(\theta_1)\sin^3(t_n\theta_1) - \\
&- \quad 4\beta\Big[\sin^2(t_n\theta_1) - {t_n}^2\sin^2(\theta_1)\Big]\left[t_n\cos(t_n\theta_1)\sin(\theta_1) + \cos(\theta_1)\sin(t_n\theta_1)\right] + \\
&+ \quad \alpha\Big[-4{t_n}^3\cos(t_n\theta_1)\sin^3(\theta_1) - 2t_n\cos[(1+t_n)\,\theta_1]\sin(\theta_1)\sin[(1-t_n)\,\theta_1]\sin(t_n\theta_1) \\
&\qquad +2\cos(\theta_1)\sin^3(t_n\theta_1) + {t_n}^2\sin^2(\theta_1)\Big(\sin[(1-t_n)\,\theta_1] - 3\sin[(1+t_n)\,\theta_1]\Big)\Big] \\
&\qquad +2t_n\cos[(1-t_n)\,\theta_1]\sin(\theta_1)\sin(t_n\theta_1)\sin[(1+t_n)\,\theta_1]\Big\} \qquad (10.2.35)
\end{aligned}
$$

$$
\begin{aligned}
B_{2n} &= Eq.(10.1.33) + \\
&+ \quad \eta \quad \frac{8(1+t_n)^2}{1+\alpha}\Big\{4\beta\,(1-t_n)\sin(\theta_1)\sin(t_n\theta_1)\left[{t_n}^2\sin^2(\theta_1) - \sin^2(t_n\theta_1)\right] -
\end{aligned}
$$

$$
\begin{aligned}
&- \Big[2{t_n}^2\cos(\theta_1)\cos(t_n\theta_1)\sin^2(\theta_1)+t_n\Big(\cos(2\theta_1)-\cos(2t_n\theta_1)\Big)\sin(\theta_1)\sin(t_n\theta_1)- \\
&\quad -2\cos(\theta_1)\cos(t_n\theta_1)\sin^2(t_n\theta_1)\Big]- \\
&- \alpha\Big[2{t_n}^2\cos(\theta_1)\cos(t_n\theta_1)\sin^2(\theta_1)+t_n\Big(2-\cos(2\theta_1)-\cos(2t_n\theta_1)\Big)\sin(\theta_1)\sin(t_n\theta_1) \\
&\quad -4{t_n}^3\sin^3(\theta_1)\sin(t_n\theta_1)-2\cos(\theta_1)\cos(t_n\theta_1)\sin^2(t_n\theta_1)\Big]\Big\} \qquad (10.2.36)
\end{aligned}
$$

$$
\begin{aligned}
C_{2n} &= Eq.(10.1.34)+ \\
&+ \eta\quad\frac{8\,(1+t_n)}{1+\alpha}\Big\{-2{t_n}^3\cos(t_n\theta_1)\sin^3(\theta_1)+2\cos(\theta_1)\sin^3(t_n\theta_1)- \\
&\quad -{t_n}^2\Big(\cos(t_n\theta_1)\cos(2t_n\theta_1)\sin(\theta_1)+\cos(\theta_1)\sin(t_n\theta_1)-\cos(2\theta_1)\sin[(1+t_n)\,\theta_1]\Big) \\
&\quad +t_n\Big(\cos(t_n\theta_1)\sin(\theta_1)+\cos(\theta_1)\cos(2\theta_1)\sin(t_n\theta_1)-\cos(2t_n\theta_1)\sin[(1+t_n)\,\theta_1]\Big) \\
&+ \alpha\Big[-4{t_n}^4\cos(t_n\theta_1)\sin^3(\theta_1)+2\cos(\theta_1)\sin^3(t_n\theta_1) \\
&\quad +{t_n}^2\Big(\cos(t_n\theta_1)\sin(\theta_1)-\cos(t_n\theta_1)\cos(2t_n\theta_1)\sin(\theta_1)+2\sin^2(\theta_1)\sin[(1-t_n)\,\theta_1]\Big) \\
&\quad +{t_n}^3\sin^2(\theta_1)\Big(\sin[(1-t_n)\,\theta_1]-3\sin[(1+t_n)\,\theta_1]\Big) \\
&\quad +t_n\Big(\cos(\theta_1)\sin(t_n\theta_1)-\cos(\theta_1)\cos(2\theta_1)\sin(t_n\theta_1)+2\sin^2(t_n\theta_1)\sin[(1+t_n)\,\theta_1]\Big)\Big] \\
&+ \beta\Big[4{t_n}^4\cos(t_n\theta_1)\sin^3(\theta_1)-4{t_n}^3\sin^2(\theta_1)\sin[(1-t_n)\,\theta_1]+ \\
&\quad +4t_n\sin[(1-t_n)\,\theta_1]\sin^2(t_n\theta_1)+4\cos(\theta_1)\sin^3(t_n\theta_1)-{t_n}^2\Big(2\sin[(1+t_n)\,\theta_1]- \\
&\quad -2\sin^2[(1-t_n)\,\theta_1]\sin[(1+t_n)\,\theta_1]-\cos[(1-t_n)\,\theta_1]\sin[2\,(1+t_n)\,\theta_1]\Big)\Big]\Big\} \qquad (10.2.37)
\end{aligned}
$$

$$
\begin{aligned}
D_{2n} &= Eq.(10.1.35)+ \\
&+ \eta\quad\frac{16(1+t_n)^2}{1+\alpha}\Big\{{t_n}^2\cos(\theta_1)\cos(t_n\theta_1)\sin^2(\theta_1)-\cos(\theta_1)\cos(t_n\theta_1)\sin^2(t_n\theta_1)+ \\
&+ 2\beta\,(-1+t_n)\sin(\theta_1)\Big[{t_n}^2\sin^2(\theta_1)-\sin^2(t_n\theta_1)\Big]\sin(t_n\theta_1)+ \\
&+ \alpha\Big[{t_n}^2\cos(\theta_1)\cos(t_n\theta_1)\sin^2(\theta_1)-2{t_n}^3\sin^3(\theta_1)\sin(t_n\theta_1)-\cos(\theta_1)\cos(t_n\theta_1)\sin^2(t_n\theta_1) \\
&\quad +t_n\sin(\theta_1)\sin(t_n\theta_1)-t_n\cos[(1-t_n)\,\theta_1]\cos[(1+t_n)\,\theta_1]\sin(\theta_1)\sin(t_n\theta_1)\Big]- \\
&- t_n\sin(\theta_1)\sin[(1-t_n)\,\theta_1]\sin(t_n\theta_1)\sin[(1+t_n)\,\theta_1]\Big\}. \qquad (10.2.38)
\end{aligned}
$$

In case of $\theta_1=-\theta_2=\pi/2$

$$
A_{1n}=8t_n(1+t_n)^2\cos(\frac{\pi t_n}{2})\left[\eta\left(1+2t_n-\cos(\pi t_n)\right)-\sin(\pi t_n)\right] \qquad (10.2.39)
$$

$$
B_{1n}=-8t_n(1+t_n)^2\cos(\frac{\pi t_n}{2})\left[1-2t_n-\cos(\pi t_n)+\eta\,\sin(\pi t_n)\right] \qquad (10.2.40)
$$

$$C_{1n} = -8t_n\,(1+t_n)\cos(\frac{\pi t_n}{2})\Big\{\eta\,\Big[-1+t_n+2{t_n}^2+\cos(\pi t_n)+t_n\cos(\pi t_n)\Big]- \\ -\sin(\pi t_n)+t_n\sin(\pi t_n)\Big\} \tag{10.2.41}$$

$$D_{1n} = -8t_n\,(1+t_n)\cos(\frac{\pi t_n}{2})\Big[\,(-1+t_n)\,[-1-2t_n+\cos(\pi t_n)]-\eta\;(1+t_n)\sin(\pi t_n)\Big] \tag{10.2.42}$$

$$A_{2n} = Eq.(10.1.40)+\eta\quad\frac{8t_n(1+t_n)^2}{1+\alpha}\cos(\frac{\pi t_n}{2})\Big\{1+2t_n-\cos(\pi t_n)+ \\ +\alpha\,\Big[1-2t_n-4{t_n}^2-\cos(\pi t_n)\Big]+2\beta\,\Big[-1+2{t_n}^2+\cos(\pi t_n)\Big]\,\Big\} \tag{10.2.43}$$

$$B_{2n} = Eq.(10.1.41)+ \\ +\quad\eta\quad\frac{8(1+t_n)^2}{1+\alpha}\Big\{\alpha\Big[4{t_n}^3+t_n[-3+\cos(\pi t_n)]\Big]+t_n\,[1+\cos(\pi t_n)]+ \\ +\quad 2\beta\Big[-1+2{t_n}^2-2{t_n}^3+t_n\,[1-\cos(\pi t_n)]+\cos(\pi t_n)\Big]\Big\}\sin(\frac{\pi t_n}{2}) \tag{10.2.44}$$

$$C_{2n} = Eq.(10.1.42)+ \\ +\quad\eta\quad\frac{8\,(1+t_n)}{1+\alpha}\cos(\frac{\pi t_n}{2})\Big\{\alpha t_n\,(1+t_n)\,\Big[1+2t_n-4{t_n}^2-\cos(\pi t_n)\Big]+ \\ +\quad 2\beta\,(-1+t_n)\,t_n\,\Big[-1+2{t_n}^2+\cos(\pi t_n)\Big]+ \\ +\quad t_n\Big(1-t_n-2{t_n}^2-\cos(\pi t_n)-t_n\cos(\pi t_n)\Big)\Big\} \tag{10.2.45}$$

$$D_{2n} = Eq.(10.1.43)+ \\ +\quad\eta\quad\frac{8(1+t_n)^2}{1+\alpha}\Big\{-2t_n\cos^2(\frac{\pi t_n}{2})+\alpha t_n\Big[3-4{t_n}^2-\cos(\pi t_n)\Big]+ \\ +\quad 2\beta\,(-1+t_n)\,\Big[-1+2{t_n}^2+\cos(\pi t_n)\Big]\,\Big\}\sin(\frac{\pi t_n}{2}). \tag{10.2.46}$$

In case of $\theta_1 = -\theta_2 = \pi$

$$A_{1n} = 16(1+t_n)^2\sin^2(\pi t_n)\,[\cos(\pi t_n)-\eta\,\sin(\pi t_n)] \tag{10.2.47}$$

$$B_{1n} = 16(1+t_n)^2\sin^2(\pi t_n)\,[\eta\,\cos(\pi t_n)+\sin(\pi t_n)] \tag{10.2.48}$$

$$C_{1n} = 8\,(1+t_n)\sin(\pi t_n)\,\Big[-2\eta\;(1+t_n)\sin^2(\pi t_n)-\sin(2\pi t_n)+t_n\sin(2\pi t_n)\Big] \tag{10.2.49}$$

$$D_{1n} = 8\,(1+t_n)\sin(\pi t_n)\,\Big[2\,(1-t_n)\sin^2(\pi t_n)-\eta\;(1+t_n)\sin(2\pi t_n)\Big] \tag{10.2.50}$$

$$A_{2n} = Eq.(10.1.48) + \eta \quad \frac{16}{1+\alpha}\,(-1-\alpha+2\beta)\,(1+t_n)^2 \sin^3(\pi t_n) \tag{10.2.51}$$

$$B_{2n} \;=\; Eq.(10.1.49) - \eta \quad 16(1+t_n)^2\cos(\pi t_n)\sin^2(\pi t_n) \tag{10.2.52}$$

$$\begin{aligned} C_{2n} \;&=\; Eq.(10.1.50) - \\ &-\; \eta \quad \frac{16\,(1+t_n)}{1+\alpha}\Big[1+\alpha\,(1+t_n)+t_n+2\beta\,(1-t_n)\Big]\sin^3(\pi t_n) \end{aligned} \tag{10.2.53}$$

$$D_{2n} \;=\; Eq.(10.1.51) + \eta \quad 16(1+t_n)^2\cos(\pi t_n)\sin^2(\pi t_n). \tag{10.2.54}$$

In case of $\theta_2 = -\pi$ and θ_1 being arbitrary

$$\begin{aligned} A_{1n} \;&=\; -8(1+t_n)^2\Big[t_n\cos(t_n\theta_1)\sin(\theta_1)+\cos(\theta_1)\sin(t_n\theta_1)\Big]\times \\ &\quad \times\Big[t_n\sin(2\theta_1)+\sin(2t_n\theta_1)-2\eta\,\Big(t_n\sin^2(\theta_1)+\sin^2(t_n\theta_1)\Big)\Big] \end{aligned} \tag{10.2.55}$$

$$\begin{aligned} B_{1n} \;&=\; -8(1+t_n)^2\Big[1-t_n+t_n\cos(2\theta_1)-\cos(2t_n\theta_1)-\eta\,\Big(t_n\sin(2\theta_1)-\sin(2t_n\theta_1)\Big)\Big]\times \\ &\quad \times\Big[t_n\cos(t_n\theta_1)\sin(\theta_1)+\cos(\theta_1)\sin(t_n\theta_1)\Big] \end{aligned} \tag{10.2.56}$$

$$\begin{aligned} C_{1n} \;&=\; -8\,(1+t_n)\,\Big[t_n\cos(t_n\theta_1)\sin(\theta_1)+\cos(\theta_1)\sin(t_n\theta_1)\Big]\times \\ &\quad \times\Big\{\eta\,\Big[-1+\cos(2t_n\theta_1)+t_n\,[-\cos(2\theta_1)+\cos(2t_n\theta_1)]+2{t_n}^2\sin^2(\theta_1)\Big]+ \\ &\quad +{t_n}^2\sin(2\theta_1)-\sin(2t_n\theta_1)+t_n\,[-\sin(2\theta_1)+\sin(2t_n\theta_1)]\,\Big\} \end{aligned} \tag{10.2.57}$$

$$\begin{aligned} D_{1n} \;&=\; -8\,(1+t_n)\,\Big[t_n\cos(t_n\theta_1)\sin(\theta_1)+\cos(\theta_1)\sin(t_n\theta_1)\Big]\times \\ &\quad \times\Big\{\,(-1+t_n)\,\Big[-1+\cos(2t_n\theta_1)-2t_n\sin^2(\theta_1)\Big]+ \\ &\quad +\eta\,\Big[t_n\sin(2\theta_1)+{t_n}^2\sin(2\theta_1)-\sin(2t_n\theta_1)-t_n\sin(2t_n\theta_1)\Big]\Big\} \end{aligned} \tag{10.2.58}$$

$$\begin{aligned} A_{2n} \;&=\; Eq.(10.1.56) + \eta \quad \frac{8(1+t_n)^2}{1+\alpha}\Big\{-1-t_n+t_n\cos(2\theta_1)+\cos(2t_n\theta_1)+ \\ &+\; 2\beta\Big[1-{t_n}^2+{t_n}^2\cos(2\theta_1)-\cos(2t_n\theta_1)\Big]+ \\ &+\; \alpha\Big[-1+t_n+2{t_n}^2-t_n\cos(2\theta_1)-2{t_n}^2\cos(2\theta_1)+\cos(2t_n\theta_1)\Big]\Big\}\sin(\pi t_n) \end{aligned} \tag{10.2.59}$$

$$\begin{aligned} B_{2n} \;&=\; Eq.(10.1.57) + \\ &+\; \eta \quad 8(1+t_n)^2\cos(\pi t_n)\Big[-1+{t_n}^2-{t_n}^2\cos(2\theta_1)+\cos(2t_n\theta_1)\Big] \end{aligned} \tag{10.2.60}$$

$$
\begin{aligned}
C_{2n} &= Eq.(10.1.58) + \\
&+ \eta \quad \frac{8\,(1+t_n)}{1+\alpha}\sin(\pi t_n)\Big\{\,(1+t_n)\,\Big[\,-1+t_n-t_n\cos(2\theta_1)+\cos(2t_n\theta_1)\Big]\,+ \\
&+ \alpha\,(1+t_n)\,\Big[\,-1-t_n+2{t_n}^2+t_n\cos(2\theta_1)-2{t_n}^2\cos(2\theta_1)+\cos(2t_n\theta_1)\Big]\,+ \\
&+ 2\beta\,(1-t_n)\,\Big[\,-1+{t_n}^2-{t_n}^2\cos(2\theta_1)+\cos(2t_n\theta_1)\Big]\Big\} \qquad (10.2.61)
\end{aligned}
$$

$$
\begin{aligned}
D_{2n} &= Eq.(10.1.59) + \\
&+ \eta \quad 8(1+t_n)^2\cos(\pi t_n)\,\Big[1-{t_n}^2+{t_n}^2\cos(2\theta_1)-\cos(2t_n\theta_1)\Big]\,a. \qquad (10.2.62)
\end{aligned}
$$

In case of $\theta_1 = \pi/2, \theta_2 = -\pi$

$$
A_{1n} = 8t_n(1+t_n)^2\cos(\frac{\pi t_n}{2})\,\Big[\eta\,\Big(1+2t_n-\cos(\pi t_n)\Big)-\sin(\pi t_n)\Big] \qquad (10.2.63)
$$

$$
B_{1n} = -8t_n(1+t_n)^2\cos(\frac{\pi t_n}{2})\,[1-2t_n-\cos(\pi t_n)+\eta\,\sin(\pi t_n)] \qquad (10.2.64)
$$

$$
\begin{aligned}
C_{1n} &= -8t_n\,(1+t_n)\cos(\frac{\pi t_n}{2})\Big\{\eta\,\Big[-1+t_n+2{t_n}^2+\cos(\pi t_n)+t_n\cos(\pi t_n)\Big]\,- \\
&\quad -\sin(\pi t_n)+t_n\sin(\pi t_n)\Big\} \qquad (10.2.65)
\end{aligned}
$$

$$
\begin{aligned}
D_{1n} &= -8t_n\,(1+t_n)\cos(\frac{\pi t_n}{2})\Big[\,(-1+t_n)\,[-1-2t_n+\cos(\pi t_n)]\,- \\
&- \eta\,(1+t_n)\sin(\pi t_n)\Big] \qquad (10.2.66)
\end{aligned}
$$

$$
\begin{aligned}
A_{2n} &= Eq.(10.1.64) + \eta \quad \frac{8(1+t_n)^2}{1+\alpha}\Big\{-1-2t_n+\cos(\pi t_n)+ \\
&+ 2\beta\,\Big[1-2{t_n}^2-\cos(\pi t_n)\Big]+\alpha\,\Big[-1+2t_n+4{t_n}^2+\cos(\pi t_n)\Big]\,\Big\}\sin(\pi t_n) \qquad (10.2.67)
\end{aligned}
$$

$$
B_{2n} = Eq.(10.1.65) + \eta \quad 8(1+t_n)^2\cos(\pi t_n)\,\Big[-1+2{t_n}^2+\cos(\pi t_n)\Big] \qquad (10.2.68)
$$

$$
\begin{aligned}
C_{2n} &= Eq.(10.1.66) + \\
&+ \eta \quad \frac{8\,(1+t_n)}{1+\alpha}\sin(\pi t_n)\Big\{2\beta\,(1-t_n)\,\Big(-1+2{t_n}^2+\cos(\pi t_n)\Big)\,+ \\
&+ \alpha\,(1+t_n)\,\Big[-1-2t_n+4{t_n}^2+\cos(\pi t_n)\Big]\,+ \\
&+ \Big[-1+t_n+2{t_n}^2+\cos(\pi t_n)+t_n\cos(\pi t_n)\Big]\,\Big\} \qquad (10.2.69)
\end{aligned}
$$

$$
D_{2n} = Eq.(10.1.67) + \eta \quad 8(1+t_n)^2\,\Big[1-2{t_n}^2-\cos(\pi t_n)\Big]\cos(\pi t_n) \qquad (10.2.70)
$$

It should be mentioned that if $+\eta$ is used for the determination of the eigenvalue, Eqs. (10.2.23) through (10.2.70) can be used for the calculation of the angular functions. Otherwise, -η should replace η in Eqs. (10.2.23) through (10.2.70).

10.3 Determination of the Regular Stress Term for a Contact Problem

To determine the regular stress term, which corresponds to the solution of $\lambda_n = 0$ in the previous Section, the stress function (see Eq. (3.3.1)) given in Section 3.3 is used. For a contact problem the displacement u in r-direction at the interface is not used as a boundary condition. The stresses and the displacement v have the same relations as in Section 3.3 for thermal loading and mechanical loading. Therefore, the regular stress term for a contact problem is the same for thermal loading and mechanical loading. Inserting Eqs. (3.3.3, 3.3.4, 3.3.6) into Eqs. (10.2.3-10.2.5) yields

$$-2C_{10}\mu(1+\nu_1) + F_{10}E_2 + 2C_{20}(1+\nu_2) - F_{20}E_2 = 0 \tag{10.3.1}$$

$$\mu A_{10} - A_{20} = 0 \tag{10.3.2}$$

$$B_{10} + D_{10} - B_{20} - D_{20} = 0 \tag{10.3.3}$$

$$A_{10} + 2C_{10} - A_{20} - 2C_{20} = 0 \tag{10.3.4}$$

$$A_{10} + 2C_{10} \pm \eta\, 2(B_{10} + D_{10}) = 0 \tag{10.3.5}$$

$$A_{10}\theta_1 + B_{10} + C_{10}\sin(2\theta_1) + D_{10}\cos(2\theta_1) = 0 \tag{10.3.6}$$

$$A_{10} + 2C_{10}\cos(2\theta_1) - 2D_{10}\sin(2\theta_1) = 0 \tag{10.3.7}$$

$$A_{20}\theta_2 + B_{20} + C_{20}\sin(2\theta_2) + D_{20}\cos(2\theta_2) = 0 \tag{10.3.8}$$

$$A_{20} + 2C_{20}\cos(2\theta_2) - 2D_{20}\sin(2\theta_2) = 0 \tag{10.3.9}$$

for plane stress with $\mu = E_2/E_1$. For plane strain, E should be replaced by $\frac{E}{1-\nu^2}$, ν by $\frac{\nu}{1-\nu}$, and α by $\alpha(1+\nu)$. For the regular stress term the coefficients F_{k0} are not relevant. From Eqs. (10.3.2) - (10.3.9) the coefficients $A_{10}, B_{10}, C_{10}, D_{10}, A_{20}, B_{20}, C_{20}, D_{20}$ can be determined. Equations (10.3.2) - (10.3.9) make up a homogeneous system. Therefore, its solution is zero in the general case. If and only if the determinant of its coefficient matrix is zero, the equation system has a non-zero solution. The determinant of its coefficient matrix under arbitrary geometry (θ_1, θ_2) is

$$\begin{aligned}\mathrm{Det}[A_{cont.}] = \frac{64}{1+\alpha}\sin(\theta_1)\sin(\theta_2)\Big\{ &-(1+\alpha)\,\theta_1\cos(\theta_1)\cos(\theta_2) + \\ &+(1-\alpha)\,\theta_2\cos(\theta_1)\cos(\theta_2) + \sin(\theta_1-\theta_2) + \alpha\sin(\theta_1+\theta_2) + \\ &+\eta\left[(\alpha-1)\,\theta_2\cos(\theta_2)\sin(\theta_1) + (1+\alpha)\,\theta_1\cos(\theta_1)\sin(\theta_2) - 2\alpha\sin(\theta_1)\sin(\theta_2)\right]\Big\}.\end{aligned} \tag{10.3.10}$$

For the geometry (θ_1, θ_2) and material combination (α, η), which leads to Det$[A_{cont.}]$=0, the regular stress term is non-zero.
In case of $\theta_2 = -\theta_1$, there is

$$\mathrm{Det}[A_{cont.}] = \frac{128}{1+\alpha}\left[\theta_1\cos(\theta_1) - \sin(\theta_1)\right]\sin^2(\theta_1)\left[\cos(\theta_1) + \alpha\eta\ \sin(\theta_1)\right]. \quad (10.3.11)$$

If $\theta_2 = -\theta_1 = \pi/2$,

$$\mathrm{Det}[A_{cont.}] = -\frac{128}{1+\alpha}\alpha\eta. \quad (10.3.12)$$

This means that for the geometry $\theta_2 = -\theta_1 = \pi/2$ the regular stress term is always zero as long as $\eta \neq 0$ and $\alpha \neq 0$.
Following Eq. (10.3.10) it can be seen that for $\theta_1 = \pi$ and θ_2 being arbitrary or $\theta_2 = -\pi$ and θ_1 being arbitrary, there always is

$$\mathrm{Det}[A_{cont.}] = 0. \quad (10.3.13)$$

Therefore, for these geometries the regular stress term always is non-zero.
For an arbitrary geometry (θ_1, θ_2) the coefficients of the regular stress term can be calculated as $A_{k0} = K_0 A^*_{k0}$, $B_{k0} = K_0 B^*_{k0}$, $C_{k0} = K_0 C^*_{k0}$, $D_{k0} = K_0 D^*_{k0}$ with

$$A^*_{10} = 32\sin(\theta_1)\left[-\cos(\theta_1) + \eta\ \sin(\theta_1)\right]\sin^2(\theta_2) \quad (10.3.14)$$

$$B^*_{10} = 8\Big[-1 + \cos(2\theta_1) + 2\theta_1\sin(2\theta_1) + \eta\ \left[2\theta_1\cos(2\theta_1) - \sin(2\theta_1)\right]\Big]\sin^2(\theta_2) \quad (10.3.15)$$

$$C^*_{10} = 16\sin(\theta_1)\Big[\cos(\theta_1) + \eta\ \left[-2\theta_1\cos(\theta_1) + \sin(\theta_1)\right]\Big]\sin^2(\theta_2) \quad (10.3.16)$$

$$D^*_{10} = 8\Big[-1 + \cos(2\theta_1) + \eta\ \left[-2\theta_1\cos(2\theta_1) + \sin(2\theta_1)\right]\Big]\sin^2(\theta_2) \quad (10.3.17)$$

$$A^*_{20} = A^*_{10}\frac{1-\alpha}{1+\alpha} \quad (10.3.18)$$

$$\begin{aligned} B^*_{20} = \frac{4\sin(\theta_1)}{1+\alpha}\Big\{ & 4\left(1-\alpha\right)\theta_2\cos(\theta_1) - 4\left(1+\alpha\right)\theta_1\cos(\theta_1)\cos(2\theta_2) + \\ & + \ \left(3+\alpha\right)\sin(\theta_1 - 2\theta_2) + \left(1+3\alpha\right)\sin(\theta_1 + 2\theta_2) \\ & + 2\eta\left[2\left(\alpha-1\right)\theta_2\sin(\theta_1) + 2\left(1+\alpha\right)\theta_1\cos(\theta_1)\sin(2\theta_2) - \left(1+3\alpha\right)\sin(\theta_1)\sin(2\theta_2)\right]\Big\} \end{aligned} \quad (10.3.19)$$

$$C_{20}^{*} = \frac{16\sin(\theta_1)}{1+\alpha}\sin^2(\theta_2)\Big\{\cos(\theta_1) - \alpha\cos(\theta_1) + \eta\Big[-2\theta_1\cos(\theta_1) + \sin(\theta_1) + \\ + \alpha\left[-2\theta_1\cos(\theta_1) + 3\sin(\theta_1)\right]\Big]\Big\} \tag{10.3.20}$$

$$D_{20}^{*} = \frac{8\sin(\theta_1)}{1+\alpha}\Big\{2\left(1+\alpha\right)\theta_1\cos(\theta_1) + 2\left(-1+\alpha\right)\theta_2\cos(\theta_1) - 2\sin(\theta_1) + \\ + \cos(\theta_1)\sin(2\theta_2) - \alpha\left[2\sin(\theta_1) + \cos(\theta_1)\sin(2\theta_2)\right] \\ + \eta\left[2\left(1-\alpha\right)\theta_2\sin(\theta_1) - 2\left(1+\alpha\right)\theta_1\cos(\theta_1)\sin(2\theta_2) + \left(1+3\alpha\right)\sin(\theta_1)\sin(2\theta_2)\right]\Big\}. \tag{10.3.21}$$

The regular stress term can be determined from Eqs. (3.3.28-3.3.30), where K_0 is an unknown constant, which has to be calculated from the stress analysis of the total contact problem.
The coefficients of the regular stress term in case of $\theta_2 = -\theta_1$ are

$$A_{10}^{*} = 32{\theta_1}^3\left(-1+\eta\,\theta_1\right)\cos^4(\theta_1) \tag{10.3.22}$$

$$B_{10}^{*} = 8{\theta_1}^2\cos^2(\theta_1)\Big[-1+\cos(2\theta_1) + 2\theta_1\sin(2\theta_1) + \eta\left(2\theta_1\cos(2\theta_1) - \sin(2\theta_1)\right)\Big] \tag{10.3.23}$$

$$C_{10}^{*} = 16{\theta_1}^3\left(1-\eta\,\theta_1\right)\cos^4(\theta_1) \tag{10.3.24}$$

$$D_{10}^{*} = 8{\theta_1}^2\cos^2(\theta_1)\Big[-1+\cos(2\theta_1) + \eta\left(-2\theta_1\cos(2\theta_1) + \sin(2\theta_1)\right)\Big] \tag{10.3.25}$$

$$A_{20}^{*} = A_{10}^{*}\frac{1-\alpha}{1+\alpha} \tag{10.3.26}$$

$$B_{20}^{*} = \frac{4\theta_1\cos(\theta_1)}{1+\alpha}\Big\{\theta_1\cos(\theta_1)\Big[-5+\alpha-4\cos(2\theta_1) - 4\alpha\cos(2\theta_1)\Big] + \\ + \left(3+\alpha\right)\sin(3\theta_1) + 2\left(1-\alpha\right)\eta\,\theta_1\cos(\theta_1)\left[2\theta_1 - \sin(2\theta_1)\right]\Big\} \tag{10.3.27}$$

$$C_{20}^{*} = \frac{16\left(1-\alpha\right){\theta_1}^3\left(1-\eta\,\theta_1\right)\cos^4(\theta_1)}{1+\alpha} \tag{10.3.28}$$

$$D_{20}^{*} = \frac{8\left(-1+\alpha\right)}{1+\alpha}\theta_1\left(-1+\eta\,\theta_1\right)\cos^2(\theta_1)\left[2\theta_1 - \sin(2\theta_1)\right] \tag{10.3.29}$$

for $\sin(\theta_1) = \theta_1 \cos(\theta_1)$, and

$$A^*_{10} = 32\,(1+\alpha)\,\eta\,\sin^4(\theta_1) \tag{10.3.30}$$

$$B^*_{10} = 8\sin^2(\theta_1)\Big[-1+\cos(2\theta_1)+2\theta_1\sin(2\theta_1)+\eta\ \left[2\theta_1\cos(2\theta_1)-\sin(2\theta_1)\right]\Big] \tag{10.3.31}$$

$$C^*_{10} = 16\eta\ \left(1-\alpha+2\alpha\eta\,\theta_1\right)\sin^4(\theta_1) \tag{10.3.32}$$

$$D^*_{10} = 8\sin^2(\theta_1)\Big[-1+\cos(2\theta_1)+\eta\ \Big(-2\theta_1\cos(2\theta_1)+\sin(2\theta_1)\Big)\Big] \tag{10.3.33}$$

$$A^*_{20} = A^*_{10}\frac{1-\alpha}{1+\alpha} \tag{10.3.34}$$

$$\begin{aligned} B^*_{20} \;&=\; \frac{8\sin^2(\theta_1)}{1+\alpha}\Big\{1-\alpha+3\cos(2\theta_1)+\alpha\cos(2\theta_1)+2\alpha\,(1+\alpha)\,\eta\,{}^2\theta_1\sin(2\theta_1)+ \\ &+\;\; \eta\,\Big[2\theta_1\Big(1-\alpha^2+\alpha\cos(2\theta_1)+\alpha^2\cos(2\theta_1)\Big)+\sin(2\theta_1)+3\alpha\sin(2\theta_1)\Big]\Big\} \end{aligned} \tag{10.3.35}$$

$$C^*_{20} = 16\eta\ \left[1+\alpha+2\alpha\eta\,\theta_1\right]\sin^4(\theta_1) \tag{10.3.36}$$

$$D^*_{20} = -8\sin^2(\theta_1)\Big[2+2\alpha\eta\,{}^2\theta_1\sin(2\theta_1)+\eta\ \Big(2\theta_1+\sin(2\theta_1)+\alpha\sin(2\theta_1)\Big)\Big] \tag{10.3.37}$$

for $\cos(\theta_1) = -\eta\,\alpha\sin(\theta_1)$.
In case of $\theta_1 = \pi$ and θ_2 being arbitrary (but $\theta_2 \neq -\pi$) the regular stress term in material 1 is

$$\begin{aligned} \sigma_{xx10} &= K_0 \\ \sigma_{yy10} = \tau_{xy10} &= 0. \end{aligned} \tag{10.3.38}$$

In material 2 the regular stress term is zero, i.e.

$$\sigma_{xx20} = \sigma_{yy20} = \tau_{xy20} = 0. \tag{10.3.39}$$

If $\theta_1 = \pi$ and $\theta_2 = -\pi$, the regular stress term is

$$\begin{aligned} \sigma_{xx10} &= K_{10} \\ \sigma_{yy10} = \tau_{xy10} &= 0 \end{aligned} \tag{10.3.40}$$

$$\begin{aligned} \sigma_{xx20} &= K_{20} \\ \sigma_{yy20} = \tau_{xy20} &= 0, \end{aligned} \tag{10.3.41}$$

with two unknown constants K_{10} and K_{20}.

10.4 The Behavior of the Eigenvalues in a Contact Problem

In Sections 10.1 and 10.2 the essential equations to determine the eigenvalues were given for a contact problem with and without friction. For a friction free contact problem, the eigenvalue depends on the contact geometry (θ_1, θ_2) and the Dundurs parameter α only. For a contact problem with friction the eigenvalue depends on the contact geometry (θ_1, θ_2), both Dundurs parameters α, β, and the friction coefficient η. As these equations are transcendental equations of λ_n or t_n, the characteristics of the eigenvalues are not obvious. In this section the behaviors of the eigenvalues, e.g. for a given joint geometry how many singular terms exist or for which material combination the eigenvalues are real and complex or how large is the possible singular stress exponent or what is the dependence of the eigenvalue on the friction coefficient η and so on, will be discussed for two types of contact geometry that often appear in engineering structures. The first type of geometry is that one material has the angle 180° while the other is arbitrary (see Fig. 10.2). The second type of geometry is that $\theta_1 = -\theta_2 = 90^\circ$ (see Fig. 10.3).

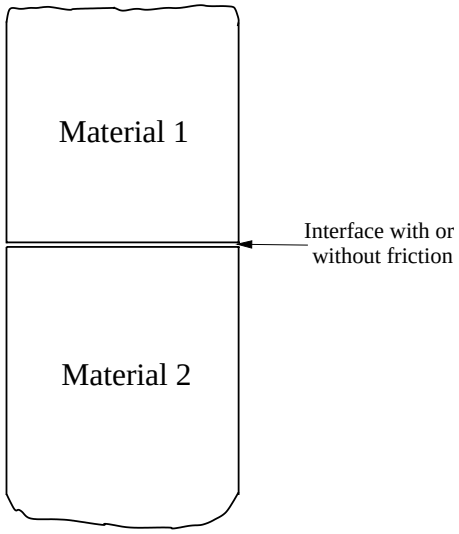

Figure 10.3: Two dissimilar materials contact: $\theta_1 = -\theta_2 = 90^\circ$.

Friction free contact problem

In this case, the behavior of the eigenvalues is very simple. The singular stress exponents depend on one Dundurs parameter α only. For the first type of contact geometry the singular stress exponents (here $\omega = \lambda$) are plotted in Fig. 10.4 at variable values of θ_1. From Fig. 10.4 it can be seen that (a) for all contact geometries, there is one singular term only and it is real. (b) For the contact geometry with $\theta_1 = 45^\circ$, there exists singular stress exponent only when α is very large ($\alpha > 0.8$). With increasing θ_1, the range of α increases where the stress exponent is singular, and for the same material combination the value of the stress exponent increases. (c) For $\theta_1 > 90^\circ$ there

always exists a singular stress exponent. (d) For $\alpha = 1$ always $\omega = 0.5$. (e) In a friction free contact problem the maximum value of the singular stress exponent is 0.5.

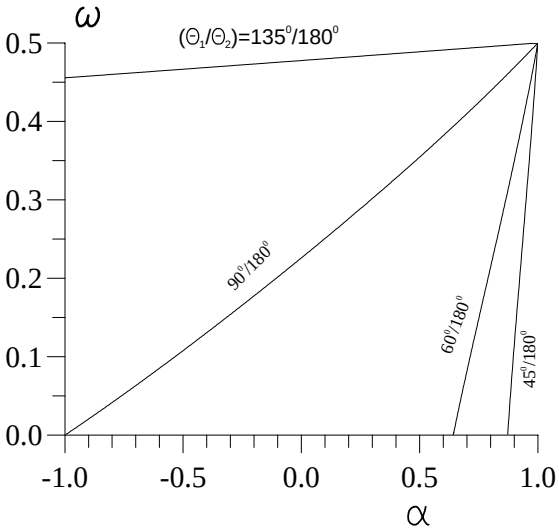

Figure 10.4: The singular stress exponent ω vs. the Dundurs parameter α for friction free contact with different contact angles.

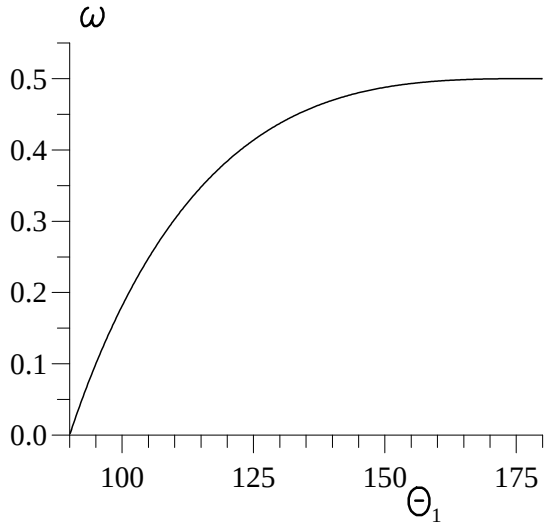

Figure 10.5: The singular stress exponent ω vs. the contact angle θ_1 for friction free contact with $\theta_1 = -\theta_2$.

For a contact geometry with $\theta_1 = -\theta_2 = 180°$ always $\omega = 0.5$ (see Eq. (10.1.17)).
For the second type of contact geometry (i.e. $\theta_1 = -\theta_2 = 90°$) there is no singular stress exponent (see Eq. (10.1.16)).
For the contact geometry with $\theta_1 = -\theta_2$ it can be seen from Eq. (10.1.15) that the eigenvalue depends not on α and β, and on θ_1 only. In Fig. 10.5 the singular stress exponent is plotted vs. the angle θ_1. It is obvious that for $\theta_1 \leq 90°$ no singular stress exponent exists.

Contact problem with friction

For a contact problem with friction the eigenvalues depend on the contact geometry (θ_1, θ_2), the material data (α, β), the friction coefficient (η), and the sign of the stress components σ_θ and $\tau_{r\theta}$ at the interface. If the sign of σ_θ and $\tau_{r\theta}$ at the interface is the same, Eq. (10.2.10) yields

$$A_{1n}\lambda_n + C_{1n}(2-\lambda_n) + \eta\,(2-\lambda_n)(B_{1n}+D_{1n}) = 0. \tag{10.4.1}$$

On the contrary, if the sign σ_θ and $\tau_{r\theta}$ at the interface is different,

$$A_{1n}\lambda_n + C_{1n}(2-\lambda_n) - \eta\,(2-\lambda_n)(B_{1n}+D_{1n}) = 0 \tag{10.4.2}$$

has to be applied. For mathematical simplification the last two equations can be written as

$$A_{1n}\lambda_n + C_{1n}(2-\lambda_n) + \eta\,(2-\lambda_n)(B_{1n}+D_{1n}) = 0 \tag{10.4.3}$$

where the value of η is positive if the sign of σ_θ and $\tau_{r\theta}$ at the interface is the same. If the sign of σ_θ and $\tau_{r\theta}$ at the interface is different, the value of η should be negative. Therefore, the parameter η in the following figures takes the value from -1 to 1. It should be mentioned that the negative value of η has no physical meaning. Here, it is only used for mathematical simplification.

For a contact geometry with $\theta_1 = 45°$ and $\theta_2 = -180°$ the isoline of the singular stress exponent $0 \leq \omega \leq 1$ is plotted in a Dundurs diagram in Fig. 10.6 for $\eta = 0.5$ (solid lines) and for $\eta = -0.5$ (dotted lines). It can be seen for this contact geometry: (a) There is only one singular term, and the eigenvalue is real. (b) Only for a large value of α ($\alpha > 0.7$ for positive η and $\alpha > 0.9$ for negative η), a singular stress exponent exists, i.e. for $\alpha < 0.7$ there is no stress singularity. To see the effect of the friction coefficient η on the stress exponent, Fig. 10.7 shows ω plotted vs. η for variable pairs of (α, β), which are the limit points in the Dundurs diagram. It is clear that: (a) If $\alpha < 0$, no singular stress exponent exists, irrespective of the value of η. (b) At a small value of α, a singular stress exponent only exists when η takes a large value. (c) At very large values of α, the singular stress exponent may exceed 0.5. (d) At the point of $\alpha = 1$ and $\beta = 0$, always $\omega = 0.5$, irrespective of the value of η.

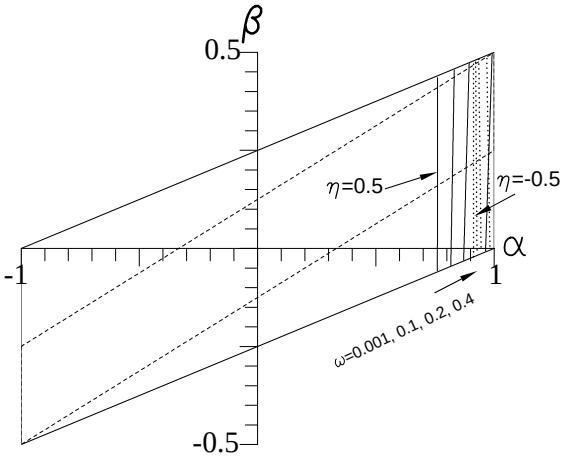

Figure 10.6: The isoline of the singular stress exponent ω in a Dundurs diagram at a friction coefficient of $\eta = 0.5$ (solid lines) and $\eta = -0.5$ (dotted lines), and $\theta_1 = 45°$ and $\theta_2 = -180°$.

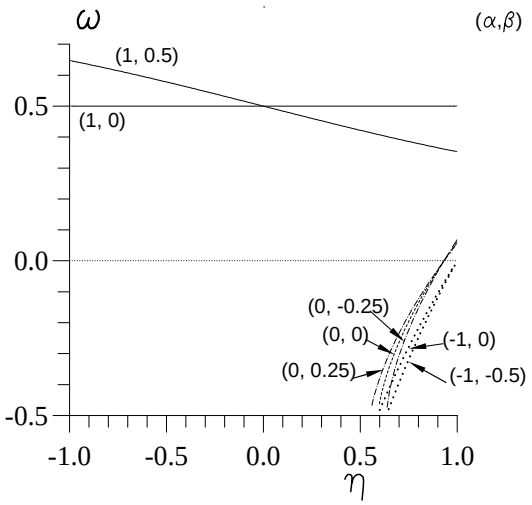

Figure 10.7: The singular stress exponent ω vs. the friction coefficient η for different pairs of (α, β), and $\theta_1 = 45°$ and $\theta_2 = -180°$.

For the contact geometries with $\theta_1 = 60°, 90°, 135°$, and $\theta_2 = -180°$ the isoline of the singular stress exponent is plotted in Figs. 10.8, 10.9, and 10.10 for $\eta = 0.5$ (solid lines) and for $\eta = -0.5$ (dotted lines). In Figs. 10.11, 10.12, and 10.13 ω is plotted vs. η for different pairs of (α, β). Comparing Figs. 10.6, 10.8, 10.9 and 10.10, and Figs. 10.7,

10.11 10.12 and 10.13, it can be seen that: (a) In a Dundurs diagram, the area where the singular stress exponent exists increases with increasing value of the angle θ_1. (b) For the same material combination (i.e. the same value of α, β, and η), it is almost true that the larger the value of θ_1 is, the larger is the singular stress exponent. To explain (b) clearly, in Fig. 10.14 the singular stress exponent is plotted vs. the angle θ_1 at variable (α, β, η).

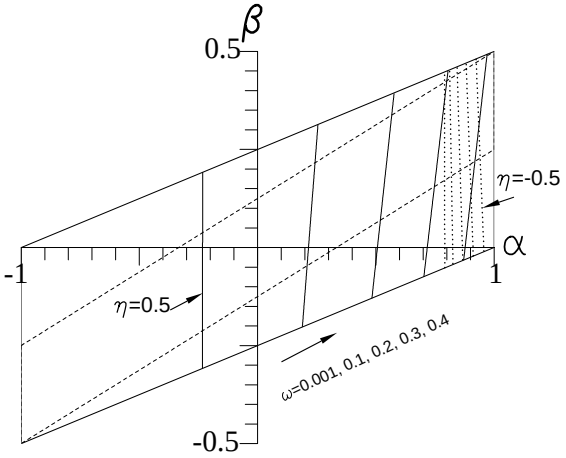

Figure 10.8: The isoline of the singular stress exponent ω in a Dundurs diagram at a friction coefficient of $\eta = 0.5$ (solid lines) and $\eta = -0.5$ (dotted lines), and $\theta_1 = 60°$ and $\theta_2 = -180°$.

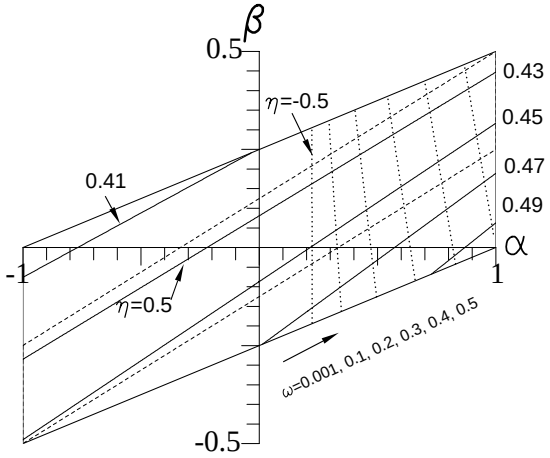

Figure 10.9: The isoline of the singular stress exponent ω in a Dundurs diagram at a friction coefficient of $\eta = 0.5$ (solid lines) and $\eta = -0.5$ (dotted lines), and $\theta_1 = 90°$ and $\theta_2 = -180°$.

For the special case of $\alpha = 1$, Eq. (10.2.21) can be simplified as

$$det[A] = -32(1 + t_n)\sin(\pi t_n)\Big[t_n^2 \sin^2(\theta_1) - \sin^2(t_n\theta_1)\Big]\Big[\cos(\pi t_n) \pm \eta\beta \sin(\pi t_n)\Big]. \quad (10.4.4)$$

From Eq. (10.4.4) it is known that (a) at $\beta = 0$, the singular stress exponent is 0.5, irrespective of the angle θ_1 and the friction coefficient η. (b) In case of $\beta \neq 0$, the singular stress exponent is independent of the angle θ_1, but depends on η. This is clearly evident from Figs. 10.7, 10.11, 10.12, and 10.13.
For the contact geometry with $\theta_1 = -\theta_2 = 90°$ and $\theta_1 = -\theta_2 = 180°$ the behavior of the singular stress exponent is shown in Figs. 10.15, 10.16, 10.17, and 10.18. As the geometry is symmetric to the line of $\theta = 0$, the singular stress exponent should be the same when exchanging material 1 and 2 (i.e. the signs of α and β change). From Figs. 10.15, 10.16, 10.17, and 10.18 it can be seen that this is true, if the sign of η is also changed. From the physical point of view, this means that due to the exchange of materials 1 and 2, the sign of the shear stress is changed. Consequently, the sign of η should be changed in the calculation. The effect of the friction coefficient η on the singular stress exponent is very clear from Figs. 10.16 and 10.18. For the contact

geometry with $\theta_1 = -\theta_2 = 90°$, there is no stress singularity if η=0 (i.e. friction free contact). However, the singular stress exponent may be larger than 0.5 for contact with friction. For the contact geometry with $\theta_1 = -\theta_2 = 180°$, the singular stress exponent is always 0.5 if η=0 (i.e. friction free contact). However, for contact with friction the singular stress exponent may be smaller or larger than 0.5.

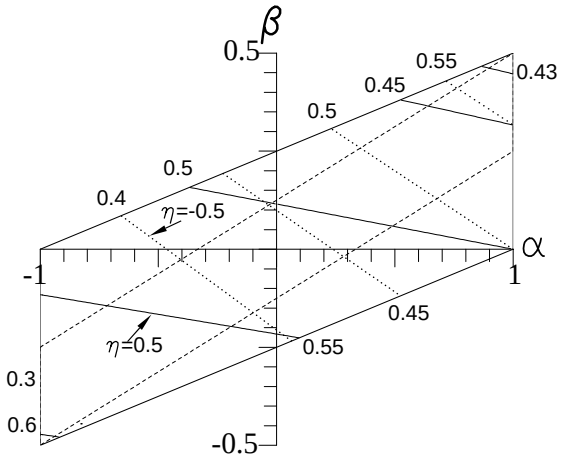

Figure 10.10: The isoline of the singular stress exponent ω in a Dundurs diagram at a friction coefficient of $\eta = 0.5$ (solid lines) and $\eta = -0.5$ (dotted lines), and $\theta_1 = 135°$ and $\theta_2 = -180°$.

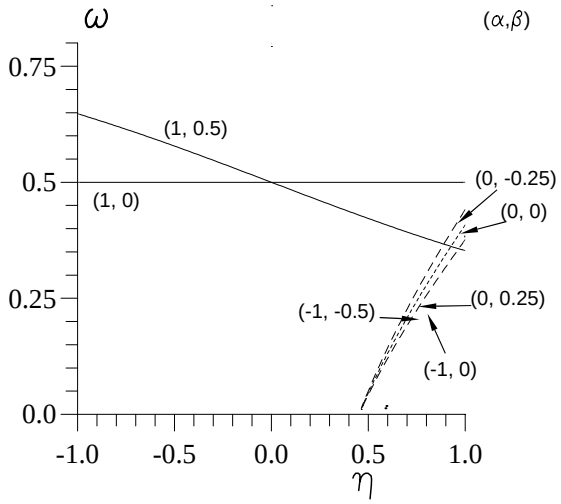

Figure 10.11: The singular stress exponent ω vs. the friction coefficient η for different pairs of (α, β), and $\theta_1 = 60°$ and $\theta_2 = -180°$.

To study the behavior of the singular stress exponent as a function of the contact geometry, three material combinations are considered. The first example is a homogeneous material contact problem. The isoline of the singular stress exponent is plotted in Fig. 10.19 for $\eta = 0.2$ and $\eta = -0.2$. Here, the x-axis is the angle θ_1 and the y-axis is the angle θ_2. Since the material is homogeneous, if we exchange the value of θ_1 and θ_2, and the sign of η, the singular stress exponent should be the same, which can be seen in Fig. 10.19.

As the second example, a real material combination of S_iC / Al is considered. The material data are E_1=410 GPa, ν_1=0.24, E_2=71 GPa, ν_2=0.35, which gives $\alpha = 0.686371, \beta = 0.140934$. The isoline of the singular stress exponent is plotted in Fig. 10.20 for $\eta = 0.2$ and $\eta = -0.2$. As the last example, the material combination of carbon steel / Al_2O_3 is chosen. The material data are E_1=215 GPa, ν_1=0.28, E_2=375 GPa, ν_2=0.27, which gives $\alpha = -0.268428, \beta = -0.078540$. The isoline of the singular stress exponent is plotted in Fig. 10.21 for $\eta = 0.2$ and $\eta = -0.2$. From Figs. 10.20 and 10.21 it can be seen that for a given material combination stress singularity disappears at a number of contact angles.

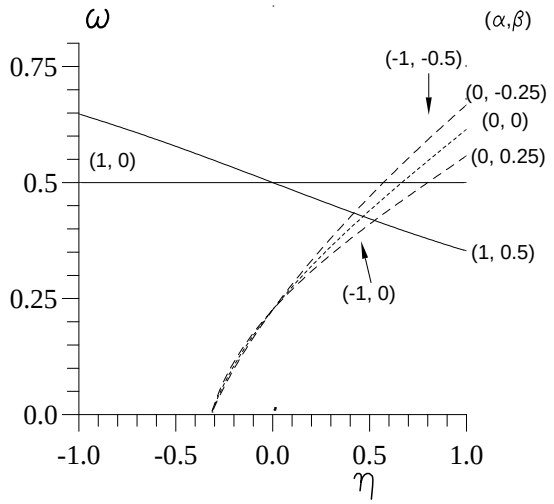

Figure 10.12: The singular stress exponent ω vs. the friction coefficient η for different pairs of (α, β), and $\theta_1 = 90°$ and $\theta_2 = -180°$.

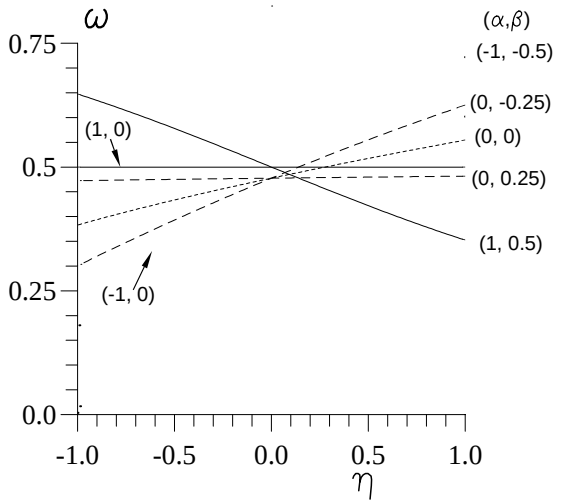

Figure 10.13: The singular stress exponent ω vs. the friction coefficient η for different pairs of (α, β), and $\theta_1 = 135°$ and $\theta_2 = -180°$.

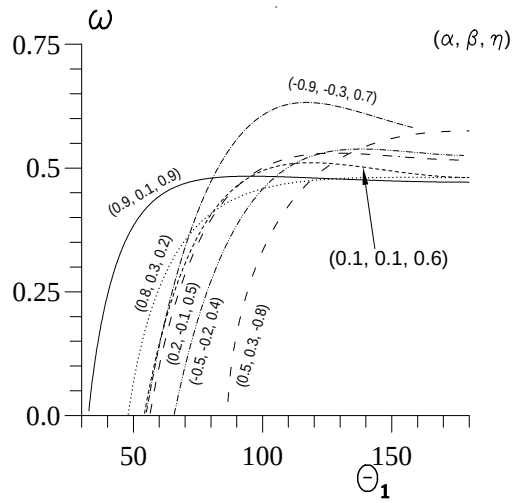

Figure 10.14: The singular stress exponent vs. the angle θ_1 at different (α, β, η) and $\theta_2 = -180°$.

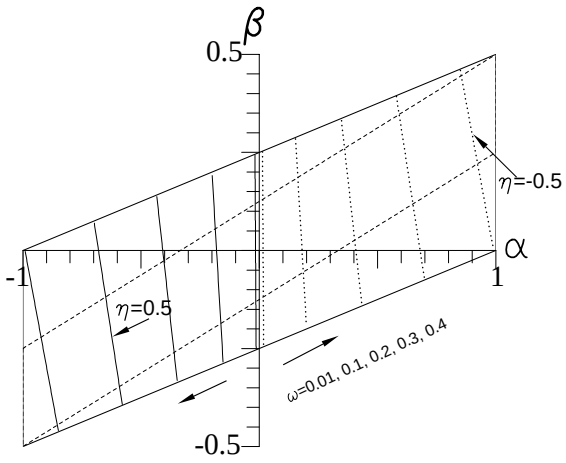

Figure 10.15: The isoline of the singular stress exponent ω in a Dundurs diagram at a friction coefficient of $\eta = 0.5$ (solid lines) and $\eta = -0.5$ (dotted lines), and $\theta_1 = 90°$ and $\theta_2 = -90°$.

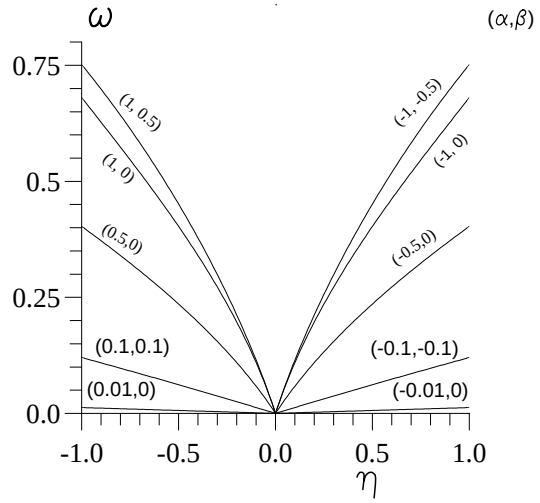

Figure 10.16: The singular stress exponent ω vs. the friction coefficient η for different pairs of (α, β), and $\theta_1 = 90°$ and $\theta_2 = -90°$.

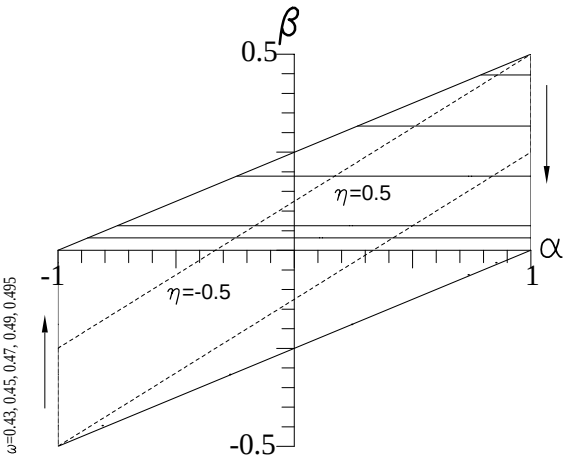

Figure 10.17: The isoline of the singular stress exponent ω in a Dundurs diagram at a friction coefficient of $\eta = 0.5$ (solid lines) and $\eta = -0.5$ (dotted lines), and $\theta_1 = 180°$ and $\theta_2 = -180°$.

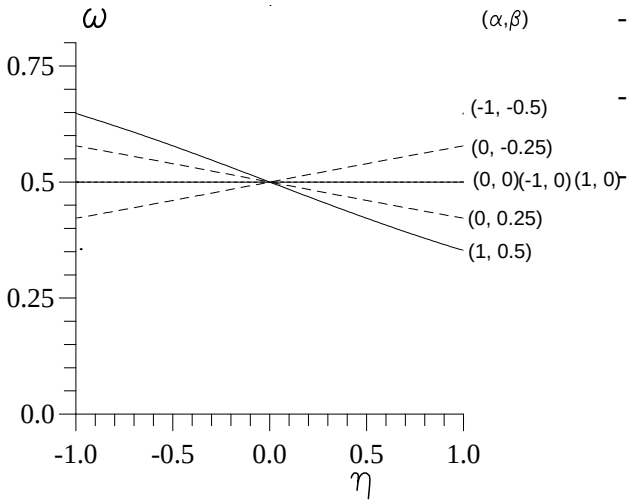

Figure 10.18: The singular stress exponent ω vs. the friction coefficient η for different pairs of (α, β), and $\theta_1 = 180°$ and $\theta_2 = -180°$.

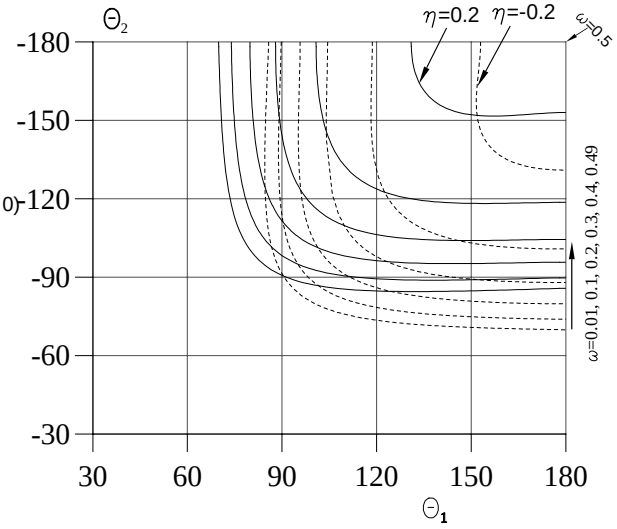

Figure 10.19: The isoline of the singular stress exponent ω at different contact angles θ_1, θ_2, friction coefficients of $\eta = 0.2$ (solid lines) and $\eta = -0.2$ (dotted lines), in homogeneous material.

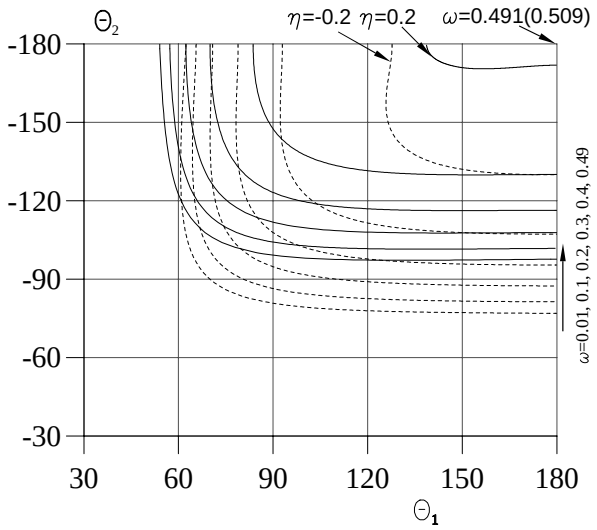

Figure 10.20: The isoline of the singular stress exponent ω at different contact angles θ_1, θ_2, friction coefficients $\eta = 0.2$ (solid lines) and $\eta = -0.2$ (dotted lines), in S_iC / Al.

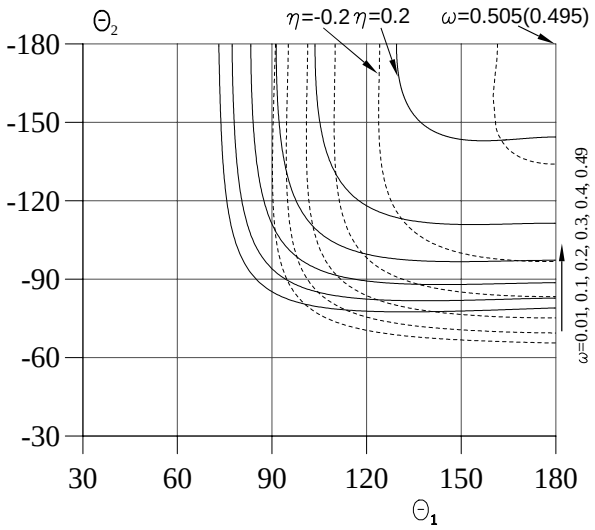

Figure 10.21: The isoline of the singular stress exponent ω at different contact angles θ_1, θ_2, friction coefficients $\eta = 0.2$ (solid lines) and $\eta = -0.2$ (dotted lines), in carbon steel / Al_2O_3.

Chapter 11

Conclusion

Stress singularities in dissimilar materials joints may occur under mechanical or thermal loading at the intersection point of a free edge and an interface or at an interface corner. For isotropic material the stress distribution near the singular point depends on the joint geometry, the loading and on the two Dundurs parameters, which are functions of the four elastic constants of the two materials. The stress distribution can be obtained by using the Airy stress function, or the corresponding relations with complex functions, or the Mellin transform method.
In this work, solutions of different singularity problems in a dissimilar materials joint are studied. The problems considered are: two dissimilar materials joint with free edges; dissimilar materials joint with edge tractions; joint with interface corner; joint with a given displacement at one edge; cracks in dissimilar materials joint; contact problem in dissimilar materials. The stress singularity can be divided into two groups: a r^{ω} singularity with the eigenvalue ω and a $r^{\omega}\ln(r)$ singularity. For the r^{ω} singularity and a real eigenvalue the stress distribution near the singular point is given by

$$\sigma_{ij}(r,\theta) = \sum_{n=1}^{N} \frac{K_n}{(r/R)^{\omega_n}} f_{ijn}(\theta) + \sigma_0 f_{ij0}(\theta) + \sum_{m=1}^{M} (r/R)^m \sigma_{ijm}^{ET}(\theta). \qquad (11.0.1)$$

The first term is the singular term, the second term is called the regular term and is especially important for thermal loading. The third term is important for edge traction loading. For complex eigenvalues $\lambda = \omega + ip$ the stress distribution is given by

$$\begin{aligned} \sigma_{ij}(r,\theta) &= \sum_{n=1}^{N} \frac{K_n}{(r/R)^{\omega_n}} \Big\{ \cos[p_n ln(r/R)] f_{ijn}^{c}(\theta) \\ &+ \sin[p_n ln(r/R)] f_{ijn}^{s}(\theta) \Big\} + \sigma_0 f_{ij0}(\theta) + \sum_{m=1}^{M} (r/R)^m \sigma_{ijm}^{ET}(\theta). \qquad (11.0.2) \end{aligned}$$

In case of a logarithmic singularity the stress distribution near the singular point can be obtained from:

$$\sigma_{ij}(r,\theta) = l_{ij} \Big\{ -2ln(r/R) f_{ij}(\theta) + t_{ij}(\theta) + (K + I_{ij}) f_{ij}(\theta) \Big\} \qquad (11.0.3)$$

or

$$\sigma_{ijn}(r,\theta) = -(r/R)^{\omega_n} ln(r/R) K_{1n} l_{ijn} f_{ijn}(\theta) + (r/R)^{\omega_n} \Big\{ K_{2n} l_{ijn} f_{ijn}(\theta) + K_{1n} \Big\{ I_{ijn} f_{ijn}(\theta) + l_{ijn} \Big[t_{ijn}(\theta) - \frac{X_{3n}}{3X_{2n}} f_{ijn}(\theta) - \frac{1}{\omega_n} f_{ijn}(\theta) \Big] \Big\} \Big\}. \tag{11.0.4}$$

The eigenvalues and the angular functions of the singular term depend on the notch angles and the elastic constants. The regular stress term depends on the notch angles, the elastic constants and the loading. For thermal loading the regular stress term always is nonzero. It can be determined analytically. However, for mechanical loading the regular stress term for most joint geometries and material combinations is zero. In some special cases, the regular stress term is non-zero. It can be determined analytically with one or two arbitrary constants, which have to be determined from the stress analysis of the total joint, as for the determination of the stress intensity factor. The stress intensity factors K_n are proportional to the applied mechanical or thermal load. They depend also on the notch angles and the elastic constants, additionally on the overall size of the joint.
Equations to calculate the stress exponents ω, p_n (for complex eigenvalue), the angular functions $f_{ijn}(\theta)$, $f^c_{ijn}(\theta)$, $f^s_{ijn}(\theta)$ and the regular stress term $\sigma_{ij0}(\theta)$ for thermal and mechanical loading are given for an arbitrary joint geometry. The methods to determine more than one stress intensity factors K_n at one time have been presented.
In general, it is true that if ω is the eigenvalue of the problem, $2-\omega$ also is the eigenvalue of the problem, except for a dissimilar materials contact problem with friction.

The most important results for each case are:

(I) Two dissimilar materials joint with free edges

- Explicit expressions are presented for the determination of the stress exponent and the regular stress term for an arbitrary joint geometry, and the angular functions for $\theta_1 = -\theta_2 = 90°$.
- An empirical relation for the determination of the stress intensity factor K was found for the most important joint with $\theta_1 = -\theta_2 = 90°$.
- For $\theta_1 - \theta_2 < 180°$ ($\theta_2 < 0$), i.e. the materials occupy an angle smaller than 180°, always there is a range in Dundurs diagram where no stress singularity exists ($\omega < 0$). With increasing total angle of the material occupied in a joint, there may exist one, two even three (e.g. for $\theta_1 - \theta_2 = 360°$) singular terms. The singular stress exponent may be larger than 0.5.
- The regular stress term for thermal loading is independent on the overall geometry of the joint.

• If one stress exponent (e.g. ω_1) goes through zero and the regular stress constant σ_0 goes to infinity, the corresponding K-factor (K_1) also goes towards infinity with a different sign, and the ratio of K_1/σ_0 at $\omega_1 = 0$ is equal to -1.

• For thermal loading the stress near the singular point, corresponding to the larger value of ω, is not always higher than the stress in a joint with a smaller ω, except for very small distances r. However, for mechanical loading the following holds: the larger is the ω, the higher is the stress near the singular point.

• For thermal loading the stress, also very close to the singular point, is strongly influenced by the regular term with the consequence that the stresses are not related to ω only.

• The absolute size of the joint has a obvious effect on the stress distribution near the singular point. The larger the value of ω is, the stronger is the effect of the size on stresses.

(II) Dissimilar materials joint with edge tractions

• The eigenvalues and the angular functions are the same as those for a joint with free edges.

• Equations to calculate the constant regular stress term $\sigma_{ij0}(\theta)$ and higher order regular stress terms $\sigma_{ijm}^{ET}(\theta)$ are given for an arbitrary joint geometry under arbitrary edge tractions. In particular, explicit expressions are presented for the determination of these regular stress terms for joint with $\theta_1 = -\theta_2 = 90°$.

• For joint with $\theta_1 = -\theta_2 = 90°$ and $H/L < 0.5$ or $H/L > 2$, under tension edge traction the stress intensity factor K can be obtained from the found empirical relations.

(III) Joint with interface corner

• Explicit expressions are presented for the determination of the stress exponent and the regular stress term for an arbitrary joint geometry, and the angular functions for $\theta_1 = 90°$.

• For a joint with an interface corner, there may be three singular terms, which are three real terms or one pair is complex. For most material combinations there are two singular terms. The maximum value of the singular stress exponent is 0.5.

• For thermal loading the regular stress term is independent of the joint geometry (i.e. θ_1).

• For joints with the same material combination, loading, and geometry, but with different interface conditions, the joint with a delamination crack (i.e. the interface being stress free) has much stronger singular stress exponents than a joint with an interface corner (interface being perfectly joined).

• For the same joint under different loading (thermal and mechanical loading) the behavior of the stress intensity factor is strongly different, even for $\theta_1 = 90°$.

(IV) Joint with a given displacement at one edge

• Explicit expressions are presented for the determination of the stress exponent and the regular stress term for an arbitrary joint geometry, and the angular functions for $\theta_1 = -\theta_2 = 90°$.

• For the same material combination and joint geometry, the singular stress exponent of a joint having a given displacement at one edge is larger than that one of a joint with free edges.

• For a joint with free edges, there is an area in Dundurs diagram where there is no singular stress exponent (i.e. $\omega < 0$), however, in a joint with a given displacement at one edge, there always exists at least one singular stress exponent.

• In a joint with a given displacement edge the maximum singular exponent is 1.

(V) cracks in dissimilar materials joint

• Four types of cracks are considered: cracks with an arbitrary angle terminating at the interface, cracks perpendicular to the interface, interface cracks and delamination cracks or interface corner cracks, which are under thermal and mechanical loading.

• Explicit expressions are presented for the determination of the stress exponent and the regular stress term for an arbitrary joint geometry, and the angular functions for joint with interface cracks and delamination cracks.

• The results have demonstrated that to obtain a good description of the stresses near the singular point over a large range analytically, the regular stress term should be considered, also for the joint with a strong singular stress exponent.

(VI) Contact problem in dissimilar materials

• The explicit expressions for calculating the stress exponents ω, p_n (for complex eigenvalue), the angular functions $f_{ijn}(\theta)$, and the regular stress term $\sigma_{ij0}(\theta)$ are given for an arbitrary joint geometry.

• If ω is the eigenvalue of the problem, $2-\omega$ also is the eigenvalue only for friction free contact problem. For contact problem with friction $2-\omega$ is not more the eigenvalue. In addition, for a friction free contact the eigenvalue is independent of the Dundurs parameter β.

• In a friction free contact problem the maximum value of the singular stress exponent is 0.5. In a contact problem with friction the maximum value of the singular stress exponent may be larger than 0.5 depending on the friction coefficient and Dundurs parameters. For all considered contact geometries, there is maximal one singular term and it is real.

• The regular stress term for a contact problem is the same for thermal loading and for mechanical loading, which is zero for most joint geometries and material combinations. In some special cases, the regular stress term is non-zero. It can be determined

analytically with one or two arbitrary constants, which have to be determined from the stress analysis of the total joint, as for the determination of the stress intensity factor.

(VII) Logarithmic stress singularities in a joint under thermal loading

- For the type of ln(r) and $r^{-\omega}$ln(r) stress singularity, equations to calculate the angular functions $f_{ij}(\theta)$ and $t_{ij}(\theta)$ are given for an arbitrary joint geometry. In particular, explicit expressions are presented for a joint geometry with $\theta_1 = -\theta_2 = 90^\circ$ and for the type of ln(r) stress singularity.
- The case of $\omega \to 0$ does not mean that the stress singularity disappears for a joint with a free edge under thermal loading.
- For joints with very small ω ($\omega < 10^{-2}$) in the type of $r^{-\omega}$ singularity, stresses near the singular point can also be described by the equations for the type of ln(r) stress singularity.
- The equations for the type of ln(r) stress singularity assuming K=0 can be applied to calculate stresses near the singular point for joints with $\omega < 0.01$ and $H_1/L > 1$, and $H_2/L > 1$. This means that the stresses near the singular point can be calculated without using any FEM. The error is less than 10% for $\omega < 0.01$ and r/L< 0.01. For $\omega < 0.005$ the error is less than 5%. If the corresponding value of K in Eq. (11.0.3) is used, the error is even smaller.
- The solution for the type of $r^{-\omega}$ln(r) singularity can be used to describe approximately the singular stress field for material combinations with two almost the same stress exponents ω (i.e. $\omega_i = \omega_j = \omega$) of $r^{-\omega}$ singularity.

The general rule is that: To describe the stress field near the singular point in a larger range, all singular terms plus the regular stress term (if it is not zero) should be used. Use of the so-called dominant singular term only is not sufficient to describe the singular stress field in the range of $r/L > 10^{-7}$.

The solutions of the singularity problem obtained in this work are useful for the selection of the material combination or the selection of the joint geometry to avoid or weaken the singularity. It can also be applied for the stress analysis near the singular point and for the optimization of the joined structure. Though only two isotropic materials joint is considered, the methods presented in this work can be used for more than two materials joint and for anisotropic materials. As long as in continuum mechanics, the solutions are also valid in micro-mechanics area.

Acknowledgements

The author would like to thank Prof. Dr. D. Munz for his support to this work, for a lot of helpful discussions and comments, and for giving his expert opinion on this work.

The author wish to express her gratitude to Prof. Dr. L. Banks-Sills, Prof. Dr. W. Becker and Prof. Dr. E. Schnack for giving their expert opinion on this work and their helpful comments.

Last but not the least, the author would like to thank her husband Dr. B. Yuan and her sons Kai and Kevin for their support to finish this work.

Bibliography

[1] Sheppard, L.M. (1988)
Global outlook for the ceramic heat engine, Adv. Ceramic Mater., 3, 309-315.

[2] Ito, M., Ishida, N. and Kato, N. (1988)
Development of brazing technology for ceramic turbocharger rotors, SAE Technical Paper Series P-207, Automotive ceramics - recent developments, 55-63.

[3] Bastawros, A.F. and Voloshin, A.S. (1990)
Thermal strain measurements in electronic packages through fractional fringe moirè interferometry, J. Electr. Pack., 112, 303-308.

[4] Kitamura, K. et al. (1991)
Experimental and analytical studies on residual stress in the tungsten-copper duplex structure for a divertor application, Fusion Eng. Design, 18, 173-178.

[5] Blanchard, J.P. and Ghoniem, N.M.(1990)
Analysis of singular Stress fields in duplex fusion components, J. of Nuclear Materials, 172, 54-70.

[6] S.Timoshenko (1925)
Analysis of bi-metal thermostats, J. of the Optical Society of America, 11, 233-255.

[7] Kuo, An-Yu (1989)
Thermal stresses at the edge of a bimetallic thermostat, Trans. ASME, J. of Appl. Mech., 56, 585-589.

[8] Hess, M.S. (1969)
The end problem for a laminated elastic strip - II. differential expansion stresses, J. Composite Materials, 3, 630-641.

[9] Delale, F., Erdogan, F. and Aydinoglu, M.N. (1981)
Stresses in adhesively bonded joints: a closed-form solution, J. Composite Materials, 15, 249-271.

[10] Eichen, J.W., Chung, C. and Kim, J.H. (1990)
Realistic modeling of edge effect stresses in bimaterial elements, Trans. ASME, J. of Elect. Packaging., 112, 16-23.

[11] Chen, Du and Cheng, Shun (1990)
Stress distribution in plane scarf and butt joints, Trans. ASME, J. of Appl. Mech., 57, 78-83.

[12] Cheng, S., Chen, D. and Shi, Y. (1991)
Analysis of adhesive-bonded joints with nonidentical adherents, J. of Engineering Mechanics, 117, 605-623.

[13] Hsueh, C.H. and Evans, A.G. (1985)
Residual stresses in metal/ceramic bonded strips, J. Am. Ceram. Soc., 68, 241-248.

[14] Xian, Ai-Ping and Si, Zhong-Yao (1990)
Residual stress in a soft-buffer-inserted metal/ceramic joint, J. Am. Ceram. Soc., 73, 3462-3465.

[15] Bigwood, D.A. and Crocombe, A.D. (1989)
Elastic analysis and engineering design formulae for bonded joints, Int. J. Adhesion and Adhesives, 9, 229-242.

[16] Grimado, P.B. (1978)
Interlaminar thermoelastic stresses in layered beams, J. of Thermal Stresses, 1, 75-86.

[17] Flanagan, G. (1994)
An efficient stress function approximation for the free-edge stresses in laminates, Inter. J. Solids Structures, 31, 941-952.

[18] Suhir, E. (1986)
Stresses in bi-metal thermostats, Trans. ASME, J. of Appl. Mech., 53, 657-660.

[19] Suhir, E. (1989)
Interfacial stresses in bimetal thermostats, Trans. ASME, J. of Appl. Mech., 56, 595-600.

[20] Pionke, C.D. and Wempner, G. (1991)
The various approximations of the bimetallic thermostatic strip, Trans. ASME, J. of Appl. Mech., 58, 1015-1020.

[21] Pao, Y.-H. and Eisele, E. (1991)
Interfacial shear and peel stresses in multilayered thin stacks subjected to uniform thermal loading, Trans. ASME, J. of Elect. Packaging., 113, 164-172.

[22] Mirman, B. (1992)
Interlaminar stresses in layered beams, Trans. ASME, J. of Elect. Packaging., 114, 389-396.

[23] Webber, J.P.H. and Morton, S.K. (1993)
An analytical solution for the thermal stresses at the free edge of laminated plates, Composites Sci. and Techno., 46, 175-185.

[24] Herakovich, C.T. (1976)
On thermal edge effects in composite laminates, Int. J. Mech. Sci., 18, 129-134.

[25] Kirchner, H.P., Conway,Jr., J.C. and Segall, A.E. (1987)
Effect of joint thickness and residual stresses on the properties of ceramic adhesive joints: I, finite element analysis of stresses in joints, J. Am. Ceram. Soc., 70, $104 - 109$.

[26] Levy, A. (1991)
Thermal residual stresses in ceramic-to-metal brazed joints, J. Am. Ceram. Soc., 74, 2141-2147.

[27] Lin, K.Y. and Tong, Pin (1980)
Singular finite elements for the fracture analysis of a V-notched plate, Int. J. for Numer. Methods in Engineering, 15, 1343-1354.

[28] Yeh, J.R. and Tadjbakhsh, I.G. (1986)
Stress singularity in composite laminates by finite element method, J. of Composite Materials, 20, 347-364.

[29] Abdi, R.E. (1991)
A special finite element for the analysis of the singularity in a bimaterial containing a crack perpendicular to the interface, Eng. Fract. Mech., 39, 1061-1065.

[30] Qian, J. and Long, Y.-Q. (1992)
Sub-region mixed FEM for calculating the stress intensity factor of an anti-plane notch in bi-material, Eng. Fract. Mech., 43, 1003-1007.

[31] Tan, M.A. and Meguid, S.A. (1997)
Analysis of bimaterial wedges using a new singular finite element, Int. J. of Fracture, 88, 373-391.

[32] Williams, M.L. (1952)
Stress singularities resulting from various boundary conditions in angular corners of plates in extension, Trans. ASME, J. of Appl. Mech., 74, 526-528.

[33] Dempsey, J.P. and Sinclair, G.B. (1981)
On the singular behavior at the vertex of a bi-material wedge, J of Elasticity, 11, 317-327.

[34] Blanchard, J.P. and Ghoniem. N.M. (1989)
An eigenfunction approach to singular thermal stresses in bonded strips, J. of Thermal Stresses, 12, 501-527.

[35] Bogy, D.B. (1971)
Two edge-bonded elastic wedges of different materials and wedge angles under surface tractions, Trans. ASME, J. of Appl. Mech., 38, 377-386.

[36] Bogy, D.B. (1972)
The plane solution for anisotropic elastic wedge under normal and shear loading, Trans. ASME, J. of Appl. Mech., 39, 1103-1109.

[37] Bogy, D.B. (1968)
Edge-bonded dissimilar orthotropic elastic wedge under normal and shear loading, Trans. ASME, J. of Appl. Mech., 35, 460-466.

[38] England, A.H. (1971)
On stress singularities in linear elasticity, Int. J. Engng Sci., 9, 571-585.

[39] Hein, V.L. and Erdogan, F. (1971)
Stress singularities in a two-material wedge, Int. J. of Fract. Mech., 7, 317-330.

[40] Kelly, P., Hills, D.A. and Nowell, D. (1992) The design of joints between elastically dissimilar components (with special reference to ceramic/metal joints), J. of Strain Analysis, 27, 15-20.

[41] Reedy, JR, E.D. (1990)
Intensity of the stress singularity at the interface corner between a bonded elastic and rigid layer, Engineering Fract. Mech., 36, 575-583.

[42] Ting, T.C.T. (1984)
The wedge subjected to tractions: a paradox re-examined, J. of Elasticity, 14, 235-247.

[43] Vasilopoulos, D. (1988)
On the determination of higher order terms of singular elastic stress fields near corners, Numer. Math., 53, 51-95.

[44] Wang, S.S. and Choi, I. (1982)
Boundary-layer effects in composite laminates: Part1: free-edge stress singularities, Trans. ASME, J. of Appl. Mech., 49, 541-548.

[45] Zwiers, R.I., Ting T.C.T. and Spilker, R.L. (1982)
On the logarithmic singularity of free-edge stress in laminated composites under uniform extension, Trans. ASME, J. of Appl. Mech., 49, 561-569.

[46] Dempsey, J.P. and Sinclair, G.B. (1979)
On the stress singularities in the plane elasticity of the composite wedge, J of Elasticity, 9. 373-391.

[47] Theocaris, P.S. (1974)
The order of singularity at a multi-wedge corner in a composite plate, Int. J. Engng. Sci., 12, 107-120.

[48] Sternberg, Eli and Koiter, W.T. (1958)
The wedge under a concentrated couple: a paradox in the two-dimensional theory of elasticity, Trans. ASME, J. of Appl. Mech., 25, 575-581.

[49] Sukumar, N. and Kumosa, M. (1992)
Stress singularities at sharp notches: interpolation formulas, Int. J. of Fracture, 58, R45-R49.

[50] Seweryn, A. and Zwoliński, J. (1993)
Solution for the stress and displacement fields in the vicinity of a V-notch of negative wedge angle in plane problems of elasticity, Engng. Fract. Mech., 44, 275-281.

[51] Dimitrov, A., Andrä, H. and Schnack, E. (2001)
Efficient computation of order and mode of corner singularities in 3D-elasticity. Int. J. Numer. Meth. Engng., 52, 805-827.

[52] Dimitrov, A., Andrä, H. and Schnack, E. (2002)
Singularities near three-dimensional corners in composite laminates. International Journal of Fracture, 115, 361-375.

[53] Dimitrov, A. and Schnack, E. (2002)
Asymptotical Expansion in Non-Lipschitz-Ian Domains - a Numerical Approach. Numerical Linear Algebra with Applications, 9, 467-492.

[54] Dimitrov, A., Buchholz, F.-G. and Schnack, E. (2002)
Free-surface effects in crack propagation: a theoretical-numerical-experimental correlation. Preprint.

[55] Iancu, O.T., Fett, T. and Munz, D. (1990)
A fracture mechanical treatment of free edge stress singularities applied to a brazed ceramic/metal compound, Int. J. Fracture, 46, 159-172.

[56] Inoue, T. and Koguchi, H. (1996)
Influence of the intermediate material on the order of stress singularity in three-phase bonded structure, Inter. J. Solids Structures, 33, 399-417.

[57] Raju, I.S. and Crews, Jr., J.H. (1981)
Interlaminar stress singularities at a straight free edge in composite laminates, Computers & Structures, 14, 21-28.

[58] Miller, G.R. and Stock, W.L. (1989)
Analysis of branched interface cracks between dissimilar anisotropic media, Trans. ASME, J. of Appl. Mech., 56, 844-849.

[59] Huang, T.-F. and Chen W.-H. (1994)
On the free-edge stress singularity of general composite laminates under uniform axial strain, Inter. J. Solids Structures, 31, 3139-3151.

[60] Ting, T.C.T. and Chou, S.C. (1981)
Edge singularities in anisotropic composites, Inter. J. Solids Structures, 17, 1057-1068.

[61] Labossiere, P.E.W. and Dunn, M.L. (1998)
Calculation of stress intensities at sharp notches in anisotropic media, Eng. Fract. Mech., 61, 635-654.

[62] Mizuno, K., Miyazawa, K. and Suga, T. (1988)
Characterization of thermal stress in ceramic/metal-joint, J. of the Faculty of Eng., Uni. of Tokyo (B) Vol.XXXIX, No.4, 401-412.

[63] Suga, T., Mizuno, K. and Miyazawa, K. (1989)
Thermal stresses in ceramic-to-metal joints, MRS Int'I.Mtg. on Adv. Mats., 8, 137-142.

[64] Gradin, Per A. (1982)
A fracture criterion for edge-bonded bimaterial bodies, J. Composite Materials, 16, 448-456.

[65] Munz, D. and Yang, Y.Y. (1994)
Stresses near the free edge of the interface in ceramic to metal joints, J. of the Euro. Cer. Soc. 13, 453-460.

[66] Qian, Z.Q. and Akisanya, A.R. (1998)
Analysis of free-edge stress and displacement fields in scarf joints subjected to a uniform change in temperature, Fatigue & Fracture of Eng. Mater. & Structures, 21, 687-703.

[67] Reedy, JR, E.D.(1991)
Intensity of the stress singularity at the interface corner of a bonded elastic layer subjected to shear, Engng. Fract. Mech., 38, 273-281.

[68] Ding, S.-L. and Kumosa, M. (1994)
Singular stress behavior at an adhesive interface corner, Eng. Fract. Mech., 47, 503-519.

[69] Micheal, M.M. (1991)
The thermal stress singularities in microelectronics, IEEE, 273-277.

[70] Wang, S.S. and Choi, I. (1982)
Boundary-layer effects in composite laminates: Part 2 : free-edge stress solutions and basic characteristics, Trans. ASME, J. of Appl. Mech., 49, 549-560.

[71] Carpenter, W.C. (1984)
A collocation procedure for determining fracture mechanics parameters at a corner, Int. J. Fracture, 24, 255-266.

[72] Fett, T. (1998)
A boundary collocation analysis of a bimaterial plate with different elastic properties, Engng. Fract. Mech., 59, 29-45.

[73] Sham, T.-L. and Brueckner, H.F. (1988)
The weight-function theory for piecewise homogeneous isotropic notches in anti-plane strain, Trans. ASME, J. of Appl. Mech., 55, 596-603.

[74] Wang, S.S. and Choi, I. (1979)
Boundary layer thermal stresses in angle-ply composite laminates, J.R.Vinson ed., Modern Devel. in Composite Mater. and Struct., 315-341.

[75] Carpenter W.C. and Byers, C. (1987)
A path independent integral for computing stress intensities for V-notched cracks in a bi-material, Int. J. Fracture, 35, 245-268.

[76] Banks-Sills, L, Yang, Y.Y. and Munz, D. (1997)
An influence function for stress intensity factors of a bimaterial notched bodies. Int. J. of Fracture, 85, 333-350.

[77] Banks-Sills, L. (1997)
A conservative integral for determining stress intensity factors of a bimaterial strip, Int. J. of Fracture, 86, 385-398.

[78] Munz, D. and Yang, Y.Y. (1992)
Stress singularity at the interface in bonded dissimilar materials under mechanical and thermal loading, ASME J. Appl. Mech. 59, 857-861.

[79] Tilscher, M., Munz, D. and Yang, Y.Y. (1994)
The relationship between the stress intensity factor and the stress exponent for bimaterial under thermal loading, Int. J. Fract. 65, R23-R28.

[80] Tilscher, M., Munz, D. and Yang, Y.Y. (1995)
The stress intensity factor in bonded quarter planes after a change in temperature, J. of Adhesion 49, 1-21.

[81] Munz, D. and Yang, Y.Y. (1993)
Stresses near the edge of bonded dissimilar materials described by two stress intensity factors, Int. J. Fract., 60, 169-177.

[82] Inoue, T. and Koguchi, H. (1997)
Relaxation of thermal stresses in dissimilar materials (approach based on stress intensity), Inter. J. Solids Structures, 34, 3215-3233.

[83] Yang, Y.Y. and Munz, D. (1995)
The stress distribution in a dissimilar materials joint for complex singular eigenvalues under thermal loading, J. of Thermal Stresses, 18, 407-419.

[84] Yang, Y.Y. (1992)
Spannungssingularitäten in Zweistoffverbunden bei mechanischer und thermischer Belastung. Bericht VDI, Reihe 18 Nr.113, VDI Verlage, Düsseldorf (in German).

[85] Yang, Y.Y. and Munz, D. (1992)
A method of determination of the regular stress term for an arbitrary joint geometry under thermal loading, KfK - Report, No. 5089.

[86] Munz, D., Fett, T. and Yang, Y.Y. (1993)
The regular stress term in bonded dissimilar materials after a change in temperature, Engng. Fract. Mech. 44, 185-194.

[87] Yang, Y.Y. and Munz, D. (1994)
Determination of the regular stress term in a dissimilar materials joint under thermal loading by the Mellin transform, J. of Thermal Stresses, 17, 321-336.

[88] Theocaris, P.S. (1987)
The Mesophase concept in composites, Springer-Verlag, Berlin.

[89] Sih, G.C. and Rice, J.R. (1964)
The bending of plates of dissimilar materials with cracks, Trans. ASME, J. of Appl. Mech., 31, 477-482.

[90] Rice, J.R. and Sih, G.C. (1965)
Plane problems of cracks in dissimilar media, Trans. ASME, J. of Appl. Mech., 32, 418-423.

[91] England, A.H. (1965)
A crack between dissimilar media, Trans. ASME, J. of Appl. Mech., 32, 400-402.

[92] Erdogan, F. (1965)
Stress distribution in bonded dissimilar materials with cracks, Trans. ASME, J. of Appl. Mech., 32, 403-410.

[93] Mak, A.F. and Keer, L.M., Chen, S.H. and Lewis, J.L. (1980)
A no-slip interface crack, Trans. ASME, J. of Appl. Mech., 47, 347-350.

[94] Erdogan, F. and Ozbek, T. (1969)
Stresses in fiber-reinforced composites with imperfect bonding, Trans. ASME, J. of Appl. Mech., 36, 865-869.

[95] Comninou, Maria (1977)
The interface crack, Trans. ASME, J. of Appl. Mech., 44, 631-636.

[96] Theocaris, P.S. and Gdoutos, E.E. (1977)
Stress singularity in cracked composite full-planes, Int. J. Fract., 13, 763-773.

[97] Willians, M.L. (1959)
The stresses around a fault or crack in dissimilar media, Bulletin of the Seismological Soc. of Amer., 49, 199-204.

[98] Smelser, R.E. (1979)
Evaluation of stress intensity factors for bimaterial bodies using numerical crack flank displacement data, Int. J. Fracture, 15, 135-143.

[99] Hutchinson, J.W., Mear, M.E. and Rice, J.R. (1987)
Crack paralleling an interface between dissimilar materials, Trans. ASME, J. of Appl. Mech., 54, 828-832.

[100] Rice, J.R. (1988)
Elastic fracture mechanics concepts for interfacial cracks, Trans. ASME, J. of Appl. Mech., 55, 98-103.

[101] Matos, P.P.L, McMeeking, R.M., Charalambides, P.G. and Drory, M.D. (1989)
A method for calculating stress intensities in bimaterial fracture, Int. J. of Fracture, 40, 235-254.

[102] Akisanya, A.R. and Fleck, N.A. (1997)
Interfacial cracking from the free-edge of a long bi-material strip, Inter. J. Solids Structures, 34, 1645-1665.

[103] Duva, J.M. (1990)
The singularity strength at the apex of a wedge undergoing finite deformations, Trans. ASME, J. of Appl. Mech., 57, 577-580.

[104] Dempsey, J.P. (1981)
The wedge subjected to tractions: a paradox resolved, J of Elasticity, 11, 1-10.

[105] Ting, T.C.T. (1985)
Asymptotic solution near the apex of an elastic wedge with curved boundaries, Quart. of Appl. Mathematics, 467-476.

[106] Kuo, M.C. and Bogy, D.B. (1974)
Plane solutions for the displacement and traction-displacement problems for anisotropic elastic wedges, Trans. ASME, J. of Appl. Mech., 41, 197-202.

[107] Willians, M.L. (1956)
The complex-variable approach to stress singularities, Trans. ASME, J. of Appl. Mech., 23, 477-478.

[108] Bogy, D.B. and Sternberg, E. (1968)
The effect of couple-stresses on the corner singularity due to an asymmetric shear loading, J. of Solids Structure, 4, 157-174.

[109] Bogy D.B. (1970)
On the problem of edge-bonded elastic quarter-planes loaded at the boundary, J. of Solids Structure, 6, 1287-1313.

[110] Yang, Y.Y. and Munz, D. (1997)
Stress singularities in a dissimilar materials joint with edge tractions under mechanical and thermal loading, J. of Solids Structure, 34, 1199-1216.

[111] Bogy, D.B. and Wang, K.C. (1971)
Stress singularities at interface corners in bonded dissimilar isotropic elastic materials, J. of Solids Structure, 7, 993-1005.

[112] van Vroonhoven, J.C.W. (1992)
Stress singularities in bi-material wedges with adhesion and delamination, Fatigue Fract. Engng Mater. Struct., 15, 157-171.

[113] Keer, L.M. and Parihar, K.S. (1978)
Elastic stress singularity at conical inclusions, J. of Solids Structure, 14, 261-263.

[114] Chen, D.-H. and Nisitani, H. (1993)
Singular stress field near the corner of joined dissimilar materials, J. of Appl. Mech., 60, 607-613.

[115] Yang, Y.Y. and Munz, D. (1995)
Stress intensity factor and stress distribution in a joint with an interface corner under thermal and mechanical loading, J. Computers & Structures 57, 467-476.

[116] Groth, H.L. (1988)
Stress singularities and fracture at interface corners in bonded joints, Int. J. Adhesion and Adhesives, 8, 107-113.

[117] Vasilopoulos, D. (1990)
An algorithm for the eigenvalues of a fixed-fixed corner, Eng. Fract. Mech., 37, 839-851.

[118] Bogy,D.B. (1970).
On the problem of edge-bonded elastic quarter-planes loaded at the boundary. Inter. J. of Solids and Structures 6, 1287-1313.

[119] Chen, D.-H. (1996)
Logarithmic singular stress field in a semi-infinite plate consisting of two edge-bonded wedges subjected to surface tractions, Int. J. Fract., 75, 357-378.

[120] Gadi, K.S., Joseph, P.F., Zhang, N.-S. and Kaya, A.C. (2000)
Thermally induced logarithmic stress singularities in a composite wedge and other anomalies, Engng. Fract. Mech., 65, 645-664.

[121] Dempsey, J.P. (1995)
Power-logarithmic stress singularities at bi-material corners and interface cracks. J. Adhesion Sci. Technol. 9, 253-265.

[122] Yang, Y.Y. (1998)
Asymptotic description of the logarithmic singular stress field and its application, J. of Solids Structure, 35, 3917-3933.

[123] Yang, Y.Y. (1999)
The type of $r^{-\omega}\ln(r)$ stress singularities in a two - dissimilar - materials joint under thermal loading, J. of Thermal Stresses, 22, 101-121.

[124] Yang, Y.Y. (1999)
Effect of the regular term on the stress field in a joint of dissimilar materials under remote mechanical load, Archive of Applied Mechanics, 69, 364-378.

[125] Adams, G.G. and Bogy, D.B. (1976)
The plane solution for the elastic contact problem of a semi-infinite strip and half plane, J. of Appl. Mech., 43, 603-607.

[126] Adams, G.G. and Bogy, D.B. (1977)
The plane symmetric contact problem for dissimilar elastic semi-infinite strip of different widths, J. of Appl. Mech., 44, 604-610.

[127] Dundurs, J. and Lee, M.-S. (1972)
Stress concentration at a sharp edge in contact problems, J. of Elasticity, 2, 109-112.

[128] Miniatt, E.C., Waas, A.M. and Anderson, W.J. (1990)
An experimental study of stress singularities at a sharp corner in a contact problem, Experimental Mechanics, 281-285.

[129] Comninou, Maria (1977)
Interface crack with friction in the contact zone. Trans. ASME, J. of Appl. Mech., 44, 780-781.

[130] Dundurs, J. (1969)
Discussion on 'edge-bonded dissimilar orthogonal elastic wedges under normal and shear loading', J. of Appl. Mech., 36, 650-652.

[131] Timoshenko, S.P. and Goodier, J.N. (1982)
Theory of elasticity. 3rd Ed, Mc Graw Hill, Singapore.

[132] Pageau, S.S, Gadi, K.S., Biggers, Jr., S.B and Joseph, P.F. (1996)
Standardized complex and logarithmic eigensolutions for n-material wedges and junctions, Int. J. of Fracture, 77, 51-76.

[133] Fraenkle, M., Munz, D. and Yang, Y.Y. (1996)
Stress Singularities in a bimaterial joint with inhomogeneous temperature distribution, Inter. J. Solids Structures, 33, 2039 - 2054.

[134] Hu, S.Y., Li, Y.L., Munz, D. and Yang, Y.Y. (1998)
Thermal stresses in coated structures, Surface and Coating Technology, 99, 125-131.

[135] Glushkov, E.V., Glushkova, N.V., Munz, D. and Yang, Y.Y. (2000)
Analytical solution for bonded wedges under thermal loading, Int. J. of Fracture, 106, 321-339.

[136] Banks-Sills, L. and Sherer, A. (2002)
A conservative integral for determining stress intensity factors of a bimaterial notch. Int. J. Fract., 115, 1-26.

[137] Fett, T. (2002)
T-stress solutions and stress intensity factors for 1-D cracks. Bericht VDI, Reihe 18, Nr.272, VDI Verlage, Düsseldorf.

[138] Gharpuray, V.W., Dundurs, J. and Keer, L.M. (1991)
A crack terminating at a slipping interface between two materials, J. of Appl. Mech., 58, 960-963.

[139] Chiang, C.R. (1991)
On the stress intensity factors of cracks near an interface between two media, Int. J. Fract., 47, R55-R58.

[140] Qian, J. (1992)
A general formula for plane corners, Int. J. Fract., 54, R41-R46.

[141] Romeo, A. and Ballarini, R. (1995)
A crack very close to a bimaterial interface, Trans. ASME, J. of Appl. Mech., 62, 614-619.

[142] Atkinson, C. (1975)
On the stress intensity factors associated with cracks interacting with an interface between two elastic media, Int. J. Engng. Sci., 13, 489-504.

[143] Glaser, C.J. (1990)
Thermal stresses in compliantly joined materials, Trans. ASME J. of Elec. Packaging, 112, 24-29.